THE
PHYSICAL REVIEW

A journal of experimental and theoretical physics established by E. L. Nichols in 1893

SECOND SERIES, VOL. 74, NO. 12 DECEMBER 15, 1948

On the Relative Abundance of the Elements*

RALPH A. ALPHER AND ROBERT C. HERMAN
Applied Physics Laboratory, The Johns Hopkins University, Silver Spring, Maryland

(Received September 1, 1948)

The theory of the neutron capture process for the formation of the elements has been reformulated, taking into account the radioactive decay of neutrons as well as the expansion of the universe. However, the calculations have been carried out for the case of a static universe. Satisfactory agreement between this theory and observed relative abundances has been obtained with the assumption that the density of matter was 5×10^{-9} g/cm^3 at the start of the capture process.

I. INTRODUCTION

THE problem of explaining the observed relative abundance of the elements is of interest both in itself and because it may give information concerning the structure and evolution of the universe. The failure of equilibrium theories[1] to give a reasonably simple explanation of the observed relative abundances, together with the changes in physical conditions which must have accompanied the early stages of the expansion of the universe, led Gamow[2] to the suggestion that a rapid non-equilibrium process was responsible. Recently a non-equilibrium theory of the building up of nuclei based on the successive capture of neutrons was suggested by Alpher, Bethe, and Gamow,[3] and the detailed results of this theory were developed by one of us.[4]

The purpose of this paper is to reformulate the theory of the neutron capture process by taking into account explicitly the radioactive decay of neutrons. The effect of the expansion of the universe on this theory is indicated in the formulation but is not included in the calculations described. This work revises previous estimates as to the physical conditions during the early stages of the expansion. Finally, some of the features of the abundance data resulting from variations in neutron capture cross section are discussed.

II. FORMULATION OF THE PROBLEM

It is suggested that the elements were formed in the following manner. Early in the expansion of the universe, the ylem consisted of neutrons only. During the early stages the universe

* The work described in this paper was supported by the Bureau of Ordnance, U. S. Navy, under Contract NOrd-7386.

[1] The following is a partial list of papers on the equilibrium theory: T. E. Sterne, Mon. Not. R. Astr. Soc. **73**, 736, 767, 770 (1938). C. von Weizsäcker, Phys. Zeits. **39**, 633 (1938). S. Chandrasekhar and L. R. Henrich, Astrophys. J. **95**, 288 (1942). G. Wataghin and P. S. de Toledo, Phys. Rev. **73**, 79 (1948). G. B. van Albada, Bull. Astr. Inst. Neth. Vol. X, No. 374, Sept. 12, 1946. See also Astrophys. J. **105**, 393 (1947). O. Klein, G. Beskow and L. Treffenberg, Ark. Mat. Astr. Fys. **33A**, No. 1 (1946). G. Beskow and L. Treffenberg, Ark. Mat. Astr. Fys. Pt. I, **34A**, No. 13 (1947); Pt. II, **34A**, No. 17 (1947). J. Géhéniau, I. Prigogine, and M. Demeurs, Physica, 's Grav. **13**, 429 (1947). F. Hoyle, Mon. Not. R. Astr. Soc. **106**, 343 (1946).

[2] G. Gamow, Phys. Rev. **70**, 572 (1946).

[3] R. A. Alpher, H. A. Bethe, and G. Gamow, Phys. Rev. **73**, 803 (1948).

[4] R. A. Alpher, Phys. Rev. **74**, 1577 (1948).

TABLE I.*

j	P_j	$(\xi_j/\xi_1)_{max}$
1	5.01	1.000
2	4.62	0.782
3	4.72	0.442
4	4.88	0.204

i	Π_i	$(\xi_i/\xi_1)_{max}$	i	Π_i	$(\xi_i/\xi_1)_{max}$
7	1.16	4.27×10^{-2}	72	97.0	1.57×10^{-10}
12	1.60	3.98×10^{-3}	77	137	8.82×10^{-11}
17	2.21	4.08×10^{-4}	82	193	5.25×10^{-11}
22	3.11	4.73×10^{-5}	87	273	3.27×10^{-11}
27	4.37	6.47×10^{-6}	92	385	2.11×10^{-11}
32	6.16	1.05×10^{-6}	104.5	134	1.96×10^{-11}
37	8.70	2.03×10^{-7}	124.5	134	1.44×10^{-11}
42	12.3	4.66×10^{-8}	144.5	134	1.10×10^{-11}
47	17.3	1.27×10^{-8}	164.5	134	8.38×10^{-12}
52	24.4	4.09×10^{-9}	184.5	134	6.34×10^{-12}
57	34.4	1.52×10^{-9}	204.5	134	
62	48.6	6.41×10^{-10}	224.5	134	
67	68.7	3.03×10^{-10}	244.5	134	

* The index i designates the center element of the group of five or twenty which the element represents.

expanded at a rate controlled by the density of radiation since this was very high compared to the density of the ylem. As the expansion proceeded, the temperature eventually dropped sufficiently so that thermally stable nuclei could be formed. Neutrons underwent radioactive decay into protons and electrons. The capture of neutrons by these protons led to deuterons, neutron capture by deuterons led to tritons, etc.

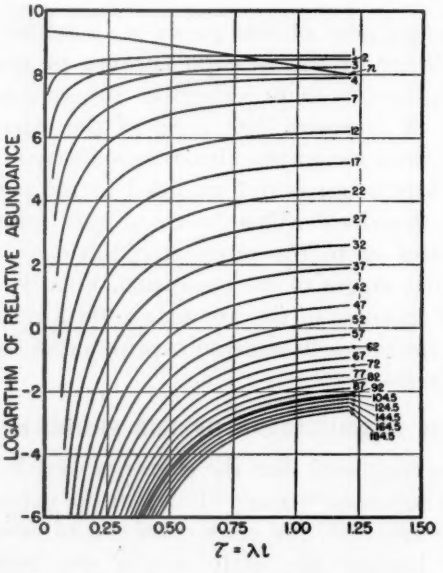

FIG. 1. Logarithm of the relative abundance *versus* $\tau=\lambda t$. The numbers on the right hand side refer to the nuclear species or group. The curve labeled n shows the change in neutron concentration.

Successive neutron captures led to the heavier elements with intervening β-decay processes adjusting the neutron-proton ratios toward stable values. If this sequence of events was the process responsible for forming the elements, it seems clear that the capture cross sections for fast neutrons of the elements must have played an important role in determining the present relative abundances. The reduction of neutron concentration as a result of their decay into protons and the dilution of all matter by the universal expansion must have controlled and terminated the element-forming process.

In the previous development of a neutron capture theory,[4] it was assumed that the effect of the expansion could be neglected, that the rate of deuteron formation was constant, and that all processes other than radiative capture of neutrons could be ignored. It was implicitly assumed that there was sufficient time between successive neutron captures for the necessary adjustment of nuclei by β-decay. In this paper the neutron-capture process is reformulated. The assumptions made in the previous paper[4] are retained with the exception that neutron decay and the universal expansion are explicitly introduced. In calculations of this reformulated theory, however, the expansion once again has been neglected because of computational difficulties.

Let V be any finite volume element in the universe, and let N_j be the number of nuclei of species j in that volume, where j represents the number of nucleons. Let n_j be given by $n_j=N_j/V$. It is assumed that the composition of the universe is always homogeneous. Then, we have

$$\frac{dn_j}{dt}=\frac{1}{V}\frac{dN_j}{dt}-\frac{n_j}{V}\frac{dV}{dt}. \tag{1}$$

It has been shown[4] that in a cosmological model consisting of a homogeneous, isotropic, perfect fluid the density of matter ρ_m varies, during the early stages of the expansion, as

$$\rho_m\cong Kt^{-\mu}. \tag{2}$$

If the universe contains matter only, the exponent μ is found to be 2; if there is a trace of matter in a universe consisting principally of radiation, the exponent is $\frac{3}{2}$. Since $\rho_m=M/V$

where M is the mass of matter in the volume element V, we have

$$\frac{1}{\rho_m}\frac{d\rho_m}{dt}=-\frac{1}{V}\frac{dV}{dt}=-\frac{\mu}{t}. \tag{3}$$

Substituting Eq. (3) into Eq. (1) we have

$$dn_j/dt=(1/V)(dN_j/dt)-(\mu n_j/t). \tag{4}$$

The change in the total number of neutrons, N_n, with time is given by

$$\frac{dN_n}{dt}=-\lambda N_n-\sum_{j=1}^{J}p_j n_n N_j, \tag{5}$$

where λ is the neutron decay constant, p_j is the effective neutron capture volume swept out per second by nuclei of species j and where J is the total number of nuclear species differing only in atomic weight A. In Eq. (5) the first term represents the radioactive decay of neutrons, while the summation term represents the rate at which neutrons are captured to form the various nuclei other than protons. Substituting Eq. (5) into Eq. (4), using $\tau=\lambda t$ as the independent variable and dividing the resulting equation by n_0, which is the particle concentration at time τ_0, we obtain,

$$\frac{d\xi_n}{d\tau}=-\left(1+\frac{\mu}{\tau}\right)\xi_n-\sum_{j=1}^{J}P_j\xi_n\xi_j, \tag{6}$$

where

$$\xi_j=n_j/n_0, \tag{6a}$$

and

$$P_j=p_j n_0/\lambda. \tag{6b}$$

The equation describing proton formation is given by,

$$d\xi_1/d\tau=\xi_n-P_1\xi_n\xi_1-(\mu\xi_1/\tau), \tag{7}$$

where it is seen that protons are formed by neutron decay and are used up only in deuteron formation by neutron capture. In general

$$(d\xi_j/d\tau)=P_{j-1}\xi_n\xi_{j-1}-P_j\xi_n\xi_j-(\mu\xi_j/\tau). \tag{8}$$

Equation (8) states that nuclei of species j are formed through the capture of neutrons by nuclei of the preceding species $j-1$, and that nuclei of species j are changed into the succeeding species $j+1$ by still another neutron capture.

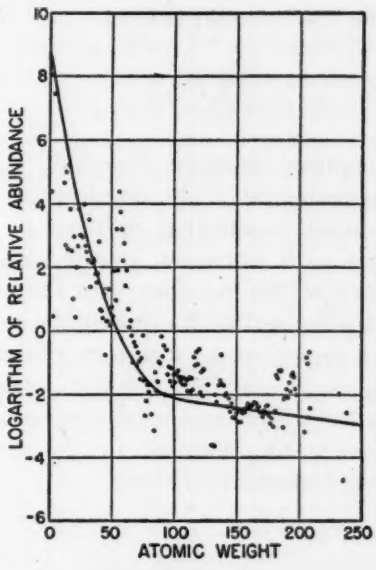

FIG. 2. Comparison of theoretical and observed relative abundances *versus* atomic weight. The observed data are those given by Harrison S. Brown. The theoretical curve corresponds to a matter density of 5×10^{-9} g/cm³ at the start of the element forming process.

In addition, the concentration of all species is diminished by the expansion of the universe according to the term $-\mu\xi_j/\tau$. Equations (6), (7) and (8) constitute a set of $J+1$ equations which should be solved simultaneously.

The computational difficulties associated with the above set of $J+1$ equations has led us to simplify these equations in the following manner:

$$\begin{aligned}
&d\xi_n/d\tau=-\xi_n-P_1\xi_n\xi_1-P_2\xi_n\xi_2-P_3\xi_n\xi_3-P_4\xi_n\xi_4,\\
&d\xi_1/d\tau=\xi_n-P_1\xi_n\xi_1,\\
&d\xi_2/d\tau=P_1\xi_n\xi_1-P_2\xi_n\xi_2,\\
&d\xi_3/d\tau=P_2\xi_n\xi_2-P_3\xi_n\xi_3,\\
&d\xi_4/d\tau=P_3\xi_n\xi_3-P_4\xi_n\xi_4\\
&\quad\cdot\\
&\quad\cdot\\
&\quad\cdot\\
&d\xi_j/d\tau=P_{j-1}\xi_n\xi_{j-1}-P_j\xi_n\xi_j.
\end{aligned} \tag{9}$$

In Eqs. (9) the terms of the type $-\mu\xi_j/\tau$, which represent the dilution of matter resulting from the expansion of the universe, have been neglected. In order to simplify the computations, only the first five of Eqs. (9) were solved simultaneously and the remaining equations were grouped in sets representing five or twenty nuclear species each and solved in succession.

Neglecting the summation term

$$\sum_{j=5}^{J} P_j \xi_n \xi_j$$

in the neutron equation does not materially affect the remainder of the computation because of the almost exponential decrease in relative abundance with increasing atomic weight. The significance of the grouping into sets of say q nuclear species is that the representative species of the ith group must capture on the average q neutrons to form the $(i+1)$st group. The equation for the change in concentration, ξ_i, of the representative element of the ith group containing q species is given by

$$d\xi_i/d\tau = \Pi_{i-1}\xi_n\xi_{i-1} - \Pi_i\xi_n\xi_i, \qquad (10a)$$

where

$$\Pi_i = \sum' P_j/q^2, \qquad (10b)$$

in which the prime indicates summation over the q species in the ith group. In the calculations the group size q was taken to be 5 for $4<A<96$ and 20 for $A \geqq 96$. The quantities p_j are given by[4]

$$p_j = p_A = 1.4\times10^{-19+0.03A}[(1+A)/A]^{\frac{1}{3}} \text{ cm}^3/\text{sec.}, \quad A<100, \qquad (11a)$$

and

$$p_A = 1.4\times10^{-16} \text{ cm}^3/\text{sec.}, \quad A>100, \qquad (11b)$$

where the capture cross sections of the elements, which do not appear explicitly, are given by[4]

$$\log_{10}(\sigma E^{\frac{1}{2}}) = 0.03A - 1.00, \quad A<100, \qquad (12a)$$

and

$$\log_{10}(\sigma E^{\frac{1}{2}}) = 2, \quad A>100. \qquad (12b)$$

In Eqs. (12), σ is in barns, and E is the collision energy in ev. It is evident from the exponential increase in σ with increasing A in Eqs. (12) that using an arithmetic average in computing the Π_i, given by Eq. (10b), is at best a first approximation. Having the p_j from Eq. (11), the P_j may be determined from Eq. (6b) by using the present value of λ, the neutron decay constant, and appropriately choosing n_0, the concentration of particles at the start of the process. The neutron decay constant is given by the Fermi theory[5] as 15 minutes, whereas recent experiments indicate it is probably of the order of $\frac{1}{2}$ hour.[6] The latter figure has been used in our calculations. There does not seem to be any basis on which to choose a value of n_0 other than the fit of theory to the observed relative abundance data, and, as a matter of fact, n_0 should be regarded as an arbitrary parameter. As will be discussed later, a value of $n_0 = 3.23\times10^{15}$ cm^{-3} appears to give a good fit. Values of the P_j for $j=1, \cdots, 4$ and the Π_i are given in Table I.

As initial conditions for the integration, it has been assumed that the process started at $\tau_0=0$, with $\xi_n=1$, and $\xi_j=0$ for $j\neq n$. It is to be understood that $\tau_0=0$ is considered the starting time of the element-forming process, and is not the starting time of the expansion. It can be shown that on the latter time scale the process probably started at about 250 seconds.

III. RESULTS AND DISCUSSION

Integration of Eqs. (9), with grouping according to Eq. (10b), has been carried out with several choices of the parameter n_0 to sufficiently high atomic weights to enable the choice of a best n_0 value. The integrations were done by the lineal element method employing intervals in $\tau=\lambda t$ of 0.01. As described previously, the neutron equation together with the equations for the first four nuclear species were solved simultaneously. The best value of n_0 was found to be $n_0=3.23\times10^{15}$ cm^{-3} and is therefore to be regarded as the initial concentration of neutrons. The integration with this value of n_0 was then carried to the group $i=184.5$. The integrations were not performed for higher atomic weights because it was found that a plot of the logarithms of the relative abundances *versus* atomic weight was a straight line beyond $A\sim100$. It was found in the integration that a slight irregularity resulted in the vicinity of the change in group size from 5 to 20, which has been ignored. The results are plotted as the logarithm of the relative abundance *versus* τ in Fig. 1. It should be noted that ξ_n, ξ_1, ξ_2, ξ_3, ξ_4 are the result of simultaneous solution of the first 5 of Eqs. (9), while ξ_7, ξ_{12}, etc. are the group representative elements. The indices 7, 12, etc. are the center

[5] See H. A. Bethe, *Elementary Nuclear Physics* (John Wiley and Sons, Inc., New York, 1947), p. 105.

[6] A. H. Snell and L. C. Miller, Bull. Am. Phys. Soc. **23**, 21 (1948).

points of the groups of elements. It may be seen in Fig. 1 that the individual ξ_j reach limiting values $(\xi_j)_{max}$ after a τ of about 1.2. The curves attain the limiting values $(\xi_j)_{max}$ given in Table I, simply because the neutrons are used up by radioactive decay and by capture. As the atomic weight increases, the time, τ, required to reach $(\xi_j)_{max}$ becomes progressively greater. However, the error involved in taking $(\xi_j)_{max}$ at a τ of about 1.2 does not exceed several percent for the elements of highest atomic weight

Values of $(\xi_j)_{max}$ taken at $\tau=1.21$ from Fig. 1 are, after appropriate normalization, the relative concentrations or relative abundances, as computed according to the neutron capture theory. These limiting values have been plotted as $[\log(\xi_j)_{max}+\text{const}]$ *vs* atomic weight, $j=A$, in Fig. 2, for comparison with the observed relative abundance data.[7] A smooth curve is drawn in Fig. 2 rather than individually computed points, in order to avoid confusion with the abundance data. The theoretical abundances computed in this paper give a better representation of the observed data than those previously reported[4] in that for atomic weights greater than 100 the theoretical values do not drop off as rapidly with increasing atomic weight. This results from the present calculations leading to abundances at limiting values rather than at an arbitrarily chosen time prior to the attainment of limiting values. In judging the goodness of representation it should be noted that the observed abundance data may be no better than plus or minus about one unit on the logarithmic plot of Fig. 2.

In a previous paper[4] it was pointed out that a correlation existed between neutron capture cross sections for given elements and the relative abundances of these elements. This correlation may be expressed as

$$\log\sigma = C_1 \log\alpha + C_2, \tag{13}$$

where α is relative abundance. If one combines Eq. (13) with Eqs. (12), one can derive for $A<100$ a relationship of the form

$$\log\alpha = C_3 A + C_4, \tag{14a}$$

and for $A>100$

$$\log\alpha = \text{constant}. \tag{14b}$$

If the constant C_1 in Eq. (13) is evaluated from the observed data, then one arrives at values for the constants in Eqs. (14) such that the two lines given by Eqs. (14) are a satisfactory first approximation to the relative abundances of those elements involved in obtaining the constants of Eq. (13).

Some of the detailed features of the observed abundances are probably obscured by the scatter of data. Certain details are nevertheless evident. These are the low abundance of the Li, Be and B isotopes,[7] the large abundance in the vicinity of iron, and the apparent series of peaks for those elements whose atomic weights correspond to the "magic number" nuclei.[4,8] The anomalous behavior of Li, Be and B is probably the result of high cross sections for proton reactions at relatively low temperatures.[4,9] No reasonable explanation has as yet been found for the large abundance peak in the vicinity of iron. The "magic number" nuclei show markedly smaller neutron capture cross sections than other nuclear species, and, in terms of a neutron-capture theory, should exhibit relatively high abundance. This is because they would tend to form only a small amount of the succeeding nuclei. Quantitative examination of this behavior indicates that the element with small σ does indeed pile up, but the abundances of the succeeding elements

[7] Harrison S. Brown, Rev. Mod. Phys. (in press). With the exception of those nuclei below oxygen in atomic weight, these data are relative abundances in the universe as a whole, stated as the number of nuclei of a given atomic weight per 10,000 atoms of silicon. Possibly because of thermonuclear reactions in stars, there appear to be differences from star to star in the relative abundances of isotopes among the lighter elements. As a result, Brown has given only elemental abundances for these lighter elements, and the precision of these data is much less than for elements above oxygen. Despite their uncertainty, these elemental abundances have been converted to nuclear abundances by using the isotopic abundance ratios of the Segrè table, and are included in Fig. 2. Relative abundances of the noble gases A, Ne, Kr, and Xe are not sufficiently well fixed, and are not given by Brown. Brown has not reported relative abundance data on Li, Be, and B. However, relative abundance data previously given by Goldschmidt (reference 4) indicate these elements to be very much less abundant than elements of neighboring atomic weights. In those cases where Brown has given upper and lower limits for the relative abundance of a particular species, the average value has been used.

With regard to the precision of the data, Brown has stated that with the exception of the light elements, the relative abundance data are good to within a factor of about 4. Fluctuations for certain individual elements may exceed a factor of 10 because of experimental difficulties in the measurement of their relative abundance.

[8] M. G. Mayer, Phys. Rev. **74**, 235 (1948).

[9] H. A. Bethe, Phys. Rev. **55**, 434 (1939).

are greatly depressed. The depression is so large that probably the abundances did not derive entirely in this manner. It is suggested that while certain elements exhibiting small σ may have piled up, the succeeding elements may have been built up in large part through neutron capture by nuclei of normal cross section which were isobars of those nuclei exhibiting small σ.

The value of $n_0 \cong 3\times10^{15}$ cm^{-3} corresponds to a density of matter at the start of the process of the order of 5×10^{-9} g/cm^3. While it has not been necessary to specify explicitly the temperature at which the process of successive neutron captures started, the temperature must have been sufficiently low such that thermal dissociation of nuclei could be neglected. On the other hand, the temperature must have been sufficiently high such that resonance effects in the capture of neutrons would not occur. The latter statement follows from the fact that small abundances are not observed for nuclei having large resonance cross sections. A temperature of about 10^5 ev$\cong10^{9}$°K is suggested.[4]

The value of n_0 which has been obtained in this study should be considered as a lower limit because, (1) the introduction of small cross sections for certain elements in the calculations would depress the computed abundance values, and therefore require a higher value of n_0, and (2) the introduction of the universal expansion would also require a higher starting value of n_0 to overcome the dilution of the ylem. It is the nature of the solutions of Eqs. (9) that too high a value of n_0 leads to theoretical relative abundances that are too high and vice versa.

We are undertaking the solution of Eqs. (6)–(8), which include the expansion, in the hope that a better value of the starting density of matter may be obtained and that through this knowledge of the early state and evolution of the universe may be improved.

If the early universe consisted of matter only, then a starting density of matter as low as $\rho_0 \cong 5\times10^{-9}$ g/cm^3 would have been attained quite late in the expansion, in fact, at a time very long compared to the neutron life time. With this state of affairs there would not have been a sufficient concentration of neutrons available to build the elements according to the process which has been described. Thus, the starting time of the neutron capture process must have been small compared to the neutron life time. We have seen that the temperature at the start of the process must have been of the order of 10^{9}°K and it appears that the density of matter must have been no more than several orders of magnitude greater than 10^{-9} g/cm^3. Since 10^{9}°K corresponds to a density of radiation of the order 1 g/cm^3 the behavior of the universe during the times of interest here must have been controlled by radiation. For a universe of essentially radiation only a temperature of about 10^{9}°K is reached in the expansion at about 250 seconds, which is satisfactorily short compared to the neutron life time.

Calculations of the relative abundances of the elements according to the neutron capture theory lead to an estimate of the temperature and density of matter and radiation at a specific epoch in the evolution of the universe. It is noteworthy that recently Gamow[10] has shown that a knowledge of these conditions yields a reasonable picture of the manner in which the galaxies were formed and has estimated their size, separation and density.

IV. ACKNOWLEDGMENTS

We wish to thank Miss Kathryn E. Pace for invaluable assistance on the calculations and Miss Shirley L. Thomas for aid in preparation of the manuscript. We are indebted to Dr. G. Gamow for many stimulating discussions. We also wish to thank Dr. Harrison S. Brown for his cooperation in giving us his relative abundance data prior to publication.

[10] G. Gamow, Nature (in press).

Experimental Determination of Rate of Energy Loss for Slow H^1, H^2, He^4, Li^6 Nuclei in Au and Al*

HOWARD A. WILCOX**
Institute for Nuclear Studies and Department of Physics, University of Chicago, Chicago, Illinois
(Received August 5, 1948)

A description is given of the use of a variable energy source of monoenergetic H^1, H^2, He^4, Li^6 nuclei, an energy analyzer, and an electron multiplier tube to measure the decrease in energy of these particles as they pass through a Au foil of known thickness; the measurements are carried out for protons from an energy of 30 kev to 400 kev, for deuterons from 30 kev to 650 kev, for alpha-particles from 30 kev to 1400 kev, and for the Li^6 nuclei from 750 kev to 850 kev. Similar measurements are carried out for the energy loss of protons and deuterons in Al over the energy range from 60 kev to 300 kev. Integrated range energy curves are given for these low energies. Although current theory predicts that the energy loss rates will be precisely equal for protons and deuterons of the same velocity, it is found that the loss rate for deuterons of low velocity is a few percent higher than that for protons of the same velocity. A qualitative explanation for the discrepancy is advanced.

I. INTRODUCTION

IT is of particular interest to determine the rate of energy loss by low velocity charged particles traversing material media, because present knowledge concerning this problem is both theoretically crude and experimentally meagre. A survey of the relevant literature shows that when the particle moves at such high velocity that it carries with it no bound electrons, the corresponding theory is accurate and well known,[1] but that when the particle moves slowly enough to carry with it some electrons in its various bound orbits, the theory becomes more qualitative.[2] Similarly, although much experimental work has been done on the velocity-energy loss relations for high energy protons and alpha-particles in various media,[3] very little has been attempted in the low energy regions,[4] probably because of the experimental difficulties encountered in detecting slow particles with the conventional Geiger counters, ionization chambers, and photographic plates.

The electron multiplier tubes, recently developed at this laboratory by J. S. Allen and used here to investigate the energy spectra of the recoil nuclei from the reactions $Be^9(p,d)Be^8$, $Be^9(p,\alpha)Li^6$, $H^2(d,n)He^3$, and $H^2(d,p)H^3$,[5-7] form an ideal tool for detecting very low energy particles, and have made possible these investigations of the velocity-energy loss relations for low energy particles in various media. This paper describes the experimental methods used in these investigations, together with the results now available.

II. THE EXPERIMENTAL METHODS

Figure 1 is a schematic diagram of the experimental arrangement. All the apparatus to the left of the "exit slit from target chamber" is used for the purpose of producing nearly monoenergetic, variable energy beams of the various kinds of particles under study, directed out to the right through this slit. On the other hand, all the

* The construction of the electron multiplier tube for this work was assisted by the joint program of the Office of Naval Research and the Atomic Energy Commission.
** Present address: Department of Physics, University of California, Berkeley, California.

[1] For a derivation of the basic formula, see N. Bohr, Phil. Mag. **25**, 10 (1913); H. A. Bethe, Ann. d. Physik **5**, 325 (1930); F. Bloch, Ann. d. Physik **16**, 285 (1933). For a correction at relativistic velocities, see H. A. Bethe, Zeits. f. Physik **76**, 293 (1932); C. Møller, Ann. d. Physik **14**, 531 (1932). For corrections due to K and L electron binding in the medium, see H. A. Bethe, Rev. Mod. Phys. **9**, 264 (1937); J. O. Hirschfelder and J. L. Magee, Phys. Rev. **73**, 207 (1948). For corrections in condensed media, see E. Fermi, Phys. Rev. **57**, 485 (1940); O. Halpern and H. Hall, Phys. Rev. **73**, 477 (1948).

[2] N. Bohr, Phys. Rev. **59**, 270 (1941); W. E. Lamb, Phys. Rev. **58**, 696 (1940); J. Knipp and E. Teller, Phys. Rev. **59**, 659 (1941).

[3] H. A. Bethe, Rev. Mod. Phys. **9**, 261 (1937).

[4] P. M. S. Blackett and D. S. Lees, Proc. Roy. Soc. **134**, 658 (1932); D. B. Parkinson, R. G. Herb, J. C. Bellamy, and C. M. Hudson, Phys. Rev. **52**, 75 (1937); C. M. Crenshaw, Phys. Rev. **62**, 54 (1942).

[5] For the Be reactions, see L. Del Rosario, Phys. Rev. **74**, 304 (1948).

[6] For the $H^2(d,n)He^3$ reaction, see H. V. Argo, Phys. Rev. **74**, 1293 (1948).

[7] The $H^2(d,p)H^3$ reaction is not yet published.

apparatus to the right of the "foil" in Fig. 1 is used for the purpose of measuring the distribution in energy of the beams of particles entering the analyzer mouth.

The idea of these experiments is the following: the apparatus is made to produce a nearly monoenergetic beam of the desired kind of particles, at some desired energy E_1, directed from the exit slit of the target chamber toward the mouth of the energy analyzer. With the foil swung out of this beam, the energy spectrum of the particles is investigated with the energy analyzer and is found to give a sharp maximum at the energy E_1. With the foil swung into the beam, the energy spectrum of the emergent particles is again investigated; the maximum is found at a lower energy E_2, and, since the thickness of the foil is not exactly constant, the energy spectrum of the emergent particles is somewhat broadened. The average energy lost in the foil by the particles is therefore $\Delta E = E_1 - E_2$. The average thickness Δx of the foil is measured, and the ratio $\Delta E/\Delta x$ gives the average rate at which the particles lose energy in the foil material. The average energy of the particles in the foil is taken to be $E = \frac{1}{2}(E_1 + E_2)$, and $\Delta E/\Delta x$ is measured as a function of E.

A. The Kevatron

The kevatron is the 400-kv Cockcroft-Walton accelerator, recently rebuilt in this laboratory and described elsewhere.[5] The accelerating voltage produced by this machine is measured using a high voltage resistance column whose value is known to ± 0.2 percent. Although the accelerating voltage tends to fluctuate slightly, it can be held always within ± 500 volts of any desired average value by means of continuous hand adjustment of a Variac feeding the primary of the high voltage transformer in the kevatron circuit.

The machine may be made to give useful beams of H^+, H_2^+, D^+, D_2^+, and He^+ ions with energies variable from about 40 kev to about 430 kev under average conditions. The desired beam is magnetically selected from the others, deflected through about 15°, and directed toward the target chamber. The beam charge which enters the target chamber is collected on the target and recorded by a beam current integrator of conventional design.

B. The Source of Particles

Two methods, the "scattering method" and the "reaction method," have been used to produce beams of the desired kinds of particles, at the desired energies, directed out through the exit slit from the target chamber.

1. The Scattering Method

In this method, the kevatron beam is limited at the entrance to the target chamber by a

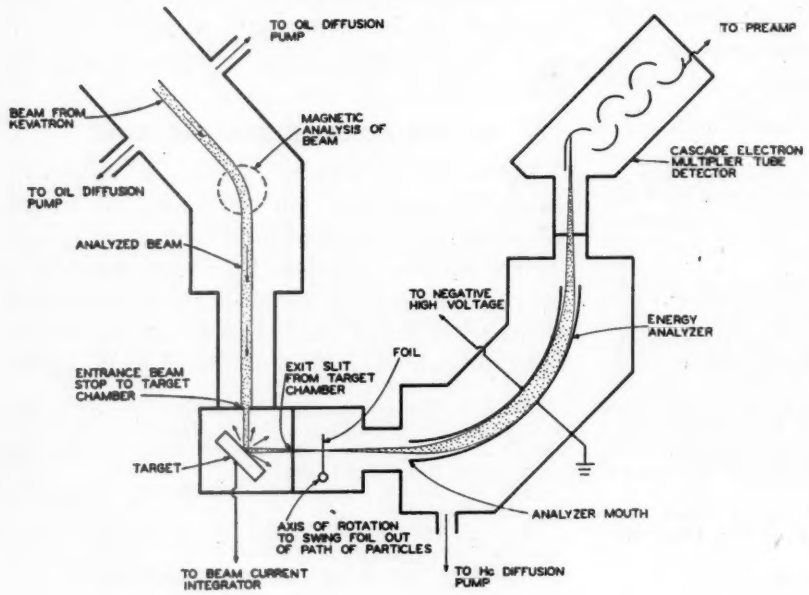

FIG. 1. Schematic diagram of experimental arrangement.

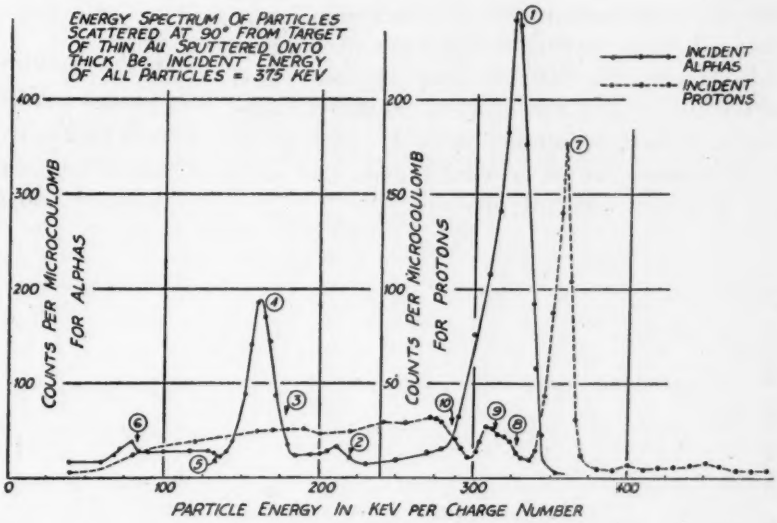
ENERGY SPECTRUM OF PARTICLES SCATTERED AT 90° FROM TARGET OF THIN Au SPUTTERED ONTO THICK Be. INCIDENT ENERGY OF ALL PARTICLES = 375 KEV
INCIDENT ALPHAS
INCIDENT PROTONS
COUNTS PER MICROCOULOMB FOR ALPHAS
COUNTS PER MICROCOULOMB FOR PROTONS
PARTICLE ENERGY IN KEV PER CHARGE NUMBER

FIG. 2. Energy spectra of particles scattered at 90° from "scattering target" (see text). Peak 1 is He^+ coming from the thin Au layer, 2 is probably He^+ from an O layer, 3 is He^+ from a C layer, 4 is He^{++} from the Au layer, 5 is He^+ from the Be base, 6 is He^{++} from the C layer; peak 7 is H^+ from the Au layer, 8 is probably H^+ from an O layer, 9 is H^+ from a C layer, 10 is H^+ from the Be base. For explanation of presence of C on target see reference 9.

2.08-mm diameter drill hole in the beam stop. After passing through this hole, the ions impinge on the target, which is a solid Be disk with a very thin sputtering of Au on the polished front surface. The kevatron beam is incident on this target at 45°, and those particles which scatter at 90° from the incident beam into the direction of the exit slit are the useful particles.

If the particles in the beam have mass number A and energy E_B, then those which leave the exit slit after scattering from the very thin Au surface layer will *all* have energy

$$[(197-A)/(197+A)]E_B \quad \text{(mass number of Au}=197), \quad (1)$$

whereas those which leave the exit slit after scattering from the thick Be base will all have energies *less* than

$$[(9-A)/(9+A)]E_B \quad \text{(mass number of Be}=9). \quad (2)$$

Thus the energy spectrum of the particles leaving the exit slit from the target chamber exhibits a sharp maximum at the energy given by (1), as is desired for these experiments.[8] Figure 2 gives typical energy spectra curves of particles scattered from this target. (When these curves were taken, the target had a slight but visible deposit of carbon on it where the beam struck;[9] evidence for the presence of this carbon layer on the surface of the target is also to be seen in the energy spectra of Fig. 2.)

2. *The Reaction Method*

In this method, a beam stop with a 3.18 mm $\times$12.7 mm slit is used at the entrance to the target chamber, and the scattering target is replaced by a target which is a solid disk of Ni with a very thin layer of Be evaporated onto its polished front surface. This target is bombarded with protons, which produce the nuclear reactions $Be^9(p,d)Be^8$ and $Be^9(p,\alpha)Li^6$. Because of the high probability of these reactions, together with the extreme thinness of the Be layer on the Ni disk, the target becomes a fairly strong source of monoenergetic H^2, He^4, and Li^6 nuclei having kinetic energies of about 645 kev, 1400 kev, and 900 kev, respectively. In order to vary these energies somewhat, a second foil is inserted between the target and the exit slit from the target chamber. This foil is so arranged that it

[8] I am indebted to Dr. S. K. Allison for the suggestion of this kind of target.

[9] Since the accelerator tube is evacuated by two large oil diffusion pumps working in parallel, some oil vapor finds its way into the target chamber and tends to deposit on the surface of the target. When the beam strikes this deposit, the oil molecules are dissociated and inert carbon begins to build up. To help prevent oil vapor from reaching the target chamber, each pump is equipped with a liquid air trap and the walls of the long (30″) beam entrance canal, terminating in the beam stop at the entrance to the target chamber, are cooled with solid CO_2. Furthermore, to help prevent any oil vapor in the target chamber from settling on the target, the latter is heated to a temperature just below that at which the adjacent brass begins to emit zinc vapor. These expedients are fairly successful, but nevertheless some carbonization of the targets is observed after prolonged bombardment.

may be rotated and its effective thickness thereby changed, thus varying the energies of the particles leaving the exit slit. Since this foil is used merely to control the energies of the particles produced in the "reaction method," its material and thickness are of no consequence and need not be known with any precision.

C. Foils

In the experiments so far completed, two foils of Au and one foil of Al were used. The Au foils were both cut from the same large sheet of Au, whose weight was $W=18.7\pm0.1$ mg and whose area was $A=99.99\pm1.21$ cm^2. Hence the average

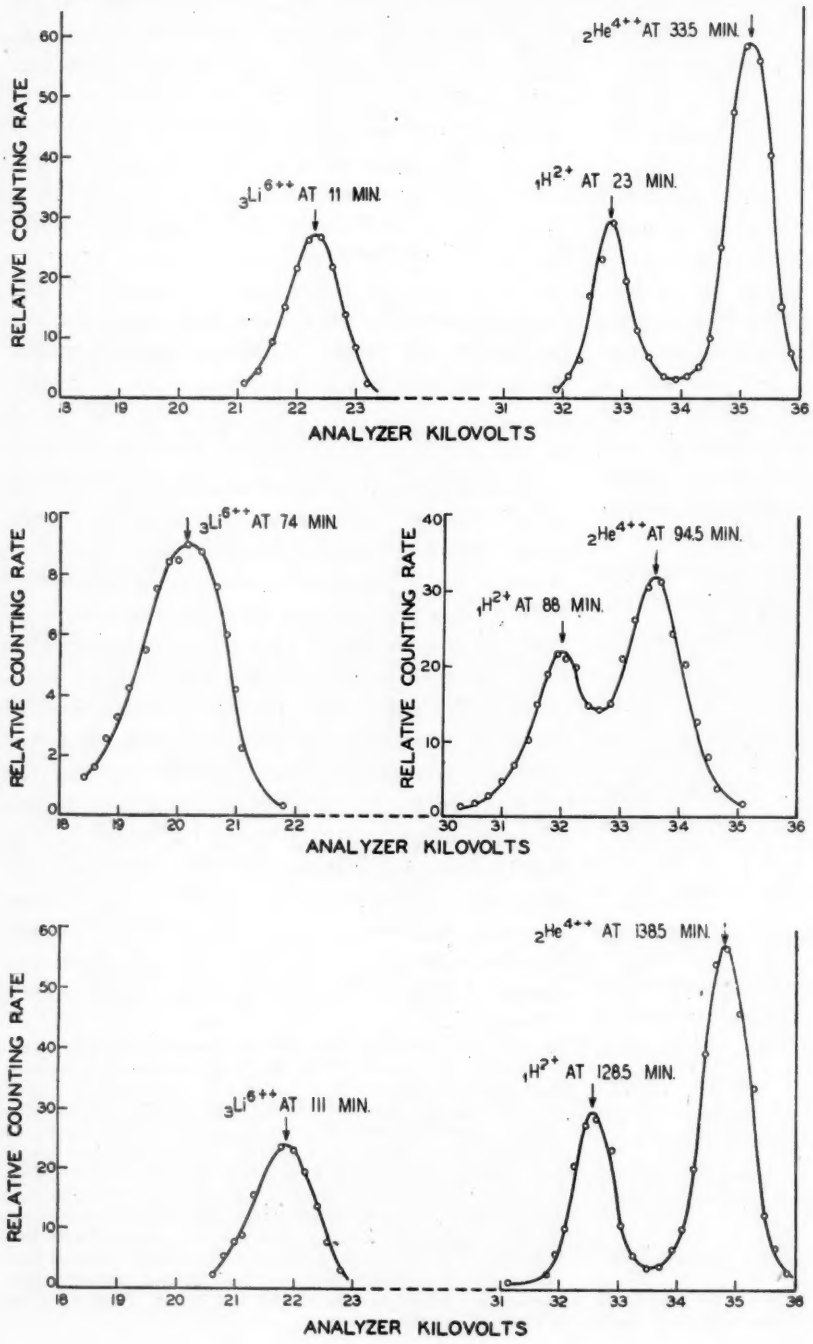

FIG. 3. Typical data from the "reaction method" (see text). Top curve is spectrum of particles without foil, middle curve is spectrum of particles emerging from Au foil, bottom curve is spectrum without foil again. Difference between top and bottom curves is due to progressive carbonization of target as explained in reference 9.

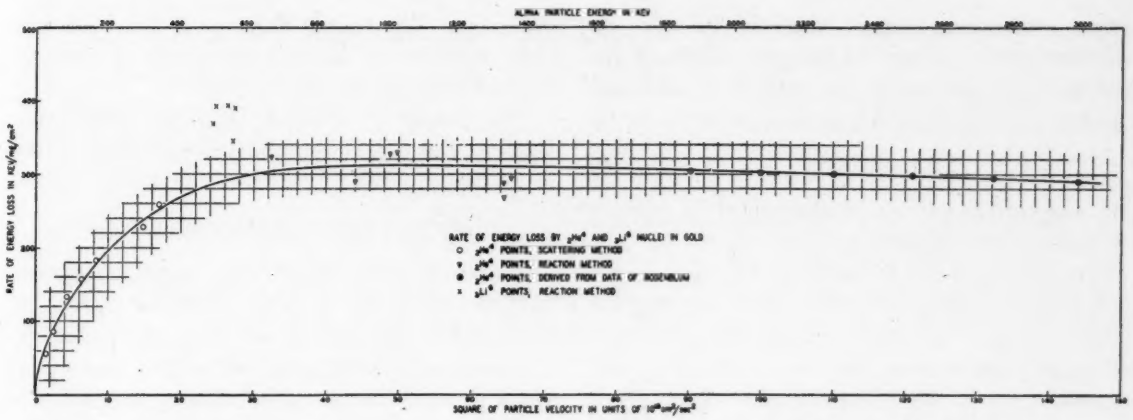
ALPHA PARTICLE ENERGY IN KEV
RATE OF ENERGY LOSS IN KEV/mg/cm²
RATE OF ENERGY LOSS BY ₂He⁴ AND ₃Li⁶ NUCLEI IN GOLD
○ ₂He⁴ POINTS, SCATTERING METHOD
▽ ₂He⁴ POINTS, REACTION METHOD
● ₂He⁴ POINTS, DERIVED FROM DATA OF ROSENBLUM
× ₃Li⁶ POINTS, REACTION METHOD
SQUARE OF PARTICLE VELOCITY IN UNITS OF

FIG. 4. Energy loss rates for He^4 and Li^6 nuclei in Au. The Li^6 energies range from 750 kev to 880 kev.

surface density of this sheet was

$$W/A=(18.7\pm0.53\%)/(99.99\pm1.21\%)$$
$$=0.187\pm1.74\%\ \text{mg/cm}^2.$$

This figure is probably reliable for both foils within the limits of error indicated, since beaten Au foil is very uniform. On the other hand, it was found that the available Al foil was not of uniform thickness. A 9.54-mm×19.1-mm portion of Al foil was used in these experiments, and subsequently a 6.35-mm disk was cut from the center of this portion, its diameter was measured with a micrometer microscope, and its weight was measured with a microbalance. The weight of this disk was $W=0.0543\pm2.8$ percent mg and the area of the disk was $A=0.317\pm1.0$ percent cm^2; hence the surface density of the Al foil used in these experiments was

$$W/A=(0.0543\pm2.8\%)/(0.317\pm1.0\%)$$
$$=0.171\pm3.8\%\ \text{mg/cm}^2.$$

To minimize the danger that vapor from the pumps will condense on the foils, the apparatus is set up so that the foil chamber and energy analyzer can be sealed off by stopcocks at the exit slit from the target chamber and at the pump outlet from the energy analyzer. By means of these arrangements, the foils are left in the static vacuum of the energy analyzer except during the actual running times of the experiments.

D. The Energy Analyzer

The energy analyzer used in these experiments is the same one used by L. Del Rosario and others; its description appears in the literature,[10] and will be only briefly summarized here. The analyzer (see Fig. 1) is a pair of quarter-circle, cyclindrical, concentric aluminum surfaces, of such radii that when a voltage difference V is applied between them and a particle of charge number z traverses them along the arc of a concentric circle, the energy of the particle is given by

$$E=20.00zV, \tag{3}$$

where E is in electron volts and V is in volts. The outer surface of the analyzer is held at the same potential as the target, namely ground potential, and the inner surface is maintained at a potential $-V$; hence, the energy of the particle before it enters the field of the analyzer is not the same as its energy when it traverses the analyzer. The true energy of a positively charged particle before entering the analyzer is determined by subtracting a positive correction Δ from its energy within the analyzer, whence

$$E_{\text{true}}=20zV-\Delta. \tag{4}$$

It has been thought for some time that the best value for Δ is about $0.20zV$. Recent work by Argo[6] on a similar analyzer, however, indicates that Δ more probably has the value $0.50zV$. Hence we use the relation

$$E_{\text{true}}=19.5zV \tag{5}$$

in these experiments.

The analyzer does not, of course, possess

[10] S. K. Allison, L. S. Skaggs, and N. M. Smith, Phys. Rev. **54**, 171 (1938).

perfect resolving power; that is to say, its "window curve" is not a δ-function. Instead, the analyzer window curve is nearly an isosceles triangle of half-width ΔV given theoretically by

$$\Delta V = 0.025 V. \quad (6)$$

This theoretical value is well realized in practice under good conditions.[5]

The potential $-V$ applied to the energy analyzer is produced by half-wave rectification of the output of a 100-kv transformer fed by a 540-cycle synchronous M-G set. This potential, smoothed by a filter capacitance of $0.1\mu f$, is continuously variable from 0 to 50 kv and is measured by means of the current it produces through a stack of Shallcross precision resistors. For values of V above about 20 kv, this stack consists of ten units, each of 5.0 ± 0.1 percent megohm resistance, making 50 megohms in all. For values of V below 20 kv, only four units of the stack are used. The current is measured using a Simpson d.c. ammeter, 1.5 ma full scale, with a 6-in. scale, approximately. A current of $2(10)^{-6}$ amp. through this meter produces a measurable deflection. The meter movement has been carefully calibrated, and its accuracy is therefore limited only by its sensitivity.

The potential V has a tendency to fluctuate slightly, but can be manually held within ± 100 v at 30 kv.

E. The Electron Multiplier Tube

The electron multiplier tube which detects the particles emerging from the analyzer is the same one studied and described by L. Del Rosario.[5] The external amplifying and scaling circuits are also the same that she used. The tube is mounted at the back of the analyzer in such a way as to catch on the first electrode the particles emerging from the analyzer. Each such particle then initiates the well-known cascade of secondary electrons down the series of electrodes in the multiplier tube. The output pulse from the multiplier tube is electronically amplified and is recorded by a conventional scale-of-64 circuit. To keep the background count within convenient limits, the apparatus was adjusted throughout these experiments so as to accept pulses from

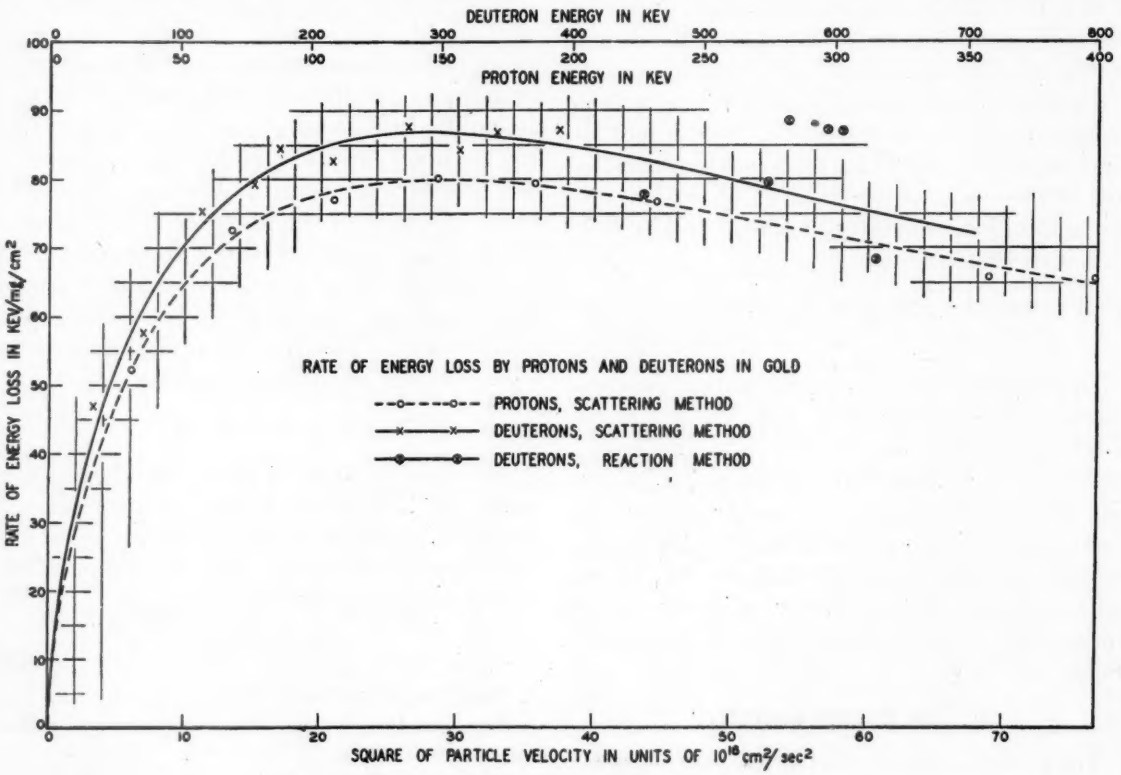
DEUTERON ENERGY IN KEV
PROTON ENERGY IN KEV
RATE OF ENERGY LOSS IN KEV/mg/cm²
SQUARE OF PARTICLE VELOCITY IN UNITS OF 10¹⁸ cm²/sec²
RATE OF ENERGY LOSS BY PROTONS AND DEUTERONS IN GOLD
PROTONS, SCATTERING METHOD
DEUTERONS, SCATTERING METHOD
DEUTERONS, REACTION METHOD

FIG. 5. Energy loss rates for protons and deuterons in Au.

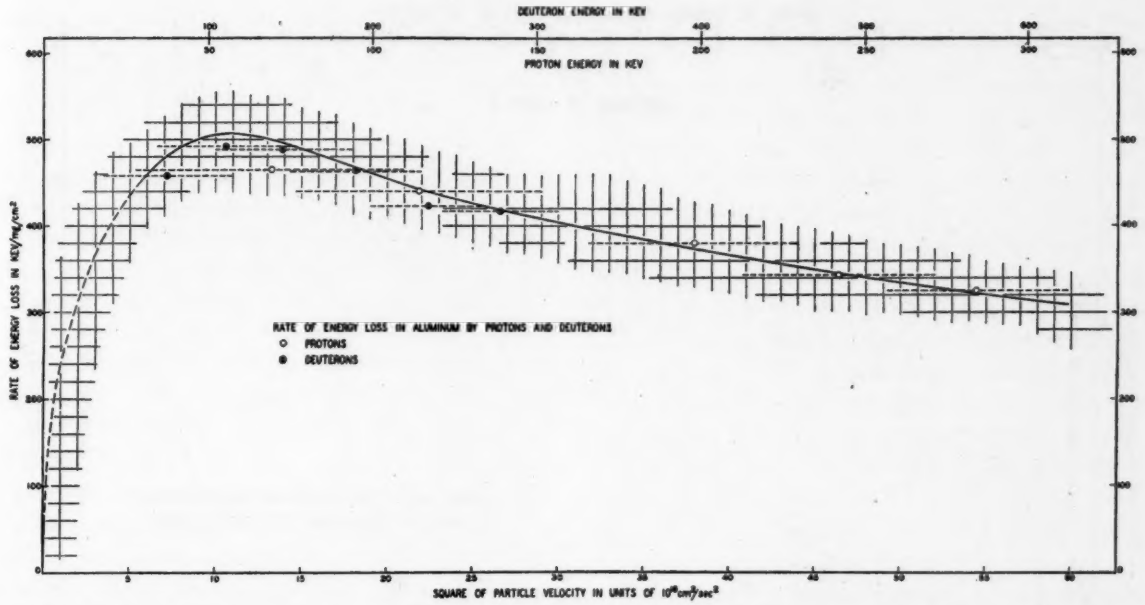
DEUTERON ENERGY IN KEV
PROTON ENERGY IN KEV
RATE OF ENERGY LOSS IN ALUMINUM BY PROTONS AND DEUTERONS
PROTONS
DEUTERONS
RATE OF ENERGY LOSS IN KEV/mg/cm²
SQUARE OF PARTICLE VELOCITY IN UNITS OF 10⁸cm²/sec²

FIG. 6. Energy loss rates for protons and deuterons in Al. The experimental ordinates are the average rates of energy loss over the energy intervals indicated by the horizontal dotted lines. See text for explanation as to why the curve is not drawn through the experimental points.

the electron multiplier tube only if they exceeded approximately 20 millivolts in amplitude.

F. Method of Taking Data

In typical operation, for each setting of the analyzer potential V the scaler is permitted to count until a predetermined quantity of beam charge, as measured by the beam current integrator (Fig. 1), has been collected on the target. In this way the relative number of particles incident on the analyzer, per unit beam charge, is determined as a function of the analyzer voltage V, which therefore gives, with the aid of Eq. (5), the energy spectrum of the particles incident on the analyzer.

The carbonization of the targets, mentioned in reference 9, causes the energies of the various particles leaving the targets to decrease slowly with time. Hence the data are actually taken by first observing the energy spectrum without the foil and noting the times at which the various peaks are observed; the energy spectrum with the foil interposed is then observed and the times of observation are again noted; finally the foil is removed and the first procedure repeated. Assuming the carbon thickens at a constant rate, it is then a simple matter to calculate from these data the energies of the particles incident on the foil at the same time as their emergent energies are observed.

III. EXPERIMENTAL RESULTS, DISCUSSION, CONCLUSIONS

Figure 3 gives typical data from the reaction method. The top curve gives essentially the energy spectrum of the particles from the Be-proton reactions before the foil is interposed, the middle curve gives the energy spectrum of the particles as they emerge from the Au foil, and the bottom curve gives the spectrum after the foil has been again removed. The times of observation of the various peaks are noted in the figure. The top and bottom curves are not quite identical because of the progressive carbonization of the targets mentioned above.

It will be observed that in the top curve of Fig. 3, for example, the various peaks in the energy spectrum are identified as belonging to doubly ionized Li^6 atoms of 870-kev energy, to singly ionized H^2 atoms of 640-kev energy, and to doubly ionized He^4 atoms of 1370-kev energy. If the analyzer voltage scale in this figure were extended in both directions, additional peaks would appear belonging to the singly and triply

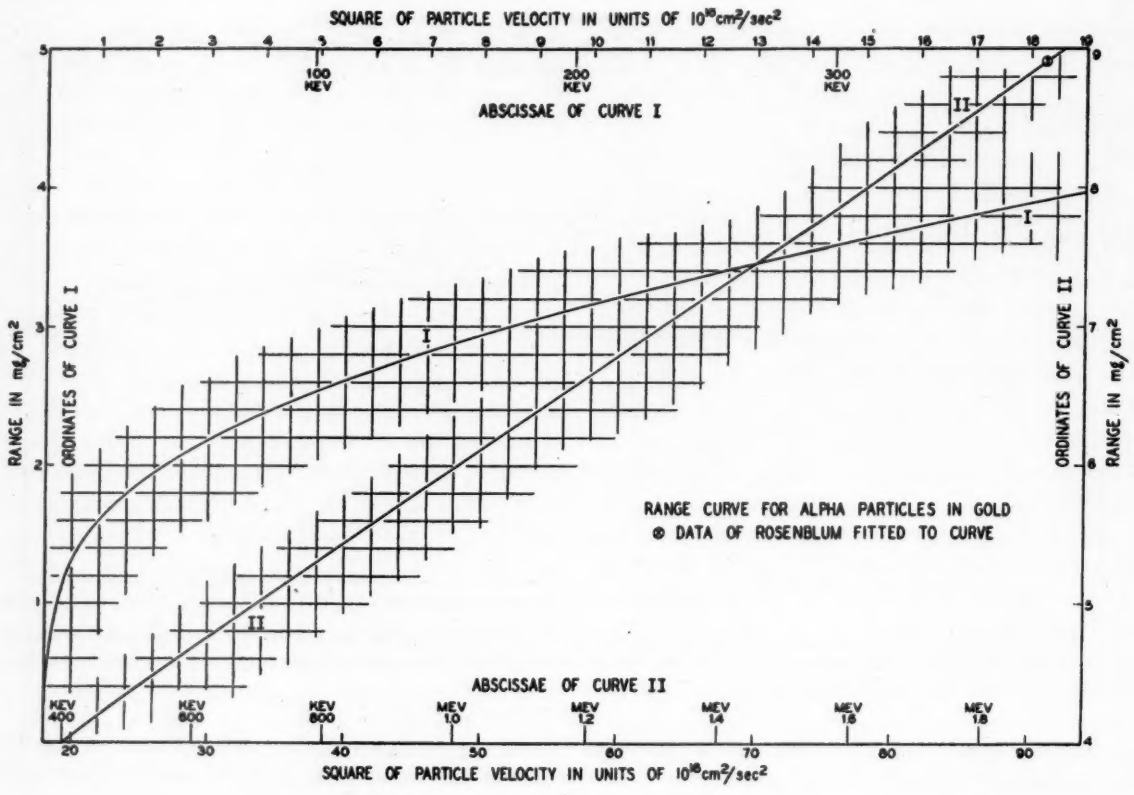

A

ionized Li^6 atoms of 870-kev energy and also to the singly ionized He^4 atoms of 1370-kev energy.

It should be noticed that the state of ionization of the various atoms before entering and after leaving the foil will have no effect whatsoever upon the rate at which they lose energy within the foil. This statement follows from the fact that inside the foil the mean free path for capture and loss of electrons is extremely short for low energy particles—hence each particle, regardless of its initial state of ionization, will capture and lose electrons hundreds of times before emerging from the foil. Upon leaving the foil, the particles will be statistically distributed among the various possible charge states in a way which depends upon their emergent energy and the surface character of the foil, but not upon their charge states when they entered the foil.

This statement is experimentally confirmed by observing the energy shifts of the various peaks when the foil is interposed. It is found, for example, that the particles in the singly ionized Li^6 peak lose exactly the same energy as the particles in the doubly ionized Li^6 peak.

Figures 4–6 give the direct results of these experiments, together with some of the results of previous investigations. In these figures $\Delta E/\Delta x$ is plotted against the square of the velocity of the particles, since current theory[1] predicts that over most of the energy range $\Delta E/\Delta x$ in a given substance will be a function only of the square of the velocity of the particle (and also of its charge number z). The "thickness" Δx of the foil is for convenience left in the form of a surface density.

The results in Fig. 4 fit in well with results derived from the work of Rosenblum[11] at higher energy.

At the very low energies obtained here, the decreased rate of energy loss by the particles immediately suggests an extrapolation to zero rate of energy loss at zero velocity; hence these figures have been so extrapolated. This procedure permits the numerical calculation of the integrated range x as a function of the particle

[11] S. Rosenblum, Ann. de physique **10**, 408 (1928).

energy, according to the formula

$$x(E)=\int_0^E (dx/dE)dE. \qquad (7)$$

Integrated ranges in Au and Al are given in Figs. 7–9 for the various particles.

The stopping power of the very thin Au foil used was so small that with a high degree of accuracy the average slopes $\Delta E/\Delta x$ over the small intervals $\Delta E=E_1-E_2$ can, in Figs. 4 and 5, be identified with the true slopes dE/dx at the arithmetic mean energies $E=\frac{1}{2}(E_1+E_2)$. In the case of the available Al foil, however, the average slopes $\Delta E/\Delta x$, over the rather large energy intervals made necessary by the thickness of the foil and indicated by the horizontal dotted lines in Fig. 6, cannot always be correctly identified with the true slopes at the arithmetic mean energies; hence the curve in Fig. 6 is not drawn precisely through the experimental points. This effect is easy to take into account, and a direct check of the average slopes on Fig. 9 shows it to be correct.

In these experiments, the main uncertainty in $\Delta E/\Delta x$ stems from the fact that ΔE is the small difference of two large numbers. Hence fluctuations in the kevatron voltage and in the analyzer voltage may cause relatively large errors in ΔE. Another source of error, peculiar to the "reaction method," arises from the unavoidable straggling of the particles in the rather thick foil used to control their energies in the manner explained in Section 2 under IIB above. Hence, in this method the energy peaks are rather broad and their exact centers are difficult to locate precisely. It is thought that this effect accounts for the increased scatter of the "reaction method" points over that for the "scattering method" points, as is clearly evident in Figs. 4 and 5.

Despite these effects, however, the curves obtained are surprisingly smooth. With sufficiently great care in the regulation of the kevatron voltage and in the regulation and measurement

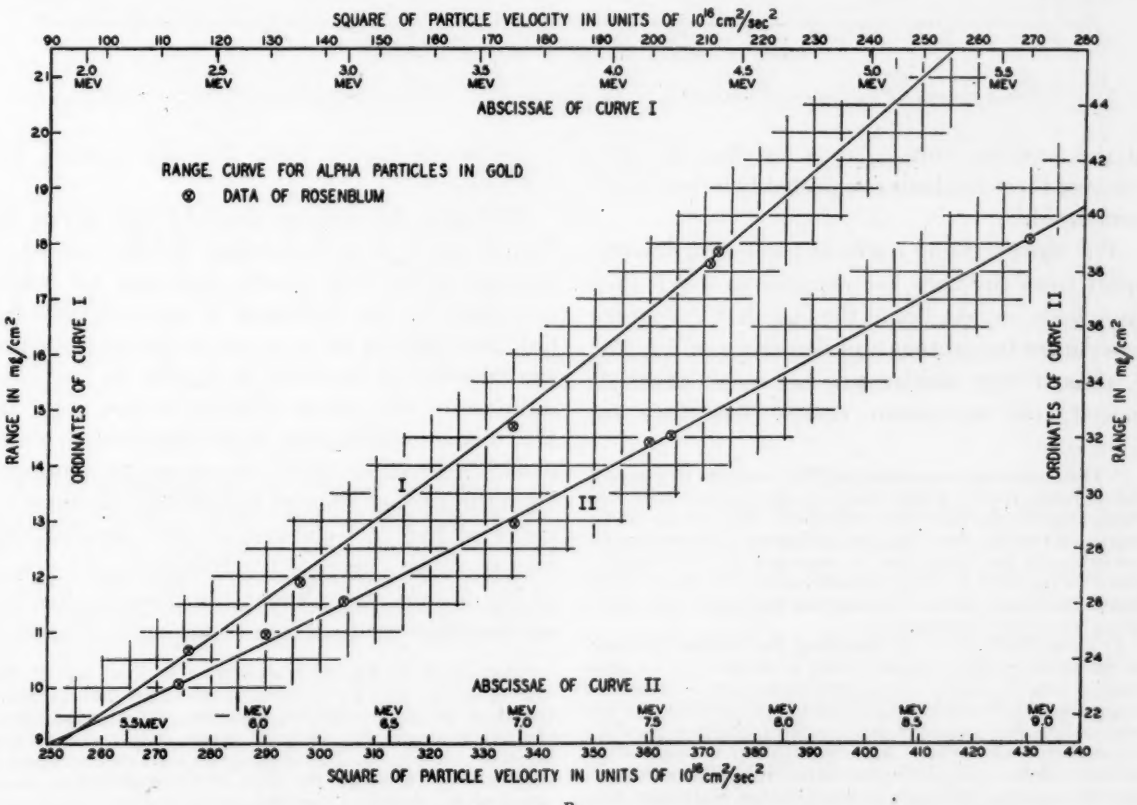
SQUARE OF PARTICLE VELOCITY IN UNITS OF 10^{16}cm^2/sec^2
ABSCISSAE OF CURVE I
RANGE CURVE FOR ALPHA PARTICLES IN GOLD
⊗ DATA OF ROSENBLUM
ORDINATES OF CURVE I
RANGE IN mg/cm^2
ORDINATES OF CURVE II
RANGE IN mg/cm^2
I
II
ABSCISSAE OF CURVE II
SQUARE OF PARTICLE VELOCITY IN UNITS OF 10^{16}cm^2/sec^2

B

FIG. 7A–B. Range curve for alpha-particles in Au. From 0 to 2 Mev, the curve is obtained by numerical integration of the curve of Fig. 4; above 2 Mev the curve is obtained from the data of Rosenblum (reference 11).

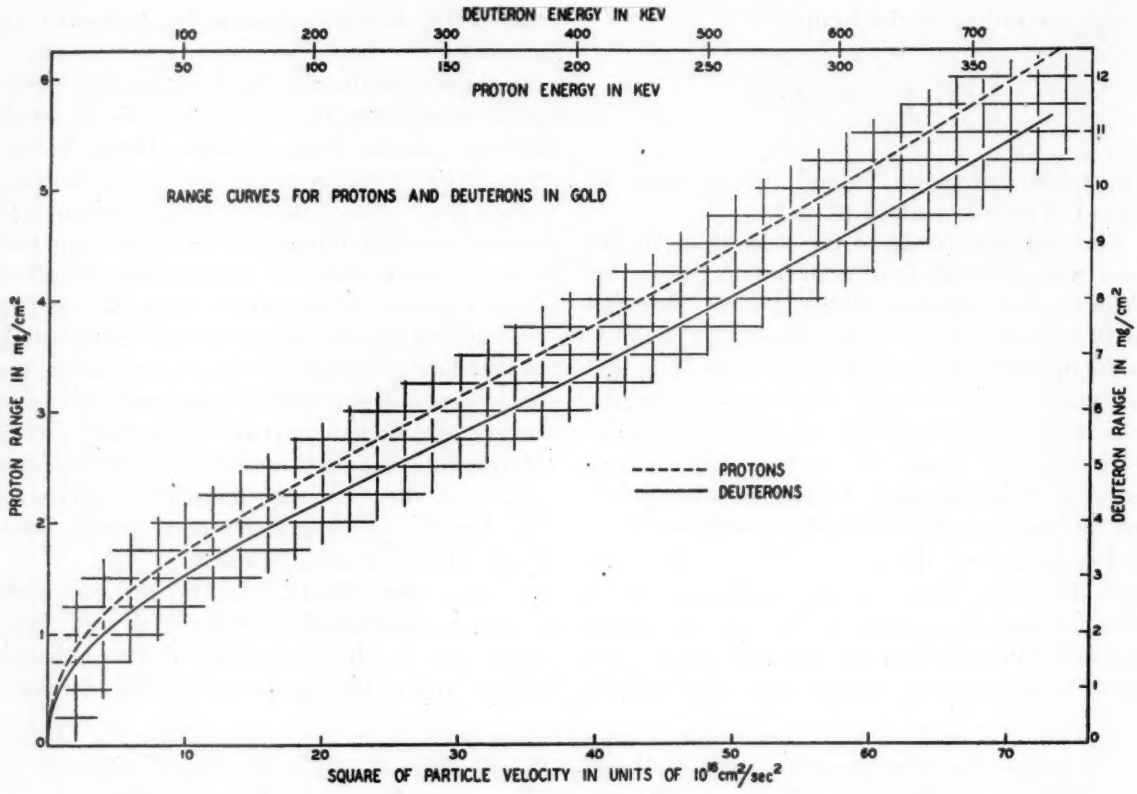

FIG. 8. Range curves for protons and deuterons in Au, obtained by numerical integration of the curves of Fig. 5.

of the analyzer voltage, it is felt that the precision of these methods can probably be improved many-fold.[12]

The most striking result of these experiments, apart from the very low energies to which they have been carried, lies in the fact that the energy loss curves for protons and deuterons in Au, Fig. 5, though very similar, are not quite identical; indeed, the maximum energy loss rate for deuterons is higher than that for protons by ~8.5 percent.

Although the similar data for Al, given in Fig. 6, are not as conclusive as the Au data because of the large energy intervals ΔE made necessary by the thickness of the available Al foil, nevertheless there seems to be evidence for the existence of the effect in Al also. In fact, the ordinate of the lowest velocity proton point in Fig. 6 is actually less by about five percent than would be predicted for a corresponding deuteron from the average slope of the integrated deuteron curve of Fig. 9. Furthermore, the slope of the proton range curve of Parkinson *et al.*,[4] given in Fig. 9, indicates a lower rate of energy loss by protons than by deuterons of the same velocity.[13]

[12] These methods can, moreover, be extended to measure the stopping power of any material which either is able to stand alone in the form of a sufficiently thin foil, or can be deposited on the very thin Au foil which is commercially available. In the latter case, a correction for the stopping power of the Au foil is easy to make since the rate of energy loss in Au is now known for protons, deuterons, and alpha particles of very low energies.

It seems likely that, by observing the relative numbers of particles in the various states of ionization as they emerge from the media, these methods can also be extended to get useful information regarding the probabilities for the various possible states of ionization of charged particles traversing solid media. This investigation is impeded at present chiefly by lack of quantitative information regarding the counting efficiency of the electron multiplier tube as a function of the energy of the incident particle, its charge, the pressure in the tube, the operating potentials for the tube, etc.

[13] In regard to Fig. 9, it should be noticed that if the rate of energy loss for protons is less than that for deuterons of the same velocity, then the proton range curve should lie above the deuteron range curve rather than below it (cf. Fig. 8). The explanation for this discrepancy may be the following: the data of Parkinson *et al.* were obtained by observing the energies of protons incident on various Al foils under such conditions that the beam currents were observed just to cease penetrating the foils. The thicknesses of the foils were then regarded as the ranges in

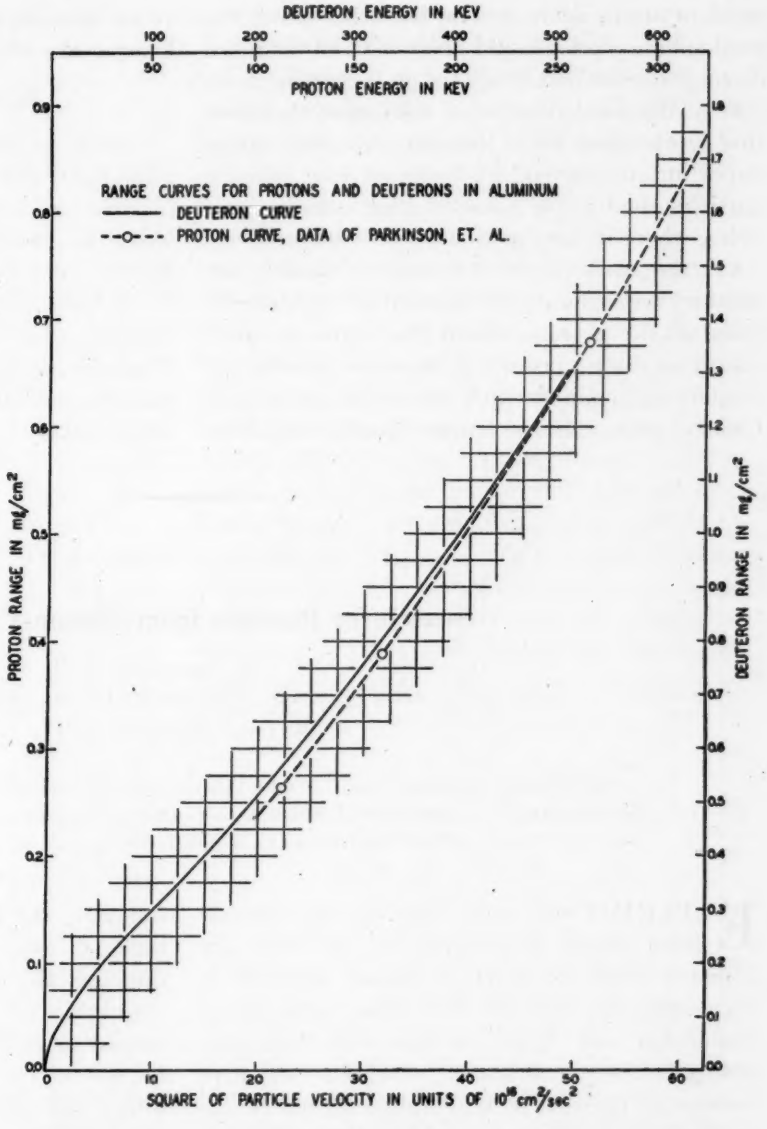

FIG. 9. Range curves for protons and deuterons in Al. The proton curve is obtained from the data of Parkinson, *et al.* (reference 4); the deuteron curve is obtained by numerical integration of the curve of Fig. 6.

The fact that the energy loss rate for deuterons is slightly higher than that for protons of the same velocity, in the region of low velocities investigated here, is in direct contradiction to the prediction by current theory that the energy loss rates for isotopic particles will be exactly the same for all equal velocities. A qualitative explanation for this difference is perhaps to be found in the mechanism of glancing, essentially "hard-sphere," elastic atomic collisions, which is entirely neglected in the usual theory. Since it is to be expected, of course, that the rather crude hard-sphere atomic model will be a fairly valid approximation only for atomic collisions in which the transfers of energy are rather small, it follows that, for incident particles of given velocity, the mechanism of hard-sphere collisions would be limited to quite glancing collisions, for otherwise the transfers of energy would be so large as to invalidate the model. As the velocity of the

Al of protons of these energies. As they point out (p. 78), however, it is likely that the proton charges are largely neutralized before the protons are stopped; and if this be the case, they will underestimate, by a small additive constant, the range in Al of protons of every energy they used. Hence it is possible that the proton curve of Fig. 9 should be shifted upward by adding to every range ordinate a small constant.

incident atoms decreases, on the other hand, the hard-sphere model would become valid for more direct collisions and hence for an increasing fraction of the total number of collisions; therefore this mechanism would become relatively more important in the energy losses of low velocity particles than in the losses of high velocity particles, where it may justifiably be neglected.

On the basis of the hard-sphere model, elementary considerations show that a deuteron loses, on the average, about four times as much energy as does a proton of the same velocity, in a (glancing) collision with a heavy atom at rest. Clearly, then, this mechanism would contribute to an increased rate of energy loss for deuterons compared with that for protons, as observed.

IV. ACKNOWLEDGMENTS

I wish to thank Dr. S. K. Allison, in whose laboratory this work was done, for his constant interest and valuable advice in the course of the work. In addition, I wish to express my thanks for the very important and active help of Mr. C. N. Yang during the early phases of these investigations. Finally, thanks are due Messrs. D. S. Bushnell and G. W. Farwell for their assistance with the tedious but necessary job of taking the many data.

PHYSICAL REVIEW VOLUME 74, NUMBER 12 DECEMBER 15, 1948

Search for Photons from Meson-Capture*

O. PICCIONI**
Laboratory for Nuclear Science and Engineering, Massachusetts Institute of Technology, Cambridge, Massachusetts
(Received August 27, 1948)

High energy photons (about 50 Mev) associated with mesons stopped in iron have been searched for. The experimental evidence shows that no such photons arise from the capture of negative mesons or from the free decay of positive ones.

EXPERIMENTS with delayed coincidences[1] have shown that no decay electrons are detected from negative μ-mesons stopped in materials with high Z. This was predicted by Tomanaga and Araki, in line with Yukawa's theory.[2] Their conclusion was that negative mesons at the end of their range should be attracted by the Coulomb field of the nuclei and then "captured" by the nuclei even for low values of Z and density of the absorber. The presence of decay electrons for both positive and negative mesons in light nuclei already indicates a strong departure from the predictions of Tomanaga and Araki and hence from Yukawa's theory, as far as μ mesons are concerned. However, the event following the capture of negative μ-mesons in a high Z absorber was somehow expected to undergo the process which was predicted on the basis of Yukawa's theory. This process should most likely lead to a nuclear disruption in which the outgoing particles would carry almost all of the 100 Mev rest energy of the mesons. From the absence of such stars in cloud chamber pictures, it was felt[3] that the idea sketched above does not correspond to the actual phenomenon.***,[4] Hence the present experiment

* Preliminary results of this work appeared in Phys. Rev. 73, 411 (1948); a complete report was given in the Washington meeting of the American Physical Society, April 29, 1948.

** Now at Brookhaven National Laboratory, Upton, Long Island, New York.

[1] Conversi, Pancini, and Piccioni, Phys. Rev. 68, 232 (1945); G. E. Valley, Phys. Rev. 72, 772 (1947).

[2] Tomanaga and Araki, Phys. Rev. 58, 90 (1940).

[3] O. Piccioni, Phys. Rev. 73, 411 (1948).

*** After this experiment was performed, Lattes and Gardner (see reference 4) reported that μ mesons had been detected with photographic plates exposed in the 184-inch cyclotron of Berkeley. Only a part (<50 percent) of the observed μ mesons produce a star at the end of their range, and these stars have mostly one prong. From the comparison with the Σ-stars, one has the impression that the μ-stars do not represent an energy of 100 Mev. Other information on this subject is available from the preliminary results of R. Sard and coworkers, who find neutrons associated with the stopping of mesons in lead. Unfortunately quantitative information is not available as yet.

[4] Lattes and Gardner, Am. Phys. Soc. 23, No. 3, p. 42 (1948).

was performed, in order to investigate whether or not high energy photons (50÷100 Mev) are produced in association with the "capture" of a negative meson, giving account of the 100 Mev energy. While it seems unlikely that such high energy photons could be emitted by the excited nuclei,[5] they could be produced by the direct interaction between the negative meson and one single proton of the nuclei. As will be shown, the evidence arising from the present experiment stands against such hypothesis of high energy photons emitted after the capture of a negative μ-meson. At the same time, the apparatus provides a negative answer to the hypothesis of high energy photons accompanying the decay of positive stopped mesons.

DESCRIPTION OF THE APPARATUS

The apparatus, with counters, absorbers and screens, is shown schematically in Fig. 1. Mesons were collimated by the telescope AB and filtered through a lead absorber 6-inches thick. The 4-inch thick aluminum plate was there to prevent the mesons which reach the tray B with a small residual range from having a big angle of scattering. That would decrease the rate of mesons absorbed in the iron. The anticoincidence tray C selected events corresponding to the stopping of a meson in the iron absorber. Geometries like the one adopted here have been widely used in slow meson experiments,[6] so that one can assume that practically all the particles stopped in the absorber are meson of 200 electron masses and natural mean life 2.2 μsec.

The counters "H" formed a "Hodoscope" set. They were connected to an apparatus which indicated individually which one of them was discharged when an AB–C event took place. Such information was taken from a picture of a cathode-ray tube. In this way it was possible to indicate roughly the track of the ionizing particles, so that one could exclude spurious events which could give the appearance of a γ-event in a simple coincidence–anticoincidence arrangement. The counters "H" were brass counters 1-inch diameter, 10-inch useful length, with a 0.003-inch diameter tungsten wire. They were filled with pure argon at the pressure of 13 cm Hg, and worked as follows. The voltage between the wall and the wire was normally kept at -5 volt (wire negative). A 0.001 μf condenser was connected between the wire and ground. When a coincidence AB occurred, the wall received a negative pulse of about 1200 volts in amplitude, 2 μsec. long, rising time 0.2 μsec. If an ionizing particle went through any one of the "H" counters at the time when an AB coincidence occurred and the pulse was given, the counter would discharge, and its condenser would be charged at a potential of about -100 v respect to ground. In this way, each pulse appearing on the wires of the H counters represents automatically a coincidence with the trays A and B, within about 2 μsec., although the pulse itself may last for a time as long as 1 second. This feature and the big amplitude of the pulse makes it easy to detect individually which one of the counters H is discharged. In the present experiment, such information was given by a cathode ray scope, by means of a rotary-scanning switch and a synchronized sweep-circuit. The efficiency of the counters H,

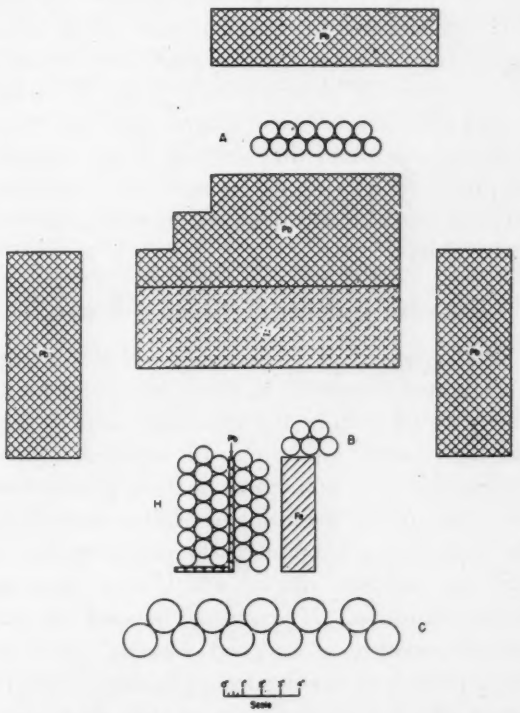

FIG. 1. Schematic of the apparatus—When an anticoincidence AB–C occurred, the "picture" of the counters H (30) was taken. The counters A, B, H, were 1 inch diameter, 10 inches long. The counters C were $1\frac{3}{4}$ inches diameter, 20 inches long.

[5] J. A. Wheeler, Phys. Rev. **71**, 320 (1947).
[6] F. Rasetti, Phys. Rev. **60**, 198 (1941).

TABLE I.

γ-energy in Mev	Fraction of γ-rays lost in iron	Ratio of useful solid angle to 4π	Max. useful thickness of lead in g/cm²	Actual thickness of lead in g/cm²		Fraction of γ-rays lost in lead		Efficiency of the useful thickness of lead		Total efficiency	
				Series I	Series II and III	Series I	Series II and III	Series I	Series II and III	Series I	Series II and III
50	0.46	0.075	11.4	7	14	0	0.22	0.48	0.65	0.019	0.02
100	0.49	0.075	15.1	7	14	0	0	0.62	0.8	0.024	0.03

working as outlined above, was proved to be better than 95 percent. Due to the geometrical disposition of the apparatus, this efficiency was more than sufficient for the purpose of the experiment. It should be noted that even if such efficiency would have been as low as, say, 75 percent, one might expect to get false pictures showing a pseudo γ-event, rather than to miss any substantial number of pictures of real γ-events. No distinction has been made between positive and negative particles. Such a distinction, which would have reduced the rate of occurrence of the investigated events, was left as a second stage of the experiment, in case evidence had been found for photons produced by stopped mesons. The type of apparatus used was particularly suitable to be transformed for that purpose, by the introduction of a magnetized iron piece and the addition of other "*H*" counters to indicate the deflection of the mesons in the magnetized iron. Since evidence was found that no high energy photons are produced by stopped mesons, the distinction between positive and negative mesons was obviously useless.

Expected Number of "Good γ-Events"

The hypothetical phenomenon which was being investigated consisted of the following: a meson which would stop in the iron and cause at least one high energy photon to be emitted with no preferential direction. Some of those photons will then come out of the iron and will be converted in the lead, giving, by pair-production, one electron and one positron, one of which may cross the three columns of "*H*" counters beyond the lead. Correspondingly as a "good γ-event" (g. γ. e.) was regarded an event selected by the anticoincidence circuit, which gave a picture showing no discharge in the two columns of the "*H*" counters placed between the iron and the lead converter, and showing a discharge in one counter for each of the three other columns. In addition it was required that the discharged counters showed a direction for the ionizing particle, compatible with the assumption of a photon coming from the iron and converted in the lead. This criterion of the direction allowed one to exclude false pictures due for instance to more than one particle crossing the apparatus simultaneously. The exclusion, however, could not be complete, and indeed it is felt that the small number of "g. γ. e." in Table II is due to such cases. On the other hand, the criterion tends to exclude also some good pictures —namely, in case the photo-electron emerging from the lead has been scattered by a big angle. However, this happens only for those electrons which emerge from the lead at the very last part of their range, so that their exclusion does not constitute a substantial reduction of the expected rate.

It is to be pointed out that it was not required that both the pair-produced electrons emerged from the lead converter. Of course, a picture compatible with the assumption of both particles emerging from the lead, if any such pictures had been found, was not subject to exclusion.

In order to evaluate the expected number of "g. γ. e." one has to take into account that when a meson is brought to rest in the iron, on the assumption that negative mesons release a high energy photon, the following conditions have to be fulfilled in order to register a "g. γ. e.".

(A) The photon has to have a direction contained in a certain solid angle.
(B) The photon has not to be absorbed in the iron.
(C) The photon has not to be absorbed in the first millimeters of lead which are in excess of the useful range of the *conversion* electrons.
(D) The photon has to be converted in the remainder part of the lead.

The detection of high energy photons emitted in the decay process was subject to the additional condition, *related* to the resolving time of the

TABLE II.

Series	Number of mesons stopped	Estimated number of negative mesons stopped	Estimated number of positive mesons stopped	Expected number of γ-events from negative mesons if γ-energy 50 Mev	γ-energy 100 Mev	Expected number of γ-events from positive mesons for γ-energy 50 Mev	Experimental number of "good γ-events"
I	2200	990	1210	19	24	12	2
II	3100	1400	1700	34	42	17	2
III	3200	1440	1760	35	43	17	0

apparatus: the decay process has to have an actual delay not bigger than 1.5 μsec.

The probability which corresponds to the condition (A) is simply the ratio of the useful solid angle, determined by the last column of the "H" counters, to the whole solid angle 4π. This ratio had the value 0.075. To the condition (B) is attached a probability which can easily be estimated from the Klein-Nishina cross sections for absorption and scattering and from the cross section for pair production.

We have to take into account that mesons are stopped uniformly at any point of a horizontal plane in the iron. This means that if Λ is the mean free path of the photons, the average probability that a photon will escape from the iron is

$$\frac{1}{T}\int_0^T e^{-t/\Lambda}dt=\frac{\Lambda}{T}(1-e^{-T/\Lambda})$$

where T is the thickness of the iron. The values of Λ for different photon-energies have been taken from Rossi and Greisen.[7]

The condition (C) is taken into account in the same way as (B), once it is established what is the useful range of the electrons, which of course plays the most important role for the evaluation of the probability corresponding to (D). Now, if the energy of the photon is W, the two particles of the produced pair will have a known distribution in energy. One particle will generally have more energy than the other one. We will take the average energy $\bar{U}$ of the most energetic particle, disregarding completely the less energetic one. For $\bar{U}$, we may take the value $0.75W$. Thus for a photon energy of 100 Mev, it will be equal to 75 Mev. The thickness of the counters is only 0.005-inch of brass, except for two or three rings $\frac{1}{8}$-inch wide, $\frac{1}{32}$-inch thick, so we do not need to take that into consideration.

In Table I are the numbers corresponding to the conditions (A)–(D), from which is derived the value of the total efficiency. The rate of stopped mesons, measured by the difference with and without absorber, was 20 per hour. A lead plate was placed below the counter "H" in order to prevent photo-electrons to discharge the anticoincidence counters, which would have caused the failure of detecting that event, with the consequence of a reduction of the efficiency.

In Table II are listed the total numbers of expected "g. γ. e." for photon energies of 50 and 100 Mev. The Series I and II differ in the thickness of the plate where the photons should be converted. The Series III has been obtained with the addition of other "H" counters, because it was felt that even the small number of "g. γ. e." appearing in Table II, Series I and II, was due to oblique rays. In Series III, in order to consider a picture as a "g. γ. e.," it was requested that the "H" counters placed in the way of the beam (Fig. 2) indicated, by their discharging, a path of

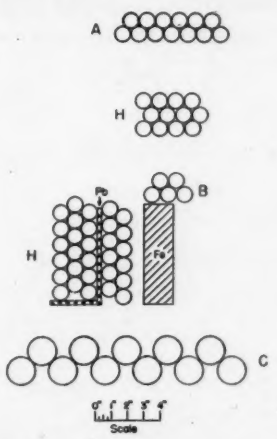

FIG. 2. Schematic of the apparatus for series III. (The screening materials are not reproduced here.)

[7] Rossi and Greisen, Rev. Mod. Phys. **13**, 240 (1941).

a single particle going toward the tray B. It was then found that pictures similar to those which constituted a "g. γ. e." in Series I and II had to be rejected, because the new "H" counters indicated that was not a straight vertical particle to cause the event. It has been checked that this new requirement did not reduce appreciably the overall efficiency of the apparatus.

DISCUSSION

Table I shows that the computation of the total efficiency comes out of the computations of various factors. One has then to be rather conservative about the precision of the assumed efficiency. However, it is to be noticed that the approximations used were mostly in the direction of underestimating the overall efficiency. For instance, in the calculation of the absorption of photons in the iron, it was assumed that the entire Klein-Nishina cross section for scattering is effective in removing photons, while it is clear that in the geometry used not all photons scattered miss the counters, and other photons which do not start in the direction of the counters may be scattered into a "useful" direction. Furthermore, it was entirely disregarded the less energetic particle of the pair. Therefore, considering that the result of the experiment does not depend on a high precision of the computed efficiency, but on a striking difference between the expected rate and the experimental one, one can conclude that the hypothesis that a big amount of the 100 Mev meson rest energy could be emitted as photons, is strongly contradicted by the experimental evidence. From the values reported in Table II, one sees that if any photons are emitted after the capture of a negative normal meson in iron, their energy must be appreciably less than 50 Mev. To set a lower limit of this energy, for which the experiment still would give a significant negative answer, one would need a more precise calculation of the efficiency of the apparatus. From a rough extrapolation of the numbers in Table II toward the low energies, one would exclude that as much as an energy of 20 Mev is irradiated after a meson stops in Fe. In the hypothesis of a neutral meson emitted, and subject to decay in two light-quanta, the present experiment indicates that the mean life of such a meson must be greater than, say, 10^{-10} sec., unless its rest-mass is much smaller than 50 Mev. Concerning the decay process of the positive mesons, if we take as a reference the value of 50 Mev for the energy of a hypothetical photon emitted, the experiment gives again a negative answer, which checks with the results of R. D. Sard and E. J. Althaus,[8] and E. P. Hincks and B. Pontecorvo.[9]

The author is indebted to Professor Bruno Rossi for the offer of a visiting research associateship at the Massachusetts Institute of Technology. In assembling the experiment and in taking data, the cooperation of Mr. John Harriman was most helpful. The writer also acknowledges with pleasure many stimulating discussions which he had with Professor V. Weisskopf and Doctor T. Welton. The experiment here reported was partially supported by Contract N5ori-78, U. S. Navy Department, Office of Naval Research.

[8] Sard and Althaus, Bull. Am. Phys. Soc. **23**, No. 2, p. 20 (1948).
[9] E. P. Hincks and B. Pontecorvo, Phys. Rev. **73**, 257 (1948).

PHYSICAL REVIEW VOLUME 74, NUMBER 12 DECEMBER 15, 1948

The Coulomb Scattering of Relativistic Electrons by Nuclei

WILLIAM A. MCKINLEY, JR.
Rensselaer Polytechnic Institute, Troy, New York

AND

HERMAN FESHBACH
Massachusetts Institute of Technology, Cambridge, Massachusetts

(Received July 8, 1948)

The cross section for the Coulomb scattering of relativistic electrons by atomic nuclei has been evaluated. The exact results obtained by Mott have been expanded in a power series in $Z/137$, where Z is the nuclear charge, the coefficients depending principally on the angle of scattering. The coefficients have been evaluated numerically. The resultant cross sections, taken together with those evaluated previously by Bartlett and Watson for Hg, yield the cross section for all Z to within 1 percent accuracy. A new approximate formula valid for $Z/137<0.2$ is obtained.

INTRODUCTION

THE experimental study of the single scattering of electrons by atomic nuclei is of the greatest fundamental importance. In the energy range in which the electron wave-length is considerably larger than the target nucleus, the Coulomb law of force is under scrutiny. For the higher energies which are now becoming available, the electron wave-length will be of the same size, or smaller, than the nucleus, so that scattering experiments should furnish information about the current and charge distribution within the nucleus.

The comparison of theory and experiment has been greatly hampered by the complexity of the theoretical formulas which have been obtained by Mott[1] in the form of a conditionally convergent infinite series. He has also derived an approximate formula, the "Mott formula,"[2] which is valid when

$$\alpha/\beta \ll 1, \quad \alpha = Ze^2/\hbar c, \quad \beta = v/c, \tag{1}$$

where Z is the nuclear charge. Sexl[3] and Urban[4] have also derived a formula valid in this range, which is in disagreement with Mott's result. Bartlett and Watson[5] have summed Mott's series for the case of Hg($Z=80$) for a range of energies up to $\beta \cong 1$. In this paper, the Mott series has been expanded in a power series in α and α/β the coefficients depending upon the angle of scattering θ. The series is accurate for middle Z elements. Used however in conjunction with the results of Bartlett and Watson, the cross section for scattering may be computed for all Z with an error of at most a few percent.

THEORY

Mott gives as the differential scattering cross section the result:

$$\sigma = q^2(1-\beta^2)F^*F \csc^2\theta/2 + G^*G \sec^2\theta/2, \tag{2}$$

where $q=\alpha/\beta$. The functions F and G are given by:

$$\begin{aligned} &F = F_0 + F_1, \quad G = G_0 + G_1, \\ &F_0 = i/2 \exp(iq \ln \sin^2\theta/2)\Gamma(1-iq)/\Gamma(1+iq), \\ &G_0 = -iq \cot^2\theta/2 F_0, \\ &F_1 = i/2 \sum_{k=0}^{\infty} [kD_k + (k+1)D_{k+1}](-)^k P_k(\cos\theta), \\ &G_1 = i/2 \sum_{k=0}^{\infty} [k^2 D_k - (k+1)^2 D_{k+1}] \\ &\qquad \times (-)^k P_k(\cos\theta), \end{aligned} \tag{3}$$

where Γ is the gamma-function and P_k the Legendre polynomial of order k. Finally

$$D_k = \frac{e^{-\pi i k}}{(k+iq)} \frac{\Gamma(k-iq)}{\Gamma(k+iq)} - \frac{e^{-i\pi\rho_k}}{(\rho_k+iq)} \frac{\Gamma(\rho_k-iq)}{\Gamma(\rho_k+iq)}, \quad \rho_k = (k^2-\alpha^2)^{\frac{1}{2}}. \tag{4}$$

[1] N. F. Mott, Proc. Roy. Soc. **A124**, 426 (1929); N. F. Mott, Proc. Roy. Soc. **A135**, 429 (1932).
[2] See reference 1.
[3] T. Sexl, Zeits. f. Physik **81**, 178 (1933).
[4] P. Urban, Zeits. f. Physik **119**, 67 (1942).
[5] J. H. Bartlett and R. E. Watson, Proc. Amer. Acad. Arts and Sci. **74**, 53 (1940).

TABLE I. The angular functions of Eq. (8).

θ	$A(\theta)$ Re	$A(\theta)$ Im	$B(\theta)$ Re	$B(\theta)$ Im	$C(\theta)$ Re	$C(\theta)$ Im
30°	−0.362	0.064	−0.086	0.498	0.580	−0.010
45	−0.510	0.114	−0.201	0.375	0.404	−0.069
60	−0.637	0.167	−0.339	0.209	0.313	−0.167
80	−0.780	0.235	−0.537	−0.033	0.289	−0.351
90	−0.840	0.266	−0.636	−0.150	0.305	−0.448
100	−0.893	0.295	−0.729	−0.263	0.332	−0.553
120	−0.980	0.344	−0.897	−0.455	0.408	−0.750
135	−1.028	0.373	−0.995	−0.568	0.464	−0.876
150	−1.062	0.394	−1.072	−0.650	0.511	−0.971
180	−1.089	0.411	−1.133	−0.720	0.551	−1.052

θ	$D(\theta)$ Re	$D(\theta)$ Im	$E(\theta)$ Re	$E(\theta)$ Im	$H(\theta)$ Re	$H(\theta)$ Im
30°	−0.107	−0.129	2.249	−0.676	1.483	1.044
45	−0.217	−0.221	1.267	−0.480	1.221	1.371
60	−0.344	−0.310	0.785	−0.347	0.953	1.174
80	−0.525	−0.417	0.437	−0.221	0.643	0.817
90	−0.614	−0.464	0.325	−0.173	0.514	0.658
100	−0.699	−0.505	0.240	−0.133	0.401	0.514
120	−0.849	−0.574	0.122	−0.072	0.219	0.281
135	−0.940	−0.612	0.065	−0.040	0.123	0.158
150	−1.007	−0.638	0.028	−0.017	0.051	0.065
180	−1.062	−0.657	0.000	0.000	0.000	0.000

θ	$I(\theta)$ Re	$I(\theta)$ Im	$J(\theta)$ Re	$J(\theta)$ Im
30°	3.105	0.471	0	1.711
45	1.261	0.733	0	1.199
60	0.354	0.781	0	0.851
80	−0.110	0.678	0	0.532
90	−0.200	0.591	0	0.413
100	−0.206	0.495	0	0.315
120	−0.174	0.305	0	0.167
135	−0.085	0.173	0	0.091
150	−0.071	0.085	0	0.040
180	−0.000	0.000	0	0

The procedure used in this paper involves the expansion of F_1 and G_1 in a power series in α and α/β. The expansion will thus be valid only for relativistic electrons $\beta\sim 1$. The first term, the "α approximation" should yield the correct Mott formula. The expansion of the coefficients D_k yields

$$D_k=(-)^{k+1}\Big\{\alpha^2\Big(\frac{i\pi}{2k^2}+\frac{1}{2k^3}\Big)+\alpha^3\Big(\frac{i\psi_2}{\beta k^2}+\frac{\pi\psi_1}{\beta k^2}+\frac{\pi}{2\beta k^3}-\frac{i\psi_1}{\beta k^3}-\frac{i}{\beta k^4}\Big)+\alpha^4\Big(\frac{2\psi_1\psi_2}{\beta^2k^2}-\frac{i\pi\psi_1^2}{\beta^2k^2}-\frac{\pi^2}{8k^3}+\frac{\psi_2}{\beta^2k^3}-\frac{i\pi\psi_1}{\beta^2k^3}-\frac{\psi_1^2}{\beta^2k^3}+\frac{3}{8}\frac{i\pi}{k^4}-\frac{i\pi}{2\beta^2k^4}-\frac{2\psi_1}{\beta^2k^4}+\frac{3}{8k^5}-\frac{3}{2\beta^2k^5}\Big)\Big\}+0(\alpha^5). \quad (5)$$

Here $\psi_n(k)$ are the polygamma-functions. The function

$$\psi_1=(d/dk)\ln\Gamma(k),$$

while

$$\psi_n=(d/dk)\psi_{n-1}(k).$$

This expansion of D_k must now be substituted in (3) to obtain F_1 and G_1. Only the sums over k involved in the α^2 term may be performed exactly, the other sums must be performed numerically.

The α^2 term will now be discussed. It should lead to the Mott formula which has been the subject of controversy inasmuch as Mott and Urban have obtained conflicting answers. We take

$$D_k\simeq\frac{(-)^{k+1}\alpha^2}{2}\Big(\frac{i\pi}{k^2}+\frac{1}{k^3}\Big).$$

Then

$$G_1\simeq\alpha^2/4\sum_{k=1}^{\infty}(\pi-i/k)(P_k+P_{k-1}),$$
$$G_0\simeq\tfrac{1}{2}q\cot^2\theta/2+0(\alpha^2), \quad (6)$$
$$F_0\simeq i/2+0(\alpha^2).$$

To evaluate G_1 we use the sum formulas given by Mott,

$$\sum_{k=1}^{\infty}(P_k+P_{k-1})=\csc\theta/2-1,$$
$$\sum_{k=1}^{\infty}\frac{1}{k}(P_k+P_{k-1})=\ln\csc^2\theta/2.$$

Introducing (6) into (3) and (3) into (2) yields for R the ratio of the scattering to Rutherford scattering*

$$R=1-\beta^2\sin^2\theta/2+\pi\alpha\beta\sin\theta/2(1-\sin\theta/2). \quad (7)$$

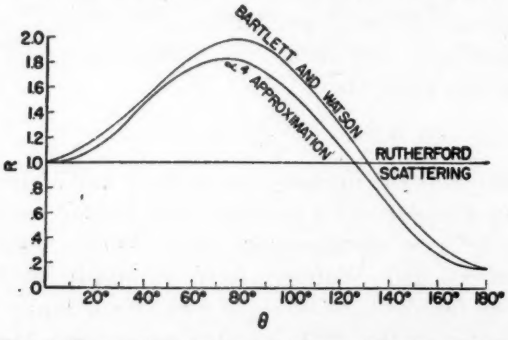

FIG. 1. Comparison between α^4-approximation and exact calculation of Bartlett and Watson for Hg. The energy of the electron is 2 Mev. R is the ratio of the scattering cross section to Rutherford scattering.

* Rutherford scattering yields cross section

$$\sigma=\Big(\frac{Ze^2}{2m_0c^2}\Big)^2\frac{1-\beta^2}{\beta^4}\csc^4\theta/2.$$

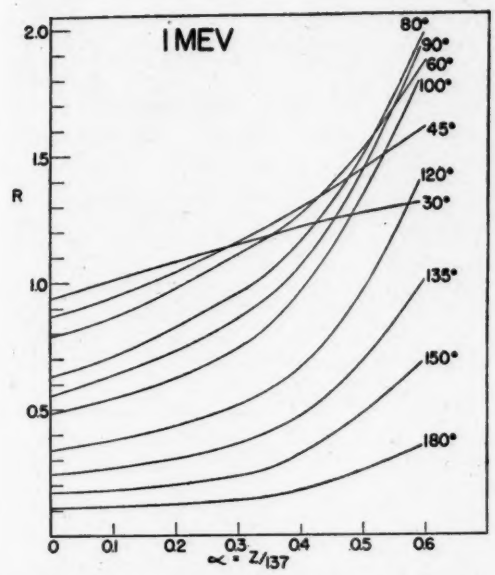

FIG. 2. The ratio R of the scattering cross section to Rutherford scattering as a function of $Z/137$ for the various scattering angles labelling each curve. Electron energy 1 Mev.

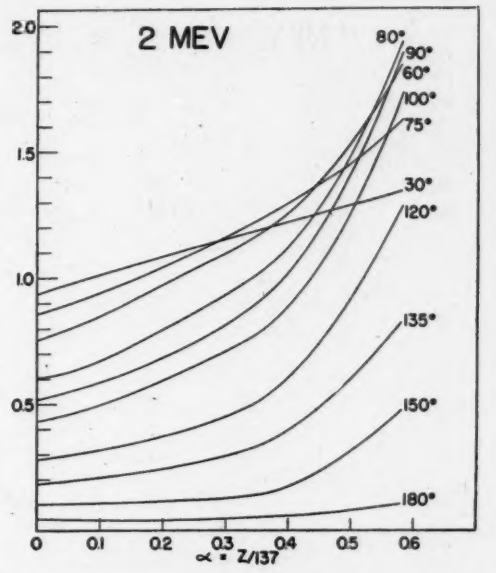

FIG. 3. The ratio R of the scattering cross section to Rutherford scattering as a function of $Z/137$ for the various scattering angles labelling each curve. Electron energy 2 Mev.

This result has been obtained by Julian Schwinger[6] by the variational-iterational procedure. In Mott's formula the factor $(1-\sin\theta/2)$ is replaced by $\cos^2\theta/2$ while Urban replaces this factor by 1. Thus both Mott's and Urban's formulas will be correct for $\theta\sim 0°$, Mott's for $\theta\sim 180°$. Both are incorrect in the intermediate angular range.

When the complete expression for D_k given by (5) is substituted into (3) one obtains expressions for F_1 and G_1 in the following form:

$$F=F_0+A(\theta)\alpha^2+B(\theta)\alpha^3/\beta+C(\theta)\alpha^4/\beta^2+D(\theta)\alpha^4,$$
$$G=G_0+E(\theta)\alpha^2+H(\theta)\alpha^3/\beta+I(\theta)\alpha^4/\beta^2+J(\theta)\alpha^4. \quad (8)$$

The function F_0 has been tabulated by Bartlett and Watson. Only $E(\theta)$ may be summed analytically (see Eq. (6)). The remaining sums must be performed numerically.[7] The important difficulties which occur are discussed in the appendix. The real and imaginary parts of the functions A through J are given in Table I.

[6] Private Communication.

[7] The polygamma-functions are tabulated in H. T. Davis, *Tables of Higher Functions*, Vol. II (University of Indiana Press, Bloomington, 1935). The Legendre polynomials are tabulated up to P_{32} by H. Tallqvist, Acta. Soc. Scient. Fennica, Vol. II (1938).

Since we have neglected terms of the order of α^5 the error in our results should be of this order. This has been verified by comparing the α^4 approximation of this paper with the results of the Bartlett and Watson for Hg for which $\alpha^5=0.068$. Figure 1 shows this comparison. Since our results extrapolate smoothly to those of Bartlett and Watson, it is possible to combine their results with ours to obtain scattering cross sections which are valid for all Z. These are summarized in the curves given in Figs. 2, 3 and 4, where we have plotted the ratio R as a function of Z for different values of θ. This ratio is independent of the electron energy for energies above 4 Mev within the accuracy of these calculations. In the regions of α in which these plots deviate from the straight line, the approximate formula (6) will be invalid. The value of α at which this occurs varies with angle. Roughly speaking formula (6) should be valid for $\alpha\leq 0.2$.

COMPARISON WITH EXPERIMENT

We have compared our results with those of the most recent experiments,[8] performed with

[8] R. J. Van de Graaff, W. W. Buechner and H. Feshbach, Phys. Rev. 69, 452 (1946); Buechner, Van de Graaff, Sperduto, Burrill, Jr. and Feshbach, Phys. Rev. 72, 678 (1947).

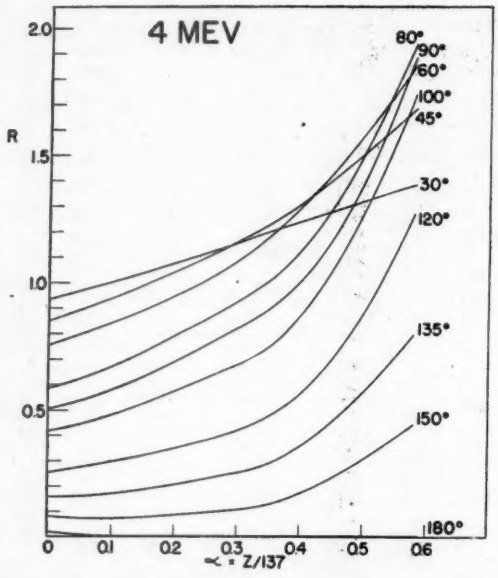

FIG. 4. The ratio R of the scattering cross section to Rutherford scattering as a function of $Z/137$ for the various scattering angles labelling each curve. Electron energy 4 Mev. The energy dependence of the ratio R may be neglected within the accuracy of these calculations above 4 Mev.

the electrostatic generator. The average of the ratios of experimental to the theoretically expected scattering is 1.01 ± 0.04. A typical example of the good agreement is plotted in Fig. 5.

ACKNOWLEDGMENT

We are indebted to Miss Barbara Siegle and Miss Elizabeth Campbell for computational aid. This research was supported in part by the Office of Naval Research.

APPENDIX

The convergence of the infinite series for the angular functions $A(\theta)-J(\theta)$ (Eq. (8)) may be examined by using the asymptotic expressions:

$$\begin{aligned} &P(\cos\theta)\xrightarrow[k\to\infty]{}\left(\frac{2}{\pi k\sin\theta}\right)^{\frac{1}{2}}\sin[(k+\tfrac{1}{2})\theta+\pi/4],\\ &\psi_1(k)\xrightarrow[k\to\infty]{}\ln k,\\ &\psi_2(k)\xrightarrow[k\to\infty]{}1/k. \end{aligned} \tag{A1}$$

All of the series involved converge absolutely except for

$$\sum_1^\infty P_k,\quad \sum_1^\infty \psi_1(k)P_k,\quad \sum_1^\infty \psi_1(k)^2P_k,$$

and, similarly,

$$\sum_1^\infty P_{k-1},\quad \sum_1^\infty \psi_1(k)P_{k-1},\quad \sum_1^\infty \psi_1^2(k)P_{k-1}.$$

The latter series converge only conditionally. Fortunately some of them may be summed:

$$\begin{aligned} &\sum_{k=1}^\infty P_k=\tfrac{1}{2}\csc\theta/2-1,\quad \sum_{1=k}^\infty\frac{P_k}{k}=\ln\frac{\csc^2\theta/2}{1+\csc\theta/2},\\ &\sum_{k=1}^\infty P_{k-1}=\tfrac{1}{2}\csc\theta/2,\quad \sum_{k=1}^\infty\frac{P_{k-1}}{k}=\ln(1+\csc\theta/2),\\ &\sum_1^\infty\frac{P_{k+1}}{k}=-2\sin\theta/2(1-\sin\theta/2)+\cos\theta\ln\frac{\csc^2\theta/2}{1+\csc\theta/2}. \end{aligned} \tag{A2}$$

In addition we have summed

$$\begin{aligned} \sum_{k=1}^\infty\psi_1(k)P_k=&-\gamma(\tfrac{1}{2}\csc\theta/2-1)\\ &+\tfrac{1}{2}\csc\theta/2\ln\tfrac{1}{4}(\csc\theta/2+1)\\ &-\ln\frac{\csc^2\theta/2}{4\csc\theta/2},\\ \sum_{k=1}^\infty\psi_1(k)P_{k-1}=&-\gamma/2\csc\theta/2\\ &+\tfrac{1}{2}\csc\theta/2\ln\tfrac{1}{4}(\csc\theta/2+1), \end{aligned} \tag{A3}$$

where γ is the Mascheroni constant, 0.5772.

In general, all the series involved, including those which converged absolutely, converged rather poorly. Because of the slow convergence it was found useful to derange the series so as to permit the use of the Euler transformation.[9] The validity of the derangement for the conditionally convergent series is guaranteed by the theorem of Levi.[10] In addition for the $\Sigma\psi_1^2(k)P_k$ series it was necessary to use asymptotic expressions for the sum for sufficiently large k:

$$\begin{aligned} \sum_N^\infty P_k\psi_1^2(k)\simeq&\tfrac{1}{2}\csc^2\theta/2\Big\{-4\csc^2\theta/2\sum_{N-1}^\infty\frac{P_k\psi_1(k)}{k}\\ &-\tfrac{1}{2}\cos\theta\sum_N^\infty\frac{P_{k-1}\psi_1^2(k)}{k}+\tfrac{1}{2}\sum_{N-2}^\infty\frac{P_k\psi_1^2(k)}{k}\\ &-\sum_{N-2}^\infty\frac{P_k\psi_1^2(k)}{k^2}+\frac{2P_{N-1}\psi_1(N-1)}{N-1}\\ &-(\cos\theta+\tfrac{1}{2})P_{N-1}\psi_1^2(N-1)\\ &-\tfrac{1}{2}P_{N-2}\psi_1^2(N-2)\Big\}+0\Big(\sum_N^\infty\frac{P_k\psi_1(k)}{k^2}\Big)\\ &+0\Big(\sum_N^\infty\frac{P_k}{k^2}\Big),\quad\text{for }\theta\simeq90°. \end{aligned} \tag{A4}$$

$$\begin{aligned} \sum_N^\infty P_k\psi_1^2(k)\simeq&\csc^2\theta/2\Big\{-2(1+\cos^2\theta/2)\sum_{N-1}^\infty\frac{P_k\psi_1(k)}{k}\\ &-\frac{\cos\theta}{4}\sum_N^\infty\frac{P_{k-1}\psi_1^2(k)}{k}+\tfrac{1}{4}\sum_{N-2}^\infty\frac{P_k\psi_1^2(k)}{k}\\ &-\tfrac{1}{2}\sum_{N-2}^\infty\frac{P_k\psi_1^2(k)}{k^2}-\cos^2\theta/2P_N\psi_1^2(N)\\ &-P_{N-2}\frac{\psi_1(N-2)}{(N-2)}-\tfrac{3}{4}P_{N-1}\psi_1^2(N-1)\\ &-\tfrac{1}{4}P_{N-2}\psi_1^2(N-2)\Big\}+0\Big(\sum_N^\infty\frac{P_k\psi_1(k)}{k^2}\Big)\\ &+0\Big(\sum_N^\infty\frac{P_k}{k^2}\Big)+0\Big(\sum_N^\infty\frac{P_k\psi_1^2(k)}{k^3}\Big),\\ &\text{for }\theta\simeq180°. \end{aligned} \tag{A5}$$

[9] T. J. I'A. Bromwich, *Introduction to the Theory of Infinite Series* (The MacMillan Company, New York, 1947).

[10] Levi, Duke Math. J. **13**, 579 (1946).

The value chosen for N was 20. These procedures were checked by applying them to series (A2) and (A3) which could be summed analytically. In addition, some internal checks were provided by the recurrence relations

$$\psi_1(k+1)-\psi_1(k)=1/k,$$
$$\psi_2(k+1)-\psi_2(k)=-1/k^2, \qquad \text{(A6)}$$

which lead to the relations:

$$\sum_1^\infty \psi_1(k)P_k=\sum_1^\infty \psi_1(k)P_{k-1}+\gamma-\ln\frac{\csc^2\theta/2}{1+\csc\theta/2},$$

$$\sum_1^\infty \psi_1^2P_k=\sum_1^\infty \psi_1^2(k)P_{k-1}-\psi_1^2(1)$$
$$-\sum_1^\infty \frac{P_k}{k^2}-2\sum_1^\infty \frac{\psi_1(k)P_k}{k^2},$$

$$\sum_1^\infty \psi_1(k)\psi_2(k)P_k=\sum_1^\infty \psi_1(k)\psi_2(k)P_{k-1}-\psi_1(1)\psi_2(1)$$
$$+\sum_1^\infty \frac{\psi_1(k)P_k}{k^2}-\sum_1^\infty \frac{\psi_2(k)P_k}{k}+\sum_1^\infty \frac{P_k}{k^3},$$

$$\sum_1^\infty \psi_2P_k=\Sigma\,\psi_2P_{k-1}-\psi_2(1)+\Sigma\,P_k/k^2. \qquad \text{(A7)}$$

Similar relations using the recurrence relations for the Legendre polynomials but were not found as useful except as used in (A4) and (A5). Another check was also provided by the asymptotic expansion for $\psi_2\to 1/k+1/2k^2+1/6k^3+\cdots$. It is estimated that the error in the computation of R is 0.1 percent.

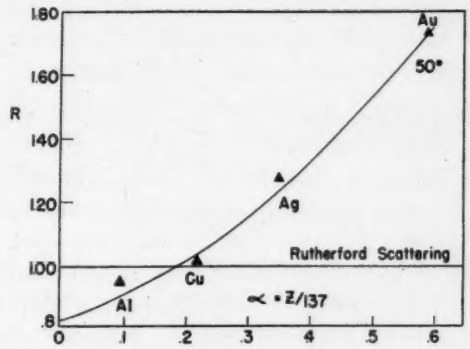

FIG. 5. Comparison of theory and experiment at electron energy of 2 Mev. The solid line is given by the theory. The triangles give the experimental points as obtained by Van de Graaff, Buechner *et al.*

PHYSICAL REVIEW VOLUME 74, NUMBER 12 DECEMBER 15, 1948

Variational Methods in Nuclear Collision Problems*

W. KOHN**
Department of Physics, Harvard University, Cambridge, Massachusetts
(Received August 19, 1948)

Variational methods, similar to the Rayleigh-Ritz method for bound state calculations, are developed for the phase shifts and elements of the scattering matrix in nuclear collisions. Numerical applications to neutron-proton and neutron-deuteron scattering involving trial functions with undetermined coefficients are described. Another variational principle, for scattering amplitudes, is shown to lead to the Born approximations and a formula recently derived by Schwinger. It may also be used in conjunction with the method of undetermined coefficients.

I. INTRODUCTION

A GREAT deal of information about the nature of nuclear forces has been derived from a comparison of experimental and theoretical studies of simple nuclear systems.

The bound states of nuclei comprising up to four particles have been theoretically treated with considerable accuracy[1] and have yielded very important results. For nuclear collisions involving more than two particles, Breit and Wigner,[2] Wheeler,[3] Heisenberg,[4] and Wigner[5] have developed general, phenomenological theories. However, no very satisfactory scheme for treating such collisions in detail has so far been given. All calculations up to the present[6] are based on an approximation of the wave function by an

* This paper is based on Part I of a thesis submitted in partial fulfillment of the requirements for the degree of Doctor of Philosophy, at Harvard University, June 1948.
** Parker Fellow, 1947–8.
[1] See, for example, W. Rarita and R. D. Present, Phys. Rev. **51**, 788 (1937); H. Margenau and D. T. Warren, Phys. Rev. **52**, 790 (1937).
[2] G. Breit and E. Wigner, Phys. Rev. **49**, 519 (1936).
[3] J. A. Wheeler, Phys. Rev. **52**, 1107 (1937).
[4] W. Heisenberg, Zeits. f. Physik **120**, 513 (1942).
[5] E. P. Wigner, Phys. Rev. **70**, 15 and 606 (1946).
[6] For example, L. Motz and J. Schwinger, Phys. Rev. **58**, 26 (1940); R. A. Buckingham and H. S. W. Massey, Proc. Roy. Soc. **179**, 123 (1941).

expression of the type

$$\Psi=\sum_i \varphi_i F_i, \tag{1.1}$$

where φ_i is the product of the internal wave functions of two colliding or separating nuclei[7] and F_i is the wave function of relative motion. The sum is taken over all pairs of nuclei whose formation is energetically possible and the signs adjusted in accordance with the exclusion principle. Wave functions of this so-called group structure type were first introduced by Wheeler.[8] While the function (1.1) has the correct symmetry and asymptotic behavior, one cannot expect it to describe too well the correct wave function in that part of the configuration space where the colliding nuclei interact, and it is just this region which determines the observable cross section.

To determine the best wave function of the group structure type, Wheeler employed a variational principle. Variational methods have also been applied by Hulthén[8] and Schwinger[9] to two-particle collisions.

The purpose of this paper is to propose variational methods, related to Hulthén's approach, which lead to stationary expressions for the observable scattering cross sections. In particular our methods lend themselves to a systematic treatment of composite collisions, which is not restricted to wave functions with group structure. The mathematical operations bear a considerable analogy to those of the Rayleigh-Ritz method for determining the binding energies of nuclei. The physical clue for this fact may be seen in the connection between binding energies and phase shifts which was pointed out by Heisenberg.[4] However, instead of attacking collision problems from this point of view, it will be simpler to investigate them independently of related bound states.

II. ONE-DIMENSIONAL PROBLEMS

In considering the collision of two particles, interacting by a short-range potential, one is led to the equation

$$\{d^2/dx^2+\kappa^2-V(x)\}u(x)=0, \tag{2.1}$$

for the partial wave of angular momentum 0; here κ is the wave number of relative motion and $V(x)$ the interaction potential. The wave function $u(x)$ has the following properties

$$u(0)=0, \tag{2.2}$$

$$x\to\infty: \quad u(x)\to A\sin\kappa x+B\cos\kappa x = A(\sin\kappa x+\tan\eta\cdot\cos\kappa x), \tag{2.3}$$

where A and B are some constants and the phase shift η is defined by $\tan\eta=B/A$.

Let the logarithmic derivative of $u(x)$ at $x=a$ be

$$L=u'(a)/u(a). \tag{2.4}$$

Then it is easily verified that u satisfies the equation

$$\int_0^a \{-(du/dx)^2+\kappa^2u^2-V(x)u^2\}dx + Lu^2(a)=0. \tag{2.5}$$

Furthermore, for a given value of L, κ^2 as calculated from (2.5) is stationary, if the trial functions, u_t, satisfy the condition (2.2). This fact is the basis of binding energy calculations. One can equally well regard (2.5) as providing a stationary expression for L, given the value of κ^2. This is the more natural approach in collision problems, in which the energy of the system is prescribed. If $x=a$ is beyond the range of interaction, $L=\kappa\cot(\kappa a+\eta)$, so that $\tan\eta$ and hence the scattering cross section, $\sigma=4\pi/\{\kappa^2(1+\cot^2\eta)\}$ can be calculated, once L is known.

To find an approximation for L from the stationary property of (2.5) we write our trial function in the form

$$u_t=c_1u_1+c_2u_2+\cdots c_nu_n, \tag{2.6}$$

where $u_i(0)=0$ and the unknown coefficients c_i are to be determined. Substituting (2.6) in (2.5), one is led to an equation of the form

$$Q\equiv\sum_{\substack{i=1\\j=1}}^{n} A_{ij}(\kappa^2)c_ic_j+L\Big(\sum_{i=1}^{n} c_iu_i(a)\Big)^2=0, \tag{2.7}$$

where we have indicated the dependence of the integrals A_{ij} on κ^2. We may, of course, assume that $A_{ij}=A_{ji}$.

The stationary property of (2.7) with respect to variations of the c_i now leads to the set of

[7] No systematic theory for nuclear collisions in which more than two end products are possible has yet been developed.

[8] L. Hulthén, Extrait, Dixième Congrès des Mathématiciens Scandinaves, Copenhague, 1946.

[9] Unpublished lectures, 1947.

equations,

$$\frac{\partial Q}{\partial c_i}=2\{\sum_{j=1}^{n} A_{ij}c_j+Lu_i(a)\cdot\sum_{j=1}^{n} u_j(a)c_j\}=0. \quad (2.8)$$

They are compatible only if the determinant of the coefficients of the c_i vanishes, i.e., if

$$\Delta\equiv|A_{ij}+Lu_i(a)\cdot u_j(a)|=0. \quad (2.9)$$

As the matrix $\|u_i(a)\cdot u_j(a)\|$ has rank 1, this is a *linear* equation for L and hence determines L uniquely.[10] This is in contrast to the usual secular determinants, whose degree in the unknown energy is as high as the number of trial functions. We shall refer to determinants of the character of Δ as collision determinants.

Another closely related variational principle can be derived as follows. Consider the expression

$$I\equiv\int_0^\infty u\{d^2/dx^2+\kappa^2-V(x)\}udx, \quad (2.10)$$

which vanishes if u is the correct solution of (2.1). Now let us consider its first variation, if the trial functions, $u_t=u+\delta u$ satisfy the conditions

$$u_t(0)=0,$$
$$x\to\infty: \quad u_t\to A\sin\kappa x+B_t\cos\kappa x. \quad (2.11)$$

Then, in virtue of the differential Eq. (2.1),

$$\delta I=\int_0^\infty (u\,d^2/dx^2\,\delta u-\delta u\,d^2/dx^2\,u)dx$$
$$=(u\,d/dx\,\delta u-\delta u\,d/dx\,u)_{x=\infty}=-\kappa A\delta B, \quad (2.12)$$

where $\delta B=B_t-B$. Hence,

$$\delta(I+\kappa AB)=0.^{11} \quad (2.13)$$

Since for the correct u, $I=0$, and $B=A\tan\eta$, the equation

$$I+\kappa AB_t=\kappa A^2\tan\eta, \quad (2.14)$$

is correct to the first order and hence serves as a variational principle for $\tan\eta$. As before, on using trial functions of the form (2.6) one is led to a collision determinant, Δ, which is linear in $\tan\eta$, so that the latter is uniquely determined by the compatibility equation, $\Delta=0$.

Numerical Illustrations

Using Eqs. (2.5) and (2.14), we have calculated scattering of neutrons by protons at zero energy. We have assumed the interaction

$$\left.\begin{aligned} V(x)&=-4.01435, \quad x\leqslant 1\\ &=0, \quad x>1\end{aligned}\right\} \quad (2.15)$$

(x measured in units of 2.80×10^{-13} cm), which gives the correct binding energy for the deuteron. The wave equation, in this case, is simply

$$d^2u/dx^2+V(x)u=0, \quad (2.16)$$

and can of course be solved exactly. For $x>1$, u has the form, $u=C(x+X)$, where X is the desired $\lim_{\kappa\to0}(\tan\eta/\kappa)$, in terms of which the scattering cross section is $4\pi X^2$. As trial functions we have used

$$u_t=\sum_1^n C_k x^k, \quad x\leqslant a(n=1,2,3). \quad (2.17)$$

Since (2.17) does not have the correct asymptotic form, required by (2.11), we have assumed that at $x=a$ it passes smoothly into a function of the form $u_t=Cx+D$.

Clearly, for a given n, a function of the type (2.17) can approximate the correct wave function better over a short than over a long interval, so that the best results are obtained with $a=1$ (see Table I).

III. THE SCATTERING AMPLITUDE

It is desirable to have methods for calculating the scattering amplitudes of the entire plane wave without having to determine, separately,

TABLE I. Approximations to $X=\lim_{\kappa\to0}\tan\eta/\kappa$; $X_{\text{exact}}=-2.080$; I.....by Eq. (2.5); II.....by Eq. (2.14).

a	c_1x		$c_1x+c_2x^2$		$c_1x+c_2x^2+c_3x^3$	
	I	II	I	II	I	II
1	−3.957	+1.338	−2.112	−2.126	−2.083	−2.084
2	+4.043	+1.338	−2.858	−4.039	−2.201	−2.206
3	+2.416	+1.338	−6.593	−51.606	−2.385	−2.520
4	+2.011	+1.338	968.870	+7.634	−2.936	−3.315

[10] This can also be made apparent by the transformation $d_1=\sum_1^n u_j(a)c_j$, $d_i=c_i$, $(i\neq1)$. Then Q has the form $Q=\sum_1^n B_{ij}d_id_j+Ld_1^2$, and the compatibility equation, $|B_{ij}+L\delta_{1i}\delta_{1j}|=0$, is evidently linear in L.

[11] L. Hulthén (see reference 8) has used an equivalent relation to determine $\tan\eta$, by restricting his trial functions by the condition $I=0$. This is a little complicated and leads to a quadratic equation for $\tan\eta$, only one of whose solutions is "good."

the phase shifts of each partial wave. This is usually accomplished by the use of successive Born approximations, i.e., by an iteration procedure. Another iteration method, giving more accurate results, has been developed by Schwinger.[9] We shall now derive a variational principle which serves as common basis of (a) Born approximations; (b) Schwinger's approximation; (c) The method of linear trial functions.

Let the wave equation of the problem be

$$\{\nabla^2+\kappa^2-V(\mathbf{r})\}\psi(\mathbf{r})=0, \tag{3.1}$$

where $\mathbf{r}$ is the usual relative position vector. We denote by ψ_1, ψ_2 the two solutions of (3.1) which correspond to plane waves incident along the vectors $\boldsymbol{\kappa}_1$ and $\boldsymbol{\kappa}_2$, respectively, ($|\boldsymbol{\kappa}_1|=|\boldsymbol{\kappa}_2|=\kappa$). They have the asymptotic form

$$\psi_i=\exp(i\boldsymbol{\kappa}_i\cdot\mathbf{r})+f(\boldsymbol{\kappa}_i,\boldsymbol{\kappa})\exp(i\kappa r)/r, \tag{3.2}$$

where $r=|\mathbf{r}|$ and $f(\boldsymbol{\kappa}_i,\boldsymbol{\kappa})$ is the scattering amplitude in the direction $\boldsymbol{\kappa}$ of a plane wave incident along $\boldsymbol{\kappa}_i$.

Next we define the bilinear form $I(\boldsymbol{\kappa}_1,-\boldsymbol{\kappa}_2)$ as

$$I(\boldsymbol{\kappa}_1,-\boldsymbol{\kappa}_2)=\int_0^\infty \psi_2\{\nabla^2+\kappa^2-V(\mathbf{r})\}\psi_1 d\mathbf{r}. \tag{3.3}$$

For the correct ψ_1, $I(\boldsymbol{\kappa}_1,-\boldsymbol{\kappa}_2)=0$. Its first variation is

$$\delta I(\boldsymbol{\kappa}_1,-\boldsymbol{\kappa}_2)=\int_S (\psi_2(\partial/\partial n)\delta\psi_1 - \delta\psi_1(\partial/\partial n)\psi_i)dS, \tag{3.4}$$

where S is a large sphere and $\partial/\partial n$ denotes differentiation along the outward normal. This follows immediately from an integration by parts.

If we admit only trial functions of the correct asymptotic form (3.2), but possibly false scattering amplitudes, $f_{i;i}(\boldsymbol{\kappa}_i,\boldsymbol{\kappa})$, then, asymptotically,

$$\delta\psi_i\to\delta f_i(\boldsymbol{\kappa}_i,\boldsymbol{\kappa})\exp(i\kappa r)/r. \tag{3.5}$$

Clearly only the plane wave part of ψ_2 contributes to the surface integral in (3.4), so that

$$\delta I(\boldsymbol{\kappa}_1,-\boldsymbol{\kappa}_2)=\int_S\left\{\exp(i\boldsymbol{\kappa}_2\cdot\mathbf{r})\frac{\partial}{\partial n}\frac{\exp(i\kappa r)}{r} - \frac{\exp(i\kappa r)}{r}\frac{\partial}{\partial n}\exp(i\boldsymbol{\kappa}_2\cdot\mathbf{r})\right\}\cdot\delta f_1(\boldsymbol{\kappa}_1,\boldsymbol{\kappa})dS. \tag{3.6}$$

Dirac[12] has shown that the factor multiplying $\delta f_1(\boldsymbol{\kappa}_1,\boldsymbol{\kappa})$ has a δ-function like character for large values of r, so that the integration simply gives $-4\pi\delta f_1(\boldsymbol{\kappa}_1,-\boldsymbol{\kappa}_2)$. Hence, corresponding to (2.14) we find

$$I(\boldsymbol{\kappa}_1,-\boldsymbol{\kappa}_2)+4\pi f_{i;1}(\boldsymbol{\kappa}_1,-\boldsymbol{\kappa}_2)=4\pi f(\boldsymbol{\kappa}_1,-\boldsymbol{\kappa}_2), \tag{3.7}$$

as a stationary expression for $f(\boldsymbol{\kappa}_1,-\boldsymbol{\kappa}_2)$ relative to independent variations of ψ_1 and ψ_2, subject to the conditions (3.5).

More generally, if we admit trial functions of the asymptotic form

$$\psi_{i;i}\to A_i\left\{\exp(i\boldsymbol{\kappa}_i\cdot\mathbf{r})+f_{i;i}(\boldsymbol{\kappa}_i,\boldsymbol{\kappa})\frac{\exp(i\kappa r)}{r}\right\}, \tag{3.8}$$

(3.7) is replaced by the homogeneous equation

$$I(\boldsymbol{\kappa}_1,-\boldsymbol{\kappa}_2)+4\pi A_i^2 f_{i;1}(\boldsymbol{\kappa}_1,-\boldsymbol{\kappa}_2)=4\pi A_i^2 f(\boldsymbol{\kappa}_1,-\boldsymbol{\kappa}_2), \tag{3.9}$$

where $I(\boldsymbol{\kappa}_1,-\boldsymbol{\kappa}_2)$ is defined as before, Eq. (3.3).

Born Approximations

The simplest admissible trial functions are $\psi_i=\exp(i\boldsymbol{\kappa}_i\cdot\mathbf{r})$ which, by (3.7), directly yield the first Born approximation,

$$-\int\exp(i\boldsymbol{\kappa}_2\cdot\mathbf{r})V(\mathbf{r})\exp(i\boldsymbol{\kappa}_1\cdot\mathbf{r}) = 4\pi f(\boldsymbol{\kappa}_1,-\boldsymbol{\kappa}_2). \tag{3.10}$$

The second Born approximation is obtained by using either

$$\psi_1=\exp(i\boldsymbol{\kappa}_1\cdot\mathbf{r});\qquad \psi_2=\exp(i\boldsymbol{\kappa}_2\cdot\mathbf{r}) - \int(\exp(i\kappa|\mathbf{r}-\mathbf{r}'|)/4\pi|\mathbf{r}-\mathbf{r}'|) \times V(\mathbf{r}')\exp(i\boldsymbol{\kappa}_2\cdot\mathbf{r}')d\mathbf{r}', \tag{3.11}$$

or

$$\psi_1=\exp(i\boldsymbol{\kappa}_1\cdot\mathbf{r}) - \int(\exp(i\kappa|\mathbf{r}-\mathbf{r}'|))/(4\pi|\mathbf{r}-\mathbf{r}'|) \times V(\mathbf{r}')\exp(i\boldsymbol{\kappa}_1\cdot\mathbf{r}')d\mathbf{r}'; \tag{3.11'}$$

$\psi_2=\exp(i\boldsymbol{\kappa}_2\cdot\mathbf{r})$.[13]

[12] P. A. M. Dirac, *The Principles of Quantum Mechanics* (Clarendon Press, Oxford, 1947), third edition, p. 191.

[13] The symmetry with respect to the functional forms of ψ_1 and ψ_2 is a general property of this method.

Higher Born approximations are obtained in a similar way.

Schwinger's Approximation

The correct ψ_1 satisfies the integral equation

$$\psi_1(\mathbf{r}) = \exp(i\boldsymbol{\kappa}_1\cdot\mathbf{r}) - \int (\exp(i\kappa|\mathbf{r}-\mathbf{r}'|)/4\pi|\mathbf{r}-\mathbf{r}'|) \times V(\mathbf{r}')\psi_1(\mathbf{r}')d\mathbf{r}'. \quad (3.12)$$

Using the well-known equation

$$f(\boldsymbol{\kappa}_1, -\boldsymbol{\kappa}_2) = -1/4\pi \int \exp(i\boldsymbol{\kappa}_2\cdot\mathbf{r}') \times V(\mathbf{r}')\psi_1(\mathbf{r}')d\mathbf{r}', \quad (3.13)$$

we can rewrite (3.12) in the homogeneous form

$$\psi_1(\mathbf{r}) = -\int G(\mathbf{r},\mathbf{r}')\,V(\mathbf{r}')\psi_1(\mathbf{r}')d\mathbf{r}, \quad (3.14)$$

where

$$G(\mathbf{r},\mathbf{r}') = 1/(4\pi f(\boldsymbol{\kappa}_1, -\boldsymbol{\kappa}_2)) \times\exp(i\boldsymbol{\kappa}_1\cdot\mathbf{r})\cdot\exp(i\boldsymbol{\kappa}_2\cdot\mathbf{r}') +\exp(i\kappa|\mathbf{r}-\mathbf{r}'|)/(4\pi|\mathbf{r}-\mathbf{r}'|). \quad (3.15)$$

Equation (3.14) has the property that regardless of what function is used for ψ_1 in the right-hand side, the left-hand side, in virtue of (3.15), is a wave function whose scattering amplitude from $\boldsymbol{\kappa}_1$ to $-\boldsymbol{\kappa}_2$ is $f(\boldsymbol{\kappa}_1, -\boldsymbol{\kappa}_2)$.

In (3.8) we now use some trial function ψ_2 and a function ψ_1 of the form

$$\psi_1 = -\int G(\mathbf{r},\mathbf{r}')\,V(\mathbf{r}')\varphi_1(\mathbf{r}')d\mathbf{r}'. \quad (3.16)$$

Since now $f_{1;1}(\boldsymbol{\kappa}_1, -\boldsymbol{\kappa}_2) = f_1(\boldsymbol{\kappa}_1, -\boldsymbol{\kappa}_2)$, (3.9) becomes simply $I(\boldsymbol{\kappa}_1, -\boldsymbol{\kappa}_2) = 0$, which when written out in full is

$$0 = \int \psi_2(\mathbf{r})\,V(\mathbf{r})\varphi_1(\mathbf{r})d\mathbf{r} + \int\int \psi_2(\mathbf{r})\,V(\mathbf{r}) \times(\exp(i\kappa|\mathbf{r}-\mathbf{r}'|))/(4\pi|\mathbf{r}-\mathbf{r}'|) \times V(\mathbf{r}')\varphi_1(\mathbf{r}')d\mathbf{r}d\mathbf{r}' + \frac{1}{4\pi f(\boldsymbol{\kappa}_1, -\boldsymbol{\kappa}_2)} \times \int \psi_2(\mathbf{r})\,V(\mathbf{r})\exp(i\boldsymbol{\kappa}_1\cdot\mathbf{r})d\mathbf{r} \times \int \varphi_1(\mathbf{r})\,V(\mathbf{r})\exp(i\boldsymbol{\kappa}_2\cdot\mathbf{r})d\mathbf{r}. \quad (3.17)$$

This is Schwinger's variational principle for the determination of $f(\boldsymbol{\kappa}_1, -\boldsymbol{\kappa}_2)$.

Linear Trial Functions

For simplicity, we use the same functional form for ψ_1 and ψ_2 and write

$$\psi_i = c_1\exp(i\boldsymbol{\kappa}_i\cdot\mathbf{r}) + \sum_{l=2}^{n} c_l u_{i;l}, \quad i=1,2, \quad (3.18)$$

where $u_{1;l}$ and $u_{2;l}$ differ only by a rotation of the coordinates and have the asymptotic form

$$u_{i;l} \to f_l(\boldsymbol{\kappa}_i, \boldsymbol{\kappa})(\exp(i\kappa r))/(r). \quad (3.19)$$

Then

$$f_i^{(1)}(\boldsymbol{\kappa}_1, -\boldsymbol{\kappa}_2) = 1/c_1 \sum_{l=2}^{n} c_l f_l(\boldsymbol{\kappa}_1, -\boldsymbol{\kappa}_2), \quad (3.20)$$

so that (3.8) gives

$$I(\boldsymbol{\kappa}_1, -\boldsymbol{\kappa}_2) + 4\pi c_1 \sum_{l=2}^{n} c_l f_l(\boldsymbol{\kappa}_1, -\boldsymbol{\kappa}_2) = 4\pi c_1^2 f(\boldsymbol{\kappa}_1, -\boldsymbol{\kappa}_2). \quad (3.21)$$

As in the one-dimensional case, $f(\boldsymbol{\kappa}_1, -\boldsymbol{\kappa}_2)$ is uniquely determined by the vanishing of the collision determinant corresponding to (3.21).

IV. COMPOSITE COLLISIONS: THEORY[14]

We consider processes of the following kind: A number of nucleons, divided into alternative pairs, collide within a region of interaction and then re-emerge into the asymptotic region, grouped again into pairs.[15]

Let φ_i be the normalized product of the internal wave functions of the nuclei constituting the pair i, and let F_i be the wave function of relative motion when they are apart. Then the function

$$\Phi_i = \varphi_i F_i, \quad (4.1)$$

will be called a mode of collision. On a hypersurface, S, separating the region of interaction from the external region, the wave function, Ψ, of the entire system has the form

$$\Psi = \sum_i \Phi_i. \quad (4.2)$$

[14] Many of the mathematical operations of this section are similar to those employed and explained by E. P. Wigner (see reference 5).

[15] It is assumed that disintegrations into three or more particles cannot occur and that at least one constituent of each pair is electrically neutral.

Let us note that, even barring accidental degeneracies, the proper functions of the Hamiltonian, H, are highly degenerate for two reasons:

(a) The spatial orientation of Ψ is arbitrary.
(b) The amplitudes of the incoming waves of the different modes are arbitrary.

A degeneracy of the type (a) was made use of in Section III to deduce a variational principle for the scattering amplitude $f(\kappa_1, \kappa_2)$ from one asymptotic state into another. In precisely the same way we shall in this section develop a variational principle for the scattering amplitude, into the mode Φ_j of nucleons colliding in the mode Φ_i. To avoid complications we remove the degeneracy (a) by considering only such functions Ψ which belong to the same proper values of the total angular momentum, J, and its z component, J_z. With this restriction the modes satisfy the orthogonality relations

$$\int_S \Phi_i \Phi_j^* dS = 0, \quad i \neq j. \tag{4.3}$$

For if the modes Φ_i and Φ_j describe different groupings of nucleons, they exist on different portions of S and hence (4.3) is satisfied; while if they describe the same groupings, the internal wave functions of the nuclei must be orthogonal so that (4.3) follows in this case also.

The Elements of the Scattering Matrix

Let $\Psi^{(1)}$ and $\Psi^{(2)}$ be two wave functions of the relative coordinates of the nucleons, belonging to the same proper values of H, J, and J_z but differing in the amplitudes of their modes. We write their asymptotic form on the surface S as

$$\begin{aligned}\Psi^{(\mu)} &= \sum_i \Phi_i^{(\mu)} \\ &= \sum_i \varphi_i (S_i/c_i)(\alpha_i^{(\mu)} \exp(-i\kappa_i r_i)/r_i \\ &\qquad - \beta_i^{(\mu)} \exp(i\kappa_i r_i)/r_i), \end{aligned} \tag{4.4}$$

where we have decomposed the function of relative motion into its angular and radial parts. r_i is the separation of the centers of gravity of the nuclei of the mode Φ_i; κ_i is the wave number and S_i the normalized angular wave function of relative motion; c_i is a constant chosen so that $|\alpha_i^{(\mu)}|^2$ represents the probability flux resulting from the mode Φ_i into the interior of S. It has the value $c_i = (2E_i/M_i)^{\frac{1}{2}} = (\hbar\kappa_i/M_i)^{\frac{1}{2}}$, where E_i is the energy of relative motion and M_i the reduced mass of the two nuclei. The sum in (4.4) is taken over all possible pairs of nuclei.

Before developing variational principles for the elements of the scattering matrix, let us note that in the case of a continuum of degenerate states the symbol δ for the first variation must be carefully defined. Thus, let Ψ_t be a trial function of the form (4.4), but with possibly incorrect α_i, β_i, and φ_i; then $\delta\Psi = \Psi_t - \Psi$, where Ψ is *some* neighboring correct function. For example, we may choose Ψ to agree with Ψ_t in the values of

(a) the amplitudes, α_i, of the incoming waves;
(b) the amplitudes, β_i, of the outgoing waves.

Consider now the integral

$$I_{12} = \int_V \Psi^{(1)*}(H-E)\Psi^{(2)} d\tau, \tag{4.5}$$

where V is the region enclosed by S, and H and E are the total Hamiltonian and energy, after the motion of the center of gravity has been separated out. We now define $\delta\Psi^{(1)}$ according to (b) and $\delta\Psi^{(2)}$ according to (a), so that $\beta_{i,t}^{(1)} = \beta_i^{(1)}$ and $\alpha_{i,t}^{(2)} = \alpha_i^{(2)}$. δI_{12} is the corresponding variation of I_{12}. It can be evaluated in terms of the α_i and β_i by transforming the volume integral arising from (4.5) to an integral over the hypersurface S by Green's theorem (cp. (2.12)) and by making use of the orthogonality relations (4.3). (For details see reference 5.) In this way one obtains

$$\delta I_{12} = -i\hbar \sum \beta_i^{(1)*} \cdot \delta\beta_i^{(2)}. \tag{4.6}$$

It should be noted that, to the first order, errors of the internal wave functions of the colliding nuclei do not appear. For the correct $\Psi^{(2)}$, $I_{12} = 0$, and hence the equation

$$I_{12} + i\hbar \sum_i \beta_i^{(1)*} \cdot \beta_{i,t}^{(2)} = i\hbar \sum_i \beta_i^{(1)*} \cdot \beta_i^{(2)}, \tag{4.7}$$

is correct to the first order.

We now introduce the scattering matrix, S_{ij}, belonging to the energy and total angular momentum under consideration, which is defined by the equations

$$\beta_i^{(\mu)} = \sum_j S_{ij} \alpha_j^{(\mu)}, \tag{4.8}$$

and embodies all observable scattering properties. Then (4.7) may be written as

$$I_{12}+i\hbar\sum_i \beta_i^{(1)*}\beta_{i,i}^{(2)}=i\hbar\sum_{i,j}\beta_i^{(1)*}S_{ij}\alpha_j^{(2)}, \quad (4.9)$$

where all quantities, except the elements S_{ij}, are determined by the trial functions. This is a homogeneous variational principle for the matrix elements S_{ij}, allowing directly the application of the method of linear trial functions. For example, to find the element S_{56} one would choose trial functions with $\beta_i^{(1)}=c^{(1)}\delta_{i5}$ and $\alpha_j^{(2)}=c^{(2)}\delta_{i6}$ in which case the right-hand side of (4.9) reduces to $i\hbar c^{(1)*}c^{(2)}S_{56}$; the stationary property of S_{56} relative to variations of the undetermined coefficients uniquely determines its value with an error of the second order in $\delta\Psi^{(\mu)}$. The wave functions can then be found in the usual way correct to the first order.

The Proper Phases of the Scattering Matrix

If the system of nucleons can group itself into n modes, the matrix S_{ij} has rank n, and n proper values, σ_m, satisfying the equations

$$\beta_i^{(\mu_m)}=\sum_i S_{ij}\alpha_i^{(\mu_m)}=\sigma_m\alpha_i^{(\mu_m)}, \qquad m=1, 2, \cdots n; \quad (4.10)$$

the $\alpha_i^{(\mu_m)}$ and $\beta_i^{(\mu_m)}$ are the amplitudes of the proper wave functions. Because of the unitary property of the matrix S_{ij}, the σ_m have unit magnitude and hence can be written as $\sigma_m=\exp(2i\eta_m)$, where the η_m are referred to as proper phases of S_{ij}. The corresponding wave functions have, asymptotically, the form of standing waves.

Schwinger[9] has suggested the use of proper phases in collision problems, and has shown that the total cross section in neutron-proton scattering with tensor forces is expressible in terms of these phases.

To find a variational principle for the η_m, consider the expression

$$I=\int_V \Psi^*(H-E)\Psi d\tau, \quad (4.11)$$

where Ψ is a proper function of S_{ij} (corresponding to one of the σ_m), with the asymptotic form

$$\Psi\rightarrow\sum \varphi_i S_i(A_i j_{l_i}+B_i n_{l_i}); \quad (4.12)$$

the j_{l_i} and n_{l_i} are the spherical Bessel and Neumann functions of the argument $\kappa_i r_i$ and of the order l_i, where l_i is the relative angular momentum of the nuclei in the mode i.

We assume now that our trial functions have the correct asymptotic form, (4.12), although possibly the internal functions φ_i and the coefficients A_i and B_i may have first-order errors. Thus, asymptotically,

$$\delta\Psi=\sum \varphi_i S_i(\delta A_i j_{l_i}+\delta B_i n_{l_i}) +\sum \delta\varphi_i S_i(A_i j_{l_i}+B_i n_{l_i}). \quad (4.13)$$

In evaluating δI, we use the fact that

$$(H-E)\Psi=0,$$

which gives

$$\delta I=\int_V \{\Psi^* T\delta\Psi-\delta\Psi T\Psi^*\}d\tau, \quad (4.14)$$

where T is the kinetic energy operator. This may be converted to a surface integral in which the asymptotic forms (4.12) and (4.13) can be used to give, after some straightforward calculation,

$$\delta I=-\sum_i (\hbar^2)/(2M_i\kappa_i)\{A_i\delta B_i-B_i\delta A_i\} =\sum_i (\hbar^2)/(2M_i\kappa_i)\{\delta(A_iB_i) -(B_i)/(A_i)\delta(A_i^2)\}. \quad (4.15)$$

Since for a proper function all ratios B_i/A_i equal $-\tan\eta_m$, it follows that

$$\delta\{I+\sum_i (\hbar^2)/(2M_i\kappa_i) \times(A_iB_i+\tan\eta_m A_i^2)\}=0, \quad (4.16)$$

where $\tan\eta_m$ is considered fixed at its correct value. As the curly bracket vanishes for a correct Ψ, the equation

$$I+\sum_i (\hbar^2)/(2M_i\kappa_i)A_{i,i}B_{i,i} =-\tan\eta_m\sum_i (\hbar^2)/(2M_i\kappa_i)A_{i,i}^2, \quad (4.17)$$

provides a stationary expression for $\tan\eta_m$. The collision determinant, Δ, arising from the method of linear trial functions is of the nth degree in the unknown $\tan\eta_m$ corresponding to the sum of n squares multiplying it.[16] The n solutions of the

[16] Certain modes differ only by interchanges of identical particles. Hence their amplitudes must agree within a factor of ±1, determined by the Pauli principle. This al-

equation $\Delta=0$ are variational approximations to the tangents of the n proper phases, η_m. The proper wave functions are then determined as usual.

To determine the cross sections of some given physical process (e.g., only certain modes incoming) one must, in general, take suitable linear combinations of the proper functions of S_{ij}, in each of which every mode is both incoming and outgoing with a certain amplitude. However, since the proper functions involve first-order errors even asymptotically (the phase shifts are determined to the second order, but the relative amplitudes of the modes only to the first order) the cross sections so calculated will also have first-order errors. Exceptions from this rule are neutron-deuteron and proton-deuteron scattering, without tensor forces (Section V), where the relative amplitudes are known exactly from symmetry considerations, so that the method of proper phases gives the physical scattering cross section correct to the second order.

V. COMPOSITE COLLISIONS: NUMERICAL APPLICATIONS

The theory developed in the preceding section has been applied to two simple systems: The neutron-proton system with the inclusion of tensor forces and the neutron-deuteron system, at low energies, assuming central forces. The first calculation is simple and could be checked against a numerical integration by Schwinger. The second calculation demands the use of a great number of trial functions, because of the three-dimensional character of the wave function. Only preliminary results have been obtained in this case.

TABLE II. $^3S_1+^3D_1$ scattering with tensor forces.

Trial functions	Uncoupled $\tan\eta_S$	Uncoupled $\tan\eta_D$	Coupled $\tan\eta_1$	Coupled $\tan\eta_2$
$u=cr+cr^3$, $w=dr^3$	6.9850	−0.3199	+6.986	−0.0003
$u=cr+cr^3$, $w=dr^3+dr^4$	6.9850	−0.3070	−1.525	−0.0002
$u=cr+cr^2+cr^3$, $w=dr^3+dr^4$	9.1398	−0.3070	−1.425	−0.0002
Correct functions	9.2314	−0.3069	−1.435[9]	0.0000[9]

lows one to reduce the number of squared unknowns multiplying $\tan\eta_m$ in (4.17) and hence the degree of the collision determinant.

Neutron-Proton Scattering with Tensor Forces

At low energies the scattering is mainly due to the $^3S_1+^3D_1$ part of the wave function. Rarita and Schwinger[17] have shown that for this partial wave the Schroedinger equation leads to two coupled equations,

$$\begin{aligned}((d^2)/(dr^2)+\kappa^2)u+\lambda(fu+gw)=0,\\ ((d^2)/(dr^2)-6/r^2+\kappa^2)w+\lambda(gu+hw)=0,\end{aligned}\tag{5.1}$$

where $u(r)$ and $w(r)$ are the radial functions of the S and D wave, respectively. Following reference 17 we set

$$\begin{aligned}&\lambda=2.62828,\\ &f(r)=-1, \quad r\leqslant 1\\ &\quad\ =0, \quad\ r>1,\\ &g(r)=2.19203f(r); \quad h(r)=4.10000f(r).\end{aligned}\tag{5.2}$$

It is simpler to base our variational procedure directly on Eqs. (5.1) rather than go back to the three-dimensional Schroedinger equation. Thus we define

$$I=\int_0^\infty \{u[(d^2/dr^2+\kappa^2)u+\lambda(fu+gw)]$$
$$+w[(d^2/dr^2+\kappa^2-b/r^2)w+\lambda(gu+hw)]\}dr. \tag{5.3}$$

If we use trial functions with the asymptotic form

$$\begin{aligned}u&=r[A_{S,t}j_0(\kappa r)+B_{S,t}n_0(\kappa r)],\\ w&=r[A_{D,t}j_2(\kappa r)+B_{D,t}n_2(\kappa r)],\end{aligned}\tag{5.4}$$

we find the following variational principle for $\tan\eta_m$:

$$I-1/\kappa(A_{S,t}B_{S,t}+A_{D,t}B_{D,t})$$
$$=1/\kappa(A_{S,t}^2+A_{D,t}^2)\tan\eta_m. \tag{5.5}$$

We have used the trial functions

$$\left.\begin{aligned}u_p&=\sum_1^p c_k r^k, \quad p=1,2,3\\ w_q&=\sum_1^q d_k r^{k+2}, \quad q=1,2\end{aligned}\right\} r\leqslant 1, \tag{5.6}$$

and the expressions (5.4) for $r>1$. $A_{S,t}$, $B_{S,t}$, $A_{D,t}$, $B_{D,t}$ were determined from the conditions that at $r=1$, the functions (5.6) pass smoothly into the free particle wave functions (5.4).

[17] W. Rarita and J. Schwinger, Phys. Rev. **59**, 436 (1941).

As checks on our calculation we have at each stage computed by the variational method the S and D phase shifts when tensor forces are absent and compared the results with the exact values which are easily obtained for the uncoupled states. The results of our calculations are collected in Table II.

It is seen that the last pair of trial functions gives good agreement with Schwinger's numerical integration, given in the last row.

Neutron-Deuteron Scattering

We have made an exploratory calculation of S scattering in the limit of vanishing neutron energy. For the interaction between the nucleons i and j we have assumed a Wigner potential

$$V_{ij} = -V_0 \exp(-(r_{ij})^2/b^2), \qquad (5.7)$$

where $V_0 = 72.00$ mc^2, r_{ij} is the distance between the nucleons, and $b = 2.24\times10^{-13}$ cm. These constants give the correct deuteron binding energy.

Let us now introduce the vectors $\boldsymbol{\rho}_1$ and $\mathbf{r}_1$ from the proton, 3, to the neutron, 2, and from the center of mass of 2 and 3 to the neutron, 1, respectively. (See Fig. 1.) Further, if P_{12} denotes interchange of the neutrons 1 and 2 we define $\boldsymbol{\rho}_2 = P_{12}\boldsymbol{\rho}_1$ and $\mathbf{r}_2 = P_{12}\mathbf{r}_1$.

As trial function we have used

$$\Psi_t = [\varphi_t(\rho_1)\chi_1]F_t(r_1) - [\varphi_t(\rho_2)\chi_2]F_t(r_2), \qquad (5.8)$$

where

$$\begin{aligned}
&\varphi_t(\rho) = (0.0904468)\exp(-(0.0637755)\rho^2);\\
&F_t(r) = c_0 + c_2 r^2 + c_4 r^4, \quad r < 8.4\times10^{-13}\text{ cm};\\
&\chi_1 = \chi_2 = \alpha(1)\alpha(2)\alpha(3)\\
&\qquad\qquad \text{for quartet scattering;} \qquad (5.9)\\
&\chi_1 = P_{12}\chi_2 = 6^{-\frac{1}{2}}[\alpha(1)\alpha(2)\beta(3)\\
&\qquad +\alpha(1)\beta(2)\alpha(3) - 2\beta(1)\alpha(2)\alpha(3)]\\
&\qquad\qquad \text{for doublet scattering.}
\end{aligned}$$

The function (5.8) has group structure, for simplicity, but our methods are not restricted to this type of trial function (see Section VI). Our polynomial expression for F_t has the wrong asymptotic form. Hence at some distance $r = a$ it was assumed to pass smoothly into the correct asymptotic form $C + D/r$. We found that the smallest a including the region of interaction was approximately 8.4×10^{-13} cm.

In order to eliminate meaningless contributions to I which come from the error of the trial function for the deuteron wave function (see (5.9)), we have replaced E in the expression (4.5) for I by the expectation value of the deuteron Hamiltonian in the deuteron *trial* function. Because of the stationary nature of the deuteron binding energy, the change is of the second order and hence theoretically legitimate.

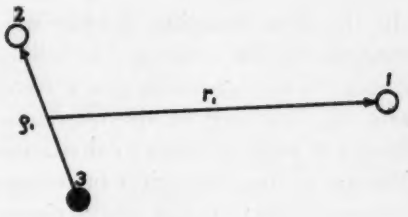

FIG. 1.

We have calculated by the formula (4.17) the quantities $X = \lim_{\kappa\to0} \tan\eta/\kappa$, where κ is the wave number and η the phase shift of the incident neutron, for quartet and doublet scattering. If we denote these by X_q and X_d, respectively, the total cross section in the limit of zero collision energy is

$$\sigma = 4\pi(\tfrac{2}{3}X_q^2 + \tfrac{1}{3}X_d^2). \qquad (5.10)$$

The values obtained were $X_q = 5.12\times10^{-13}$ cm and $X_d = 4.20\times10^{-13}$ cm. In the case of X_d it appears that inclusion of more terms in F_t may appreciably alter the result. The cross section corresponding to our calculated values of X_q and X_d is 2.9 barns. This compares reasonably well with the recently published experimental value of 3.3 ± 0.2 barns.[18]

No great significance is claimed for the result of this calculation which was carried out primarily to provide a rough test of our method. It should be extended by using more elaborate trial functions as well as different types of interaction.

VI. DISCUSSION

The methods which we have described bear a strong analogy to the Rayleigh-Ritz method for the determination of the binding energies of bound nuclei. The chief new features, in collision problems, are the following.

(a) The trial functions must, asymptotically, become sums of products, as do the actual wave functions (see (4.4) or (4.8)).

[18] Rainwater, Havens, Jr., Dunning, and Wu, Phys. Rev. 73, 733 (1948).

(b) In the determination of elements of the scattering matrix the integral I is bilinear (see, for instance, (4.5)), involving two different trial functions, as compared to the quadratic forms encountered in binding energy calculations. This is a reflection of the degeneracy of collision functions, corresponding to the arbitrariness of the amplitudes of the incident waves.

(c) The scattering properties are determined as solution of a determinantal equation, whose degree in the unknown is determined by the problem itself and not by the number of trial functions, as in bound state problems. For elements of the scattering matrix this degree is 1; for the tangents of the proper phase shifts it equals the number of physically different modes into which the system can split.

In numerical calculations one requires matrix elements of the Hamiltonian and total energy just as in binding energy problems. Thus the labor involved is approximately the same except for the somewhat more complicated trial functions in collision calculations. Here, to assure convergence to the correct answer, one must use trial functions of the form

$$\Psi_t=\sum_i \varphi_{i;t}(a_i f_i+b_i g_i)S_i/c_i+\sum_n c_n\psi_n, \quad (6.1)$$

where $f_i\rightarrow\sin\kappa_i r_i/r_i$, $g_i\rightarrow\cos\kappa_i r_i/r_i$, the $\varphi_{i;t}$ are trial functions for the internal wave functions of the colliding nuclei and the ψ_n are a complete set of functions vanishing rapidly at infinity. The first sum is required to describe the asymptotic behavior, the second to describe the region of interaction. In binding energy calculations only the second sum is required.

On the other hand, the necessity of solving high order determinantal equations does not arise in reasonably simple collision problems, which is a simplification over binding energy calculations.

In view of the great theoretical interest attaching to the scattering of light nuclei, more extensive calculations along the indicated lines, perhaps with the aid of electronic computing machines, would appear desirable.

ACKNOWLEDGMENTS

The writer wishes to express his sincere thanks to Professor J. S. Schwinger for suggesting collisions of light nuclei as a research topic and for giving invaluable counsel at all stages of the investigation. This work was carried out while the writer was recipient of a Parker Fellowship at Harvard University.

On the Virtual Excited State of the Be^9 Nucleus*

CONRAD LONGMIRE**
University of Rochester, Rochester, New York
(Received August 11, 1948)

An attempt has been made, on the basis of a simple model, to understand the energy and width of the virtual level of the Be^9 nucleus, which was found by Davis and Hafner by inelastic scattering of protons from Be^9. The model used for the Be^9 nucleus was that of a neutron moving in a potential well provided by the remainder of the nucleus. There is no striking agreement numerically between the model and experiment, but a loose interpretation by means of the model is possible.

DAVIS and Hafner[1] have found an excited state of the Be^9 nucleus at an energy of 2.41 Mev above the ground state, or 780 kev above the energy of dissociation into Be^8 and a neutron. This virtual level was found through the inelastic scattering of protons from a thin Be^9 target, with magnetic-spectrographic analysis of the scattered protons. The experiment sets an upper limit of about 100 kev for the width of the level.

This letter concerns an attempt to understand the energy and width of the virtual level on the basis of a simple model. The model chosen was that of a neutron (the least bound neutron in the Hartree model of Be^9) moving in a potential well provided by Be^8, the remainder of the nucleus. That such a model might be used successfully in describing low energy processes involving Be^9 was first suggested by Guth,[2] who based his argument on the low binding energy (1.63 Mev) of the one neutron compared with about 8 Mev for the average binding energy per particle. Here the figure 1.63 Mev, the dissociation energy of Be^9, was determined experimentally by Collins, Waldman, and Guth[3] using both electron bombardment and photo-dissociation of Be^9, and also by Skaggs[4] by measuring the energy released in the reaction Be^9 (p, d) Be^8. The neutron-well model has been used with some success by Caldirola[5] to calculate the cross section for disintegration of Be^9 by electrons.

In the ground state, the neutron is in a P-state, since an S-state is ruled out for this particle by the exclusion principle (which must be continually fed into the Hartree model). Assuming the reasonable well-radius 5×10^{-13} cm, a well-depth of 11.96 Mev is required to make the neutron bound by 1.63 Mev. These are the constants used by Caldirola. With these constants there are no other bound states. However, the calculation neglects the spin-orbit coupling for the neutron, so that a bound $P_{\frac{1}{2}}$-state is not ruled out. (The ground state is thought to be a $P_{3/2}$-state.[6,7]

For the purposes of the present calculation, we define a virtual state in the following manner. With the normalization of the neutron wave function maintained in a unit sphere, the coefficient A_i of the Bessel function in the neutron wave function inside the well is calculated as a function of the neutron energy. If $|A_i|^2$ possesses a sharp maximum at some energy, we say there is a virtual state at this energy. That this definition of the state is correct for the inelastic scattering process can be seen by considering that the cross section is proportional to the square of a matrix element from which $|A_i|^2$ can be factored approximately. The remainder of the matrix element will hardly affect the shape of the state if the width of the peak in $|A_i|^2$ is small compared to the well-depth.

With Caldirola's values for the radius and depth of the well, there are no S- or P-states

*Part of work on Doctoral thesis.
** National Research Predoctoral Fellow; now at the Department of Physics, Columbia University, New York.
[1] K. E. Davis and E. M. Hafner, Phys. Rev. **73**, 1473 (1948).
[2] E. Guth, Phys. Rev. **55**, 411 (1939).
[3] Collins, Waldman, and Guth, Phys. Rev. **56**, 876 (1939).
[4] L. S. Skaggs, Phys. Rev. **56**, 24 (1939).
[5] P. Caldirola, Nuovo Cimento, **4**, 39, No. 12 (1947).
[6] E. Feenberg and E. Wigner, Phys. Rev. **51**, 95 (1937).
[7] M. E. Rose and H. A. Bethe, Phys. Rev. **51**, 205 (1937).

near the observed energy. The second radial S-state occurs at 8.3 Mev, and is much too broad. In fact, virtual S-states with low radial quantum numbers have widths of the order of the well-depth, or larger, and can not properly be called levels. Since the first radial P-state is just bound, the second radial P-state is much too high. However, one might argue that the observed state is the lowest $P_{\frac{1}{2}}$-state, with a potential differing from that for the ground state because of the spin-orbit coupling. But even when the well-depth is decreased to bring the lowest P-state to the observed energy, the state is much too broad. The evidence here against a $P_{\frac{1}{2}}$-state is not conclusive, however, for the model may be at fault. Perhaps stronger evidence is the large separation from the ground state, compared to the presumably similar doublets[8,9] of He^5 and Li^7. It is possible that the $P_{\frac{1}{2}}$-state is so close to the ground state that it was obscured by the elastic scattering in the work of Davis and Hafner.

Again with Caldirola's constants, the lowest D-state is at 3.7 Mev and is much too broad. However, there is not much reason to believe that the effective potential provided for the neutron by Be^8 remains the same for different angular momenta. The D-state is brought down to the observed energy when the well-depth is increased to 17.6 Mev. The width of the level is then about 100 Kev, and this narrowness is due to the angular momentum barrier. The width would be less for a smaller well-radius and a correspondingly greater well-depth; however, the constants required to push the width much below 100 kev seem unreasonable. Thus, if the actual value for the width turns out to be much smaller (100 kev is the width due to the experimental lack of resolution), the neutron-well model would have to be rejected.

The author also calculated the angular distribution of the inelastically scattered protons from the virtual level of Be^9, using the method of distorted waves, for 7-Mev incident protons. Although the crudeness of the model would not permit one to believe the fine details of such a calculation, it was felt that the general predictions, if any, might provide a test for the model. One such prediction is that the sum of forward plus backward scattering should predominate over scattering at right angles, provided the force between the incident proton and the neutron outside Be^8 in the Be^9 nucleus is of the ordinary (non-exchange) type. This is a consequence of the facts: (a) the incident protons have no angular momentum about their direction of motion; (b) protons with angular momentum up to $4\hbar$ or $5\hbar$ are scattered; (c) most of the scattering occurs with a change in the proton angular momentum by a vector of length zero or $1\hbar$ (other matrix elements are small). Therefore, the protons after scattering have mostly small components of angular momentum about the incident direction. The spatial distribution of such states is predominantly in the forward and backward directions, and is symmetric. However, the result of interference between the states is that only the average of forward and backward scattering predominates over that at right angles. The statements made here were borne out by the calculation; the average predominance of forward and backward compared to 90° scattering turned out to be about 3:1.

If the neutron-proton force is completely of the exchange type, then, by similar reasoning, the distribution of inelastically scattered protons should be approximately spherically symmetric. For an exchange force, the effective initial proton state is the actual initial state of the neutron, for which the angular momentum is uniformly distributed in direction. After scattering, the uniformity should still hold approximately. The scattering would then be in principle spherically symmetric, but there could be quite large "accidental" variations. However, calculation to check this conclusion was not carried through.

Experiments by Davis on the angular distribution are in progress. Preliminary indications[10] are that the scattering is approximately spherically symmetric. If this is borne out, it would suggest an exchange force for the neutron-proton interaction. However, this evidence is certainly not strong, for either exchange forces or the validity of the neutron-well model.

Assuming that the scattering is spherically symmetric, and using the experimental value of

[8] H. Staub and H. Tatel, Phys. Rev. **58**, 820 (1940).
[9] D. R. Inglis, Phys. Rev. **50**, 783 (1936).

[10] K. E. Davis, private communication.

the differential cross section at 37°, the total cross section for inelastic scattering from the virtual state is $(5.0\pm1.0)\times10^{-26}$ cm². The calculation, with ordinary forces, gave 4.5×10^{-26} cm², and it is not likely that the value for exchange forces would be widely different. It appears, therefore, that the neutron-well model gives approximately the correct value for the product of width times height of the state, as defined by $|A_i|^2$.

The author is very grateful to the National Research Council for financial aid, and to Professor R. Marshak for suggesting and guiding the work reported.

PHYSICAL REVIEW VOLUME 74, NUMBER 12 DECEMBER 15, 1948

Tc^{92} and Tc^{93} by Relative Cross-Section Measurements

D. N. KUNDU* AND M. L. POOL
Ohio State University, Columbus, Ohio

(Received September 3, 1948)

Under 5-Mev proton and 10-Mev deuteron bombardments on natural Mo and on electromagnetically enriched Mo isotopes, activities of 2.7-hour, 47-minute, and 4.5-minute half-lives are found to be produced from Mo^{92}. The relative cross sections for the production of these activities are 25:127:1, respectively. On comparing these figures with those for the $(p, n):(p, \gamma)$ reactions from Mo^{95}, the 47-minute activity is assigned to Tc^{92}, and the 2.7-hour and the 4.5-minute activities to Tc^{93}. Tc^{92} decays by K-capture only attended with 1.5-Mev γ-rays. For the 2.7-hour Tc^{93}, the decay is 93 percent by K-capture and 7 percent by emission of positrons of maximum energy 0.83 Mev. There are also γ-rays of energy 2.0 Mev associated with this activity.

I. INTRODUCTION

A NUMBER of technicium activities are known to which no definite mass numbers have been assigned. The situation has remained inconclusive in spite of the recent use of electromagnetically enriched isotopes of Mo as target materials. The reason is that the usual method of assigning mass numbers to artificially produced radioisotopes by production through appropriate cross reactions from neighboring elements is not immediately available for deciding the issue due to the lack of suitable stable target isotopes. Relative cross-section measurements may be expected to be of use in such cases. In a previous paper,[1] enriched Mo isotopes were used to obtain the relative cross sections for (p, n) to (p, γ) reactions of Mo^{95}. These results have been utilized to assign mass numbers to three technicium activities of half-lives 2.7 hours, 47 minutes, and 4.5 minutes.

II. REVIEW OF Tc ACTIVITIES

2.7 Hours.—A technicium activity with a provisional value of a 2-hour half-life was reported[2] as a result of deuteron bombardments of Mo. This activity was later[3] shown to be a 2.7-hour positron emitter obtained by bombarding Mo with protons. To correlate these facts with the observations by others[4] that a similar activity is produced by alpha-bombardments of columbium, the 2.7-hour period was assigned[5] to Tc^{96}. Recently, by using a deuteron beam on enriched Mo^{92}, it has been shown[6] that the 2.7-hour activity is produced from Mo^{92}. However, no definite assignment of the activity to Tc^{92} or Tc^{93} could be made. The decay is claimed to take place by emission of positrons of maximum energy 1.2 ± 0.2 Mev and a hard γ-ray of 2.4 ± 0.5 Mev.

* Research Fellow of the National Institute of Health, Bethesda, Maryland.

[1] D. N. Kundu and M. L. Pool, Phys. Rev. **74**, 1574 (1948).

[2] G. T. Seaborg and E. Segrè, Phys. Rev. **55**, 808 (1939).

[3] L. A. Delsasso, L. N. Ridenour, R. Sherr, and M. G. White, Phys. Rev. **55**, 113 (1939).

[4] L. D. P. King, W. J. Henderson, and J. R. Risser, Phys. Rev. **55**, 1118 (1939).

[5] G. T. Seaborg, Rev. Mod. Phys. **16**, 1 (1944).

[6] E. E. Motta and G. E. Boyd, Phys. Rev. **73**, 1470 (1948).

40–53 Minutes.—With proton bombardment of Mo, a 40±5-minute Tc activity was reported to presumably decay by positron emission.[3] The value of the half-life given by others was 53±3 minutes.[7] Later observers[8] confirmed the value of 53 minutes. The maximum energy of the positrons was found to be 2.45 Mev. Also observed were x-rays of Mo and Tc and five γ-rays of energies ranging from 0.380 to 2.74 Mev associated with low energy electrons due to internal conversion of the γ-rays. Probable assignment was made to numbers 92 or 94. Recent workers,[9] using enriched Mo^{94} under a deuteron beam, have given the value of the half-life as 50±2 minutes. They have confirmed the energy of the positrons but have found only one γ-ray of energy 0.9±0.1 Mev. The assignment of this activity to Tc^{94} was considered as probable. The same observers[6] have also announced a 40±5-minute activity obtained with deuteron bombardment of Mo^{97} and Mo^{98}. The decay was by the emission of charged particles of 2.0±0.5 Mev. No assignment of mass number was made.

To anticipate some results of the present paper, a 47-minute Tc activity appears which also has to be placed at positions 92 or 93.

4.5 Minutes.—A 4.5-minute Tc activity was found by the above group of workers[6] when

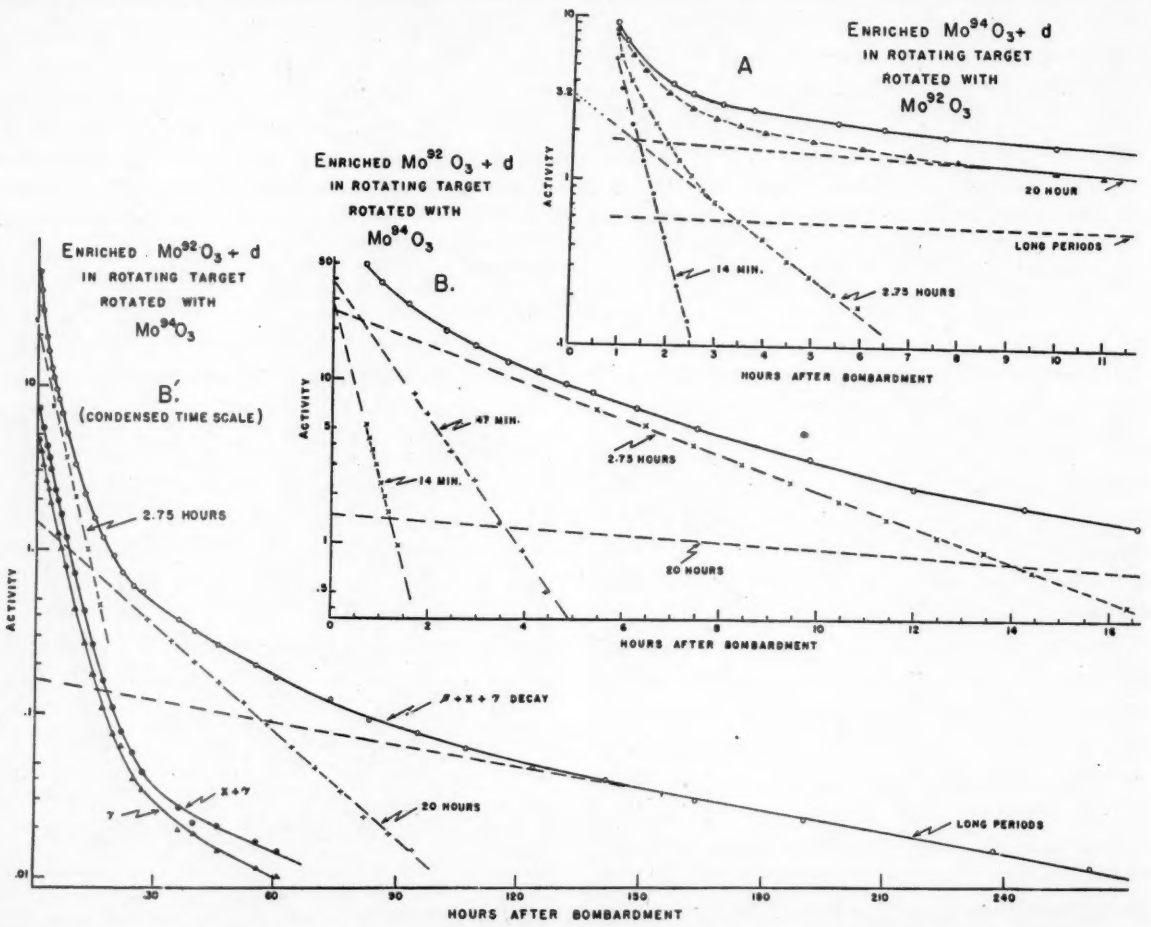

FIG. 1. Decay curves obtained by deuteron bombardment on MoO_3 enriched separately in Mo^{92} and Mo^{94}. The two enriched samples were placed on opposite sides of a rotating target and bombarded under the same beam. The 47-minute and the 2.75-hour activities are produced from Mo^{92}. The small amount of 2.75-hour activity seen in (*A*) is due to the small amount of Mo^{92} present in the enriched Mo^{94} sample. The (x+γ)- and the γ-decay curves are also shown (*B'*).

[7] D. Ewing, T. Perry, and R. McCreary, Phys. Rev. **55**, 1136 (1939).
[8] P. C. Gugelot, O. Huber, H. Medicus, P. Preiswerk, P. Scherrer and R. Steffen, Helv. Phys. Acta. **19**, 418 (1946); **20**, 240 (1947); O. Huber, P. Marmier, H. Medicus, P. Preiswerk, and R. Steffen, Phys. Rev. **73**, 1208 (1948).
[9] E. E. Motta and G. E. Boyd, Phys. Rev. **74**, 220 (1948).

enriched Mo^{92} was bombarded with deuterons. The activity decays by emitting positrons of 4.3 ± 0.5 Mev and γ-rays of 1.3 ± 0.3 Mev. The assignment to either Tc^{92} or Tc^{93} was suggested.

It is thus apparent that the question as to which of these various activities are to be ascribed to Tc^{92} and Tc^{93} is of considerable interest. It is the purpose of this paper to show how the application of reaction cross-section measurements point toward reasonable mass assignments.

III. EXPERIMENTAL

Proton of 5 Mev and deuteron of 10 Mev were used to bombard natural molybdenum and three different samples of MoO_3 electromagnetically enriched in Mo^{92}, Mo^{94}, and Mo^{98}, respectively.** The methods of measurements of the charged particles, x-rays, and γ-rays are the same as described previously.[1] In order that the decay of both the positive and the negative particles may be followed separately, the sample was placed between the pole faces of a large electromagnet and the particles of the desired sign bent circularly into a Geiger counter. The counts per minute were automatically recorded.[10] To decide whether a particular activity produced was associated with one or the other of two target isotopes, the two enriched isotopes were placed on opposite sides of a rotating target holder and bombarded simultaneously under the same beam and the relative intensities compared. Chemistry was done after bombardments to identify the elements whenever necessary.

IV. RESULTS

2.7 Hours.—A Cb+α bombardment did not produce the 2.7-hour Tc activity, showing that this activity is not due to Tc^{96} as once supposed.[5]

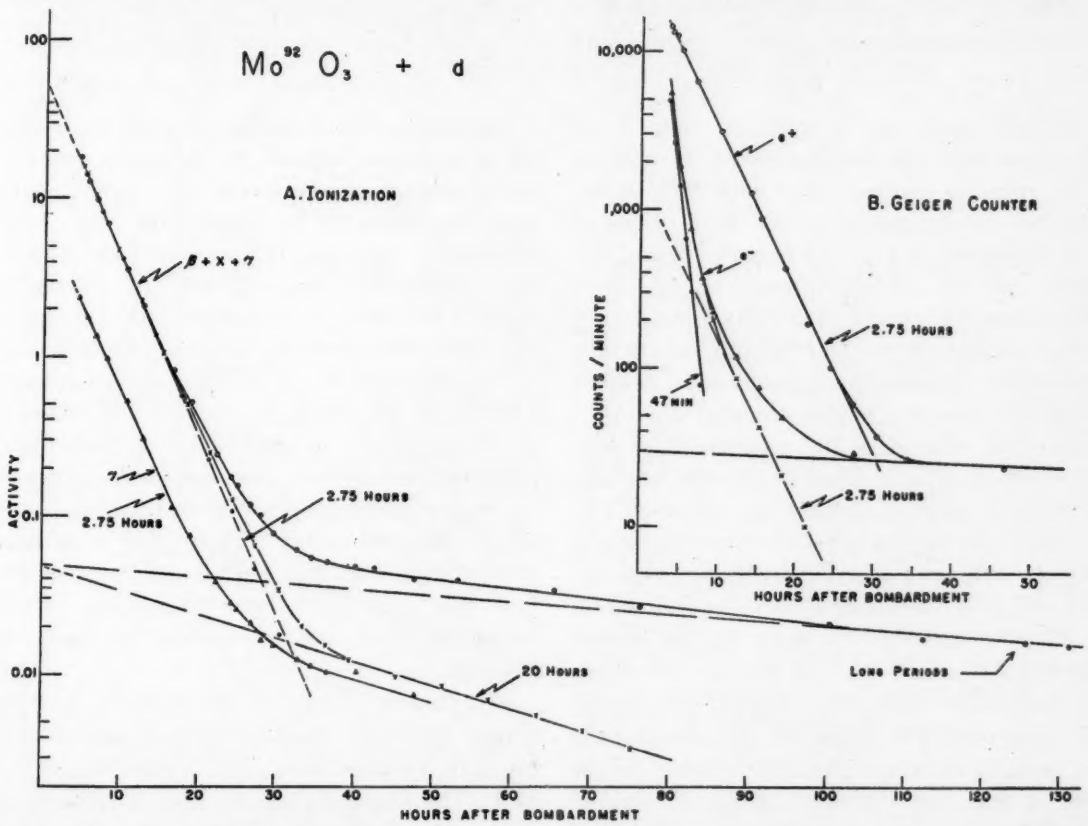

FIG. 2. Decay curves of enriched $Mo^{92}O_3$ d on electrometer showing 2.75-hour half-life and the associated γ-rays (A). The decay curves using Geiger counters on the positive and negative particles separately are shown in (B). The 47-minute activity is seen to emit negatively charged particles.

** Kindly supplied by the Y-12 Plant, Carbide and Carbon Chemicals Corporation, through the Isotope Division, United States Atomic Energy Commission, Oak Ridge, Tennessee.

[10] L. L. Woodward and D. A. McCown, Rev. Sci. Inst. in press.

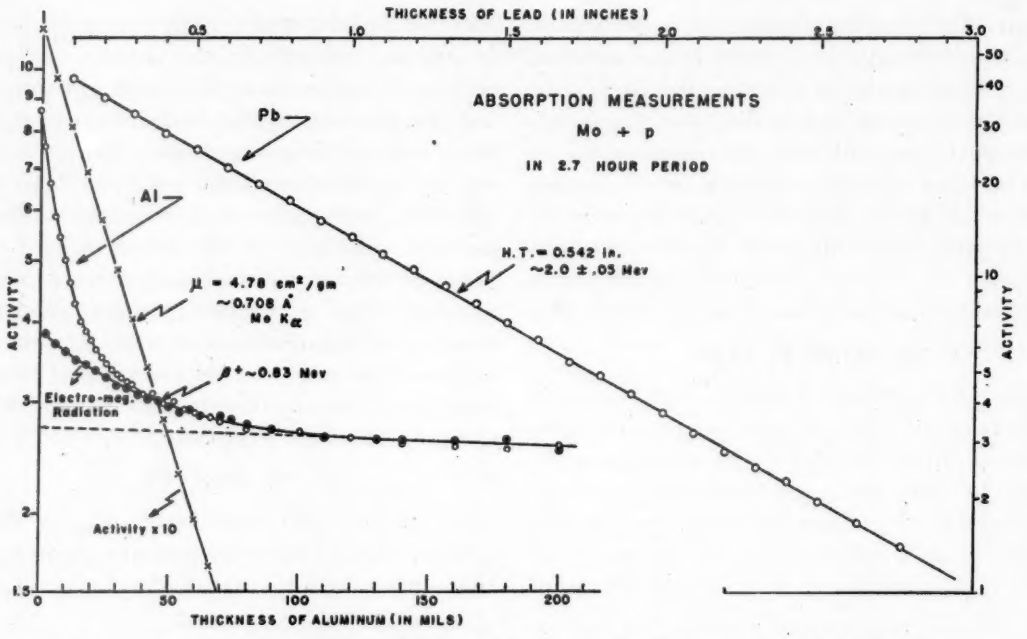

FIG. 3. Absorption curves in aluminum and head of Mo+p in the 2.7-hour period showing x-rays corresponding to MoK_α line, positrons of energy 0.83 Mev and γ-rays of 2.00 Mev.

The activity, however, is produced under both proton and deuteron bombardment on natural Mo. By rotating enriched Mo^{92} with Mo^{94} under a deuteron beam, decay curves were obtained which are shown in Fig. 1. From the figure, the intensity of the 2.7-hour period in the Mo^{92} sample is seen to be more than eight times that in the Mo^{94} sample. In the Mo^{94} sample, all the Mo isotopes with mass numbers greater than 93 were present in a larger percent than in the Mo^{92} sample. This eliminates the assignment of any mass numbers greater than 93 to this activity. The 2.7-hour, therefore, belongs to either Tc^{92} or Tc^{93}. The decay curves followed separately on the positively and negatively charged particles are shown in Fig. 2. The charged particles emitted by the 2.7-hour activity are seen to be mostly positrons. The exact amount will be calculated later. Negatively charged particles of this period originating from conversion of the gamma-rays and Compton electrons are also observed to the extent of about five percent of the number of positrons. In the same figure, from an interval of over ten half-lives, a value of 2.75 ± 0.05 hours is obtained. As shown in Fig. 3, lead absorption measurements of the gamma-ray lead to an energy of 2.00 ± 0.05 Mev.

The absorption measurements with aluminum are of particular interest. Without the use of the electromagnet, the beta-end point might erroneously be taken to be about 100 mils, corresponding to an energy of approximately 1.4 Mev. On applying the magnetic field to remove the charged particles, it is observed that the part of the absorption curve beyond about 50 mils is due to electromagnetic radiation of wave-length 0.708A which is the K_α line of Mo. The end point for the positrons, as is clearly seen from Fig. 3, superimposed on the curve for x-rays gives the maximum energy as 0.83 Mev, contrary to the observations of others.[6] This value is obtained after adding 2.68 mils to the end point as read from the curve, in order to correct for the thickness of air and window of the ionization chamber.

47 Minutes.—Separate bombardments of enriched Mo^{92} and Mo^{94} with deuterons show in Fig. 4 that a 47-minute activity is produced from Mo^{92}. The charged particles associated with the decay are all negative. The decay curve corresponding to $Mo^{94}+d$, however, does not show any 47-minute period. Also in the decay curve for the proton bombardment on Mo^{98}, there is no positron activity of 47-minute half-life. There is,

however, a very weak short period of the order of 55 minutes, which consists of negatively charged particles. The proton bombardments of Mo^{92} and Mo^{94} lead to the same observations with regard to this 47-minute period. In Fig. 5 the positron decay curve of the Tc from the $Mo^{94}+d$ bombardment also shows no 47-minute activity. The electrometer measurements substantiate this observation. In order to study more closely the connection of the 47-minute activity with Mo^{92} or Mo^{94}, we go back to Fig. 1, which shows the results obtained with the rotating target. The 47-minute period is obtained from $Mo^{92}+d$ sample and no observable amount is found in the decay curve of $Mo^{94}+d$.

Absorption measurements with aluminum foils show in Fig. 6 once again that without the use of the magnetic field, the beta-end point might wrongly be taken at about 150 mils, corresponding to 2.05 Mev. The removal of the charged particles by the magnet shows this part to be x-rays of wave-length 0.71A, corresponding to the K_α radiation of Mo. The maximum energy of the negatively charged particles is 0.54 Mev after applying corrections for air and ion-chamber window. The energy of the γ-rays is found to be 1.50 ± 0.05 Mev from the same figure. The quantitative estimation of the x- and γ-rays as compared with the number of charged particles will be made in the next section. The decay takes place by K-capture alone.

4.5 Minutes.—No detailed study of this activity was made beyond noting that in $Mo+p$ bombardments of very short duration (15 minutes), there was an activity of the order of five minutes, in addition to the 14-minute activity of Tc^{101}. The x-rays, if any, and the γ-rays were too weak to be properly analyzed.

V. RELATIVE CROSS SECTIONS AND ASSIGNMENTS

From the activity values at the end of the bombardments, the saturation intensities for the electrons, x-rays, and γ-radiations are calculated

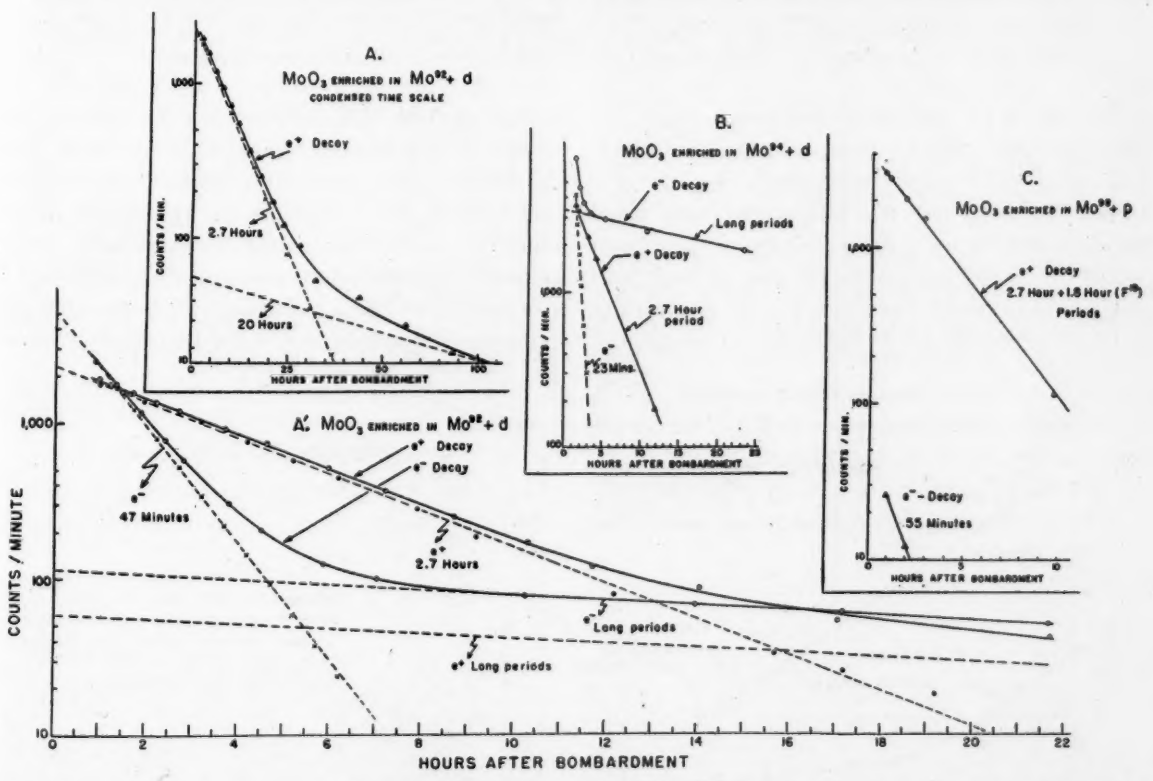

FIG. 4. Decay curves from separate bombardments of enriched Mo^{92} and Mo^{94} with deuterons and of enriched Mo^{98} with protons. No 47-minute activity is found in (*B*) $Mo^{94}+d$. The 47-minute activity is seen very clearly in (*A'*) $Mo^{92}+d$ on the curve for negative particle emission. No 40-minute positron activity is observed in (*C*) $Mo^{98}+p$. The 2.7-hour activities seen in (*B*) and (*C*) are due to small amounts of Mo^{92} present in the enriched Mo^{94} and Mo^{98} samples.

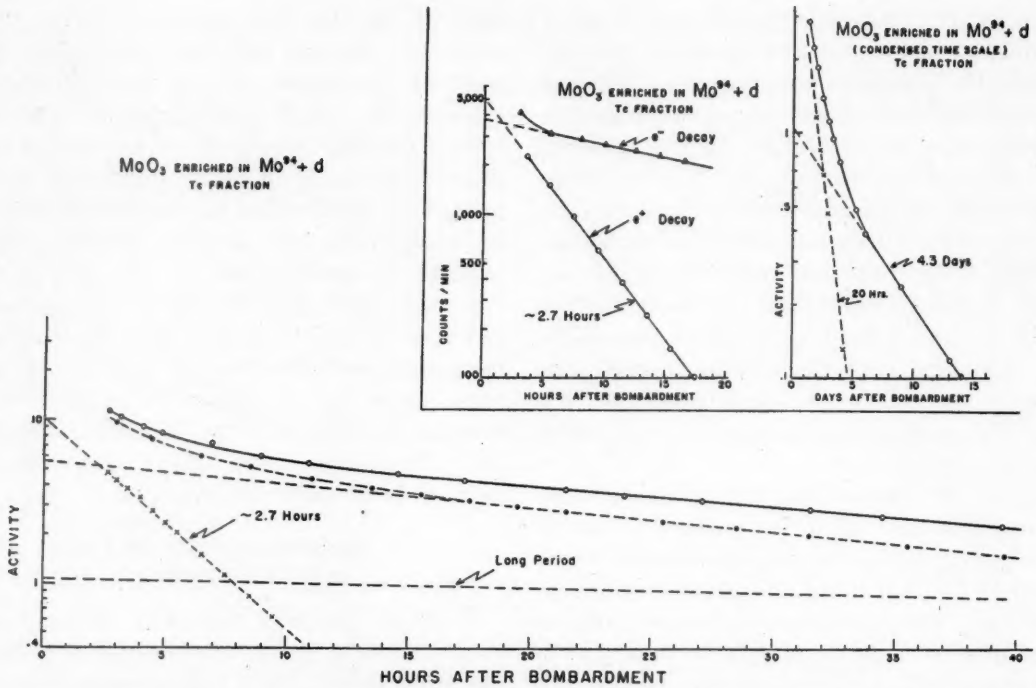

FIG. 5. Decay curves of the Tc fraction of enriched $Mo^{94}+d$. No 47-minute activity is seen either on the electrometer measurements or on the counter measurements for positive and negative particles. The 4.3-day activity is produced from Mo^{95} and Mo^{96} present in small amounts in the enriched Mo^{94} sample. The small amount of the 2.7-hour activity is similarly due to the presence of Mo^{92} in the enriched Mo^{94} sample.

to be 2.67, 0.52, and 0.605 ionization units, respectively, for the 2.7-hour activity and 3.34, 2.67, and 0.273 units, respectively, for the 47-minute activity. For the ionization chamber of the electrometer used, each electron of maximum energy of about 0.83 Mev on the average will produce 123 as much ionization as each x-quantum of 1A; the corresponding figure for an electron of energy of 0.54 Mev will be 58.5. Thus there are about 24 x-quanta per positron emitted by the 2.7-hour activity and 50 x-quanta per electron observed in the 47-minute period. In the same chamber, each x-ray quantum and each γ-ray quantum produce ionization of the same order compared to the ionization due to charged particles. Therefore, in the 2.7-hour period, there

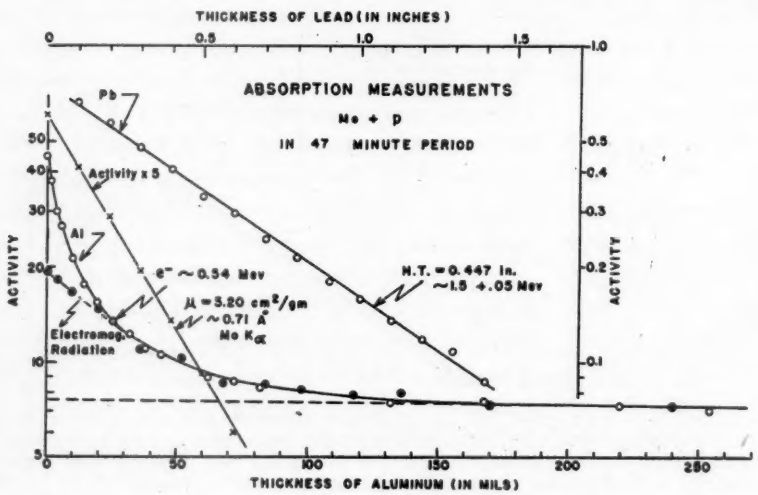

FIG. 6. Absorption curves in aluminum and lead of $Mo+p$ in the 47-minute period showing x-rays corresponding to MoK_α line, electrons of energy 0.54 Mev and γ-rays of 1.50 Mev.

are 0.9 x-quantum per γ-quantum and in the 47-minute period, 9.8 x-quanta per γ-quantum. Combining, we find that for the 2.7-hour activity, for each positron measured, there are 13.6 x-quanta and 15 γ-quanta which are being measured. For the 47-minute material, per electron measured, there are 21.4 x-quanta and 3.1 γ-quanta. These x-rays were found to be K_α line of Mo. Both these activities, therefore, decay by K-capture primarily. Each x-quantum is taken as due to one disintegration. For determining the relative cross sections, it would, thus, be enough to base the computation on the x-ray quanta alone.

The ratio of the cross sections σ_{92} (47 min.)/σ_{92} (2.7-hour) = 2.67/0.52 = 5.1. The relative cross sections for the $(p, n)/(p, \gamma)$ reaction from Mo^{95} was found to be 6.5. On this basis, the 47-minute activity is produced by (p, n) and the 2.7-hour activity by (p, γ) reactions, respectively. The 47-minute activity is thus assigned to Tc^{92} and the 2.7-hour activity to Tc^{93}.

With regard to the 4.5-minute activity, the saturation intensity for positrons was 5.49 units, whereas in the same bombardment the saturation positron intensity of the 2.7-hour activity was 5.24 units. We saw that for the 2.7-hour period there are 25 disintegrations to each positron measured. Therefore, the cross section for the production of the 4.5-minute activity is about 1/25 of that for the production of the 2.7-hour activity, and, therefore, only about 1/127 of that for the 47-minute period. On the basis of this cross section consideration, the 4.5-minute activity is assigned to Tc^{93} as an isomer to the 2.7-hour activity.

VI. DISCUSSION

The assignment and relative cross sections are summarized in Fig. 7. The similarities in the relative proton reactions from Tc^{92} and Tc^{95} are readily seen. These seem quite reasonable in view of the similarity of the decay characteristics of the 47-minute, 2.7-hour, 20-hour, and 4.3-day activities.

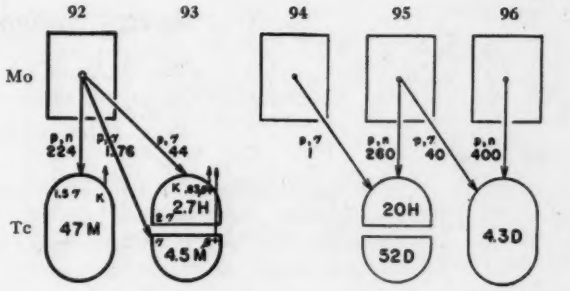

FIG. 7. Relative cross sections of proton reactions from Mo^{92} are compared with those from Mo^{94}, Mo^{95}, and Mo^{96}. Assignment of the 47-minute activity to Tc^{92} and of the 2.7-hour and 4.5-minute activities to Tc^{93} are made and the characteristic radiations are shown.

The characteristic radiations of the 47-minute activity studied in the present paper have been shown to be different from those of the 40- and 50-minute activities observed by others.[6,9] It is, however, difficult to see how the 10-Mev deuterons failed to produce the 50-minute half-life reported as being produced by 16-Mev deuterons from Mo^{94}, especially when it was shown[1] that the (d, n) and $(d, 2n)$ reactions proceed with comparable readiness.

The help received from the Development Fund and the Graduate School of the Ohio State University is gratefully acknowledged. The chemical separations were ably done by H. L. Finston and R. M. Dyer. Thanks are also due the National Institute of Health, Bethesda, Maryland, for a Research Fellowship to one of the authors, and the Ghosh Board of the Calcutta University for facilities of traveling to this country.

Energy Straggling of Protons

C. B. MADSEN AND P. VENKATESWARLU
Institute for Theoretical Physics, University of Copenhagen, Denmark
(Received August 9, 1948)

The energy straggling of protons of different energies penetrating foils of mica or beryllium of different thicknesses has been measured using the resonance radiation from aluminium and fluorine targets as energy indicators. The experimental results are in good agreement with the theory of straggling.

THE method of using the sharp resonances in the proton capture processes as energy indicator for protons, in the way previously described in an investigation of the stopping power of beryllium,[1] makes it also possible to measure the energy straggling caused by a thin foil. In fact, the resonance peaks show not only a shift, when a foil is inserted in the proton beam, but also a broadening, which is sufficiently great to justify a more quantitative comparison with the theory of energy straggling.

The energy of the protons in a homogeneous beam will, by the passage of a thin foil, be distributed over a finite range corresponding to a standard deviation Ω which, according to the theory,[2] should be approximately given by

$$\Omega^2 = (4\pi e^4/M)\cdot(Z/A)\cdot(t), \qquad (1)$$

where M is the mass and e the charge of the protons, Z the atomic number and A the mass number of the foil material, and where t is the thickness of the foil measured in weight per unit area.

In the previous investigation of the stopping power of beryllium[1] only an upper limit for the energy straggling in this substance was obtained, because it was not known, to what extent the foils, which had been prepared by evaporation, were homogeneous in thickness.

According to Eq. (1) the standard deviation should be proportional to the square root of the thickness t, and the factor of proportionality should be approximately independent of both the energy and of the foil material for not too small an energy of the protons, because the ratio of Z to A is close to the value $\frac{1}{2}$ for all elements (except hydrogen).

It is, therefore, also possible to compare the theory with experiments carried out with foils consisting of a mixture of different elements. The measurements were consequently mainly performed with foils of mica, which has the advantage that it can easily be split into very thin foils of homogeneous thicknesses, and that the homogeneity can be checked by optical means both before and after the experiments.

The technique and apparatus were the same as in the earlier work,[1] but it proved necessary to defocus the proton beam to 5 mm in diameter and to use currents less than 0.1 micro amp. in order to prevent destruction of the foils. Measurements at the lowest proton energies were carried out with the molecular beam H_2^+ of the van de Graaff generator, because the focusing was unstable at low voltages, but this should not influence the result as the molecules will split up as soon as they hit the foil.

The mica foils were prepared in thicknesses down to 0.3 mg per cm^2. They were used in the form of small disks with a diameter of 11 mm, but their thicknesses were determined before they were cut out, by measuring weight and area of pieces more than ten times bigger, which in mercury light had shown the same interference color over the whole of their area. A few foils were also silvered and investigated in an interferometer[3] by the method of Tolansky,[4] and the thicknesses were found to be constant at least within 0.1 percent, also for foils bombarded. Only two foils, which unfortunately had been heated too much by the proton current, showed 10 to 20 interference fringes at small spots, but were homogeneous over the whole area between the

[1] C. B. Madsen and P. Venkateswarlu, Phys. Rev. **74**, 648 (1948).
[2] Cf. N. Bohr, Kgl. Danske Vid. Selsk. mat.-fys. Medd. **XVIII**, 8 (1948), formula (3.4.5).
[3] We are very much indebted to cand. mag. Rahbek for carrying out this investigation.
[4] S. Tolansky, Proc. Roy. Soc. **A186**, 261 (1945) and **A191**, 182 (1947).

spots. The undisturbed area was about 90 percent of the whole area. These spots could also be seen directly as a metallic-like tint, probably caused by a decomposition of the mica, but the weight and the stopping power, as well as the straggling had the same values as for other foils of the same thickness.

The thicknesses of a few small foils, the areas of which could not be measured with sufficient accuracy, because of irregularities in the edges, were determined by comparing their stopping powers to that of a foil of known thickness.

Furthermore, the interferometer measurements did not only give information about the homogeneity of the foils, but also about their absolute thicknesses measured in angstrom units. The relative thicknesses of the different foils, determined by weighing, by the optical means and from the stopping power, agreed within the experimental accuracy.

TABLE I. The columns contain: 1. foil material, 2. foil thickness in mg per cm², 3. resonance used as indicator (figures in kev), 4. stopping power 's' of the foil, measured in kev per mg/cm², 5. standard deviation Ω_1 without foil, in kev, 6. standard deviation Ω_2 with foil, in kev, 7. straggling Ω in kev and 8. $\Omega/(t)^{\frac{1}{2}}$ in kev $(\text{mg/cm}^2)^{-\frac{1}{2}}$. The theoretical value of $\Omega/(t)^{\frac{1}{2}}$ is according to formula (1):

$$(2Z\cdot 2\pi e^4/AM)^{\frac{1}{2}}=(2Z/A)^{\frac{1}{2}}8.85 \text{ kev } (\text{mg/cm}^2)^{-\frac{1}{2}}.$$

Substance	t mg/cm²	Resonance	s kev/mg/cm²	Ω_1 kev	Ω_2 kev	Ω kev	$\Omega/(t)^{\frac{1}{2}}$ kev/(mg/cm²)$^{\frac{1}{2}}$
1	2	3	4	5	6	7	8
Be	0.222	Al-503	327	4.4	6.1	4.2	8.9
—	0.222	Al-630	283	1.45	5.1	4.9	10.4
—	0.222	Al-630	283	4.2	5.3	3.3	6.9
—	0.222	Al-986	219	1.4	5.0	4.8	10.2
—	0.222	Al-986	219	1.7	4.2	3.9	8.2
—	0.222	Al-1112	195	2.9	5.5	4.7	9.9
—	0.222	Al-1112	195	2.9	5.3	4.5	9.4
—	0.222	Al-1255	188	1.7	4.9	4.6	9.7
—	0.245	Al-986	216	1.25	4.2	4.0	8.2
—	0.609	F-339	377	4.2*	9.5*	7.2	9.2
—	0.609	Al-986	207	2.5	6.6	6.1	7.9
			experimental mean value for Be				8.99
			value for Be according to Eq. (1)				8.3
Mica	0.336	F-339	300	3.6*	5.8*	4.5	7.8
—	0.336	Al-630	218	3.4	5.6	4.4	7.6
—	0.336	Al-986	176	1.7	5.2	4.9	8.5
—	0.336	Al-986	176	1.7	5.0	4.7	8.1
—	0.441	Al-986	172	1.6	6.4	6.2	9.3
—	0.441	Al-986	172	1.6	6.1	5.9	8.8
—	0.441	Al-986	172	1.6	5.9	5.7	8.5
—	0.441	Al-986	172	1.5	6.3	6.1	9.2
—	0.66	Al-986	170	1.7	8.0	7.8	9.6
—	0.66	Al-986	170	1.7	7.6	7.4	9.2
—	0.76	Al-986	170	3.5	8.0	7.2	8.3
—	1.02	Al-986	170	1.7	8.7	8.5	8.5
—	1.02	Al-986	170	1.9	9.0	8.8	8.7
—	1.02	Al-986	170	1.9	9.4	9.2	9.1
—	1.02	Al-986	170	2.1	9.5	9.3	9.2
—	1.02	Al-986	170	2.1	9.1	8.9	8.8
—	1.23	Al-986	174	3.0	9.5	9.0	8.3
—	1.71	Al-986	166	3.8	12.5	11.9	9.1
			experimental mean value for mica				8.70
			value for mica according to Eq. (1)				8.8

* 0.42 times the half-width. Standard deviation not determined (see text).

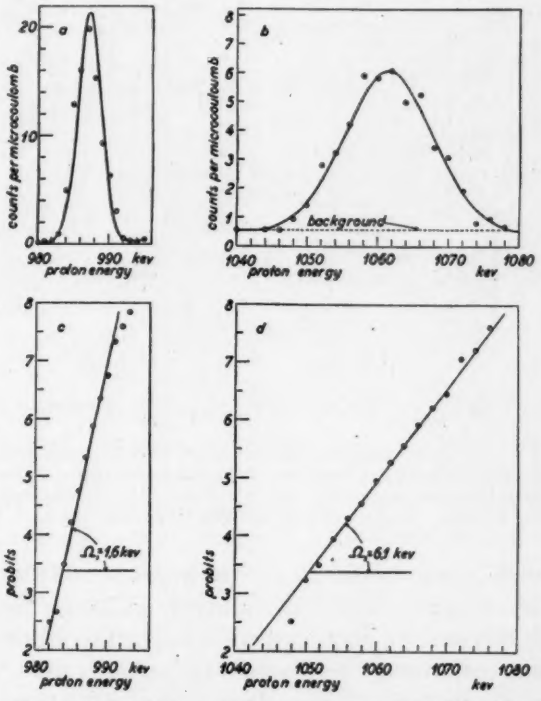

FIG. 1. The 986 kev Al resonance measured (a) without foil and (b) with a mica foil of thickness 0.441 mg per cm² inserted in the proton beam. In (c) and (d) the results from (a) and (b) are transformed into straight lines, the slopes of which give the standard deviations.

The sharp aluminum resonances, especially the 986 kev resonance, have been used as indicators in the high energy region, whereas the rather broad, but strong fluorine line at 339 kev has been used at the lowest energies, because the scattering and stopping powers of the foils are greater at low energies, and very low proton currents are therefore demanded. Targets with stopping powers ranging from 4 to 10 kev were used, depending on the foil thicknesses.

In Fig. 1 is shown an example from a measurement in the 1 Mev region. In Fig. 1a is plotted a measurement without foil and in Fig. 1b a measurement with a foil of thickness 0.441 mg per cm² inserted in the beam. In order to determine the standard deviation corresponding to the values plotted in these figures, the distribution is approached by the Gaussian, even though it should not be the case in Fig. 1a, where the

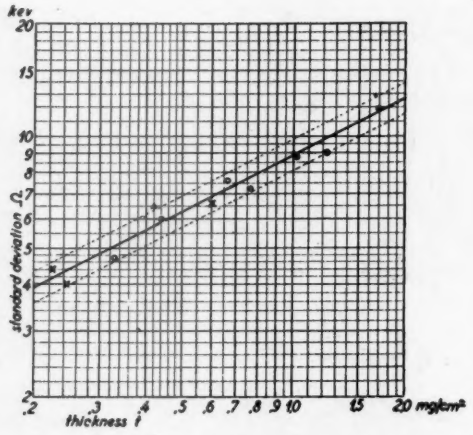

FIG. 2. The straggling Ω for beryllium foils (crosses) and mica foils (circles) as function of the thickness of the foils. The full drawn line is the theoretical Eq. 1 for substances with $2Z=A$. The dotted lines are the 10 percent lines.

width is mainly due to the thickness of the aluminum target used. The standard deviations for the two series of measurements can then be found by transforming the results into straight lines,[5] the slopes of which give the standard deviations Ω_1 and Ω_2 corresponding to the measurements without and with the foil respectively. By this method one takes into account all the points of the resonance peak except those which are only slightly above the background, and the determination of the standard deviations should, therefore, be rather unambiguous. The straight lines are drawn in Figs. 1c and 1d. The two curves on Figs. 1a and 1b are Gaussian curves with the standard deviations found in Figs. 1c and 1d respectively.

The true straggling Ω is calculated from Ω_1 and Ω_2, by the formula

$$\Omega=(\Omega_2^2-\Omega_1^2)^{\frac{1}{2}}, \qquad (2)$$

since the standard deviations add up geometrically.

In the measurements with fluorine as indicator the transformed curves deviated very much from straight lines, because of the long tails of the Breit-Wigner curve. In these cases, therefore, the straggling was found directly, by determining that Gaussian distribution, which combined with the curve obtained without foil, gave the best fit to the curve obtained with foil inserted.

The results of all the straggling measurements are given in Table I, and in Fig. 2 the mean of the values obtained for each foil is plotted in double logarithmic scale as a function of the thicknesses of the foils. The measurements with the sharp and strong line Al-986 are the most reliable.

Both from the curve and from the figures in the last column of the table it is seen that the results for beryllium and mica agree well with formula (1), whereas previous measurements by Briggs[6] of the straggling of fast α-rays in mica gave values, which were about 40 percent larger than those corresponding to the equivalence for α-rays of expression (1). Later measurements by Bennett[7] are however more in agreement with ours, giving values only about 15 percent in excess of the theoretical estimate.

The simple theoretical formula (1) is expected to represent a good approximation for fast particles in substances of comparatively small atomic number, in which case all the atomic electrons may be assumed to contribute effectively to the stopping and straggling process. This assumption should be well fulfilled in the case of beryllium for the proton energies in question, and also for mica it is approximately justified, at any rate for the experiments with proton energies of the order of 1 Mev. For smaller energies it may be necessary to take into account, that the strongest bound electrons no longer contribute to the phenomenon.[2] This circumstance might in fact explain the somewhat smaller straggling found at the lower proton energies, although too much significance cannot, of course, be given to the experimental evidence regarding this point.

The authors wish to express their gratitude to Professor Niels Bohr for the great interest taken in this work and for the hospitality extended to them at the Institute for Theoretical Physics at Copenhagen. Cordial thanks are, furthermore, due cand. mag. K. J. Brostrøm and mag. scient. Torben Huus for numerous stimulating discussions.

One of us (CBM, on leave from the University of Aarhus) is indebted to the Carlsberg Foundation and to the Danish Society for Treatment of Cancer, and the other (PV) to the Rask-Ørsted Foundation for grants enabling us to take part in the work in Copenhagen.

[5] R. A. Fisher and F. Yates, *Statistical Tables* (Oliver and Boyd Ltd., London, 1938).

[6] G. H. Briggs, Proc. Roy. Soc. **A114**, 313 (1927).

[7] W. E. Bennett, Proc. Roy. Soc. **A155**, 419 (1936).

On the Theory of the Recoil in β-Decay

O. KOFOED-HANSEN
Institute for Theoretical Physics, University of Copenhagen, Copenhagen, Denmark
(Received August 9, 1948)

On the basis of the Fermi theory of β-decay a formula for the recoil spectrum is derived, and the average values of the momentum and energy of the recoil are calculated. Some properties of the recoil spectrum are discussed in the case when the β-decay is followed by γ-ray emission. It is shown that the average recoil energy is independent of a possible angular correlation between successive β- and γ-rays. Finally the influence of a finite mass of the neutrino and the neglect of the kinetic energy of the recoil in the energy balance is discussed.

THE DESCRIPTION OF β-DECAY

A β-DECAY process where a nucleus A decays into a recoil nucleus R, an electron and a neutrino, may be described, because of the conservation laws for energy and momentum, by two independent parameters, e.g., the absolute value p_β of the momentum of the β-particle and the angle $\theta_{\beta\nu}$ between the directions of emission of the electron and the neutrino.

The probability $P(p_\beta, \theta_{\beta\nu})dp_\beta d\theta_{\beta\nu}$ of a process in which these two parameters lie within the intervals p_β, $p_\beta+dp_\beta$ and $\theta_{\beta\nu}$, $\theta_{\beta\nu}+d\theta_{\beta\nu}$, respectively, has been calculated on the basis of the Fermi theory of β-decay by D. R. Hamilton[1] for an allowed and a first forbidden transition. The expressions for forbidden transitions are rather complicated, but the main result is, as an addition to the expressions for allowed transitions, a factor which varies as the square of the recoil momentum, p_R, and such a factor can very easily be taken into account in the calculation of the recoil spectrum. In the treatment of the recoil phenomena we may thus start with the following general expression, in which we also include the effect of a finite neutrino mass,

$$P(p_\beta, \theta_{\beta\nu})dp_\beta d\theta_{\beta\nu} = \tfrac{1}{2}g p_R^{2n} p_\beta^2 (\Delta - E_\beta)[(\Delta - E_\beta)^2 - m_\nu^2]^{\frac{1}{2}} \cdot \{1 + \alpha(p_\beta[(\Delta - E_\beta)^2 - m_\nu^2]^{\frac{1}{2}}/(E_\beta(\Delta - E_\beta)) \times \cos\theta_{\beta\nu} \pm (m_\nu)/(E_\beta(\Delta - E_\beta))\} \cdot \sin\theta_{\beta\nu} dp_\beta d\theta_{\beta\nu}. \quad (1)$$

The influence of the Coulomb field on the wave functions of the electron has been neglected. g is a constant which includes the nuclear matrix element. The integer n is zero for allowed transitions and equal to unity for first forbidden processes. Δ is the mass difference between the masses M_A and M_R of the nucleus in the initial state A and the final state R, respectively. E_β is the energy of a β-particle with the momentum p_β measured in a system of units where $m_\beta = 1$ and $c = 1$. m_ν is the mass of the neutrino. We put $m_\nu = 0$, but later on we shall discuss the influence of a finite mass of the neutrino. α accounts for the different possibilities of coupling between the nucleons and the light particles and has the values $+1$, $+\frac{1}{3}$, $-\frac{1}{3}$, -1, and -1 in the case of an interaction with the invariance properties of a vector, tensor, axial vector, scalar, and a pseudoscalar, respectively. In the last term inside the brackets the $-$ sign is to be taken, except in the case of pseudoscalar interaction where the $+$ sign is to be applied. For allowed transitions and $m_\nu = 0$ all the different expressions contained in (1) lead to the same shape of the β-spectrum—the well-known Fermi type—and even for first forbidden processes the deviations from this shape are small.

THE RECOIL SPECTRUM

By introducing in formula (1) p_R as a new variable we get for the differential probability that the recoil momentum lies in the interval p_R, p_R+dp_R

$$P(p_R)dp_R = (g/24)\{(1+\alpha)p_R^{2n+2} \times (\Delta^2 - 1 - p_R^2)^2/(\Delta^2 - p_R^2)^2 \cdot (p_R^4 - p_R^2(4\Delta^2 - 1) + 3\Delta^2(\Delta^2 + 1)) - 6\alpha p_R^{2n+2}(\Delta^2 - 1 - p_R^2)^2/(\Delta^2 - p_R^2)\} dp_R, \quad (2)$$

and the maximum value of the recoil momentum is given by the relation

$$(p_R^{\max})^2 = \Delta^2 - 1. \quad (3)$$

[1] D. R. Hamilton, Phys. Rev. 71, 456 (1947).

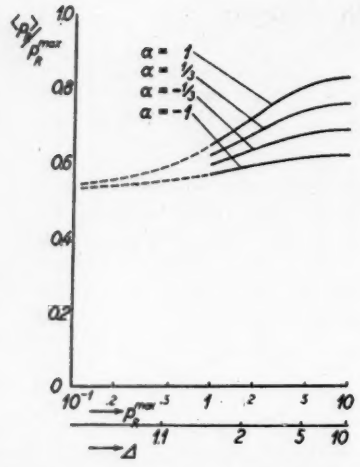

FIG. 1. Allowed transitions. The ratio $\langle p_R\rangle/p_R^{\max}$ plotted against $p_R^{\max}$ for different values of α.

In the case of very low values of Δ, just in the neighborhood of unity, the electron may be treated non-relativistically, and (2) gives the same momentum distribution for the recoil, as formula (1) for the electron. That the momentum distribution for the recoil and for the electron is the same for $\Delta\rightarrow 1$ follows from the fact that in this limit we may neglect the momentum of the neutrino in the momentum conservation. However, the special form of the recoil spectrum given by (2) is hardly valid in this energy region because our approximation neglects the influence of the Coulomb field of the recoil. With increasing Δ the deviations of (2) from the β-spectrum become more and more pronounced, and the curves for different values of α have also a rather different shape. Still, near the maximum value of p_R they all approach the p_R axis as a parabola. For very high values of Δ the region of such a parabolic decrease is strongly limited by the factor $(\Delta^2-p_R^2)$ in the denominator, and this effect is enhanced for forward-going distributions of $\theta_{\beta\nu}$. Thus for fixed Δ the abscissa of the maximum of the distribution curve (2) is higher for forbidden processes than for allowed transitions and furthermore increases with α. These shifts of the distribution curves towards higher energies are illustrated by the following calculation of the average values of p_R and of the kinetic energy $E_R^{\rm kin}$ of the recoil, a calculation which also may be useful for the comparison with experiments.[2] Since $2M_RE_R^{\rm kin}$ is equal to p_R^2 we can easily find these average values from (2). We get expressions containing integrals of the types

$$\int_0^{[\Delta^2-1]^{\frac{1}{2}}} p_R{}^m \frac{(\Delta^2-1-p_R^2)^2}{(\Delta^2-p_R^2)^3}[p_R^4-p_R^2(4\Delta^2-1)+3\Delta^2(\Delta^2+1)]dp_R, \quad (4a)$$

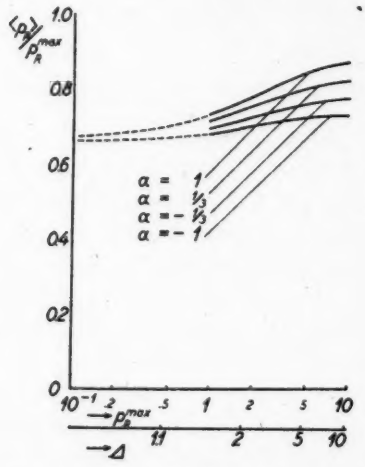

FIG. 2. First forbidden transitions. The ratio $\langle p_R\rangle/p_R^{\max}$ plotted against $p_R^{\max}$ for different values of α.

and

$$\int_0^{[\Delta^2-1]^{\frac{1}{2}}} p_R{}^m \frac{(\Delta^2-1-p_R^2)^2}{(\Delta^2-p_R^2)}dp_R, \quad (4b)$$

which may easily be computed. The results for the average values $\langle p_R\rangle$ and $\langle p_R^2\rangle$ are illustrated in Figs. 1–4, where the ratios $\langle p_R\rangle/p_R^{\max}$ and $\langle p_R^2\rangle/(p_R^{\max})^2$ are plotted as functions of $p_R^{\max}$ for the four possible values of α, for both the case of allowed and that of first forbidden transitions.

The values for $\alpha=\pm\frac{1}{3}$ may be found from the values corresponding to $\alpha=\pm 1$ by linear interpolation. This is exact for $n=0$ and a rather good approximation for $n=1$. As already mentioned, our treatment in which the influence of the Coulomb field of the nucleus on the electron is neglected fails for values of Δ near unity, and the curves in the figures are therefore not drawn with full line in this energy region.

[2] J. C. Jacobsen and O. Kofoed-Hansen, Phys. Rev. **73**, 675 (1948).

PROCESSES INVOLVING THE EMISSION OF γ-RAYS

The emission of γ-rays from the recoil nucleus may change the recoil spectrum considerably.

In the calculation of the recoil spectrum after the γ-ray emission, the question of angular correlation of successive β- and γ-rays must be taken into account. Both theoretically[3] and experimentally[4] this question is not cleared up in all details. However, from an assumption on this angular correlation one may find the probability $P(p_R, \theta_{R\gamma})dp_R d\theta_{R\gamma}$ that the recoil after the emission of the β-particle but before the emission of the γ-quantum has a momentum lying in the interval p_R, p_R+dp_R and that simultaneously the angle between the direction of $\mathbf{p}_R$ and the direction of emission of the γ-ray lies in the interval $\theta_{R\gamma}$, $\theta_{R\gamma}+d\theta_{R\gamma}$. By transforming to new variables and integrating, we get an expression for the probability density $P(p_R')$ for the distribution of the recoil momentum p_R' after the emission of the γ-ray, an expression which, however, is rather complicated. It is easier to calculate the average values of the final recoil momentum and

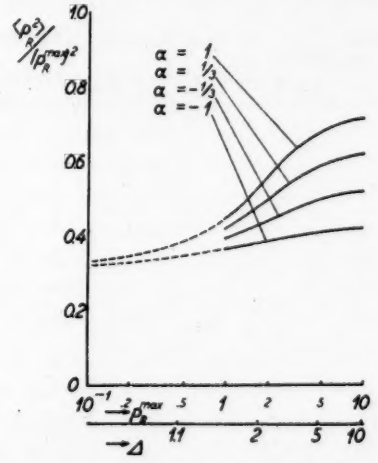

FIG. 3. Allowed transitions. The ratio $\langle p_R^2\rangle/(p_R^{\max})^2$ plotted against $p_R^{\max}$ for different values of α.

energy

$$\langle p_R'\rangle = \langle [p_R^2+p_\gamma^2-2p_R p_\gamma \cos\theta_{R\gamma}]^{\frac{1}{2}}\rangle, \quad (5)$$

and

$$\langle (p_R')^2\rangle = \langle p_R^2+p_\gamma^2-2p_R p_\gamma \cos\theta_{R\gamma}\rangle, \quad (6)$$

using directly the probability function $P(p_R, \theta_{R\gamma})$. p_γ is the momentum of the γ-ray. It may be pointed out that especially (6) is very easily evaluated, since the symmetry properties embodied in the electromagnetic radiation process demand that $P(p_R, \theta_{R\gamma})$ must satisfy the relation

$$P(p_R, \pi-\theta_{R\gamma}) = P(p_R, \theta_{R\gamma}), \quad (7)$$

so that (6) is reduced to

$$\langle (p_R')^2\rangle = \langle p_R^2\rangle + p_\gamma^2, \quad (8)$$

an expression which may be generalized to any number of successive γ-rays following the β-transition. The final average recoil energy, but not the average recoil momentum, is thus completely independent of a possible angular correlation between successive β- and γ-rays.

THE INFLUENCE OF A FINITE MASS OF THE NEUTRINO

If the neutrino has a finite mass, the maximum value of the recoil energy is obtained in a process in which the electron and the neutrino are emitted in the same direction and with the same velocity. We find

$$(p_R^{\max})^2 = \Delta^2-(1+m_\nu)^2. \quad (9)$$

By means of this relation the mass of the neutrino could be found in principle from a measured value of $p_R^{\max}$. Unfortunately, this maximum value may here, just as in the case of the β-spectrum, only be estimated by an extrap-

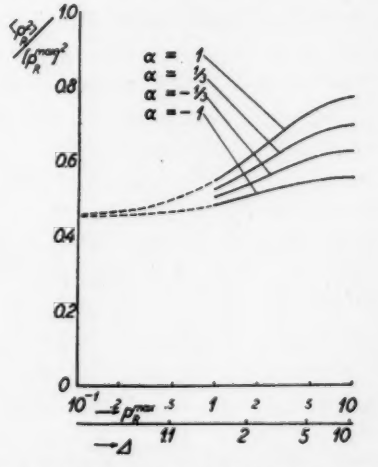

FIG. 4. First forbidden transitions. The ratio $\langle p_R^2\rangle/(p_R^{\max})^2$ plotted against $p_R^{\max}$ for different values of α.

[3] This question is closely connected with the question of angular correlation of successive γ-rays. (D. R. Hamilton, Phys. Rev. **60**, 168 (1941)). For the question of correlation of successive γ-rays compare, e.g., G. Goertzel, Phys. Rev. **70**, 897 (1946).

[4] W. M. Good, Phys. Rev. **70**, 978 (1946).

olation, a procedure which is not independent of theoretical assumptions.

For simplicity let us confine ourselves to the special case $\alpha=-1$. We find, from formula (1),

$$P(p_R)dp_R=(g/4)p_R{}^{2n+2}\times[(\Delta^2-1-m_\nu{}^2-p_R{}^2)^2-4m_\nu{}^2]^{\frac{1}{2}}/(\Delta^2-p_R{}^2)\cdot(\Delta^2-1-m_\nu{}^2-p_R{}^2\pm 2m_\nu)dp_R, \quad (10)$$

or approximately

$$P(p_R)dp_R\cong(g/4)p_R{}^{2n+2}\times[\Delta^2-(1\mp(m_\nu/2))^2-p_R{}^2]^2/(\Delta^2-p_R{}^2)dp_R, \quad (11)$$

which means that the most straightforward extrapolation would lead to

$$(p_R{}^{ex})^2=\Delta^2-(1\pm m_\nu/2)^2, \quad (12)$$

which is seen to depend on the assumption on the coupling between the light particles and the nucleons.

THE INFLUENCE OF THE KINETIC ENERGY OF THE RECOIL

For all known β-decaying nuclei the mass ratio M_R/M_A lies close to unity, and in all these cases the kinetic energy of the recoil may be neglected in the energy conservation. However, in case the mass ratio M_R-M_A deviates considerably from unity, the neglect of the kinetic energy of the recoil in the energy conservation is no satisfactory approximation.[5] The energies involved will in general be so large that the rest mass of the electron may be neglected, and the recoil particle may be treated in a relativistic way.

The maximum energy of the recoil becomes equal to

$$E_R{}^{max}=(M_A{}^2+M_R{}^2)/(2M_A), \quad (13)$$

and for the recoil energy distribution for allowed transitions we get[6]

$$P(E_R)dE_R=(g/24)p_RE_R\times\{[3(M_A-E_R)^2-(E_R{}^2-M_R{}^2)](1+\alpha)-12M_A(E_R{}^{max}-E_R)\alpha\}dE_R. \quad (14)$$

For increasing values of M_A and M_R but for fixed $\Delta=M_A-M_R$ formula (14) approaches the expression obtained from (2) for $\Delta\gg 1$. The distribution curve (14) has no parabolic decrease but goes steeply towards zero at $E_R{}^{max}$.

I wish to thank Professor N. Bohr for his kind interest and valuable advice in this work. My thanks are also due Professor C. Møller and Dr. S. Rozental for helpful discussions.

---

[5] J. J. Horowitz, O. Kofoed-Hansen, and J. Lindhard, Phys. Rev. **74**, 713 (1948).

[6] It must be remembered that formula (14) is only valid on the same conditions as formula (8) from reference 5.

PHYSICAL REVIEW VOLUME 74, NUMBER 12 DECEMBER 15, 1948

The Self-Oscillations of a Charged Particle

D. BOHM AND M. WEINSTEIN
Palmer Physical Laboratory, Princeton University, Princeton, New Jersey
(Received July 19, 1948)

It is found that certain rigid charge distributions can oscillate without radiation even when no forces are present, other than their own retarded fields. The periods are of the order of the time required for light to cross the particle. The energy of these oscillations is always positive, and there are therefore no exponentially increasing unstable motions of the type possessed by the Dirac classical electron.

The frequencies of these oscillations are such, that when quantized, the energy of the first excited state is of the order of the meson self-energy. Hence, it is suggested that some kinds of mesons may be electrons in such an excited state of self-oscillation.

It is indicated that the principle of causality may have to be reformulated in terms of causal connections over finite intervals of time if one wishes to regard the electron plus its associated electromagnetic field as a single system.

I. INTRODUCTION

CURRENT relativistic, quantum field theories are based on the assumption that the elementary charges have no extension in space. It is well known that this assumption leads to infinite results in the higher approximations.[1,2] With the aid of the canonical transformations introduced by Schwinger[3] and Tomonaga,[4] however, it has been possible to classify these infinities in a relativistically invariant way, such that the infinite parts can be uniquely identified as contributions to the mass and to the renormalization of the electronic charge, while the remaining finite terms, which are also unique, give various small but real effects such as the displacements of energy levels observed by Lamb and Retherford.[5] Although this procedure is very satisfactory in that it yields many results which agree with experiment, at least up to second order in $e^2/\hbar c$, it is by no means certain that in higher orders one can continue to isolate the infinite terms in a logically consistent and unambiguous way.[6] It is, in fact, widely felt that some totally new idea is required, which will make the infinite terms finite and unique but at the same time will leave the results of the present theory unaltered wherever these are finite and unambiguous.

A direct way to obtain finite results has always been open, namely, to assume that the electronic charge has a finite extension in space. This idea, however, has never been successfully applied because of the difficulty of specifying the charge distribution in a way that is consistent with the relativistic interpretation of causality. In order to illustrate the problems involved, let us consider, for example, the behaviour of a perfectly rigid electron at which is directed a pulse of electromagnetic radiation. As soon as the pulse strikes the edge of the charge distribution the electron as a whole is set into motion. Thus an impulse is transmitted across the electron instantaneously, contradicting the relativistic law of causality. Although it has often been suggested that the failure of causality for very short intervals of time may be permitted,[7,8] a procedure more in line with our present ideas is to take a model in which the electron is not rigid, but transmits impulses with the speed of light or less. This approach, however, presents problems of its own, for we must then include in our theory a specification of not only the structure of the electron, but also of the dynamical laws governing the transmission of impulses through this structure. In a quantum theory of an extended charge the nonrigid model leads to still another problem, this

[1] R. Serber, Phys. Rev. **49**, 545 (1936).
[2] V. F. Weisskopf, Phys. Rev. **56**, 72 (1939).
[3] J. A. Schwinger, Pocono Conference Notes (by J. A. Wheeler); See also J. A. Schwinger, Phys. Rev. **73**, 416 (1948).
[4] S. Tomonaga, Progress of Theoretical Physics **1**, 27 (1946).
[5] W. E. Lamb, Jr. and R. C. Retherford, Phys. Rev. **72**, 241 (1947).
[6] A. Pais, *Positon Theory* (Princeton University Press, Princeton, to be published).
[7] J. A. Wheeler and R. P. Feynman, Rev. Mod. Phys. **17**, 157 (1945).
[8] D. Blokhinzev, J. Phys. USSR **10**, 167 (1946).

time when one tries to give a quantum description of the shape of the electron. In a state of steady motion, for example, the electron is flattened in the direction of motion because of the Lorentz contraction. When the electron is scattered, however, it undergoes an indivisible change of momentum. What shape does it have during the process of transition? If it may be said to have any shape at all, that shape must be some symmetrical function of initial and final velocities which corresponds neither to initial nor to final shapes. The way to deal with these problems is certainly not yet understood.

Because the theory of an extended charge involves so many difficulties and ambiguities, there has been little impetus to develop this general line of approach. We wish to show, however, that the motion of a rigid, and therefore non-relativistic, extended charge has some unexpected properties, which suggest that the effort to develop a relativistic theory of the extended charge is worth more intensive study. In particular, we find that these new properties may lead to the possibility of describing mesons and perhaps other kinds of particles as excited states of electrons. In this way, the same step that removes the infinities may also reduce the number of elementary particles.

II. SUMMARY OF PROCEDURE AND RESULTS

In this work we consider only a spinless rigid electron with an arbitrary spherically symmetric distribution of charge, which we assume at the outset to be specified. The equations of motion of the center of mass of the charge are solved, taking into account exactly the action of the retarded fields produced by the charge itself. For a general charge distribution we make the assumption that $(v/c)\ll 1$, i.e., only non-relativistic motions are considered. In the special case of a spherical shell charge, however, we can solve the equations exactly for arbitrary values of v/c between 0 and 1, but one must remember that, despite the appearance of arbitrary v/c, this treatment is still not relativistically invariant because the charge is assumed to be rigid.

In agreement with Markov,[9] who uses a similar treatment for the case of small v/c, we find that there are no "self-accelerated" exponential motions of the type discussed by Dirac.[10] Instead, however, we find that for a certain general class of charge distributions, an electron *under the action of no external forces*, is capable of undergoing oscillatory motion. The period, τ_0, depends somewhat on the form of the charge distribution, but it is of the general order of magnitude of the time required for light to cross the electron. These "self-oscillations" consist of simple harmonic motion of the center of mass of the particle; they do not represent a dynamical property of the internal structure of the electron. Nor do they constitute a form of instability, as does the "self-acceleration" of the Dirac classical electron, because they grow only in proportion to their excitation by an external source of energy. The amplitude of the oscillations, A, is less than the mean radius of the electron, a, for since the charge can move in the same direction for at most half a period, $A\sim v_M(\tau_0/2)\sim(v/c)a$. Oscillations are made possible by the fact that each part of the electron moves in a field which was produced by other parts of the electron in the past, so that for certain charge distributions undergoing motion with the proper period the net force can vanish. This implies also that no radiation is emitted,* so that the charge and its own electromagnetic field form a closed system.

These fairly general results were derived on the assumption that $(v/c)\ll 1$. For the special case of a spherical shell charge, however, an exact solution can be obtained. We find that for arbitrary periodic motion of such a charge, with period $\tau_0=2a/c$, the electromagnetic self-force vanishes provided that $v/c<1$. Thus if a spherical shell charge possesses no non-electromagnetic mass, it can continue to move indefinitely in such a periodic orbit, under the action of no external forces and without radiation once it has been set in motion in this way. This type of charge distribution has already been studied by Schott,[11] who shows that for arbitrary spinless periodic motion with the above period there is no radiation. He also shows[12] that for uniform motion in a circular

[9] M. Markov, J. Phys. USSR **10**, 159 (1946).

[10] P. A. M. Dirac, Proc. Roy. Soc. **A167**, 148 (1938).

* The self-force can be regarded as the sum of two terms, one of which yields the rate of radiation while the other leads to forces similar to those of inertia.

[11] G. A. Schott, Phil. Mag. **15**, 752 (1933).

[12] G. A. Schott, Proc. Roy. Soc. **A159**, 570 (1937).

orbit the total self-force vanishes. This is a special case of our result.

In general, for motions which are neither rectilinear nor circular, the retarded fields will produce a couple.[13] In all cases which we consider, however, the self-torque can be shown to vanish, a result necessary for the consistency of the assumption of no spin.

III. EFFECTS OF QUANTIZATION

While we have not, as yet, quantized these self-maintaining oscillations, one can obtain a general idea of the effect of quantization by estimating the energy levels corresponding to the excitation of the first excited states. Let us do this for the special case of the spherical shell charge. The energy of excitation, ΔE, is obtained by multiplying the angular frequency, ω, by $\hbar$, giving

$$\Delta E=\hbar\omega=n\pi(\hbar c/a),$$

where n is an integer. If we take

$$a\sim\frac{e^2}{mc^2}$$

we get

$$\Delta E\sim n\pi\frac{\hbar c}{e^2}mc^2\sim 400nmc^2.$$

Thus the energy of the first excited state with $n=1$ is not far from the rest energy of a π meson. By choosing different values of n we can obtain a spectrum of masses; still other masses and different spectra can be obtained by changing the charge distribution.

The idea then suggests itself that perhaps some kinds of mesons are really excited states of the electron. The decay from one kind of meson to another, or from meson to electron would then correspond simply to the loss of this excitation energy. The exact values of the energy obtained from this crude theory are probably not very significant, first, because they depend on the shape assumed for the charge distribution, and second, because the theory given thus far is not relativistically invariant. The essential point of this work is simply to suggest that the same step which makes the theory finite can also bring in the idea of unifying a whole spectrum of particles into a single particle. Theories involving a range of masses for the same particle have already been suggested on other grounds.[14–16]

One can easily see that for weakly coupled fields, like the electromagnetic, there is little physical significance to the non-relativistic limit in the quantum theory.[6] In order to excite the oscillation with $n=1$ to the first quantum state, for example, it is necessary to give the electron 400 times its own rest energy, and therefore to bring it into the relativistic range of velocities. Before such a theory can be applied at all, it must be extended to the relativistic quantum domain. The spherical shell charge does yield a solution for arbitrary v/c, but does not take into account the need for a non-rigid electron which can change its shape and transmit impulses with the speed of light or less. One possible approach to this problem is to try to make some relativistically invariant assumptions about the properties that we have discussed, and then to quantize the resulting theory. On the other hand, one may attempt to go directly to a quantum theory by guessing a formulation which leads to finite results, being guided by the idea that such a theory should contain the possibility of describing many masses as different states of the same particle. The authors are at present exploring both lines of approach and hope to publish some results soon.

The idea that an extended charge should be capable of self-oscillations is on a considerably more solid footing when applied to a strong-coupling meson theory, for the lowest quantized state of excitation in such a theory need not carry the particle into the relativistic region of velocities. To see this, we note that if the coupling constant is g, the contribution of the meson field to the particle mass is

$$m\sim g^2/ac^2.$$

The ratio of the energy of the first excited state to the self-energy of the particle at rest is then

$$\Delta E/mc^2\sim\pi(\hbar c/g^2),$$

and for large $g^2/\hbar c$ the ratio is small, so that one need not go to a relativistic theory. Thus, in a strong-coupling theory, even with scalar mesons

[13] G. A. Schott, Proc. Roy. Soc. **A159**, 548 (1937).

[14] H. J. Bhabha, Rev. Mod. Phys. **17**, 200 (1945).
[15] F. Bopp, Zeits. f. Naturforschung **1**, 237 (1946).
[16] D. Blokhinzev, J. Phys. USSR **11**, 72 (1947).

one should be able to obtain proton isobars in which the energy of excitation is contained in the motion of the center of mass of the proton. If one combines two such oscillations, which are orthogonal and 90° out of phase, one gets circular motion so that the particles obtain an additional contribution to their intrinsic angular momentum which would be some multiple of $\hbar$ in the quantized theory. In this way one can obtain spin isobars even with a scalar meson theory.

IV. REFORMULATION OF PRINCIPLE OF CAUSALITY

We observe that after the electromagnetic field has been eliminated the equation of motion of the electron (10), is an integral equation which can therefore have, in general, a greater arbitrariness in its boundary conditions than does the usual second order differential equation of motion of mechanics. Let us consider, for example, a spherical shell charge. The solution, as we have pointed out, is an arbitrary periodic function with period $\tau_0=2a/c$. Within the basic period of time, τ_0, the position of the center of mass, $\xi(t)$, may therefore be given an arbitrary form. One could do this, for example, by Fourier analyzing the function within a region of width τ_0 and specifying the amplitude of each Fourier component. The solution of the integral equation then consists simply in repeating the arbitrary function periodically, from one basic period to the next.

One can use this result as the basis of an interesting reformulation of the principle of causality as applied to the motion of the electron. Within a block of time of length τ_0 the behaviour of the electron is arbitrary, i.e., it seems to follow no causal laws. The causal laws are constituted by the requirement that from one block of time to the next the motion must repeat itself. (All of this is in the absence of external fields; such fields would cause the motion to be not quite periodic.) As a result, time seems to take on a twofold character. Over a block of time of length τ_0 it acts just like a space-coordinate in that there are no particular relations between the particle coordinates at neighboring instants. It is only between one block of time and the next that such causal connections appear.

The disappearance of causal laws as applied to the electron within a block of time is compensated by the appearance of new degrees of freedom, which may be taken as the amplitudes of the Fourier components of ξ. Strictly speaking, these are not really new degrees of freedom, but are merely a re-description in terms of the particle coordinates of some of the arbitrariness resulting from the old degrees of freedom, i.e., the electromagnetic field, which has been eliminated. When the electromagnetic field is taken into account, of course, the system does obey causal laws, which involve the field quantities as well as the particle coordinates. The apparent lack of causality over a basic period of time, τ_0, merely reflects the fact that if we specify only the particle coordinates, it is necessary to know the motion over the entire length of time needed for light to cross the electron before we can know the total field existing over the electron at any instant, and therefore, before we can predict the subsequent behaviour of the electron.** The essential conclusion to be drawn from this fact is that if one wishes to regard the electron plus its associated field as a single system, one may be forced to reformulate the principle of causality in terms of causal connections over finite intervals of time.

In a sense, this dual property of time may be regarded as a sort of quantization of time, since there will now be a minimum interval which can be involved in causal relations. Although shorter intervals of time can exist, they have new properties. For example, no predictions of the electronic motion can be made over intervals shorter than τ_0. The arbitrariness of the Fourier components of ξ within the period, τ_0, would in a quantized theory, be interpreted as the possibility of creating various kinds of mesons. Since the amplitude of each Fourier component can be specified only after the motion is known over the whole period, one would be unable to give a meaning to the problem of specifying the kind of

** It might be thought, at first sight, that the lack of causality is connected with the assumed rigid structure of the electron, which can transmit impulses faster than light. We are, however, discussing here a non-relativistic theory, within the framework of which one can postulate the transmission of impulses with arbitrary velocity. It is only when we make a Lorentz transformation that the transmission of impulses faster than light leads to a breakdown of causality, since events which are connected by such impulses may have future and past interchanged as a result of the transformation. The attempt to make a relativistic theory of a rigid electron would introduce an element of genuine lack of causality, which could not be explained in terms of eliminated field quantities.

meson which exists in a time less than τ_0. Thus one would obtain a new kind of complementarity between time and the nature of the particle with which one was dealing.

This discussion is intended merely to show how an attempt to devise a systematic relativistic quantum theory of extended charges might readily lead to important revisions of some of our concepts of causality.

V. THE EQUATION OF MOTION AND ITS SOLUTIONS

The equation of motion of a rigid charged particle, including the action of its own electromagnetic field, has already been studied extensively.[9–13,17] For the sake of completeness however, we include a brief derivation which, although it repeats a certain amount of work already existing in the literature, provides the result in a form convenient for our purposes.

We begin by assuming a certain spherically symmetrical charge density which we denote by

$$\rho(\mathbf{x}, t) = ef(|\mathbf{x}-\xi(t)|)$$

where $\xi(t)$ is the position vector of the center of mass and e is the total charge, so that

$$\int d\mathbf{x} f(|\mathbf{x}|) = 1.$$

This, of course, is equivalent to assuming a rigid charge distribution. The current density is then

$$\mathbf{j}(\mathbf{x}, t) = \frac{e}{c}\dot{\xi}(t) f(|\mathbf{x}-\xi(t)|),$$

which implies that the particle has no spin, i.e., currents arise only from the motion of the center of mass.

In deriving the fields produced by this charge-current distribution, it will be convenient to choose the gauge in which the vector potential, $\mathbf{a}_\perp$, is divergenceless. In this case one can easily show that the scalar potential, ϕ, satisfies the equation

$$\Delta\varphi = -4\pi\rho, \tag{1}$$

i.e., it is not retarded. Hence the field resulting from ϕ can produce no net force, and so far as the motion of the center of mass of the particle is concerned, we need pay attention only to the transverse fields arising from $\mathbf{a}_\perp$, which satisfies

$$\left(\Delta - \frac{1}{c^2}\frac{\partial^2}{\partial t^2}\right)\mathbf{a}_\perp = -4\pi\mathbf{j}_\perp, \tag{2}$$

where $\mathbf{j}_\perp$ is the divergenceless part of the current density. The next step is to Fourier analyze this equation. In the subsequent work we will denote the kth Fourier component of a function, $g(\mathbf{x}, t)$, by

$$g_k(t) = \frac{1}{(2\pi)^{\frac{3}{2}}}\int g(\mathbf{x}, t)(\exp -i\mathbf{k}\cdot\mathbf{x})d\mathbf{x},$$

where

$$g(\mathbf{x}, t) = \frac{1}{(2\pi)^{\frac{3}{2}}}\int g_k(t)(\exp i\mathbf{k}\cdot\mathbf{x})d\mathbf{k}.$$

Then $\mathbf{a}_{k\perp}(t)$ must satisfy

$$\left(c^2k^2 + \frac{\partial^2}{\partial t^2}\right)\mathbf{a}_{k\perp} = 4\pi c^2\mathbf{j}_{k\perp}. \tag{3}$$

The solution corresponding to the retarded potential*** is

$$\mathbf{a}_{k\perp}(t) = \frac{4\pi c}{k}\int_{-\infty}^{t} dt'(\mathbf{j}_k(t'))_\perp \operatorname{sin}ck(t-t'). \tag{4}$$

Now

$$\mathbf{j}_k(t) = \frac{e}{c}\dot{\xi}(t) f_k(\exp -i\mathbf{k}\cdot\xi(t)), \tag{5}$$

where

$$f_k = \frac{1}{(2\pi)^{\frac{3}{2}}}\int d\mathbf{x} f(|\mathbf{x}|)(\exp -i\mathbf{k}\cdot\mathbf{x}),$$

and since

$$(\mathbf{j}_k)_\perp = \frac{\mathbf{k}\times(\mathbf{j}_k\times\mathbf{k})}{k^2},$$

the vector potential† becomes

[17] H. A. Lorentz, *Theory of Electrons* (B. G. Teubner, Liepzig, 1909).

*** If one chooses $+\infty$ for the lower limit, one obtains the advanced potential.

† It should be noted that, in general, a convergence factor is necessary to give meaning to the integral defining $\mathbf{a}_{k\perp}$. This procedure, however, will always yield a unique result with a bounded charge because when one re-Fourier analyzes to find the potentials as functions of x and t, the effect of the k integration is to restrict the time during which contributions are made to the t' integral to a short interval.

$$\mathbf{a}_\perp(\mathbf{x},t)=\frac{4\pi e}{(2\pi)^{\frac{3}{2}}}\int_{-\infty}^{t}dt'\int\frac{d\mathbf{k}}{k}f_k\sin ck(t-t')$$

$$\times\exp i\mathbf{k}\cdot(\mathbf{x}-\xi(t'))\frac{\mathbf{k}\times(\dot{\xi}(t')\times\mathbf{k})}{k^2}. \quad (6)$$

The fields are given by

$$\varepsilon_\perp=-\frac{1}{c}\frac{\partial\mathbf{a}_\perp}{\partial t},\quad \mathbf{H}=\mathrm{curl}\mathbf{a}_\perp, \quad (7)$$

and the self-force is just

$$\mathbf{F}_{\mathrm{self}}=\int d\mathbf{x}[\rho(\mathbf{x},t)\varepsilon_\perp(\mathbf{x},t)+\mathbf{j}(\mathbf{x},t)\times\mathbf{H}(\mathbf{x},t)]. \quad (8)$$

Inserting the results of Eq. (7) into Eq. (8) and making the substitutions $t-t'=\tau$, $\xi(t)-\xi(t-\tau)=\mathbf{s}$, we obtain

$$\mathbf{F}_{\mathrm{self}}=-4\pi e^2\int_0^\infty d\tau\int\frac{d\mathbf{k}}{k}|f_k|^2$$

$$\times(\exp i\mathbf{k}\cdot\mathbf{s})\left[k\cos ck\tau\frac{\mathbf{k}\times(\dot{\xi}(t-\tau)\times\mathbf{k})}{k^2}\right.$$

$$\left.-i\sin ck\tau\frac{\dot{\xi}(t)}{c}\times(\mathbf{k}\times\dot{\xi}(t-\tau))\right]. \quad (9)$$

The equation of motion for the electron is

$$m\ddot{\xi}=\mathbf{F}_{\mathrm{self}}+\mathbf{F}_{\mathrm{ext}}, \quad (10)$$

where $\mathbf{F}_{\mathrm{ext}}$ is the external force and m is the non-electromagnetic mass.

Approximation of Small Velocities

Let us now investigate the limit in which $(v/c)\ll 1$. In this approximation the magnetic term in Eq. (9) may be neglected in comparison with the first term, which is of order v/c. Now $\mathbf{s}=\xi(t)-\xi(t-\tau)$ is essentially just the distance covered by the particle during the time τ. One can easily see that the integrand of Eq. (9) is large only over a time $\tau\sim 2a/c$, which is of the order of that needed for light to cross the electron, so s is of the order of $2a(v/c)$. Retaining only first order terms in v/c, we can replace $(\exp i\mathbf{k}\cdot\mathbf{s})$ by unity to obtain

$$\mathbf{F}_{\mathrm{self}}=-4\pi e^2\int_0^\infty d\tau\int d\mathbf{k}|f_k|^2\cos ck\tau$$

$$\times\left[\dot{\xi}(t-\tau)-\frac{\mathbf{k}(\mathbf{k}\cdot\dot{\xi}(t-\tau))}{k^2}\right].$$

Note that this equation is linear: small v/c leads to a linear approximation.††

The above expression can be put into a more convenient form by integration by parts over τ. The integrated part vanishes as $\tau\to\infty$ for any form of f_k resulting from a bounded charge distribution,††† while at $\tau=0$ it vanishes because of the appearance of $\sin ck\tau$ as a factor. After angular integration the self force becomes

$$\mathbf{F}_{\mathrm{self}}=\frac{-32\pi^2e^2}{3c}\int_0^\infty d\tau\ddot{\xi}(t-\tau)\int_0^\infty dkk|f_k|^2\sin ck\tau.$$

With the substitution

$$G(\tau)=\frac{-32\pi^2}{3c}\int_0^\infty dkk|f_k|^2\sin ck\tau \quad (11)$$

the above expression becomes

$$\mathbf{F}_{\mathrm{self}}=e^2\int_0^\infty d\tau G(\tau)\dddot{\xi}(t-\tau), \quad (12)$$

and the equation of motion, in the absence of external forces, is

$$m\ddot{\xi}=e^2\int_0^\infty d\tau G(\tau)\ddot{\xi}(t-\tau)$$

$$=\frac{-32\pi^2e^2}{3c}\int_0^\infty d\tau\ddot{\xi}(t-\tau)$$

$$\times\int_0^\infty dkk|f_k|^2\sin ck\tau. \quad (13)$$

This equation is accurate for arbitrarily large accelerations, but only for small v/c. It is essentially the same equation obtained by Markov[9] in a similar way.

---

†† It is readily shown that in the linear approximation the self torque vanishes because of symmetry.

††† This may be seen, for example, by expressing f_k in terms of $f(x)$.

Self-Oscillations

We shall now demonstrate that Eq. (13) possesses oscillatory solutions, and examine the conditions under which these solutions exist. Inserting $\xi=\mathbf{A}(\exp -i\omega t)$ into (13), we get

$$m\omega^2=\frac{-32\pi^2e^2}{3c}\omega^2\int_0^\infty d\tau(\exp i\omega\tau)\times\int_0^\infty dkk|f_k|^2\sin ck\tau$$

$$=e^2\omega^2\int_0^\infty d\tau(\exp i\omega\tau)G(\tau), \quad (14)$$

which defines the permissible frequencies of self-oscillation, if any. Since m must be real, (14) is equivalent to the two conditions

$$m=\frac{-32\pi^2e^2}{3c}\int_0^\infty d\tau\times\int_0^\infty dkk|f_k|^2\sin ck\tau\cos\omega\tau, \quad (15)$$

$$0=\int_0^\infty d\tau\int_0^\infty dkk|f_k|^2\sin ck\tau\sin\omega\tau. \quad (16)$$

Condition (16) can be put into a more convenient form by performing the τ integration. Since the integrand is an even function of τ, this condition can be rewritten

$$0=\int_{-\infty}^\infty d\tau\int_0^\infty dkk|f_k|^2\times[\cos\tau(ck-\omega)-\cos\tau(ck+\omega)].$$

The integrals over τ are just δ functions, giving

$$f_{\omega/c}=0. \quad (16')$$

It is readily shown that when condition (16′) is satisfied the radiation vanishes to order v/c.

The spectrum of frequencies at which self-oscillations can take place depends strongly on the shape of the charge. First, in order to satisfy condition (16′), it is necessary that at least one Fourier component of the charge distribution shall vanish. In addition, at this frequency, condition (15) must be satisfied, but so long as the distribution processes at least one vanishing Fourier component it will be possible, in general, to choose the non-electromagnetic mass, m, in such a way as to satisfy (15). Those distributions with vanishing Fourier components may be characterized roughly as either sharply varying, or non-monotonic. Both the spherical shell and the uniform sphere, for example, can undergo self-oscillations. On the other hand, smoothly varying, monotonic distributions, such as the Gaussian and exponential, have no vanishing Fourier components, while a smoothly varying but non-monotonic distribution like $xe^{-x/a}$ has one.

The following are a few examples of frequencies of self oscillation.

(*a*) *Spherical Shell*

$$f(x)=\frac{\delta(x-a)}{4\pi a^2}; \quad f_k=\frac{1}{(2\pi)^{\frac{1}{2}}}\frac{\sin ka}{ka}. \quad (17)$$

In this case it is most convenient to use Eq. (14) directly. We obtain from (11) and (17),

$$G(\tau)=\begin{cases}-\dfrac{1}{3a^2c}, & \tau<\dfrac{2a}{c},\\[2ex] 0, & \tau>\dfrac{2a}{c}.\end{cases}$$

The condition for self oscillation (14) is

$$m=\frac{ie^2}{3\omega ca^2}[(\exp 2i\omega a/c)-1].$$

Solutions are possible only when $m=0$. The frequencies are $\omega=n\pi c/a$, where n is an integer.

(*b*) *Uniform Sphere*

$$f(x)=\begin{cases}\dfrac{3}{4\pi a^3}, & x<a\\[2ex] 0, & x>a\end{cases}; \quad (18)$$

$$f_k=\frac{3}{(2\pi)^{\frac{1}{2}}}\frac{1}{(ka)^2}\left[\frac{\sin ka}{ka}-\cos ka\right].$$

Although the uniform sphere has an infinite number of vanishing Fourier components, condition (15) limits the spectrum to a single frequency, $\omega^2=2e^2/ma^3$. For a given e and a, however, there

are many possible ways of choosing m, given by the solutions of

$$\tan(2e^2/mc^2a)=(2e^2/mc^2a).$$

If $a\sim e^2/mc^2$, the largest value of m which will permit self-oscillation is of the same order as e^2/ac^2.

(c) $$f(x)=\frac{1}{24\pi a^4}xe^{-x/a};$$

$$f_k=\frac{1}{3(2\pi)^{\frac{1}{2}}}\frac{(3-k^2a^2)}{(1+k^2a^2)^3}. \tag{19}$$

This distribution has only one frequency, $\omega=\sqrt{3}(c/a)$, for which $f_{\omega/c}$ vanishes. To satisfy condition (15) we must choose $m=e^2/192ac^2$. Since the electromagnetic mass is of the order of e^2/ac^2, in this case the mechanical mass must be much less than the electromagnetic mass.

Absence of "Self-Accelerated" Solutions

Markov[9] has suggested that Eq. (13) should have no exponentially increasing solutions of the type obtained by Dirac.[10] One can obtain this result very simply by attempting to find solutions of the form $\xi=A(\exp(\lambda-i\omega_0)t)$ where ω_0 and λ are real and positive, i.e., by replacing ω in Eq. (14) by $\omega_0+i\lambda$. Because of the appearance of the factor $e^{-\lambda\tau}$ in the integrand, the integral over τ converges, and can be carried out first, yielding

$$m+\frac{32\pi^2e^2}{3}\int_0^\infty dkk^2|f_k|^2 \times\frac{[(\lambda^2-\omega_0^2+c^2k^2)+2i\lambda\omega_0]}{(\lambda^2-\omega_0^2+c^2k^2)^2+4\lambda^2\omega_0^2}=0. \tag{20}$$

There can be no solution unless the imaginary part of the integral vanishes, but since the imaginary part of the integrand is everywhere positive this cannot happen unless either $\lambda=0$ or $\omega_0=0$. If $\omega_0=0$ the integrand is everywhere positive, and there is a solution only for negative m. Peierls has already shown that the Dirac classical electron is equivalent to one in which an infinite negative mass almost cancels the infinite positive contribution of the point charge. The extended electron, therefore, has no motions of the "self-accelerating" type possessed by the Dirac classical electron so long as the non-electromagnetic mass is positive or zero.

Stability of Motion of Extended Electron

From the above result one can immediately conclude that the motion of the extended electron is stable. In order to investigate the stability of the electron at rest, for example, we must see whether small displacements remain small for all time. Now, the assumption of small v/c leads immediately to the validity of Eq. (13). Thus if we assume a displacement, $\xi=Ae^{\lambda t}(\exp-i\omega_0t)$, which is small at the time t, it will be smaller still throughout all the earlier time during which contributions are made to Eq. (13). On the other hand, it is inadmissible to test for the stability with the aid of the Lorentz expansion in a series of derivatives of ξ, just because the ratio $(d^{n+1}\xi/dt^{n+1})/(d^n\xi/dt^n)$ may not be small, even though ξ itself is small.

Another way to investigate the stability of the resting electron is to see whether the energy of a moving electron is always greater than that of a fixed electron.‡ Remembering that the electrostatic potential is not retarded, since the electron does not change its shape‡‡ one can conclude that the electrostatic energy is independent of the velocity. It can be shown,[18] furthermore, that the total electromagnetic energy is just the sum of the electrostatic contribution and that due to $\mathbf{a}_\perp$. Now, $\mathbf{a}_\perp=0$ when the electron is at rest, so the increase in energy which is due to the motion is given by

$$W=\frac{1}{8\pi}\int d\mathbf{x}\left[\frac{1}{c^2}\left(\frac{\partial\mathbf{a}_\perp}{\partial t}\right)^2+(\nabla\times\mathbf{a}_\perp)^2\right], \tag{21}$$

and since $\mathbf{a}_\perp$ cannot vanish everywhere for a moving electron this is clearly a positive quantity. The state of rest is therefore a stable one.

‡ We have seen that the instability of the Dirac classical electron can, in fact, be traced to the assumption of an infinite negative mechanical mass which almost cancels the electromagnetic mass. It is this negative mass which supplies the electromagnetic energy generated in the exponential "self-accelerated" motion.

‡‡ One assumes that the charge is rigid, which means that the tendency of the electrostatic force to blow up the charge is automatically counteracted by some other force which holds the electron together. Since this force does no work, it need not be considered in any study of the motion of the electron.

[18] W. Heitler, *Quantum Theory of Radiation* (Clarendon Press, Oxford, 1936).

It is instructive to evaluate W for the case of small v/c. If one expresses $\mathbf{a}_\perp$ in terms of its Fourier components one obtains

$$W=\frac{1}{8\pi c^2}\int d\mathbf{k}[|\dot{\mathbf{a}}_{\mathbf{k}\perp}|^2+c^2k^2|\mathbf{a}_{\mathbf{k}\perp}|^2], \quad (22)$$

where $\mathbf{a}_{\mathbf{k}\perp}$ is given in Eq. (4). In the linear approximation we can neglect ξ in the exponential, and with this simplification one obtains

$$W=\frac{16\pi^2e^2}{3}\int_0^\infty d\tau\int_0^\infty d\tau'\int_0^\infty dkk^2|f_k|^2 \times\cos ck(\tau-\tau')\dot{\xi}(t-\tau)\cdot\dot{\xi}(t-\tau'). \quad (23)$$

As an example we consider the spherical shell charge, for which f_k is given in Eq. (17). We get, for a self-oscillation,

$$W=\frac{e^2}{6a^2c}\int_0^{2a/c}d\tau\dot{\xi}^2(t-\tau)=\frac{M\bar{v}^2}{2}, \quad (24)$$

where $M=(2/3)(e^2/ac^2)$ is the electromagnetic mass.

Exact Treatment for Self-Force of Spherical Shell Charge

Let us begin with the exact Eq. (9) for the self-force. We shall consider a typical term and show that it vanishes for an arbitrary periodic motion of period $2a/c$.

The electric term in the self-force is

$$\mathbf{F}_e=-4\pi e^2\int_0^\infty d\tau\int d\mathbf{k}|f_k|^2 \times(\exp i\mathbf{k}\cdot\mathbf{s})\cos ck\tau\left[\dot{\xi}(t-\tau)-\frac{\mathbf{k}(\mathbf{k}\cdot\dot{\xi}(t-\tau))}{k^2}\right].$$

Integration over angles in $\mathbf{k}$ space yields

$$\mathbf{F}_e=-16\pi^2e^2\int_0^\infty d\tau\left[\dot{\xi}(t-\tau)-\frac{3\mathbf{s}}{s^2}\mathbf{s}\cdot\dot{\xi}(t-\tau)\right] \times\int_0^\infty\frac{dk}{s^2}|f_k|^2\cos ck\tau\left(\cos ks-\frac{\sin ks}{ks}\right) -16\pi^2e^2\int_0^\infty d\tau\left[\dot{\xi}(t-\tau)-\frac{\mathbf{s}}{s^2}\mathbf{s}\cdot\dot{\xi}(t-\tau)\right] \times\int_0^\infty dkk|f_k|^2\frac{\sin ks}{s}\cos ck\tau.$$

Writing

$$K(\tau)=\int_0^\infty\frac{dk}{s^2}|f_k|^2\cos ck\tau\left(\cos ks-\frac{\sin ks}{ks}\right), \quad (25)$$

$$M(\tau)=\int_0^\infty\frac{dk}{s}k|f_k|^2\cos ck\tau\sin ks. \quad (26)$$

$\mathbf{F}_e$ can be rewritten

$$\mathbf{F}_e=-16\pi^2e^2\int_0^\infty d\tau \times\left(K(\tau)\left[\dot{\xi}(t-\tau)-\frac{3\mathbf{s}}{s^2}\mathbf{s}\cdot\dot{\xi}(t-\tau)\right] +M(\tau)\left[\dot{\xi}(t-\tau)-\frac{\mathbf{s}}{s^2}\mathbf{s}\cdot\dot{\xi}(t-\tau)\right]\right). \quad (27)$$

We first consider the term containing $K(\tau)$. Now, when dealing with a distribution of infinitesimal thickness, like a spherical shell, one must define the integrals as limits of distributions of finite thickness. Since it is not always possible to permit these distributions to approach zero thickness before the results have been obtained, we shall at the outset spread the distribution by writing

$$f_k=\frac{1}{(2\pi)^{\frac{1}{2}}}\frac{i\lambda}{k+i\lambda}\frac{\sin ka}{ka}, \quad (28)$$

which approaches a spherical shell in the limit $\lambda\to\infty$. With this value for f_k, $K(\tau)$ becomes

$$s<c\tau<2a-s: K(\tau)=\frac{1}{64\pi^2a^2s^2\lambda} \times[(\exp-\lambda(2a-c\tau))-2(\exp-\lambda c\tau)] \times\left(\cosh\lambda s-\frac{\sinh\lambda s}{\lambda s}\right) +\text{terms proportional to } (\exp-\lambda(2a+c\tau\pm s)),$$

$$c\tau>2a+s: K(\tau)=\frac{1}{64\pi^2a^2s^2\lambda} \times(\exp-\lambda(c\tau-2a))\left(\cosh\lambda s-\frac{\sinh\lambda s}{\lambda s}\right) +\text{terms proportional to } (\exp-\lambda(c\tau+2a\pm s)).$$

We first observe that the terms in $K(\tau)$ proportional to $(\exp-\lambda(2a+c\tau\pm s))$ will make no contribution to the integral in the limit $\lambda\to\infty$. This follows from the fact that $s=|\xi(t)-\xi(t-\tau)|$ is always less than or equal to $c\tau$.¶ The remaining terms make contributions only near the points at which the arguments of the exponentials in $K(\tau)$ vanish, i.e., only near $c\tau\pm s=0$ and $2a-c\tau\pm s=0$. The only two points satisfying these relations are $\tau=0$, and $\tau=2a/c$. This is because, from the fact that $s<c\tau$, and from the periodicity, one can conclude also that $s<|2a-c\tau|$. This means that contributions to the τ integral come only from the infinitesimal regions near $\tau=0$ and $\tau=2a/c$, where s is small. In these regions we can therefore expand s in powers of τ and $|\tau-2a/c|$:

$$\begin{aligned} &s\sim v(t)\,\tau && \text{near} \quad \tau=0,\\ &s\sim v(t)\left|\tau-\frac{2a}{c}\right| && \text{near} \quad \tau=\frac{2a}{c}. \end{aligned} \tag{29}$$

With these values for s,

$$(1/\lambda s^2)[\cosh\lambda s-(\sinh\lambda s)/\lambda s]$$

can be replaced by $\lambda/3$,¶¶ so that $K(\tau)$ becomes

$$K(\tau)=\frac{\lambda}{3.64\pi^2a^2}\times\begin{cases}(\exp-\lambda(2a-c\tau))-2(\exp-\lambda c\tau), & 0\leqslant\tau\leqslant\dfrac{2a}{c},\\ (\exp-\lambda(c\tau-2a)), & \tau\geqslant\dfrac{2a}{c}.\end{cases} \tag{30}$$

Thus $K(\tau)$ clearly approaches

$$K(\tau)=\frac{1}{3\times32\pi^2a^2}(\delta(c\tau-2a)-\delta(c\tau)), \tag{31}$$

and since

$$\dot{\xi}(t-\tau)-\frac{3\mathbf{s}}{s^2}\mathbf{s}\cdot\dot{\xi}(t-\tau)$$

approaches $-2\dot{\xi}[t-(2a/c)]$ and $-2\dot{\xi}(t)$ as τ approaches zero and $2a/c$ respectively, we obtain for the exact value of the force resulting from the term containing $K(\tau)$,

$$\frac{e^2}{3a^2c}\left[\dot{\xi}\left(t-\frac{2a}{c}\right)-\dot{\xi}(t)\right]$$

which vanishes if $\xi(t)$ is a function with period $2a/c$. It is readily verified that $M(\tau)$ leads to the same set of δ functions, so that the second term in $\mathbf{F}_s$ also vanishes. One can treat the magnetic term and the self-torque in the same way and show that these are also zero.

¶ Since s is essentially just the distance covered by the particle in time τ, $s<c\tau$ follows from the fact that $(v/c)<1$.

¶¶ One must let $\lambda\to\infty$ in such a way that $(3/\lambda^2s^2)\times[\cosh\lambda s-(\sinh\lambda s)/\lambda s]$ remains close to unity in the region where the integrand is appreciable. Because $|2a-c\tau|$ and $c\tau$ are both greater than s, the exponential factors will then make the result small, except near $\tau=0$ and $\tau=2a/c$. The contributions of the regions where the above factor is not unity are negligible for large λ, because the exponential factor far more than makes up for the increase in the $\cosh\lambda s$ and $\sinh\lambda s$ functions.

PHYSICAL REVIEW VOLUME 74, NUMBER 12 DECEMBER 15, 1948

Deuteron and Triton Methods

WILLIAM RARITA
Brooklyn College, Brooklyn, New York, and Massachusetts Institute of Technology, Cambridge, Massachusetts
(Received September 2, 1948)

Some methods are reported of calculating accurately the depths of different shape potentials of the deuteron for non-central forces.

Starting with a square well, we know the radial S and D wave functions u and w outside the well. Inside the range of interaction we assume a general expansion in terms of modes. These modes for u and w we take to be Bessel functions of order one-half and five-halves, respectively. The wave-lengths of these modes are determined by requiring the continuity of the logarithmic derivative. Using the variational principle for one mode and then two such modes, we get 95 percent and 99 percent of the full binding energy.

With an exponential times a power of the interparticle distance as our modes, we decided to relax the joining condition so as to require only continuity at the potential edge. The results for the square well were excellent. This method was extended to the exponential and meson potentials. The accurate depths for these potentials were calculated with these modes as initial trial wave function for the iteration-variational method developed by Feshbach and Schwinger.

The relaxed continuity procedure was successfully applied to the triton problem without and with tensor forces.

INTRODUCTION

ALTHOUGH the simple square well for the interaction potential between nucleons has had[1] an astounding success in correlating the known facts of two-body nuclear phenomena, yet there is a great need to extend methods and results to other shape potentials for two reasons: first, to test the sensitivity of the theory to shape of potential and, second, to see whether agreement between theory and experiment can be improved. It is in this spirit that we suggest some methods that we have found useful or promising.

DEUTERON BINDING ENERGY

Starting with the problem of the deuteron binding energy, we discuss what may be called the method of modes. We shall first test our procedure on the square well potential for which an exact solution already exists. To be explicit, we introduce a special set of modes found to be highly convergent. The presence of tensor forces requires the consideration of both the S and D radial waves function u and w, respectively.[2] The u and w outside the well are simple and exactly known. The assumed expansions inside the interaction range r_0 are

$$u=\Sigma A_i(\kappa_i r)^{\frac{1}{2}}J_{1/2}(\kappa_i r)=\Sigma u_i,$$

and

$$w=\Sigma B_j(\lambda_j r)^{\frac{1}{2}}J_{5/2}(\lambda_j r)=\Sigma w_j. \quad (1)$$

The u_i and w_j are the modes. The modes are here expressed in terms of Bessel functions of order one-half or five-halves. The u_i are simple: $u_i\sim\sin\kappa_i r$ and the w_j are the usual combination of $\sin\lambda_j r$ and $\cos\lambda_j r$ in terms of the interparticle distance r. The wave-lengths κ_i and λ_j are determined by requiring separately the continuity of the logarithmic derivative of u_i (and w_j) at the edge of the well to the outside known u (and w). Incidentally, the u_i and the w_j form a complete orthogonal set of functions on the interval inside the well. Substituting these expressions for u and w into the usual integral expression for the energy[3] and varying the coefficients A_i, B_j, we get a set of linear algebraic equations for which we can calculate the energy and the wave functions u and w completely. In particular, we can evaluate the electric quadrupole moment of the deuteron. To indicate the rapid convergence we give some results. From the known potential depths of the exact calculation,[1] one mode for u and w yields 95 percent of the full binding energy. Two such modes for u and w increase the energy to 99 percent.

We also tried a different set of modes for the internal functions. These modes were taken as

[1] W. Rarita and J. Schwinger, Phys. Rev. 59, 436 (1941).
[2] We employ the notation of reference 1.
[3] See appendix of a forthcoming paper by H. Feshbach and W. Rarita.

TABLE I.

r_0 (in 10^{-13} cm)	V_0 (Mev)	γV_0 (Mev)	γ	%D	Shape
1.18	15.2	75.2	4.9_4	5.3	Meson
1.73	84.9	72.5	0.854	3.3	Exponential
2.80	13.9	10.8	0.775	3.9	Square

an exponential times a power series in the interparticle distance r.

$$u=\Sigma A_i r^i \exp(-\lambda r)=\Sigma u_i$$

and (2)

$$w=\Sigma B_j r^{j+2} \exp(-\mu r)=\Sigma w_j.$$

The parameters λ and μ are most practically fixed by minimizing the energy with a single mode for the S and D functions. We decided at this point to relax the joining condition so as to demand only continuity at the potential edge of u_i and w_j to the outside exact functions u and w. This relaxation of boundary condition on u_i and w_j produced a more rapid convergence of the energy to its final value. For one mode in u and w the energy is 76 percent. If the more rigid condition of the logarithmic continuity of the derivative is imposed, the calculated energy drops to 66 percent. We also determined the ratio R of the computed potential depth to the exact depth assuming the correct energy and the correct ratio γ of tensor depth to ordinary depth. For three mode expansions, R is 1.0035 and the corresponding ratio of the calculated to the exact electric quadrupole moment is 1.0087.

The two methods explained above can be extended to other shape potentials commonly assumed in nuclear work. We merely have to take the inside region as that in which the potential is appreciable. The outside region is where the potential is essentially negligible. A wise choice of this distance expedites the calculations. We have, in fact, carried out such calculations for the exponential and the meson potential with gratifying results. For the meson potential $V_0 r_0/r \exp(-r/r_0)$ having the Breit range, we fitted the binding energy and the electric quadrupole moment Q and applied our relaxed continuity method with three terms in expansion (2). The calculated ordinary potential depth was within a few percent of the correct value. The wave functions u and w were even more difficult to evaluate accurately. The ratio γ varied rapidly with change in Q. The most reliable values for the various depths quoted below were obtained by using the three modes as the initial trial wave function for the iteration-variational method developed by Feshbach and Schwinger.[4] Two iterations gave excellent results. We also give the results for the exponential potential $V_0 \exp(-2r/r_0)$ for the range once determined by Rarita and Present.[5] In Table I, V_0 represents the ordinary depth. The percent D state is also included. The exact results for the square well are inserted for comparison.

TRITON BINDING ENERGY

The methods expounded above were in great part incited by the desire to find a suitable way to solve for the square well the triton binding energy problem. A promising method is the generalization of the second deuteron procedure. But now the inside region is not well defined from the outside region. Although the surfaces of separation can no doubt be found, it seems to be counter to the spirit of the variational method to solve any part of the problem in a needlessly complicated form. Accordingly, we take the inside region to be that in which the three nuclear particles are within the interaction range.

We first discuss the case of square wells without tensor forces (S state). For the simple wave (for notation and further discussion, see reference 3) function $A+B \exp[-\lambda(r_1+r_2+\rho)]$ inside and $C \exp[-\mu(r_1+r_2+\rho)]$ outside and with mere continuity imposed at joining, the triton binding energy calculated was 80 percent of the experimental value. If continuity up to the first derivative is exacted, the energy drops to 74 percent. If analytic continuity, as expressed by an exponential term times a power series in the three interparticle distances r_1, r_2, ρ is assumed, the energy is 72 percent for the exponential term alone and 77 percent for the third-order terms of the power series.

For the actual case in the presence of tensor forces, a similar joining in the D state gave 35 percent. The corresponding analytic result is 32 percent.

[4] H. Feshbach and J. Schwinger, to be published soon.
[5] W. Rarita and R. Present, Phys. Rev. **51**, 788 (1937).

Calculations were also made for the deuteron in a closely parallel form to serve as a control. The analogous S state calculation gives 76 percent for the analytic joining and 92 percent for the new type of joining. With tensor forces, the results are 66 percent and 77 percent for analytic and mere continuity joining, respectively.

The author enjoyed the hospitality of the Massachusetts Institute of Technology. He takes pleasure in thanking Hannah Paul for her fine computing work.

PHYSICAL REVIEW VOLUME 74, NUMBER 12 DECEMBER 15, 1948

Scattering of Particles in Air Showers*

L. EYGES**
Cornell University, Ithaca, New York
(Received August 24, 1948)

The radial distribution of singly scattered particles in air showers is discussed. The probability $\mathcal{P}(x')dx'$ that a singly scattered particle is found in the annular ring between x' and $x'+dx'$ is $\mathcal{P}(x')dx'=0.16(dx'/x'^3)$, where x' is the "Moliere unit." In the deduction of this formula Belenky's expression for the mean square length of a shower, which remains valid below the critical energy, is evaluated. The main process contributing to particles at large distances from the shower axis involves the radiation, and subsequent rematerialization, of electrons below the critical energy.

I. INTRODUCTION

EXTENSIVE cosmic-ray showers are initiated at the top of the atmosphere by particles with energies up to 10^{17} ev. In traversing the atmosphere the electrons and positrons in the shower are scattered by the electrostatic fields of the air nuclei, and over most of the shower's length can be deflected to distances of the order of hundreds of meters from the shower axis. The particles at the largest distances from the axis will be predominantly those which have been scattered once through a large angle (single scattering). For experiments such as those of Skobeltzyn *et al.*[1] it is important to know the radial distribution of these particles. Moliere[2] has calculated this, but the details of the calculation are not given. Moreover, he uses the Arley approximation, neglecting radiation processes below the critical energy, which gives too few low energy electrons, as Moliere himself recognizes. In this paper we have independently calculated the distribution function for singly scattered electrons without using the Arley approximation. It turns out that the most important process contributing to the electrons at large distances is radiation and rematerialization of electrons below the critical energy. Surprisingly enough, however, our result does not differ greatly from Moliere's. It therefore seems clear that Skobeltzyn's[1] assumption that the radial distribution falls off exponentially at large distances is not correct.

II. DERIVATION OF THE SINGLE-SCATTERING FORMULA

In this section we will derive a formula for the distribution of particles which have been once scattered through a sufficiently large angle that the probability of a second scattering through an angle of the same order is small. Hence these particles will retain their original direction except for small deviations resulting from multiple scattering. In this derivation several approximations will be made, without a discussion of their validity. The justification for these approxi-

---

* Part of a thesis presented to Cornell University in partial fulfillment of the requirements for the degree of Doctor of Philosophy.

** Present address: Department of Mathematical Physics, The University, Birmingham, 15, England.

[1] D. V. Skobeltzyn, G. T. Zatsepin, and V. V. Miller, Phys. Rev. 71, 315 (1947).

[2] G. Moliere, *Cosmic Radiation* ed. Heisenberg (Dover Publications, New York, 1946), p. 26.

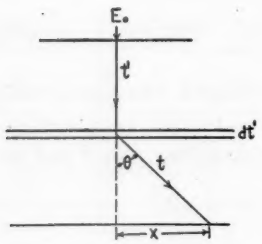

FIG. 1.

mations can only be made after evaluation of the formula, which is done in Sections III and IV. The validity of the approximations is then taken up in Section V.

The probability that an electron of energy E is scattered into the solid angle $2\pi \sin\theta d\theta$ in travelling a distance dt' (radiation units) is:[3]

$$d\sigma = \frac{1}{8\ln(181Z^{-\frac{1}{3}})}\frac{E_s^2}{E^2}\frac{\sin\theta d\theta}{(1-\cos\theta)^2}dt', \quad (1)$$

where $E_s = 21$ Mev is the 'characteristic scattering energy,' and Z is the average atomic number of the scatterer, air in our case. We will assume that although θ is large it is still small enough that the approximations $\sin\theta \approx \theta$, $1-\cos\theta \approx \theta^2/2$ are reasonably good. Using them (1) becomes:

$$d\sigma = \frac{1}{2\ln(181Z^{-\frac{1}{3}})}\frac{E_s^2}{E^2}\frac{d\theta}{\theta^3}dt'. \quad (2)$$

Consider now a shower initiated by a particle of energy E_0. Let the number of particles of energy E at depth t' be $\pi(E_0, E, t')$.

The number of particles of energy E scattered in the layer dt' is $\pi(E_0, E, t')d\sigma$. In traversing an additional thickness t of material these particles suffer a lateral displacement (Fig. 1)

$$x = t\sin\theta \approx t\theta \quad (3)$$

and produce a shower of their own with a total number of particles $\Pi(E, 0, t)$. The number of particles in x, dx at the thickness T is then given by the integral

$$\frac{E_s^2}{2\ln(181Z^{-\frac{1}{3}})}\frac{dx}{x^3}\int_0^{E_0}\frac{dE}{E^2} \times \int_0^T \pi(E_0, E, t')\Pi(E, 0, T-t')(T-t')^2 dt', \quad (4)$$

where we have used $(d\theta/\theta^3) = (dx/x^3)t^2 = (dx/x^3)(T-t')^2$. This integral would be very difficult to evaluate; in fact, it seems impossible to do it analytically. We are saved by one fact; the radial distribution is almost independent of T. The reason is that the distribution depends mainly on the energy distribution of electrons a few radiation lengths back in the shower, and this energy distribution is itself an insensitive function of T. The electrons at more than a few radiation lengths back have no effect on the radial distribution at T, since if they have high enough energy to produce particles at T they will not be scattered, and if they are low enough in energy to be scattered appreciably, will produce no particles at T.

From these arguments we may expect that the radial distribution, *averaged over the shower length*, will be a good approximation to the radial distribution at any point in the shower except near the very beginning and end. This average radial distribution is a much easier quantity to find than the distribution defined by (4). Thus consider the expression for the total number of particles at x integrated over the shower length. This number is:

$$\frac{E_s^2}{2\ln(181Z^{-\frac{1}{3}})}\cdot\frac{dx}{x^3}\int_0^{E_0}\frac{dE}{E^2} \times \int_0^\infty \pi(E_0, E, t')dt' \int_0^\infty t^2\Pi(E, 0, t)dt. \quad (4')$$

The *probability* that a particle is found at x is then this number divided by the total number of particles, integrated over t, which is:

$$\int_0^\infty \Pi(E_0, 0, t)dt = E_0/\beta, \quad (5)$$

where β is the "critical energy." If we use two quantities familiar in shower theory: the "track length,"

$$z_\pi(E_0, E) = \int_0^\infty \pi(E_0, E, t)dt, \quad (6)$$

and the "mean square length" of a shower

$$\langle t^2(E)\rangle_{Av} = \frac{\int_0^\infty \Pi(E, 0, t)t^2 dt}{E/\beta} \quad (7)$$

[3] B. Rossi and K. Greisen, Rev. Mod. Phys. **13**, 262 (1941).

the probability distribution is

$$\mathcal{P}(x)dx=\frac{dx}{x^3}\cdot\frac{E_s^2}{E_0\cdot 2\ln(181Z^{-\frac{1}{2}})}\times\int_0^{E_0}dE\cdot\frac{z_\pi(E_0,E)}{E}\langle t^2(E)\rangle_{Av}.$$

If we use the 'Moliere unit' of length $x'=E_s x/\beta$ and for convenience in later work introduce the dimensionless variables $\epsilon=2.4E/\beta$, $\epsilon_0=2.4E_0/\beta$ into the integral we get

$$\mathcal{P}(x')dx'=\frac{dx'}{x'^3}\frac{\beta^2}{9.06E_0}\int_0^{\epsilon_0}\langle t^2(\epsilon)\rangle_{Av}\frac{z_\pi(\epsilon_0,\epsilon)}{\epsilon}d\epsilon,$$

where $9.06=2\ln(181\cdot 7.22^{-\frac{1}{2}})$. We will now anticipate a future result by defining a new function $G(\epsilon)$ by the equation

$$\frac{z_\pi(\epsilon_0,\epsilon)}{\epsilon}=\frac{\epsilon_0}{\beta}G(\epsilon)=\frac{2.4E_0}{\beta^2}G(\epsilon). \tag{8}$$

$\mathcal{P}(x')$ is then:

$$\mathcal{P}(x')dx'=\frac{dx'}{x'^3}\cdot.265\int_0^{\epsilon_0}\langle t^2(\epsilon)\rangle_{Av}G(\epsilon)d\epsilon. \tag{9}$$

It is clear that the normalization of $\mathcal{P}(x')$ is such that the number of particles in the annular ring between x' and $x'+dx'$ at any depth in the shower is the *total* number of particles at that depth times the probability $\mathcal{P}(x')$ given by (9).

The dependence of the distribution (9) on x' is the same as that given by Moliere. To find the numerical coefficient one must have expressions for z_π and $\langle t^2(\epsilon)\rangle_{Av}$ which remain valid for energies considerably below the critical energy, which is the region where most of the scattering occurs. Such expressions have been given by Belenky[4] in the form of integrals. These are evaluated in the next section.

III. EVALUATION OF $\langle t^2(\epsilon)\rangle_{Av}$

Belenky's expression for $\langle t^2(\epsilon)\rangle_{Av}$ is a sum of five integrals

$$\langle t^2(\epsilon)\rangle_{Av}=\tau_1(\epsilon)+\tau_2(\epsilon)+\tau_3(\epsilon)+\tau_4(\epsilon)+\tau_5(\epsilon). \tag{10}$$

The integral $\tau_1+\tau_3$ which we shall call τ_{13}, is simpler than either τ_1 or τ_3 taken separately, hence we will work with this. The expressions for the τ's are:

$$\tau_{13}(\epsilon)=\frac{2}{q^2}\left(1+\frac{1}{\sigma}\right)^2\int_0^{\epsilon}\times\int_{z'}^{\epsilon}\psi_p(\epsilon,z)\psi_p(\epsilon,z')dzdz', \tag{11a}$$

$$\tau_2(\epsilon)=\frac{2}{q\sigma^2}\int_0^{\epsilon}\psi_p(\epsilon,z)dz, \tag{11b}$$

$$\tau_4(\epsilon)=\frac{2}{q^2}\left(1+\frac{1}{\sigma}\right)\frac{1}{\sigma}\int_0^{\epsilon}\int_{z'}^{\epsilon}\psi_p(\epsilon,z)\times[\psi_\Gamma(z,z')-\psi_p(z,z')]dzdz', \tag{11c}$$

$$\tau_5(\epsilon)=\frac{2}{q^2}\left(1+\frac{1}{\sigma}\right)\int_0^{\epsilon}\int_{z'}^{\epsilon}z\psi_p(\epsilon,z)\times\frac{\partial\psi_p(z,z')}{\partial z}dzdz', \tag{11d}$$

where $q=2.4$ and

$$\psi_p(\xi,\eta)=\eta e^{\eta}\int_{\eta}^{\xi}\frac{e^{-x}}{x^2}dx \tag{12}$$

$$\psi_\Gamma(\xi,\eta)=\psi_p(\xi,\eta)-\frac{\eta}{\xi^2}[1-(\exp-\xi+\eta)]. \tag{13}$$

σ is the photon absorption coefficient per radiation unit, i.e., the sum of the absorption coefficients for pair-production and the Compton effect. For high energies $\sigma=\text{constant}=7/9$. We will be interested mainly in the energy range 10^7 to 10^8 ev, where σ varies somewhat and is in fact less than 7/9. We shall assume for the present that it is constant, however, and correct for the variation later.

Now we define four new quantities, I_{13}, I_2, I_4 and I_5 as the integrals which appear in Eqs. (11). Thus,

$$\tau_{13}=\frac{2}{q^2}\left(1+\frac{1}{\sigma}\right)^2 I_{13}, \tag{14a}$$

$$\tau_2=\frac{2}{q\sigma^2}I_2, \tag{14b}$$

$$\tau_4=\frac{2}{q^2}\left(1+\frac{1}{\sigma}\right)\frac{1}{\sigma}I_4, \tag{14c}$$

[4] S. Belenky, J. Phys. U.S.S.R. 8, 305 (1944).

TABLE I.

	Small ϵ	Large ϵ
$I_2(\epsilon)$	$\epsilon/2-\epsilon^2/12$	$\ln\epsilon-0.425$
$I_{13}(\epsilon)$	$\epsilon^2/12$	$\frac{1}{2}(\ln^2\epsilon-0.85\ln\epsilon-0.43)$
$I_4(\epsilon)$	$-\epsilon^2/36$	$-\frac{1}{2}(\ln\epsilon-1.735)$
$I_5(\epsilon)$	$\epsilon^2/12$	$\ln\epsilon-1.425$

and

$$\tau_5=\frac{2}{q^2}\left(1+\frac{1}{\sigma}\right)I_5. \tag{14d}$$

The integrals can be evaluated in terms of elementary functions, exponential integrals, and rapidly converging series of incomplete Γ-functions.

The expressions for the four integrals I_{13}, I_2, I_4, I_5 can be put simply in terms of three new functions P, Q, and R. Let

$$\ln\gamma=0.5772\cdots=\int_0^1(1-e^{-t}/t)dt-\int_1^\infty e^{-t}/t dt, \tag{15}$$

$$P(\epsilon)=(1/\epsilon)-(e^{-\epsilon}/\epsilon)-1, \tag{16}$$

$$Q(\epsilon)=\ln\epsilon+\ln\gamma+\int_\epsilon^\infty e^{-x}/x dx, \tag{17}$$

$$R(\epsilon)=(1-e^{-\epsilon})\left(\frac{\ln^2\epsilon}{2}+\frac{\ln\epsilon}{\epsilon}\right)-\ln\epsilon-\frac{1}{2}\int_0^\epsilon \ln^2 x e^{-x}dx. \tag{18}$$

Then,

$$I_2(\epsilon)=P(\epsilon)+Q(\epsilon), \tag{19a}$$

$$I_{13}=\ln\gamma[P+Q]+R+2\int_0^\epsilon e^{-x}\times\left[\frac{1}{2!2}+\frac{x^2}{4!4}+\frac{x^4}{6!6}\cdots\right]dx+\int_0^\epsilon e^{-x}\left[\frac{1}{2!}-\frac{x}{3!2}+\frac{x^2}{4!3}+\cdots\right]dx+\int_0^\epsilon\left(\frac{e^{-x}}{x^2}-\frac{1}{x^2}+\frac{1}{x}\right)dx\int_\epsilon^\infty\frac{e^{-y}}{y}dy, \tag{19b}$$

$$I_4=-\frac{3}{2}P-\frac{Q}{2}-\int_0^\epsilon e^{-x}\times\left[\frac{1}{2!2}+\frac{x}{3!3}+\cdots\right]dx, \tag{19c}$$

$$I_5=2P+Q. \tag{19d}$$

There are two independent partial checks on the correctness of these expressions. For ϵ large enough so that $e^{-\epsilon}$ and $1/\epsilon$ are negligible, our expressions agree with those of Belenky.[4] For small ϵ they agree with results obtained by first expanding the integrand in the original integrals and then integrating. The asymptotic forms for small and large ϵ are given in Table I.

As we shall see later, the main contribution to our formula for single scattering will come from small ϵ, and hence from I_2 which varies as ϵ. The other integrals I_{13}, I_4 and I_5 vary as ϵ^2; this is easy to understand. Consider

$$\langle t^2(\epsilon)\rangle_{Av}=\frac{2.4}{\epsilon}\int_0^\infty \Pi(E,0,t)t^2dt. \tag{20}$$

For small ϵ, i.e., energies below the critical energy, where the range R is proportional to ϵ, $R=k\epsilon$ say, if we assume that the particle loses energy mainly by collision loss, we will have one particle for $t<k\epsilon$ and no particles for $t>k\epsilon$. Thus

$$\Pi(\epsilon,0,t)=1 \quad t<k\epsilon,$$
$$\Pi(\epsilon,0,t)=0 \quad t>k\epsilon.$$

Then (20) becomes

$$\langle t^2(\epsilon)\rangle_{Av}=\frac{2.4}{\epsilon}\int_0^{k\epsilon} t^2dt\propto\epsilon^2. \tag{21}$$

I_{13}, I_4, I_5 are thus the contribution to $\langle t^2(\epsilon)\rangle_{Av}$ of this collision process. It is clear that I_2 must correspond to a different kind of process. I_2 represents the contribution to $\langle t^2(\epsilon)\rangle_{Av}$ of a particle which produces a photon very soon after its single scattering, which photon travels a long distance and then materializes into a slow electron. This can be seen from Belenky's derivation of $\langle t^2(\epsilon)\rangle_{Av}$. His result is in the form of integrals over products of track lengths. $I_2(\epsilon)$ comes from the track length γ_r i.e., the track length of photons, in a shower initiated by a photon, and in particular from that part of the expression

which corresponds to the original photon continuing for a considerable distance and then materializing. The importance of this process can be seen from the fact that the photon mean free path remains roughly constant (between 1.2 and 1.6 radiation lengths) down to 10^7 ev, whereas the electron mean free path decreases very rapidly for electrons below the critical energy.

We have calculated numerically $\langle t^2(\epsilon)\rangle_{Av}$ for the region in which the asymptotic forms do not hold. The results are listed in Table II. The dominant integral τ_2 is listed separately.

TABLE II.

ϵ	$\langle t^2(\epsilon)\rangle_{Av}$	$\tau_2(\epsilon)$	ϵ	$\langle t^2(\epsilon)\rangle_{Av}$	$\tau_2(\epsilon)$
0.20	0.141	0.133	2.00	1.503	1.037
0.40	0.286	0.259	3.00	2.241	1.388
0.60	0.435	0.377	4.00	2.939	1.674
0.80	0.586	0.487	5.00	3.589	1.913
1.00	0.738	0.592	6.00	4.197	2.119
1.20	0.890	0.690	7.00	4.764	2.299
1.40	1.044	0.784	8.00	5.295	2.459
1.60	1.197	0.873	9.0	5.795	2.602
1.80	1.350	0.957	10.0	6.627	2.732
2.00	1.503	1.037			

IV. NUMERICAL INTEGRATION

We must now calculate

$$\int_0^{\epsilon_0} \langle t^2(\epsilon)\rangle_{Av} G(\epsilon) d\epsilon. \tag{22}$$

Belenky has given as the expression for z_τ

$$z_\tau(\epsilon_0, \epsilon) = -\frac{\epsilon_0}{\beta}\frac{\partial \psi_p(\epsilon_0, \epsilon)}{\partial \epsilon}. \tag{23}$$

From Eq. (8) then

$$G(\epsilon) = -\frac{1}{\epsilon}\frac{\partial \psi_p(\epsilon_0, \epsilon)}{\partial \epsilon}, \tag{24}$$

where ψ_p is given by (12). After some transformation we get

$$\frac{\partial \psi_p}{\partial \epsilon} = 1 - (\epsilon e^\epsilon + e^\epsilon)\int_\epsilon^\infty \frac{e^{-x}}{x}dx - (\epsilon e^\epsilon + e^\epsilon)\int_{\epsilon_0}^\infty \frac{e^{-x}}{x^2}dx.$$

Since ϵ_0 is at least 10^{12} ev for air showers and the main contribution to the integral (22) comes from around 10^8 ev, we can neglect the last term and get:

$$G(\epsilon) = -\frac{1}{\epsilon}\left[1 - e^\epsilon(1+\epsilon)\int_\epsilon^\infty \frac{e^{-x}}{x}dx\right]. \tag{25}$$

Using our tabulated values for $\langle t^2(\epsilon)\rangle_{Av}$ the integral was done numerically. It is important to know what ranges of ϵ contribute most; Table III gives this information. For $\epsilon<2$ a correction was made for the fact that $\sigma(\epsilon)$, the photon absorption coefficient, varies somewhat.

If we use this result in (9) we get as the final distribution:

$$\mathcal{P}(x')dx' = 0.162dx'/x'^{3}. \tag{26}$$

This is to be compared with Moliere's distribution, in which the numerical coefficient is ≈ 0.1 instead of 0.162.

V. VALIDITY OF THE APPROXIMATIONS

We turn now to a discussion of the assumptions and approximations on which this result is based. The first point to consider—it is at the base of the whole calculation—is whether the large angle scattering we have assumed is really possible. Williams has shown that the finite size of the nucleus limits the scattering probability so that for angles greater than a certain θ_{max} the scattering probability goes rapidly to zero. For air ($Z=7.22$), θ_{max} is given by[3]

$$\theta_{max} \approx (66/E(\text{Mev})). \tag{27}$$

For $\epsilon=2$, $E=72$ and $\theta_{max}=52°$. From Table III we see that roughly 2/3 of the contribution to the integral (22) comes from $\epsilon<2$, i.e., from energies which admit angles greater than 52°. It seems plausible then, especially in view of the fact that the angle defined by (27) is not a perfectly sharp cut-off, that the assumption of large angle single scattering is justified.

We now consider the angular approximations in the scattering formula (1). We have used $(4d\theta/\theta^3)$ as an approximation to the correct expression $[\sin\theta d\theta/(1-\cos\theta)^2]$. In terms of $x/t=\zeta=\sin\theta$ we have replaced the exact expression

$$\frac{d(\cos\theta)}{(1-\cos\theta)^2} = \frac{\zeta d\zeta}{[1-(1-\zeta^2)^{\frac{1}{2}}]^2(1-\zeta^2)^{\frac{1}{2}}}$$

by the approximate expression $(4\zeta d\zeta/\zeta^4)$. The

TABLE III.

a	b	$\int_a^b \langle t^2(\epsilon)\rangle_{Av} G(\epsilon)d\epsilon$
0	0.2	0.028
0.2	0.4	0.121
0.4	1	0.154
1	2	0.105
2	10	0.167
10	∞	0.026
0	∞	0.601

ratio r of the exact expression to the approximate one is:

$$r=\zeta^4/4(1-\zeta^2)^{\frac{1}{2}}[1-(1-\zeta^2)^{\frac{1}{2}}]^2. \tag{28}$$

Introducing $(1-\zeta^2)^{\frac{1}{2}}=\cos\theta=\eta$ we get

$$r=\frac{\left(\frac{1+\eta}{2}\right)^2}{\eta}. \tag{29}$$

r thus turns out to be

$$\left(\frac{\text{arithmetic mean of } \eta \text{ and } 1}{\text{geometric mean of } \eta \text{ and } 1}\right)^2.$$

We might expect from this that r remains close to 1 over a large region, and this turns out to be the case. Thus for $\theta=53°$, $r=1.07$, $\theta=66°$, $r=1.22$ and for $\theta=78°$, $r=1.80$. Beyond 80° the approximation rapidly becomes worse, and blows up completely at 90°. For large angles we see that $r>1$, i.e., that our approximation gives too small a result. This error is partially compensated by another approximation we have made. It is clear from Fig. 1 that t must always be greater than x. This means that the last integral in (4) should not be

$$\int_0^\infty t^2\Pi(E, 0, t)dt \tag{30}$$

but

$$\int_x^\infty t^2\Pi(E, 0, t)dt. \tag{31}$$

The error involved in this replacement is hard to estimate, but obviously is an increasing function of x. It is true however that most of the contribution to (31) comes from large t, hence the approximation represented by (30) is probably not intolerable. We can see that large t contribute most by considering the expressions for $\langle t^2(\epsilon)\rangle_{Av}$ and $\langle t(\epsilon)\rangle_{Av}^2$.

For small ϵ Belenky has found $\langle t(\epsilon)\rangle_{Av}=0.94I_2(\epsilon)$ where I_2 is given by (15). Thus

$$\langle t(\epsilon)\rangle_{Av}\approx 0.47\left(\epsilon-\frac{\epsilon^2}{12}+\cdots\right).$$

We get from Table I and Eqs. (11) that

$$\langle t^2(\epsilon)\rangle_{Av}=0.69\left(\epsilon+\frac{\epsilon^2}{18}+\cdots\right).$$

We see that for ϵ as large as 2, which includes the most important energy range for our integral (22) that $\langle t^2(\epsilon)\rangle_{Av}$ is considerably larger than $\langle t(\epsilon)\rangle_{Av}^2$, confirming that most of the contribution to the integral comes from large t.

It is a pleasure to thank Professor H. A. Bethe for suggesting this problem and for essentially deriving Eq. (9), as well as for several helpful discussions.

PHYSICAL REVIEW VOLUME 74, NUMBER 12 DECEMBER 15, 1948

Starting Potential of the Geiger-Mueller Counter Discharge

P. B. WEISZ
Socony-Vacuum Laboratories, Research and Development Department, Paulsboro, New Jersey
(Received August 5, 1948)

The starting voltage for the pulse-equalizing Geiger-Mueller tube discharge has been measured for mixtures of argon and hydrocarbons and helium and hydrocarbons. The results are discussed in the light of the known ionization potentials of the homologous series of normal hydrocarbons and the energy levels of the phenomena which contribute directly—by ionization—or indirectly—by metastable intermediates—to the production of the ions in the initial process.

INTRODUCTION

LITTLE has been discussed concerning the relationship between the "starting potential" for the Geiger-Mueller (G-M) counter discharge and the physical constants of the gases present. A brief study was made on the resulting "starting potentials" when a series of different gas constituents was used under otherwise identical conditions of geometry and gas pressures with gases for which the important electronic energy levels were known.

Quite often the word "starting potential" is used simply to identify the voltage necessary across a G-M tube so that it will "count." This is no clear definition since the ability for the apparatus to record "counts" is primarily determined by the minimum sensitivity of the associated circuits. If these were sensitive enough, a small collecting potential across the tube would be sufficient to have the apparatus "count" as a pulse recording ionization chamber. A definition which is truly related to the setting-in of the Geiger-Mueller discharge mechanism is that adopted by Korff.[1] It is the voltage at which pulse-size equalization sets in.

At this voltage, the discharge spreading mechanism is assumed to be complete to the point where a further growth of the discharge is limited by the positive space-charge sheath of gaseous ions. For a quantitative discussion regarding the voltage at which the discharge growth becomes "complete" in this sense it would be necessary to know more about the mechanism of spreading than is known at this time. We may assume that this condition requires the production of a minimum number of electrons (and ions) in the ordinary avalanche process, leading to just sufficient numbers of photons capable of progressively producing "neighbor"-avalanches down the length of the anode wire. The ordinary avalanche process has been treated to some extent theoretically and experimentally by Rose and Korff.[2] They show that the amplification factor $A=N_f/N_0$, where N_0 is the initial number of ionization electrons and N_f the final number after avalanche multiplication and without photon propagation of the discharge, is a rapid function of voltage applied across the electrodes of the form

$$A=\exp\{aV_0^{\frac{1}{2}}[(V_0/V_t)^{\frac{1}{2}}-1]\}. \qquad (1)$$

This relationship was arrived at by making such assumptions as that all electron production is due to a simple ionization process setting in at one critical electron energy expressed as an "average ionization potential" of the gases, having a cross section rising linearly with increasing electron energies and treating the electron energy distribution in terms of an "average electron energy." In this manner the pertinent physical constants of the gases are contained in a and V_t of (1), which in essence lumps them into experimentally available quantities.

In studying the starting potential, we assume that the number of basic avalanches, each of which grows in a manner indicated by (1), is in itself multiplied by a propagating mechanism (such as photon-emission and photo-ionization) to provide spreading of the discharge and pulse equalization. In the sub-starting voltage region of operation where (1) is valid, measurements of

[1] S. A. Korff, *Electron and Nuclear Counters* (D. Van Nostrand Companv. Inc., New York, 1946), p. 15.

[2] M. E. Rose and S. A. Korff, Phys. Rev. 59, 850 (1941).

TABLE I. (Argon).*

$I_A = 15.77$ ev	(ion potential)
$M_{A,1} = 11.72$ ev	(metastable states)
$M_{A,2} = 11.54$ ev	

* From R. F. Bacher and S. Goudsmit, *Atomic Energy States* (Mc Graw-Hill Book Company, Inc., New York, 1932), calculated with the conversion factor 1 ev $\leqq$ 8067.49 cm^{-1}.

the voltage at which gas amplification factor is attained for different gases should reflect such physical constants as the ionization potential and cross section. Similarly, if the mechanism of spreading does not vary sufficiently for a series of different gases, the starting potential may still reflect such physical constants as are still responsible for the development of the basic avalanches.

Some experiments will be shown concerning G-M starting potentials obtained for a series of different gases and will be discussed in the light of the basic electron multiplication mechanism. The attainment of low starting potentials will also be discussed in view of the results obtained.

EXPERIMENTAL

All data were obtained on two tubes of identical construction, containing 15-cm long cylindrical copper cathodes and 0.003-inch diameter tungsten wire anodes. The tubes were first evacuated and baked in a furnace at 300°C for about 15 minutes, the pressure in the vacuum system being somewhat better than 1 micron. Subsequently, oxygen was admitted for 10 minutes, allowing oxidation of the copper cathode

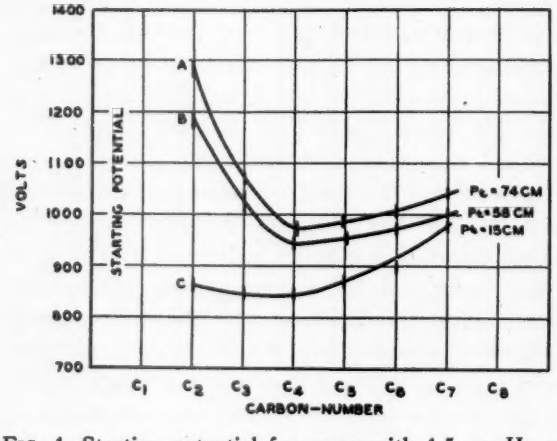

FIG. 1. Starting potential for argon with 1.5 cm Hg of partial pressure of saturated *n*-hydrocarbons.

to a reddish color to proceed, the gas again evacuated, and the furnace removed after another 10 minutes of pumping. During this pumping period the center wire was "flashed" in the usual manner.

A variable counter voltage was applied from an electronically stabilized H.V. rectifier, the voltage being readable to ± 20 volts or better. The pulses were observed on a DuMont type 224 oscilloscope over a 1-megohm dropping resistor to the counter anode wire.

The vacuum system was operated on a Welsh Duo Seal mechanical pump with a dry ice-acetone main trap and mercury manometers. The mixtures were made in a separate flask allowing sufficient time for mixing, and the gas mixtures were admitted to both tubes.

The starting potential for each mixture was determined by progressively increasing the operating voltage until all pulses appeared in equal size on the oscilloscope screen. The estimate of pulse equalization may appear to be vague; however, the transition from essentially random pulse distribution to complete equalization is so rapid with voltage near the starting potential that this potential can be determined without difficulty within an interval no larger than the error of voltage measurement.

This measurement can be carried out with a radiation source sufficient to make convenient observation of pulse size, but must not be so strong that an appreciable number of statistical pulse intervals would be smaller than the recovery time of the tube.* Roughly speaking, the number of pulses per second should not be greater than $1/100\tau$, where τ is the recovery time in seconds. For a recovery time of the order of 100 μsec. as was the case in the tubes used, the pulse rate was held below 100/sec.

A series of runs was made using in every case a mixture of argon and a polyatomic quenching gas, at total pressures of 15, 58, and 74 cm Hg, with the quenching gas constituting a partial pressure of 1.5 cm Hg throughout. As quenching gases the normal (straight-chain) hydrocarbons from methane through heptane were used.

* Ionizing events occurring within such time intervals from preceding ones may result in smaller pulse sizes because of the shielding effect of the unremoved positive ions; see H. G. Stever, Phys. Rev. 61, 38 (1942).

Figure 1 shows the starting potentials obtained for these runs as a function of the total pressure, and the carbon number of the hydrocarbon (C_1=methane, C_2=ethane, etc.).

As will be seen in the subsequent discussion, it was of interest to try the same quenching gases with another monatomic gas which has all metastable energy levels above all of the ionization potentials of the quenching gases, and helium was therefore chosen for the comparison. Figure 2 shows a run using helium plus 1.5 cm Hg of quenching gases, at total pressures of 15 and 67 cm Hg.

Finally, a run was made to determine starting potentials for decreasing concentrations of a given quenching gas in argon at constant total pressure. Such runs were carried out for the three gases *n*-butane, *n*-heptane, and ethyl-alcohol, each at two total pressures of 15 and 67 cm Hg. Figure 3a, b, c shows the results of these measurements. Besides the equalization voltage (starting potential) an approximate "breakdown" voltage was measured as the voltage at which "pulse trains" first appeared. The latter appears as the curve to the right of the curve pair.

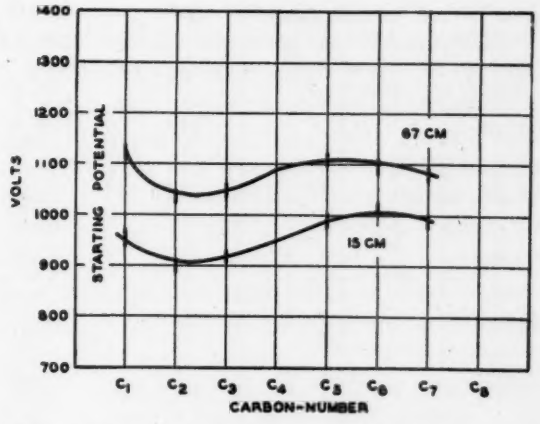

FIG. 2. Starting potentials for helium with 1.5 cm Hg of partial pressure of partial pressure of saturated *n*-hydrocarbons.

DISCUSSION

It is obvious that for the process of electron multiplication in the gas we have[2]

$$-dN = N(r)dr \int_{E_0}^{E_{\max}} (n(E_1 r))/(\lambda(E))dE, \quad (2)$$

where $N(r)$ is the number of electrons at a radius r from the center of the tube, E the electron energy such that $n(E, r)dE$ is the fraction of all electrons at r having energies between E and $E+dE$, and at such energy having a mean free path $\lambda(E)$ for collisions resulting in the production of a secondary electron. Rose and Korff made the simplifying assumption that a discrete lower limit of energy E_0 exists which is equal to an "average ionization potential." If we wish to analyze the ability of a given gas to create secondaries in more detail, we must consider the following:

(a) The ionizing collision may not be the only electron-generating collision process. It is possible that collisions leading to metastable excited atoms of A will become electron donors subsequently when these atoms collide with molecules of Q, if the ionization potential I_Q is equal or smaller than the energy of the metastable state M_A.

(b) In a mixture of A and Q the "effective" ionization potential may therefore involve the potential representing the energy of such metastable states if they are produced in sufficient quantity to indirectly participate in secondary electron production. Such ionization by metastables states is quite important, as has been pointed out frequently in connection with gas discharge problems.[3] Penning[4] has studied this effect for the breakdown between parallel plane electrodes.

(c) In a mixture of A and Q with effective electron-producing energy levels J_A and J_Q (i.e., ionization or metastable energies), the lower of the two will be the one contributing more to the multiplication process, since the lower energy process will inhibit the growth of the electron energy distribution $n(E, r)$ so as to reduce the number of electrons permitted to gain sufficiently high energies for the more energetic production processes. This will be the more important the greater the energy difference between the two levels is, or—in other words—the larger the number of possible collisions is for electrons while gaining energy from J_Q to J_A (with $J_Q < J_A$).

(d) In the case of some polyatomic gases the cross section for ionization of the parent molecule is smaller than the cross section for collisions leading to an ionized and unionized fragment. The appearance potential (which is the term used in mass spectrometry) for this ionization-dissociation process is usually higher than that for simple ionization.

(e) It was already pointed out by Rose and Korff[2] that the energy distribution of the electrons and consequently the ability to multiply is markedly influenced by the availability of cross sections for vibrational energy transfers. The sum of such available cross sections would be expected to increase with molecular complexity.

---

[3] See, e.g., M. J. Druyvesteyn and F. M. Penning, Rev. Mod. Phys. 12, 87 (1940).

[4] F. M. Penning, Zeits. f. Physik 46, 335 (1927).

TABLE II.

Molecule (Q) or fragment (F)		I_Q or I_F ev	ρ_F/ρ_A
Methane	CH_4^+	13.04	1.00
	CH_3^+	14.3***	0.86
Ethane	$C_2H_6^+$	11.76	1.00
	$C_2H_4^+$	12.84*	3.82
Propane	$C_3H_8^+$	11.21	1.00
	$C_2H_5^+$	12.21**	3.45
n-butane	$C_4H_{10}^+$	10.80	1.00
	$C_3H_7^+$	11.14*	7.95
n-pentane	$C_5H_{12}^+$	10.55	1.00
	$C_3H_7^+$	11.1*	11.3
n-hexane	$C_6H_{14}^+$	10.43	1.00
	$C_4H_9^+$	10.90***	7.15
n-heptane	$C_7H_{16}^+$	10.35	1.00
	$C_3H_7^+$	?	7.60
Ethyl-alcohol	$C_2H_5OH^+$	11.3±0.2†	1.00
	CH_2OH^+	11.3±0.2†	6.1

* D. P. Stevenson and J. A. Hipple, J. Am. Chem. Soc. **64**, 1588 (1942).
** D. P. Stevenson and J. A. Hipple, J. Am. Chem. Soc. **64**, 2769 (1942).
*** R. E. Honig, this laboratory, unpublished.
† C. S. Cummings and Walker Bleakney, Phys. Rev. **58**, 787 (1940).

(f) It is not impossible that cross sections leading to dissociating excited states, without ionization, of polyatomic molecules may also be active in influencing the progress of the electron energy distribution.

These considerations should be applicable to suitably designed measurements of the gas amplification factor itself for various gases and gas mixtures, and they may reflect themselves similarly in measurements of starting potentials.

The normal hydrocarbon series of compounds was chosen for the measurements because a great deal is known regarding their behavior under electron bombardment from mass spectrometer studies, including ionization potentials, appearance potentials of fragment ions, as well as relative cross section for the various processes.

In order to discuss the system argon—*n*-hydrocarbon it seems best, therefore, to present all pertinent information concerning these gases. Table I shows the pertinent energy data for argon.

Table II shows the ionization potentials I_Q of the hydrocarbons[5] from methane to *n*-heptane, the appearance potential I_F of the fragment ion process of largest cross section, ρ_F, and the cross section of the latter relative to that of the parent-ionization process, ρ_Q. The appearance potentials were taken from sources indicated by the footnotes. The relative cross sections of parent and fragment ion processes were calculated from mass spectral data[6] for electrons of 50-ev energy.

Examination of these data reveals that all ionization potentials of the gases in Table II are below that of argon. However, considering the argon metastable energy levels, methane and ethane are found to have ionization and appearance potentials above both metastable levels. In case of ethane, the ionization potential of 11.76 ev is so close to that of 11.72 ev ($M_{A,2}$), that the degree of uncertainty in the measurement of I_{ethane} and consideration of additional kinetic energies raises the possibility that one of the metastable states ($M_{A,2}$) may produce ethane ions.

In case of propane, the parent ion is formed by an energy lower than both $M_{A,1}$ and $M_{A,2}$, yet the fragment ion formation, which in electron-propane interaction is the more probable one, cannot be brought about by either metastable state.

Beginning with butane, however, all hydrocarbon ions and most abundant ion fragments can be formed at energies clearly less than either of the metastable argon states.

Figure 1 shows a rapidly dropping starting potential for ethane and propane reaching the minimum with butane for the mixtures richest in argon (98 percent in curve *A* and 97.3 percent in curve *B*). In view of the data just mentioned, this may reasonably be explained by the fact that as we pass through C_3 (propane) the metastable argon states become, progressively, electron "donors" at a level of 11.54 to 11.72 ev, as compared to 15.77 ev required ionization energy.

Past C_3 the ionization potentials of the gases do not change much. The slow rise in starting potential could be due to a number of processes. It may be due to providing more available cross sections for energy losses in line with (5) or (6) of the above discussion. It would also involve

[5] R. E. Honig, J. Chem. Phys. **16**, 105 (1948).

[6] Catalog of Mass Spectral Data, American Petroleum Institute Research Project 44, National Bureau of Standards, Washington, D. C.

the nature of the competitive reactions for the destruction of metastables for the various gases Q having different resonance levels leading to fragmentation+ionization with the reaction

$$M_A + A \rightarrow A + A + \text{kin. energy},$$

or any non-ionizing de-excitation by dissociation.

It is to be noted that methane could not be used in these experiments because no Geiger-Mueller discharge region can be produced with the partial gas pressures used.

Experiments with He as the inert gas, shown in Fig. 2, were carried out because in this case the only metastable state of He ($M_{He} = 19.81$ ev) lies entirely above the ionization potentials and the important fragment-ionization potentials of all the compounds used here. Thus, the effect of dropping starting potentials from methane through propane should not exist in case of helium if the assumed mechanism is the one responsible. Figure 2 confirms this supposition. Furthermore, even methane, now presenting critical ionization potentials less than both ionization and metastable argon levels, was operable as an added gas yielding a small Geiger-Mueller region ("plateau"). There is some structure to the curves of Fig. 2 which is not easily interpretable. The same argument applies as in case of the slow rise of the argon curve.

CONSIDERATIONS REGARDING OPERATION OF G-M COUNTERS AT LOW VOLTAGES

Some general conclusions might be stated concerning the problem of constructing G-M tubes operable at low voltages.

It would appear that to attain this end the two requirements will be: (a) providing an electron "donor" mechanism at the lowest possible energy level; (b) to remove as much as possible any mechanisms leading to inelastic energy losses for electrons of energies lower than the levels responsible for condition (1).

It must be emphasized, of course, that in any particular case the assumptions made at the beginning of this paper are valid, namely, that the discharge propagating mechanism not be radically different in the case of comparison between different gases. Furthermore, other considerations must be fulfilled, some concerned with other requirements for the quenching mechanism to function properly (e.g., concerning de-excitation on the cathode wall), some others of practical nature (e.g., chemical compatibility with materials used).

An experiment was carried out to ascertain how far the above principles could be realized with the gases used in this work, namely, by choosing a quenching gas such as butane or higher molecular weight hydrocarbon so as to take full advantage of the argon-metastable states and using this gas at the lowest operable concentration so as to reduce non-ionizing inelastic energy losses as far as possible.

By progressively diluting an initial mixture of argon and butane and also one of argon and

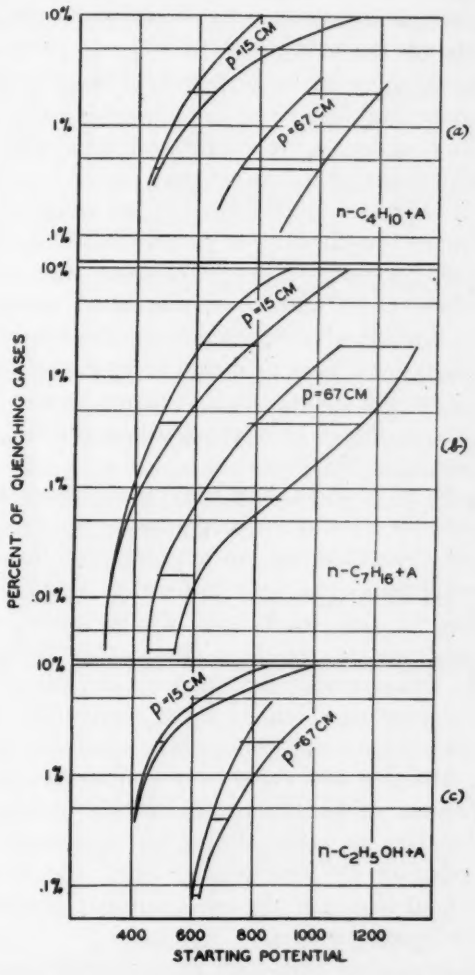

FIG. 3. Starting potentials and approximate breakdown potentials for argon with small admixtures of hydrocarbon quenching gases.

heptane with additional argon, the starting potentials and breakdown voltages, as defined above, were obtained for constant total pressure but decreasing partial pressures of the quenching gas.

A rough order-of-magnitude estimate of quenching gas concentration which might be able effectively to convert argon metastables to ions of the quenching gas can be made as follows: we assume that the discharge must be fully developed before an appreciable part of the ion sheath passes the dead-time radius. Since the dead-time interval for the tubes used here is of the order of 20 to 30 μsec., we will require that the metastable-to-ion transition take place in a time of the order of 10^{-5} sec. or smaller. At a pressure of about $\frac{1}{2}$ atmospheric pressure (and room temperature) the mean molecular collision time is of the order of 10^{-10} second. Thus during the allowed time there is a mean of 10^5 collisions possible between a metastable molecule and any molecule, or $\eta \times 10^5$ collisions with a quenching gas molecule, where η is the relative concentration of quenching gas to argon. Depending on the efficiency of the metastable-to-ion transfer process, a very small concentration may be sufficient, for with these numerical assumptions a concentration of quenching gas somewhat exceeding 0.001 percent would yield appreciable metastable-ion conversion if the cross section for this process should be nearly equal to the kinetic collision cross section.

Figure 3a, b, and c show the starting potentials obtained for three quenching gases at decreasing relative concentration. An approximate "breakdown-voltage" was also measured. While the purpose of this work was not to study the practicability of different gases, this "breakdown" measurement gives at least an indication of a "counting" range. It is seen that, for example, the starting voltage is reduced considerably, down to 400 volts for a concentration of 0.1 percent of heptane in 15 cm Hg of argon. Similar data on ethyl alcohol are presented for the purpose of comparison, since the latter compound is one of the most familiar practical quenching gases.

When dealing with such small concentrations of added gases, the significance of the measurements has to be examined in the light of possible effects of impurities, of course. In case of the argon experiments, the following impurities or impurity limits may be present:

Vacuum system:	H_2O:	0.001 percent
(from vapor pressure at -78°C)		
	Hg	10^{-7} percent
(from vapor pressure at -78°C)		
Argon:[7]	N_2:	0.4 percent
	H_2:	0.001 percent
	O_2:	0.001 percent

For the purpose of these measurements, only impurities of gases having ionization potentials below 11.72 ev would have to be considered. Of the gases listed, only Hg, H_2O, and O_2 fall into this class, and it is seen that their concentration is appreciably below the minimum concentration of hydrocarbons used in this work.

The gases used in this investigation are polyatomic and result in self-quenching type counter tube characteristics. Simpson[8] has briefly reported low starting potential tubes of the non-self-quenching type using small concentration of metastable-destructive gases added to argon and helium similar to those used by Penning[4] in his work on the breakdown potential of these gases. Liebson[9] has reported low voltage operation with similarly small concentration of iodine and bromine in argon or neon, which he reported to have self-quenching action despite their diatomic nature.[10] Presumably, iodine ($I = 9.7$ ev) was used to quench metastables in the case of argon and bromine ($I = 12.8$) in the case of neon ($M = 16.7$ ev).

In conclusion it should be said that it was not the purpose of this work to investigate the *practical* aspects of hydrocarbon compounds as quenching gases. Their practical counting characteristics are poor, particularly their limited lifetime resulting presumably from a tendency to form polymer deposits.

The author wishes to thank Mr. W. P. Kern for his assistance in carrying out experimental work.

---

[7] Information supplied by the Matheson Company, East Rutherford, New Jersey.
[8] J. A. Simpson, Jr. Phys. Rev. **72**, 181 (1947).
[9] S. H. Liebson, Phys. Rev. **72**, 181 (1947).
[10] Possible mechanisms were subsequently discussed by R. D. Present, Phys. Rev. **72**, 243 (1947).

Note on Polarization Effects in Compton Scattering

A. WIGHTMAN
Palmer Physical Laboratory, Princeton University, Princeton, New Jersey
(Received September 1, 1948)

A derivation of the probability of Compton scattering for an arbitrary initial and final photon polarization is sketched. The result is applied to the case of two successive Compton scatterings, and some possibilities of experimental verification are discussed. A remark is made on a simplification of the calculations of Compton scattering when it is used to analyze the polarization of annihilation quanta.

THE aim of this note is to treat the Compton effect for polarized light and make two applications of the result. Although Nishina has already dealt with this problem[1] it is convenient to sketch in Section I another derivation which puts the result in a form more suitable for the present applications.[2] In Section II the result of Section I is used to obtain the azimuthal variation in intensity of initially unpolarized light which has undergone two Compton scatterings. The result has already been obtained by Nishina for the case of right angle scattering,[3] but to get the maximum variation intensity, as is desirable experimentally, one must go to angles other than ninety degrees. In Section III the result of Section I is used to show how a suitable choice of coordinates permits one to deduce directly from the Klein-Nishina formula the result of Pryce and Ward[4] for the coincidence rate in an experiment on the polarization of annihilation quanta.

I. DERIVATION OF THE TRANSFORMATION MATRIX

We wish to calculate the differential cross section for scattering of a photon of momentum $\mathbf{k}_0$ with an arbitrary initial polarization state to a final momentum $\mathbf{k}$ and an arbitrary final polarization state. To specify the initial and final polarization states we use statistical matrices U and W respectively.[5] U and W have two rows and columns labeled by two independent polarization states. The differential cross section is of the form

$$\sum_{lmst} U_{lm} S_{lm,st}(\mathbf{k}_0, \mathbf{k}) W_{st}. \tag{1}$$

To identify the matrix elements of S, write Eq. (18) p. 149 of QTR for the scattering of an initial photon specified by the polarization vector $\sum_{l=1,2} c_l \boldsymbol{\varepsilon}_l$ to a final state specified by the polarization vector $\sum_{s=1,2} d_s \boldsymbol{\zeta}_s$

$$\frac{d\sigma}{d\Omega} = e^4 \left(\frac{k}{k_0}\right)^2 \frac{E}{\mu} \sum_u A v_{u_0} \times \left| \sum_{u'u''} \frac{(u_0, \sum c_l \boldsymbol{\varepsilon}_l \cdot \boldsymbol{\alpha} u')(u', \sum d_s^* \boldsymbol{\zeta}_s^* \cdot \boldsymbol{\alpha} u)}{\mu + k_0 - E'} + \frac{(u_0, \sum d_s^* \boldsymbol{\zeta}_s^* \cdot \boldsymbol{\alpha} u'')(u'', \sum c_l \boldsymbol{\varepsilon}_l \cdot \boldsymbol{\alpha} u)}{\mu - k - E''} \right|^2. \tag{2}$$

(Equation (18) has been averaged over the initial and summed over the final spin states of the electron, the possibility of complex polarization vectors is not excluded.) This expression for the differential scattering cross sections may be rewritten in the form

$$\frac{d\sigma}{d\Omega} = \frac{1}{4} \left(\frac{e^2}{mc^2}\right)^2 \left(\frac{k}{k_0}\right)^2 \sum_{lmst} c_m^* c_l d_t^* d_s S_{lm,st}, \tag{3}$$

where the matrix S is defined by the equation

$$S_{lm,st} = \frac{4\mu}{E} \sum_u A v_{u_0} \times \left(\sum_{u'u''} \frac{(u_0, \boldsymbol{\alpha} \cdot \boldsymbol{\varepsilon}_m u')(u', \boldsymbol{\alpha} \cdot \boldsymbol{\zeta}_s^* u)}{\mu + k_0 - E'} + \frac{(u_0, \boldsymbol{\alpha} \cdot \boldsymbol{\zeta}_s^* u'')(u'', \boldsymbol{\alpha} \cdot \boldsymbol{\varepsilon}_m u)}{\mu - k - E''} \right)^* \times \left(\sum_{u'u''} \frac{(u_0, \boldsymbol{\alpha} \cdot \boldsymbol{\varepsilon}_l u')(u', \boldsymbol{\alpha} \cdot \boldsymbol{\zeta}_t^* u)}{\mu + k_0 - E'} + \frac{(u_0, \boldsymbol{\alpha} \cdot \boldsymbol{\zeta}_t^* u'')(u'', \boldsymbol{\alpha} \cdot \boldsymbol{\varepsilon}_l u)}{\mu - k - E''} \right), \tag{4}$$

[1] Y. Nishina, Zeits. f. Physik. 52, 869 (1929).
[2] The present derivation runs parallel to that of W. Heitler *Quantum Theory of Radiation* (Oxford University Press, London, 1936), pp. 146–60 for the Klein-Nishina formula. Heitler's book will be referred to hereafter as QTR.
[3] Reference (1) page 876.
[4] M. H. Pryce and J. C. Ward, Nature 160, 435 (1947).
[5] For the use of a statistical matrix to describe a state see, for example, Kemble *Principles of Quantum Mechanics* (McGraw-Hill Book Company, Inc., New York, 1937), p. 434.

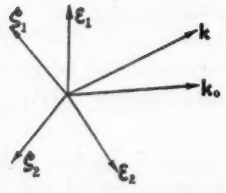

FIG. 1. Polarization vectors $\boldsymbol{\varepsilon}_1$ and $\boldsymbol{\varepsilon}_2$ for incoming photon $\mathbf{k}_0$, and $\boldsymbol{\zeta}_1$ and $\boldsymbol{\zeta}_2$ for scattered photon $\mathbf{k}$. $\boldsymbol{\zeta}_1$, $\boldsymbol{\varepsilon}_1$ and $\mathbf{k}$ lie in a plane perpendicular to the plane which contains $\boldsymbol{\zeta}_2$, $\boldsymbol{\varepsilon}_2$ and $\mathbf{k}_0$.

The case considered here is that in which the initial and final states are pure states. They have the statistical matrices

$$U_{lm}=c_m^*c_l, \quad W_{st}=d_t^*d_s,$$

respectively. U and W are normalized to unit trace:

$$\sum_m U_{mm}=1, \quad \sum_s W_{ss}=1.$$

In the more general case of mixed states it will be impossible to decompose the elements of the statistical matrices U and W into simple products. However, the principle of superposition insures that the matrix S itself will remain unaltered in this situation.

The evaluation of $S_{lm,\,st}$ can be carried out by the methods described in QTR. The details will not be reproduced here. The result is

$$S_{lm,\,st}=\boldsymbol{\varepsilon}_l\cdot\boldsymbol{\zeta}_t^*\boldsymbol{\varepsilon}_m^*\cdot\boldsymbol{\zeta}_s\left[3+\frac{E}{\mu}+\frac{k-k_0}{\mu}\frac{\mathbf{k}_0\cdot\mathbf{k}}{k_0k}\right]$$
$$+\left[\boldsymbol{\varepsilon}_l\cdot\boldsymbol{\varepsilon}_m^*\,\boldsymbol{\zeta}_s\cdot\boldsymbol{\zeta}_t^*-\boldsymbol{\varepsilon}_l\cdot\boldsymbol{\zeta}_s\,\boldsymbol{\varepsilon}_m^*\boldsymbol{\zeta}_t^*\right]$$
$$\times\frac{E-\mu}{\mu}\left(1-\frac{\mathbf{k}_0\cdot\mathbf{k}}{k_0k}\right). \quad (5)$$

A useful basis for the polarization states of initial and scattered photon is that of Fig. 1. The unit vectors are chosen so that

$$\boldsymbol{\varepsilon}_1\cdot\boldsymbol{\varepsilon}_2=\boldsymbol{\zeta}_1\cdot\boldsymbol{\zeta}_2=0, \quad \boldsymbol{\varepsilon}_1\times\boldsymbol{\varepsilon}_2=\frac{\mathbf{k}_0}{k_0}, \quad \boldsymbol{\zeta}_1\times\boldsymbol{\zeta}_2=\frac{\mathbf{k}}{k},$$

and so that $\boldsymbol{\zeta}_1$ lies in the plane of $\boldsymbol{\varepsilon}_1$ and $\mathbf{k}$, while $\boldsymbol{\zeta}_2$ lies in the plane of $\mathbf{k}_0$ and $\boldsymbol{\varepsilon}_2$. As a result $\boldsymbol{\varepsilon}_1\cdot\boldsymbol{\zeta}_2=0$, but $\boldsymbol{\varepsilon}_2\cdot\boldsymbol{\zeta}_1$ will be zero only when $\mathbf{k}$, $\mathbf{k}_0$ and $\boldsymbol{\varepsilon}_1$ lie in the same plane. If the symbol $\parallel$ be used as equivalent to the subscript 1 and the symbol $\perp$ as equivalent to the subscript 2, then S takes the following form

$$S_{lm,\,st}=\begin{array}{c|cccc}
 & \parallel\parallel & \perp\perp & \parallel\perp & \perp\parallel \\
\parallel\parallel & \frac{k}{k_0}+\frac{k_0}{k}-2 & \frac{k}{k_0}+\frac{k_0}{k}-2 & 0 & 0 \\
 & +4(\boldsymbol{\varepsilon}_1\cdot\boldsymbol{\zeta}_1)^2 & & & \\
\perp\perp & \frac{k}{k_0}+\frac{k}{k}-2 & \frac{k}{k_0}+\frac{k_0}{k}-2 & 4(\boldsymbol{\varepsilon}_2\cdot\boldsymbol{\zeta}_2)(\boldsymbol{\varepsilon}_2\cdot\boldsymbol{\zeta}_1) & 4(\boldsymbol{\varepsilon}_2\cdot\boldsymbol{\zeta}_2)(\boldsymbol{\varepsilon}_2\cdot\boldsymbol{\zeta}_1) \\
 & +4(\boldsymbol{\varepsilon}_2\cdot\boldsymbol{\zeta}_1)^2 & +4(\boldsymbol{\varepsilon}_2\cdot\boldsymbol{\zeta}_2)^2 & & \\
\parallel\perp & 4(\boldsymbol{\varepsilon}_1\cdot\boldsymbol{\zeta}_1)(\boldsymbol{\varepsilon}_2\cdot\boldsymbol{\zeta}_1) & 0 & -(\boldsymbol{\varepsilon}_1\cdot\boldsymbol{\zeta}_1)(\boldsymbol{\varepsilon}_2\cdot\boldsymbol{\zeta}_2) & (\boldsymbol{\varepsilon}_1\cdot\boldsymbol{\zeta}_1)(\boldsymbol{\varepsilon}_2\cdot\boldsymbol{\zeta}_2) \\
 & & & \times\left(\frac{k}{k_0}+\frac{k_0}{k}-2\right) & \times\left(3+\frac{E}{\mu}+\frac{k-k_0}{\mu}\frac{\mathbf{k}_0\cdot\mathbf{k}}{k_0k}\right) \\
\perp\parallel & 4(\boldsymbol{\varepsilon}_1\cdot\boldsymbol{\zeta}_1)(\boldsymbol{\varepsilon}_2\cdot\boldsymbol{\zeta}_1) & 0 & (\boldsymbol{\varepsilon}_1\cdot\boldsymbol{\zeta}_1)(\boldsymbol{\varepsilon}_2\cdot\boldsymbol{\zeta}_2) & -(\boldsymbol{\varepsilon}_1\cdot\boldsymbol{\zeta}_1)(\boldsymbol{\varepsilon}_2\cdot\boldsymbol{\zeta}_2) \\
 & & & \times\left(3+\frac{E}{\mu}+\frac{k-k_0}{\mu}\frac{\mathbf{k}_0\cdot\mathbf{k}}{kk_0}\right) & \times\left(\frac{k}{k_0}+\frac{k_0}{k}-2\right)
\end{array}. \quad (6)$$

It will be noted that the four matrix elements in the upper lefthand corner are just four cases of the Klein-Nishina formula, apart from a proportionality factor.

When the incident photon is unpolarized the scattering probability is determined by the sum

$$S_{,\,st}=\tfrac{1}{2}\sum_m S_{mm,\,st}.$$

When the polarization of the scattered photon is to be averaged over, the scattering probability is determined by the sum

$$S_{lm,}=\tfrac{1}{2}\sum_{s} S_{lm,ss}.$$

The two sums just defined have the form

$$S_{,st}=\begin{matrix} & \| & \perp \\ \| & \left(\frac{k}{k_0}+\frac{k_0}{k}-2+2[(\varepsilon_2\cdot\zeta_1)^2+(\varepsilon_1\cdot\zeta_1)^2]\right. & \left.2(\varepsilon_2\cdot\zeta_2)(\varepsilon_2\cdot\zeta_1)\right) \\ \perp & \left.2(\varepsilon_2\cdot\zeta_2)(\varepsilon_2\cdot\zeta_1)\right. & \left.\frac{k}{k_0}+\frac{k_0}{k}-2+2(\varepsilon_2\cdot\zeta_2)^2\right) \end{matrix}, \tag{7}$$

and

$$S_{lm,}=\begin{matrix} & \| & \perp \\ \| & \left(\frac{k}{k_0}+\frac{k_0}{k}-2+2(\varepsilon_1\cdot\zeta_1)^2\right. & \left.2(\varepsilon_1\cdot\zeta_1)(\varepsilon_2\cdot\zeta_1)\right) \\ \perp & \left.2(\varepsilon_1\cdot\zeta_1)(\varepsilon_2\cdot\zeta_1)\right. & \left.\frac{k}{k_0}+\frac{k_0}{k}-2+2[(\varepsilon_2\cdot\zeta_2)^2+(\varepsilon_2\cdot\zeta_1)^2]\right) \end{matrix}. \tag{8}$$

When axes are chosen so that $\mathbf{k}_0$, $\mathbf{k}$ and $\boldsymbol{\varepsilon}_1$ lie in the same plane, $\varepsilon_1\cdot\zeta_1=0$. Then all three matrices (6), (7), and (8) take on an especially simple form. In particular $S_{,st}$ and $S_{lm,}$ are diagonal. This circumstance finds application in Section III. It could be proved directly from the symmetry of the problem under reflection in the plane of $\mathbf{k}_0$, $\mathbf{k}$ and $\boldsymbol{\varepsilon}_1$.

II. THEORY OF DOUBLE COMPTON SCATTERING

In the process to be considered, a photon of momentum $\mathbf{k}_0$ undergoes Compton scattering; the resultant scattered photon of momentum $\mathbf{k}_1$ is again scattered to produce a final scattered photon of momentum $\mathbf{k}_2$, which is counted. The relative number of counts is to be determined as a function of the azimuth of $\mathbf{k}_2$ around the axis of $\mathbf{k}_1$.

If the statistical matrix of polarization of $\mathbf{k}_0$ is $U_{ij}^{(0)}$ before the first scattering, the statistical matrix of $\mathbf{k}_1$ will be proportional to

$$U_{kl}^{(1)}=\sum_{ij} U_{ij}^{(0)}S^{(1)}{}_{ij,kl}. \tag{9}$$

The second scattering will produce a statistical matrix for $\mathbf{k}_2$ proportional to

$$\sum_{kl} U_{kl}^{(1)}S^{(2)}{}_{kl,mn},$$

(see Fig. 2).

We consider the case that the original photons have random polarization. Thus the original statistical matrix $U^{(0)}$ is one-half the unit matrix. We take $\boldsymbol{\varepsilon}_1$ in the plane of $\mathbf{k}_0$ and $\mathbf{k}_1$. The matrix S takes a very simple form, for in this coordinate system,

$$1-(\varepsilon_2\cdot\zeta_1)^2-(\varepsilon_1\cdot\zeta_1)^2=\sin^2\theta_1\cos^2\phi_1=\sin^2\theta_1,$$

$$1-(\varepsilon_2\cdot\zeta_2)^2=1-\frac{\cos^2\theta_1}{1-\sin^2\theta_1\cos^2\phi_1}=0,$$

$$\varepsilon_2\cdot\zeta_1=0,$$

so that we have from section one,

$$\tfrac{1}{2}\sum_{iklm} S^{(1)}{}_{ii,kl}S^{(2)}{}_{kl,mm}=4[\gamma_{01}\gamma_{12}-\gamma_{01}\sin^2\theta_2 -\gamma_{12}\sin^2\theta_1+2\sin^2\theta_1\sin^2\theta_2\cos^2\phi_2],$$

where

$$\gamma_{01}=\frac{k_1}{k_0}+\frac{k_0}{k_1}, \quad \text{and} \quad \gamma_{12}=\frac{k_2}{k_1}+\frac{k_1}{k_2}.$$

For scatterers consisting of single electrons separated by the distance R, the number of photons $\mathbf{k}_2$ going into the solid angle $d\Omega_2$ per

FIG. 2. Momentum vectors for the two successive Compton scatterings.

TABLE I. Optimum ratio of maximum to minimum number of counts for photons initially unpolarized but twice Compton scattered. The azimuth of the second counter is varied while the angles of scattering θ_1 and θ_2 are held fixed at values chosen to give the largest N max/N min.

K_0(Mev)	θ_1	θ_2	(N max/N min) max
0.5	~83°	~85°	3.85
1.0	~80°	~83°	2.14
5.0	~73°	~80°	1.17

second is[6]

$$dN=\frac{I}{16}\left(\frac{e^2}{mc^2}\right)^4\left(\frac{1}{4\pi R^2}\right)\left(\frac{k_1}{k_0}\right)^2\left(\frac{k_2}{k_1}\right)^2 \times 4[\gamma_{01}\gamma_{12}-\gamma_{01}\sin^2\theta_2-\gamma_{12}\sin^2\theta_1 +2\sin^2\theta_1\sin^2\theta_2\cos^2\phi_2]d\Omega_2, \quad (10)$$

where I is the current of incident photons (number per cm² per sec.). For fixed angles of scattering, θ_1 and θ_2, N varies from a maximum at $\phi_2=0$ (then $\mathbf{k}_2$ is in the plane of $\mathbf{k}_0$ and $\mathbf{k}_1$) to a minimum at $\phi_2=\pi/2$. The ratio N max/N min is

$$\frac{\gamma_{01}\gamma_{12}-\gamma_{01}\sin^2\theta_2-\gamma_{12}\sin^2\theta_1+2\sin^2\theta_1\sin^2\theta_2}{\gamma_{01}\gamma_{12}-\gamma_{01}\sin^2\theta_2-\gamma_{12}\sin^2\theta_1}. \quad (11)$$

The maximum of this ratio as a function of θ_1 and θ_2 is a monotonically decreasing function of energy which is only about 1.04 at $k_0=17$ Mev. Although an experiment to test (10) at 17 Mev appears uninteresting because of the smallness of the effect, the data of Table I have been computed in the hope that a test may be possible at lower energies.

Unfortunately, the small absolute number of counts is expected to make the experimental test quite difficult e.g., at $k_0=1$ Mev with $R=10$ cm and scatterers 1 cm on a side and containing 10^{24} electrons, only ~1 in 10^7 of the photons striking the first scatterer will be twice scattered into unit solid angle about the direction which gives the maximum number of counts. Possibly, some geometrical arrangement or focussing device could be used to increase the absolute intensity.

[6] This result can be obtained directly from the Klein-Nishina formula, once it is known that after the first scattering photons polarized parallel and perpendicular to the plane of scattering are incoherent.

III. REMARKS ON AN EXPERIMENT ON THE POLARIZATION OF ANNIHILATION QUANTA

The use of Compton scattering as an analyser of the polarization of annihilation photons was originally suggested by Wheeler[7] and has been investigated by numerous physicists.[8] Here we only wish to show under what conditions it is possible to neglect interference between the probability amplitudes of the photons.[9]

In the suggested experiment slow positons are allowed to annihilate, acting as a source of pairs of annihilation quanta traveling in (nearly) opposite directions. (See Fig. 3.) After having gone through a scattering block, each photon (or a negaton which it has knocked on) is given a chance to trip a counter. Coincidences are measured as a function of relative azimuth $\phi_1-\phi_2$.

The following simple argument shows that the interference of the photon amplitudes can be quite essential. For, neglecting interference we might reason (incorrectly) as follows: Calculate the probabilities that photons (1) and (2) are right and right, left and left, right and left, and left and left circularly polarized respectively. Then, multiply each of these probabilities by the probability that, given that state, a coincidence should result when the counters are at a given relative azimuth $\phi_1-\phi_2$. Then, sum over the four states. Now, for circularly polarized photons the probability of Compton scattering is independent of azimuth. Consequently the sum (which is proportional to the number of coincidences) should be independent of azimuth. This result is known to be wrong.[4]

A virtue of the general formalism developed in Section I is that one can see when the neglect of interference is justified.[7] The probability of a coincidence is proportional to

$$w=\sum_{1,1',2,2',3=3',4=4'}U_{12,1'2'}S^{(1)}{}_{11',33'}S^{(2)}{}_{22',44'},$$

[7] J. A. Wheeler, Annals N. Y. Acad. Sci. 48, 219 (1946).

[8] See reference 4. Snyder, Pasternack and Hornbostel, Phys Rev. 73, 440 (1948). E. Bleuler and D. Ter Haar, Science 108, 10 (1948). R. P. Feynman, unpublished. I am indebted to Professor Feynman for the opportunity to read his elegant treatment of two quantum annihilation. His method suggested the use of the statistical matrix in the present work.

[9] In paragraph 2 of their paper, Snyder, Hornbostel and Pasternack give a very simple justification of the neglect of interference for the particular bases of polarization vectors below.

where $U_{12,1'2'}$ is the statistical matrix of photons (1) and (2), and $S^{(1)}{}_{11',33'}$ is the transformation matrix from the statistical matrix of (1) to (3), $S^{(2)}{}_{22',44'}$ the transformation matrix from the statistical matrix of (2) to that of (4).

For simplicity, consider the case in which the position and negaton annihilate at zero velocity. Then to conserve angular momentum the resultant photons must be in a state of zero angular momentum, for the following reason: From the polarization states of the two photons one can make up four polarization states of the combined system of which three have angular momentum 2 and the fourth angular momentum 0. Now a negaton and positon at rest have at most total angular momentum 1. Consequently, the resultant annihilation photons must be a pure state of angular momentum 0. (In passing we note that this is in agreement with the standard result that annihilation is forbidden in first approximation for a slow negaton-positon pair in a triplet spin state.) As a result the matrix U takes a simple form. Using the basis for polarization vectors of figure one, we find

$$U=\tfrac{1}{2}\begin{array}{c} \\ \parallel\parallel \\ \perp\perp \\ \parallel\perp \\ \perp\parallel \end{array}\begin{array}{c} \begin{array}{cccc} \parallel\parallel & \perp\perp & \parallel\perp & \perp\parallel \end{array} \\ \left.\begin{array}{cccc} 0 & 0 & 0 & 0 \\ 0 & 0 & 0 & 0 \\ 0 & 0 & 1 & -1 \\ 0 & 0 & -1 & 1 \end{array}\right\} \end{array}.$$

Thus

$$\begin{aligned} w=4\{&U_{\perp\perp,\perp\perp}S_{\parallel,\parallel}{}^{(1)}S_{\perp,\perp}{}^{(2)}+U_{\perp\parallel,\perp\parallel}S_{\perp,\perp}{}^{(1)}S_{\parallel,\parallel}{}^{(2)} \\ &+U_{\perp\perp,\perp\parallel}S_{\parallel,\perp}{}^{(1)}S_{\perp,\parallel}{}^{(2)}+U_{\perp\parallel,\perp\perp}S_{\perp,\parallel}{}^{(1)}S_{\parallel,\perp}{}^{(2)}\} \\ =2(&S_{\parallel,\parallel}{}^{(1)}S_{\perp,\perp}{}^{(2)}+S_{\perp,\perp}{}^{(1)}S_{\parallel,\parallel}{}^{(2)} \\ &-S_{\parallel,\perp}{}^{(1)}S_{\perp,\parallel}{}^{(2)}-S_{\perp,\parallel}{}^{(1)}S_{\parallel,\perp}{}^{(2)}). \end{aligned}$$

The coincidence rate is given by the expression:

$$\begin{aligned} &NN_1t_1N_2t_2wd\Omega_1d\Omega_2 \\ &=\frac{1}{4}\left(\frac{e^2}{mc^2}\right)^4 NN_1t_1N_2t_2\left(\frac{k}{k_0}\right)_1^2\left(\frac{k}{k_0}\right)_2^2 \\ &\quad\times[\gamma_1\gamma_2-2\gamma_1\sin^2\theta_2-2\gamma_2\sin^2\theta_1 \\ &\qquad+2\sin^2\theta_1\sin^2\theta_2\sin^2\phi_1-\phi_2]d\Omega_1d\Omega_2, \end{aligned}$$

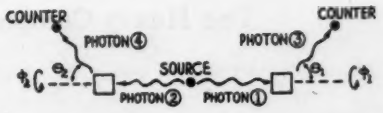

FIG. 3. Geometry of experiment on the polarization of annihilation quanta.

where $N\equiv$number of annihilations per second which result in photons striking scatterers, $N_i\equiv$number of electrons per unit volume in scatterer i, $t_i\equiv$thickness of scatterer i, $d\Omega_i\equiv$solid angle of counter at i,

$$\gamma_i\equiv\left(\frac{k}{k_0}+\frac{k_0}{k}\right)_i,$$

Moreover, when the coordinate system is chosen so that one of the counters is in the plane determined by ε_1 and the momentum of an annihilation quantum, then the off-diagonal elements of either $S^{(1)}$ or $S^{(2)}$ vanish so that

$$w=2(S_{\parallel,\parallel}{}^{(1)}S_{\perp,\perp}{}^{(2)}+S_{\perp,\perp}{}^{(1)}S_{\parallel,\parallel}{}^{(2)}).$$

Thus, the coincidence rate can be written down immediately from the diagonal elements of S_{qr}, or, equivalently, from the Klein-Nishina formula. (This simplification also extends to the case in which the negaton-position pair annihilates with velocity greater than zero, provided the annihilation is considered in the frame in which the pair has zero total momentum.[10] In the general case of arbitrary $U_{ij,kl}$ and arbitrary basis for the polarization vectors one can determine from Eq. (12), whether the neglect of interference of the photon amplitudes is permissible in any given case.) Apart from effects of finite geometry, the expression agrees in its angular dependence with the result of the above authors.

I wish to thank Dr. A. Pais, Professor J. A. Wheeler, and Professor E. P. Wigner for helpful discussion.

[10] The U for this case has been calculated by Feynman in the unpublished manuscript mentioned in reference 4.

PHYSICAL REVIEW VOLUME 74, NUMBER 12 DECEMBER 15, 1948

The Heavy Component of Primary Cosmic Rays*,**

PHYLLIS FREIER, E. J. LOFGREN,*** E. P. NEY, AND F. OPPENHEIMER
University of Minnesota, Minneapolis, Minnesota

(Received September 7, 1948)

Further evidence is presented for the existence of heavy nuclei as components of the primary cosmic radiation. Preliminary results are given for the distribution in atomic numbers of these components. Lower limits of the energies of the particles on entrance into the atmosphere are calculated. These are, in general, above the cut-off imposed by the earth's magnetic field. The mean free path for nuclear collisions is of the order of 14 cm of photographic emulsion. This is longer than that expected from the geometrical cross section and may indicate velocity dependence of nuclear forces. An example of a track that stops in emulsion is shown. This particle gives further evidence for the nuclear character of the rays, because as it slows down it captures planetary electrons and decreases its rate of energy loss. An approximate value of the hydrogen-helium ratio of 4 is reported.

I. INTRODUCTION

IN a previous publication[1] evidence was presented for the existence of heavy nuclei as components of the primary cosmic rays. Further experiments with free balloons at 80,000 to 95,000 ft. have shown that this component consists of nuclei with atomic numbers ranging from that of helium to those of the region around molybdenum. Because these nuclei have average energies which increase regularly with their atomic number, they appear to have been accelerated as partially or completely stripped nuclei probably by the same mechanism as the more abundant proton component. Conclusions regarding the very heavy nuclei can best be drawn from the work with photographic emulsions, while the cloud chamber is more suitable for study of the lighter component.

II. OBSERVATION IN PHOTOGRAPHIC EMULSIONS

In four high altitude flights at 55° geomagnetic latitude (Camp Ripley, Minnesota) a total of approximately 300 penetrating particles heavier than α-particles have been observed in photographic plates. Previously[1] estimates of atomic numbers were made on the basis of the volume of developed silver in the solid core of the tracks. However, a much better estimate can be made by counting the number of δ-rays (knock-on electrons) of greater than a given energy which the particle produces at a known speed. This number can be compared with the corresponding number for α-particles produced in the Berkeley cyclotron.[2] To make accurate estimates of the atomic number in this manner, it is necessary that the particles stop in the stack of photographic plates or at least be near the end of their range in order that β, the ratio of the velocity of the particle to the velocity of light, may be determined.

Another method for estimating Z is possible for the particles which actually stop in an emulsion. Two of these have been observed. At the end of the range, the solid silver filament reaches a maximum diameter, then becomes thinner as the particle slows down to the speed of its several electron shells. That is, as the particle slows down, it captures electrons and thus neutralizes some of its nuclear charge. This "thin down length" should be a function of Z, since the thinning starts when the K electrons are caught and the K electron velocities are proportional to Z.

Figure 1 shows an example of the effect for the particle whose atomic number is estimated

* Assisted by the joint program of the Office of Naval Research and Atomic Energy Commission.

** The photographic emulsion experiments and techniques described in this paper were developed jointly with H. Bradt and B. Peters of the University of Rochester. The data presented in this paper and in the accompanying one of Bradt and Peters is an extension of the earlier data on heavy particles that we published with them. We wish to convey our gratitude for discussions with them.

*** Now at Radiation Laboratory, University of California.

[1] Freier, Lofgren, Ney, Oppenheimer, Bradt, and Peters, Phys. Rev. 74, 213 (1948).

[2] Plates exposed to 380-Mev α-particles were supplied by Eugene Gardner.

by δ-ray counts to be 15. The thinning down takes place in a path length of 140 microns. The importance of this effect is that it gives further evidence that the heavy component of the cosmic radiation really consists of atomic nuclei. The effect is not observed for fission tracks because their ranges are only 10 to 20 microns.

An approximate calculation of Z from the "thin down length" can be made by using the Bohr model of the atom and assuming that capture of electrons takes place when the speed of the nucleus is that of electrons in the various atomic shells. The mass of the heavy nucleus is assumed to be $2Z$ times the proton mass. The heavy nucleus then has an energy of $0.05Z^3$ Mev when it picks up its first electron. If one assumes that at all lower energies the energy $E=0.05Zz^2$ Mev, where z is the effective charge at the energy E and Z is the nuclear charge, one can obtain the "thin down length" as a function of Z by numerical integration of Eq. (1).

$$L=\int_0^Z (dx)/(dz)dz=\int_0^Z (dE/dz)/(dE/dx)dz, \quad (1)$$

dE/dz is obtained from the assumed relationship between energy and charge; dE/dx for a particle of effective charge, z, is equal to z^2 times dE/dx for a proton of the same velocity. dE/dx for protons was obtained by differentiating the experimental range-energy curves for protons in Ilford emulsions.[3] Figure 2 shows the variation of the calculated "thin down length" with Z. Z for the particle of Fig. 1 is 17 by this method, in good agreement with 15 obtained from δ-ray counts.

III. RESULTS OF δ-RAY COUNTING IN EMULSIONS

Eight heavy particles satisfied the condition for estimating Z by δ-ray counts. Two particles actually stopped in emulsion, but one of them penetrated some of the cloud-chamber lead and its range in the photographic plates is very short. The others stopped in the glass between emulsions, and ionized heavily near the end of their range. To justify the δ-ray method, δ-rays were counted in several emulsions along two tracks.

[3] Lattes, Fowler, and Cuer, Proc. Phys. Soc. 59, 884 (1947).

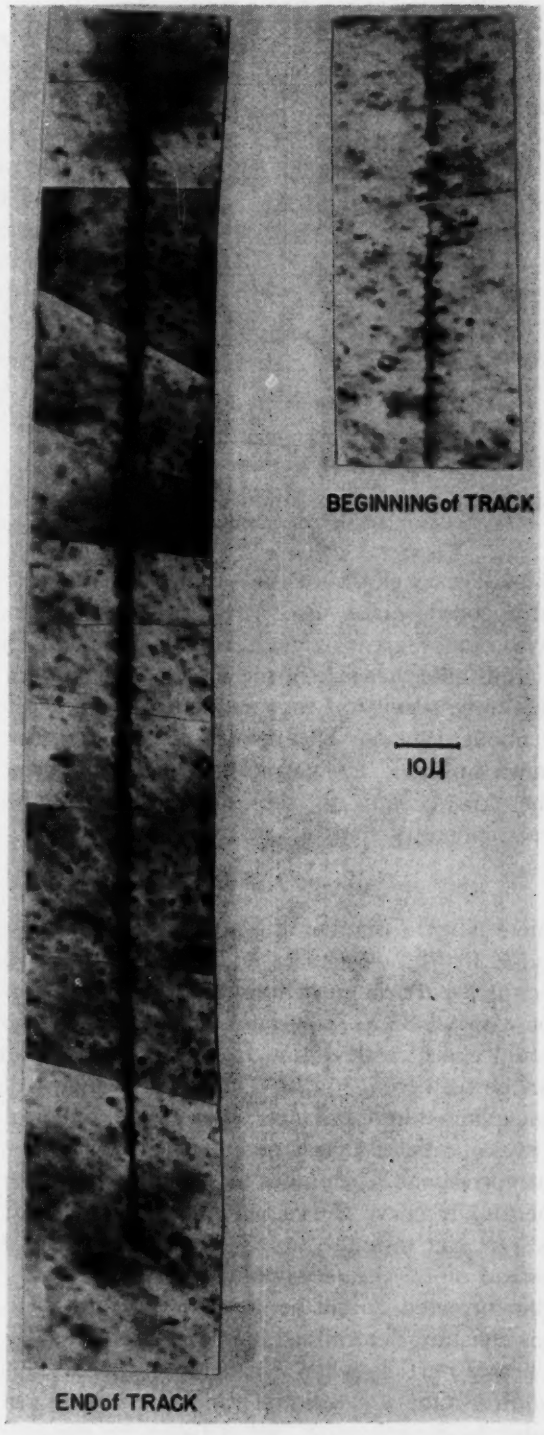

FIG. 1. Photomicrograph of track with $Z=15$ (estimated from δ-rays) stopping in emulsion. The insert shows the track when it enters the stack of photographic plates with $\beta \leqq 0.7$. The thin down shown at the left occurs after the particle has penetrated 9.6 g/cm² of glass and emulsion.

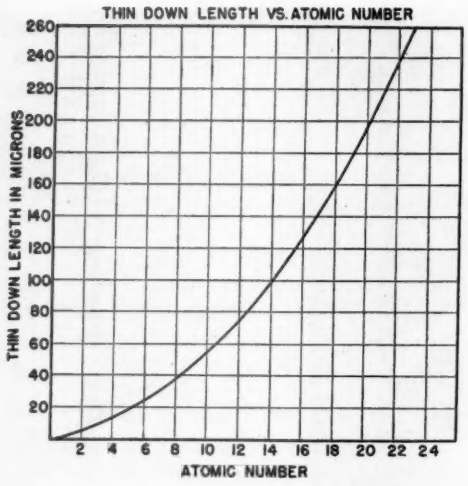

FIG. 2. Graph of the theoretical relation between "thin down length" and atomic number.

This allows a check on the assumption that the δ-ray count varies as Z^2/v^2. All δ-rays which have ranges great enough to bring them 1.5 microns on either side of the track were counted. This corresponds to δ-rays with energies in excess of about 10 kev. The results of this test are shown in Table I. The method was as follows: The δ-ray count on the α-particle gives the proportionality constant K, in the equation,

$$N=(Z^2)/(\beta^2)K, \qquad (2)$$

where N is the number of δ-rays per 100 microns, and Z for the α-particles is 2. The measured K for the α-particle must, however, be increased in the ratio of 8.2/7.5, because at a β of 0.35 one would expect a deviation from the $1/v^2$ law, as can be seen from Fig. 3. This curve, which will be explained in detail later, shows the number of δ-rays of greater than a given energy divided by the corresponding number for $v=c$. Reference to the 10-kev curve shows that if the δ-rays went as $1/v^2$ the ordinate at $\beta=0.35$ should be 8.2 instead of 7.5 (i.e., it should be $1/(0.35)^2=8.2$). The corrected K will be used throughout. With this constant determined, one can then get Z for a heavy particle when β can be obtained. This requires that the residual range be known. In order to determine Z and β from the residual range and the δ-ray count, one first guesses a value of β and determines Z from Eq. (2). This value of Z and the residual range allow calculation of the quantity $Z^2R/\mu c^2$. (R is the residual range and μ is the rest mass appropriate for the Z.) For most of the particles considered μc^2 is 2 (0.93) Z Bev. By using range energy curves one can determine $P/\mu c$ and β and compare this with the β originally chosen. By successive approximations both Z and β can then be determined. The curves used for this transformation were obtained from a publication by Rossi[4] with the ordinate modified to read $Z^2R/\mu c^2$ and the values corrected to apply to charged particles in glass. The curves are reproduced in Fig. 4. In order to check the Z^2/v^2 law, Z and β were determined for the particle in the first emulsion in which it was seen. For every other residual range β can be determined using the same Z, and the product, $N\beta^2$, examined for constancy. Columns A and B are the results obtained by different observers. The δ-ray counts of both observers gave $Z=13$ for H_{29} and $Z=15$ for H_4. It should be borne in mind in examining Table I that the Z estimate depends on $(N\beta^2)^{\frac{1}{4}}$.

The results of the Z estimation for the eight chosen particles are shown in Table II. The track for which the highest Z was estimated is shown in Fig. 5. The heavy particles described were obtained in two flights, one of which remained aloft for about 30 hours. The altitude was unknown after the first six hours, but the incidence of heavy particles was less than that predicted from the other flight of known altitude and duration. For this reason we believe the balloon went to lower altitudes as the flight progressed. This means that for this flight one cannot calculate energy of entrance into the, atmosphere because the residual atmosphere was unknown for most of the flight. Because of the reason stated and the fact that other equipment was around, one can only compute a lower limit on the energy of entrance into the atmosphere. The minimum energy of entrance into the atmosphere was calculated for both flights by using the residual atmosphere at maximum altitude for the direction in which the particle entered the stack.

In many cases where the particles do not stop, it is possible from δ-ray counting to obtain limits on the atomic number (Table III). The upper limit is obtained by assuming that the

[4] B. Rossi, Rev. Mod. Phys. 20, 537 (1948).

particle is at minimum ionization when it enters the stack, the lower limit by assuming that the observed range is the actual range. By applying this procedure to twenty-eight tracks, a preliminary Z spectrum was obtained. The spectrum is shown in Fig. 6. Particles with Z's of 10–15 may have been discriminated against by our visual method of choosing heavy tracks for study.

IV. OBSERVATION IN VARIOUS EMULSIONS

The results reported for the photographic technique were all obtained with Ilford C-2 nuclear research emulsions. Preliminary experiments have been done with Eastman NTB and some special diluted (low silver content) Ilford plates furnished by Eugene Gardner. The core of the tracks in the NTB plates was not as pronounced as in the Ilford C-2 plates, but the δ-rays appeared to be better in NTB's. The diluted Ilford plates showed δ-rays, and the density of ionization in the core was less. It seems feasible with highly diluted plates to obtain atomic numbers by grain counting. Experiments are now in progress with diluted Eastman plates furnished through the courtesy of Dr. Julian Webb.

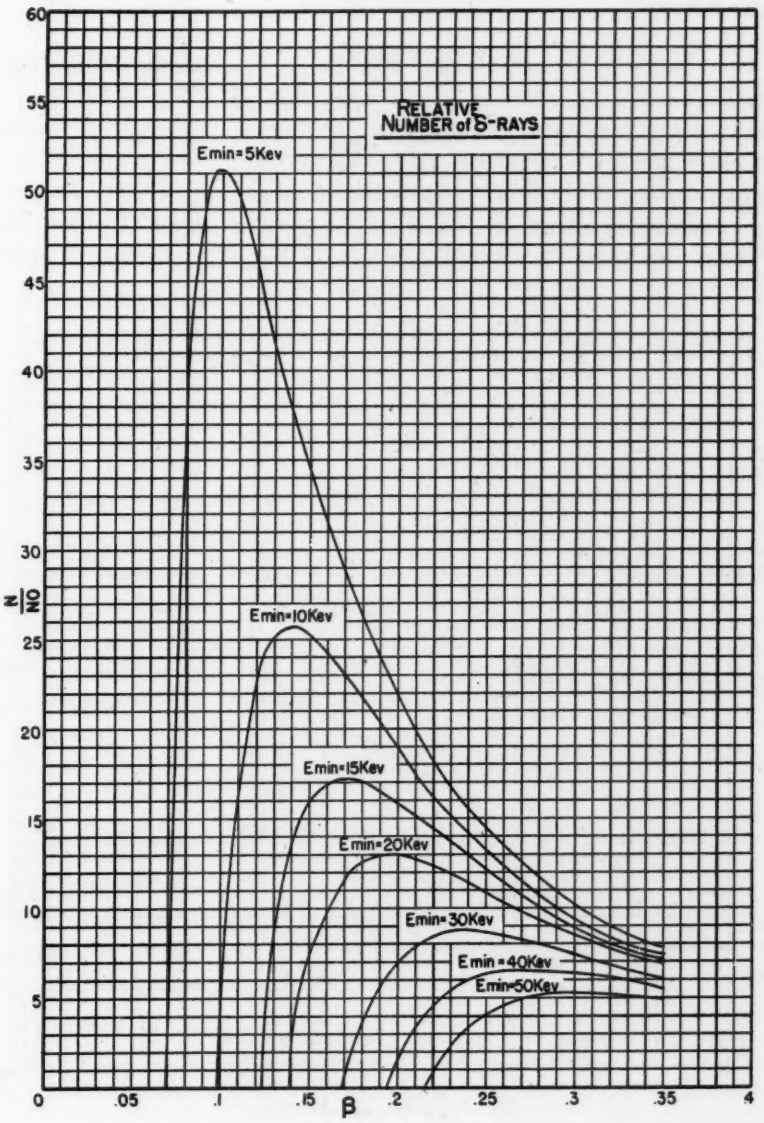

FIG. 3. Graph of the number of knock-on electrons of energy greater than E_{min} relative to the corresponding number when $v=c$ as a function of β.

TABLE I.

Track	Residual range g/cm²	β^2	β	$\frac{A}{*N\beta^2}$	$\frac{B}{*N\beta^2}$
α-particle	5.2	0.12	0.35	0.14	0.17
H.4 $Z=15$	9.6	0.47	0.69	8.7	9.1
	9.4	0.46	0.68	8.8	9.0
	4.85	0.35	0.59	7.9	8.2
	4.6	0.34	0.58	8.0	8.2
H.29 $Z=13$	9.4	0.43	0.66	5.6	6.4
	7.8	0.41	0.64	5.8	7.0
	7.0	0.38	0.62	5.7	7.9
	6.0	0.35	0.59	5.4	6.8
	4.3	0.31	0.56	5.6	6.0
	2.6	0.25	0.50	5.9	8.5
	1.0	0.17	0.41	6.4	8.0

* The value of N here for the α-particle has been corrected for the $1/v^2$ law deviation.

TABLE II. Results of the Z estimate for the eight chosen particles.

Track	Estimated Z	Energy on entering stack of plates	β on entering plates	Minimum energy on entering atmosphere	Minimum β on entering atmosphere	Angle with vert.	*Energy to penetrate earth's field
H.1	41	54 Bev	0.8	110 Bev	0.9	30°	45 Bev
H.4A	15	12	0.7	22	0.8	45°	17
H.29	13	8.5	0.7	16	0.8	35°	15
H.16	19	15	0.7	33	0.85	48°	22
H.12	12	4.5	0.55	13	0.8	41°	12.5
H.19	22	13.5	0.6	56	0.9	68°	25
H.22	10	4.5	0.6	9	0.75	10°	12
H.5A	20	9	0.6	41	0.9	64°	24

* The energy was calculated for a Stoermer variable of 0.2. According to G. Lemaitre and M. S. Vallarta, Phys. Rev. 43, 89 (1933), Fig. 1, p. 92, particles would be able to come in from the whole sky at 55° latitude for this value of the Stoermer variable.

V. FLUX OF HEAVY PRIMARIES

It is possible to estimate the primary flux of particles of $Z>10$ from the angular distribution at a given altitude. The fact that the distribution is not isotropic at 15-g/cm² residual atmosphere is a consequence of the high rate of energy loss of these particles. Those that come in at large angles cannot penetrate the residual atmosphere. The flight from which the data were obtained reached a maximum altitude of 94,000 feet (15 g/cm²). The angular distribution is shown in Fig. 7. Forty particles make up the distribution. If one assumes that the probability of detection is unity and that all particles from

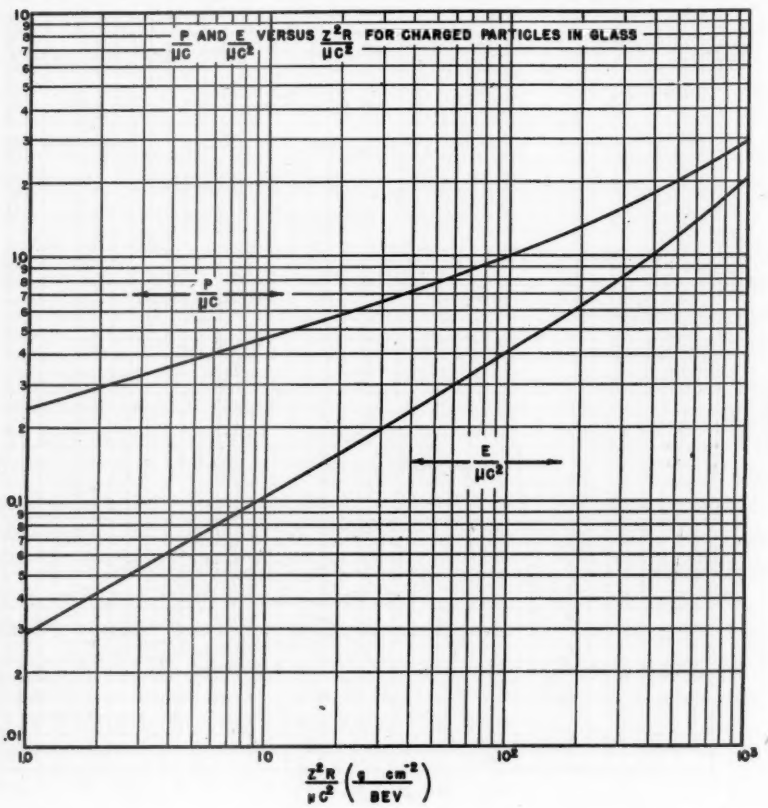

FIG. 4. Graph of $[\beta(1-\beta^2)^{-\frac{1}{2}}]$ and $[(1-\beta^2)^{-\frac{1}{2}}-1]$ as a function of $Z^2R/\mu c^2$ for charged particles in glass.

angles near the vertical penetrate the residual atmosphere, the flux of heavy primaries would be 3.2×10^{-4} particles/cm² sec. steradian, using the data from 0–20°. The foregoing estimate, however, is based on six particles observed in this interval. If one uses 0–30°, twelve particles are involved and the flux would be 1.9×10^{-4} particles/cm² sec. steradian. All particles with energies above the magnetic cut-off energy and Z less than about 25 will penetrate from the vertical. Because the mean free path for nuclear processes is so long (see Section VI) the correction for particles which stop in the 15 g/cm² by making stars is negligible. In Fig. 6 we have also plotted the relative numbers of hydrogen and helium nuclei with respect to the heavy nuclei. The hydrogen helium ratio was measured in the cloud chamber (see Section VIII). The hydrogen to total heavy particle ratio was obtained using 3.2×10^{-4}/cm² sec. steradian for the flux of heavy particles and comparing this with the figure of 12×10^{-2} particles/cm² sec. steradian for the total primary flux.[5]

VII. MEAN FREE PATH FOR NUCLEAR PROCESSES

Because one cannot observe what happens to particles while they are in the glass, it is difficult to use total path of glass and emulsion to estimate free paths. It is true that some particles disappear between emulsions without increasing their ionization while others become heavy before disappearing. It may well be that the first group disappears by making stars. Probably the best estimate of free path comes from comparing the total path observed in emulsion with the number of stars produced in the emulsion. Only one† heavy particle-produced star has been observed in 56 g/cm² of emulsion. This corresponds to a free path of 14 cm. If one assumes that the radius of a nucleus is $1.5\times10^{-13}A^{\frac{1}{3}}$ cm, that the average Z of the heavy particles is 20, and that the cross section for events is the geometric nuclear cross section, then the free path for star production should be 5 cm. The experimental result indicates a cross section which is smaller than the geometrical cross section. In measuring the mean free path, our observations are mostly on particles with high β's. This "transparency" of nuclei to high energy bombarding particles[6]

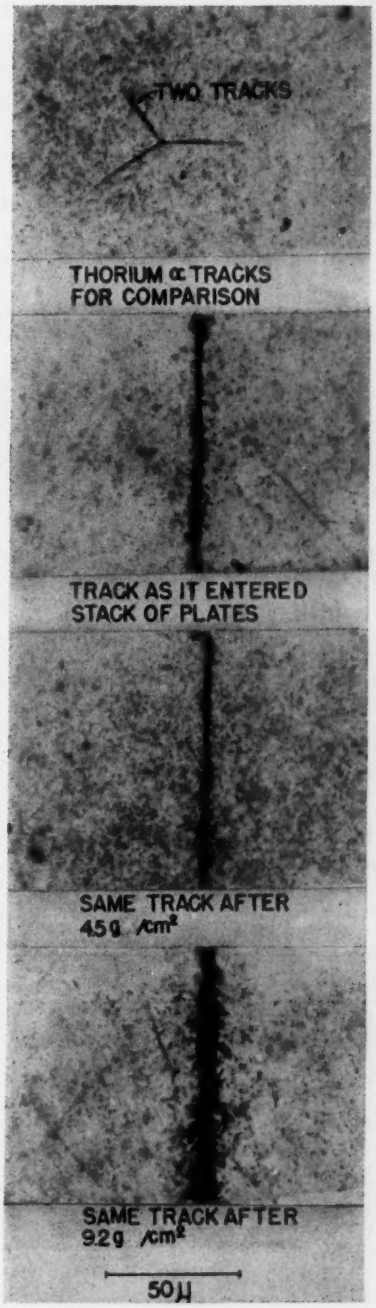
TWO TRACKS
THORIUM α TRACKS FOR COMPARISON
TRACK AS IT ENTERED STACK OF PLATES
SAME TRACK AFTER 4.5 g /cm²
SAME TRACK AFTER 9.2 g /cm²
50 μ

FIG. 5. Photomicrograph of sections of the heaviest track observed. The atomic number of this track was estimated to be 41 by δ-ray counting.

[5] J. A. Van Allen and H. E. Tatel, Phys. Rev. **73**, 245 (1948).

† *Note added in proof:* Three stars produced by particles with $s>10$ have been observed, yielding a mean-free path of 12 cm of emulsion.

[6] R. Serber, Phys. Rev. **72**, 1114 (1947).

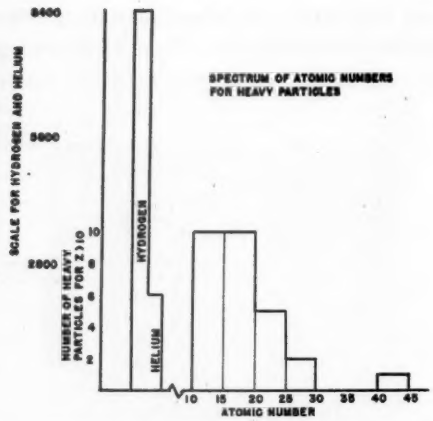

FIG. 6. Spectrum of atomic numbers. The scales for the ordinate read in relative numbers of atoms.

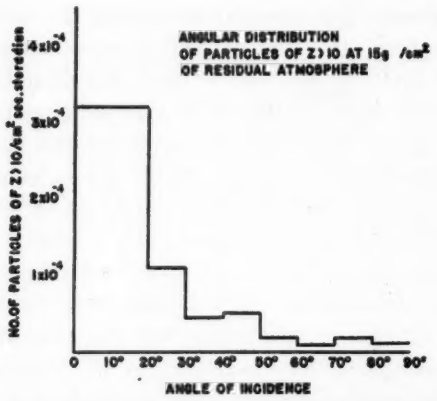
ANGULAR DISTRIBUTION
OF PARTICLES OF Z ≥ 10 AT 15g /cm²
OF RESIDUAL ATMOSPHERE
NO. OF PARTICLES OF Z ≥ 10/Am² sec. steradian
ANGLE OF INCIDENCE

FIG. 7. Angular distribution at 94,000 feet. A total of forty particles was used for this distribution.

might well be more pronounced at the high β's encountered here than with the lower β's of cyclotron accelerated particles. Our result therefore suggests a velocity dependence of nuclear forces.

The single example of a heavy particle-induced star is shown in Fig. 8. The Z of the incoming particle is estimated to be from 8 to 14. One particle, not clearly evident in the picture, proceeds within 2° of the direction of the incident particle. It is probably a fast α-particle or proton. Of the remaining particles one is identified is an α-particle and the other three as particles with $Z \geqq 2$. A possible interpretation is that the star was produced when the heavy nucleus struck a proton in the emulsion.

TABLE III. Particles for which minimum and maximum Z are available.

Particle	Z minimum	Z maximum
H.21	14	19
H.3	15	21
H.7	19	27
H.34	18	26
H.20	10	16
H.30A	14	21
H.30	8	14
H.28A	12	18
H.16A	11	18
H.22A	12	19
H.7A	23	34
H.27A	15	22
H.13A	12	19
H.14A	25	33
H.19A	18	22
H.20A	10	15
H.24	14	19
H.27	18	25
H.28	16	23
H.35	10	16

VII. CLOUD-CHAMBER OBSERVATIONS OF NUCLEI

The equipment developed for cloud-chamber experiments with free balloons has been described.[7] One cloud-chamber picture of a heavy penetrating particle has been published.[1] Several more examples have been obtained. Two of these are shown in Figs. 9 and 10. For the particle of Fig. 9, probable limits on the Z can be set from the δ-rays alone. The curves from which the conclusions are drawn are shown in Fig. 3. Figure 3 was calculated by the method outlined by Hazen.[8] It shows as a function of Z the number of δ-rays of energy greater than E min. at a given particle velocity divided by the number with energy greater than E min. when $v=c$. The number of δ-rays of energy greater than E min. at $v=c$ for a singly charged particle is called N_0. N_0 is 0.0056 per cm in nitrogen at 76 cm mercury pressure and 15°C for E min. $=20$ kev.[9] Our cloud chamber was filled with argon and a 30 percent–70 percent water alcohol mixture at 115 cm pressure and 20°C. N_0 for

TABLE IV. Estimates of the H/He ratio.

Date of flight	g/cm² residual atmosphere	Number of pictures considered	No. of penetrating singly charged particles	No. of particles identified as He	Total No. of particles	H/He ratios
July 23	14 g/cm²	44	14	3	17	4.7
July 16	25	30	5	2	7	2.5
Average						4

[7] E. J. Lofgren, E. P. Ney, and F. Oppenheimer, Rev. Sci. Inst. (in press).
[8] Wayne E. Hazen, Phys. Rev. 65, 70 (1944).
[9] G. Hornbeck and I. Howell, Proc. Am. Soc. 84, 33 (1941).

these conditions should be 0.010 per cm for E min. = 20 kev. In Fig. 9, the particle has four δ-rays in 5 cm of path under the top lead plate. Three of these definitely originate in the gas and the fourth probably does also. The longest of these is about 2 cm long, which corresponds to an energy of 45 kev. This means that β for the particle must be greater than 0.2. See Fig. 3. The 4δ-rays are all longer than 0.5 cm, or 20 kev. From Fig. $3N/N_0$ for 20 kev and $\beta=0.2$ is 13. N for a singly charged particle of $\beta=0.2$ would then be $13(0.01)=0.13$ δ-rays/cm. The observed number is $\frac{4}{5}$ δ-rays/cm, which is 6 times that of a singly charged particle. This means that $Z\geqq(6)^{\frac{1}{2}}$. $Z\geqq 3$ is the lower limit. To get the upper limit, one assumes that the particle is at minimum ionization. It has $0.8/0.01=80$ times as many δ-rays as a singly charged particle at $v=c$, and hence $Z\leqq(80)^{\frac{1}{2}}$ or $Z\leqq 9$. The δ-ray estimate then sets $3\leqq Z\leqq 9$. The track passes in and out of the illuminated region and can only be seen passing through one $\frac{1}{4}$-inch lead plate.

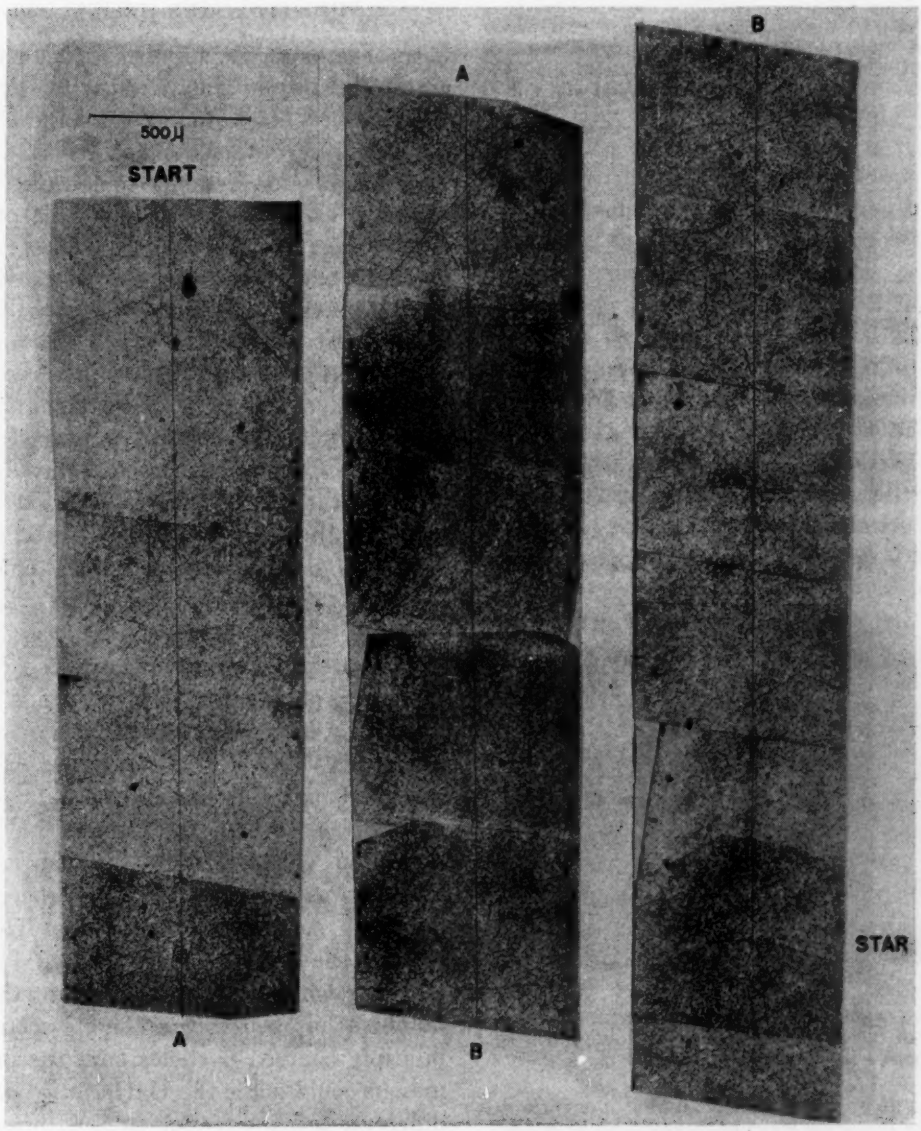

FIG. 8. Photomicrograph of heavy particle (Z estimated between 8 and 14) ending in the emulsion with a nuclear collision.

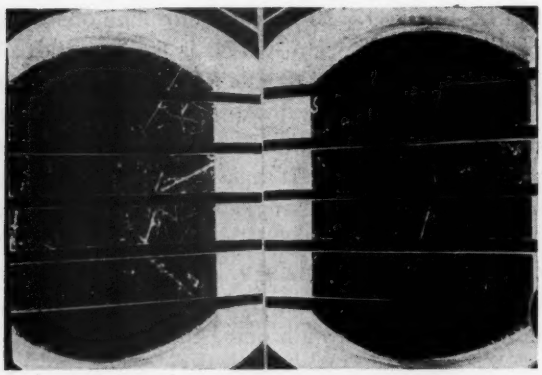

FIG. 9. A cloud-chamber stereophotograph of a heavy particle (upper right) penetrating a lead plate and ionizing heavily on both sides. The δ-rays in the section below the plate are quite evident. The particle passes in and out of the illuminated region.

For the track of Fig. 10, the particle passes through 30 g/cm² of lead. It comes into the illuminated region from the rear and passes out through the side plate. It has four δ-rays of greater than 20-kev energy in the region where δ-rays could be seen. This leads to an upper limit for Z of 6. Its ionization is estimated to be about $\frac{1}{10}$ that of a 10-Mev α-particle. If one assumes the value of $\frac{1}{10}$ the ionization of a 10-Mev α-particle, one gets a value of 60-Mev/(g/cm²) for the rate of energy loss and an energy of 75×10^6 electron volts.[10] Such an α-particle would have a range of 1 g/cm², as opposed to the observed range of greater than 30 g/cm². From the above argument it seems likely that the atomic number is $3\leqq Z\leqq 6$.

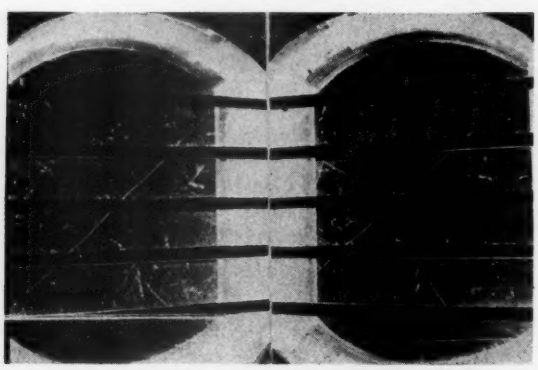

FIG. 10. A particle heavier than an α-particle comes in at the back of the chamber, penetrates three ¼-inch lead plates, and passes out through the left side plate.

[10] The rate at energy loss of a 10-Mev α-particle was obtained from Bethe's calculation reported by R. Serber—private communication. The other rates of energy loss and ranges were obtained from the collection by Aron, Hoffman, and Williams—private communication.

Figure 11 shows an interesting case of a heavy particle for which no estimate could be made because of the age of the track. The track has been pulled apart by the clearing field, and two columns of ionization may be seen in each section. The same picture shows a star in the lead plate with the production of two penetrating particles.

VIII. HYDROGEN-HELIUM RATIO

By examining a number of cloud-chamber pictures, an approximate value for the ratio of the number of protons to the number of α-particles was obtained. It is believed that the figures apply to primary cosmic rays. The cloud chamber used had five ¼-inch lead plates and, for studying the H–He ratio, photographs were chosen in which all sections of the cloud chamber were operating well. One flight had 44 such pictures at 95,000 feet (14 g/cm² of residual atmosphere), another had 30 pictures at 80,000 to 85,000 feet (25 g/cm² of residual atmosphere). The only particles considered were those which entered the chamber in such a way as to penetrate at least 3 lead plates and which scattered less than the limit imposed by turbulence (1 or 2°). This requirement and the high altitude discriminate against mesons. The tracks which satisfied these conditions were classified as to ionization and thereby placed in two groups, depending on whether their ionization was minimum for a singly charged particle or about four times this value. In only one case did the ionization change appreciably in penetrating ¾ inch of lead. Because of the manner in which the ionization changed with residual range, this particle was identified as a low energy proton. Table IV summarizes the results. The average value of the H/He ratio is 4. It should be pointed out that what was measured were the relative numbers of penetrating singly charged and multiply charged particles, and the presence of mesons could make the H/He ratio considerably different. It is interesting to note, however, that this value is consistent with astrophysical estimates. Using spectroscopic methods, Menzel

and Goldberg[11] determined 4 as the value for the H/He ratio on the sun, and Aller and Menzel[12] find 10 as the ratio for planetary nebulae.

IX. CONCLUSIONS

When experiments are made at altitudes corresponding to 25 g/cm² of residual atmosphere or less, heavily ionizing particles appear, and these heavily ionizing particles show the properties of the nuclei of the elements.

Because of their energy and their angular distribution at the altitudes investigated, they appear to be present as a component of primary cosmic rays.

Examination of Table II leads to the conclusion that the kinetic energies of the heavy nuclei so far investigated range from 0.5 to 1.5 Bev per nucleon. Serber[13] has estimated that the primaries (assumed to be protons) have an average energy of about 7 Bev.

The hydrogen-helium ratio for these particles is not inconsistent with hydrogen-helium ratio for the sun or for planetary nebulae. The relative abundance of the heavy elements with respect to hydrogen and helium seems to be consistent with that assumed by astrophysicists.

X. ACKNOWLEDGMENTS

This research was done under the partial support of the joint program of the Office of Naval Research and the Atomic Energy Commission, Contract N5ori-147. It was also materially assisted by the University of Minnesota Technical Research Fund subscribed to by General Mills, Inc., the Minneapolis Honeywell Regulator Company, the Minneapolis Star Journal and Tribune Company, the Minnesota Mining and Manufacturing Company, and the Northern States Power Company. The writers wish to express their appreciation to George Freier who developed the calculation for z from the "thinning down" of the track in Fig. 1. They also wish to thank Professor John T. Tate for his advice during the course of the work, Dr. C. L. Critchfield and Dr. J. Weinberg for helpful discussions, and Mr. B. W. Downs for making the calculations which form the basis of Fig. 3.

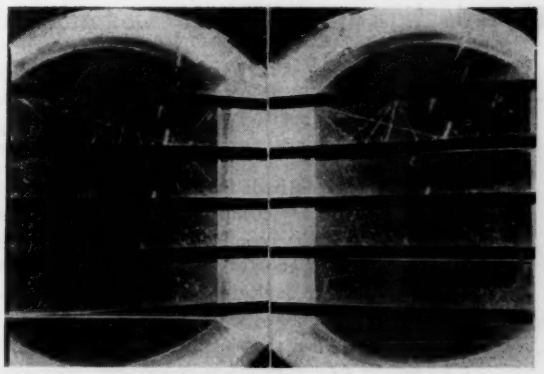

FIG. 11. A stereophotograph of a heavy particle that penetrated five ½-inch lead plates. It traversed the cloud chamber early, and the two columns of ionization are pulled apart by the clearing field. It ionizes like a slow α-particle, but it has a range very much greater. Three other interesting events also occur. In the center of the top plate a star is formed by non-ionizing radiation. This star has one fragment which penetrates one-inch of lead and another which penetrates ¼ inch. In the left side of the upper lead plate, a shower of penetrating particles is initiated by an ionizing particle. Two of the particles in this shower can be seen penetrating three-quarters of an inch of lead without radiation or detectable scattering. There is also a rather large shower of fast particles originating at the right side of the second from the top lead plate.

[11] L. Goldberg and L. H. Aller, *Atoms, Stars, and Nebulae* (The Blakiston Company, Philadelphia, 1943).
[12] L. H. Aller and D. H. Menzel, Astrophys. J. **102**, 239 (1945).
[13] R. Serber, Phys. Rev. **54**, 317 (1938).

PHYSICAL REVIEW VOLUME 74, NUMBER 12 DECEMBER 15, 1948

Investigation of the Primary Cosmic Radiation with Nuclear Photographic Emulsions

H. L. BRADT AND B. PETERS
University of Rochester, Rochester, New York

(Received September 15, 1948)

Several methods for determining the charge and energy of heavy nuclei found to be present in the primary cosmic radiation, are discussed. The application to a number of tracks of the heavy primary cosmic-ray component in Ilford C_2 emulsions shows the presence of nuclei from the neighborhood of carbon in the periodic system up to the neighborhood of iron ($Z \approx 20 \div 30$).

A nuclear explosion caused by the collision of a $\gtrsim$3-Bev carbon or oxygen nucleus with a silver nucleus of the emulsion is discussed.

It is shown that both the magnitude of the flux and the distribution of ranges of the nuclei of the heavy primary cosmic-ray component may give valuable information regarding the origin of cosmic rays.

NUCLEAR photographic emulsions are particularly well suited for investigations at very high altitudes, because of their small weight, simplicity, large stopping power, and continuous sensitivity.

Recent developments in the technique of manufacturing emulsions sensitive to ionizing particles have greatly enhanced their value as a research tool.

The silver halide grains in the emulsion are made developable by the ionization produced by a charged particle. Since the same process is responsible for the energy loss of the particle in its passage through matter, the grain density, like the specific energy loss, will increase with increasing charge and decreasing velocity of the particle and will be independent of its mass.

In the Ilford C_2 boron-loaded emulsion, a proton track can be followed over a range of approximately 10,000 microns from its end until it is lost in the background. This determines the smallest observable specific energy loss K_0, from which the maximum observable energies and ranges for other particles can be obtained.

These are listed in Table I together with the quantity $K_0/K_{\min}$, which is the ratio of the smallest observable specific energy loss to the minimum value which the specific energy loss can assume.

The corresponding table (Table II) for the recently improved Eastman NTB emulsions is based on the fact that electron tracks can be observed of lengths up to 38μ. Thus the most sensitive photographic emulsions will record all multiply charged particles and singly charged particles up to a kinetic energy equal to 1/7 of their rest mass.

DETERMINATION OF CHARGE Z AND ENERGY E OF THE HEAVY PRIMARIES

The heavy primaries observed at 94,000 feet will be completely stripped by the passage through more than 14 g/cm^2 of air overhead and will remain stripped as long as their velocities are large compared to that of their inner shell electrons. This condition is certainly fulfilled for any particle capable of penetrating several g/cm^2 of material. We can therefore approximate the mass of the particles by the relation $M \approx 2Z$.

In general we can measure three quantities characteristic of the heavy particle tracks, or at least determine lower limits for them:

(1) the range R (in g/cm^2);
(2) the track density D (the number of developed silver grains per unit length or, if the track consists of a solid column of developed silver, the width of this column);
(3) the number n of secondary electrons (δ-rays) ejected per unit length (the energy of the secondary electrons lying in a given arbitrary energy interval).

If some portion of the track consists of a series of resolved, developed silver grains on the trajectory, we can obtain the specific energy loss K of the particle by comparison with a track of equal grain density produced by a known particle of known energy or residual range (proton or α-particle). This is possible because the probability of making a certain fraction of the traversed grains developable depends only on the ionization and therefore on the specific energy

TABLE I. Ilford C_2 emulsions, boron loaded.

	max. energy E_{max}	Range in emulsion R	K_0/K_{min}	$\beta_{max}=V/C$
proton	50 Mev	10,250 microns	6.0	0.308
π-meson ($313m_e$)	8.5 Mev	1700 μ		
μ-meson ($200m_e$)	5.5 Mev	1100 μ		
electron	27 kev	6 μ		
α-particle	1.4 Bev	300,000 $\mu\mu$	1.5	0.677
heavier ions	all energies	all ranges	<1.0	

TABLE II. Eastman improved NTB emulsion.

	max. energy $E_{max.}$	Range in emulsion R	K_0/K_{min}	$\beta_{max}=V/C$
proton	147 Mev	70,000μ	2.8	0.490
π-meson	24.5 Mev	11,700μ		
μ-meson	16.5 Mev	7,800μ		
electron	80 kev	38μ		
α-particle	all energies	all ranges	<1.0	
heavier	all energies	all ranges	<1.0	

loss and not explicitly on the charge of the particle.

If, however, the particle is heavy or comparatively slow, the track no longer consists of a linear array of silver grains. The track then consists of a solid column of developed silver whose thickness can be many times larger than the diameter of the grains in the emulsion. The width of such tracks is far too large to be accounted for by the increased range of the effective electric field from multiply charged nuclei. The width is due to a great number of secondary electrons ejected with sufficient energy to make a few silver grains developable in the immediate neighborhood of the trajectory. Thus the width of such heavy tracks cannot be simply related to the specific energy loss and an estimate of charge based on such a relation which was made in the first communication[1] must be considered as misleading.

For heavy tracks we can only put a lower limit on the specific energy loss and hence obtain only a lower limit for charge and energy.

However, the large number of δ-rays ejected from these heavy tracks make it possible to determine the charge without knowing the specific energy loss. Some electrons will be ejected with sufficient energy to make recognizable δ-ray tracks of several microns length, and the number of such δ-rays per unit length (δ-ray density) in conjunction with the range can be used to determine charge and energy.

We shall therefore discuss separately the determination of charge and energy from range and specific energy loss which is applicable to lighter tracks and the determination from range and δ-ray density which is always applicable but more reliable for heavy tracks where the δ-ray density is high. Table V shows that both methods give consistent results within the accuracy assigned to each measurement.

A. Determination of Charge Z and Energy E from Range and Specific Energy Loss

In order to determine the specific energy loss of the particle for any portion of its track, we have to find a portion of equal grain density on a track produced by a known particle of known energy or residual range. At present α-particles are the heaviest particles available for comparison purposes. Their specific energy loss reaches its maximum value very near the end of their range and does not exceed $K_\alpha=0.9$ Mev/mg/cm^2. Thus only values of K below this value can be accurately determined.

If the specific energy loss K and the range R can be measured, the charge and energy of the ions can be determined by the following procedure: Let E, R, K, β denote the kinetic energy, range, specific energy loss, and velocity in units of c of the particle, and let primed symbols designate the same quantity for a proton of equal velocity. We then have the relations:

$$\beta\equiv\beta',$$
$$E/2Z=E' \text{ representing the kinetic energy per nucleon,}$$
$$K=Z^2\varphi(\beta)=Z^2K',$$
$$R=(M/Z^2)R'\approx(2/Z)R'.$$

The three quantities $E/2Z=E', Z/(K)^{\frac{1}{2}}=1/(K')^{\frac{1}{2}}$, and $R(K)^{\frac{1}{2}}=2R'(K')^{\frac{1}{2}}$ are known functions of the velocity:[2] therefore, for given values of R and K, the value of $Z/(K)^{\frac{1}{2}}$ and hence the charge Z and energy E can be determined. Figure 1 shows the relation between the quantities $E/2Z$ and $Z/(K)^{\frac{1}{2}}$ *vs.* $R(K)^{\frac{1}{2}}$. As can be seen from the graph, if only lower limits of R or K are known, one obtains a lower limit for Z and $E/2Z$. As an

[1] Phyllis Freier, E. J. Lofgren, E. P. Ney, F. Oppenheimer, H. L. Bradt, and B. Peters, Phys. Rev. **74**, 213 (1948). The present work is a continuation of a preliminary investigation made jointly with Freier, Lofgren, Ney, and Oppenheimer. We are greatly indebted to them for the many discussions we have had.

[2] J. H. Smith, Phys. Rev. **71**, 32 (1947).

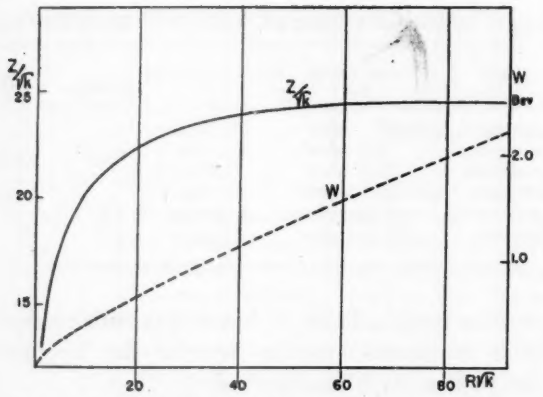

FIG. 1. Determination of the charge Z and the kinetic energy E from the range R and the specific energy loss K. Plotted are $Z/(K)^{\frac{1}{2}}$ and $W=E/2Z$ (kinetic energy per nucleon) *versus* $R(K)^{\frac{1}{2}}$. Range R in g/cm² Al equivalent (1 cm emulsion ≈ 1.07 cm glass ≈ 2.8 g/cm² Al). Specific energy loss K in Mev/(mg/cm²).

example, we consider a track which has a grain density equal to that of an α-particle with a residual range of 800–1000μ in the emulsion, as determined by grain counting. The specific energy loss K thus lies between the limits $0.11<K<0.125$ Mev/mg/cm². The particle travels through 17000μ in a single emulsion without any apparent change in grain density. The track enters the emulsion from the vertical and ends in the center of a large nuclear explosion leading to the emission of 22 fragments (Fig. 2).

Since for this particle we have certainly $K>0.11$ Mev/(mg/cm²), we deduce with $R>1.7$-cm emulsion (~4.8 (g/cm²) Al) from the graph as lower limit for the charge $Z>5$ and as lower limit for the energy $E_{\text{kin}}>2$ Bev. Although a charge $Z=5$ is consistent with a specific energy loss of $K>0.11$ Mev/(mg/cm²) and a range $R>4.8$ g/cm², such a particle would have to increase its specific energy loss after traversing 4.8 g/cm² of material to a value $K>0.16$ Mev/(mg/cm²), while we observe a value of $K<0.125$ for all portions of the track. Taking into account that the increase in specific energy loss must lie within the observed limits, we find that the particle must have a charge of $Z\geqq 6$.

An upper limit for Z is obtained from the argument that the minimum specific energy loss of the particle may not exceed 0.125 Mev/(mg/cm²). Since the minimum value for a proton is 0.00166 Mev/(mg/cm²) we obtain

$$Z^2\cdot 0.00166<0.125 \text{ or } Z<9.$$

The particle is therefore a fast moving carbon, nitrogen, or oxygen nucleus. If carbon, its energy is *ca.* 3.2 Bev where the track enters the emulsion and *ca.* 2.6 Bev near the star. If nitrogen, its energy lies between 5.1 and 6.5 Bev. If oxygen, its energy lies between 11 and 19 Bev.*

It is of some interest to discuss the star (Fig. 2) at the end of the above track. The star is very probably due to the disintegration of a silver nucleus by the particle responsible for the track. By counting the number of fragments and assigning the least possible charge to each fragment consistent with its track thickness, we obtain a minimum estimate of 37 charges emanating from the star. But the probability is high that a number of energetic protons which escape detection are also emitted and therefore the actual number of charges emitted is probably considerably higher. With the reasonable assumption that the carbon, nitrogen, or oxygen nucleus is incident on a silver atom and is the cause of the explosion, we estimate the energy dissipated in the explosion to be at least 3 to 4 Bev, in good agreement with the energy assigned to the incoming particle.

If the track density of a heavy particle is everywhere higher than that of an α-particle we get only a lower limit on the charge which, in the case of very heavy tracks, is far below the real value. For 25 very heavy tracks investigated, these (certainly, in most cases, far too low) lower limits range from $Z>8$ to $Z>16$. In these cases, however, much more accurate values for the charge can be obtained by the second method which we shall discuss now.

B. Determination of the Charge Z by Range and δ-Ray Density Measurements

For heavy tracks, the counting of the number of secondary electrons (δ-rays) in a given range interval per unit length can provide, together with the range measurement, a more accurate value for the charge Z than the rather qualitative estimate of the specific energy loss K from the track density.

* We have obtained in the meantime 12 tracks of light ions with ranges sufficiently long to permit much more accurate charge determinations. For these tracks we could determine Z uniquely by the above method. Z values of six, seven and eight have been found showing that atoms of carbon, nitrogen and oxygen are present in the primary cosmis radiation.

The number of δ-rays per centimeter with energies in the interval between W and $W+dW$ is given by Mott:[3]

$$dn=(2\pi NZ^2e^4/m_e v^2)(dW/W^2)\times[1-\tfrac{1}{2}(1-\beta^2)(W/m_e c^2)+(Z\pi\beta/137)[\tfrac{1}{2}((1-\beta^2)/\beta^2)(W/m_e c^2)]^{\frac{1}{2}}\times[1-\tfrac{1}{2}((1-\beta^2)/\beta^2)(W/m_e c^2)]],$$

where W, m_e are the kinetic energy and mass of the electrons; Z, v are the charge and velocity of the ion; and N is the number of electrons per cm³ of stopping material.

We will be able to detect the tracks of δ-rays in the Ilford emulsion, provided they lie in a direction favorable for observation and provided their energies lie approximately between 10 kv and 30 kv. The upper energy limit is given by the sensitivity of our emulsion and the lower limit by the criterion used to exclude confusion with background grains (the δ-ray track must show at least four grains in a row). In the non-relativistic approximation the maximum energy of the δ-rays is given in terms of the velocity v of the ion by

$$W_{\max}=2\cdot m_e c^2\cdot(v/c)^2.$$

The smallest value of the velocity which will lead to the production of δ-rays up to 30 kev is therefore determined by the condition

$$v^2/c^2\geq 30\text{ kev}/2mc^2=0.03.$$

For an α-particle this means that the formula can be applied for residual ranges greater than 325 mg/cm² aluminum or 1200μ in the emulsion. For six times ionized carbon the residual range is 110 mg/cm²≈400μ and for heavier ions still shorter. For most tracks it is therefore applicable to within a very short distance from the end of the track. For δ-rays between 10 kev and 30 kev the relativistic correction term in the brackets will give a correction of less than eight percent up to $Z=30$. Since none of the tracks measured so far gives a value for Z larger than about 30, we shall in general neglect the term in the brackets.

The number of δ-rays with energies between W_1 and W_2 is then given by

$$n_{\text{theor}}=2\pi N(e^2/m_e c^2)^2\times[(m_e c^2/W_1)-(m_e c^2/W_2)](Z^2/\beta^2).$$

Whatever our criteria in selecting δ-rays for

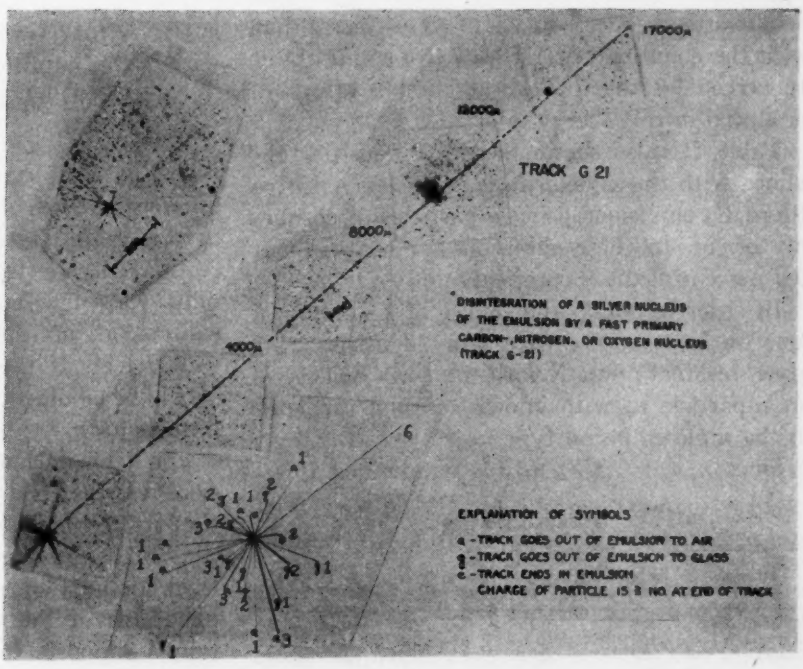
17000μ
12000μ
8000μ
4000μ
TRACK G 21
DISINTEGRATION OF A SILVER NUCLEUS OF THE EMULSION BY A FAST PRIMARY CARBON-, NITROGEN-, OR OXYGEN NUCLEUS (TRACK G-21)
EXPLANATION OF SYMBOLS
a - TRACK GOES OUT OF EMULSION TO AIR
g - TRACK GOES OUT OF EMULSION TO GLASS
e - TRACK ENDS IN EMULSION
CHARGE OF PARTICLE IS 8 NO. AT END OF TRACK

FIG. 2. Disintegration of a silver nucleus by a fast primary carbon, nitrogen, or oxygen nucleus (track G-21). The charge of the particle responsible for the 17,000μ long track G-21 has been determined to be $Z=6$, 7, or 8 from the specific energy loss $0.11<K<0.125$ Mev/(mg/cm²) and the δ-ray density

$$n=(2.8\pm0.5)(\delta\text{-rays}/100\mu).$$

[3] N. F. Mott, Proc. Roy. Soc. **124**, 425 (1929). Mott's cross section for the elastic scattering of electrons by the Coulomb field of a nucleus of charge Z has been transcribed to the coordinate system in which the electron is initially at rest.

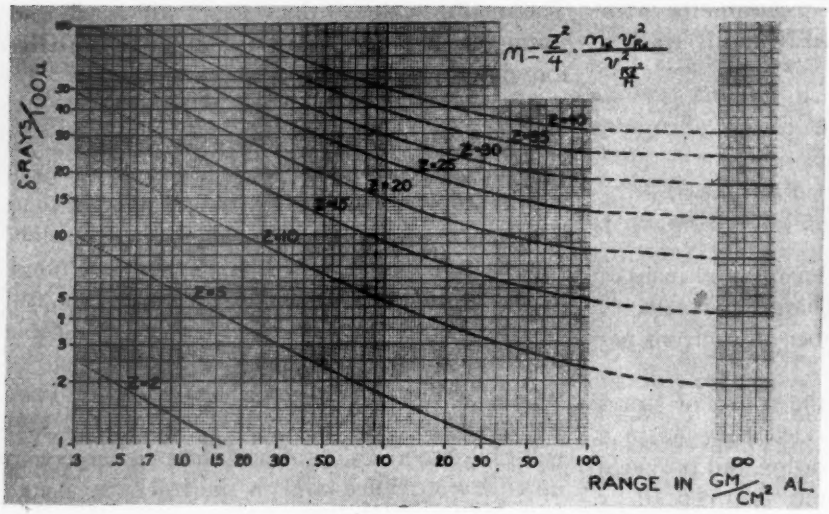

δ-Ray Density *vs.* Range

FIG. 3. Determination of the charge Z by range and δ-ray density measurements. Plotted is the number of δ-rays per 100μ n_δ *versus* the range R for Z values between 2 and 40, calculated with the unrelativistic formula $n_\delta=(Z^2/4)[n_\alpha\beta^2(R_\alpha)/\beta^2((Z/2)R)]$, with

$$n_\alpha\beta^2(R_\alpha)=0.075(\delta\text{-rays}/100\mu).$$

counting, we should always obtain a constant fraction of the theoretical δ-ray density and for a given set of criteria the densities obtained should vary like Z^2/β^2 in an emulsion of given sensitivity.

We have made δ-ray counts for improved Eastman NTB emulsions irradiated with α-particles from the 184″ Berkeley cyclotron.** The results are given in Table III. We estimate that with the counting criteria used, we count about 16 percent of the theoretical number of δ-rays produced in this energy interval.

Table III also shows the δ-ray densities obtained with the same criteria in the less sensitive Ilford C_2 emulsions using α-particles of cosmic-ray origin. In these emulsions we count about ten percent of the theoretical number.

In order to obtain the charge of an unknown ion, we have to compare δ-ray densities at a given residual range R with the δ-ray density of an α-particle n_α with known residual range R_α in the same emulsion type.

Since $n/n_\alpha=(Z^2/Z_\alpha^2)(\beta_\alpha^2/\beta^2)$ and since β^2 is a known function of the variable $RZ^2/M\approx RZ/2$,

$$\beta^2=\psi(RZ/2),$$

we obtain the relation

$$n=(Z^2/4)n_\alpha[\psi(R_\alpha)/\psi(RZ/2)]$$

For $n_\alpha\psi(R_\alpha)$ we use the values listed in Table III:

$n_\alpha\psi(R_\alpha)=0.12(\delta\text{-rays}/100\mu)$ for Eastman NTB emulsions and
$=0.079(\delta\text{-rays}/100\mu)$ for Ilford C_2 emulsions.

TABLE III.

Emulsion type	α-particle energy	β^2	δ-rays/100μ n	$n\beta^2$
Eastman NTB	368 Mev	0.164	0.76±0.08	0.125±0.01
Eastman NTB	168	0.084	1.3 ±0.2	0.11 ±0.02
Ilford C_2	60	0.032	2.5 ±0.05	0.079±0.016

** We are greatly indebted to Dr. E. Gardner for making the exposures for us.

In Fig. 3 we have plotted log$n$ *versus* log$R$ for different values of Z. The main uncertainties in this graph, apart from the relativistic correction, derive from the fact that we have only very few suitable α-particle tracks for calibration in the Ilford plates exposed at 94,000 feet. If the accepted value for $n_\alpha\psi(R_\alpha)$ should be modified, this will only lead to a change of scale for n.

For a particle which traverses several emulsions and then ends in one of the emulsions, such that its residual range is accurately known, we can obtain, by selecting different sections of the track for δ-ray counts, several independent determinations of the charge. The consistency obtained supports the assumption that the δ-ray density varies very nearly like Z^2/β^2.

Let us take as example the track G-20 of a particle which enters the stack of plates under an

angle of 10° from the vertical, traverses two glass plates and three emulsions, and comes to rest in the fourth emulsion (Fig. 4, Table IV). The track appears in the first emulsion about as heavy as an α-particle track.

The observed variation of δ-ray density with residual range follows closely the $1/\beta^2$-law** and agrees reasonably well with the one calculated (using the relativistic correction) for a charge $Z=20\pm2$. The energy of a calcium nucleus of range $R=5.4$ (g/cm²) Al equivalent would be $E_{\text{kin}}=10.8$ Bev and the specific energy loss in the first emulsion $K=1.2$ Mev/(mg/cm²), not inconsistent with the appearance of the track.

In cases where the actual range of the particle is not known but only a lower limit for it, the variation of the δ-ray density along the track can be used to obtain a value for both Z and R. If n does not change measurably over several g/cm² track length, the value of Z obtained will be good, though only a lower limit can be deduced for the range or the energy. For example, we find for the δ-ray density along the 17,000μ track G-21 of the light nucleus producing the nuclear explosion discussed above, the average value

$$n_{\delta}=(2.8\pm0.5)\delta\text{-rays}/100\mu.$$

(Only near the star does the δ-ray count give a slightly larger value.) This δ-ray density cor-

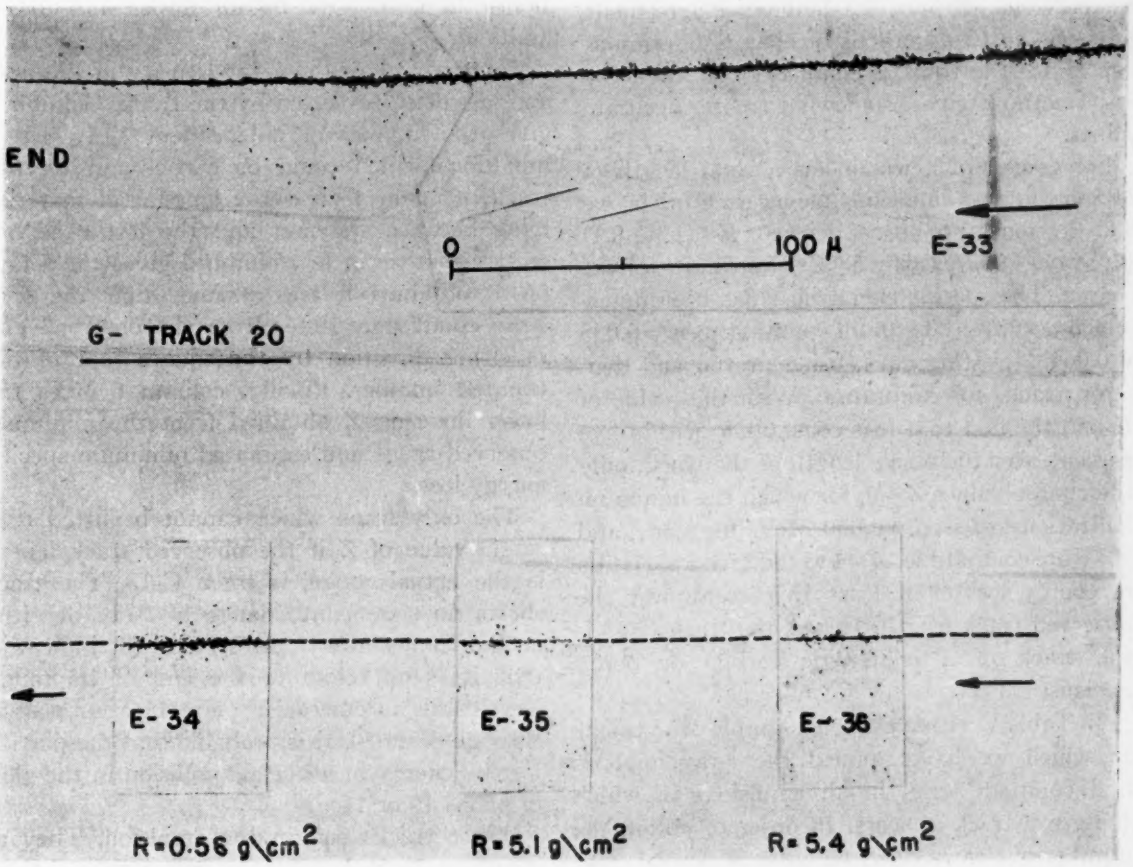

FIG. 4. Track G-20 of a particle with charge $Z=20\pm2$ entering the stack of plates in emulsion E-36 and coming to rest in emulsion E-33. The portions of the track in emulsion E-36 and E-35 shown in Fig. 4 correspond to a velocity $\beta=v/c\approx0.62$. In emulsion E-34, where the track is already considerably heavier, the velocity is reduced to $\beta=v/c\approx0.34$. The track density reaches a maximum in emulsion E-33 for a remaining range of approximately 100μ; then the track tapers off, due to the gradual filling up of the electronic shells.

** The increase of δ-ray density with decreasing range seems to be only slightly less rapid than calculated, a fact which may be due to the larger chance of missing δ-rays while counting in portions of the track with very high δ-ray densities.

TABLE IV. Observed and calculated δ-ray densities for track G-20 ending in emulsion E-33.

Emulsion	Remaining Range R Glass	Emulsion	R in g/cm²/Al	n_{exp}	$n_{calc.}$ $Z=17$	$Z=19$	$Z=21$
	cm	cm					
36	1.68	0.37	5.4	23.5±1.6	16	19	23
35	1.68	0.25	5.1	24.3±1.5	17	20	24
$34_{(1)}$		0.20	0.56	53.0±3.0	47	55	66
$34_{(2)}$		0.14	0.39	65.0±4.0	56	66	74

responds to a charge $6<Z<12$. The value of 2.8 δ-rays/100μ is the value expected for a carbon nucleus of 2.6 Bev, a nitrogen nucleus of 6.1 Bev, or an oxygen nucleus of 11 Bev.

Comparing this with the values obtained for this particle from grain density measurements in the previous chapter, we find good agreement between the two methods of charge determination. Since the track is comparatively thin, the first method gives somewhat more accurate values.

For track G-23, which has a total length of 2.35 cm in two emulsions facing each other, we find a constant δ-ray density $n=(1.1\pm0.1)\times$(δ-rays/100μ), giving $5\leq Z\leq 7$ as limits for the charge. The specific energy loss has been determined accurately by grain counting to $K=0.055\div0.064$ Mev/(mg/cm²), using proton and deuteron tracks for calibration. With this value of K and the fact that it is constant to within five percent over the whole length of the track, only the charge values $Z=6$, for which the minimum ionization loss is $K=0.060$ Mev/(mg/cm²), and $Z=5$ are compatible. $Z=4$ would give a variation of energy loss of at least 15 percent over the observed track length. Hence, the track G-23 is the track of a relativistic carbon or boron nucleus.

In Table V we have listed a sample of 15 tracks to which we have applied the δ-ray analysis and counted δ-rays in all emulsions in which the given track appears. In order to obtain the number of δ-rays/100μ, we have in general combined the counts in the two emulsions facing each other. As a measure of uncertainty, we have used the square root of the number of counts obtained in these two emulsions.

In those cases where we know the range, a single measurement of δ-ray density gives us a value of Z and other measurements along the track can be used to test the consistency of the value obtained. This is the situation for the G-20 track already discussed and occurs also for track G1*** which stops in the glass between plates 10 and 11 and where therefore the range is known for any part of the track with an accuracy of 1.2 g/cm². We can carry out four independent measurements of δ-ray density on the latter track and they are all consistent with a value $20<Z<24$.

Most of the particles listed in Table V go through the entire stack of plates and leave tracks in varying numbers of plates, depending on their angle of incidence. From the observed minimum range and δ-ray count at any place along the track, we obtain upper and lower limits for Z.

Column 2 gives the δ-day density in the first and last plate traversed by the track. Column 3 gives the number of independent δ-ray determinations which could be carried out on the track. Column 4 gives the amount of material lying between the first and the last observed section of the track. Column 5 gives the limits on Z obtained if one assumes that the true δ-ray count may differ from the observed one in either direction by the square root of the counted number. Finally, column 6 gives the lower limit on Z obtained from the minimum observed range and estimated minimum specific energy loss.

The only track which cannot be fitted to a single value of Z if the observed track length is the actual range, is track G-13. The track shows no significant change of δ-ray densities in the four plates 7, 8, 9, and 10, indicating that it is not close to the end of its range. Yet it fails to emerge in plate 11 after passing through plate 10. It is probable that the particle lost its energy in a nuclear collision in the glass of plates 10 or 11.

Three tracks end in the emulsion. They all show a gradual decrease in track thickness towards the end of their range which is to be expected when the particle is slow enough to

*** This is the track discussed in reference 1. Due to the unjustified assumption of proportionality between the amount of reduced silver and energy loss, the estimate of the charge and energy of this particle given in that paper is too high.

collect electrons (see Fig. 4). Their appearance is similar to that of fission tracks. The range over which the decrease of track width takes place is, in one case, about 70μ, in the two other cases, about 100μ. In principle, the charge could be obtained from a measurement of the tapering. However, a satisfactory theory of energy loss of multiply charged ions of low velocity does not as yet exist.

In an aggregate of 15-cm track length of heavy primary tracks in the emulsion, we have seen four particles coming to rest but only one event (see above) which may be interpreted as a nuclear explosion caused by a heavy primary.

Since the energy per nucleon seems to be comparable to that of the proton component, one may expect meson production of high multiplicity from the nuclear collision of a heavy primary with a nitrogen or oxygen nucleus. It is therefore possible that heavy primaries will contribute appreciably to the number of large penetrating air showers at high altitudes. Helium nuclei if present in large numbers would contribute appreciably to meson production. However, in view of the relatively small number of primaries heavier than He and the strong competition of energy loss by ionization, *their* contribution to the total meson intensity would still be small.

THE HEAVY PRIMARIES AND THE ORIGIN OF COSMIC RAYS

Originally, it was not expected that the photographic technique would give any information on the primary cosmic radiation, supposed to consist of high energy protons, because even at high geomagnetic latitudes protons cannot reach the earth unless they possess several Bev kinetic energy and therefore leave no visible tracks in the emulsion. It turned out, however, that the photographic emulsions are an excellent tool for the study of the heavier nuclei of the primary cosmic radiation, among which we have found atomic numbers roughly between carbon and iron. The fact that such nuclei with energies of the order of 1 Bev per nucleon enter the earth's atmosphere may have some bearing on the question of the origin of cosmic rays. This fact obviously favors some mechanism for adiabatic acceleration as opposed to some catastrophic process, such as might result from a nuclear explosion. Any adiabatic mechanism for acceleration should be equally effective for protons and, since hydrogen is by far the most abundant constituent of stellar bodies and interstellar matter, the heavy primary radiation should be accompanied by a much stronger proton component. By means of this argument the presence of heavy nuclei among the primary cosmic rays gives added weight to the already well established hypothesis that the primary radiation consists predominantly of protons.

TABLE V.

1	2	3	4	5	6
Track G	δ-rays/100μ in first and last section n	Number of sections used for δ-ray count	ΔR in g/cm^2 Al between first and last section	Limits for Z from δ-rays	Estimate of Z from ionization density
1	19.7±0.4 52.7±0.8	7	3.75	$20<Z<24$	$Z\gtrsim 22$[a,b]
2	5.2±0.8 9.3±1.0	5	3.72	$8<Z<12$	$Z>8$
3	20.1±2.5 28.1±3.0	11	4.64	$25<Z<35$	$Z\gtrsim 25$[b]
4	10.7±1.8 21.5±2.0	6	2.26	$10<Z<15$	$Z>10$
5	9.2±1.8 17.6±2.2	11	6.8	$15<Z<16$	$Z>13$
7	4.9±0.7 6.3±0.7	8	11.0	$9<Z<18$	$Z>15$
9	5.2±0.9 7.0±1.0	4	2.66	$7<Z<18$	$Z>11$
10	8.8±0.7 8.8±0.7	11	6.48	$18<Z<22$	$Z\approx 25$[a]
11	10.9±1.8 10.9±1.8	11	7.4	$17<Z<24$	$Z>15$
13	10.1±1.5 10.4±1.5	4	1.75	$15<Z<24$	$Z>10$[e]
20	23.5±1.6 65.0±4.0	4	2.96	$18<Z<22$	$Z>15$[d]
21	2.8±0.5 (3.6±0.5)	1	3.4	$6\leq Z<12$	$6\leq Z<9$[e]
22	4.0±0.4 4.3±0.4	2	4.4	$10<Z<15$	$10<Z<14$
23	1.1±0.1 1.1±0.1	2	4.4	$Z\leq 7$	$Z=5$ or 6
24	11.0±1.0 11.7±1.0	2	4.9	$17<Z<26$	$Z>15$

[a] Particle stops in the glass after traversing eight plates.
[b] $K\cong 1.4$ Mev/(mg/cm^3) estimated from comparison with track G-20.
[c] Probably loses its energy in nuclear collision in the glass.
[d] Ends in emulsion.
[e] Produces nuclear explosion in emulsion (Fig. 2).

It is clear that a comparison of the relative frequencies of nuclei heavier than hydrogen among the primary cosmic rays with the known abundance of the elements in the stars and interstellar space may shed light on the origin of cosmic radiation. Most interesting would be a measurement of the relative abundance of He, the element whose abundance is next to that of hydrogen. The astrophysical data suggest for planetary nebulae, the sun, and τ Scorpii a helium abundance of 1 to 2 He atoms for each 10 atoms of hydrogen,[4] a ratio which is in fair agreement with that calculated for the sun by Christy and O'Reilly,[5] using the recently measured cross sections relevant for the carbon cycle (He:H atomic ratio = 1:15).

Heavier elements such as oxygen, sodium, magnesium, silicon, potassium, calcium, and iron are known to occur in stellar bodies, planetary nebulae, and in interstellar space. The abundance of carbon and nitrogen is estimated by O'Reilly and Christy to be of the order of one percent by weight for the sun. For interstellar space, the relative abundance of various elements has been derived from spectroscopic data by Struve and Dunham,[6] leading to an estimate of 1:100 by atom for the oxygen: hydrogen ratio and an estimate of the order of 1:10,000 for the relative abundance of all the elements heavier than oxygen. Our preliminary data indicate that the flux of nuclei with $Z \gtrsim 10$ is about one thousandth of the flux of primary protons. This value is in fair agreement with the results of Freier, Lofgren, Ney, and Oppenheimer reported in this issue of the Physical Review.

The flux of nuclei of the carbon, nitrogen and oxygen group is about five times larger than the flux of the heavier nuclei, corresponding to one carbon, nitrogen or oxygen nucleus per 200 primary protons. These values have to be considered as lower limits, since the absorption of heavy primaries due to collisions in the residual air above the plates is not negligible.

A detailed comparison of the chemical composition of cosmic-ray primaries with the relative abundance of elements in stellar and interstellar matter as obtained from astrophysical data may be very instructive. In particular, we have some evidence that the abnormally low abundance of Li, Be and B and the high abundance of Fe in stellar matter repeats itself in the cosmic-ray flux. Thus far no tracks of primary Li, Be or B nuclei have been found.

Measurements to determine accurately the flux of nuclei as a function of their charge are in progress.

Further information bearing on the origin of cosmic rays can be obtained by investigating whether there exists a minimum range for heavy primaries of giving charge Z. Calculations by J. Ashkin† show that if heavy primaries traverse an appreciable fraction of the galaxy with the observed velocities, they will be stripped of electrons by the matter in interstellar space, assuming a density of one hydrogen atom per cm^3 or an effective hydrogen layer of 15 mg/cm^2 for the galaxy. Upon entering the sun's or earth's magnetic field the heavy primaries should therefore be subject to a magnetic energy cut-off, $E_Z{}^c$, which, in terms of the cut-off for protons $E_1{}^c$, is given by

$$E_Z{}^c = Z[((E_1{}^c+1)^2+3)^{\frac{1}{2}}-2], \quad (M \approx 2Z).$$

The particles should therefore possess a minimum energy and minimum range dependent on their charge.

If, however, the particles come from the sun, they will in general not be expected to be completely stripped (though this may occur occasionally) and partially stripped ions with comparatively low velocities should not be prevented by the earth's magnetic field from reaching its atmosphere. Thus the study of the geomagnetic effect for heavy primaries, by deciding whether they arrive completely stripped or only partially so, may contribute to a solution of the problem of the origin of cosmic rays.

[4] L. H. Aller and D. H. Menzel, Astrophys. J. **102**, 263 (1945).
[5] J. O'Reilly and R. F. Christy, Pasadena Meeting of the American Physical Society, June 1948.
[6] C. S. Beals, Monthly Notices, Roy. Astr. Soc. **102**, 96 (1942).

† Dr. J. Ashkin states: "Taking $v/c = 0.3$ as an intermediate velocity of the ion, the stripping cross section in the Born approximation for most of the electrons of an ion like calcium ($Z = 20$) is of the order of 10^{-20} cm^2 for impact with a hydrogen atom at rest. This corresponds to a mean free path of 10^{20} cm. Since the mean free path decreases with the second power of the velocity for smaller velocities, any reasonable fraction of the total 10^{22} cm of the galaxy should be sufficient to remove most of the electrons of the ion."

Experiments to decide whether there exists a minimum range for particles of given Z equal to that calculated for complete stripping (using stopping material up to 120 (g/cm²) in the form of photographic plates) are in progress.

We wish to extend our thanks to Messrs. S. Tamor and Tom Putnam of the University of Rochester for valuable help in carrying out measurements and preparing graphs, and to the cosmic-ray group of the University of Minnesota and the Aeronautical Research Group of General Mills for assistance in the exposure.

This work was assisted by the Joint Program of the Office of Naval Research and the Atomic Energy Commission.

PHYSICAL REVIEW VOLUME 74, NUMBER 12 DECEMBER 15, 1948

On the Energy of Cosmic Radiation Allowed by the Earth's Magnetic Field

M. S. VALLARTA
Instituto de Física, Universidad de México, México, D. F.

(Received August 9, 1948)

Curves giving proton energies (a) below which no energy is allowed by the earth's magnetic field, (b) above which all energies are permitted, for all latitudes in case (a), for latitudes from 0° to 40° geomagnetic in case (b), are given for the following directions: (1) vertical, (2) zenith angle 45°, north, south, east and west azimuths. In addition the distance and angular corrections due to the longitude effect are given for geographic latitudes up to 40°.

IN the course of discussions on the east-west asymmetry of cosmic radiation which took place on occasion of the Symposium on Cosmic Rays held at the California Institute of Technology in honor of Robert A. Millikan's eightieth birthday, it became clear that additional information on the energy of cosmic radiation allowed through the earth's magnetic field was required to interpret high altitude experiments now being carried out. Such information is presented in the curves given in this paper.

In Fig. 1 the lower curve, labeled E_1, gives the least energy that a proton must have in order to penetrate through the earth's magnetic field in the vertical direction at the geomagnetic latitude given by the abscissa. This energy is determined either by the Störmer cone or by the simple shadow cone,[1] the former for low latitudes and the latter for intermediate and high latitudes.

The upper curve labeled E_2 gives the energy that a proton must have in the vertical direction, at the geomagnetic latitude given by the abscissa, above which all energies are allowed by the earth's magnetic field. This energy limit is determined by the main cone.[2]

Between the upper and lower curves lies the region of penumbra, in which only certain energies between these two limits are allowed, in the given direction, and others are forbidden.[3]

At low latitudes (less than 15°) the dark bands predominate in this region and the least allowed energy is practically given by the lower curve. At intermediate latitudes (between 15° and 35°) the dark and light bands are about equally important, but one cannot predict without further very difficult analysis whether an energy between these limits will actually arrive in the vertical direction. At 20°, for instance, it is known, that only energies higher than those given by E_2 (main cone) can actually arrive. At high latitudes light bands predominate in the penumbra and the least allowed energy is practically given by the lower

[1] E. J. Schremp, Phys. Rev. **54**, 158 (1939).

[2] G. Lemaitre and M. S. Vallarta, Phys. Rev. **50**, 493 (1936).

[3] G. Lemaitre, Ann. de la Soc. Sci. de Bruxelles **54**, 162 (1935); R. Albagli Hutner, Phys. Rev. **55**, 614 (1939); Tchang Yong-Li, Ann. de la Soc. Sci. de Bruxelles **59**, 285 (1939); René de Vogelaere (unpublished, private communication to the author).

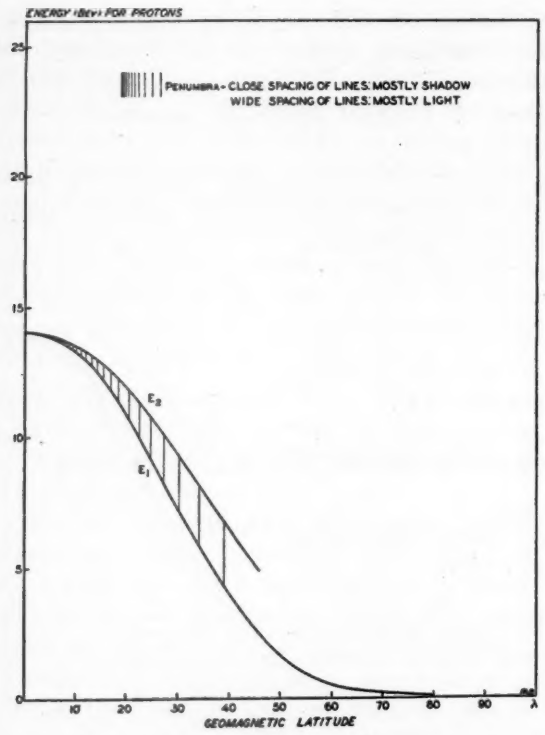

FIG. 1. Proton energies allowed by the earth's magnetic field in the vertical direction, as a function of geomagnetic latitude.

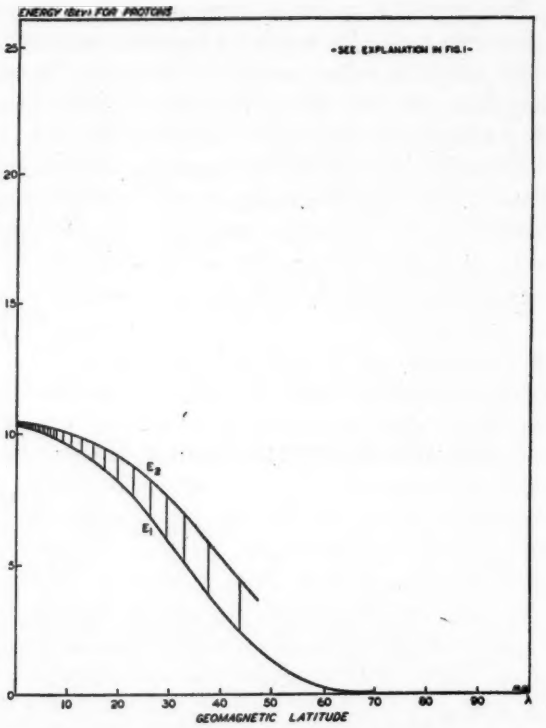

FIG. 3. Proton energies allowed by the earth's magnetic field in the direction 45° west, as a function of geomagnetic latitude.

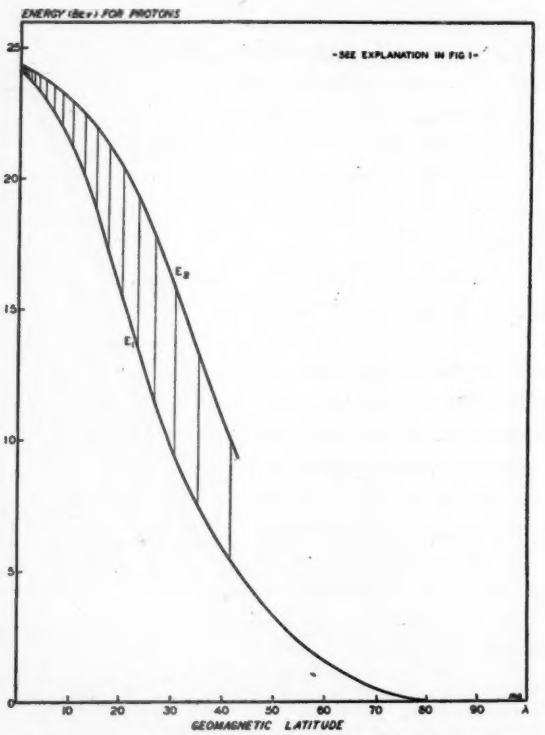

FIG. 2. Proton energies allowed by the earth's magnetic field in the direction 45° east, as a function of geomagnetic latitude.

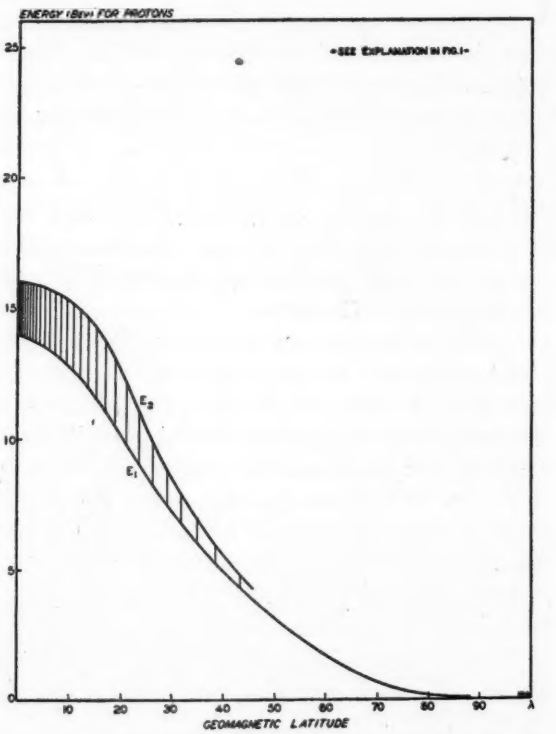

FIG. 4. Proton energies allowed by the earth's magnetic field in the direction 45° north, as a function of geomagnetic latitude.

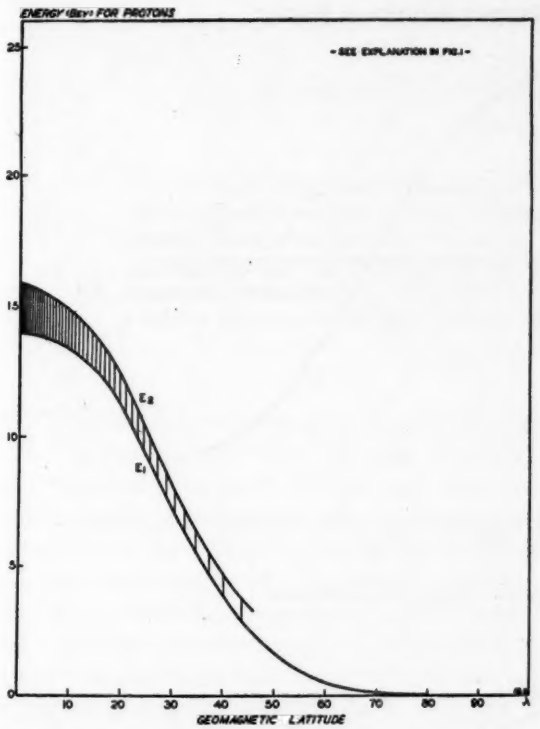

FIG. 5. Proton energies allowed by the earth's magnetic field in the direction 45° south, as a function of geomagnetic latitude.

curve E_1. This circumstance is indicated by the spacing of vertical lines between the two curves. Close spacing means that all energies between the two curves are ruled out, distant spacing signifies that all energies above the lower curve are practically allowed.

Figures 2 and 3 give the same information as Fig. 1, with the same explanation as in the preceding paragraph, but now for zenith angle 45° in the azimuths east and west, respectively. It is seen that in these cases the penumbra is quite important at certain latitudes.

Figures 4 and 5 give the same data for zenith angle 45° and azimuths north and south, respectively. It is seen that the energy difference responsible for the north-south asymmetry is much less than that responsible for the east-west asymmetry. However, since the allowed cones for positive particles are symmetrical, with respect to the meridian plane, to those for negative ones, the north-south asymmetry depends on the sum of positive and negative primaries, while the east-west asymmetry depends on their difference. Thus the knowledge of both the east-west and north-south asymmetries gives information on the ratio of positive to negative primaries. Therefore the north-south asymmetry should be studied experimentally as well as the east-west effect, in spite of the fact that the former is much smaller. It should also be noted that the penumbra hardly plays a part in the north-south effect. Curve E_2 in Figs. 4 and 5 has been determined from the main cone.[4]

The corrections to Figs. 1 to 5 because of the

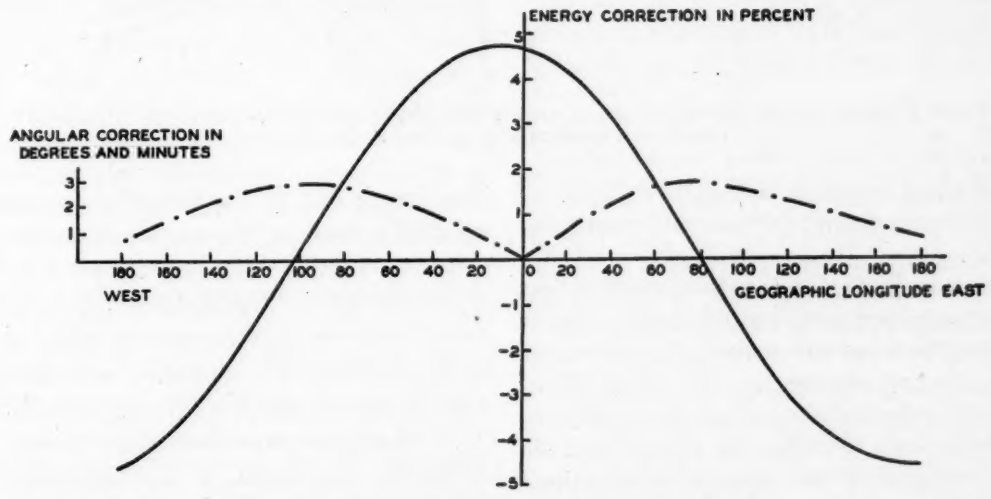

FIG. 6. Distance and angular (dotted line) corrections as a result of longitude effect along the geographic equator, as a function of geographic longitude.

[4] G. Lemaitre and M. S. Vallarta, Phys. Rev. **49**, 719 (1936); G. Lemaitre, M. S. Vallarta and L. Bouckaert, **47**, 434 (1935).

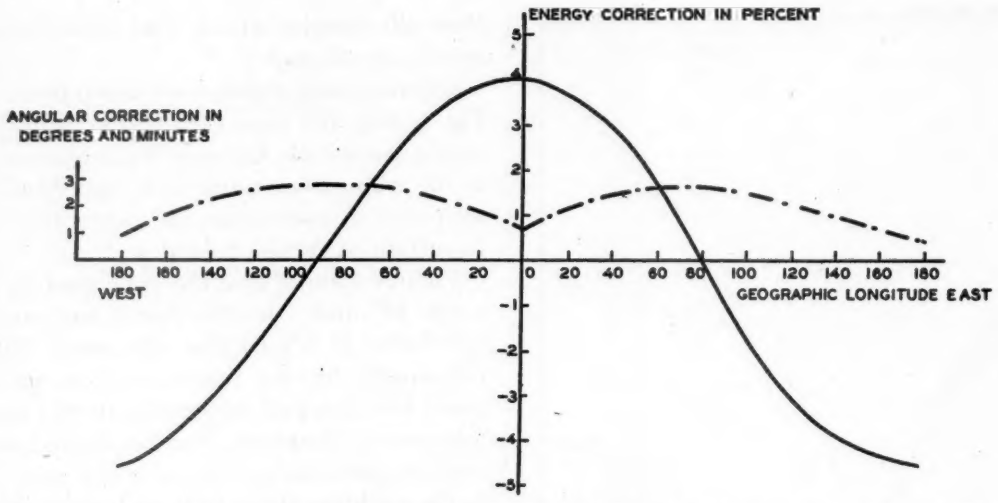
ENERGY CORRECTION IN PERCENT
ANGULAR CORRECTION IN DEGREES AND MINUTES
180 160 140 120 100 80 60 40 20 0 20 40 60 80 100 120 140 160 180
WEST
GEOGRAPHIC LONGITUDE EAST

FIG. 7. Distance and angular corrections as a result of longitude effect at the geographic latitude 20° north, as a function of geographic longitude.

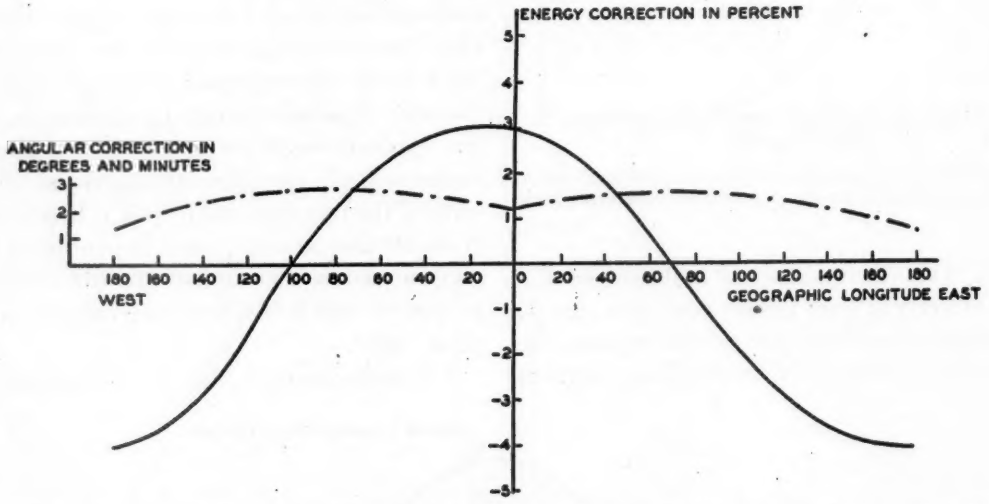
ENERGY CORRECTION IN PERCENT
ANGULAR CORRECTION IN DEGREES AND MINUTES
180 160 140 120 100 80 60 40 20 0 20 40 60 80 100 120 140 160 180
WEST
GEOGRAPHIC LONGITUDE EAST

FIG. 8. Distance and angular corrections as a result of longitude effect at the geographic latitude 40° north, as a function of geographic longitude.

longitude effect are given in Figs. 6, 7 and 8, for geographic latitudes 0°, 20° and 40° north, respectively.

There are two corrections to be made. The first is the distance correction and takes into account the distance between the earth's magnetic center and the point of observation; the second (dot-dash curve) is the angular correction and refers to the angle between the magnetic vertical and the ordinary vertical of the point of observation.[5] The first is due to the fact that, according to Schmidt's analysis, the earth's magnetic center does not coincide with its ordinary center, the second depends on the circumstance that the line connecting the earth's magnetic center with the point of observation (magnetic vertical) does not always coincide with the ordinary vertical.

It is a pleasure to acknowledge the help of the Comisión Impulsora y Coordinadora de la Investigación Científica of Mexico which made this research possible.

[5] M. S. Vallarta, Phys. Rev. 47, 647 (1935); G. Lemaitre, Nature 140, 23 (1937).

The Absorption of Gamma-Radiation*

CLYDE L. COWAN
Department of Physics, Washington University, St. Louis, Missouri

(Received July 16, 1948)

Absorption coefficients for gamma-radiation ranging from 0.32 to 2.8 Mev penetrating various elements ranging from low to high Z were measured. A geometry was employed which yielded results whose accuracy was limited only by statistics and background corrections. The source, absorbers of area just sufficient to completely intercept all detected gamma-rays, and a Geiger tube were suspended outdoors about 25 feet above the ground. The results are in excellent agreement with theoretical predictions.

THE large number of wide variety of radioisotopes which have become available to the physical laboratory in the past few years through the facilities of the Atomic Energy Commission have made it possible to investigate further the validity of the modern theories of the interaction of gamma-radiation with matter. Of the various experimental techniques which lend themselves to this work, that of measurement of absorption coefficients is probably the simplest in application and interpretation, though somewhat limited in the degree of accuracy attainable. A number of investigators[1] have utilized absorption measurements for this purpose, obtaining in general good agreement with the predictions of theory. It is the purpose of the present work to extend these measurements over a wider range of gamma-ray energy and for absorbers of widely differing atomic number, employing a technique calculated to reach a higher degree of accuracy by reducing to a minimum the effects of the geometry and environment of the measuring apparatus.

Three processes are primarily responsible for the attenuation of a beam of gamma-radiation when it penetrates matter: the Compton effect, the photoelectric effect and, for quantum energies above 1.02 Mev, pair creation. Applying the methods of Dirac's electron and radiation theories, a number of physicists[2] have developed the theories of these effects, the results and predictions of which are now well known.[3] It is possible, however, that other processes such as multiple Compton scattering[4] and pair creation in the fields of the atomic electrons[5] may account for some slight additional observable attenuation. Further, with sufficiently accurate measurements, one might hope to find small deviations from the theory of Klein and Nishina as a result of the effect of nuclear binding of the orbital electrons.[6]

APPARATUS

The nature of the absorbing and scattering processes for gamma-rays makes stringent demands on geometry if the errors in the measured values of the coefficients are to be kept small.

* Part of a dissertation to be presented to the graduate school of Washington University in partial fulfillment of requirements for the degree of Doctor of Philosophy.

[1] E. McMillan, Phys. Rev. **46**, 868 (1934); W. Gentner and J. Starkweicz, J. de Phys. et rad. **6**, 340 (1935); G. Groetzinger and L. Smith, Phys. Rev. **67**, 53 (1945); J. Halpern and H. R. Crane, Phys. Rev. **55**, 258 (1939); D. E. Alburger, Phys. Rev. **73**, 344 (1948); McDaniel, von Dardel and Walker, Phys. Rev. **72**, 985 (1947); W. A. Fowler and C. C. Lauritsen, Phys. Rev. **51**, 391 (1937); C. M. Davisson and R. D. Evans, Bull. Am. Phys. Soc. **23**, 45 (1948), and others have found agreement with theory. J. M. Cork and R. W. Pidd, Phys. Rev. **66**, 227 (1944), observed values of absorption coefficients appreciably below theoretical predictions.

[2] O. Klein and Y. Nishina, Zeits. f. Physik **52**, 853 (1929); Y. Nishina, Zeits. f. Physik **52**, 869 (1929); A. Sommerfeld and G. Schur, Ann. d. Physik **4**, 409 (1930); M. Stobbe, Ann. d. Physik **7**, 661 (1930); F. Sauter, Ann. d. Phys. **9**, 217 (1931), **11**, 454 (1931); Hulme, McDougall, Buckingham, and Fowler, Proc. Roy. Soc. **149**, 131 (1935); H. Hall, Phys. Rev. **45**, 620 (1934); J. R. Oppenheimer and M. S. Plesset, Phys. Rev. **44**, 53 (1933); W. Heitler and F. Sauter, Nature **132**, 892 (1933); H. Bethe and W. Heitler, Proc. Roy. Soc. **146**, 83 (1934).

[3] An excellent summary of these results is contained in W. Heitler's *The Quantum Theory of Radiation* (Clarendon Press, Oxford, 1944).

[4] W. Heitler and L. Nordheim, Physica **1**, 1049 (1934); O. Halpern and N. M. Kroll, Phys. Rev. **72**, 82 (1947); C. J. Eliezer, Proc. Roy. Soc. **187**, 210 (1946).

[5] K. M. Watson, Phys. Rev. **72**, 1060 (1947); P. Nemirovsky, J. Phys. USSR **11**, 94 (1947); A. Borsellino, Helv. Phys. Acta. **20**, 136 (1947).

[6] H. Casimir, Helv. Phys. Acta. **6**, 287 (1933); W. Franz, Zeits. f. Physik **90**, 623 (1934); G. Wentzel, Zeits. f. Physik **43**, 1 and 779 (1927); F. Bloch, Phys. Rev. **46**, 674 (1934).

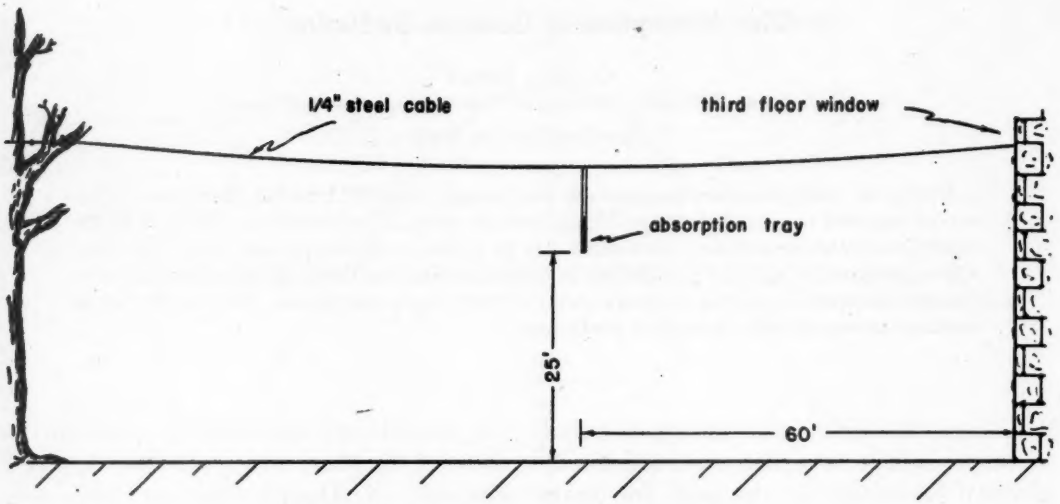

FIG. 1. The out-of-doors suspension employed.

The definition of the absorption coefficient assumes that a given photon will penetrate the full thickness of the absorber unchanged or it will encounter only one absorbing or scattering event, after which no particles which leave the scene of the event are detected in the envelope of the primary beam. Thus, a second or third scattering of the degraded photon which causes it to reach the detector represents a systematic error in the measurements. Furthermore, the beam is assumed to be composed of monoenergetic gamma-quanta which are traveling in parallel paths. An experimental geometry is thus demanded which includes a source of monoenergetic gamma-radiation traveling in a small well-collimated beam, an absorber which is just sufficiently wide to cover the solid angle defined at the source by the detector, and high efficiency gamma-ray detector whose characteristics are invariant to any environmental changes.

In order to approach this idealized geometry, an essentially bare source with small absorbers and a small Geiger tube, all mounted on a light aluminum frame suspended out of doors and as far from massive objects as possible, was employed (Fig. 1). A $\frac{1}{4}$-inch steel cable was run from a hand winch anchored in a third-floor laboratory to a tree about 130 feet distant from the building. An "absorption tray" was suspended from the cable and about 6 feet below it by two nickel wires and Lucite insulators approximately 60 feet from the building. The tray, 2 inches by 4 inches in cross section and 28 inches long, was made of $\frac{1}{16}$-inch aluminum sheet and carried the source, absorbers and Geiger tube as illustrated in Fig. 2.

The gamma-ray source for each measurement was enclosed in a light aluminum tube. As measurements were made throughout the year, the Geiger tube was designed to meet extremes of weather. Alcohol-argon fillings were useless below temperatures of 40°F, but ethyl ether-argon and ethylene-argon fillings were excellent for all-weather counting. The weatherproof Geiger tube is illustrated in Fig. 3. The tube was connected directly to a 100-foot co-axial lead of 11$\mu\mu$f capacity per foot. The lead was hung from the steel cable and connected to a guard cathode follower and scaling circuit and a high-voltage supply located near the winch. The cathode follower neutralized the effect of the long lead very

TABLE I. Linear absorption coefficients measured in the present work. The values in parentheses are the corresponding theoretical values. The coefficients are listed against the corresponding emitters and the effective gamma-ray energy. Units are cm^{-1}.

Source	Gamma-energy (Mev)	Pb	Sn	Cu	Al	C
Cr-51	0.32		1.05 (1.04)	0.937 (0.928)	0.292 (0.280)	0.170 (0.170)
Cs-137	0.65	1.26 (1.27)	0.521 (0.513)	0.617 (0.622)	0.195 (0.197)	0.128 (0.123)
Zn-65	1.11	0.724 (0.712)	0.372 (0.360)	0.478 (0.475)	0.155 (0.152)	0.091 (0.086)
Sb-124	1.72	0.533 (0.538)	0.302 (0.290)	0.371 (0.392)		0.0742 (0.071)
Na-24 (from 5 to 12 cm Pb)	2.30	0.473 (0.479)	0.266 (0.264)			0.0599 (0.060)

satisfactorily without seriously interfering with the shielding. The only pick-up disturbances noted were caused by near-by lightning discharges. The absorption tray was lowered to ground level by paying out cable from the winch when absorber changes were required.

BACKGROUND EFFECTS

One serious limitation on the accuracy of absorption measurements is the comparative magnitude of background and transmitted radiation (i.e., "signal-to-noise" ratio). A study of the apparatus was, therefore, made as follows: background measurements were taken with no source in the tray and both with and without 20 cm of lead absorber in position, a count being taken for every two feet of altitude from ground level to the maximum height of 25 feet. It was found that

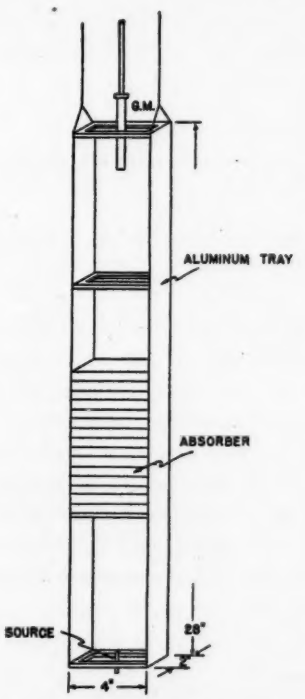

FIG. 2. The absorption tray. The construction afforded adequate rigidity to prevent relative movement of the Geiger tube and the source as the weight of absorber was increased. When the activity of the source was large, the Geiger tube was employed in the position shown. For extremely weak sources, the tube was rotated 90° so that in a broadside position, the increased counting rate with no increase in background could be utilized. A test was made for changes in measured absorption coefficient for absorbers of area half that shown and with the tube in the vertical position. No detectable change was found, indicating that the absorbers used were sufficiently small.

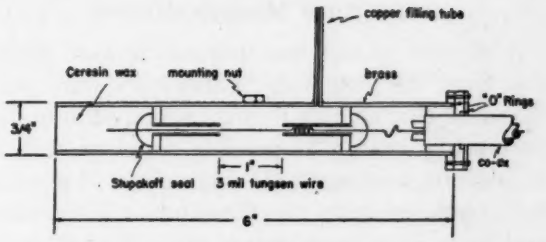

FIG. 3. The weatherproof Geiger tube. The filling of 30 percent ethylene—70 percent argon proved very satisfactory, yielding a tube of high stability, long plateau and no temperature dependence.

background thus measured was the normal cosmic-ray intensity and was not a function of height, nor was it affected by the presence of absorber in the tray. The background *versus* height measurements were then repeated with a 3 mc antimony-124 source and 20 cm of lead absorber in the tray. With this arrangement the background was quite high at ground level and dropped rapidly with increasing height, reaching a constant value of about four times natural background at about 12 feet above the ground. Doubling the mass of the aluminum tray by fastening $\frac{1}{16}$-inch aluminum sheets to it raised this excess or "induced" background by only $\frac{1}{2}$ percent. Only the ground and the air could then account for the induced background.

A lead cap 2-inches thick was made which fitted over the top of the Geiger tube and shielded the tube from the greater part of the solid angle around it while leaving the active region of the tube largely exposed to the ground. With the source and lead absorbers now in place and with the apparatus 25 feet above the ground, the induced background fell to 5 percent of the natural background, indicating that the air was responsible for the back scattering. As the simple geometry described in the last section was designed to eliminate scattering of transmitted photons by matter near the Geiger tube, the intensity of which would vary with absorber thickness, the lead cap was removed for the absorption measurements. A theoretical study of the scattering of gamma-radiation by the atmosphere was made by Dr. H. Primakoff of this department with the result that the induced background could be assigned to air scattering (Fig. 4).

ABSORPTION MEASUREMENTS

A number of radioisotopes which were available from the Oak Ridge Laboratory were purchased so that as wide a range of monochromatic gamma-ray energy as possible could be tested. In addition, antimony-124 and sodium-24 sources were obtained from the Washington University cyclotron. In several cases it was not possible to obtain monochromatic radiation, but it was possible to use sources which either emitted gamma-lines close together or quite far apart. A study of these complex spectra revealed that when the lines were quite close together, the measurements should yield a coefficient which should be characteristic of gamma-radiation possessing the mean energy of the spectrum. On the other hand, when the lines were well separated, the line possessing the highest absorption coefficient should effectively disappear from the transmitted radiation for relatively small absorber thickness, leaving a quite usable intensity of the higher energy radiation for further measurement. In the case of the radiation from sodium-24, the lines cannot be resolved as above nor are they close enough together to appear monochromatic. The resulting absorption coefficient measured would then be a function of the absorber thickness. The data are usable, however, when taken over only 6 to 10 cm of, say, lead absorber for which range the deviation from a pure exponential absorption caused by the complex character of the spectrum was less than experimental error. Matching this portion of the absorption curve to a synthetic curve constructed by assigning theoretical coefficients to the known lines in the spectrum and adding the resultant curves is a valid test of the theory at this energy. Whenever possible, sources possessing long half-lives relative to the time required for a complete absorption coefficient determination were chosen. The gamma-spectra of the sources were analyzed by the various beta-spectrograph groups in the laboratory whenever

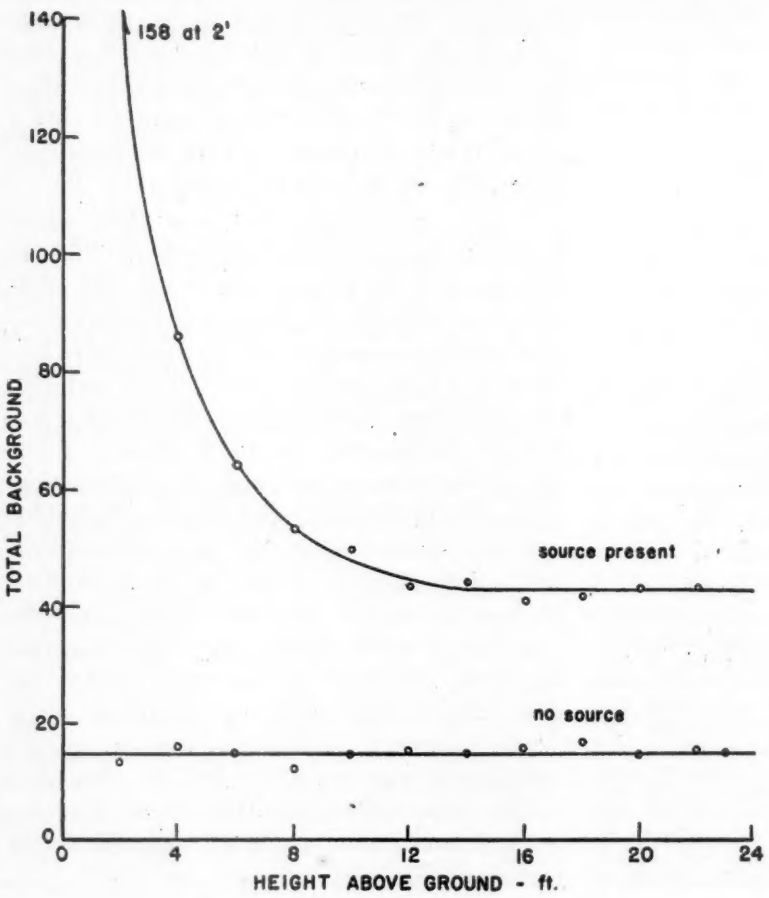

FIG. 4. Background *versus* height of the absorption tray above ground. The statistical deviation for each point is approximately 5 percent.

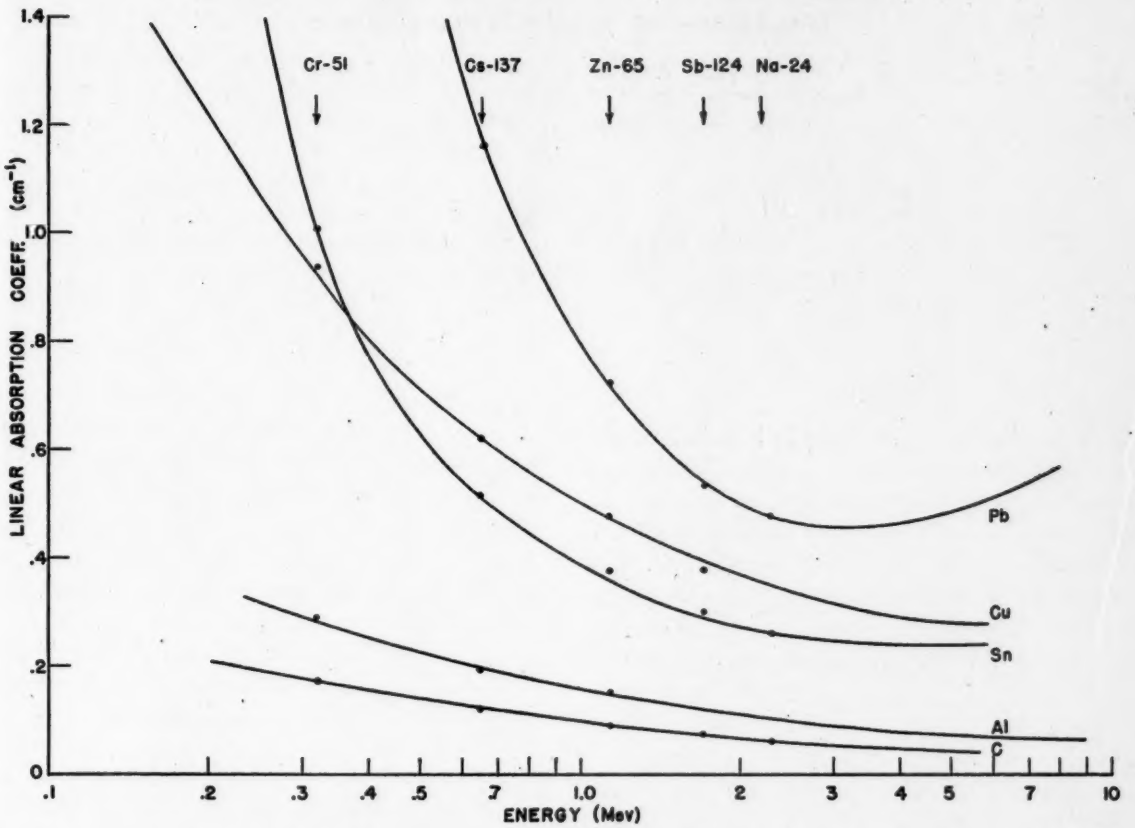

FIG. 5. The points are the results of the present measurements and the lines are the predictions of theory. The line for carbon was calculated for graphite of density 1.59 g/cm³.

there was doubt as to their true composition. A chemical purification of the radioisotopes was also carried out where indicated.

All counts taken were sufficiently large so that standard deviation was less than one percent. Corrections were made for the effect of Geiger tube insensitive time and, where necessary, for decay of the source during measurement. Attenuation of the gamma-beam by absorber was carried to a point no farther than ten times the total (natural plus induced) background.

RESULTS

Absorption coefficients thus measured are listed in Table I along with theoretically predicted values. Figure 5 is a plot of the predictions of theory (solid lines) on which the experimental values are placed. It is seen that within the experimental error the values are in excellent agreement with theoretical ones from low to high Z and over the energy range covered. No evidence could be found for observable secondary attenuating effects such as double Compton scattering.

ACKNOWLEDGMENTS

The author wishes to thank Professors A. L. Hughes, F. Rassetti, H. Primakoff, and F. N. D. Kurie for their interest and helpful discussions; K. Morganstern and T. Stix for their assistance in taking the voluminous data; L. Sylvester and O. Retzloff for invaluable glass and machine shop work required in developing the Geiger tube, and the office of Naval Research for its support through Contract N6ori-117, Task Order I.

The Alpha-Ray Spectrum of Polonium*

WALTER G. WADEY**
Randall Laboratory, University of Michigan, Ann Arbor, Michigan
(Received August 25, 1948)

Measurements of the alpha-ray spectra of polonium mounted on nickel, silver, and cadmium by means of a 180-degree-focusing magnetic spectrograph are reported and discussed. The weak line series reported by Chang was not apparent. The hypothesis is proposed that the alpha-ray spectra seen to date have not been caused by the element polonium, but by the diffusion of the polonium into the mounting metal.

I. INTRODUCTION

THE nucleus of the element polonium has been shown to emit gamma-radiation of 0.80-Mev energy and also softer gamma-radiation whose energy has not been confirmed.[1–4] The existence of multiple gamma-rays from polonium has been confirmed by the detection of gamma-gamma coincidences in this laboratory by M. L. Wiedenbeck. An alpha-ray line at 5.300 Mev has been accurately measured.[5,6] Its intensity has been determined to be about 100,000 times that of the gamma-radiation.[2,3]

In 1946, W. Y. Chang[7] reported the discovery of a long series (12 actually measured) of very weak alpha-ray lines spaced at about 0.1-Mev intervals below the 5.300-Mev line. He found their intensities to be about 10,000 times weaker than that of the 5.300-Mev line, inconsistent with the gamma-ray data, as pointed out by Feather.[8] Chang recognized that the existence of the weak line series was in severe conflict with the present theory of alpha-ray emission in that if both are taken at their face value, they imply large spin differences (of the order of 10) between the alpha-ray transitions, and spin differences of this order have never been observed elsewhere in alpha-ray spectra. He also plotted log λ *versus* energy for the line series and showed that the sequence diverged sharply from the Geiger-Nuttall relation of the uranium family.

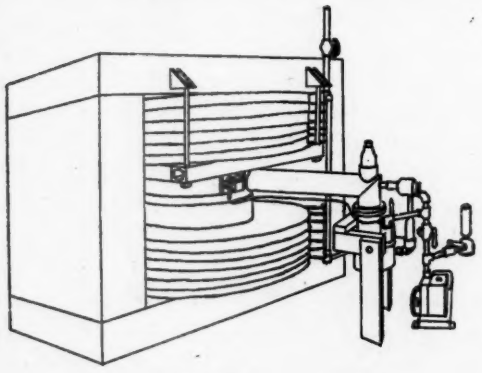

FIG. 1. View of spectrograph.

II. SPECTROGRAPH

In order to investigate the alpha-ray spectrum of polonium further, a 180-degree-focusing magnetic spectrograph of 24-inch pole diameter was designed and constructed. A general view is shown in Fig. 1 and a scale drawing of the vacuum chamber in Fig. 2.

The design was based on Kai Siegbahn's theory of beta-ray spectrographs.[9] For the resolving power R, defined as

$$R=\delta(Hr)/Hr,$$

he derives the formula

$$R=Q/r+2(1-\cos\alpha) \qquad (1)$$

and the relation for greatest intensity at a given resolution:

$$Q\cong 2r(1-\cos\alpha), \qquad (2)$$

* A condensation of a dissertation submitted in partial fulfillment of the requirements for the degree of Doctor of Philosophy in the University of Michigan.
** Now at Yale University, New Haven, Connecticut.
[1] I. Curie and F. Joliot, J. de phys. et rad. **2**, 20 (1931).
[2] H. C. Webster, Proc. Roy. Soc. **A136**, 428 (1932).
[3] W. Bothe, Zeits. f. Physik **96**, 607 (1935).
[4] S. DeBenedetti and F. H. Kerner, Phys. Rev. **71**, 122 (1947).
[5] S. Rosenblum and G. Dupouy, J. de phys. et rad. **4**, 262 (1933).
[6] W. B. Lewis and B. V. Bowden, Proc. Roy. Soc. **A145**, 235 (1934).
[7] W. Y. Chang, Phys. Rev. **69**, 60 (1946).
[8] N. Feather, Phys. Rev. **70**, 88 (1946).
[9] Kai Siegbahn, Arkiv. f. Mat., Astr. o Fys. **30A**, No. 20 (1944).

where H is the magnetic field strength, r the radius of curvature of the particle path, Q the source width, and α the half-angle of divergence of the particle paths in the horizontal plane. $\sin\alpha = s/d$, where $2s$ is the width of the slit and d is the distance from source to slit. The constants of the spectrograph were $d = 25.42_5$ mm $\pm 0.02_5$ mm, $2s = 1.72_7$ mm ± 0.05 mm, $Q = 0.32_3$ mm $\pm 0.01_2$ mm, which give at the maximum radius of 260 mm

$$R = 0.23 \text{ percent.}$$

The alpha-rays were detected with Eastman nuclear track plates (type NTA) inclined at a 45-degree angle to the plane of the particle paths and accurately located within the spectrograph in order that positions on the plates could be correlated with positions in the spectrograph.

The inclination of the plates necessitated corrections to the measured plate positions, as may be seen from Fig. 3, where XYZ is a space coordinate system with OZ the vertical axis and OY horizontal in the plane of the spectrograph slit midway between the top and bottom of the vacuum chamber. The monoenergetic image of a line source is a line, BO, called the "track line." This geometrical correction allows us to correct the measured value of a, the distance from the slit to the point concerned, to that value which would have been observed if φ had been zero:

$$\delta a = (y_0 - y)(\cos\theta)d/a, \qquad (3)$$

where y_0 is the value of the coordinate across the plate in the plane of the slit, y is the point coordinate, θ is the plate inclination angle (45 degrees), and a is the distance from the image to the slit.

A simple calculation shows that if the position of the plate is known to within 1 mm and the position of the line in the plate with reference to the end of the plate to within 0.25 mm, the momentum will be known to within 0.1 percent. The spectrograph construction and method of plate measurement enabled them to be measured to within 0.1 mm. Expansion of the "frame" (see Fig. 2) introduced no error because of the use of the quartz rod which determined the slit-plate distance.

The vacuum chamber had a brass wall and iron lids, top and bottom, leaving $1\frac{3}{4}$ inches clear inside. It was lined with 0.010-inch cellulose acetate. The "trunk" and "slide" permitted daylight loading of the spectrograph. All parts in the vacuum chamber were made of 24S-T aluminum alloy, except for the quartz rod and brass screws.

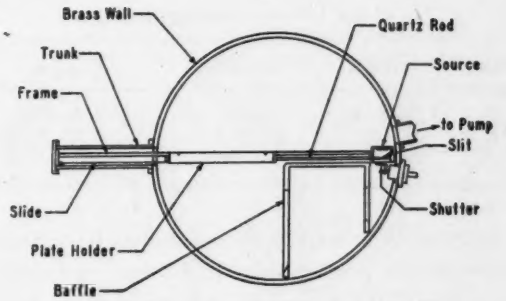

FIG. 2. Spectrograph vacuum chamber, to scale.

The electromagnet was powered by a motor-generator controlled by a current-regulating circuit (a slight modification of the circuit devised by Lawson and Tyler[10]) which maintained the magnet current within very close limits indefinitely. Simple annular shims gave the magnetic field distribution shown in Fig. 4, varying only 0.4 percent over the 260-mm maximum radius at the field strength used, 15,000 gauss.

III. EXPERIMENTAL PROCEDURE

The sources consisted of polonium metal deposited by the Canadian Radium and Uranium Corporation[11] on one $1\frac{7}{16}$-inch by 0.020-inch edge of a strip of metal $1\frac{7}{16}$ inches by 0.020 inch by $\frac{1}{8}$ inch. We were informed that "deposition was made spontaneously by immersion in a polonium solution relatively free from metallic ions. The plating time was approximately 6 hours" for a 0.1-mc source. The sources are listed in Table I.

The mountings were made at this laboratory

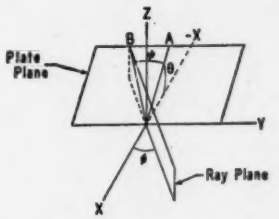

FIG. 3. Track-plate geometry.

[10] J. L. Lawson and A. W. Tyler, Rev. Sci. Inst. 10, 304 (1939).

[11] 630 Fifth Avenue, New York 20, New York.

TABLE I. List of sources used.

Source	Strength	Mounting	Prepared
B	0.25 mc	nickel	Dec. 8, 1947
E	0.1 mc	silver	Jan. 19, 1948
F	0.1 mc	cadmium	Jan. 26, 1948

as follows: For source *B*, machined from nickel sheet which presumably had been rolled into sheet form; for source *E*, rolled down to 0.020-inch from 0.065-inch sheet and machined; and for source *F*, rolled down to 0.020 inch from a piece about 0.065 inch thick cut from a cast rod. Each was carefully cleaned of burrs and the edge to be plated polished on a buffing wheel, and each appeared smooth and clean under a 15× glass both before and after coating. In the spectrograph the source was masked to 0.012-inch width by two aluminum jaws.

Exposures were made at pressures of less than 0.10 micron. Immediately after the completion of exposure the plates were developed on the time-temperature curve passing through 5 minutes at 68 degrees Fahrenheit in D-11 or 2 minutes at 68 degrees Fahrenheit in D-8. All plate handling and processing was done in total darkness.

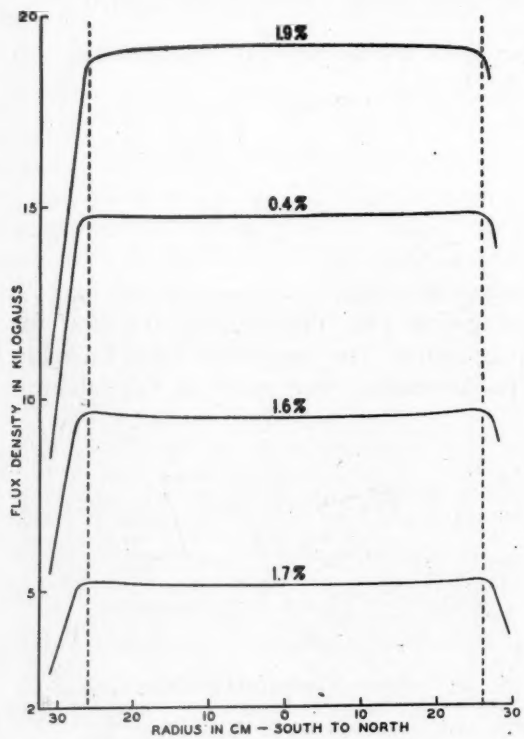

FIG. 4. Magnetic field distribution.

The data were obtained by measuring the alpha-ray track density as a function of position on the plate. This was done by sampling the tracks by dark-field microscopic examination at systematic intervals down the plate. Areas were marked by an ocular grating of 49 squares calibrated by a stage micrometer. Plate coordinates were taken from a special calibrated mechanical stage with verniers on both motions reading to 0.1 mm. The appearance of the microscope field may be seen in Fig. 5, taken from plate No. 39 at 5.15 Mev. The magnification used throughout was about 150×, and counting was done over the central vertical strip of seven squares (each about 0.1 mm by 0.1 mm).

Most of the tracks were parallel and of the same length. These were the tracks counted. The others, caused by contamination of the vacuum chamber or scattering, were readily disregarded because of their different range and direction. The large blobs were dirt on the emulsion. For the spectra studied, the track density varied over a range of 7000 to 1—too great a range to be counted on one plate, so three accurately measured exposure times were used for each spectrum and the data combined. It is conservatively estimated that the error in counting tracks was about 2 percent.

IV. DATA

(a) Reduction

The original data were numbers of tracks per square as a function of the plate coordinates x and y. It was necessary to reduce them to track densities per hour of exposure as a function of alpha-particle energy. From the geometry and constants of the spectrograph:

$$r=(1/2)(521.3-\delta a)-x/2, \qquad (4)$$

where δa is given by formula (3). From these values of r, the values of the momentum Hr were obtained using:

$$Hr=r\cdot(Hr)_0/r_0,$$

where $(Hr)_0$ was the known value for the 5.300-Mev line, $3.316_5\times10^5$ gauss cm. The quantity r^0 was the measured position of the 5.300-Mev line.

In order to convert from momentum to energy, a table was prepared, accurate to four digits, over the range 3.513 Mev to 5.343 Mev, based on the general relativistic relation:

$$E_t = c(p^2 + m^2c^2)^{\frac{1}{2}} \text{ ergs.}$$

This relation, the equation between the magnetic and centrifugal forces on the particle, and the values of the physical constants[12] give the generating formula:

$$E = 4.822_2 \cdot 10^{-11} \cdot (Hr)^2 - 3.12 \cdot 10^{-25} \cdot (Hr)^4 \text{ Mev.}$$

The track density data were converted from tracks per square to tracks per square millimeter per hour of exposure, corrected for source decay, and for the change from momentum space to energy space.

(b) Polonium on Nickel

To correlate this data with that of Chang,[7] the first spectrum studied was that of 0.25 millicurie of polonium mounted on nickel. The data were taken from plates No. 34, 35, and 36, listed in Table II. (The data from plate No. 28 confirmed the absence of alpha-particles of energy higher than 5.300 Mev. At the field strength used, alpha-particles up to 11.4 Mev would have been seen.)

The reduced data are plotted in Fig. 6. Each point represents a counted field. The data from plate No. 34 are those below 5.2 Mev and to the right of the drawn-in curve at 5.3 Mev. The data from plates No. 35 and 36 are plotted to an intensity scale reduced 500 times and connected by a solid line. Plate No. 39 was exposed as a check. Data at 4.0 Mev and 5.0 Mev fell within the data plotted in Fig. 6.

(c) Polonium on Silver

In order to investigate the possibility that the spectrum might be influenced by the mounting, the next source studied was 0.1 millicurie of polonium mounted on silver. Data were obtained from plates No. 44, 46, and 47, with No. 45 providing a satisfactory check. The exhaustive counting done for the nickel-mounted source was not done for these plates, and the data are presented in Fig. 7 with the expected mean deviations indicated as calculated from the formula

$$\delta N = N/u^{\frac{1}{2}},$$

where u is the total number of tracks counted to determine N.

[12] R. T. Birge, Rev. Mod. Phys. **13**, 233 (1941).

TABLE II. List of plates exposed.

Plate No.	Date	Source	Exposure	Current	Developer
28	12/12/47	*B*	1:55 hr.	148*A*	D-11
34	12/16/47	*B*	25:00 hr.	50*A*	D-11
35	12/17/47	*B*	16 min.	50*A*	D-11
36	12/18/47	*B*	101 sec.	50*A*	D-11
39	12/19/47	*B*	25:00 hr.	50*A*	D-8
44	1/21/48	*E*	25:00 hr.	50*A*	D-8
45	1/23/48	*E*	25:00 hr.	50*A*	D-8
46	1/24/48	*E*	3600 sec.	50*A*	D-8
47	1/25/48	*E*	300 sec.	50*A*	D-8
48	1/28/48	*F*	25:00 hr.	50*A*	D-8
49	1/30/48	*B*	25:00 hr.	50*A*	D-8

(d) Polonium on Cadmium

Data from 0.1 millicurie of polonium mounted on cadmium were obtained from plate No. 48. The results are plotted in Fig. 8.

Finally plate No. 49 was exposed to the nickel-mounted source, and its data showed that there had been no change in the spectrograph characteristics during the course of the experiments.

V. CONCLUSIONS

(a) Discussion of Data

The spectrum on nickel, of which the most extensive study was made and for which the

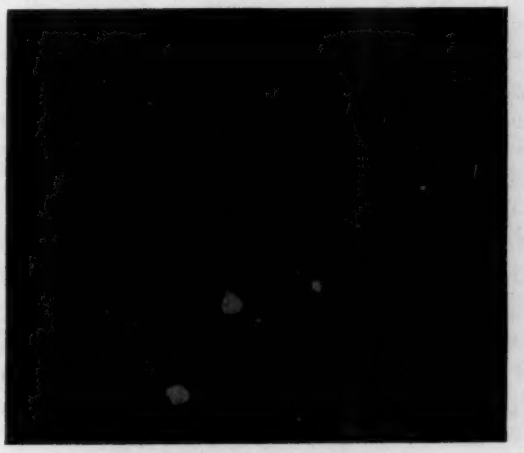

FIG. 5. Microscope field showing tracks from polonium on nickel at 5.15 Mev.

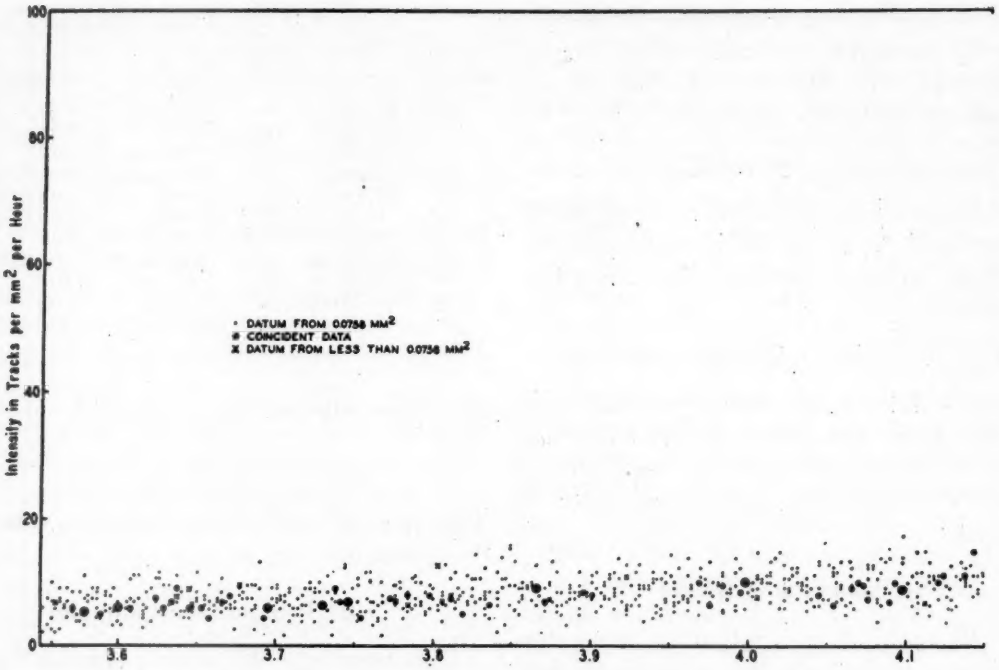

FIG. 6(a). Alpha-ray spectrum of polonium mounted on nickel.

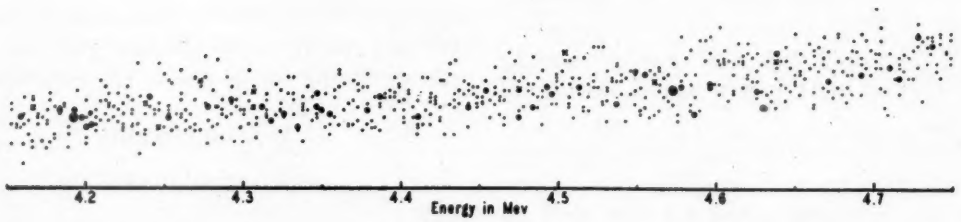

FIG. 6(b).

statistics are very good, shows no evidence of the weak line series discovered by Chang. The other spectra are similar in this regard, but differ considerably in detail. On nickel, the spectrum has a line at 5.300 Mev and falls gradually to low values on the low energy side.

On silver, the 5.300-Mev line has the same half-width, but shows a striking plateau from 5.1 Mev to 5.25 Mev. On cadmium, the plateau begins at a higher energy and intensity, has greater slope, but ends at about the same energy as on silver. (The ratios of maximum intensities are not believed significant, since the source strengths were not known accurately.)

Thus, it can readily be seen that the mounting metal had a strong influence on the spectrum obtained. The structural data[13] on the metals concerned are listed in Table III.

The question arises, why did the weak line series which was so clearly apparent in the data of Chang not appear here? The resolution of the instrument was adequate since the half-width of the 5.300-Mev line as measured by this instrument was 0.012 Mev and the half-widths of the lines seen by Chang were about 0.03 Mev. The examination intervals were close enough to resolve these lines also. Straggling in the source or scattering in the vacuum chamber might have raised the intensity at the lower energies so as

[13] *Handbook of Chemistry and Physics* (Chemical Rubber, Cleveland, 1939), twenty-third edition, p. 1590.

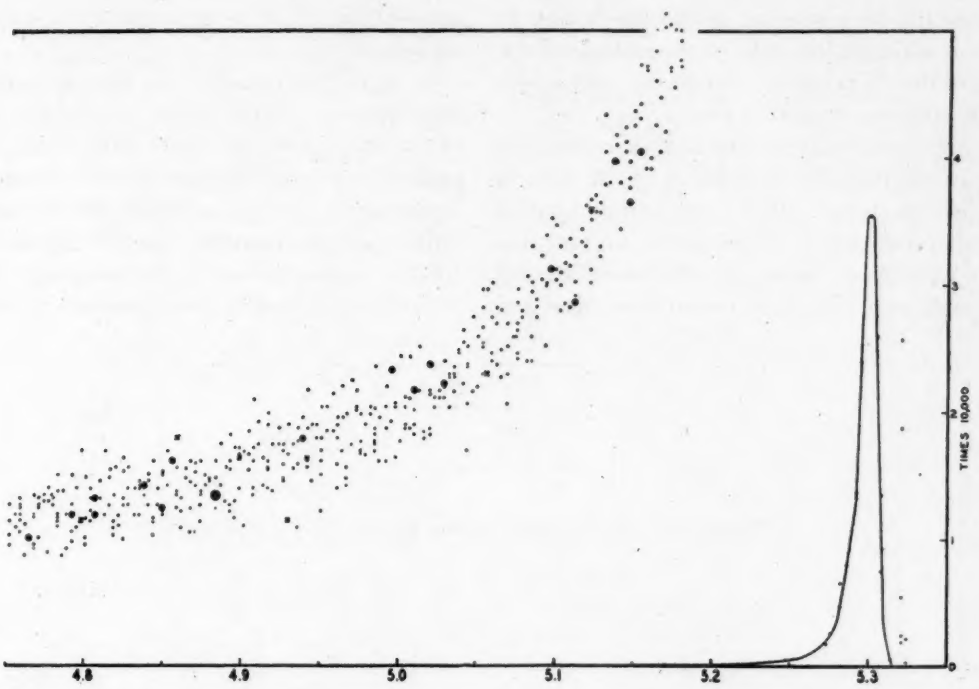

FIG. 6(c).

to cover up the weak line series. However, Chang states[7] that "the intensities at 0.25 Mev or more below the energy of the main group are less than 0.1 percent of the maximum intensity," and in Fig. 6, at 5.05 Mev, the intensity is 0.15 percent of maximum. Thus we see that the data are strictly comparable, and we are driven to the conclusion that there was no instrumental error, but that the weak line series seen by Chang did not come out of the sources used for these experiments.

(b) Suggested Explanation

The following hypothesis is proposed: None of the alpha-ray spectra seen here nor that seen by Chang is the true alpha-ray spectrum of polonium, but, with the exception of the 5.300-Mev line, all the observed spectra are due to the diffusion of the polonium into the metallic mounting.

This hypothesis would eliminate the theoretical difficulty regarding the spins and Feather's[8] objection to the intensities since it would indicate that the true spectral line intensities are of a lower order of magnitude than the intensities obtained to date and so have never been seen. It is substantiated by a paper of A. B. Focke[14] in which he reported a study of the alpha-radiation from polonium introduced into bismuth as an impurity in single crystals. He concluded that "polonium is segregated into small regions which have nearly regular spacings when viewed in several different directions."

It seems probable that when polonium is introduced into a crystal by diffusion it should also be segregated. This would cause just such regularly spaced weak alpha-ray lines as were seen by Chang. A further fact tending to confirm this explanation is the shape of the lines seen by Chang. This type of spectrograph inherently gives a line shape which is very sharp on the high energy side. The lines in Chang's paper are symmetrical and not at all sharp. This agrees with the work of Focke, since there would surely be a symmetrical distribution of the polonium atoms within the crystal about each point of segregation.

Another check is a calculation of the range of 5.300-Mev alpha-particles in nickel correspond-

[14] A. B. Focke, Phys. Rev. **46**, 623 (1934).

ing to the 0.1-Mev spacing of the line series. It is 10^{-5} cm which is the order of magnitude of the spacing of the "slip-bands" of metals[15] and agrees with the spacings found by Focke.[14]

This argument would make it appear that the line series should have been found in the data of *this* paper. However, all the mountings used in these experiments were rolled during preparation so that each was thoroughly cold-worked, and the crystals were oriented at random so that any such effect would be expected to average out to nothing.

It may be possible to use polonium salts mounted on plastic films to obtain the true alpha-ray spectrum, and such work is being undertaken at this laboratory. If the above explanation proves correct, the technique of alpha-ray spectrography may be a useful method for the investigation of the structure of metals since it would enable the structure to be studied

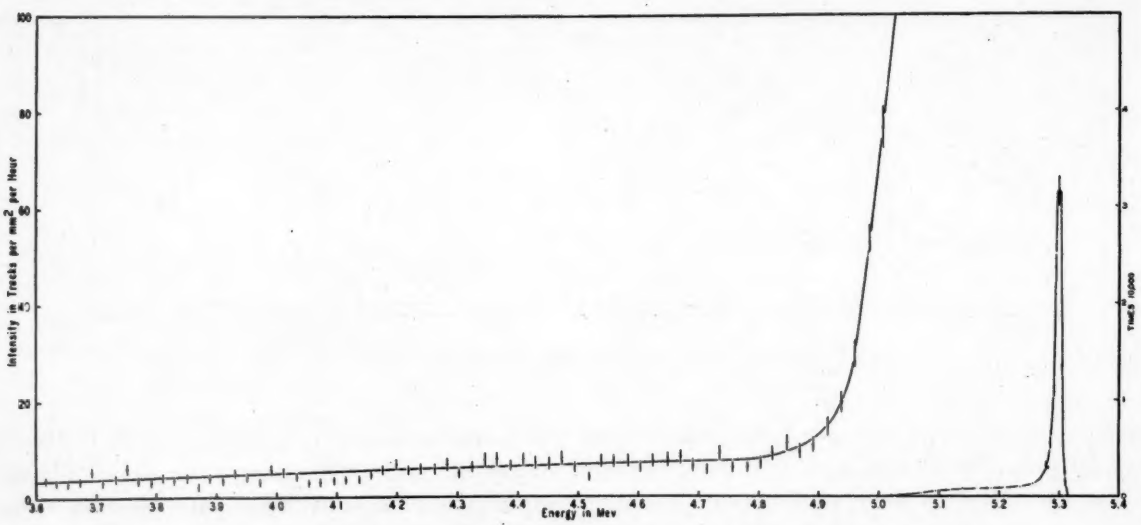

FIG. 7. Alpha-ray spectrum of polonium mounted on silver.

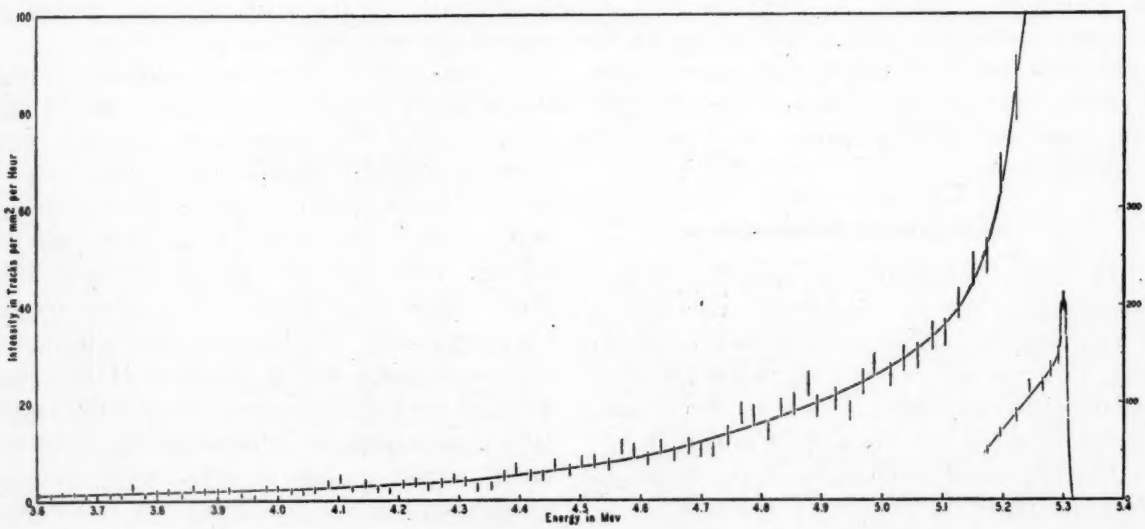

FIG. 8. Alpha-ray spectrum of polonium mounted on cadmium.

[15] F. Seitz, *The Physics of Metals* (McGraw-Hill Book Company, Inc., New York, 1943), p. 74. Also R. D. Heidenreich and W. Shockley, J. App. Phys. **18**, 1029 (1947).

without the application of stress or the introduction of a significant quantity of the radioactive impurity.

Table III. Structural data of metals concerned.

Metal	System	Lattice constants
Po	monoclinic	7.42, 4.29, 14.10
Ni(β)	cubic, face-centered	3.517
Ag	cubic, face-centered	4.0776
Cd	hexagonal, close-packed	2.97, —, 5.61

VI. ACKNOWLEDGMENTS

The author wishes to express his appreciation for the great interest and many helpful suggestions of Professor M. L. Wiedenbeck and for the benefit of discussions with Professors G. E. Uhlenbeck, H. R. Crane, D. M. Dennison, and G. Y. Rainich. It is also a pleasure to thank the University of Michigan for granting him a Horace H. Rackham Special Fellowship during the work on this problem.

PHYSICAL REVIEW VOLUME 74, NUMBER 12 DECEMBER 15, 1948

Statistical Error in Absorption Experiments

M. E. Rose and M. M. Shapiro
Oak Ridge National Laboratory, Oak Ridge, Tennessee

(Received July 26, 1948)

In certain exponential absorption experiments, notably measurements of cross sections by transmission, it is important to achieve minimum statistical error in a limited time or to minimize the counting time required to measure the absorption coefficient with a preassigned accuracy. The conditions required to attain these ends, i.e., the geometry for optimum transmission, and the best apportionment of counting times among the incident and transmitted beams and background, have been investigated for a wide range of relative backgrounds (10^{-3} to 10^{3}), and for two geometries: I. Beam area fixed, absorber thickness alone is varied. II. Beam area and absorber thickness are both disposable parameters, while the total amount of absorber intercepting the beam remains fixed. In both cases the incident flux density and the background rate are assumed constant. The optimum transmissions are shown to be, in general, considerably smaller than those commonly used in absorption experiments. Thus, in Case I, a useful rule is to employ a transmission of about 0.1 for low backgrounds, 0.2 for moderate backgrounds, and 0.3 for high backgrounds. The following have also been determined: (a) minimum statistical error for a given total counting time, (b) statistical error and the best distribution of counting times for non-optimum geometry, and (c) sensitivity of the accuracy or total counting time to deviations from optimum transmission.

INTRODUCTION

THERE are many physical measurements of absorption or transmission of radiation in which the transmission is an exponential function of the absorber thickness. Measurements of this kind occur, for example, in the fields of optics, x-rays, and nuclear physics. In the latter field the purpose is usually to determine a total cross section.

In most measurements of this type, the thickness of absorber can be chosen at will within reasonable limits, i.e., the transmission is a disposable parameter. Suppose for the sake of definiteness that the detector is a counter. If a thick absorber is interposed in the beam, the transmitted intensity is low and a relatively long time is required to collect an adequate count. In fact, for sufficiently low transmissions, the transmitted beam may become comparable in magnitude to the background. This obviously results in inefficient counting. On the other hand, if a very thin absorber is used, the intensity of the transmitted beam approaches that of the incident beam, and again the geometry is statistically unfavorable. Therefore, some intermediate value of the transmission should be employed, and of course this is commonly done.

It may sometimes be desirable to know what value of the transmission is *best* if the greatest accuracy is to be obtained in a given time or if a preassigned accuracy is to be attained in the least time. Moreover, the dependence of this optimum

transmission on background is essential. In addition, it is important to determine the sensitivity of the precision of measurement or the total counting time to deviations from optimum geometry. Further questions are concerned with the best apportionment of the total counting time among incident beam, transmitted beam and background, and its dependence on the background and the thickness of absorber. These questions become important when the total available counting time is strictly limited by radioactive decay of the absorbing material, or by other considerations. They are also relevant in other situations in which high counting efficiency is desirable. The answers to these questions depend upon the way in which the background varies and upon certain geometric properties of the beam, the absorber, and the detector.

The present discussion is based on the following assumptions: (a) The flux density in the incident beam is constant in time and independent of geometry. (b) The total background rate is likewise constant. (c) The detector completely intercepts the beam. (d) The efficiency of the detector is the same for the incident and transmitted beams. (e) The transmission is an exponential function of the absorber thickness; i.e., the absorber thickness is small compared to the scattering mean free path. To the extent that the optimum transmission is significantly less than unity, which will almost always be true, this also implies that the absorption cross section must be much larger than the scattering cross section.

Two cases will be considered:

I. The total counting rate of the incident beam is fixed (i.e., the cross-sectional area of the beam is fixed); the thickness of absorber can be varied. This is the usual situation.

II. The total counting rate of the incident beam is *not* fixed but disposable by changing the area of the beam, subject to the condition that the total amount of absorber in the path of the beam remains fixed. Adjustment of the beam area may be advantageous when the amount of absorber available for the measurement is small, and it is desired to exploit the absorber fully by placing all of it in the path of the beam.

CALCULATION OF OPTIMUM CONDITIONS

By virtue of the assumption of constant background a transmission measurement consists in obtaining three counting rates. This simplicity may not be present in the case of individual experimental arrangements. For example, the background may depend on absorber thickness, in which case at least one additional counting rate must be determined. However, such cases can easily be treated by the procedure described below.

Designating the counting times for the incident and transmitted beams, including background, by t_0 and t_1, respectively, and the counting time for the background by t_2, we have for the counting rates

$$r_i = c_i/t_i, \tag{1}$$

where c_0, c_1, and c_2 are the total counts for these three measurements, respectively. The flux densities in the incident and transmitted beams, exclusive of background, are denoted by s_0 and s_1, respectively, so that

$$s_i = (r_i - r_2)/a \qquad (i=0, 1), \tag{2}$$

where a is the cross-sectional area of the beam. The transmission T can then be written as

$$T = s_1/s_0 = (r_1 - r_2)/(r_0 - r_2) = e^{-x}, \tag{3}$$

where

$$x = N\sigma/a, \tag{4}$$

N is the total number of atoms in the path of the beam, and σ is the total cross section per atom of absorber.

We use the symbol Δ prefixed to any quantity to indicate the standard error in that quantity. The relative standard error $\Delta\sigma/\sigma$ in the cross section σ is obtained by applying the law of propagation of error to

$$\sigma = -(a/N)\ln T, \tag{5}$$

so that

$$(\Delta\sigma/\sigma)^2 = [(\partial\sigma/\partial a)(\Delta a/\sigma)]^2 + [(\partial\sigma/\partial N)(\Delta N/\sigma)]^2 + [(\partial\sigma/\partial T)(\Delta T/\sigma)]^2.$$

We shall confine our attention to the contribution of the third term, i.e., assume that Δa and ΔN are negligible. Subject to this condition, we have

$$p \equiv |\Delta\sigma/\sigma| = |(\partial\sigma/\partial T)(\Delta T/\sigma)|. \tag{6}$$

From (4), (5), and (6),

$$p^2 = (\Delta T/T\ln T)^2 = (\Delta T/T)^2/x^2. \tag{7}$$

To evaluate p^2, we apply the law of propagation

of error to $(\Delta T/T)^2$ using (3):

$$(\Delta T/T)^2=[((\Delta r_1)^2+(\Delta r_2)^2)/(r_1-r_2)^2] +[((\Delta r_0)^2+(\Delta r_2)^2)/(r_0-r_2)^2]. \quad (8)$$

Since the errors in measuring the times t_i are almost invariably negligible, we have, from (1),

$$\Delta r_i/r_i=\Delta c_i/c_i. \quad (9)$$

Here and in the following i takes on values 0, 1, and 2. With $(\Delta c_i)^2=c_i$, it follows that

$$(\Delta r_i)^2=r_i/t_i. \quad (10)$$

Substituting from (2), (3), and (10) into (8),

$$\left(\frac{\Delta T}{T}\right)^2=\frac{1}{s_0^2a^2}\left[e^{2x}\left(\frac{r_1}{t_1}+\frac{r_2}{t_2}\right)+\frac{r_0}{t_0}+\frac{r_2}{t_2}\right]. \quad (11)$$

It is convenient to introduce the *total* counting time τ,

$$\tau=t_0+t_1+t_2, \quad (12)$$

and to replace the partial counting times t_i by the relative counting times α_i:

$$\alpha_i=t_i/\tau, \quad (13)$$

with

$$\sum_i \alpha_i=1. \quad (14)$$

Using (11) and (13) and multiplying both sides by τ, (7) can be written:

$$p^2\tau=(1/xs_0a)^2[(r_2+s_2a)/\alpha_0 +(r_2e^{2x}+as_0e^x)/\alpha_1+(r_2e^{2x}+r_2)/\alpha_2]. \quad (15)$$

As might have been expected, the total counting time is inversely proportional to the square of the relative error in the cross section.

We shall now investigate the optimum geometry and apportionment of counting times, treating in turn the two cases previously described.

I. Cross-Sectional Area of Beam Fixed

Let the *relative background* m be defined by

$$m=r_2/(r_0-r_2)=r_2/s_0a. \quad (16)$$

Substitution of this in (15) yields

$$p^2\tau=(1/x^2s_0a)[(m+1)/\alpha_0 +(me^{2x}+e^x)/\alpha_1+m(e^{2x}+1)/\alpha_2]. \quad (17)$$

From this it is evident that whether it be required (a) to minimize τ for a preassigned p or (b) to minimize p for a fixed τ, the optimum conditions are the same. The adjustable parameters in either case are x, which refers to the geometrical

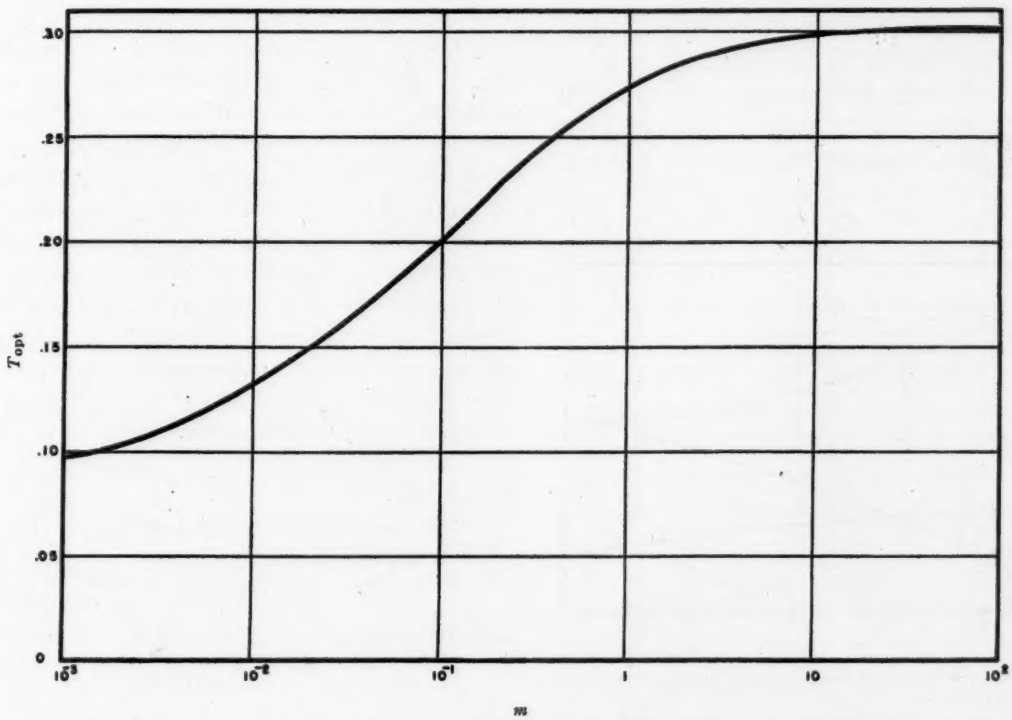

FIG. 1. Variation of optimum transmission with relative background in Case I.

arrangement, and the α_i, which refer to the apportionment of counting times.

Requirement (a) may occur when *there is no essential restriction on the total counting time*, and an upper limit is preassigned to the relative error p. To be sure, p can then be made arbitrarily small, regardless of geometry or apportionment of counting times, merely by counting long enough. However, it is sometimes worth while to select experimental conditions which will keep p below the prescribed limit *in the least time*. For example, in a long series of transmission measurements the time saved can be significant.

Requirement (b) applies when the *total available counting time is limited*, e.g., by radioactive decay of the absorber material or in cosmic-ray experiments at high altitudes. Here p cannot be made arbitrarily small, but the experimental conditions can be chosen so as to minimize it.

For the calculation it is convenient to introduce the notation:

$$\begin{aligned} f_0^2 &= (m+1)/x^2, \\ f_1^2 &= (me^{2x}+e^x)/x^2, \\ f_2^2 &= m(e^{2x}+1)/x^2, \end{aligned} \tag{18}$$

so that

$$p^2\tau = (1/s_0 a)\sum_i f_i^2/\alpha_i. \tag{19}$$

Designating differentiation with respect to x by primes, the solutions are given by

$$\sum_i f_i f_i'/\alpha_i = 0. \tag{20}$$

Minimizing with respect to the α_i and taking (14) into account, we obtain

$$\alpha_i = f_i/\sum_i f_i. \tag{21}$$

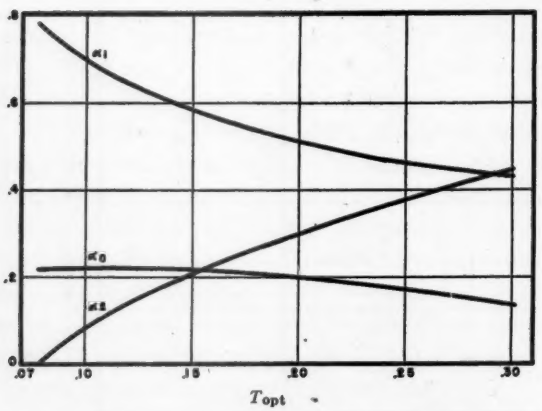

FIG. 2. Optimum apportionment of counting times as a function of optimum transmission in Case I. Each α_i is a fraction of the total time: α_0 for the incident beam, α_1 for the transmitted beam, and α_2 for the background.

Substitution of (21) into (20) gives

$$\sum_i f_i' = 0, \tag{22}$$

or, more explicitly,

$$me^{2x}[1/f_1+1/f_2]+e^x/2f_1-x\sum_i f_i=0. \tag{22a}$$

It is seen that the optimum values of the parameters x and α_i depend on the relative background m alone.

A. Optimum Transmission

By numerically solving Eq. (22a) for x as a function of m, the optimum transmission $T_{\text{opt}}=\exp[-x_{\text{opt}}]$ is evaluated as a function of the relative background m. In Fig. 1, T_{opt} is plotted over a wide range of m, from 10^{-3} to 10^2. It will be noticed that even for very large backgrounds, T_{opt} does not exceed 0.31, and, in general, the optimum transmissions are considerably smaller than those frequently used in absorption experiments.

The results in Fig. 1 may be crudely summed up by the following useful rule: From the point of view of counting efficiency, a transmission of about 0.1 should be employed for low backgrounds, 0.2 for moderate backgrounds, and 0.3 for high backgrounds. The meaning of "low," "moderate," and "high" will be evident from Fig. 1. This rule is applicable when the cross-sectional area of the beam is fixed and the absorber thickness can be adjusted; moreover, the conditions (a) to (e) specified in the introduction are assumed to hold at least approximately. If the background changes significantly during an experiment and it is inconvenient to change the absorber thickness, then a fairly good procedure is to use a transmission appropriate to an average background. This is a consequence of the insensitivity of T_{opt} to m. As will be evident from the subsequent discussion,* these rules have wider applicability than might be supposed at first glance.

When the background is absent ($m=0$), Eq. (22a) reduces to

$$(x-2)^2 = 4e^{-x} \tag{23}$$

and the solution is

$$e^{-x} = T_{\text{opt}} = 0.076.$$

* See I*D* below, also Fig. 5.

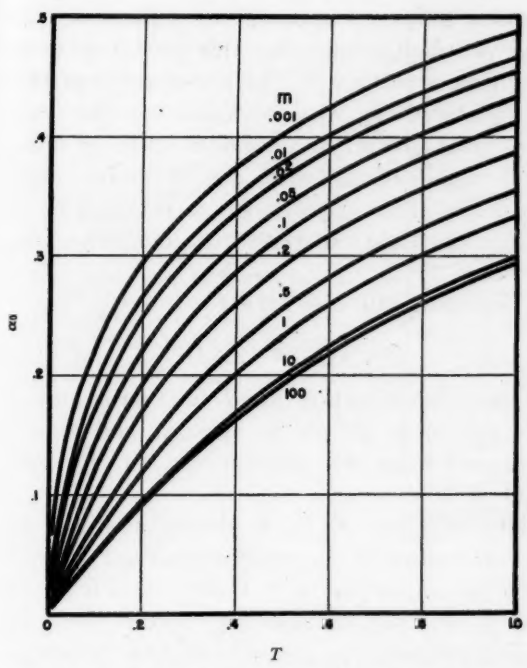

FIG. 3. Fraction of time devoted to counting the *incident* beam, as a function of transmission (when absorber thickness is not necessarily optimum), for various values of the relative background m. Optimum apportionment of counting times is assumed.

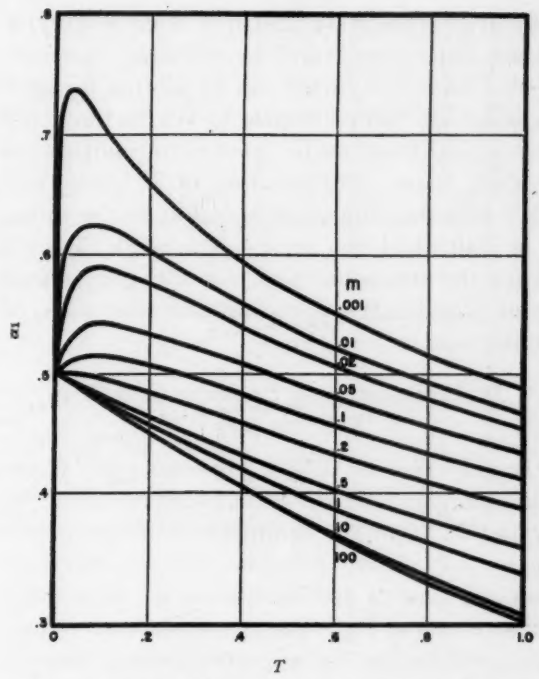

FIG. 4. Fraction of time devoted to counting the *transmitted* beam, as a function of transmission (when absorber thickness is not necessarily optimum), for various values of m. The fraction of time α_2 to be devoted to the background is obtained from this figure, Fig. 3, and Eq. (14).

This special case has been previously considered by Rainwater and Havens.[1]

B. Optimum Counting Times for Optimum Transmission

The best apportionment of counting times for any value of m is obtained by substituting into (21) the root of (22a) for that m, i.e., by putting the optimum transmission into (21). Although the optimum fractional times α_i are functions of m alone, they can be plotted against T_{opt} instead of m, since to each m there corresponds a unique T_{opt}. In Fig. 2 the α_i's are so plotted. The curve labeled α_0 gives the fractional time which should be devoted to counting the incident beam, α_1 the transmitted beam, and α_2 the background. It will be recalled from Fig. 1 that increasing values of T_{opt} correspond to increasing m. Figure 2 shows that at low T_{opt} (and therefore low backgrounds) the background rate r_2 is relatively unimportant and need not be measured with great precision; most of the time τ should be devoted to measuring r_1 which is small compared with r_0. As the background increases, r_2 contributes more significantly to the quantities r_0-r_2 and r_1-r_2 (the true counting rates for incident and transmitted beams), and it becomes necessary to measure r_2 more and more accurately. The required time is obtained mainly at the expense of r_1, which of course increases with T_{opt}, so that it can be measured adequately in less time.

C. Deviations from Optimum Geometry: Optimum Counting Times When Arbitrary Transmission Is Used

In some experiments it may be too difficult or even unwise[2] to employ the optimum transmissions derived here. For *any* transmission T which may be used, however, there is still an optimum apportionment of counting times. These α_i's are given by (21), as before, but they are now functions of *two* independent parameters, T and m,

[1] J. Rainwater and W. W. Havens, Phys. Rev. **70**, 146 (1946).

[2] For example, in spectrometry, where higher order effects introduce errors which are sometimes difficult to measure, the magnitude of these effects may be reduced by using higher transmissions. Another example is given in reference 1, p. 147.

instead of m alone (or T alone). Accordingly, for all non-optimum (as well as optimum) transmissions a family of curves can be plotted for each α_i, as in Figs. 3 and 4. Figure 3 gives the fractional time α_0 which should be devoted to counting the incident beam, as a function of T for various relative backgrounds corresponding to the values of m with which the curves are labeled. Figure 4 shows the fractional time for the transmitted beam. The fractional background time α_2 is, of course, simply $1-\alpha_0-\alpha_1$.

D. Deviations from Optimum Geometry: Effect on p or τ

It may now be asked: How sensitive is the relative error p or the total counting time τ to deviations from the optimum thickness of absorber, i.e., what price is paid in increased counting time or decreased accuracy for a given departure from T_{opt}? The answer depends in part upon whether the *best* apportionment of times or some arbitrary set α_i is used. Since situations in which the optimum α_i should not be used (when counting efficiency matters) are difficult to conceive, we shall assume that this partial optimum condition is realized.** The sensitivity can then be measured by the deviation of the ratio $(p^2\tau)/(p^2\tau)_{\text{opt}}$ from its minimum value of unity. Large values of this ratio are, of course, undesirable, as they imply large uncertainty or an unduly long time required to attain a preassigned accuracy.

Combining (19) and (21),

$$p^2\tau=(1/s_0a)(\textstyle\sum_i f_i)^2. \tag{24}$$

$p^2\tau$ depends on both m and T (i.e., on m and x). The minimum of $p^2\tau$ is $(p^2\tau)_{\text{opt}}$, and this is evaluated from the solution of (22a) for each value of m.

The ratio $p^2\tau/(p^2\tau)_{\text{opt}}$ is plotted in Fig. 5 for various values of m (numbers affixed to each curve) as a function of T. It is evident from the flatness of the minima in Fig. 5 that moderate deviations from T_{opt} are only slightly disadvantageous, i.e., it matters little if the geometry used is not *very* close to the optimum. On the other

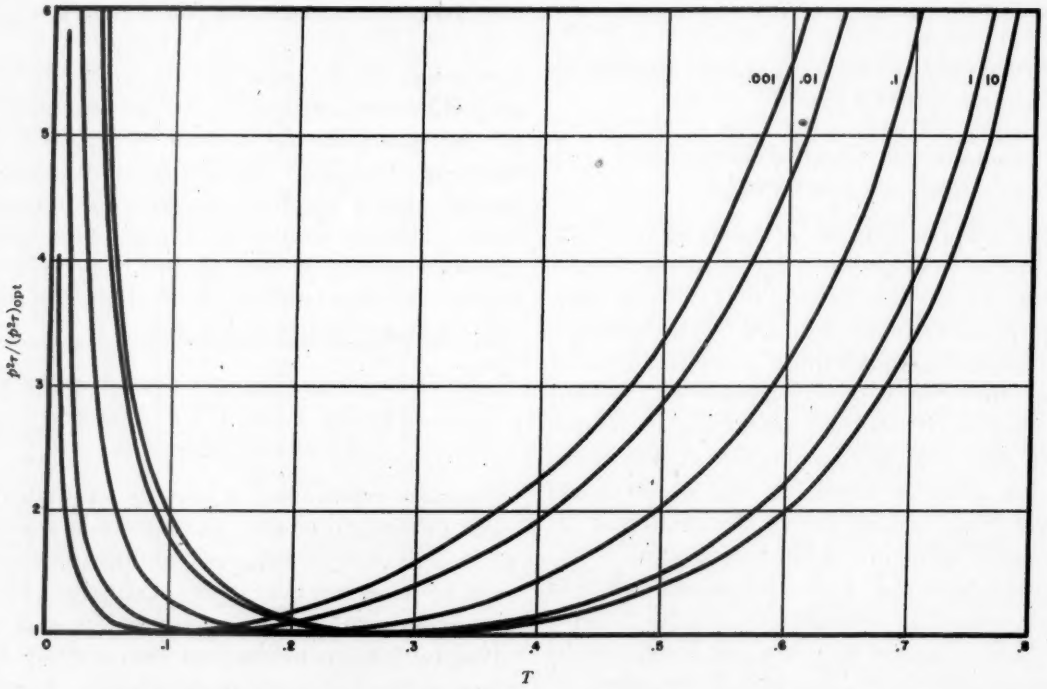

FIG. 5. Curves showing the sensitivity of the error or counting time to deviations from optimum transmission for various values of the relative background m (numbers affixed to each curve) in Case I. The minima correspond to optimum transmissions.

** It should be noted that the best apportionment of α_i for non-optimum T is in general different from that shown in Fig. 2, as discussed in the previous section. The apportionment for *any* T is given in Figs. 3 and 4.

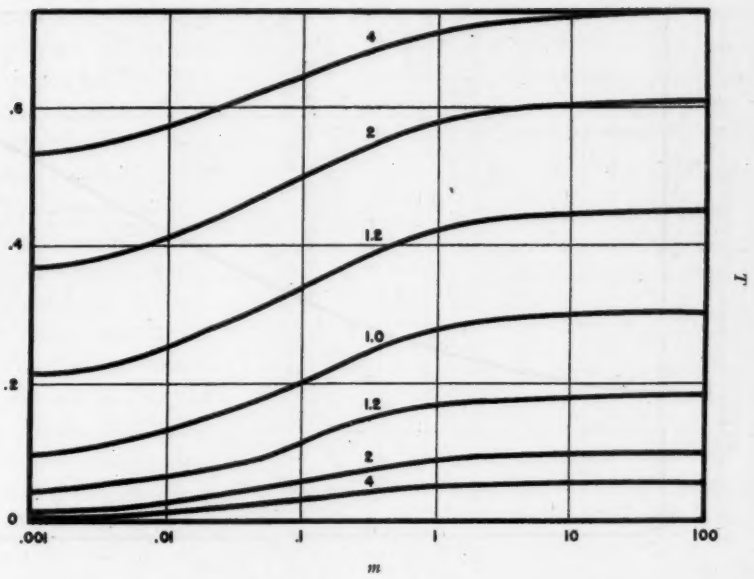

FIG. 6. Permissible range of transmissions in Case I when the ratio $p^2\tau/(p^2\tau)_{opt}$ is not to exceed 1.2, 2, or 4, respectively. Upper and lower limits on T are plotted against relative background. The curve labeled 1.0, showing optimum transmissions, is included for comparison.

hand, the steep portions of the curves, and especially those for $T<T_{opt}$ show that for large departures from T_{opt} a significant and rapidly rising increase in error or counting time is incurred. Thus, from the curve for the smallest relative background, $m=10^{-3}$, it is clear that a transmission as small as 0.01 is decidedly disadvantageous, as would be expected. The same curve, however, also shows that using a transmission of 0.61 instead of the optimum (≈ 0.1), necessitates a sixfold increase in the counting time to achieve a given accuracy, or, in a given counting time, increases the relative error p by a factor $(6)^{\frac{1}{2}}$.

In general, for low backgrounds, transmissions exceeding 0.6 should be avoided if possible, and even for very high backgrounds it is unwise to exceed 0.75. Inspection of Fig. 5 confirms the working rule previously deduced from Fig. 1, i.e., that transmissions of about 0.1, 0.2, and 0.3, respectively, are suitable for use with low, moderate, and high backgrounds.

Figure 5 can be used to ascertain the permissible range of transmissions if $p^2\tau$ is not to exceed $(p^2\tau)_{opt}$ by more than some preassigned factor. For example, suppose $m=0.1$ and it is desired not to exceed the minimum counting time (for a given accuracy) by more than a factor 2. From the curve labeled 0.1 in Fig. 5 it is seen that the transmission should lie in the range $0.06 \leqslant T \leqslant 0.5$.

The permissible range of transmissions as a function of relative background is shown more directly in Fig. 6 for several maximum values, 1.2, 2, and 4, of $p^2\tau/(p^2\tau)_{opt}$. The numbers on the curves are values of this ratio. Thus, if

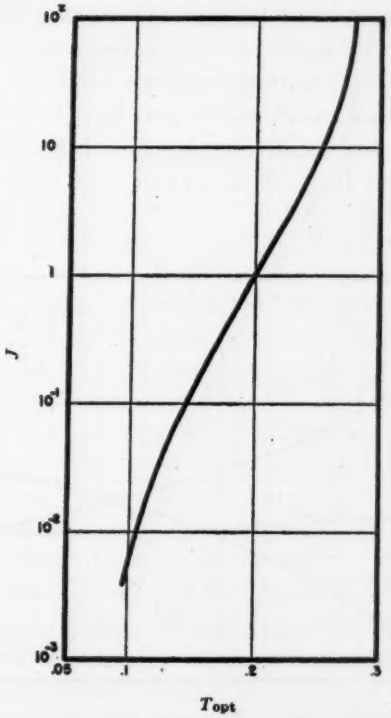

FIG. 7. The product of $(p^2\tau)_{opt}$ and the absolute background counting rate *versus* optimum transmission in Case I. For a given T_{opt} and background, either the relative error p or the total counting time τ is obtainable from this curve.

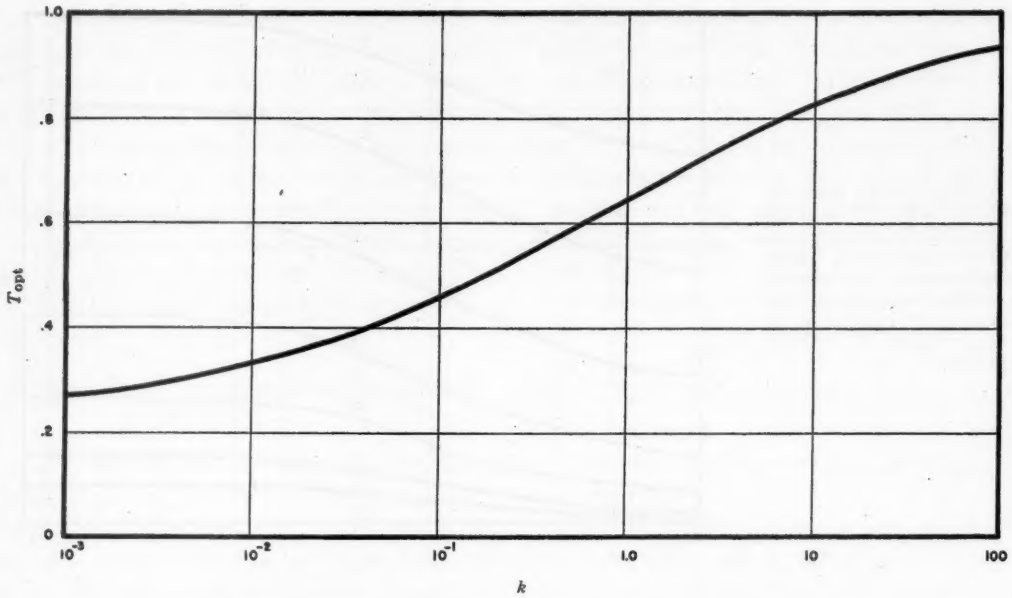

FIG. 8. Optimum transmission *versus* relative background in Case II.

$p^2\tau/(p^2\tau)_{opt}$ is not to exceed 2, the highest permissible transmission is shown by the upper curve "2," and the lowest by lower curve "2." For example, if the relative background is 0.01 and it is desired not to spend more than twice the minimum time in obtaining a given accuracy, the allowable range of transmissions runs from 0.03 to 0.42. If the total counting time is fixed, the relative error in σ will then exceed the minimum error by at most $\sqrt{2}$.

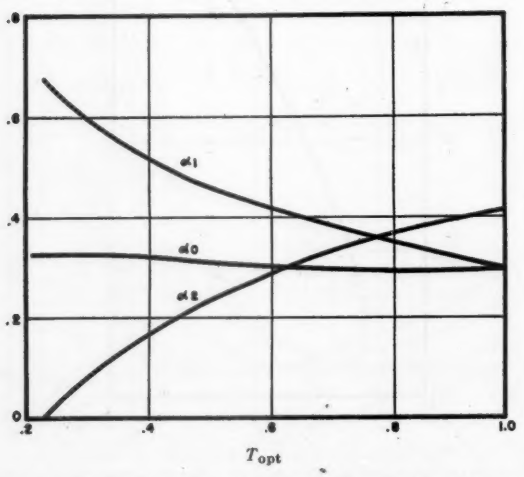

FIG. 9. Optimum apportionment of counting times as a function of optimum transmission in Case II. Each α_i is a fraction of the total time: α_0 for the incident beam, α_1 for the transmitted beam, and α_2 for the background.

E. Evaluation of $(p^2\tau)_{opt}$

For a given relative background or a given T_{opt}, it may be desired to estimate quickly the value of $(p^2\tau)_{opt}$. The latter depends on the absolute background as well as on m (or k, see II below).

Using (16), Eq. (24) can be rewritten

$$p^2\tau r_2 = m(\textstyle\sum_i f_i)^2. \qquad (24a)$$

When for a given m the corresponding x_{opt} is substituted in the right-hand side of (24a), this becomes

$$J \equiv (p^2\tau)_{opt} r_2 = m(\textstyle\sum_i f_i)_{opt}^2. \qquad (24b)$$

The right hand side can be expressed as a function of m alone or of T_{opt} alone. In Fig. 7, J is plotted against T_{opt}.

II. Beam of Variable Cross-Sectional Area

When only a small sample of absorber is available for a cross-section measurement by transmission, it may be advantageous to place all of it in the path of the beam. We suppose that the cross-sectional area a of the beam and the area of the absorber sample are adjustable so that the two can be kept equal. It is further assumed that the total counting rate of the incident beam, unlike that in Case I, is not fixed, but varies in proportion to a, subject to the condition that the

total amount of absorber in the path of the beam remains fixed. This condition implies, of course, that the thickness of absorber varies as $1/a$. The problem is whether to make the absorber thick and the beam narrow, or the absorber thin and the beam wide. Here again, to a given relative background there corresponds an optimum transmission; however, the latter now determines not only the optimum absorber thickness but also the optimum beam area. It is fairly evident that the value of the best transmission here will differ from that for Case I. It is true that in both cases the thickness of absorber changes, but in Case II the beam area also changes, while the total number of atoms in the path of the beam remains fixed. In Case I the reverse is true, the beam area is fixed, and the number of atoms in the path of the beam varies with the thickness.

The derivation of T_{opt} is parallel to that in Case I: $p^2\tau$ is again minimized with respect to x and two of the α_i. It is convenient here to introduce a new parameter in place of m (cf. (16)). The latter is suitable when a is independent of T, but this is not true in Case II, where a choice of a at once determines T. We define instead a new "relative background."

$$k=r_2/s_0N\sigma, \tag{25}$$

in which the product $N\sigma$, which is constant here, takes the place of a, which is constant in Case I.[3]

Replacing x^2a^2 by $N^2\sigma^2$ (cf. (4)), and introducing k, Eq. (17) can be rewritten

$$p^2\tau=(1/s_0N\sigma)[(k+1/x)/\alpha_0 +(ke^{2x}+e^x/x)/\alpha_1+k(e^{2x}+1)/\alpha_2], \tag{26}$$

which corresponds to (17) in Case I. Similarly, corresponding to the f_i^2 in (18) we define

$$\begin{aligned}\varphi_0^2&=k+1/x,\\ \varphi_1^2&=ke^{2x}+e^x/x,\\ \varphi_2^2&=k(e^{2x}+1),\end{aligned} \tag{27}$$

so that (26) can be written

$$p^2\tau=(1/s_0N\sigma)\sum_i \varphi_i^2/\alpha_i. \tag{28}$$

Minimizing with respect to x, α_0, and α_1, subject to (14), gives

$$\sum_i \varphi_i\varphi_i'/\alpha_i=0, \tag{29}$$

$$\alpha_i=\varphi_i/\sum_i \varphi_i, \tag{30}$$

[3] Comparison of definitions (25) and (16) shows that $m=kx$.

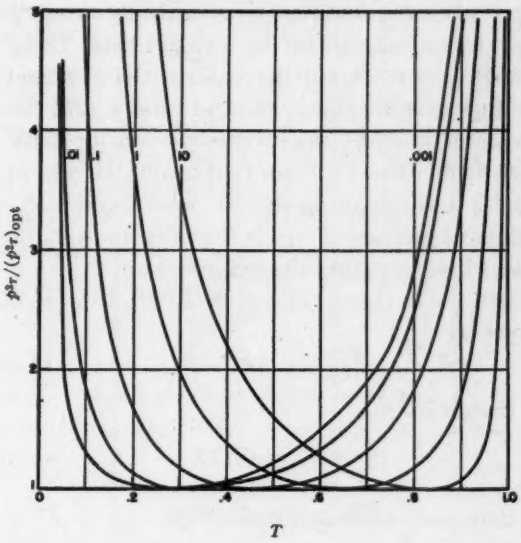

FIG. 10. Sensitivity of the error or counting time to deviations from optimum transmission for various relative backgrounds k (numbers affixed to each curve) in Case II.

and substitution of (30) into (29) gives the result

$$\sum_i \varphi_i'=0, \tag{31}$$

which can be written explicitly as

$$2kx^2e^{2x}(1/\varphi_1+1/\varphi_2) +e^x(x-1)/\varphi_1-1/\varphi_0=0. \tag{31a}$$

A. Optimum Transmission

This equation in x and k has been solved numerically, and the results are given in Fig. 8. Here $e^{-x}=T_{\text{opt}}$ is plotted against k. The optimum transmissions are higher than those shown in Fig. 1 for all values of the relative background; in particular, they approach 1.0 rather than 0.31 for large k. The difference can be explained as follows. As we have seen, a transmission is statistically unfavorable when either of the true counting rates r_1-r_2 or r_0-r_2 is too small. In both cases which we have discussed, a larger background can be partly offset by increasing r_1; hence T_{opt} increases with relative background. In Case I, however, as r_1 increases it approaches r_0 *which is fixed* (since a is fixed) so that beyond a certain point (which turns out to be $T=0.31$), it is no longer advantageous to increase r_1. In Case II, for larger relative backgrounds r_1 is increased as before by thinning the absorber. However, a is simultaneously enlarged so that the increase in the trans-

mitted counting rate is automatically accompanied by an *increase in* the incident rate. Thus, although $(r_0-r_1)/r_0$ still decreases with increasing T, it does so more slowly than in Case I, and the decrease is offset by the increased counting rates of *both* incident and transmitted beams. Hence, in Case II, it is advantageous for very large backgrounds to increase T up to the maximum value allowed by expanding the beam area.

When the background is zero ($k=0$), Eq. (31a) reduces to

$$(x-1)^2=e^{-x}, \tag{32}$$

and the solution is

$$e^{-x}=T_{\text{opt}}=0.228.$$

B. Optimum Counting Times When T_{opt} Is Used

Equation (30) gives the best apportionment of counting times for a given value of k, provided that the root of (31a) corresponding to that k is substituted in (30). Since there is a one-to-one correspondence between k and T_{opt}, the optimum fractional times α_0, α_1, and α_2 can be plotted against the optimum transmission (instead of against k). This has been done in Fig. 9.

C. Deviations from Optimum Geometry. Optimum α_i for Arbitrary T

When a non-optimum transmission is used, the best α_i's are, as might be expected, identical with those deduced for Case I. These α_i's *could* be obtained by substituting into (30) the relevant value of x (i.e., $-\ln T$) and k. But it is no longer necessary or even useful to employ k, since T, and therefore a, is now fixed (k was introduced in place of m in deriving T_{opt} because the latter contains a, which in Case II depends on T). It is better instead to revert to m as a measure of the relative background.[4] Moreover, Eq. (21) is identical with Eq. (30) for a given value of T. This can be seen by replacing[3] k with m/x in (27) and substituting the resulting φ_i into (30). Thus, for non-optimum transmissions, the best α_i's are the same, regardless of whether the experimental conditions are those of Case I or Case II. Two of the α_i's are plotted, as we have seen, in Figs. 3 and 4, respectively, and the third is obtained by subtracting the sum of the first two from 1 (cf.(14)).

D. Deviations from Optimum Geometry. Effect on p or τ

As in Case I, the sensitivity of p or τ to departures from optimum geometry can be deduced from the variation of the ratio $p^2\tau/(p^2\tau)_{\text{opt}}$ with transmission. In the present case $p^2\tau$ is evaluated from (28) and (30) with the result:

$$p^2\tau=(1/s_0N\sigma)(\textstyle\sum_i \varphi_i)^2. \tag{33}$$

$(p^2\tau)_{\text{opt}}$ for a given k is evaluated by substituting in (33) the solution of (31a) for that value of k.

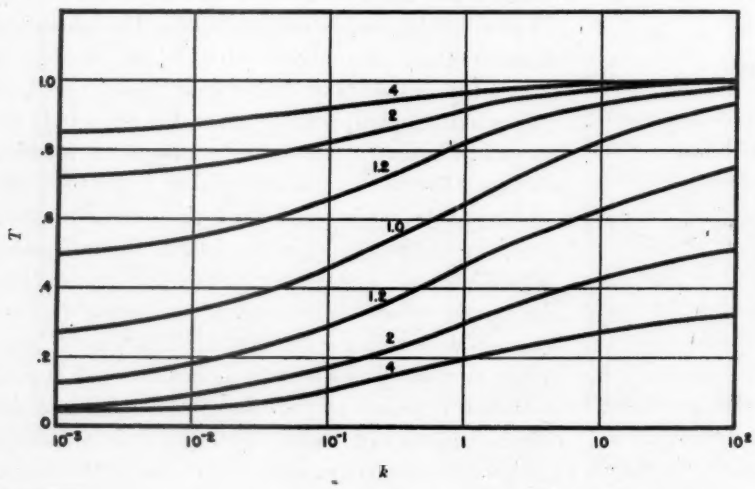

FIG. 11. Permissible range of transmission *versus* relative background in Case II when the ratio $p^2\tau/(p^2\tau)_{\text{opt}}$ is not to exceed 1.2, 2, or 4, respectively. Upper and lower limits on T as well as the optimum transmission (curve labeled 1.0) are given.

[4] To determine m only r_0 and r_2 need be measured; to determine k, on the other hand, r_1 must be measured as well, as is evident from the definitions of these quantities. In fact, by Eqs. (16), (25), and (3),

$$k=m/x=-r_2[(r_0-r_2)\ln(r_1-r_2)/(r_0-r_2)]^{-1}.$$

As was done for Case I in Fig. 5, the ratio $p^2\tau/(p^2\tau)_{opt}$ is plotted in Fig. 10 for various values of the background parameter k (numbers affixed to each curve) as a function of T. Again it is clear that moderate deviations from T_{opt} are unimportant, whereas excessive deviations may lead to large errors or long counting times.

Equation (33) can also be used to compute the permissible range of transmissions if $p^2\tau$ is not to exceed its minimum value $(p^2\tau)_{opt}$ by more than some preassigned factor. In Fig. 11 (the analog of Fig. 6) this permissible range of T is given as a function of k for the values 1.2, 2, and 4 of $p^2\tau/(p^2\tau)_{opt}$. As in Fig. 6, there are two curves for each of these values, the upper curve showing the upper limit on T and the lower one showing the lower limit.

E. Evaluation of $(p^2\tau)_{opt}$

In the same way as in Section I *E*, but now using (25), Eq. (33) can be rewritten

$$(p^2\tau)_{opt}r_2 = k(\textstyle\sum_i \varphi_i)^2, \qquad (25a)$$

and substituting x_{opt}, obtained from (31), this becomes

$$G \equiv (p^2\tau)_{opt}r_2 = k(\textstyle\sum_i \varphi_i)_{opt}^2. \qquad (25b)$$

In Fig. 12, G is plotted against T_{opt}.

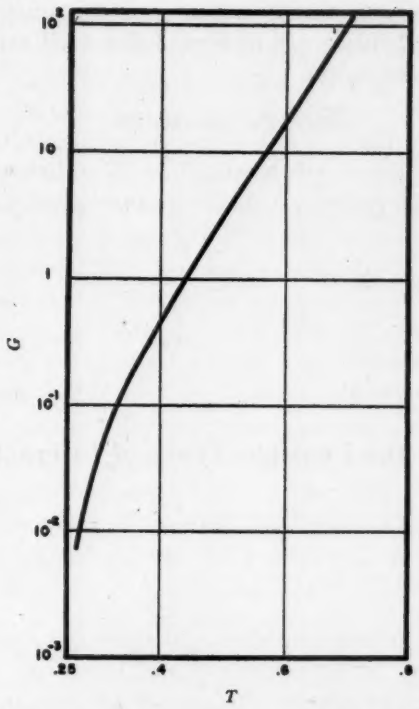

FIG. 12. The product of $(p^2\tau)_{opt}$ and the absolute background rate *versus* optimum transmission in Case II. For a given T_{opt} and background, either the relative error p or the total counting time τ is obtainable from this curve.

DISCUSSION

The utility of this investigation depends largely on the insensitivity of $p^2\tau$ to moderate deviations from T_{opt}, as shown by the flatness of the minima in Fig. 5. This is evident from the following considerations: T_{opt} depends on m in Case I and on k in Case II. A knowledge of m, however, depends on the measurement of r_0 and r_2 (cf. (16)); k depends on these two parameters and on r_1 as well.[4] Thus we are confronted with the paradoxical requirement of measuring two (or, in Case II, all three) of the counting rates from which T is deduced before we can calculate the statistically favorable conditions for making these very measurements. Moreover, in order to choose the optimum absorber thickness, once T_{opt} has been determined, the cross section (or, more generally, the absorption coefficient) must be known. Since the latter depends on T, all three of the counting rates must be known in advance, even in Case I. In practice, however, this is not a real difficulty. It has been shown that $p^2\tau$ changes so slowly in the neighborhood of T_{opt} that moderate deviations from T_{opt} are unimportant. Thus a rough preliminary measurement of the counting rates suffices to give an estimated absorber thickness which can be used for practical purposes. The time consumed by these preliminary measurements should, in general, be quite short compared with that for the final measurements, since the time required for a count is inversely proportional to the square of the permissible error, and the latter may be fairly large without leading to a significantly poor estimate of T_{opt}.

The results presented here apply when the primary considerations are the statistical ones described above. It is recognized that circumstances may arise in which other considerations are important. It may then be desirable or even necessary to use non-optimum transmissions. The foregoing remarks about deviations from optimum geometry indicate to what extent this may be done without incurring unduly large statistical errors. In addition, regardless of what transmis-

sion is used, the optimum apportionment of counting times given in Figs. 3 and 4 will still be applicable.

ACKNOWLEDGMENT

The authors are indebted to Miss Rosemary Crook for carrying out the numerical computations. This document is based on work performed under Contract Number AT-33-1-GEN-53 for the Atomic Energy Commission, and the information convered therein will appear in the National Nuclear Energy Series (Manhattan Project Technical Section) as part of the contribution of the Oak Ridge National Laboratory.

PHYSICAL REVIEW VOLUME 74, NUMBER 12 DECEMBER 15, 1948

On the Possible Types of Interaction between Spinorial and Tensorial Fields

SATOSI WATANABE
Tokyo, Japan
(Received October 28, 1948)

THE present author has pointed out that all the known (spinorial or tensorial) field equations in absence of interaction can be rewritten in covariant form in a 5-dimensional flat space: $ds^2=(dx^1)^2+(dx^2)^2+(dx^3)^2-(dx^0)^2+(dx^5)^2$, in which the fifth coordinate x^5 is considered as the canonical conjugate of the intrinsic mass.[1] The striking simplicity of the formulæ thus obtained invites us to postulate the 5-dimensional covariance also as a heuristic principle to determine the correct formulation of mutual interaction of fields.[2,3]

It must be admitted for the time being that this attempt does not lead to definite results whose meanings are unambiguously definable in the 4-dimensional framework, due to the facts:

(1) that there is at present no theoretical clue to the correct method of mass-quantization,

(2) that, in presence of interaction, the mass constant m appearing in field equations loses its meaning as the mechanical mass satisfying $P^2-E^2+m^2=0$ (P: momentum, E: energy, $c=1$), and

(3) that there appears in the 5-dimensional formalism a force which tends to change the intrinsic mass.

These difficulties prohibit us from translating the 5-dimensional formulæ directly into the current 4-dimensional language by such a simple convention as $\partial/\partial x^5=im$ ($\hbar=1$) which has been successful in the case of absent interaction. In spite of these ambiguities pertaining to the definition of intrinsic mass, the postulate of 5-dimensional covariance can nevertheless be instrumental as a criterium for determining what types of interaction are and what types are not admissible from the proposed standpoint. In the case of interaction between a spinorial (electronic or nucleonic) field and a tensorial (electromagnetic or mesonic) field, all the currently accepted types except the following three turn out, in fact, to be incompatible with the above postulate. The "allowed" types seem to provide a desirable reformulation of the electromagnetic and nuclear interaction, involved to a lesser degree in the divergence difficulties than the current theory.

If ψ is a spinor with four components having the same transformation property as the Dirac wave function, we can construct only three 5-dimensional tensors by combination of its components, *viz.*:

a pseudo-scalar:

$$s=\psi^*\alpha_1\alpha_2\alpha_3\beta\psi \tag{1}$$

a vector:

$$v^i=\psi^*(\alpha_1,\ \alpha_2,\ \alpha_3,\ 1,\ \beta)\psi \qquad (i=1\ 2\ 3\ 0\ 5) \tag{2}$$

a second-rank antisymmetric pseudo-tensor:

---

[1] S. Watanabe, Sci. Pap. I.P.C.R. **39**, 157 (1941).
[2] S. Watanabe, Sci. Pap. I.P.C.R. **42**, 1 (1944).
[3] S. Watanabe, Proc. Phys. Math. Soc. **25**, 561 (1943).

$$t^{ij}=\psi^*\begin{pmatrix} & 1 & 2 & 3 & 0 & 5 \\ 1 & 0 & i\alpha_3\beta & -i\alpha_2\beta & i\alpha_2\alpha_3\beta & i\alpha_2\alpha_3 \\ 2 & & 0 & i\alpha_1\beta & i\alpha_3\alpha_1\beta & i\alpha_3\alpha_1 \\ 3 & & & 0 & i\alpha_1\alpha_2\beta & i\alpha_1\alpha_2 \\ 0 & & & & 0 & i\alpha_1\alpha_2\alpha_3 \\ 5 & & & & & 0 \end{pmatrix}\psi. \quad (3)$$

Hence, the 5-dimensional invariants, which can be made from these quantities combined with components of a tensorial field, are

$$(A)\ su,\ (B)\ v_iu^i,\ (C)\ t_{ij}u^{ij},\ (i,j=1,2,3,0,5), \quad (4)$$

where u is a pseudo-scalar, u^i a vector, and u^{ij} a pseudo-tensor in the 5-dimensional sense. The interaction terms in the 4-dimensional Lagrangian must consist of those which are derivable from each one of these three classes.

u is necessarily a potential and u^{ij} field strengths (derivatives of potentials), but u^i may either be potentials or field strengths. The 4-dimensional mesonic potentials can be identified with the u^{i5}-components of the field strengths.[1] Coexistence of (A) and (B), or of (B) and (C), as the interaction of one kind of tensorial field with a spinorial field, is impossible, for u in (A) or u^{ij} in (C) has a *pseudo*-tensorial property, whereas u^i in (B) has a *non-pseudo*-tensorial property. Mixture of (A) and (C) for one tensorial field is also excluded, for if u in (A) is the potential, then its field strengths constitute a pseudo-vector, but not a pseudo-tensor of second rank.

The invarient (B) is composed of two 4-dimensional invariants, *viz.*:

$$(B)\quad v_\mu u^\mu \text{ and } vu \quad (\mu=1,\ 2,\ 3,\ 0) \quad (5)$$

with $v=v_5$, where u^μ is a non-pseudo 4-vector and u a 4-dimensional non-pseudo-scalar. The invariant (C) is decomposed into two 4-dimensional invariants, *viz.*:

$$(C)\quad t_{\mu\nu}u^{\mu\nu} \text{ and } t_\mu u^\mu \quad (\mu,\ \nu=1,\ 2,\ 3,\ 0) \quad (6)$$

with $t_\mu=t_{\mu 5}$, where $u^{\mu\nu}$ is a pseudo-tensor and u^μ a pseudo-vector in the 4-dimensional sense.

In the 5-dimensional formalism, u^μ and u in (5) must satisfy a simultaneous set of wave equations, and the two terms of (5) must appear in the Lagrangian with the same interaction constant. This, however, does not necessarily imply that u^μ and u should correspond to the same mass-constant in the 4-dimensional formalism. And correspondingly, the interaction constants of u^μ and u cannot be supposed to take the same value in the 4-dimensional theory.

The interaction through the fifth component u is preeminently a mass-changing agent, which interferes in a sense with the foundation of the 4-dimensional theory, which assigns a fixed value to the mass. Such a mass-changing force, however, has the property that the total mass of the interacting systems is conserved. So, if each ψ-particle is supposed to have a fixed mass, then the mass-changing force can act only "within" the particle, which amounts to setting a certain lower limit to the mass of the u-particle, for the mass is the reciprocal of the force-range. These problems, however, cannot be consistently dealt with without an adequate method of mass-quantization.

It will therefore be assumed hereafter that u^μ and u are independent fields. For the same reason, any *a priori* connection between $u^{\mu\nu}$ and u^μ of (6) will be disregarded, except for their pseudo-tensorial property. This assumption may be justified only as a provisional convention, for lack of a better access. Especially, an asymmetry of treatment with regard to the ψ-field and the u-field is undeniable, for v_μ and v of (5), or $t_{\mu\nu}$ and t_μ of (6), are considered as belonging to the same ψ-field with one fixed mass-constant.

Conforming to the interaction type (B), the Dirac equation of an electron will take the form:

$$\left\{\frac{\partial}{\partial x^0}+ieu^0+\alpha_k\left(\frac{\partial}{\partial x^k}-ieu^k\right)+i\beta(m-fu)\right\}\psi=0 \quad (k=1,\ 2,\ 3). \quad (7)$$

The present author showed in a previous work that the scalar field μ plays the role of an internal cohesive force within the electron.[4] Pais, Sakata, and others have recently shown that the electron equation of the type (7) is exempt from an infinite self-energy, when the interaction constants are suitably chosen.[5]

It will be of interest to note that here the quantity, $m-fu$, which has the meaning of a

[4] See particularly §5 of the paper cited in reference 2.

[5] A. Pais, Phys. Rev. **68**, 227 (1945); S. Sakata and O. Hara, Prog. Theor. Phys. **2**, 30 (1947); See also S. Tomonaga, Phys. Rev. **74**, 224 (1948).

mechanical mass, changes with the time, even in the 4-dimensional theory, according to

$$\frac{d}{dx^0}(m-fu)=-f\alpha_k\frac{\partial u}{\partial x^k}-f\frac{\partial u}{\partial x^0}. \tag{8}$$

If, on the contrary, $m-fu$ is to be a constant, then m must be considered as a variable.

For the type (C) the Lagrangian density of interaction will become

$$L'=-2ft_\mu u^\mu-gt_{\mu\nu}u^{\mu\nu}+\text{conj. complex}, \tag{9}$$

where u^μ and $u^{\mu\nu}$ are a pseudo-vector and a pseudo-tensor, respectively, and may belong to two different mass-constants, m_1 and m_2. t_μ and $t_{\mu\nu}$ are given by (3), but a charge-dependent operator should be inserted between ψ^* and ψ, if the theory is applied to the nucleons. We cannot at present decide whether u^μ should be regarded as the potential of a pseudo-vector field or as the field strengths of a pseudo-scalar field. Araki has carried out detailed calculations on the latter of these alternative assumptions, and gotten very satisfactory results for nuclear force, meson's lifetime, β-decay constant, and nucleonic magnetic moment.[6] It is easy to see that the strong singularity of nuclear forces can be eliminated by the assumption (9) if the interaction constants are so chosen that

$$f^2/m_1^2=g^2/m_2^2. \tag{10}$$

The relation (10) is written for the case in which u^μ and $u^{\mu\nu}$ in (9) are multiplied by suitable powers of m_1 and m_2, respectively, so that f and g may become dimensionless constants in the unit system: $c=\hbar=1$.[7]

It may thus be said that the two types (B) and (C) have successful applications in the actual wave fields. Class (A) is still to be investigated as a possibility. Most of the interaction assumptions hitherto proposed, including the Møller-Rosenfeld mixture, cannot be brought in accord with the postulate of 5-dimensional covariance.[3]

[6] G. Araki, Phys. Rev. **74**, 986 (1948).

[7] The possibility is not excluded that the two mass-constants m_1 and m_2 should correspond to two of the observed varieties of mesons.

Neutrons in the Penetrating Showers of the Cosmic Radiation

G. Cocconi, V. Cocconi-Tongiorgi, and K. Greisen
Laboratory of Nuclear Studies, Cornell University, Ithaca, New York
(Received October 13, 1948)

In connection with another experiment on neutrons in the cosmic radiation, a preliminary experiment has been performed at Echo Lake, Colorado (3200 m above sea level), in order to ascertain the presence of neutrons in the penetrating showers.

The arrangement used is drawn in Fig. 1. Tray a consisted of 20 G-M counters in parallel, each $1''\times16''$. Nine counters of the same size, connected in three groups of three counters each as in Fig. 1, constituted the trays b, c, and d. Each of these counters was separated from its neighbors by $\frac{3}{4}''$ Pb. The first and the last counters had side shields of $2''$ Pb. With thick lead absorbers in Σ, coincidences $a+b+c+d$ are due to penetrating showers, of which the great majority are locally generated and not associated with extensive air showers.[1] The few percent that are associated with extensive showers were recognized in this experiment by the coincidences S among three unshielded counter trays of large area, 2000 cm² each (S_1, S_2, and S_3 in Fig. 1).

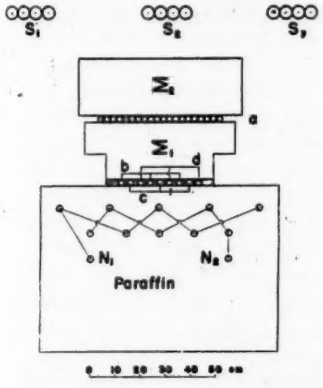

FIG. 1. Arrangement of counters

Anticoincidences $A=a+b+c+d-S$ were recorded and interpreted as local penetrating showers not accompanied by extensive showers.

The neutron detector system consisted of a large paraffin block ($38''\times26''\times26''$) in which 12 proportional counters were imbedded, each $1''\times20''$, filled with enriched BF_3 (96 percent B^{10}) at 1.5 atmos. pressure (calculated efficiency for slow neutrons 30 percent). The BF_3 counters were connected in two groups, N_1 and N_2, each of 6 counters in parallel (see Fig. 1).

The amplified pulses of the two channels N_1 and N_2 were put in delayed coincidence (7 μsec. delay) with the anticoincidences A. Delayed coincidences $A+N_1$, $A+N_2$, and $A+N_1+N_2$ were registered.

The recording circuits had 6 μsec. resolving time for the channels connected to G-M counters and 200 μsec. for the channels connected to BF_3 counters.[2]

Measurements have been taken with $\Sigma_1=9''$ Pb and $\Sigma_2=0$, $\Sigma_1=8''$ Fe and $\Sigma_2=2''$ Fe, $\Sigma_1=9''$ C and $\Sigma_2=13.5''$ C (graphite).

The results are collected in Table I. The last row refers to a test measurement taken with a 0.75-mm Cd foil around each of the BF_3 counters.

Chance coincidences were always negligible. Of course, only the anticoincidences A observed under lead can be attributed entirely to local showers of penetrating particles; the thickness of the graphite absorber and probably of the iron was not enough to prevent the recording of some local electron showers also. Notwithstanding this, it is reasonable to assume that practically all events in which anticoincidences and neutrons have been recorded were associated with penetrating showers, as it is known[2] that the number of neutrons in the air showers is not greater than a few percent of the electrons.

From a comparison of the data $A+N_1$ (or $A+N_2$) and $A+N_1+N_2$, it is possible to get information about the average number of neutrons associated with penetrating showers in different materials. In fact,

$$(A+N_1+N_2)/(A+N_1)=1-e^{\nu\epsilon},$$

where ν = average number of neutrons striking the paraffin block with energy low enough that they are slowed down, and ϵ = efficiency of the neutron detector system.

[1] G. Cocconi and K. Greisen, Phys. Rev. **74**, 62 (1948).

[2] For details see V. Tongiorgi, Phys. Rev. **73**, 923 (1948).

The values of the product $\nu\epsilon$ for Pb, Fe, and C are shown in the last column of Table I. As for ϵ, we think that 0.06 may be a reasonable estimate, assuming 0.3 for the counter efficiency and 0.2 for the probability that a neutron striking the paraffin reaches the counters. This last figure can easily be wrong by a factor 2 in either direction. By assuming isotropic distribution of the neutrons in the penetrating showers and taking into account the solid angles defined by the paraffin block with the different absorbers, one deduces that the total numbers of neutrons per penetrating shower are about 30, 18, and 10 for Pb, Fe, and C, respectively.

We want to emphasize that these figures refer only to those neutrons of energies such that our paraffin is able to slow them down, i.e., energies not larger than about 10 Mev.

From these results, we think that it is possible to conclude:

1. The presence of so many neutrons of moderate energies in the penetrating showers, in which particles of much higher energies are also contained, suggests that two different processes are probably involved. While the production of the penetrating particles is due to an interaction among nucleons, the evaporation of excited nuclei may be the main process responsible for the production of the observed neutrons

2 The very high number of neutrons observed is hardly understandable if one assumes that only a single nucleus is involved. Probably, besides the nucleus in which teh penetrating particles have been generated, other nearby nuclei can be excited by the particles produced in the primary act (high energy protons, neutrons, photons, mesons, etc.) and consequently evaporate neutrons.

3. Besides the neutrons of few Mev, heavy ionizing particles are very likely to be evaporated by the excited nuclei also. These particles may be observed as stars. In our opinion, at least a fraction of the stars generated by the cosmic radiation is directly correlated with penetrating showers, these stars being the by-product of the more energetic process in which the penetrating particles find their origin. Cloud-chamber pictures support this conclusion in that they frequently show heavily ionizing particles (stars) at the origin of a penetrating shower.

TABLE I. Summary of results.

$\Sigma=\Sigma_1+\Sigma_2$	Time (hr.)	A	$A+N_1$	$A+N_2$	$\frac{A+N_1}{+N_2}$	$\nu\epsilon$
9″ Pb	14.55	479	183	167	92	0.76
8″+2″ Fe	17.9	1663	251	230	71	0.35
9″+13.5″ C	22.8	3940	138	120	20	0.17
9″ Pb (Cd screens)	20.75	598	2	0	0	—

The authors are grateful to the Research Corporation for a grant which covered the expense of performing the experiment described above. The cost of constructing the apparatus was provided through a Navy contract. The facilities of the Inter-University High Altitude Laboratories Association and the help of Professors Cohn and Pona of Denver University were an invaluable aid in performing the experiment.

Letters to the Editor

PUBLICATION of brief reports of important discoveries in physics may be secured by addressing them to this department. The closing date for this department is five weeks prior to the date of issue. No proof will be sent to the authors. The Board of Editors does not hold itself responsible for the opinions expressed by the correspondents. Communications should not exceed 600 words in length.

Experimental Upper Limit for the Mean Life of the 478.5-Kev Excited State of Li^7

L. G. ELLIOTT AND R. E. BELL
Chalk River Laboratories, National Research Council of Canada, Chalk River, Ontario
October 28, 1948

THE γ-ray accompanying the reaction $B^{10}(n,\alpha)Li^7$ is known to arise from the de-excitation of the Li^{7*} nucleus formed when the short range α-group is emitted. This γ-ray has been studied in a magnetic lens-type β-ray spectrometer. The γ-ray source was a cylindrical pellet of B_4C of length 2 mm and diameter 8 mm placed in a beam of thermal neutrons from the Chalk River pile. A 7.2-mg/cm^2 Au foil of diameter 6 mm was mounted as a radiator on the end of the pellet away from the neutron beam and facing into the spectrometer. Photoelectrons ejected from this Au foil were then studied with a spectrometer line-width of about 2 percent in momentum.

The energy of the Li^{7*} γ-ray was measured by comparison with the γ-ray from radioactive Au^{198} (2.7 day). The result is 478.5 ± 1.5 kev based on DuMond, Lind, and Watson's energy value[1] of 411.2 ± 0.1 kev for the Au^{198} γ-ray. This value agrees well with the value 480 ± 2 kev obtained by Rubin, Snyder, Lauritsen, and Fowler[2] by measurement of the energy of the inelastically scattered protons from $Li^7(p,p')Li^{7*}$, and with the value 479 ± 2 kev, obtained by Hornyak and Lauritsen[3] by measurement of the energy of the γ-ray from $Li^7(p,p')Li^{7*}$.

The Q of the reaction $B^{10}(n,\alpha)Li^7$ is 2.83 ± 0.11 Mev from the masses, so that in the case in which Li^7 is left in the excited state the Li particle has a kinetic energy of 0.85 Mev, corresponding to a particle velocity 1.61 percent of the velocity of light. If the mean life of the Li^7 excited state is very short compared with the time (order of 10^{-13} sec.) for an appreciable slowing of the Li particles in the B_4C source material, the γ-rays would be emitted while the Li nuclei are still moving with their initial velocity. The γ-ray quanta would then have a distribution in energy given by the maximum Doppler broadening 3.22 percent and corresponding to a total spread of 15.4 kev. The photoelectrons ejected by such a γ-ray would have the same spread in energy and would produce a line in the spectrometer which is broader than that due to a γ-ray of the same energy from an ordinary radioactive source.

The experimental shapes of the K photoelectron lines produced by the Au^{198} 411.2-kev and ThC″ 585-kev γ-rays used for comparison are shown in Fig. 1a. The tail on the low energy side of each curve is due to the finite thickness of the photoelectron radiator and is more marked in the case of the lower energy γ-ray. By interpolating to the energy 478.5 kev the shape of the line due to the Li^{7*} γ-ray if no Doppler broadening were present (i.e., if the mean life $\gg10^{-13}$ sec.) has been obtained and is shown as a dotted curve in Fig. 1b. Using this curve, the line shape to be expected in the spectrometer if the full Doppler broadening were present (i.e., if the mean life $\ll10^{-13}$ sec.) has been calculated by numerical integration and is shown as a full line in Fig. 1b. The shape corresponding to any given mean life τ of the excited state of Li^7 may be calculated from the range and initial velocity of the Li particles if one assumes a relation between the rate of loss of energy of the Li particles and their residual range. Since a Li particle of 0.85 Mev ionizes according to the last part of the Bragg curve for a single particle, the rate of energy loss is roughly proportional to the residual range. Using Gilbert's range value[4] of 0.48 air-cm, the range in the B_4C source material as calculated from the Bragg-Kleeman rule is 1.97×10^{-4} cm. The curve for a mean life of 2.0×10^{-13} sec. has been computed and is shown as a broken line in Fig. 1b. The experimental points lie between this curve and the curve corresponding to the full Doppler broadening in a position corresponding to a mean life of about 1×10^{-13} sec. Taking the experimental errors into account, an upper limit for the mean life of the Li^7 excited state is 2.0×10^{-13} sec.

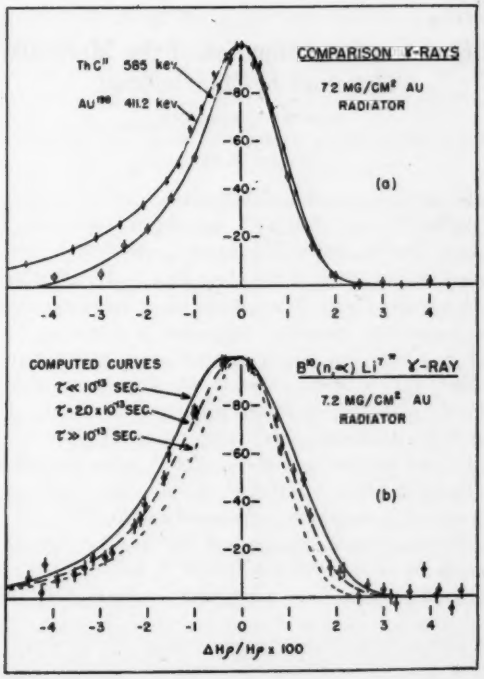

FIG. 1. (a) The shape observed in the spectrometer for the K photoelectron lines due to the comparison γ-rays. (b) The experimental points corresponding to the observed shape of the K photoelectron line due to the $B^{10}(n,\alpha)Li^{7*}$ γ-ray are shown as circles. The curves have been computed. All experimental points have the background subtracted, are normalized to 100, and plotted as a function of percent deviation from the $H\rho$ at the maximum.

The time of slowing of the Li particles in FeB is smaller by a factor of about 0.5 than in B_4C. A further experiment using this compound as a γ-ray source together with an improved spectrometer resolving power may make it possible to give a definite value for the mean life of this excited state in Li^7 rather than only an upper limit.

The angular momentum of Li^7 in the ground state is $\frac{3}{2}$ and the 478.5-kev excited state is commonly supposed[5] to have angular momentum $\frac{1}{2}$ forming with the ground state a doublet, $^2P_{3/2}$ and $^2P_{1/2}$. On this basis the transition takes place by magnetic dipole radiation. The transition probability for this case may be calculated closely by considering the interaction of the magnetic moment $(e/2Mc)(L+5.6S)$ of the $2p$ proton in Li^7 with the radiation field. The square of the matrix element[6] representing this interaction is

$$\frac{8}{3}\left(\frac{2.3eh}{4\pi Mc}\right)^2,$$

which together with the energy 478.5 kev available for the transition gives a calculated mean life for the Li^7 excited state of 1.5×10^{-13} sec. This is seen to be consistent with the experimental upper limit of 2.0×10^{-13} sec.

[1] DuMond, Lind, and Watson, Phys. Rev. **73**, 1392 (1948).
[2] Rubin, Snyder, Lauritsen, and Fowler, Bull. Am. Phys. Soc. **23**, No. 5, 15 (1948).
[3] W. Hornyak and T. Lauritsen, Bull. Am. Phys. Soc. **23**, No. 5, 16 (1948).
[4] C. W. Gilbert, Proc. Camb. Phil. Soc. **44**, 447 (1948).
[5] G. Breit and J. R. Stehn, Phys. Rev. **53**, 459 (1938).
[6] We are indebted to Dr. J. A. Spiers for help with this calculation.

Microwave Determination of the Molecular Structure of Chlorosilane

A. HARRY SHARBAUGH
General Electric Research Laboratory, Schenectady, New York
October 28, 1948

THE second rotational transition, $J=1$ to $J=2$, of SiH_3Cl^{35} and SiH_3Cl^{37} has been measured and analyzed. The Hughes-Wilson Stark modulation technique was used for detection of the absorption lines, and absorption frequencies were determined by comparison with a crystal-controlled secondary frequency standard.

In Fig. 1 is shown the theoretical hyperfine pattern for a nuclear spin of $\frac{3}{2}$ for chlorine which is in satisfactory agreement with the observed spectrum. No lines caused by excited vibrational states were observed. The unperturbed transition frequency ν_0 is 26,695.2$_4$ Mc for SiH_3Cl^{35} and 26,049.6$_9$ Mc for SiH_3Cl^{37}. From these frequencies, the I_B and B_0 values were calculated and listed in Table I. Since the quadrupole moments of Cl^{35} and Cl^{37} have been measured to be $-7.921\pm0.05\times10^{-26}$ and $-6.189\pm0.05\times10^{-26}$ cm^2,[1] respectively, we may evaluate $\partial^2V/\partial Z^2$ at

TABLE I. Nuclear and molecular constants of chlorosilane.

	ν_0(Mc/sec.)	I_B(g-cm^2) $\times10^{40}$	$eQ\left(\frac{\partial^2V}{\partial Z^2}\right)$(Mc)	B_0(cm^{-1})
SiH_3Cl^{35}	26,695.2$_4$	125.7$_1$	−40.$_0$	0.2226$_3$
SiH_3Cl^{37}	26,049.6$_9$	128.8$_2$	−30.$_8$	0.2172$_5$

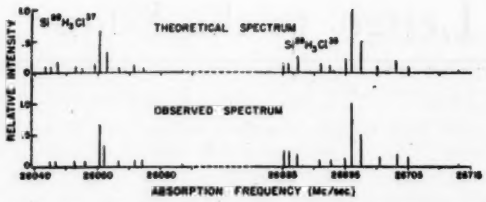

FIG. 1. Microwave absorption spectrum of monochlorsilane (SiH_3Cl).

the chlorine nucleus of chlorosilane to be about 7×10^{15} e.s.u. This is to be compared with the value 13×10^{15} e.s.u. as determined by Gordy[2] and his co-workers for methyl chloride.

Assuming the value of 1.456A for the Si−H distance determined from infra-red measurements on silane,[3] we may calculate from the I_B values in Table I, the Si−Cl internuclear distance to be 2.035A, and the H−Si−H angle to be 103° 57′. These are to be compared with the value 2.16A for Si−Cl computed from Pauling's covalent single-bond radii and the tetrahedral angle of 109° 28′. Electron diffraction measurements[4] on this compound yield a value of 2.06±0.05A for the Si−Cl distance.

The lines arising from $K=0\rightarrow0$ and $K=1\rightarrow1$ transitions were expected from theory to show second- and first-order Stark effect, respectively. This was strikingly observed in the experiment when only the $K=1\rightarrow1$ lines appeared at field of 10–20 volts/cm, being augmented by the $K=0\rightarrow0$ lines when the field was increased to several hundred volts/cm. The determination of the quadrupole coupling constants, $eQ(\partial^2V/\partial Z^2)$, was based on the frequencies of the $K=0\rightarrow0$ lines only, since these could be measured more accurately than the $K=1\rightarrow1$ lines because of experimental considerations.

The author makes grateful acknowledgment to Dr. A. E. Newkirk of this laboratory for the preparation of the chlorosilanes, Dr. Paul Zemany of this laboratory for purity checks on the mass spectrometer, and Dr. Robert Karplus of the Institute for Advanced Study for his helpful advice.

[1] Davis, Field, Zabel, and Zacharias, Phys. Rev. **73**, 525 (1948). See also reference 2.
[2] W. Gordy, J. W. Simmons, and A. G. Smith, Phys. Rev. **74**, 243 (1948).
[3] C. H. Tindal, J. W. Straley, and H. H. Nielsen, Phys. Rev. **62**, 151 (1942).
[4] R. L. Livingston and L. O. Brockway, J. Am. Chem. Soc. **68**, 719 (1946).

Argon and Neon (pn) Thresholds

H. T. RICHARDS AND R. V. SMITH,
Department of Physics, University of Wisconsin, Madison, Wisconsin
November 1, 1948

FROM mass values[1] one calculates a $Q=-1.1\pm1.1$ Mev for the reaction $A^{40}(pn)K^{40}$. Observation of the neutron threshold should give precisely the mass difference between the important isobars A^{40} and K^{40}. A gas target was recently available on the Wisconsin electrostatic generator so a quick search was made for this threshold. A BF_3 counter surrounded by paraffin served as neutron detector. The high resolution electrostatic analyzer[2] was

not used for these measurements since the somewhat non-uniform aluminum foil (0.00035 in. thick) which separates the gas target from the vacuum system limits the energy homogeneity of the proton beam.

Below $E_p=2.4$ Mev the neutron yield from the argon was so very low that an accurate determination of threshold was not possible in the short time at our disposal. However, a very intense sharp rise in the neutron yield from the argon was observed for $E_p=2.4$ Mev (see Fig. 1). It is, of course, possible that the mass values are in error and that this rise is near the argon threshold. An alternate and more probably explanation[3] is that the large angular momentum difference between K^{40} ($I=4$) and A^{40} ($I=0$?) makes the pn reaction near threshold very highly forbidden. The sudden sharp rise for $E_p=2.4$ Mev could be the threshold for the formation of K^{40} in an excited state of angular momentum 1 or 0. The lifetime of the excited state will be of the order of 10^{-6} sec. if $\Delta I=4$ and of the order of 10^{-9} sec. if $\Delta I=3$, so such an isomeric state would be difficult to observe experimentally. (These lifetime estimates assume the energy level to be 1.3 Mev above the ground state.)

The rise in background (argon gas replaced by hydrogen) neutron yield which starts at 2.35 Mev probably comes from protons hitting oxide surfaces ahead of the gas target. The aluminum foil is 230 kv thick for 2.35-Mev protons so the energy of the protons outside the foil is 2.6 Mev which is sufficient for the $O^{18}(pn)F^{18}$ reaction.

At $E_p=2.9$ Mev the argon pn cross section is about 10^{-25} cm^2 so the neutron yield is comparable[4] with the $Li^7(pn)Be^7$ reaction. The neutron energy at the 2.4-Mev threshold should be 1.4 kv so if suitable thin targets of argon could be used it might provide a variable energy neutron source superior for low energy neutrons to the lithium reaction.

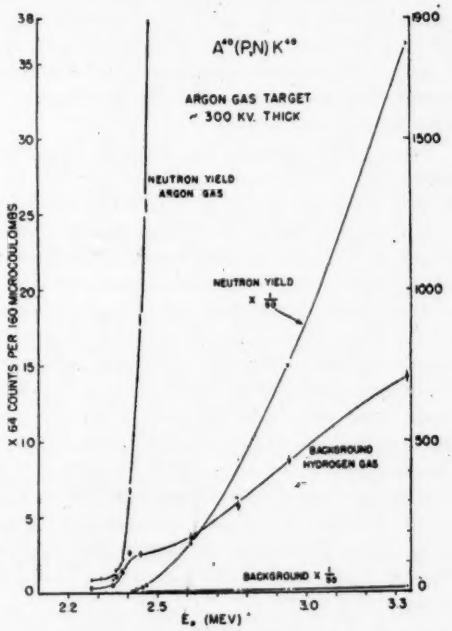

FIG. 1. Neutron yield, argon target.

A quick search was also made for a pn threshold with neon gas in the target. Bethe's mass values[1] predict a $Q=-2.1$ Mev for the $Ne^{22}(pn)Na^{22}$ reaction, but his mass of Na^{22} is a considerably in error since it has been shown by $\beta\gamma$-coincidences[5,6] that the beta-decay of Na^{22} goes entirely to 1.3-Mev excited state of Ne^{22}. No neutron yield from neon gas in the target could be detected for protons up to 3.35 Mev, which energy was the maximum available for the protons after passing through the aluminum foil to the gas target. The present negative neutron results and the beta-gamma-cascade decay of Na^{22} are consistent if the mass of Na^{22} is taken as 22.00152 m.u. when Ne^{22} is taken as 21.99844 m.u.

This work was supported in part by the Wisconsin Alumni Research Foundation and in part by the Atomic Energy Commission.

[1] H. A. Bethe, *Elementary Nuclear Theory* (J. Wiley & Sons, Inc., New York, 1947), p. 126.
[2] Warren, Powell, and Herb, Rev. Sci. Inst. **18**, 558 (1947).
[3] E. P. Wigner, private communication.
[4] R. Taschek and A. Hemmendinger, Phys. Rev. **74**, 373 (1948).
[5] Maier-Leibnitz, Zeits. f. Physik. **122**, 233 (1944).
[6] Good, Peaslee, and Deutsch, Phys. Rev. **69**, 313 (1946).

Deuterium (pn) Threshold

R. V. SMITH AND H. T. RICHARDS
Department of Physics, University of Wisconsin, Madison, Wisconsin
November 1, 1948

A DEUTERIUM gas target has recently been in use on the Wisconsin electrostatic generator for another experiment.[1] While the target is available, we have, therefore, made a quick search for the threshold of the simple but important reaction

$$D+H\rightarrow 2H+n+Q,$$

whose Q is, of course, negative and equal to the binding energy of the deuteron. Conservation of momentum requires that the proton energy at threshold be $(3/2)Q$ or about 3.3 Mev. Although the above reaction has been observed for 5.1-Mev protons,[2] it was anticipated that observation of the threshold would be difficult for two reasons: (1) From statistical arguments one expects the cross section for a three-particle disintegration to be very low at threshold; (2) the outgoing protons have a Coulomb barrier to penetrate. However, there are two other factors which assist in the threshold detection. First, momentum conservation confines all the neutrons to the forward direction at threshold, and second, the neutron energy at threshold is already 370 kv because of the velocity of the c.g. system.

These last factors were exploited by choosing a long but small diameter hydrogen recoil counter for the neutron detector and placing it directly in front of the target. It was possible in this manner to obtain a detection efficiency of $>10^{-3}$ and yet at the same time reduce background counting rate to a small fraction of that present in a BF_3 counter surrounded by paraffin. With this arrangement the results shown in Fig. 1 were obtained in one evening's run.

Since the high resolution electrostatic analyzer was not used in this experiment and because of some uncertainty in the thickness of the aluminum foil at the entrance to the gas target, no attempt was made to obtain good enough statistics to extrapolate to a precise value of the threshold. However, it is possible that this reaction may be capable of giving an independent and precise measurement of the binding energy of the deuteron. Preparations are now being made to develop a non-gaseous deuterium target in order that the high resolution electrostatic analyzer may be used to advantage for this purpose.

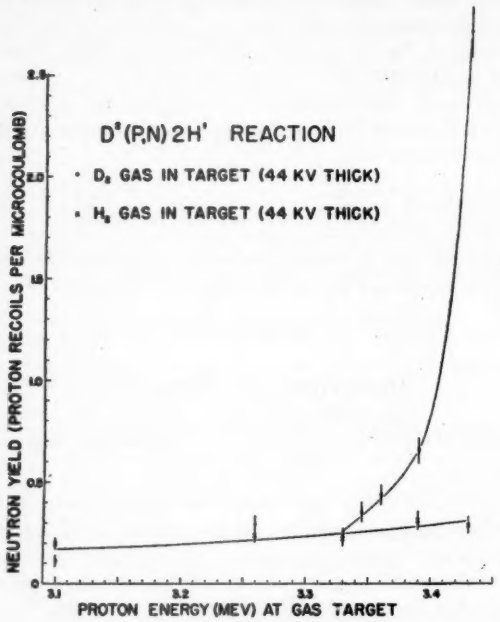

FIG. 1. Neutron yield curves.

The cross section for the reaction appears to be about 10^{-30} cm² for $E_p = 3.4$ Mev.

This work has been supported in part by the Wisconsin Alumni Research Foundation and in part by the Atomic Energy Commission.

[1] G. T. Hunter and H. T. Richards, "Angular distribution of d-d neutrons" (report in preparation).
[2] W. H. Barkas and M. G. White, Phys. Rev. **56**, 288 (1939).

On the Investigation of Supersonic Flow Patterns by Means of the Shock Tube

C. W. MAUTZ, F. W. GEIGER,* AND H. T. EPSTEIN
Randall Laboratory of Physics, University of Michigan, Ann Arbor, Michigan
November 5, 1948

THE shock tube was developed by Smith[1] at Princeton University as a tool for studying the reflections of shock waves in the laboratory. The flow behind a shock proceeding into a gas at rest may, according to the strength of the shock, move with speed less than, equal to, or greater than the sound speed. (If ξ is the shock strength,

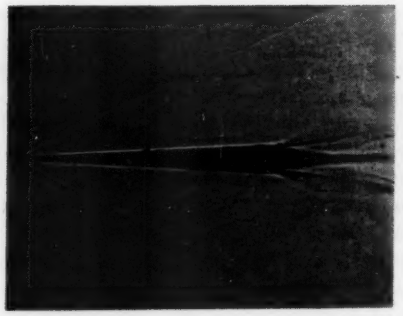

FIG. 1. Sample photograph in air. Mach number approximately 2.42.

defined to be the ratio of the pressure in front of a shock to the pressure behind that shock, then

$$\xi \gtrless 1+\frac{\gamma}{4}(\gamma+1)-\gamma\left[1+\frac{1}{16}(\gamma+1)^2\right]^{\frac{1}{2}},$$

where γ is the specific heat ratio, if the speed behind the shock is $\lessgtr \alpha$, the sound speed.) It has, therefore, occurred to the writers to employ the shock tube as an apparatus for the study of trans- and supersonic flow around objects and to modify the tube if necessary in order to gain this end.

The tube, which is being used by two of us (C.W.M. and F.W.G.), is the original Princeton tube, which was kindly furnished by the Princeton Physics Department. This tube has a 2×7-inch section, an over-all length of 9½ feet, a compression chamber length of 1½ feet, and an effective length (distance between the cellophane diaphram and the middle of the test section) of 5 feet 4 inches. In operating the tube, the pressure in the expansion chamber is reduced, and the diaphragm is pierced, whereupon a shock wave moves toward the test section. The shock strength is determined by velocity measurement using an R.C.A. electronic timer; shadowgraphs are taken at predetermined times during and after the passage of the shock through the test section.

The theory of the flow in an idealized tube has been developed, and experimental investigations of the uniformity and duration of the flow have been carried out for various values of ξ using air in the expansion chamber. The length of the compression chamber was increased in order to provide uniform flow of such duration that the steady state would be reached for the models used. (In the shorter tube, a rarefaction wave, starting from the diaphragm, traveled along the tube, was reflected from the compression end, and reached the test section before the steady state had been reached.) With the modified tube the variations in the flow Mach number, as calculated from the measured bow wave angle formed on a 5-degree wedge, were less than 0.02 for supersonic Mach numbers up to 1.35 for periods of 250 microseconds or longer, depending on the Mach number. Within this time interval the modified shock tube might indeed be regarded as an intermittent wind tunnel.

Photographs have been taken using helium and air in the compression chamber and using air, carbon tetra-

chloride, and Freon-12 in the expansion chamber. Figure 1 is an example of the type of photograph obtained in air. Here the observed Mach number is about 2.42.

The shock tube has potentialities as a transonic facility since the initial Mach number may be set at or near unity without difficulty.

This research is sponsored by the Office of Naval Research under Contract No. N6-ONR-25 T.O. No. 4 with the Engineering Research Institute of the University of Michigan.

* On leave of absence from Cornell Aeronautical Laboratory, Buffalo, New York.

[1] Lincoln G. Smith, *Photographic Investigation of the Reflection of Plane Shocks in Air*, N.D.R.C. Report No. A-350 and O.S.R.D. Report No. 6271, November, 1945.

Errata and Addenda: Mechanical Properties of Long-Chain Molecule Liquids at Ultrasonic Frequencies

[Phys. Rev. 73, 1074 (1948)]

W. P. MASON, W. O. BAKER, H. J. MCSKIMIN, AND J. H. HEISS
Bell Telephone Laboratories, Murray Hill, New Jersey

THE sixth line of the summary should read 40 rather than 14 kilocycles. Curves for polymer *A* in Figs. 2, 3, and 14 were wrongly plotted, and appear corrected in the figures shown herewith. Three rectangular points for polymer *A* have been added in Fig. 2. These are shear viscosities at 14 megacycles, measured as noted on p. 1079 of the original paper. The viscosities in Fig. 11 (of the original paper) and Fig. 14 may be denoted by $\lambda'+2\mu'$, where λ' is compressional viscosity and μ' is ("second") shear viscosity. The high frequency shear measurements now permit additional independent estimation of λ', and

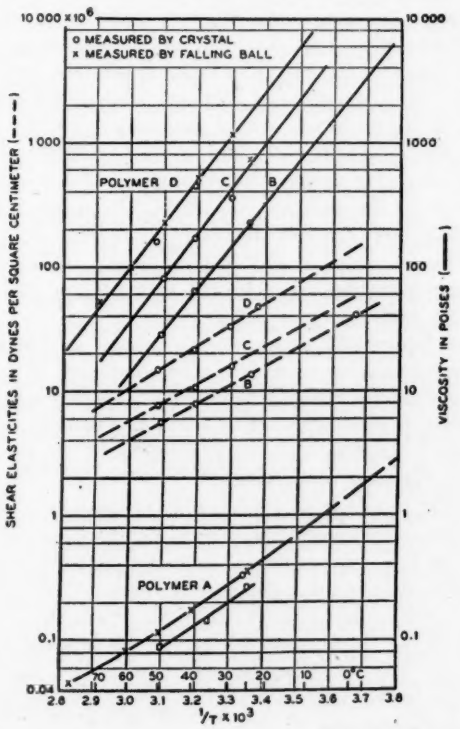

FIG. 2. Shear viscosity and shear elasticity of polyisobutylene liquids.

TABLE I. Comparison of shear and compressional viscosities (in poises) for polyisobutylene *A'*.

Shear viscosity, $\eta=\mu'$, from "static" and torsional crystal measurements	Shear viscosity μ' directly measured at 14 mc	$\lambda'+2\mu'$ from longitudinal wave measurements, 2–8 mc	λ', compressional viscosity, by difference
0.57	0.48	0.94	~0

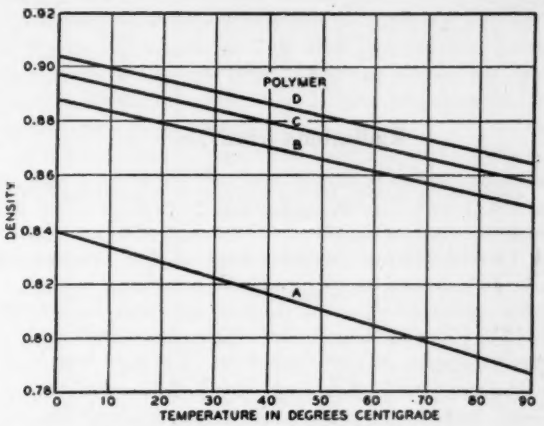

FIG. 3. Density of polyisobutylene liquids as a function of temperature.

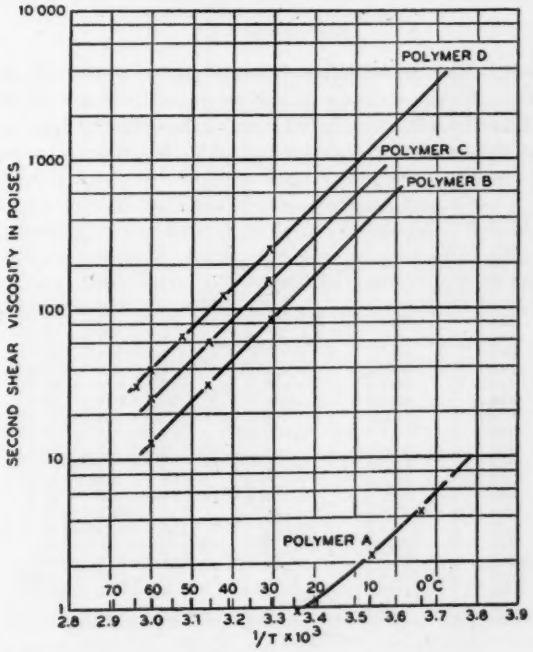

FIG. 14. Viscosities $\lambda'+2\mu'$ from longitudinal wave measurements (representing primarily 2 × (second shear viscosity)) of polyisobutylene liquids as function of temperature.

agree with the earlier conclusion that it is much less than μ', at least in the megacycle range. Typical values on a polymer A', similar to polymer A at 25°C, are found in Table I. Some measurements on higher molecular weight polymers seem to indicate larger λ' values, always, however, much less than μ'. Accordingly, it has been possible, at least in several cases, to account quantitatively for the attenuation of logitudinal waves in liquids by a shear viscosity.

Radiations from Te^{121}

R. D. Hill and J. W. Mihelich
Department of Physics, University of Illinois, Urbana, Illinois
October 25, 1948

ACCORDING to previous work in this laboratory,[1] Te^{121} decays by two isomeric transitions, namely, a highly converted γ-ray transition of approximately 50 kev of 143-day half-life followed by a partly converted 220-kev γ-ray of approximately 5×10^{-8}-sec. half-life.[2] The Te^{121} in its ground state then decays by K-electron capture of 17-day half-life[3] into Sb^{121} which subsequently emits a partly converted 610-kev γ-ray.

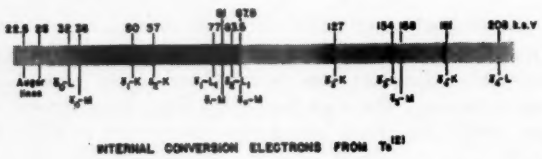

FIG. 1. Internal conversion electrons from Te^{121}.

In the present experiments we set out to measure more accurately the energies of the electrons involved in the 143-day transition. A Te^{121} source of the order 0.1 mg/cm² and 0.01 millicurie was inserted in a 180-degree focusing β-ray spectrograph,[4] and a number of spectra were taken during a period of about 5 months. The spectrum, which is shown in Fig. 1, turned out to be more complex than was anticipated and was found to contain 18 lines, indicating with certainty the presence of 4 transitions of energies: 82, 88.5, 159, and 213 kev. There is also the possibility of a 36.5-kev transition, based on the assumption that the 32.4- and 34.9-kev conversion lines are due to L- and M-conversions. The K-conversion which would lie at approximately 5 kev was not found, and this may be due to either experimental conditions or may be consistent with theory if the transition is weak and of high angular momentum change. The observed conversion lines and their assignments are shown in Table I.

TABLE I. Conversion electron spectrum of Te^{121}.

B_ρ (oersted-cm)	Line energy (kev)	Assignment	γ-ray energy (kev)
504.9	22.2	$K\alpha_1-L_I$	22.2 + 4.95 = 27.15
544.6	25.6	$K\beta_1-L_I$	25.6 + 4.95 = 30.55
616.9	32.4	γ_0-L	32.4 + 4.35 = 36.75
641.3	34.9	γ_0-M	34.9 + 1.0 = 35.9
774.7	50.3	γ_1-K	50.3 +31.8 = 82.1
824.6	56.5	γ_2-K	56.5 +31.8 = 88.3
970.2	77.0	γ_1-L_I	77.0 + 4.95 = 81.95
974.2	77.3	γ_1-L_{III}	77.3 + 4.35 = 81.65
995.6	80.6	γ_1-M	80.6 + 1.0 = 81.6
1016	83.8	γ_2-L_I	83.8 + 4.95 = 88.75
1019	84.1	γ_2-L_{III}	84.1 + 4.35 = 88.45
1041	88.0	γ_2-M	88.0 + 1.0 = 89.0
1278	127.3	γ_3-K	127.3 +31.8 =159.1
1422	154.9	γ_3-L	154.9 + 4.95 =159.85
1448	159.4	γ_3-M	159.4 + 1.0 =160.4
1557	181.2	γ_4-K	181.2 +31.8 =213.0
1689	208.7	γ_4-L	208.7 + 4.95 =213.65
1706	212.2	γ_4-M	212.2 + 1.0 =213.2

We have also obtained the relative intensities of the conversion lines and followed their decay. The relative sensitivity of the spectrographic film was first calibrated as a function of exposure and of electron energy using the known number-energy distribution of the β-rays from P^{32}.

It has been found that the intensities of all the conversion lines decay with a half-life of approximately 143 days, and that there is no contribution to their intensities from the 17-day activity. It therefore seems probable that all four transitions, including the 82 and 88.5 kev which have been previously assigned[5] to 30-day $Te^{122\text{ or }124}$, belong to Te^{121}.

The K- to L-conversion ratios for the 82-, 88.5-, 159-, and 213-kev transitions have been determined as 0.77, 0.92, 7.7, and 4.2, respectively. Following the theoretical analysis of Hebb and Nelson,[6] the effective angular momentum changes associated with 2^l-electric multipole transitions can now be obtained, and are closest to: $l=3$ for 82 kev, $l=3$ for 88.5 kev, $l=2$ for 159 kev, and $l=3$ for 213 kev. The associated lifetimes, allowing for electric multipole conversions, are of the order 3×10^{-4} sec., 2×10^{-4} sec., 1.5×10^{-9} sec., and 10^{-6} sec., respectively.

The relative intensities of the conversion electrons from all shells of the separate 82-, 88.5-, 159-, and 213-kev transitions are 87, 100, 16, and 12, respectively. The intensities of the 32.4- and 34.9-kev lines of the nominae 36.5-kev transition are only 0.3 and 1.0, on the saml arbitrary scale.

There appears to be no obvious scheme in which the observed transition energies can be combined. In particular, one cannot conclude from these experiments which transition is responsible for the 143-day half-life, as the 36.5-kev transition alone has too low an intensity to precede the other transitions.

We are indebted to Professor J. G. Hamilton of the University of California for arranging the bombardment of an Sb target by deuterons in the 60-inch cyclotron at Berkeley. We are also indebted to Professor R. B. Duffield for separating the active Te from Sb. We wish to thank Professor M. Goldhaber for his active interest in the problem. The investigation was assisted by the joint program of the Office of Naval Research and the Atomic Energy Commission.

[1] Burson, Bittencourt, Duffield, and Goldhaber, Phys. Rev. **70**, 566 (1946).
[2] P. T. Bittencourt and M. Goldhaber, Phys. Rev. **70**, 780 (1946).
[3] J. E. Edwards and M. L. Pool, Phys. Rev. **69**, 140 (1946).
[4] R. D. Hill, Phys. Rev. **74**, 78 (1948).
[5] C. V. Kent and J. M. Cork, Phys. Rev. **62**, 297 (1942).
[6] M. H. Hebb and E. Nelson, Phys. Rev. **58**, 486 (1940).

Note on the Photo-Conductivity of Cadmium Sulfide Crystals*

RUDOLF FRERICHS AND A. J. F. SIEGERT
Department of Physics, Northwestern University, Evanston, Illinois
November 1, 1948

THE photo-current in CdS crystals irradiated with alpha-, beta-, or gamma-rays or light is 100 to 10^4 times larger[1] than the total charge brought up per second to the conduction band by the radiation. The carriers of this excessive current must enter the crystal from the metal electrodes, but must be prevented from passing through the crystal in the dark. To explain this effect we assume that in CdS the energy E_0 of the lowest empty level lies already sufficiently low to allow electrons to enter before irradiation. These electrons are trapped and give rise to a negative space charge which raises the empty band until in the dark further electrons are prevented from entering.[2] By irradiation, however, this space charge is reduced and the crystal becomes conducting.[3] Since thus the main effect of the irradiation is to regulate the flow of electrons, the current can exceed by far the number of electrons lifted to the conduction band per second. The effect is very similar to the increase of current in an amplifier tube when the space charge is reduced by a positive grid.

In order for irradiation to reduce the negative space charge, a fixed positive charge must remain in the insulator under irradiation while electrons leave. For this it is sufficient to assume that there are normally filled traps at an energy E_2, below the empty band, where $E_0-E_2 > 300°K$, and the electrons from these traps can fill the holes produced by irradiation in the filled bands. Since at room temperature the current under irradiation rises without delay, we conclude that electrons from the conduction band are lifted up by the irradiation and are trapped in states of an energy E_1, which is also below E_0 but much closer to it than E_2.

At a temperature sufficiently below $(E_0-E_1)/k$, electrons should be prevented from leaving the crystal until most of the upper traps are filled.

The resulting delay in the rise of conductivity can be observed at liquid air temperature. A crystal of CdS which has been kept in the dark for a sufficiently long time reached a resistance $\gg 3\cdot 10^{13}$ ohms if cooled to $-189°C$. If at $t=0$ irradiation starts with a constant intensity of gamma-rays, the resistance is lowered at $t=3$ sec. to $3\cdot 10^{12}$ ohms. With continued irradiation it then stays constant to $t=36$ sec. After this delay it drops very fast, reaches $4\cdot 10^{10}$ ohms at $t=72$ sec. and a saturation value of $2\cdot 10^8$ ohms after one hour. In these experiments the field strength applied to the crystal was always small (2.9 volts/mm) in order to avoid ionization effects in the surroundings of the crystal.

The current during the delay period can be considered as the primary current. (Its magnitude and the duration of the delay are compatible with reasonable assumptions for the "Schubweg" and the number of traps.) During the delay time the net result of the irradiation is the transfer of electrons from the lower traps to the upper traps, a process which does not produce any change of the space charge. If the irradiation is interrupted at $t=36$ sec., the crystal can be kept in this "metastable state" at $-189°C$ for a long time. A crystal in this state is similar to an excess semiconductor, and, without further irradiation, it becomes strongly conducting for a short time if it is heated to room temperature. After this experiment the crystal has returned to its normal state and the above-mentioned delay experiment can be repeated. However, if the crystal is not warmed and thus remains in the metastable state, the delay does not occur, but with further irradiation (even after a long intermission) the current rises instantaneously.

If the crystal in its metastable state and without applied voltage is heated on one side, we find the expected sign of the thermoelectric e.m.f. (i.e., positive on the hot junction).

One of the authors (A. J. F. Siegert) wishes to thank Professor F. Seitz for a stimulating discussion.

* The experimental part of this work was sponsored by the U. S. Navy, Bureau of Ships.

[1] R. Frerichs and R. Warminsky, Naturwiss. 33, 251 (1946); R. Frerichs, Phys. Rev. 72, 594 (1947), Table I; H. Kallman drew the attention of Frerichs to this fact in 1947. Recently Kallman and Warminsky have studied this amplification in a paper in print in Ann. d. Physik. The model here proposed is entirely different from the one used by these authors.

[2] N. F. Mott and R. W. Gurney, *Electronic Processes in Ionic Crystals* (Oxford University Press, London, 1940), p. 169.

[3] Similar to the mechanism proposed by N. F. Mott and R. W. Gurney, see reference 2, pp. 186–188.

Diurnal Variations of Meteor Trails

CHARLES A. LITTLE, JR.
Department of Terrestrial Magnetism, Carnegie Institution of Washington, Washington, D. C.
November 1, 1948

METEOR trails have been observed by means of radar equipment operating on 27 megacycles.

The diurnal variation in the distribution of meteor occurrence with time of day has been established by visual observations and by radio observations of Appleton and Naismith[1] and of Hey and Stewart.[2] The seasonal change in the nature of this distribution as specified by these authors, however, differs significantly from the present observations which were made between April 17 and June 19, 1948 (Fig. 1), which correspond closely to the

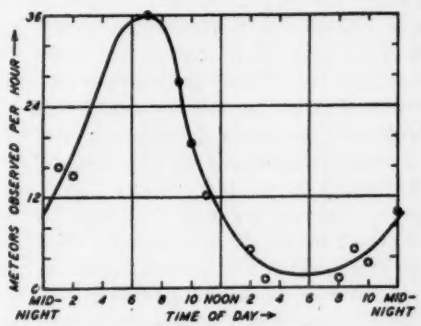

FIG. 1. The distribution of meteor occurrence over a 24-hour period.

published curves for mid-winter rather than for mid-summer. Since the present observations are at a different latitude and at a later epoch than the earliest published observations, the form of the diurnal burst distribution throughout the year seems to be more complex than originally supposed.

Observations which were made between April 17 and June 19, 1948, show a diurnal variation in the distance of meteor trails. During the night hours the distance of meteor trails centers around 75 miles and scatters within 65 to 90 miles. There is a sharp increase in the average distance of meteor trails to a maximum of about 130 miles at 9:00 a.m. local time (Fig. 2). At this time practically

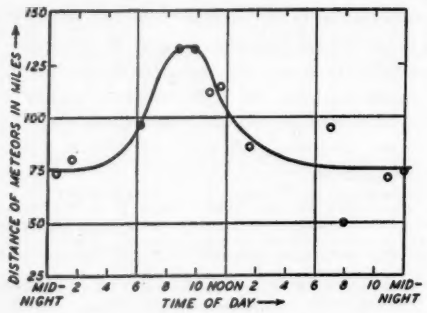

FIG. 2. The distribution of meteor distance over a 24-hour period.

no meteor trails are observed less than a distance of about 100 miles. Evidence of this variation has not been indicated in any of the earlier work.

It is expected that more observations will be made during the winter months.

[1] E. Appleton and R. Naismith, Proc. Phys. Soc. **59**, 461–473 (1947).
[2] J. S. Hey and G. S. Stewart, Nature **158**, 481–482 (1946).

The Nuclear Spin B^{10} and Spin-Orbit Coupling in Li^7

DAVID R. INGLIS
Department of Physics, Johns Hopkins University, Baltimore, Maryland
November 4, 1948

A RECENT measurement[1] of the nuclear spin of B^{10} has shown that it is $I=3$, rather than $I=1$ as was commonly assumed on the basis of a comparison with other light odd-odd nuclei. The value $I=1$ was also expected because a theoretical treatment[2] involving reasonable simplifications gave $^3S_1$ as the ground state. The same treatment gave two ^3D's as the next and not very highly excited multiplets, which could interact through non-tensor perturbations or excited configurations in such a way as to make[2] the lowest multiplet a ^3D. The simple theory of the spin-orbit coupling[3] of light nuclei based on central (non-tensor) interactions gives the sign of spin-orbit coupling which makes the ground state $^3D_3$ if the lowest multiplet is indeed ^3D. This is in agreement not only with $I=3$, but also with the magnetic moment $\mu=1.8$, approximately equal to the deuteron moment plus one, as expected for $^3D_3$ in a nucleus which is symmetrical with respect to protons and neutrons. Similar agreement with the expected sign of spin-orbit coupling has also been found[4,5] in the entire sequence Li^7, Be^9, B^{11}, C^{13}, and N^{15} (in spite of the neglect of tensor interactions).

The ground state of Li^7 is taken to be $^2P_{3/2}$. The possibility has been discussed[3] (*a*) that the 450-kev state, observed, for example, by short-range protons in $Li^6(d,p)Li^7$, is the other half of the doublet, $^2P_{1/2}$, in spite of the failure of an estimate on the basis of simple assumptions to give so large a doublet splitting. An alternative possibility is (*b*) that the doublet splitting is so small that the transitions to both states, $^2P_{3/2}$ and $^2P_{1/2}$, are unresolved in the long-range proton group, and that the 450-kev "state" is an unresolved ^2F, in spite of the fact that the most likely evaluation of parameters in reference 2 would place this next multiplet, ^2F, one or several Mev above the ^2P. It is a choice of one doublet wider than estimated or two narrow doublets closer together than estimated.

The reaction $B^{10}(n,\alpha)Li^7$ has been observed only with thermal neutrons, and the short-range group of alphas leading to the 450-kev excited state has about thirteen

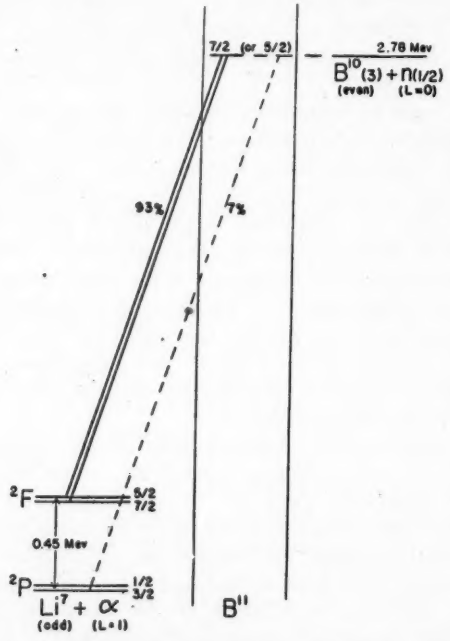

FIG. 1. Transition scheme of $B^{10}(n,\alpha)Li^7$ with thermal neutrons, accounting for the scarcity of long-range alphas.

times the intensity of the long-range group,[6] in sharp contrast with the $Li^6(d,p)$ reaction, of which the long range is a little more intense than the short.[7] It seems plausible that this extreme preference for the short-range transition in the B^{10} reaction should be associated with the large nuclear spin of B^{10}. The thermal neutrons enter in an *s* state, giving rise to states of the compound nucleus having $I_r=5/2$ or $7/2$. The energies of the long-range and short-range disintegrations are only about 2.8 Mev and 2.3 Mev, requiring barrier penetration and strongly favoring small angular momenta of the alpha. We assume that

the parity of B^{10} is even and that the low multiplets of Li^7 are odd, as in the simple models. Then the states of the compound nucleus are even, almost all the outgoing alphas have one unit of angular momentum, and Li^7 states as low as $I=3/2$ can be reached if $I_r=5/2$, or as low as 5/2 if $I_r=7/2$. The strong preference for the transition to the excited state seems thus to exclude the possibility (a) that the excited state is $^2P_{1/2}$, and to favor the possibility (b) that the excited state is an unresolved $^2F_{7/2,5/2}$ and that the compound state which is most influential at thermal energy has $I_r=7/2$ (Fig. 1).

Thus the simple theory[3] of spin-orbit coupling in light nuclei seems to remain significant in determining the nuclear spins, but the multiplet splittings to which it presumably gives rise are apparently too small to have been resolved by observation of energy groups in nuclear reactions.

[1] W. Gordy, H. Ring, and A. B. Burg, Phys. Rev. **74**, 1191 (1948). See also M. Goldhaber, Phys. Rev. **74**, 1194 (1948), Millman, Kusch, and Rabi, Phys. Rev. **56**, 165 (1939).
[2] E. Feenberg and M. Phillips, Phys. Rev. **51**, 597 (1937). Note on p. 606 the remark, "For this reason, the possibility that the normal state of B^{10} is ^3D cannot be excluded."
[3] D. R. Inglis, Phys. Rev **50**, 783 (1936). The estimated magnitude of the coupling is quite sensitive to the assumed nuclear radius ($\sim r_0^{-4}$ if ψ contains $\exp(-r^2/r_0^2)$). The length parameter used in the original estimate was taken from a central-field or "Hartree" treatment of the Li nuclei (D. R. Inglis, Phys. Rev. **53**, 880 (1938), the parameter being $\alpha\sigma=22\times1.2$) and is the "radius" of a three-dimensional oscillator potential appropriate to the average needs of the s and p nucleons in minimizing the energy. That estimate gave 0.15 Mev for the doublet splitting of a nucleon in Li^7, but in retrospect the length parameter seems too small for a p proton and the estimated energy too large. The expected splitting is reduced also by the possibility of departures from the single-particle wave functions of a sort to divide the orbital angular momentum among all the nucleons as in the alpha-model (see reference 5), for example.
[4] M. E. Rose and H. A. Bethe, Phys. Rev. **51**, 205 (1937).
[5] D. R. Inglis, Phys. Rev. **56**, 1175 (1939). See also W. H. Furry, Phys. Rev. **50**, 784 (1936).
[6] J. K. Bøggild, Kgl. Danske Vid. Sels. Math.-Fys. Medd. **23**, 4, 26 (1945).
[7] L. H. Rumbaugh, R. B. Roberts, and L. R. Hafstad, Phys. Rev. **54**, 657 (1938).

Metastable State of Sc^{46}

M. GOLDHABER* AND C. O. MUEHLHAUSE
*Argonne National Laboratory,** Chicago, Illinois*
November 5, 1948

AFTER bombarding Sc, in the form of the oxide, with slow neutrons, an intense activity of 20-sec. half-life period was observed. The decay curve (Fig. 1) was obtained by putting the sample inside an air ionization chamber. An Al absorption curve (Fig. 2) indicates internal conversion electrons with a range of ~30 mg/cm² corresponding to an energy of 165 kev. The small background left indicates that there is little if any β-branching to Ti^{46}. The energy of the metastable state was also obtained by taking a Pb absorption curve of the unconverted γ-rays with a Geiger-Mueller counter (Fig. 3). From the half-value thickness, 0.50 g/cm², we obtain a value of 180 kev for the γ-ray energy. The ratio of internal conversion electrons to γ-rays was found to be of the order 1. This is compatible with a "2^4-pole" isomeric transition.

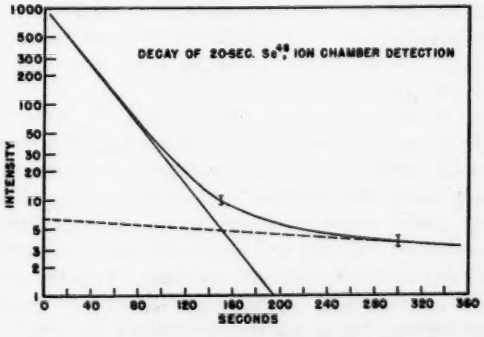

FIG. 1. Decay curve. The error in reading the ion current is negligible in the initial part of the decay curve. The activity remaining after the 20-sec. period had decayed was not investigated further.

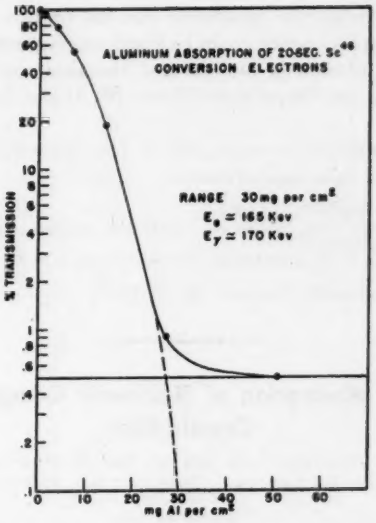

FIG. 2. Absorption of electron component.

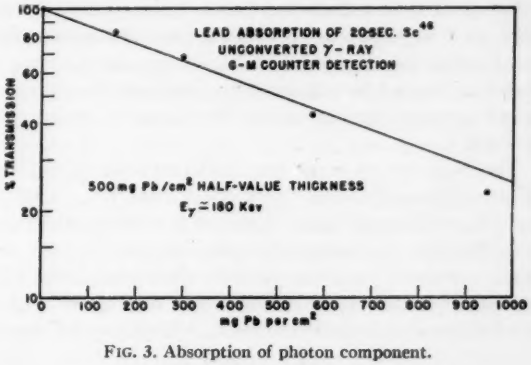

FIG. 3. Absorption of photon component.

An approximate absorption cross section of about 10×10^{-24} cm² was found for "pile neutrons." A significant fraction of the 85-day ground state, which has a slow neutron capture cross section[1] of 22×10^{-24} cm², must therefore be formed indirectly through the metastable state. For the neutrons used, a "1/v absorber" (e.g., Al) shows a Cd ratio of about 39. For the 20-sec. and 85-day Sc activity we find Cd ratios which are approximately equal: 53 and 59, respectively. This indicates that a negative energy neutron level is responsible for the strong absorption of thermal neutrons in Sc.

We excluded the possibility that the observed activity was due to Hf,[2] which could be a serious contaminant from the point of view of lifetime and chemical similarity, by measuring the Cd ratio for 19-sec. Hf. It was found to be 3.1.

We should like to thank Mr. E. Der Mateosian for help in some of these measurements.

* Now at University of Illinois.
** Research work carried out under the auspices of the Atomic Energy Commission.

[1] L. Seren, H. N. Friedlander, and S. H. Turkel, Phys. Rev. **72**, 888 (1947).
[2] A. Flammersfeld, Naturwiss. **32**, 68 (1944).

On the Absorption of Nucleonic Component in Cosmic Rays

G. Bernardini, G. Cortini, and M. Manfredini
Istituto Fisico dell'Universita', Centro di Fisica Nucleare del C.N.R., Rome, Italy
October 25, 1948

IN a previous letter[1] it was observed that the nuclear stars may be considered as "local indicators" of the nucleonic component. In this letter, from the comparison of the absorption of the star-producing radiation in air and Pb it was suggested that the related cross section was

$$\sigma \simeq k \cdot A^{\frac{1}{2}} \cdot 10^{-26} \text{ cm}^2, \qquad (1)$$

where A is the atomic weight and $k \simeq 3$.

We can add now that the results of similar experiments performed in Al appear to validate the cross section, Eq. (1). Further new data obtained following the scanning of plates in Pb and in balloons have increased the precision of our previous measurements. The data are summarized in Table I.

The cross section in air was evaluated from the number of stars observed at the Laboratorio della T.G. (3500 m) and the number of those observed in plates which have been flown in balloons. The evaluation of σ in air was made assuming an exponential absorption and then averaging on the range of pressures during the flights. We find an absorbtion thickness $L_a = 135 \pm 4$ and following

$$\sigma_{\text{air}} = 0.177 \cdot 10^{-24} \text{ cm}^2.$$

From such a value and from the data collected in Table I we can argue that the general absorption law of the nucleonic component is indicated by Eq. (1). This conclusion may be stressed observing the numbers listed in Table II. We have given in the first column the experimental values of σ and in the second the values σ' obtained from Eq. (1) putting $k = 2.95$.* The excellent agreement between the data in the first and second columns is certainly a happy case, but we believe that Bernardini *et al.*[1] express roughly the effective cross section for nucleons of high energy ($T \gtrsim Mc^2$) with nucleus. It appears to be proportional to the geometrical cross section, *but smaller* by a factor of 2 or 3.

TABLE I. Summary of data on star production.

Thickness of absorber in g/cm²		0	13.5	23.4	61	104	152
stars / cm³ day	Al	15.3 ±0.8	12.8 ±0.7		10.7 ±1.0	8.4 ±0.7	
	Pb			18.0 ±0.8		13.1 ±1.0	9.7 ±1.0

TABLE II. Values of σ and σ'. L is the absorption thickness.

	$\sigma \cdot 10^{24} = \frac{A}{N} \cdot \frac{1}{L} \cdot 10^{24}$	$\sigma' \cdot 10^{24} = 2.95 \cdot A^{\frac{1}{2}} \cdot 10^{-2}$
Pb	1.07	1.05
Al	0.27	0.26
Air	0.18	0.18

Considering the stars as "indicators" of nucleonic component, another, perhaps interesting, result appears from our plates. Lattes, Occhialini, and Powell[2] deduced a relation between the total number of mesons which are stopped by the emulsion and the number of mesonic tracks which have a projection longer than a definite length t. We have employed such a relation to compare the number, N_s, of stars at different altitude with the number, N_m, of slow mesons. For this purpose we have considered the stars having at least three prongs. Besides, we have also taken into account the results of Lattes, Occhialini, and Powell[2] at Pic du Midi. We find that the ratio N_m/N_s increases strongly at high altitude (near 20 km high). In the plates which were flown to 22 km the value of such ratio is about 7 ± 1 times larger than the corresponding values at 2800 m (Pic du Midi) and at 3500 m (Laboratorio T. G.).**

The observed mesons were generally "ρ" mesons, i.e., they do not give rise to stars. That is understandable if we consider that they were effectively "μ" mesons whose mean-life is much longer than the mean-life of "π" mesons. However, taking into account the low density of air at high altitude, we argue that the greater part of the mesons observed in such balloon plates arose from a "local generation." (In the balloon ship, near the plates, there are the storage batteries, etc.) On the contrary, in the low atmosphere the number of slow mesons appears to increase with the altitude more slowly than the nucleonic component,[3] and G. Morpurgo[4] demonstrated that from sea level to 4000 m high most of such slow mesons are the residue of μ-mesons coming from the upper layer of the atmosphere. Hence we deduce that in the meson generation the number of mesons increases strongly when their energy decreases. Considering that at 22 km high the atmospheric depth is about $\frac{1}{3}L_a$, our results appear to give support to the "multiple" generation hypothesis.

On 22 tracks of mesons and protons of rather long length (at least 600 microns) we have made a grain count. We find several tracks demonstrating an intermediate mass between 200 and 2000, but similar tracks were found in the plates which remained at sea level and at the Laboratorio T. G., and we believe that they are probably "old" protons. Our opinion is perhaps supported by the fact that such "heavy" tracks appear to end in the emulsion without giving rise to any nuclear process.

We wish to express our warm thanks and appreciation to Professor Marcel Schein of the University of Chicago

and to Professor Merle Tuve of the Carnegie Institution of Washington for supplying our laboratory with part of the balloons used for these experiments.

[1] G. Bernardini, G. Cortini, and A. Manfredini, Phys. Rev. **74**, 845 (1948).
* Corrected from the stars generated at sea level.
[2] C. M. G. Lattes, G. P. S. Occhialini, and C. F. Powell, Nature **160**, 486 (1947).
** For further details see G. Cortini, A. Manfredini, and A. Persano, Nuovo Cimento, in press.
[3] Bruno Rossi, Rev. Mod. Phys. **20**, 537 (1948).
[4] G. Morpurgo, Nuovo Cimento **5**, 285 (1948).

Evidence for a Complex Disintegration of I^{131} *

GEORGE E. OWEN, DAVID MOE, AND C. SHARP COOK
Department of Physics, Washington University, St. Louis, Missouri
November 1, 1948

THE negatron spectrum of I^{131}, obtained from Oak Ridge as a chemically separated decay product of Te^{131}, has been studied. This study was initiated because of a discrepancy reported by Miskel[1] between two methods of determining the absolute disintegration rate of I^{131}.

The present investigation was conducted with a semi-circular uniform field magnetic spectrometer having a radius of curvature of 5.7 cm. The dimensions of the vacuum chamber, however, are quite large with relation to the usual chamber size for an instrument having this radius of curvature such that it is believed that scattering within the instrument is small. The interior of the vacuum chamber is constructed of Aquadag coated Lucite.

The G-M counter utilized a thin window which passed electrons above 3 kev, this window being made of composite films of Formvar and Zapon. These films, after being placed over the exit slit, were dried under a lamp. Windows prepared in this manner appear to be more satisfactory than those prepared only of Formvar or Zapon.

Three sources were used in this investigation; a thin source of 0.18 mg/cm² mounted upon a 0.25-mil Al backing, a second source of 0.32 mg/cm² mounted upon a 0.06 mg/cm² Zapon backing, and a fairly thick source of 0.79 mg/cm² mounted upon a 0.25-mil Al backing. The thickness of the 0.32-mg/cm² source was determined by weighing and that of the others was in turn determined by comparison of relative intensities. The results are derived from a combination of the data from the two thinner sources. The thickest source, with its correspondingly higher counting rate, was used to confirm the existence of the low intensity peaks.

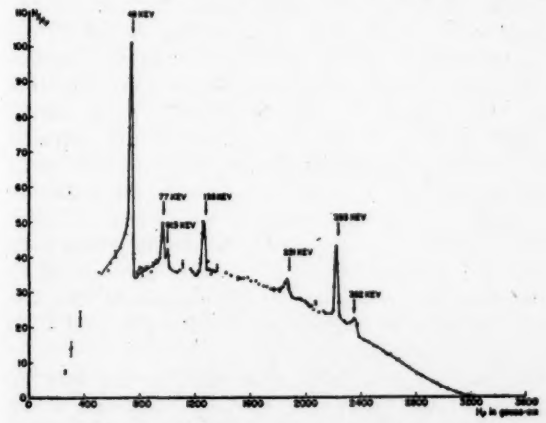

FIG. 1. Momentum distribution of the negatrons from I^{131}. Energies shown are those of the internal conversion lines. Sample statistical errors are indicated for selected points within the several regions of the spectrum. Other points within the same region have approximately the same statistical error.

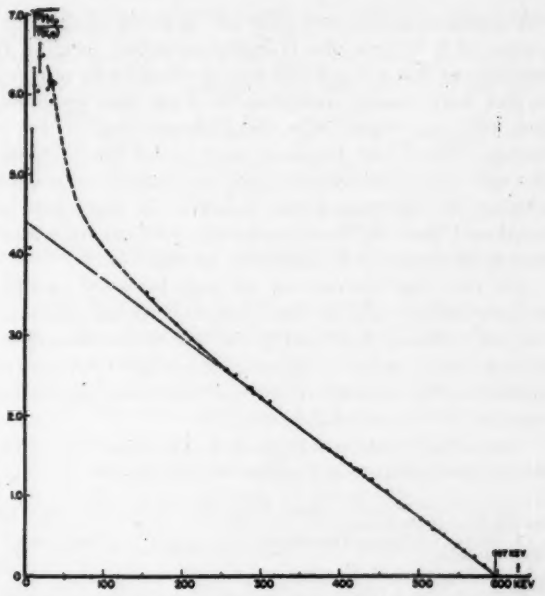

FIG. 2. Kurie plot of the negatron spectrum of I^{131}. $f(Z,\eta)$ is here the Fermi relativistic function rather than the Kurie non-relativistic approximation. The internal conversion line regions are not plotted.

Figure 1 shows the negatron momentum spectrum of I^{131}. In addition to the internal conversion lines at 48 kev and 334 kev reported by Downing, Deutsch, and Roberts,[2] several weaker lines have been found in the current investigation. One of these, at 251 kev, was found by the M.I.T. group in their internal conversion, beta-coincidence data.

If one assumes a gamma-ray whose energy is 83±2 kev then the lines at 48, 77, and 81.5 kev correspond, respectively, to this gamma's K, L, and M conversion lines. Likewise the lines at 333 and 362 kev correspond to the K and L lines for a gamma whose energy is 368±7 kev. Assuming that the other conversion lines are produced in the K shell of Xe, energies can be ascribed to the associated gamma-rays of 163±3 kev and 286±6 kev. Consistent fluctuations within 85–120-kev and 260–320-kev regions suggest the possibility of more low intensity conversion peaks, but with the present arrangements these are too weak to be accurately determined.

The Kurie plot is shown in Fig. 2. Here the true Fermi relativistic Coulomb function is used rather than the more commonly used Kurie non-relativistic approximation. Extrapolation of the higher energy data gives a maximum beta-energy of 597±5 kev. The internal conversion peaks have been omitted from the plot.

A considerable rise above the extrapolated straight line portion of the Kurie plot is indicated at low energies. If one believes that a Kurie plot can significantly be resolved to give lower energy components of the beta-spectrum, then this may mean that the beta-spectrum of I^{131} is complex. There are, however, indications[3] that a Kurie plot may rise at low energies above its straight line portion without its spectrum being complex. It may also be mentioned that the large number of internal conversion lines in this region may contribute to this rise.

The fact that the sum of the high intensity gammas 83 kev+368 kev and the sum of the low intensity gammas 163 kev+286 kev both add to 450 kev within the experimental errors makes it possible that these two sets of gammas follow parallel transitions from a single excited state of Xe^{131} to its ground state.

The authors wish to express their appreciation of many helpful discussions with Professor H. Primakoff.

* Assisted by the joint program of the Office of Naval Research and Atomic Energy Commission.
[1] J. Miskel, Chemistry Department, Washington University, private communication.
[2] J. R. Downing, M. Deutsch, and A. Roberts, Phys. Rev. 61, 686 (1942).
[3] C. S. Cook and L. M. Langer, Phys. Rev. 73, 601 (1948); Phys. Rev. 74, 227 (1948). Because the accurate shape of the spectrum in the low energy region was not of prime importance there was no correction applied based on the shape of the internal conversion lines. See G. E. Owen and H. Primakoff, Phys. Rev. 74, 1406 (1948).

The Photoelastic Properties of Diamond

ELIAS BURSTEIN AND PAUL L. SMITH
Crystal Section, Naval Research Laboratory, Washington, D. C.
October 25, 1948

IN a recent communication[1] the authors discussed the photoelastic properties of crystals in terms of atomic concepts and included a discussion of the photoelastic constants of diamond obtained by Ramachandran.[2] Ramachandran's values had been questioned by West and Makas[3] who stated that the magnitudes of the stress-optic constants $(\pi_{11}-\pi_{12})$ and π_{44} were in error by a factor of 10^2 and that the signs of the constants were wrong. Examination of Ramachandran's data, however, showed that the values of the constants for diamond were given correctly in units of cm^2/g.[4] Furthermore, it was felt that there was not sufficient evidence to warrant the rejection of Ramachandran's signs and that, since there is no way of calculating the atomic anisotropy contributions which play an important rule in determining the signs of the photoelastic constants, only an independent experimental check could settle the question.

West and Makas[5] have since made qualitative observations which confirmed their earlier conclusions about the sign and Ramachandran[6] has recently stated that he has redetermined the signs and agrees with West and Makas that the signs as given in his paper are incorrect. He attributed the error in his paper to an inadvertent reversal in sign of the compensator constant. The authors have independently confirmed these conclusions by measurements on two of the diamonds used by Ramachandran.[7]

In view of the change in sign of the diamond data it is necessary to reconsider their significance. A re-examination of Ramachandran's data shows that the reversal in sign of $(\pi_{11}-\pi_{12})$ and π_{44} changes only the signs of the individual constants and not their magnitudes. The corrected photoelastic constants are:

$$p_{11}=-0.125 \qquad \pi_{11}=-0.43\times10^{-2}\ \text{meter}^2/\text{Newton}$$
$$p_{12}=+0.325 \qquad \pi_{12}=+0.37$$
$$p_{44}=-0.11 \qquad \pi_{44}=-0.27$$
$$p_{11}-p_{12}=-0.45 \qquad \pi_{11}-\pi_{12}=-0.80.$$

From these, a recalculation of the atomic anisotropy constants and related quantities gives the following values:

$$\lambda_{11}=+0.42 \qquad \lambda_{11}-\lambda_{12}=-0.38$$
$$\lambda_{12}=+0.80 \qquad \lambda_0=+0.5$$
$$\lambda_{44}=+2.2 \qquad \rho(dn/d\rho)=+1.24.$$

As Mueller[8] has pointed out, the density contribution to p_{11} and p_{12} is positive in all crystals. In cubic crystals with D lattices, the Lorentz-Lorenz and Coulomb contributions are generally smaller than the density contribution. Positive values of p_{11} and p_{12} should, therefore, be obtained if only these three contributions are important. This is found to be true for many crystals where the atomic anisotropy contribution is small. The atomic anisotropy contribution can, however, be larger than the combined density, Lorentz-Lorenz, and Coulomb contributions and can thereby yield negative values for both p_{11} and p_{12} as in MgO ($p_{11}=-0.3$; $p_{12}=-0.08$).[9]

In diamond where Coulomb contributions are zero, the Lorentz-Lorenz contribution to p_{11} is negative. Even though λ_{11} is relatively small (compare, for example, $\lambda_{11}=1.2$ for NaCl which has a positive p_{11}) the net effect is a negative p_{11}. On the other hand, the Lorentz-Lorenz contribution to p_{12} is positive, and the λ_{12} is not sufficiently large to make p_{12} negative.

The Lorentz-Lorenz contribution to p_{44} in diamond is positive. Here, however, the atomic anisotropy contribution λ_{44}, is large, being about 10 to 20 times as large as those for the alkali halides, so the resultant p_{44} is negative. The relatively large λ_{44} can be attributed to the covalent nature of the bonding in diamond and the distortion of the bond angles by a shearing strain. In ionic crystals central forces predominate and shearing strains do not cause large effects. The λ_{44}, therefore, should be a measure of the amount of homopolar bonding in a crystal. Until data are available on the polarizability and optical strengths of the ions, however, only qualitative estimates of this constant can be obtained from photoelastic data. It is, therefore, not as useful for estimating the amount of homopolar bonding as λ_0 which is more easily obtained. A distortion of the bond angles is also obtained for normal strains and accounts in part for the fact that λ_{11} and λ_{12} of diamond are of the same order of magnitude. (See also the discussion of the relative magnitudes of λ_{11} and λ_{12} in the previous communication.)

The authors' conclusion that the $\lambda_{11}-\lambda_{12}$ may be negative for CsCl, ZnS, and diamond structures is not invalidated by the change in sign of the diamond constants.

The change in refractive index with density, however, is now found to be positive instead of negative as given in the former note.[1] This leaves MgO as the only crystal

known to have a negative $dn/d\rho$. Since dn/dT for diamond is positive, it appears that there can be a large temperature contribution $(\partial n/\partial T)\rho$ to dn/dT even though λ_0 is small. Thus a positive dn/dT does not necessarily indicate a negative $dn/d\rho$ although a negative $dn/d\rho$ is generally accompanied by a positive dn/dT.

We wish to acknowledge valuable discussions on the optical properties of diamond with Sir C. V. Raman and Dr. Ramachandran.

[1] E. Burstein and P. L. Smith, Phys. Rev. **74**, 229 (1948). (Due to typographical errors some of the values in the table are incorrectly given. The following corrections should be noted: MgO, $p_{11} = -0.32$; KBr, $p_{44} = -0.026$; diamond, $p_{44} = +0.11$ and $pdn/d\rho = -1.24$.)
[2] G. N. Ramachandran, Proc. Ind. Acad. Sci. **A25**, 266 (1947).
[3] C. D. West and A. S. Makas, J. Chem. Phys. **16**, 427 (1948).
[4] In tabulating the available photoelastic data Ramachandran did not properly convert Pockels' data (in mm²/kg) to his units which led him to conclude erroneously that the stress-optic constants of diamond were very much smaller than those of other known crystals.
[5] Personal communication.
[6] Personal communication.
[7] These were specimens No. NC 60 and NC 73 of the Raman collection which were kindly loaned to the authors by Sir. C. V. Raman.
[8] H. Mueller, Phys. Rev. **47**, 947 (1935).
[9] Not only is p_{11} negative in MgO but its absolute magnitude is one of the largest known. Since the Lorentz-Lorenz and Coulomb contributions are positive, this indicates a very large λ_{11} which is in keeping with the large amount of homopolar bonding and the large λ_0 in MgO.

Isotopes of Carbon and Oxygen in the Earth's Atmosphere

LEO GOLDBERG, ORREN C. MOHLER, AND ROBERT R. MCMATH
McMath-Hulbert Observatory, University of Michigan, Ann Arbor, Michigan
November 5, 1948

IN earlier notes,[1] the writers have described certain features of the high resolution infra-red solar spectrum obtained at the McMath-Hulbert Observatory with an all-reflecting spectrometer and a Cashman PbS cell. The solar spectrum at approximately 2μ is completely dominated by the three telluric absorption bands, ω_0, ω_1, and ω_2, which are known to arise as a result of vibrational-rotational transitions between the lower state 000 and the excited states 201, 121, and 041 in the CO_2 molecule.[2] The bands are well resolved into their rotational structures, and are of enormous intensity, the strongest lines being completely saturated at moderate solar altitudes.

According to a tabulation by J. M. Cork,[3] the abundances of the C^{13} and O^{18} isotopes are, respectively, 1.1 percent and 0.20 percent those of the more abundant isotopes. The great strength of the normal $C^{12}O_2^{16}$ bands indicates that companion bands involving the isotopes C^{13} and possibly O^{18} should also be present. Previously, observations of isotope bands of CO_2 have been limited to the fundamental ν_3 band of $C^{13}O_2^{16}$, which was discovered in the laboratory by A. H. Nielsen.[4] Inspection of the solar map in the 2μ region reveals the presence of several relatively faint band structures, for some of which the line spacings are nearly identical with those of the ω_0, ω_1, and ω_2 bands; for others the spacings are approximately one-half those of the main CO_2 bands. Two of these bands have already been called attention to by McMath and Mohler.[5] In this connection it should be pointed out that alternate rotational components of the $C^{12}O_2^{16}$ molecule are absent, due to the fact that the oxygen nuclei are identical. Substitution of C^{13} for C^{12} shifts the band position in the direction of lower frequency, but alters the rotational structure only very slightly. On the other hand, the replacement of one of the O^{16} atoms by an isotope of mass 18 destroys the symmetry of the molecule and should result in the appearance of the missing rotational lines.

TABLE I. Calculated and observed band centers for CO_2 molecule in cm^{-1}.

	000–201	000–121	000–041
$C^{13}O_2^{16}$	5104.4 *5099.4*	4981.5 *4977.8*	4852.7 *4853.6*
$C^{12}O_2^{18}$	5006.0	4892.1 *4888.8*	4737.9 *4747.9*
$C^{13}O^{16}O^{18}$	5041.7	4909.4 *4904.8*	4797.5

To assist in the identification of possible isotope bands, calculations have been made of the wave numbers of the 000–201, 000–121, and 000–041 bands of both $C^{13}O_2^{16}$ and $C^{12}O^{16}O^{18}$, in accordance with the theory of Adel and Dennison.[6] The molecular constants derived by Adel and Dennison for ordinary CO_2 were modified for the isotope molecules according to a first approximation suggested by Dennison.[7] The results of the calculation are given in arabic figures in Table I. As a check on the method of computation, the wave numbers of the ω_0, ω_1, and ω_2 bands were also calculated and found to agree perfectly with the original results of Adel and Dennison. Band positions measured at Lake Angelus are also given in Table I in italics.

The 000−121 and 000−041 bands of $C^{13}O_2^{16}$ appear to be definitely present in the infra-red solar spectrum. The center of the 000−121 band falls at the high frequency end of the positive branch of ω_2. The positive branch of the isotope band, however, occurs in a clear region of the spectrum, and 16 members of this branch have been identified. In addition, 7 members of the negative branch have been located in the spaces between the components of the positive branch of ω_2. The 000−041 band of $C^{13}O_2^{16}$ is very weak and appears only on low sun tracings, which is to be expected in view of the relative weakness of ω_2. Thirteen members of the positive branch of the 000−041 band have been detected, together with 11 members of the negative branch. The band spacings in both isotope bands are nearly identical with those in the corresponding bands ω_1 and ω_2.

At least one band of $C^{12}O^{16}O^{18}$ corresponding to the transition 000−121 has also been discovered. Twenty-one members of the positive branch and 12 of the negative branch can easily be distinguished, although the lines of the negative branch are superimposed on those of the positive branch of the 000−121 band of $C^{13}O_2^{16}$. As predicted by theory, the spacing of the $C^{12}O^{16}O^{18}$ band is approximately half that of the corresponding band of $C^{13}O_2^{16}$. The 000−201 and 000−041 bands of $C^{12}O^{16}O^{18}$ as well as the 000−201 band of $C^{12}O_2^{18}$ appear to fall in regions of strong absorption by ordinary CO_2, and although these bands have not yet been detected with certainty,

it is expected that further analysis will reveal at least a few of the lines.

In view of the difficulties that arise in the comparison of the intensities of very strong and very weak absorption lines, it is not possible at the present time to derive cacurate isotope abundances from the line intensities. It may be said, however, that the relative intensities of the $C^{12}O_2^{16}$ and $C^{12}O^{16}O^{18}$ lines are consistent with the generally accepted values for the abundances of C^{13} and O^{18}. The full details of this investigation will appear in the near future in the Astrophysical Journal.

In conclusion, we should like to express our appreciation to Professor D. M. Dennison of the University of Michigan and Dr. W. S. Benedict of the National Bureau of Standards for helpful advice, particularly in connection with the calculation of the CO_2 energy levels.

[1] L. Goldberg, O. C. Mohler, and R. R. McMath, Phys. Rev. 73, 1203 (1948); 74, 352 (1948); 74, 623 (1948); Astrophys. J., in press.
[2] The quantum number l is equal to zero for all of these levels and hence for simplicity has been omitted.
[3] J. M. Cork, *Radioactivity and Nuclear Physics* (D. van Nostrand and Company, Inc., New York, 1947), p. 273.
[4] A. H. Nielson, Phys. Rev. 53, 983 (1938).
[5] R. R. McMath and O. C. Mohler, Pub. A.S.P. 60, 119 (1948).
[6] Cf. D. M. Dennison, Rev. Mod. Phys. 12, 175 (1940).
[7] D. M. Dennison, private communication.

On the Formation of Shielded Isobars by the Nuclear Photo-Effect

J. S. SMART
*Department of Physics, University of Minnesota, Minneapolis, Minnesota**
November 3, 1948

THE most promising recent attack on the problem of the formation of the elements is the neutron capture theory of Gamow and Alpher.[1-3] However, one of the major objections to the theory is that it does not predict the existence of isobars. If the nuclei are all formed with an excess of neutrons, the only nuclear species of mass A that can be formed is the one with the lowest Z necessary for stability. Most sets of isobars are of the form X_z^A and Y_z^A+2. It is the second or "shielded" isobar which cannot be reached by β-decay.

We suggest that the shielded isobars were formed as a result of photo-emission of neutrons. Alpher[3] has pointed out that, during the early stages of universal expansion, the radiation density was several orders of magnitude greater than the matter density. Under such conditions the (γ,n) reaction could compete favorably with other nuclear reactions despite its small cross section.

We have examined 55 sets of even-even isobars; of these the shielded isobar could have been formed by a (γ,n) reaction with a stable odd nucleus in 41 cases. In the other 14 cases it could have been formed by two consecutive (γ,n) reactions. There is some qualitative support to this idea. Let N_F be the abundance of a shielded element and N_I be the abundance of the initial nucleus in the (γ,n) reaction. Then (N_I+N_F) is the original abundance of the initial nucleus, and $N_F/(N_I+N_F)$ is the fraction that has been converted into a shielded isobar. We have computed this fraction for the 41 shielded elements mentioned above. Its average value is roughly 40 times larger for the cases where the initial nucleus has an odd number of neutrons than for the cases where the initial nucleus has an even number of neutrons. This is to be expected because the binding energy of the last neutron is smaller when the neutron number is odd and there would be more photons with enough energy to eject an odd neutron. It is also of some significance that the photo-effect mechanism would not produce any shielded elements which do not exist.

To test this idea quantitatively, we shall try to estimate the (γ,n) reaction probability. To give the proper number of shielded isobars its probability should be of the same order of magnitude but somewhat less than the capture and β-decay probabilities. The number of photons per unit volume with energy sufficient to eject a neutron is given by

$$N_0=\frac{8\pi}{c^3}\int_{B_n/h}^{\infty}\frac{\nu^2 d\nu}{e^{h\nu/kT}-1}\cong 8\pi\left(\frac{kT}{hc}\right)^3 x_0^2 e^{-x_0}$$

where $x_0=B_n/kT\gg 1$ and B_n is the binding energy of the last neutron. As a rough average value for the (γ,n) cross section we have used 10^{-5} B_n barn with B_n given in Mev.[4] We have thus ignored the frequency variation of the cross section, but this is unimportant for an approximate calculation since by far the most critical energy dependence of the probability comes from the exponential term in N_0. The capture probability values used for comparison were taken from a paper by the author which will be submitted for publication in the near future. We find that the (γ,n) probability would have the correct order of magnitude at a temperature $kT=0.1$ Mev. Alpher[3] has pointed out that the formation process must have occurred at temperatures ranging between 10^8 and 10^9 electron volts, so that the result we have obtained is quite consistent with the requirements of the neutron capture theory.

Work on this problem was completed at the Naval Ordnance Laboratory. The author is greatly indebted to Professor C. L. Critchfield for helpful discussions and advice, and to Dr. R. A. Alpher for the privilege of seeing some of his results before publication. The relative abundance data used in making calculations was furnished by Dr. Harrison Brown.

* Now at Naval Ordnance Laboratory, White Oak, Silver Spring, Maryland.
[1] G. Gamow, Phys. Rev. 70, 572 (1946).
[2] R. A. Alpher, H. Bethe, and G. Gamow, Phys. Rev. 73, 803 (1948).
[3] R. A. Alpher, private communication.
[4] V. Weisskopf, *Lecture Series in Nuclear Physics* (Government Printing Office, Washington, D. C., 1947), p. 112.

High Velocity Particles Produced at Impact

J. HOWARD MCMILLEN AND R. L. KRAMER
Naval Ordnance Laboratory, White Oak, Maryland
November 1, 1948

IN the course of an investigation[1-3] of the impact produced when steel spheres impinge on water, spark shadowgrams were made showing the spheres just after they had struck a grid of copper wires. These shadowgrams show that the impact between the sphere and copper

produces a burst of small copper fragments of unusually high velocity. While their direction was mainly forward, many had components of velocity which were opposite to that of the sphere. The particles appeared to originate "explosively" from the point of impact. The steel sphere velocity was 7000 ft./sec. The spheres were $\frac{1}{8}$ inch and the copper wires were 0.005 inch in diameter.

An estimate of the fragment velocities was made by measuring the path lengths and comparing them with the distance traveled by the intact sphere after impact. It was found that the velocities ranged up to 20,000 ft./sec. (Mach Number 18) in the forward direction. Velocity components in the opposite direction as high as 5000 ft./sec. were observed. Interest in this threefold increase in velocity is aroused because the mechanism by which it is attained is not understood. It is clear that it cannot be explained by a simple momentum exchange between elastic bodies.

The fragment tracks resemble a record expected of a column of heated air. At these high velocities, the shock-wave half-angle would be only about 2 degrees. Optical effects due to the sharpness of the shock-wave cone angle confuse the shadowgram record of the shock-wave. The fragments were too small to be measured on the spark shadowgrams.

This investigation was supported by the Office of Naval Research.

[1] J. H. McMillen and R. L. Kramer, Phys. Rev. **73**, 1255 (1948).
[2] J. H. McMillen and E. N. Harvey, J. App. Phys. **17**, 541 (1946).
[3] J. H. McMillen, Phys. Rev. **68**, 198 (1945).

Erratum: "A Solid State Interpretation of the Structure Near the Limit of the Continuous X-Ray Spectrum"

[Phys. Rev. **72**, 276 (1947)]

JESSE W. M. DUMOND
Norman Bridge Laboratory of Physics, California Institute of Technology, Pasadena, California

THE author is indebted to Dr. B. R. A. Nijboer and Dr. R. van Wageningen for pointing out a serious error in the above paper in the computation of the quantity ΔV, the measure of the blurring of the isochromats coming from cathode-ray retardation in the target material. (See page 278 of that article for the definition of ΔV.)

The author computed these retardations from the formula of E. J. Williams,[1]

$$dV/dx = 1.06 \times 10^9 \rho \beta^{-1.4},$$

in which dV/dx is the energy lost by a fast electron in *electron kilovolts* per centimeter of path, ρ is the density of the material, and $\beta = v/c$ is the speed of the fast electrons relative to the speed of light. A confusion between kilovolts and volts led to an error of 10^{-3} in computing the values of ΔV which are too small as computed in the paper by that factor. This completely invalidates the conclusion that absorption of the emerging x-rays in the target material is the factor which causes the more accentuated appearance of the Ohlin valleys and reversals of slope in the low voltage isochromats than in the high voltage ones.

The author now sees no alternate explanation to the one proposed by B. R. A. Nijboer[2] to explain the existence of these reversals of slope. This calls into play the banded electron energy level structure of the target material in a dual role, once in its effect on the x-ray transitions near the quantum limit, permitting, with higher probability, transitions in which the final energy state of the cathode, ray electron after the transition has certain preferred values and once again in its effect on the retardation of the fast cathode-ray electrons entering the target imposing also a banded structure on the energy losses sustained by such electrons before the transition occurs and the x-ray quantum is emitted.

The greater prominence of the Ohlin structures on low voltage isochromats than on high may simply be due to the fact that x-ray crystal monochromators have a resolution defined by a nearly constant $\Delta\lambda$. On an *energy scale* in electron volts, therefore, the uncertainty ΔV corresponding to $\Delta\lambda$ becomes much smaller at long wave-lengths or low voltages. The scale of the detail in the Ohlin structures is, however, apparently the same in electron volts measured from the short wave-length limit in high voltage isochromats as in low, a result which is to be expected if it is explained by Nijboer's theory.

[1] E. J. Williams, Proc. Roy. Soc. (London) **A130**, 310 (1931). It should be pointed out that Williams' formula (18), page 326 of the above reference, is incorrectly stated as regards the units in which it is expressed, apparently because of a confusion of milligrams with grams. This same error is also present where this formula is given in Compton and Allison's text, *X-Rays in Theory and Experiment*, page 76. The error which forms the subject of the present letter is not, however, ascribable to these earlier mistakes.
[2] B. R. A. Nijboer, Physica **12**, 461 (1946).

Nuclear Reactor at Brookhaven National Laboratory

L. B. BORST, M. FOX, D. H. GURINSKY, I. KAPLAN, R. W. POWELL, C. WILLIAMS, AND W. E. WINSCHE
Brookhaven National Laboratory, Upton, Long Island, New York

THE Brookhaven nuclear reactor has been designed to provide a unique facility to serve the research needs of the scientific, engineering, and industrial institutions located in the northeastern part of the United States. One of the major design considerations has been the desire that the reactor should be able to support an extensive research program, with emphasis on reliable, safe, and continuous operation.

The construction of the reactor and auxiliary laboratories is nearing completion and initial operation is expected early in 1949. In order to facilitate the planning of research by scientists and institutions interested in taking part in the activities of The Brookhaven National Laboratory, as description of the reactor and its experimental facilities is given.

The reactor is an air-cooled unit constructed of graphite and unenriched uranium metal. The maximum thermal neutron flux is expected to be about 5×10^{12} neutrons per square centimeter per second. The shield is perforated by

one 12-inch square hole for large size experimental equipment and by a number of 4-inch square holes, extending through the reactor and both shields, which permit the insertion of small experimental equipment into the body of the reactor, or are capable of releasing collimated neutron beams. The top shield of the reactor consists of removable 4-foot square blocks to accommodate thermal columns and large equipment designed to utilize the leakage thermal neutron flux (in excess of 10^{11} neutrons per square centimeter per second). The over-all dimension of the reactor including the shield in the direction of the experimental holes is approximately 38 feet. It will be possible to conduct research on three vertical faces, and on the top and bottom of the reactor.

A laboratory building specially designed for handling radioactive materials is directly connected to the reactor building proper, for research in physics, chemistry, engineering, biology, and medicine.

Construction has been started on a "hot" laboratory for work on sources of intense radiation in a building adjacent to the reactor building and connected to it by a mono-rail and by pneumatic tubes for transporting irradiated material. Within the "hot" laboratory will be three distinct types of facilities: (1) "hot-cells" for processing samples up to 50 curies of 2-Mev γ-activity by remotely controlled apparatus; (2) "semi-hot cells" for work with samples of 1 millicurie to 1 curie of 2-Mev γ-rays using semi-remote control techniques including tongs and special manipulators; and (3) "semi-works" area in which large apparatus can be erected with appropriate portable shielding. The "hot" laboratory building also includes analytical laboratories, shops, store rooms for hot and cold material, personnel locker space, offices, etc. Completion of this laboratory will be delayed until after the completion of the reactor.

Every assistance will be given to scientists desiring to use the facilities of the reactor "hot" laboratory.

Erratum: Interferometric Studies of Faster-than-Sound Phenomena. Part I. The Gas Flow around Various Objects in a Free, Homogeneous, Supersonic Air Stream

[Phys. Rev. 73, 1359 (1948)]

R. LADENBURG, J. WINCKLER AND C. C. VAN VOORHIS
Palmer Physical Laboratory, Princeton University, Princeton, New Jersey

MR. A. W. HAWKINS (E. I. duPont de Nemours and Company) has drawn our attention to the fact that Eq. (1) of our article (p. 1360),

$$\frac{A}{A_1}=\frac{1}{M}\left(1+\frac{\gamma-\frac{1}{2}}{2}M^2\right)^{\frac{1}{2}(\gamma+1)/(\gamma-1)},$$

has to be replaced by the following equation:

$$\frac{A_1}{A}=\frac{1}{M}\left[\frac{2}{\gamma+1}\left(1+\frac{\gamma-1}{2}M^2\right)\right]^{\frac{1}{2}(\gamma+1)/(\gamma-1)}.$$

The Magnetic Moments of the Neutron and Proton

KENNETH M. CASE*
Harvard University, Cambridge, Massachusetts
October 27, 1948

IN the light of the recent advances made in quantum electrodynamics it seems worth while to consider whether similar techniques applied to meson theories will yield sensible results. The basic idea is that mass and charge renormalization terms arising from the meson interactions are explicitly recognized and lumped with the originally assumed mass and charge. In the present theory these terms are infinite. However, it is hoped that in a future correct theory these terms will be but small additions to the original ones. The assumption is made that the remaining, finite, predictions of the present theory will be essentially unaltered in the correct treatment, as yet unknown. The justification of this philosophy is perhaps more tenuous for the meson case with its strong interaction than for the much more weakly coupled electromagnetic field.

Using this recognition procedure the magnetic moments of the neutron and proton were calculated in both the charged and symmetrical pseudoscalar theories using the pseudovector coupling. The proton-neutron field was treated completely relativistically. The results expressed in nuclear magnetons were: *charged theory*,

$$\mu_p=1+\frac{1}{4\pi}(g^2/4\pi\hbar C)\frac{C_1(\mu/M)}{(\mu/M)^2},$$

$$\mu_n=-\frac{1}{4\pi}(g^2/4\pi\hbar C)\frac{[C_1(\mu/M)+C_2(\mu/M)]}{(\mu/M)^2},$$

symmetrical theory,

$$\mu_p=1+\frac{1}{4\pi}(g^2/4\pi\hbar C)\frac{[C_1(\mu/M)+\frac{1}{2}C_2(\mu/M)]}{(\mu/M)^2}$$

$$\mu_n=-\frac{1}{4\pi}(g^2/4\pi\hbar C)\frac{[C_1(\mu/M)+C_2(\mu/M)]}{(\mu/M)^2},$$

where g is the coupling constant with the dimensions of charge, μ=meson mass, and M=nucleon mass. C_1 and C_2 are slowly varying functions of the mass ratio. For U/M between zero and 0.3 these functions may change by something like 10 percent. For $\mu/M=0.1$ the numerical values are $C_1=0.55$ and $C_2=1.00$.

The first interesting point to be noted is that these quantities are finite. That is, after appropriate mass and charge renormalization no further cut-off is needed to insure convergence of the integrals for the magnetic moments. Expressed as integrals over momentum the integrals behave asymptotically as $1/P^3$. Practically all of the contribution comes from below $P=MC$ which is, therefore, the effective cut-off. While a non-relativistic theory would lead one to believe that such a cut-off would yield much too large values for the magnetic moments, this turns out to be false. The non-relativistic effects which one calculates are largely cancelled by the vacuum polarization phenomena which are contained only in the relativistic treatment.

Fitting the neutron moment to the experimental value yields values of $(g^2/4\pi\hbar C)$ between 0.2 and 0.3—in reasonable agreement with other determinations.

The interesting quantity

$$R=\frac{\mu_p-1+\mu_n}{\mu_p-1-\mu_n}$$

is independent of the coupling constant. For $\mu/M=0.1$ we find *charged theory*, $R=-0.50$; *symmetrical theory*, $R=-0.20$; *experimentally*, $R=-0.03$.

Thus R turns out to be considerably too large with the given mass ratio. However, while C_1 and C_2 are but slightly dependent on μ/M the ratio R is probablysome what more sensitive to the mass ratio. By changing this ratio somewhat and considering mesons of other spins and other coupling it is at least possible that agreement with experiment may be achieved.

The most important result would seem to be that the techniques which have succeeded so well in electrodynamics will be equally successful in obtaining sensible answers from meson theories.

In conclusion I would like to express my gratitude to Professor J. Schwinger for suggesting the problem and for many helpful discussions.

I am also indebted to the National Research Council for a Predoctoral Fellowship.

* Now at The Institute for Advanced Study, Princeton, New Jersey

The Magnetic Moment of Boron[11]

JOHN R. ZIMMERMAN* AND DUDLEY WILLIAMS
Mendenhall Laboratory of Physics, Ohio State University, Columbus, Ohio
October 28, 1948

SINCE our original report on the use of super-regenerative oscillators for the determination of nuclear gyromagnetic ratios,[1] several improvements have been made in the oscillator circuits and in detection methods. Since these improvements have been made, the sensitivity of our method has become comparable with the bridge methods of Purcell and Pound[2] and the nuclear induction method of Bloch.[3] We have now observed nuclear magnetic resonances for H^1, H^2, Li^7, B^{11}, F^{19}, Na^{23}, P^{31}, Cu^{63}, Cu^{65}, Br^{79}, Br^{81}, and I^{127}. Inasmuch as the gyromagnetic ratio of B^{11} has not yet been measured by the recently developed methods applicable to solids and liquids, it seems desirable to make a preliminary report on the subject at this time, especially since the results obtained to date are at slight variance with the earlier results obtained by molecular beam methods.[4]

The results reported in this note are based on a comparison of the gyromagnetic ratio of B^{11} with that of Na^{23}. Taking the magnetic moment of Na^{23} as 2.217 ± 0.002 nuclear magnetons and its spin[5] as $\frac{3}{2}$, we obtain a value of 1.800 ± 0.005 for the gyromagnetic ratio g of B^{11}. In arriving at this value for g we have made a slight correction for diamagnetism of the electrons[6] in boron and have assumed a positive moment for B^{11}. Assuming a spin[7] $I=\frac{3}{2}$ for B^{11}, we obtain a value of 2.700 ± 0.008 nuclear magnetons for the nuclear moment of B^{11}.

The gyromagnetic ratio obtained in the present work is slightly higher than the value $g=1.788\pm0.005$ obtained in molecular beam experiments.[4] Before much significance can be attached to the slight difference in the results obtained by the two methods, we feel that further work should be done. The results reported here were obtained with an aqueous solution of $Na_2B_2O_4$, for which material the Na^{23} and B^{11} resonances were both observed. We plan to make additional measurements of the B^{11} resonance in other compounds. The accuracy of measurements of gyromagnetic ratios by super-regenerative methods can be increased by a factor of 10 by making certain obvious variations in our present arrangement. We are making these changes and plan to make a more detailed report on the work in the near future.

We should like to express our appreciation to Professor E. M. Purcell for helpful discussions during the early stages of our work and to the Graduate School and University Development Fund of the Ohio State University for grants of funds used in the purchase of equipment.

* Charles A. Coffin Fellow.
[1] J. R. Zimmerman and D. Williams, Phys. Rev. 73, 94 (1948).
[2] E. M. Purcell, H. C. Torrey, and R. V. Pound, Phys. Rev. 69, 37 (1946).
[3] F. Bloch, W. W. Hansen, and M. Packard, Phys. Rev. 69, 127 (1946).
[4] S. Millman, P. Kusch, and I. I. Rabi, Phys. Rev. 56, 165 (1939).
[5] J. M. B. Kellogg and S. Millman, Rev. Mod. Phys. 18, 323 (1946).
[6] W. E. Lamb, Phys. Rev. 60, 817 (1941).
[7] S. Millman, P. Kusch, and I. I. Rabi, Phys. Rev. 56, 303 (1939).

On the Ground State of the Deuteron

FRANCIS LOW
Department of Physics, Columbia University, New York, New York
November 8, 1948

A CONVENIENT formula for the estimation of the depth-range relation of various potentials in the theory of the deuteron is

$$-\int_0^b V(r)rdr\geqq\hbar^2/M, \tag{1}$$

where b is the range of the neutron-proton force, $V(r)$ is the potential energy, and M the proton or neutron mass. Furthermore, $\hbar^2/M$ is a lower bound to the integral.

It may be of interest to note that (1) can be replaced by the exact equation

$$-\int_0^\infty V(r)u(r)\sinh\alpha r=\alpha\hbar^2/M, \tag{2}$$

where α is the reciprocal deuteron radius, $\alpha=(-ME/\hbar^2)^{\frac{1}{2}}$, and $u=\psi/r$, ψ being the wave function for the ground state of the deuteron, so normalized that

$$\lim_{r\to\infty}\frac{u(r)}{e^{-\alpha r}}=1.$$

Since (2) may be rewritten

$$-\int_0^\infty V(r)\frac{u(r)}{e^{-\alpha r}}\frac{(1-e^{-2\alpha r})}{2\alpha}=\frac{\hbar^2}{M},$$

and since $u(r)/e^{-\alpha r}\leq1$ and $(1-e^{-2\alpha r})/2\alpha\leq r$, it is obvious that $\hbar^2/M\leq-\int_0^\infty V(r)rdr\geqq-\int_0^b V(r)rdr$ and hence that (2) implies (1), provided $2\alpha b\ll1$ and $u(r)/e^{-\alpha r}\geqq1$ over most of the range $0\leq r\leq b$.

The following proof of (2) is the work of Dr. Conrad Longmire.

We note that $w=\sinh\alpha r$ satisfies the equation

$$d^2w/dr^2-\alpha^2w=0, \tag{3}$$

and that the wave equation for the ground state is

$$d^2u/dr^2-\alpha^2u=(M/\hbar^2)Vu. \tag{4}$$

Multiplying (3) by u and (4) by w, subtracting, integrating by parts from 0 to R, we have

$$w(r)\frac{du(r)}{dr}\Big|_0^R-u(r)\frac{dw(r)}{dr}\Big|_0^R=\frac{M}{\hbar^2}\int_0^R V(r)u(r)w(r)dr.$$

The lower limit does not contribute since $u(0)=w(0)=0$; the upper limit gives, for R sufficiently large,

$$-\alpha\sinh\alpha Re^{-\alpha R}-\alpha\cosh\alpha Re^{-\alpha R}=-\alpha.$$

Hence $-\alpha\geqq(M/\hbar^2)\int_0^R Vuwdr$, the equality holding exactly in the limit $R\to\infty$.

On the Half-Life of Rb^{87}

O. Haxel, F. G. Houtermans, and M. Kemmerich*
Max Planck Institut and II. Physikalisches Institut der Universität Göttingen, Germany
October 28, 1948

SEVERAL authors[1] have determined the half-life of Rb^{87} by measuring the rate of β-particle emission per mg RbCl. Their results vary between $T=4.5\cdot10^{10}$ yr. (Orban) and $12\cdot10^{10}$ yr. (Mühlhoff), the latter being the only value among the older papers obtained by modern counting technique. Hahn *et al.*[2] have calculated T by measuring the Sr/Rb ratio in a lepidolite of $2\cdot10^9$ yr. age, known from radioactive measurements of minerals from the same geological origin using the α-decay of U. Mattauch[2] had found by isotope analysis that the Sr contained in the lepidolite was exclusively of radioactive origin. They found $T=6.4\cdot10^{10}$ yr. The discrepancy between Mühlhoff's result and the value obtained by the geological method seemed rather embarrassing, not only because of the importance of T for the Rb/Sr-method of measuring geological ages, but also because it seemed to indicate a discrepancy between the time scale of α- and β-decay in a sense postulated by a cosmological theory of Jordan,[3] involving a variation of the rate of β-decay and other fundamental constants with the age of the universe.

We therefore measured very thin layers of RbCl produced by evaporation on a silver coated Zapon foil of about 0.1 mg/cm², suspended freely between a counter arrangement which allowed the measure of particles from both sides of the foil simultaneously, as well as the number of coincidences between counts on both sides.

With decreasing thickness of the RbCl layer from 2.0 to 0.05 mg RbCl/cm², the number of electrons per mg RbCl min. increases regularly for the back side of the foil, while the front side shows a considerably higher increase, the extrapolated activity for zero thickness being 13.6 and 19.6 counts/min. mg RbCl for the back and front side, respectively. This indicates a high percentage of very soft electrons from Rb, which are stopped by the supporting Zapon foil. Coincidence measurements (resolving time $3\cdot10^{-5}$ sec.) gave the surprising result that a considerable number of Rb counts on both sides coincided, up to 30 percent of the front side number for zero thickness, thus proving that more than one particle is emitted per decay process. All our results can be understood quantitatively with the assumption that for every decay of Rb^{87} one soft electron of energy up to 10 kev is emitted as well as one faster electron with the known energy limit of 135 kev. Since the electron spectrum[4] for Rb is not known well enough, it is not possible to identify either group as the decay electrons, while the other should be ascribed to a group of internal conversion electrons of 100 percent conversion rate. The presence of discrete lines shown by Ollano,[4] the difficulty of explaining a conversion electron of so low an energy emitted within $3\cdot10^{-5}$ sec., and a better fitting of Rb^{87} into a Sargent diagram by assuming a very low β-energy limit, seem even to favor the assumption that the slow electrons are the decay electrons.

By the independence of the coincidences from the argon pressure in the counters, we could prove that they were not due to back scattering from the gas. The efficiency of the counters was tested to be 100 percent by coincidence experiments, and the solid angle extended by the counters to be 2π within an error limit of 5 percent by using them as proportional counters and testing them with α-rays from a uranium deposit. Whatever the nature of the coincidences, the number of decays under the above assumptions is given by the sum of the kicks on both sides minus the number of coincidences. We thus found $n=27.2$ decays/mg RbCl min., and $T=(6.5\pm0.6)\cdot10^{10}$ yr.

The experiments with freely suspended Zapon foils, however, involve a comparatively large error in measuring the exact amount of Rb deposited. To check our results in another series of experiments, areas of 60 cm² were covered with RbCl by evaporation on Al foils and placed on the inside wall of a G-M counter of known efficiency. The weight of RbCl could be measured to about 3 percent, and the number of electrons leaving the front face of the layer could be followed down to a layer thickness of 0.025 mg/cm² RbCl. This brought after slight corrections for back-scattering and the influence of counter ends, a further increase to 23 electrons/min. mg RbCl and $n=30.7$ decays/min. mg RbCl, with $T=(5.8\pm0.5)\cdot10^{10}$ yr. As a weighed average of both series of experiments we consider $6.0\pm0.6\cdot10^{10}$ as a result of our measurements, in fair agreement within error limits with the geological value.

While our work was still in progress, a paper by Eklund[5] came to our knowledge. He measured T with a counter calibrated by mixed α- and β-particles from a uranium deposit. Eklund also found the beginning of the increase of the number of particles for thin layers down to 0.1 mg RbCl/cm², but he did not discern particles coinciding with those emitted to the back side. He found $T=5.8\cdot10^{10}$ yr., in excellent agreement with our value, but this seems to be due to the fact that by using insufficiently thin layers and neglecting coincidences, two considerable error sources compensated each other to a high extent.

The agreement of the present rate of decay of Rb^{87} with the average rate for the last $2 \cdot 10^9$ years within the mutual error limits leaves no reason to doubt the agreement of age determinations from α- and β-decay of Rb^{87} and UI. A further narrowing of both errors seems nevertheless desirable because of the principal importance of this question. A full account of our experiments will be published shortly.[7]

* The first part of this paper was read at the meeting on Sept. 5th, 1947, at Göttingen and the second part on Sept. 9th, 1948, at Clausthal, of the Deutsche Physikalische Gesellschaft für die britische Zone.

[1] O. Hahn and M. Rothenbach, Physik. Zeits. 20, 194 (1919). W. Mühlhoff, Ann. d. Physik 7, 205 (1930). G. Orban, Sitzungsber. Akad. Wien IIa 140, 121 (1931).
[2] O. Hahn, J. Mattauch, F. Strassmann, and E. Walling, Naturwiss. 25, 189 (1937). F. Strassmann and E. Walling, Ber. d.d. chem. Ges. 71, 1 (1938).
[3] P. Jordan, Physik. Zeits. 45, 183 (1945); P. Jordan and F. G. Houtermans, Zeits. f. Natur. 1, 125 (1946).
[4] Z. Ollano, Nuovo Cimento 18, 11 (1941). W. F. Libby and D. D. Lee, Phys. Rev. 55, 245 (1939).
[5] S. Eklund, Ark. f. Mat. Astr. Physik. 33a, 60 (1946).
[6] O. Haxel and F. G. Houtermans, Zeits. f. Physik 124, 705 (1948). M. Kemmerich, Zeits. f. Physik (in press).

Radiative X-Ray Transition within the *L* Shell of Sulfur

D. H. TOMBOULIAN
Department of Physics, Cornell University, Ithaca, New York
November 8, 1948

WHEN the L levels of an atom in the crystal lattice are ionized by electron impact, transitions of electrons from the conduction band into the vacant x-ray level give rise to emission bands characteristic of the solid. Though such transitions into the L_{II} and L_{III} levels are observed in the case of the light elements,[1,2] emission spectra corresponding to valence electron transitions into the L_I level have not been detected. The absence of the L_I emission band may be ascribed to other competing processes such as radiative transitions $L_I \rightarrow L_{III}$ within the shell and radiationless transitions $L_I \rightarrow L_{III}$ with a transfer of energy to a valence electron.

In a previous paper[3] the $L_I \rightarrow L_{III,II}$ radiative transitions were tentatively identified in the case of Na, Mg, and Al with the aid of the screening doublet law. Since the wave-length predictions were based on an extrapolation, the proposed assignments were regarded as provisional. Recently, in connection with further studies of L-emission spectra, a relatively narrow line appeared on several spectrograms when sulfur was present on the target. The width of the line is 1.5 ev at half-maximum. The peak of this isolated line occurs at 203A. This is in excellent agreement with the previous prediction[3] of the wave-length of the $L_I \rightarrow L_{II,III}$ radiative transition of sulfur. With this additional identification it may be concluded that the absence of the L_I emission band is in part due to a radiative process within the L shell of the light elements. The peak wave-lengths of the $L_I \rightarrow L_{III,II}$ transitions observed to date lie at 375, 317, 290, and 203 angstroms for Na, Mg, Al, and S, respectively. Radiationless transitions $L_I \rightarrow L_{III}$ which are energetically possible must play a prominent role in further weakening of the soft x-ray emission bands involving L_I as the initial state.

The author wishes to thank Professor L. G. Parratt for interesting discussions and Mr. E. Pell for technical assistance. The work was carried out under Contract N6 ori-91 with the Office of Naval Research.

[1] H. W. B. Skinner, Phil. Trans. Roy. Soc. London 239, 95 (1940).
[2] W. M. Cady and D. H. Tomboulian, Phys. Rev. 59, 381 (1941).
[3] D. H. Tomboulian and W. M. Cady, Phys. Rev. 59, 422 (1941).

On the Reflection-Transmission Effect in Experiments on Polarization of Electrons

L. J. F. BROER*
Zeeman Laboratory, University of Amsterdam, Holland
November 8, 1948

IT is contended by Shull, Chase, and Myers[1] that the difference between their measurements on the polarization of electron beams and the earlier attempts[2] to find this effect can be attributed to the so-called reflection-transmission effect of Chase and Cox.[3] We have made a more detailed examination of the connection between these two effects, the results of which we will communicate here.

When an electron beam is scattered over an angle θ, the intensity ratio of both states of polarization normal to the incident and scattered beams is given by[4]

$$\frac{I_+}{I_-}=\frac{1+\epsilon \sin\theta}{1-\epsilon \sin\theta}. \tag{1}$$

When the electrons are scattered twice over a right angle, the ratio of the total intensities of the beams antiparallel and parallel to the incident beam is therefore

$$\eta=\frac{I_a}{I_p}=\frac{(1+\epsilon)^2+(1-\epsilon)^2}{2(1-\epsilon^2)}=\frac{1+\epsilon^2}{1-\epsilon^2}. \tag{2}$$

In the experiments of Shull *et al.* 360-kev electrons were scattered by gold foils. They found $\eta_t=1.11$, $\epsilon=0.23$, in agreement with theory, when the beam passed through both foils (transmission position). When the foils were placed in reflection position, as had been done in the earlier experiments, the intensity ratio was only $\eta_r=1.02$.

The reflection-transmission effect consists in a difference in intensity between the 90° scattering as both sides of a foil orientated at 45° with the incident beam. The intensity ratio between the reflected and transmitted beams will be denoted by α. Now Shull *et al.* suggest that the difference between η_t and η_r can be understood by supposing the excess electrons in the case of reflection to be unpolarized. Under this assumption, which will be discussed later on, a relation between η_r, η_t, and α can be derived. Analogous to (2) we will have

$$\eta_r=\frac{(\alpha+\epsilon)^2+(\alpha-\epsilon)^2}{2(\alpha^2-\epsilon^2)}=\frac{\alpha^2+\epsilon^2}{\alpha^2-\epsilon^2}. \tag{3}$$

The experimental value of ϵ from the transmission experiment is 0.23. For α a value of 1.6 can be deduced from the data given by Shull *et al.* This would give $\eta_r=1.04$ as compared to the experimental value 1.02. As the accuracy of η is stated by the authors to be 2 percent, the calculated and observed values might be reconcilable. But, as the

calculated value $\eta_r=1.04$, based on an experimental value of ϵ in agreement with theory, is not sensitive to changes in α, the negative result of the earlier experimenters,[2] who did essentially find $\eta_r=1.00\pm0.02$ or 0.01, cannot be said to be clearly explained. In fact, if η_r were 1.02 and $\alpha=1.6$, this would entail $\eta_l=1.05$, $\epsilon=0.16$, well outside of the limits of both theoretical and experimental determinations.

In the second place, Shull *et al.* seem to overlook the fact that their hypothesis in which the excess electrons are not polarized is at variance with the mechanism proposed by Goertzel and Cox[5] to account for the reflection-transmission effect. These authors suppose that the excess scattering in the reflection position of the foils is caused by electrons undergoing two deflections of about 45° and traveling in the plane of the foil between these collisions. The same effect in transmission would require at least one deflection of about 135°, which is ruled out by the Rutherford factor $\csc^4\theta/2$. The polarization of the excess electrons can be found by numerical integration over the azimuth angle in the plane of the foil, using (1) and the Rutherford factor. The result is that the polarization ratio due to this double scattering amounts to

$$\frac{I^+}{I^-}=\frac{1+1.24\epsilon+0.42\epsilon^2}{1-1.24\epsilon+0.42\epsilon^2} \tag{4}$$

when no depolarization between the two collisions occurs. From the calculations of Rose and Bethe[6] it can be inferred that in this case the depolarization can be neglected. Using the value $\epsilon=0.23$ one obtains from (4) a polarization ratio 1.77 for the double scattering as compared with 1.60 for single scattering over 90°. (With complete depolarization between the two collisions we would still obtain a ratio of 1.34.) Therefore, the polarization of the scattered beam should be at least as large in reflection as in transmission. The conclusion is that the results of Shull *et al.* seem to disagree with those of Dymond, Thomson, and Richter as well as with the theory of the reflection-transmission effect given by Goertzel and Cox.

* At present: Lyman Laboratory of Physics, Harvard University, Cambridge, Massachusetts.

[1] C. G. Shull, C. T. Chase, and F. E. Myers, Phys. Rev. **63**, 29 (1943).
[2] E. Dymond, Proc. Roy. Soc. **A145**, 657 (1934); G. Thomson, Phil. Mag. **17**, 1058 (1934); E. Richter, Ann. d. Physik. **28**, 533 (1937).
[3] C. T. Chase and R. T. Cox, Phys. Rev. **58**, 243 (1940).
[4] N. Mott, Proc. Roy. Soc. **A135**, 429 (1932).
[5] G. Goertzel and R. T. Cox, Phys. Rev. **63**, 37 (1943).
[6] M. Rose and H. Bethe, Phys. Rev. **55**, 227 (1939).

PHYSICAL REVIEW VOLUME 74, NUMBER 12 DECEMBER 15, 1948

Proceedings of the American Physical Society

Minutes of the Meeting of the Ohio Section at Wilmington on October 30, 1948

THE Ohio Section of the American Physical Society held its scheduled Fall Meeting of the season 1948–1949 at Wilmington College, Wilmington, Ohio. In spite of the distance from the larger centers, there was an attendance of fifty-five. Titles of the papers presented and abstracts of five of them are appended.

LEON E. SMITH
Secretary-Treasurer

Program

An Infra-Red "Lens," ROBERT A. OETJEN, *The Ohio State University.*

Measurement of Nuclear Magnetic Moments by Means of Super-Regenerative Oscillator Circuits, JOHN R. ZIMMERMAN AND DUDLEY WILLIAMS, *The Ohio State University.*

Microwave Spectra of the Linear Molecules OCS, ClCN, and BrCN, JOHN D. ROGERS AND DUDLEY WILLIAMS, *The Ohio State University.*

Microwave Absorption by Paramagnetic Salts, YU TING, ROY C. WEIDLER, AND DUDLEY WILLIAMS, *The Ohio State University.*

Electronic Method of Measuring X-Ray Intensities, NATHAN SPIELBERG, *The Ohio State University.*

The Quartz Research Program at Antioch College, A C. SWINNERTON, *Antioch College.*

The Measurement of the Electrical Conductivity of Water Solutions Near the Critical Temperature, VERNON MATHIS, *Antioch College.*

The Growth of Quartz Crystals in Sodium Chloride Solutions, THOM MCMANUS, *Antioch College.*

A Theory of Quartz Crystal Growth, JAMES F. CORWIN, *Antioch College.*

Acoustical Birefringence, WILLIAM J. PRICE, *Battelle Memorial Institute.*

Invited Paper

Some Phenomena of Transonic and Supersonic Aerodynamics. BERNARD H. GOETHERT, *Air Materiel Command, Wright-Patterson Air Force Base.*

Contributed Papers

An Infra-Red "Lens."* ROBERT A. OETJEN, *The Ohio State University.*—An arrangement of mirrors is described whereby a diverging beam of radiation may be changed to a converging beam. Since there is no absorbing glass in the path of the radiation, it may be used for radiation of all wave-lengths including the infra-red. Both the object and image are on the axis of the system, hence extra-axial abberations are kept to a minimum. The components of the system include two concave mirrors and a double-sided flat with a hole in the center.

* The work described in this paper was carried out, in part, under contract between the Air Materiel Command, Wright-Patterson Air Force Base, and the Ohio State University Research Foundation.

Measurement of Nuclear Magnetic Moments by Means of Super-Regenerative Oscillator Circuits.* JOHN R. ZIMMERMAN** AND DUDLEY WILLIAMS, *Ohio State University.*—The super-regenerative oscillator circuit described in earlier reports has been modified with a resulting increase in sensitivity. Nuclear resonances for H^1, H^2, F^{19}, Li^7, Na^{23}, Br^{79}, Br^{81}, and I^{127} have now been observed. Magnetic fields were measured by means of a fluxmeter calibrated in terms of the field at which the proton resonance at known frequencies was observed. Resulting measurements of magnetic fields were accurate to one part in 300, and these measurements at present limit the accuracy with which nuclear magnetic moments can be determined. Plans have been made for mounting two coils containing samples in the same large magnetic field, and no difficulties are anticipated in improving the accuracy of determining nuclear magnetic moments in terms of the proton moment to one part in 10^4. The sensitivity of the present method seems to be comparable with that attained by other methods.

* This work was supported by grants from the Graduate School and the Development Fund of Ohio State University.
** Charles A. Coffin Fellow.

Microwave Spectra of the Linear Molecules OCS, ClCN, and BrCN.* JOHN D. ROGERS AND DUDLEY WILLIAMS, *Ohio State University.*—The microwave absorption spectra of the linear molecules OCS, ClCN, and BrCN have been measured in the region between 19,000 and 27,000 megacycles. Rotational transitions $J=1\rightarrow J=2$ for OCS and ClCN and $J=2\rightarrow J=3$ for BrCN have been observed and moments of inertia have been calculated. Hyperfine structure observed in the spectra of BrCN and ClCN, and measurement of this permits the calculation of nuclear quadrupole interaction terms $eQ(\partial^2 V/\partial Z^2)$; the hyperfine structure for ClCN is best explained by assuming a value of $\frac{3}{2}$ for the chlorine spin. Some of the OCS and BrCN molecules are in the first excited bending vibrational state at room temperature; from the observed spectra the *l*-type doubling constants and the vibration-rotation constants α_2 can be determined for these molecules. The experimental data obtained can be readily interpreted in terms of existing theory, and agreement between the present values for molecular constants and the values obtained in the earlier work of Townes is excellent. The conventional single reflector modulation technique and the new Stark technique described at the Symposium on Molecular Spectra June 1948, were both employed in this study.

* This work was done in connection with a contract between the O.S.U. Research Foundation and Watson Laboratories of the Air Materiel Command.

Microwave Absorption by Paramagnetic Salts.* YU TING, ROY C. WEIDLER,** AND DUDLEY WILLIAMS, *Ohio State University.*—Absorption of microwave radiation of wave-length 3.16 cm by powdered paramagnetic crystals has been observed by methods involving a resonant cavity. The *Q* of the cavity used was of the order of 1500 when the cavity was empty and loaded only by a crystal detector with a small iris opening to the cavity. Samples of the salts in small polystyrene containers were introduced into the cavity which was located in the gap between the pole pieces of an electromagnet. Resonant absorption peaks were noted when the magnetic field was in the neighborhood of 3300 gauss. Absorption by $K_2Cr_2(SO_4)_4\cdot 24H_2O$, $CuSO_4\cdot 5H_2O$, $MnSO_4\cdot H_2O$, $MnSO_4\cdot 4H_2O$, and $MnC_2O_4\cdot 2H_2O$ has been noted. Typical absorption curves will be shown, and the sensitivity obtainable with this method will be compared with that obtainable by the bridge methods used by Whitmer and others.

* This work was done in connection with a contract between the Ohio State University Research Foundation and Watson Laboratories of Air Materiel Command.
** Captain, USAF, assigned to Ohio State University from Air University, Maxwell Field, Alabama.

Acoustical Birefringence. W. J. PRICE, *Rensselaer Polytechnic Institute.**—The pulsed ultrasonic method at 10 Mc/sec. has been used to study acoustical birefringence in single crystals of ammonium dihydrogen phosphate. The acoustic medium was a 45-degree X-cut single crystal in the form of a rectangular parallelepiped with dimensions approximately one inch. An X-cut quartz transducer cemented to a face perpendicular to a 45-degree direction produced two modes, a quasi-compressional mode and a quasi-transverse mode. By means of an X-cut quartz crystal used as a receiver on the opposite surface, it was observed that the quasi-compressional and the quasi-transverse modes traveled in directions lying in the X-plane of the ADP and making angles of 22.5° and 11°, respectively, with the normal to the transducer. A Y-cut quartz transducer polarized in the X-direction of the ADP produced a transverse mode which traveled along the surface normal. Huygen's principle has been applied to predict the direction of the beam and the results are in good agreement with the observations.

* Now at Battelle Memorial Institute, Columbus, Ohio.

Author Index to Volume 74

References with (A) are to abstracts of papers presented at meetings of the American Physical Society, and those with (T) designate title only. References with (L) are to Letters to the Editor.

Adams, G. D. Absorption of high energy quanta: I.—1707
—— **and A. T. Nordsieck.** Absorption of 10–20 mev quanta —1255(T)
Ahrens, L. H. Molecular spectroscopic evidence of the existence of strontium isotopes Sr^{88}, Sr^{87}, and Sr^{86}—74
—— **and Robley D. Evans.** Radioactive decay constants of K^{40} as determined from the accumulation of Ca^{40} in ancient minerals—279
Aiken, Howard. Computing machines—1204(T)
Albert, R. D. and C. S. Wu. Beta-spectrum of S^{35}—847(L)
Alburger, David E. Spectrometer measurement of cyclotron-induced gamma-radiation—1240(A)
—— (see Pollard, Ernest)—926
Aldrich, L. T. (see Fairbank, Henry A.)—345(L)
—— (see McInteer, B. B.)—946
—— **and Alfred O. Nier.** Argon 40 in potassium minerals —876
—— **and Alfred O. Nier.** Occurrence of He^3 in natural sources of helium—1590
—— **and Alfred O. Nier.** Variation of He^3/He^4 abundance ratio in natural sources of helium—1225(A)
Allen, James S. (see Morrish, A. H.)—1260(A)
——, **H. R. Paneth, and A. H. Morrish.** Preliminary results of a He^6 neutrino experiment—1224(A)
Aller, L. H., C. W. Ufford, and J. H. Van Vleck. Forbidden lines in O II—1208(A)
Allison, Samuel K. and Harold V. Argo. Design and performance of a 15-cm electrostatic analyzer—1561(A)
——, **H. V. Argo, W. R. Arnold, L. del Rosario, H. A. Wilcox, and C. N. Yang.** Measurement of short range nuclear recoils from disintegrations of the light elements—1233(A)
Alpher, Ralph A. Neutron-capture theory of the formation and relative abundance of the elements—1577
—— **and Robert Herman.** On the relative abundance of the elements—1737
——, **R. Herman, and G. A. Gamow.** Thermonuclear reactions in the expanding universe—1198(L)
Althaus, E. J. (see Sard, R. D.)—1364
Alvarez, Luis W. Properties of the 4-second neutron emitter of low Z—1217(A)
Anderson, H. L. Nuclear magnetic moments of hydrogen 3 and helium 3—1203(T)
Andrew, Alan and W. W. Carter. Isotopic shift in the helium line spectrum—838(L)
—— **and W. R. Smythe.** Concentration of helium 3—496(L)
Andrews, C. L. Diffraction pattern of electromagnetic waves in the planes of apertures—1231(A)
Andrews, Donald H. Superconducting noise and rectification—1234(A)
Antonoff, George. Effect of length of capillary on capillary rise of polar liquids—1227(A)
—— Structure of liquids from other than X-ray evidence—1254(T)
Apker, L., E. Taft, and J. Dickey. Photoelectric emission and contact potentials of semiconductors—1462
Apte, A. S. (see Majumdar, R. C.)—538
Araki, Gentaro. Divergence difficulty and mixed meson theory—985(L)
—— On the magnetic moment of nucleons according to the pseudovector meson theory—986(L)
—— Theory of elliptically polarized photons—472
Argo, Harold V. Direct determination of the energy of the He^3 nucleus from the D−D reaction—1293
—— (see Allison, Samuel K.)—1233(A), 1561(A)
Arner, W. J. and D. E. Sharp. Discoloration of glass by radium radiations—116(A)
Arnold, W. R. (see Allison, S. K.)—1233(A)
Arroe, O. H. Hyperfine structure of 30 Zn^{67}—1263(A)
Ashkin, J. (see Szilard, L.)—1216(A)
Austern, N. (see Mack, J. E.)—1262(A)
Auld, Mary Jane. Present problems in the use of the electrostatic analyzer—129(A)
—— **and F. T. Rogers, Jr.** "Band width" for energy in the electrostatic analyzer—128(A)
Avery, R. and R. G. Sachs. Further remarks on the magnetic moments of H^3 and He^3—1320
Axel, P. (see Sala, O.)—1249(A)

Babcock, Horace W. Magnetic variable stars as sources of cosmic rays—489(L)
—— Stellar magnetic fields—1555(T)
Baker, Saul (see Wayland, Harold)—1563(A)
Baker, W. O. (see Mason, W. P.)—1873(L)
Balakrishnan, C. (see Knowles, A. J.)—627(L)
——, **J. D. Craggs, and A. A. Jaffe.** Discharge spread in Geiger counters with methane and methane/argon fillings—410
Ballario, C., M. Benini, and G. Calamai. On the positive excess of the meson component at sea level under different zenithal angles—1729(L)
Band, William (see Meyer, Lothar)—394, 1235(A)
—— **and Lothar Meyer.** Effect of relaxation on the theory of second sound in helium II—1235(A)
—— **and Lothar Meyer.** Influence of relaxation on the two velocity field model of helium II—386
Bandel, H. W. and W. N. English. Point-to-plane corona characteristics—1557(A)
Banks, Floyd R., Jr. Effects of chlorine and sulphur on photo-conductivity in silver chloride—1207(A)
Barber, W. C. East-west asymmetry of cosmic rays at 33,000 feet—1556(A)
Barbour, Ian G. On the use of nuclear plates in a magnetic field—507(L)
Bardeen, J. (see Brattain, W. H.)—231(L)
—— **and W. H. Brattain.** Transistor, a semi-conductor triode—230(L)
Barkas, Walter H., Eugene Gardner, and C. M. G. Lattes. Meson mass estimation by grain counting in photographic emulsions—1558(A)

Barlow, J. S. and F. T. Rogers, Jr. On the positive particles occurring from P^{32} in the cloud chamber—700(L)
Barnóthy, J. On the intrinsic moment of the electron—113(L)
—— Specific charge of the positron—844(L)
—— **and M. Forro.** Neutral decay-products of cosmic radiation at great depth—1300
Bashkin, S. and H. T. Richards. Simple all-electronic cloud-chamber control circuit—1260(A)
Bass, Arnold M. and H. Sponer. Fluorescence of fluorobenzene—1247(A)
Bauer, Carl August. Absorption of cosmic radiation in meteorites—225(L)
—— Rate of production of helium in meteorites by cosmic radiation—501(L)
Beams, J. W. (see Dillon, J. F.)—117(A)
—— (see McQueen, J. H.)—1551(L)
—— (see Snoddy, L. B.)—126(A)
Bearden, J. A. (see Schwarz, Guenter)—1209(A)
Beatty, Suzanne Van Dijke. Table of interplanar spacings in Angstrom or K.X. units in terms of 2θ for different target materials—625(L)
Beck, Guido. Contribution to the theory of the Cherenkov effect—795
Beeber, R. J. (see Hubbard, J. C.)—708(L)
Beeman, W. W. (see Hanson, H. P.)—1261(A)
—— (see Kaesberg, Paul)—71, 1255(A)
Begovich, Nicholas. High frequency loading—1563(A)
Belinfante, F. J. First-order variational principle for classical electrodynamics—779
Bell, P. R. and R. C. Davis. Scintillation counting with anthracene—1245(A)
Bell, R. E. (see Elliott, L. G.)—1869(L)
—— **and L. G. Elliott.** Gamma-rays from the reaction $H^1(n, \gamma)D^2$ and the binding energy of the deuteron—1552(L)
Belock, H., E. Bromberg, S. Fifer, U. Manfredi, R. McCoy, and H. Zagor. REAC: Direct current analog computer—1230(A)
Benade, A. H. (see Sard, R. D.)—1237(A)
Bender, R. S., F. C. Shoemaker, S. G. Kaufmann, and G. M. B. Bouricius. Elastic scattering of protons by aluminum in the neighborhood of the 985-kev resonance—1205(A)
Benedict, W. S. New bands in the vibration-rotation spectrum of water vapor—1246(A)
—— (see Mohler, Orren C.)—702(L)
—— (see Nelson, R. C.)—703(L)
Benedikt, Elliot T. On the integral equations of motion—1213(A)
—— On the theory of a new magneto-electric effect—1563(A)
Benfield, A. E. Thermal consequences of the capture of neutrinos by the earth—621(L)——Erratum——1192(L)
Benini, M. (see Ballario, C.)—1729(L)
Bennett, Willard H. Radiofrequency mass spectrometer—1222(A)
Berezin, Evelyn (see Zar, Jacob L.)—111(L)
Berggren, Jane L. and Robert K. Osborne. Beta-ray spectra of C^{14} and S^{35}—1240(A)
Bergman, C. E. and G. H. Fett. Theory and applications of the parallel T resistance-capacitance network—1206(A)
Bergmann, Peter G. Low angle scattering of colloidal solutions—1209(A)
Berlin, T. H. (see Greenberg, J. Mayo)—1243(A)
Bernardini, G., G. Cortini, and A. Manfredini. Nuclear evaporations produced by cosmic rays—845(L)
——, **G. Cortini, and M. Manfredini.** On the absorption of nucleonic component in cosmic rays—1878(L)
Bernstein, S. (see Szilard, L.)—1216 (A)
——, **F. L. Talbott, J. K. Leslie, and C. P. Stanford.** Yield of photo-neutrons from U^{235} fission products in Be—1258(A)
Berry, H. W. Secondary electron emission by fast neutral molecules and neutralization of positive ions—848(L)
Bershader, D. and R. Ladenburg. Interferometric analysis of two-dimensional supersonic flow through small channels—1229(A)
Bever, Renate S., Virgil E. Bottom, and Louis R. Weber. Modes of vibration in contoured quartz plates—1562(A)
Beyer, R. T. (see Davis, W. H.)—1208(A)
—— **and J. A. Krumhansl.** Barkhausen noise in ferromagnetic electrical circuit elements—1206(A)
Bhabha, H. J. and S. K. Chakrabarty. Further calculations on the cascade theory—1352
Bhattacharya, P. C. Experiments on the separation of low energy mesotrons from electrons—38
Bird, R. Byron (see Hirschfelder, Joseph O.)—1265(A)
Birks, J. B. Microwave magnetic dispersion in carbonyl iron powder—843(L)
—— Natural and induced ferromagnetic resonance—988(L)
Birnbaum, George. Recording microwave refractometer—1211(A)
—— (see Lyons, Harold)—1210(A)
Bishop, A. S., John Burfening, Eugene Gardner, and C. M. G. Lattes. Detection of positive meson producted by the 184-in. cyclotron—1558(A)
Bitter, Francis. Nuclear magnetic resonance experiments at the Massachusetts Institute of Technology—1203(T)
Blachman, Nelson M. and Ernest D. Courant. Scattering of particles by the gas in a synchrotron—140
Blair, J. Morris (see Sleator, William, Jr.)—1260(A)
——, **George Freier, Eugene Lampi, William Sleator, Jr., and J. H. Williams.** Angular distribution of 1 to 3.5-Mev deuterons scattered by deuterons—1594
——, **George Freier, Eugene Lampi, William Sleator, Jr., and J. H. Williams.** Angular distribution of the products of the D−D reaction: 1 to 3.5 Mev—1599
——, **George Freier, Eugene E. Lampi, William Sleator, Jr., and John Williams.** Scattering of 2.4- to 3.5-Mev protons by protons—553
——, **W. Sleator, Jr., George Freier, E. E. Lampi, and J. H. Williams.** Angular distribution of the disintegration products from the D−D reaction: 1 to 4 Mev—1259(A)
——, **William Sleator, Jr., George Freier, E. E. Lampi, and J. H. Williams.** Proton-proton scattering: 2.4 to 3.5 Mev—1205(A)
Blatt, John M. On the neutron-proton force—92, 1205(A)

Blau, M. and J. A. De Felice. Development of thick emulsions by a two-bath method—1198(L)
Bless, A. A. Bioelectric potentials as an index of X-ray action—1209(A)
—— (see Jones, M. W.)—126(A)
Bloch, F., D. Nicodemus, and H. H. Staub. Quantitative determination of the magnetic moment of the neutron in units of the proton moment—1025
Bloch, I. (see Breit, G.)—397
Bloom, Evelyn G., Fred L. Mohler, J. H. Lengel, and C. E. Wise. Metastable transitions in mass spectra of hydrocarbons—1222(A)
Bockhop, Dorothy, A. C. Helmholz, and J. M. Peterson. Radioactive products of high energy deuteron bombardment of Cu—1559(A)
Bockstahler, Lester I. and Harmon Plumb. Characteristics of liquid air as a low temperature bath—1235(A)
Bohm, D. and E. P. Gross. Plasma oscillations as a cause of acceleration of cosmic-ray particles—624(L)
—— **and M. Weinstein.** Self-oscillations of charged particles—1789
Bonner, T. W. (see DeBenedetti, S.)—1645
——, **J. E. Evans, J. C. Harris, and G. C. Phillips.** Resonances in the disintegration of carbon by deuterons—1227(A)
Borkowski, C. J. and E. Fairstein. Methane proportional counter for beta-counting—1243(A)
Borowitz, Sidney. Depolarization of neutrons during diffusion—1215(A)
—— **and Morton Hamermesh.** Depolarization of neutrons during diffusion—1285
Borst, L. B. and J. J. Floyd. Radioactive decay of K^{40}—989(L)
——, **M. Fox, D. H. Gurinsky, I. Kaplan, R. W. Powell, C. Williams, and W. E. Winsche.** Nuclear reactor at the Brookhaven National Laboratory—1883(L)
Bottom, Virgil E. Hall effect in tellurium measured by a.c. method—1218(A)
—— (see Bever, Renate S.)—1562(A)
Bouricius, G. M. B. (see Bender, R. S.)—1205(A)
Bouricius, W. G. (see Breit, G.)—1546(L)
Bowers, W. A. Focusing properties of the electrostatic analyzer—128(A)
—— On the relative yields of (γ, n) reactions—1538(L)
Boyd, G. E. (see Motta, E. E.)—220(L), 344(L)
Boyd, L. R. (see Wineland, W. C.)—118(A)
Boydston, R. W. Durable and optically improved front surfaced mirrors processed exclusively by thermal evaporation—124(A)
—— Hard and durable non-absorbing optical beam splitters produceable by evaporated multilayer thin filming methods—125(A)
Boyer, R. L. Determination of detonation temperatures in high explosives—1221(A)
Braden, C. H., G. E. Owen, J. Townsend, C. S. Cook, and F. B. Shull. Discrepancies caused by source charging in beta-spectrometers—1539(L)
Bradner, Hugh and J. D. Gow. Half-lives of aluminum^{25} and aluminum^{26}—1559(A)
Bradt, H. L. (see Freier, Phyllis)—213
—— **and B. Peters.** Investigation of the primary cosmic radiation with nuclear photographic emulsions—1828
Brady, Edward L. and Martin Deutsch. Angular correlation of successive gamma-ray quanta. II—1541(L)
Bragg, J. K. Interaction of nuclear electric quadrupole moments with molecular rotation in asymmetric-top molecules. I—533
Brattain, W. H. (see Bardeen, J.)—230(L)
—— **and J. Bardeen.** Nature of the forward current in germanium point contacts—231(L)
Bray, Ralph. Dependence of resistivity of germanium on electric field—1218(A)
Breit, G. Some effects of the intrinsic magnetic moment of the electron—656
—— **and I. Bloch.** Resonances in $Li^7(p, n)Be^7$—397
—— **and G. E. Brown.** Effect of nuclear motion on the fine structure of hydrogen—1278
—— **and W. G. Bouricius.** Boundary value condition for proton-proton scattering—1546(L)
Bremner, J. W. (see Poole, J. H. J.)—836(L)
Brentano, J. C. M. and D. H. Davis. Change of photoconductivity of cadmium sulfide between room temperature and the temperature of liquid air—711(L)
Brickwedde, F. G. Redefinition of the thermodynamic scale of temperatures—1220(A)
Bridge, H. and W. Hazen. Shower production by penetrating particles at 14,000 feet—579
——, **W. E. Hazen, B. Rossi, and R. W. Williams.** Study of cosmic-ray bursts—1083
Brillouin, L. Waves and electrons traveling together—a comparison between traveling wave tubes and linear accelerators—90
Britten, R. J. (see Fullbright, H. W.)—1251(A)
Brocklehurst, R. E. and L. F. Vassamillet. Measurement of the coefficient of expansion of microgram samples of metals—114(T)
Broer, L. J. F. On the reflection-transmission effect in experiments on polarization of electrons—1887(L)
Bromberg, E. (see Belock, H.)—1230(A)
Brown, F. W., III (see Lamb, W. A.)—104(L)
Brown, G. E. (see Breit, G.)—1278
Brown, Harrison S. (see Inghram, Mark G.)—343(L)
Brown, Sanborn C. (see Everhart, Edgar)—1210(A)
—— (see Farmer, Earle C.)—902
—— (see Herlin, Melvin A.)—291, 910, 1650, 1209(A)
Brubaker, W. M. Present problems in conduction of electricity in gases—116(T)
Buechner, W. W. (see Strait, E. N.)—1226(A), 1257(A)
——, **E. N. Strait, C. G. Stergipoulos, and A. Sperduto.** Excited level in Li^7 from the $Li^6(d, p)Li^7$ and $Be^9(d, \alpha)Li^7$ reactions—1569
——, **R. J. Van de Graaff, E. A. Burrill, and A. Sperduto.** Thick-target x-ray production in the range from 1250 to 2350 kilovolts—1348
——, **R. J. Van de Graaff, E. N. Strait, C. G. Stergiopoulos, and A. Sperduto.** Magnetic analysis of disintegration products—1226(A)
Buehler, J. H. (see Ramsay, B. P.)—118(A)
—— (see Wolf, H. E.)—118(A)

Bundy, F. P. (see Strong, H. M.)—1221(A)
——, **A. B. Gregg, and H. M. Strong.** Measurement of gas pressures in the exhaust flames of rocket motors by spectroscopic methods II—1221(A)
Burbury, D. W. P. (see Fenton, A. G.)—589
Burfening, John (see Bishop, A. S.)—1558(A)
Burg, Anton B. (see Gordy, Walter)—1191(L)
Burgy, M., D. J. Hughes, and J. Wallace. Double transmission and depolarization of neutrons—1207(A)
Burling, R. L. and F. N. D. Kurie. On γ-induced β-disintegration: experimental—109(L)
Burrill, E. A. (see Buechner, W. W.)—1348
Burson, S. B. and C. O. Muehlhause. Decay scheme of 47-hr Sm^{153}—1264(A)
Burstein, Elias and Paul L. Smith. Photoelastic properties of cubic crystals—229(L)
—— **and Paul L. Smith.** Photoelastic properties of diamond —1880(L)
Bush, R. R. (see Fulbright, H. W.).—1323, 1203(A)
—— (see White, M. G.)—1242(A)
—— **and H. W. Fulbright.** Nuclear energy levels from inelastic scattering of protons—1206(A)
Byatt, W. J. and F. T. Rogers, Jr. Maximum normal stresses in mild steel during bending—121(A)
——, **F. T. Rogers, Jr., and Arthur Waltner.** Cloud-chamber observations of the decay of tritium—699(L)

Cady, W. M. (see Marlow, Douglas)—1228(A)
Calamai, G. (see Ballario, C.)—1729(L)
Calbick, C. J. (see Christensen, H.)—1219(A)
Caldwell, E. E. and F. T. Rogers, Jr. Output voltage from carbon-pile type of voltage-regulator—120(A)
Caldwell, Wallace C. and Lloyd P. Smith. Photo-conductivity of silver chloride and thallium bromide in the visible and near infra-red—1207(A)
Cameron, A. E. (see White, J. R.)—991
Cardell, J. (see McCormack, R. L.)—1204(T)
Carmichael, H. Studies of bursts at sea level—1667
Carter, Robert L. and William V. Smith. Saturation effect in the microwave absorption of ammonia—123(A)
Carter, W. W. (see Andrew, Alan)—838(L)
Case, Kenneth M. Magnetic moments of the neutron and proton—1884(L)
Cassels, J. M. Polarization of neutrons by magnetized iron—111(L)
—— **and R. Latham.** Inelastic scattering of neutrons—103(L)
Castle, J. (see Spence, J.)—704(L)
Chaffe, E. L. (see Hickman, R. W.)—354(T)
Chako, Nicholas. Extensional and thickness vibrations of two-dimensional crystals—126(A)
Chakrabarty, S. K. (see Bhabha, H. J.)—1352
Champion, F. C. and R. R. Roy. Emission of protons from light nuclei on bombardment with α-particles of short range—5
Chang, T. S. Note on the general properties of S matrices —1213(A)
—— Relativistic field theories—1250(A)
Chang, W. Y. Alpha-ray spectra of RaC, and RaC′—1195(L)
—— Search for heavy particles from stopped mesons—1236(A)
—— **and T. Coor.** Alpha-ray spectra of RdTh, ThC and ThC′—1196(L)
Chao, C. Y. Cosmic-ray showers produced by penetrating particles—492(L)
Cheka, J. S. Investigation of the fading of latent images of neutron-induced proton tracks in special fine grain particle emulsions—127(A)
Cheng, Laura (see Hubbard, J. C.)—708(L)
Chew, Geoffrey F. Elastic scattering of high energy nucleons by deuterons—809
Chou, Chang-Ning. Cosmic-ray bursts at sea-level and under thirty meters of clay—1659
Christensen, H. and C. J. Calbick. Sintering process study by electron micrography—1219(A)
Christy, R. F. (see Cohen, E. Richard)—1566(A)
—— (see O'Reilly, J.)—1559(A)
Chu, K. Y. and M. L. Wiedenbeck. Coincidences between beta-rays and conversion electrons in europium—494(L)
Chubbuck, J. B. and I. Perlman. Neutron deficient isotopes of cerium and lanthanum—982(L)
Chupp, W. W. and E. M. McMillan. Production of N^{17} by deuteron bombardment—1217(A)
Clark, C. L. Electron ballistics in the Yale linear accelerator—1243(A)
Cleland, Marshall (see Townsend, J.)—99(L), 499(L)
Cobb, Jock and A. K. Solomon. Detection of beta-radiation by photographic film—354(A)
Cobine, J. D. and C. J. Gallagher. Current density of the arc cathode spot—1524
Cocconi, G. and K. Greisen. On the penetrating showers of cosmic radiation—62
——, **V. Cocconi Tongiorgi, and K. Greisen.** Neutrons in the penetrating showers of the cosmic radiation—1867
Cocconi, Vanna Tongiorgi. On the origin of the neutrons associated with the extensive cosmic-ray showers—226(L)
Cohen, E. Richard and R. F. Christy. Analysis of the Be^9+p resonances at 0.988 and 1.077 Mev—1566(A)
Cohen, Martin J. Proposed self-controlled cloud chamber—1244(A)
Coles, Donald K. Microwave absorption line frequencies of methyl alcohol and their Stark effect—1194(L)
—— Precision measurement of molecular rotation frequencies—1203(T)
Collins, George B. Decay times of scintillations—1543(L)
Conforto, A. M. (see Sard, R. D.)—97(L)
Conwell, Esther. Non-product wave function for a negative ion—268
—— Wave functions for H^- obtained by variation method —277
Cook, C. Sharp (see Owen, George E.)—1879(L)
—— (see Langer, Lawrence M.)—1263(A)
—— (see Braden, C. H.)—1539(L)
—— **and Lawrence M. Langer.** Auger electrons following K-capture in Cu^{64}—1241(A)
—— **and Lawrence M. Langer.** Shape of the positron spectrum of Cu^{61}—227(L)

——, **Lawrence M. Langer, and H. Clay Price, Jr.** Study of the beta-spectra of C^{14} and S^{35}—548
——, **L. M. Langer, H. C. Price, Jr., and M. B. Sampson.** Shape of the positron spectrum of N^{13}—502(L)
Cook, Richard K., Martin Greenspan, and Pearl G. Weissler. Thermal voltages of a quartz crystal—1714
Cooke, S. P. Hall and Kerr effects at microwave frequencies—701(L)
Cool, R. L. (see Fowler, E. C.)—101(L), 850(L)
Cooper, D. (see Kissinger, C. W.)—349(L), 1237(A)
Cooper, Eugene P. On the failure of beta-decay theory at low energies—1565(A)
Cooper, J. N. (see Shaw, C. H.)—114(T)
—— **and C. H. Shaw.** Ohio State electrostatic generator—114(T)
Coor, T. (see Chang, W. Y.)—1196(L)
Corben, H. C. Use of phase space in classical and quantum theory—788
Cork, J. M., R. G. Shreffler, and C. M. Fowler. Converted gamma-radiation from silver, cadmium, indium, praseodynium, and rhenium—1657
——, **R. G. Shreffler, and C. M. Fowler.** Gamma-radiation from tellurium and samarium—1249(A)
——, **R. G. Shreffler, and C. M. Fowler.** Neutron induced radioactivity in certain rare-earth elements—240
Cornog, I. C. (see Franzen, W.)—1234(A)
——, **W. Franzen, and W. E. Stephens.** Range of protons from $N^{14}(n, p)C^{14}$—1
Cortini, G. (see Bernardini, G.)—845(L), 1878(L)
Cottington, R. L. (see Hardy, R. C.)—1220(A)
Courant, Ernest D. Photoelectric production of protons in nuclei—1226(A)
—— (see Blachman, Nelson M.)—140
Cowan, Clyde L. Absorption of gamma-radiation—1841
—— (see Hughes, A. L.)—1238(A)
—— (see Morganstern, K. H.)—499(L)
Craggs, J. D. (see Balakrishnan, C.)—410
—— (see Knowles, A. J.)—627(L)
Crain, C. M. Dielectric constant of several gases at a wave-length of 3.2 centimeters—691
Crawford, G. W. Tensiometer for elastic properties of very small wires—119(A)
—— (see Linz, Arthur, Jr.)—119(A)
—— **and F. T. Rogers, Jr.** Note on the d.c. characteristics of the string galvanometer. II—118(A)
Crawley, Clyde B. Study of the mean radiant temperature and the air temperature in a panel heated house—120(A)
—— (see Howard, R.)—125(A)
Creutz, E. (see Falk, C. E.)—1226(A)
Critchfield, Charles L. Analysis of proton-proton scattering—1205(A)
Crittenden, E. C. (see Smith, C. S.)—114(T)
Crouch, M. F. (see Sard, R. D.)—97(L)
Csongor, Eva (see Szalay, A.)—1063
Cullwick, E. G. Tentative explanation of the observed mass of mesons and other particles—707(L)
Cunningham, B. B. (see Miller, D. R.)—347(L)
Cunningham, G. L., W. I. LeVan, and William D. Gwinn. Rotational spectrum of ethylene oxide—1537(L)
Curcio, J. A. (see Sanderson, J. A.)—1221(A)
Curtiss, C. F. and J. O. Hirschfelder. Equilibrium assumption in the theory of absolute reaction rates—1265(A)
Curtiss, L. F. Radioactivity and neutron standards—1203(T)

Dabbs, J. W. T. (see Moak, C. D.)—1249(A)
Dailey, B. P. (see Shulman, R. G.)—846(L)
——, **K. Rusinow, R. G. Shulman, and C. H. Townes.** Pure rotational spectrum of AsF^3—1245(A)
Danielson, Gordon C., Bernd T. Matthias, and John M. Richardson. Dielectric behavior of single domain crystals of $BaTiO^3$—986(L)
Darrow, K. K. Outline of the topics of the symposium—1203(T)
Daunt, John G. Erratum: the magnetic threshold curves of superconductors—985(L)
—— Special lecture: the behavior of the helium isotopes in the liquid phase—114(T)
——, **A. R. Miller, A. B. Pippard, and D. Shoenberg.** Temperature dependence of penetration depth of a magnetic field in superconductors—842(L)
——, **R. E. Probst, and S. R. Smith.** Experiments on He^3 at low temperatures—495(L)
Davidson, Norman and A. E. Larsh, Jr. Conductivity pulses in liquid argon—220(L)
Davidson, W. L. X-ray diffraction evidence for ZnS formation in zinc activated rubber vulcanizates—116(A)
Davis, D. H. (see Brentano, J. C. M.)—711(L)
Davis, Karl A. (see Edwards, John E.)—116(A)
Davis, Luther, Jr. Nuclear spin and magnetic moment of Na^{22}—1193(L)
—— **and Carroll W. Zabel.** Electric quadrupole moments of the chlorine nuclei—1211(A)
Davis, R. C. (see Bell, P. R.)—1245(A)
Davis, R. E., W. E. Johnson, K. Lark-Horovitz, and S. Siegel. Neutron-bombarded germanium semiconductors—1255(A)
Davis, W. H., A. O. Williams, Jr., and R. T. Beyer. Self-consistent field for Ca XIII—1208(A)
Davison, Perry W. Recent results of investigation of reaction $S(dp)$—1233(A)
Davisson, Charlotte M. and Robley D. Evans. Gamma-ray absorption measurements—1239(A)
Davisson, J. W. Electrical breakdown in LiF below room temperature—1218(A)
Day, F. H. (see Deal, L. J.)—127(A)
Deal, L. J., J. H. Robertson, and F. H. Day. Energy dependence of film meters—127(A)
DeBenedetti, S., J. E. Francis, Jr., W. M. Preston, and T. W. Bonner. Angular dependence of coincidences between fission neutrons—1645
—— **and F. K. McGowan.** Short-lived isomers of nuclei—728
Decker, K. M. (see Schulkin, M.)—840(L)
De Felice, Joseph A. Removal of latent image in the Powell photographic plate technique—1244(A)
—— (see Blau, M.)—1198(L)
de Hoffmann, F., B. T. Feld, and P. R. Stein. Delayed neutrons from U^{235} after short irradiation—1330

de Launay, Jules and M. C. Steele. On temperature dependence of penetration depth in superconductors—1235(A)
del Rosario, Leticia. Use of an electron multiplier tube as a new technique in disintegration experiments—304
—— (see Allison, S. K.)—1233(A)
Dempster, A. J. Neutron absorption in samarium—505(L)
—— Packing fraction measurements of the heavy elements—1225(A)
de Saussure, G. (see Medicus, H.)—839(L)
Deutsch, Martin (see Brady, Edward L.)—1541(L)
—— (see Fluharty, R. G.)—1241(A)
—— (see Metzger, Franz)—1640
—— **and Franz Metzger.** Correlation between direction and polarization of successive gamma-ray quanta—1542(L)
Devons, S. and M. G. N. Hine. γ-radiation from Be^8—976(L)
Dickey, J. (see Apker, L.)—1462
Dickson, D. (see Slack, C. M.)—1230(A)
Dillon, J. F. and J. W. Beams. Improved axial magnetic suspension—117(A)
Dirac, P. A. M. Theory of magnetic poles—817
Dollmann, E. M. (see Salant, E. O.)—694(L)
Dougherty, C. B. (see Hornyak, W. F.)—1727(L)
—— (see Lauritsen, T.)—1566(A)
——, **W. F. Hornyak, T. Lauritsen, and V. K. Rasmussen.** Internal conversion pairs in carbon—712(L)
Dresden, M. Approximate methods in momentum space—1236(A)
Dropkin, J. J. (see Parker, W. L.)—1242(A)
Duffield, R. B. (see McElhinney, J.)—1257(A)
DuMond, Jesse W. M. Erratum; Solid state interpretation of the structure near the limit of the continuous x-ray spectrum—1883(L)
—— (see Lind, David)—1561(A)
—— (see Watson, Bernard B.)—1561(A)
——, **David Lind, and Bernard B. Watson.** Precision spectroscopy of nuclear gamma-rays with a focusing curved quartz crystal—1561(A)
Dunipace, D. W. Optics of curved glass—116(A)
Dunlap, W. C., Jr. and E. F. Hennelly. Non-rectifying germanium—976(L)
Dunning, J. R. (see Havens, W. W., Jr.)—1216(A)

Eberlein, W. F. Characteristic values of spheroidal wave functions—190
Eckert, W. J. IBM selective sequence electronic calculator—1204(T)
Eden, R. J. Analytic behavior of Heisenberg's S-matrix—982(L)
Edwards, John E. and Karl A. Davis. Combination electron diffraction and x-ray tube—116(A)
Eggen, D. T. and M. L. Pool. Radioactive isotopes of Ru and Tc—57
—— **and M. L. Pool.** Radioactive Ru and Tc—1248(A)
Eggler, C. (see Hughes, D. J.)—1239(A)
——, **D. J. Hughes, and C. Huddleston.** Formation of Be^{10}—1239(A)
Ehrke, L. F. (see Slack, C. M.)—1230(A)
Einbinder, Harvey. Generalized virial theorems—803
—— Quantum statistics and the $\aleph$ theorem—805
Eisenbud, L. Neutron helium resonance scattering—1206(A)
Eisenhart, L. P. Enumeration of potentials for which one-particle Schroedinger equations are separable—87
Eisenstein, J. (see Feshbach, H.)—1223(A)
Ekstein, H. and S. Siegel. Erratum; achromatization of Debye-Scherrer lines—625(L)
Elder, F. R., R. V. Langmuir, and H. C. Pollock. Radiation from electrons accelerated in a synchrotron—52
Elliott, L. G. (see Bell, R. E.)—1552(L)
—— **and R. E. Bell.** Experimental upper limit for the mean life of the 478.5-kev excited state of Li^7—1869(L)
Elliott, Norman. Magnetic susceptibility of uranium tetrafluoride, UF_4—498(L)
Ellis, Cecil B. On closed shells in nuclei—1547(L)
English, W. N. Corona from a water drop—179
—— Effect of point material on corona onset—1556(A)
—— Positive and negative point-to-plane corona in air—170
—— (see Bandel, H. W.)—1557(A)
—— (see Moore, D. B.)—1557(A)
Epstein, H. T. Electron microscopy of monolayers—1256(A)
—— (see Mautz, C. W.)—1872(L)
Estermann, I. Interaction of molecules with solid substances—1555(T)
Estes, Dorothy V. (see Sanderson, J. A.)—1221(A)
Evans, J. E. (see Bonner, T. W.)—1227(A)
Evans, John (see Lagemann, R. T.)—124(A)
Evans, Robley D. (see Ahrens, L. H.)—279
—— (see Davisson, Charlotte M.)—1239(A)
Everhart, Edgar and Sanborn C. Brown. Method of measuring the complex conductivity of an ionized gas at microwave frequencies—1210(A)
Eyges, Leonard. Multiple scattering with energy loss—1534(L)
—— Scattering of particles in air showers—1801

Fagg, Lawrence W. (see Mock, Dana L.)—1536(L)
Fairbank, Henry A., Charles A. Reynolds, C. T. Lane, B. B. McInteer, L. T. Aldrich, and Alfred O. Nier. Increase in vapor pressure of liquid helium due to He^3 in solution—345(L)
Fairstein, E. (see Borkowski, C. J.)—1243(A)
Falk, C. E., E. Creutz, and F. Seitz. Angular distribution of neutrons from (d, n) reactions—1226(A)
Falkoff, D. L. (see Ling, D. S.)—1224(A)
Fan, H. Y. Theory of rectification of an insulating layer—1505
Farmer, Earle C. and Sanborn C. Brown. Study of the deterioration of methane-filled Geiger-Mueller counters—902
Farnsworth, H. E. Production and tests of metal single crystal surfaces—1219(A)
Feenberg, Eugene. Note on perturbation theory—206
—— Theory of scattering processes—664
Feer, Daniel B. Emission of radiation in the disintegration of mesons—1238(A)

Feld, B. T. (see de Hoffmann, F.)—1330
—— (see Knight, G.)—354(A)
—— (see Szilard, L.)—1216(A)
Fenton, A. G. and D. W. P. Burbury. Measurements of the east-west asymmetry of cosmic rays at Hobart, Tasmania—589
Ferry, John D. (see Marvin, Robert S.)—1256(A)
Feshbach, Herman. On Feenberg's perturbation formula—1548(L)
—— (see McKinley, William A., Jr.)—1759
——, **J. Eisenstein, and J. S. Schwinger.** On tensor forces and the variation-iteration method—1223(A)
Fett, G. H. (see Bergman, C. E.)—1266(A)
Feynman, R. P. Relativistic cut-off for classical electrodynamics—939
—— Relativistic cut-off for quantum electrodynamics—1430, 1212(A)
Fifer, S. (see Belock, H.)—1230(A)
Finkelnburg, Wolfgang. Electrode vapor jets in arc and spark discharges—222(L)
—— Theory of the production of electrode vapor jets by sparks and arcs—1475
Finkelstein, R. J. Quantization of unitary field theories—1563(A)
Finston, H. L. (see McCown, D. A.)—1263(A), 1263(A)
—— (see Woodward, L. L.)—1263(A)
Fireman, E. Double beta decay—1238(A)
Fisher, John C. Fracture of liquids—1256(A)
Fitzgerald, Edwin R. (see Marvin, Robert S.)—1254(A)
Fitzpatrick, J. A. (see Hubbard, J. C.)—107(L), 708(L)
——, **Thomas Kankovsky, and William J. Thaler.** Intensity as a factor in precision measurements in ultrasonics—1227(A)
Flanary, H. G., F. B. Pauls, and L. A. Pardue. Current integrator for small currents—125(A)
Flint, H. T. Quantization of space and time—209
Floyd, J. J. (see Borst, L. B.)—989(L)
Fluharty, R. G. and Martin Deutsch. Search for crossover gamma-ray transitions in Co^{60} and Se^{46}—1241(A)
Foley, H. M. (see Kusch, P.)—250
Follin, James W., Jr. Source of the solar magnetic field—1232(A)
Fonda, Gorton R. (see Studer, Frank J.)—1241(A)
Foner, S. N., A. Kossiakoff, and F. T. McClure. Ionization efficiency curves from mass spectrometer data—1222(A)
Forró, M. Comments on the theories interpreting the magnetism of celestial bodies—218(L)
—— (see Barnóthy, J.)—1300
Forstat, Harold (see Jesse, William P.)—1259(A)
Forster, Harriet H. Energy spectrum and altitude dependence of slow protons and stars up to 30,000 feet—1556(A)
Fowler, C. M. (see Cork, J. M.)—240, 1657, 1249(A)
Fowler, E. C., R. L. Cool, and J. C. Street. Example of the beta-decay of the light meson—101(L); Erratum—850(L)
Fowler, W. A. (see Rubin, S.)—1564(A)
—— (see Snyder, C. W.)—1564(A)
—— **and R. N. Hall.** Low energy $C^{12}(p, \gamma)$ cross section—1558(A)
Fowles, G. R. S-level shift in ionized helium—219(L)
Fox, F. E. and V. Griffing. Concentration of ultrasonic beams by curved reflectors—1228(A)
Fox, M. (see Borst, L. B.)—1883(L)
Fox, R. E., A. Langer, and J. A. Hipple. Appearance potential of metastable ions in some hydrocarbon gases—1222(A)
Franchetti, S. and M. Giovanozzi. On the high energy part of the K^{40} β-spectrum—102(L)
Francis, J. E., Jr. (see DeBenedetti, S.)—1645
Franzen, W. (see Cornog, I. C.)—1
——, **I. C. Cornog, and W. E. Stephens.** $N^{14}(n, p)$ reaction and the proton range-energy curve—1234(A)
Freier, George (see Blair, J. Morris)—553, 1594, 1599, 1205(A), 1259(A)
—— (see Sleator, William, Jr.)—1260(A)
Freier, Phyllis, E. J. Lofgren, E. P. Ney, and F. Oppenheimer. Heavy component of primary cosmic rays—1818
——, **E. J. Lofgren, E. P. Ney, F. Oppenheimer, H. L. Bradt, and B. Peters.** Evidence for heavy nuclei in the primary cosmic radiation—213
Frerichs, Rudolf and A. J. F. Siegert. Note on the photoconductivity of cadmium crystals—1875(L)
Fretter, W. B. Penetrating showers in lead—1555(T)
Frick, Walter, Edward J. Lofgren, Frank Oppenheimer, and Edward P. Ney. Equipment for photographing cosmic-ray cloud-chamber tracks at 100,000 ft.—1258(A)
Friedland, S. S. On the life of self-quenching counters—898
—— **and A. D. Krumbein.** Deadtime theory—1244(A)
Friedlander, G. (see Perlman, M. L.)—442
——, **M. Goldhaber, and G. Scharff-Goldhaber.** Long-lived metastable state of Te^{125}—981(L)
Fulbright, H. W. (see Bush, R. R.)—1206(A)
—— (see White, M. G.)—1242(A)
—— **and R. J. Britten.** High pressure ion chamber using fast electron collection—1251(A)
—— **and R. R. Bush.** Inelastic scattering of protons from light nuclei—1323
—— **and R. R. Bush.** New method of studying nuclear energy levels—1205(A)
Fuson, Nelson. Recent study of the infra-red sensitivity of superconducting bolometers—1234(A)

Gallagher, C. J. (see Cobine, J. D.)—1524
Gamow, G. A. Origin of elements and the separation of galaxies—505(L)
—— (see Alpher, R. A.)—1198(L)
Gardner, Eugene (see Barkas, Walter H.)—1558(A)
—— (see Bishop, A. S.)—1558(A)
—— (see Lattes, C. M. G.)—1555(T), 1236(A)
—— **and C. M. G. Lattes.** Production of mesons by the 184-inch Berkeley cyclotron. Part I. Experimental arrangement—1236(A)
Garrett, W. M. Dipole, quadrupole, and octupole field and search coils using loops and solenoids—1231(A)
Gartlein, C. W. Aurora spectra showing broad hydrogen lines—1208(A)
Gaus, Louise (see Michels, Walter C.)—1241(A)
Geib, I. G. Formation of radioactive zinc dimethyl dithiocarbamate in the vulcanization of rubber—117(A)

Geiger, F. W. (see Mautz, C. W.)—1872(L)
George, Waller and Richard LaTorre. Breaking strength dispersion in nylon yarns—1256(A)
Gerjuoy, Edward (see Halpern, Otto)—1562(A)
Geschwind, S. (see Townes, C. H.)—626(L)
Ghiorso, A. (see Perlman, I.)—1730(L)
——, **W. W. Meinke, and G. T. Seaborg.** Artificial collateral chains to the thorium and actinium families—695(L)
Gill, E. W. B. Frictional electricity—842(L)
Ginsburg, N. Additional rotational energy levels of H_2O and D_2O molecules—1052
Giovanozzi, M. (see Franchetti, S.)—102(L)
Gittings, H. T. (see Taschek, R. F.)—1553(L)
Glendenin, L. E. and A. K. Solomon. Comparison of the beta-spectra of C^{14} and S^{35}—700(L)
Goldberg, Edward (see Inghram, Mark G.)—343(L)
Goldberg, Leo (see McMath, Robert R.)—623(L)
—— (see Mohler, Orren C.)—352(L)
——, **Orren, C. Mohler, and Robert R. McMath.** Isotopes of carbon and oxygen in the earth's atmosphere—1881(L)
Goldberger, M. L. Interaction of high energy neutrons and heavy nuclei—1269
Goldhaber, Gerson. Gamma-ray spectrum from $F^{19}+H^1$ using photographic emulsions containing D_2O—1725(L)
Goldhaber, M. Note on the spins of nuclei of mass number ten—1194(L)
—— (see Friedlander, G.)—981(L)
—— (see Meyerhof, W. E.)—348(L)
—— (see Sala, O.)—1249(A)
—— **and C. O. Muehlhause.** Metastable state of Sc^{46}—1877(L)
—— **and C. O. Muehlhause.** Nuclear isomers produced by slow neutron capture—1248(A)
—— **and E. Teller.** On nuclear dipole-vibrations—1046
Goldsmith, G. J. Separation of the isomers of indium 112 and indium 114 in an electric field—1249(A)
Goldstein, L. and D. W. Sweeney. On neutron-proton scattering models—1565(A)
Golian, S. E., C. Y. Johnson, and M. Kuder. Rocket borne cloud chamber I—1215(A)
Good, W. M., E. O. Wollan, and W. A. Strauser. Stopping of fission fragments—1225(A)
Gordy, Walter (see Kessler, Myer)—123(A)
—— (see Simmons, James W.)—123(A), 1246(A)
—— (see Smith, A. G.)—123(A), 370
——, **Harold Ring, and Anton B. Burg.** Nuclear spins and quadrupole moments of B^{10} and B^{11}—1191(L)
——, **James W. Simmons, and A. G. Smith.** Microwave determination of the molecular structures and nuclear couplings of the methyl halides—243
Gorter, C. J. Irreversible processes in liquid helium II—1544(L)
Goss, Norman. Recrystallization of zinc at room temperature—116(A)
Goudsmit, S. A. Time-of-flight mass spectrometer—622(L)
—— **and W. T. Scott.** Proposed method for measuring scattering of particle tracks—1537(L)
Gow, J. D. (see Bradner, Hugh)—1559(A)
Gráf, T. On the half-life of K^{40}—831(L)
—— On the total half-life period of K^{40}—1199(L)
—— Significance of the radioactivity of potassium in geophysics. II—831(L)
Green, Alex E. S. Interaction energy in quantum field theory—1545(L)
Green, J. B. and Howard N. Maxwell. Zeeman effect of gold—1208(A)
Greenberg, J. Mayo and T. H. Berlin. Gas scattering in the electron synchrotron—1243(A)
Greene, R. F. (see Isenberg, I.)—1255(A)
Greenfield, M. A. Diffusion of neutrons without change in energy in a medium with an isotropic scattering—1215(A)
Greenspan, Martin (see Cook, Richard K.)—1714
Gregg, A. B. (see Bundy, F. P.)—1221(A)
Greisen, K. I. (see Cocconi, G.)—62, 1867
—— (see Treat, J. E.)—414
Griffing, V. (see Fox, F. E.)—1228(A)
Groetzinger, Gerhart and Gordon W. McClure. Production of neutrons by the capture of cosmic-ray mesons at sea level—341
Gross, E. P. (see Bohm, D.)—624(L)
Grunlund, Jean M. (see Yaffe, L.)—696(L)
Gugelot, P. C. (see White, M. G.)—1242(A)
—— **and M. G. White.** Neutron diffusion in shielding materials—1215(A)
Guindon, William G. Radial dependence of the tensor force in the deuteron—145; Erratum—699
Gunlock, H. F. and M. L. Pool. Evidence for a double isomer in Rh^{103}—1264(A)
Gurinsky, D. H. (see Borst, L. B.)—1883(L)
Guth, Eugene and Charles J. Mullin. On models for Be^9—832(L)
—— **and Charles J. Mullin.** Theory of the photo-disintegration of Be^9—833(L)
——, **C. J. Mullin, and J. F. Marshall.** Theory of electro-disintegration of Be^9—834(L)
Gutowsky, H. S. (see Pake, G. E.)—979(L)
Gwinn, William D. (see Cunningham, G. L.)—1537(L)

Haber-Schaim, U. On the motion of point electrons—836(L)
Haddock, F. T. (see Schulkin, M.)—840(L)
Haeff, Andrew V. Space-charge wave amplification effects—1532(L)
Hafner, E. M. (see Inglis, D. R.)—1257(A)
Hagen, J. P. (see Schulkin, M.)—840(L)
Haggenmacher, J. E. Melting pressure of helium II—1539(L)
Hahn, T. M., Jr. (see Wineland, W. C.)—118(A)
Hainer, R. M. (see King, Gilbert W.)—1247(A)
Hall, R. N. High frequency proton source—1558(A)
—— (see Fowler, W. A.)—1558(A)
Halliday, David (see Wheatley, John)—1211(A)
—— **and John Wheatley.** Paramagnetic resonance absorption in aqueous solutions of manganese sulfate—1724(L)
—— **and John Wheatley.** Paramagnetic resonance absorption in chrome alum—1712

—— **and John Wheatley.** Paramagnetic resonance absorption in single crystals of chrome alum and in aqueous solution of manganous salts—1210(A)
Halpern, I. Thin target (α,n) cross sections of Be, Mg, and Al—1234(A)
—— (see Woodward, W. M.)—1225(A)
Halpern, Otto and Edward Gerjuoy. On diffraction under small angles by three-dimensional lattices—1562(A)
Halpern, W. (see Somers, H. S., Jr.)—1210(A)
Hamermesh, Morton (see Borowitz, Sidney)—1285
Hamilton, Donald R. Polarization and direction of propagation of successive quanta—782
Hammer, C. F., A. G. Pieper, and R. Rollefson. Infra-red dispersion of N_2O and C_2H_4—1262(A)
Hanna, G. C. (see Kirkwood, D. H. W.)—497(L)
Hansen, W. W. and R. F. Post. Method of measuring cavity impedance—1560(A)
Hanson, A. O. (see McElhinney, J.)—1257(A)
Hanson, H. P. and W. W. Beeman. MnK absorption edges of manganese and manganese compounds—1261(A)
Hardin, W. D. (see Reynolds, G. T.)—1549(L)
Harding, John M. and Joseph E. Henderson. Properties of Cerenkov radiation near the threshold—1560(A)
Hardy, R. C. and R. L. Cottington. Viscosity of D_2O and of H_2O from 5° to 125°C—1220(A)
Harish-Chandra. Motion of an electron in the field of a magnetic pole—883
Harris, J. C. (see Bonner, T. W.)—1227(A)
Harris, S. P. and A. S. Langsdorf, Jr. Neutron scattering resonances in elements from scandium to arsenic—1216(A)
Hart, J. C. (see Smith, C. S.)—114(T)
Hatton, J. (see Rollin, B. V.)—346(L), 508(L)
Havas, Peter. On the classical equations of motion of point charges—456
Havens, W. W., Jr. (see Wu, C. S.)—1248(A)
——, **L. J. Rainwater, C. S. Wu, and J. R. Dunning.** Recently improved slow neutron velocity spectrometer with some of the results obtained—1216(A)
Hawkings, R. C., R. F. Hunter, W. B. Mann, and W. H. Stevens. Half-life of C^{14}—696(L)
Haxel, O., F. G. Houtermans, and M. Kemmerich. On the half-life of Rb^{87}—1886(L)
Hayden, Richard J. Mass spectrographic mass assignment of radioactive isotopes—650
—— (see Hess, D. C., Jr.)—1531(L)
—— (see Inghram, Mark G.)—98(L)
Haynes, S. K. Beta- and gamma-spectra of gallium irradiated by slow neutrons—423
—— **and H. C. Thomas.** Use of Auger electrons in coincidence experiments—128(A)
Hazen, W. (see Bridge, H.)—579; 1083
Hein, R. E. and A. F. Voigt. Activities produced by bombardment of TiO_2 with pile neutrons—1265(A)
Heiss, J. H. (see Mason, W. P.)—1873(L)
Heitler, W. Theory of meson production—1204(T)
Helmholz, A. C. Nuclear isomerism—1555(T)
—— (see Bockhop, Dorothy)—1559(A)
—— **and C. L. McGinnis.** Assignment of 48-min. and 2-min. isomers of Cd—1559(A)
Hemmendinger, Arthur (see Taschek, Richard)—373
Henderson, Joseph E. (see Harding, John M.)—1560(A)
Henderson, R. S. On the fine structure in the inversion spectrum of ammonia—107(L); Erratum—626(L)
—— **and J. H. Van Vleck.** Coupling of electron spins in rotating polyatomic molecules—106(L)
Henkel, R. L. and B. Petree. Stabilized high voltage supply for electrostatic analyzer—1260(A)
Hennelly, E. F. (see Dunlap, W. C., Jr.)—976(L)
Henry, Hugh F. Cathode spark velocities in $CuSO_4$ solutions—1232(A)
Herb, R. G. Review of electrostatic generator techniques and recent results—1254(T)
—— (see Sala, O.)—1260(A)
——, **S. C. Snowden, and O. Sala.** Absolute voltage determinations of three nuclear reactions—1256(A)
Hereford, Frank L. Polarization effects in ionization loss of fast particles—1224(A)
—— Specific primary ionization and energy loss of fast electrons in matter—574
Herlin, Melvin A. Electrical discharges in gases at microwave frequencies—1254(T)
—— **and Sanborn C. Brown.** Breakdown of a gas at microwave frequencies—291
—— **and Sanborn C. Brown.** Electrical breakdown between coaxial cylinders at microwave frequencies—1209(A)
—— **and Sanborn C. Brown.** Electrical breakdown of a gas between coaxial cylinders at microwave frequencies—910
—— **and Sanborn C. Brown.** Microwave breakdown of a gas in a cylindrical cavity of arbitrary length—1650
Herman, Robert C. (see Alpher, Ralph A.)—1198(L), 1737
——, **C. F. Meyer, and H. S. Hopfield.** Theory of electron retrapping in infra-red phosphors—1242(A)
Hershkowitz, Joseph (see Zar, Jacob L.)—111(L)
Hess, David C., Jr. Isotopic constitution of europium, gadolinium, and terbium—773
—— (see Inghram, Mark G.)—98(L), 343(L), 627(L)
—— **and Mark G. Inghram.** New naturally occurring isotope of dysprosium—1724(L)
——, **M. G. Inghram, and R. J. Hayden.** Relative abundance of the zinc isotopes—1531(L)
Hewitt, William H., Jr. Microwave resonance absorption in ferromagnetic semiconductors—1211(A)
Heydenburg, N. P. (see Inglis, D. R.)—1257(A)
——, **C. M. Hudson, D. R. Inglis, and W. D. Whitehead, Jr.** Angular distribution of alphas from $Li^6(d,\alpha)\alpha$ and $Li^7(p,\alpha)\alpha$—405
——, **C. M. Hudson, D. R. Inglis, and W. D. Whitehead, Jr.** Energy and angle variation in $Li^6(d,\alpha)\alpha$—1226(A)
Hibdon, Carl T. (see Krisberg, N. L.)—44, 1249(A)
Hickam, W. M. Analysis of solids by the mass spectrometer—1222(A)
Hickman, R. W. and E. L. Chaffe. Physics laboratories, and researches in progress at Harvard University—354(T)
Hicks, B. L. On the calculation of steady diabatic flows—1230(A)

Hicks, Harry G. (see Wilkinson, Geoffrey)—1733(L)
Hill, R. D. Internal conversion electrons from Sm^{153}-47 hour—78
—— **and J. W. Mihelich.** Radiations from Te^{131}—1874(L)
Hincks, E. P. and B. Pontecorvo. Absorption of charged particles from the 2.2-μsec. meson decay—697(L)
Hine, G. J. (see Marinelli, L. D.)—1245(A)
Hine, M. G. N. (see Devons, S.)—976(L)
Hipple, J. A. (see Fox, R. E.)—1222(A)
Hirschberg, J. G., Jr. Rydberg denominators in the principal series of the alkali metal atoms—1262(A)
Hirschfelder, Joseph O. (see Curtiss, C. F.)—1265(A)
——, **R. Byron Bird, and Ellen L. Spotz.** Transport properties of non-polar gases—1265(A)
Hirzel, O. and H. Wäffler, On the radioactivity of K^{40}—1553(L)
Hoffman, Banesh. Trajectories of charged meson test particles in the similarity geometry—1238(A)
Hofstadter, Robert. Alkali halide scintillation counters—100(L); Erratum—628(L)
Hoge, Harold J. Vapor pressure of O_2 from the triple point to the critical point—1221(A)
Holden, A. N. (see Townes, C. H.)—1113
Holstein, T. Imprisonment of resonance radiation in ionized gases—1254(T)
Hoover, J. I., W. H. Jordan, C. D. Moak, L. Pardue, H. Pomerance, J. D. Strong, and E. O. Wollan. Measurement of neutron absorption cross sections with a pile oscillator—864
Hopfield, H. S. (see Herman, R. C.)—1242(A)
Hornbeck, J. A. (see Molnar, J. P.)—1254(T)
Hornbostel, J. (see Salant, E. O.)—694(L)
Hornyak, W. F. (see Dougherty, C. B.)—712(L)
——, **C. B. Dougherty, and T. Lauritsen.** Beta-decay spectra of B^{12} and Li^8—1727(L)
—— **and T. Lauritsen.** First excited state of Li^7—1565(A)
Horowitz, J. J., O. Kofoed-Hansen, and J. Lindhard. On the β-decay of mesons—713
Hough, P. V. C. Angular distribution of pair-produced electrons and Bremsstrahlung—80
Houtermans, F. G. (see Haxel, O.)—1886(L)
Howard, R. and C. B. Crawley. Supercooling of water—125(A)
Hsiang, J. S. (see Whitmer, C. A.)—1478
Hsueh, Chao-Wang. Internal intensity ratio of H_α and of D_α—670
Hu, F. C. (see Ma, S. T.)—500(L)
Hu, Ning. On the application of Heisenberg's theory of s-matrix to the problems of resonance scattering and reactions in nuclear physics—131
Huang, Su-Shu. Continuous absorption coefficient of the helium atom—1262(A)
Hubbard, J. C., J. A. Fitzpatrick, B. T. Kankovsky, and William J. Thaler. Distortion of progressive ultrasonic waves—107(L)
——, **J. A. Fitzpatrick, W. J. Thaler, Laura Cheng, and R. J. Beeber.** Study of turbulence by light diffraction—708(L)
Huddleston, C. (see Eggler, C.)—1239(A)
Hudson, C. M. (see Heydenburg, N. P.)—405, 1226(A)
Hudspeth, Emmett L. (see Swann, C. P.)—1243(A)
—— **and C. P. Swann.** Deuteron bombardment of boron and fluorine—1227(A)
—— **and Charles P. Swann.** Observations associated with the reaction $B^{11}(d,p)$—1722(L)
Hughes, A. L. (see Morganstern, K. H.)—499(L)
—— (see Townsend, J.)—99(L), 499(L)
—— **and Clyde L. Cowan.** Measurement of absorption coefficients for gamma-rays in various materials—1238(A)
Hughes, D. J. (see Burgy, M.)—1207(A)
—— (see Eggler, C.)—1239(A)
—— **and C. Eggler.** β-spectrum of Be^{10}—1239(A)
Hull, G. F., Jr. (see Wilson, M. Carr)—711(L)
Hull, T. E. and L. Infeld. Factorization method, hydrogen intensities, and related problems—905
Humphreys, R. F. (see Motz, H. T.)—1232(A)
—— **and H. T. Motz.** Corrections to range data—1232(A)
Hunter, Joseph L. Acoustic interpretation of interferometer data—116(A)
—— Piezoelectric measurement of acoustic absorption and reflection in fluids—114(T)
—— Supersonic absorption in resonant liquid column with a free face—1228(A)
Hunter, R. F. (see Hawkings, R. C.)—696(L)
Hutchison, T. S. (see Reekie, James)—610
Hyde, Earl K. (see Studier, Martin H.)—591
Hylleraas, Egil A. Calculation of a perturbing central field of force from the elastic scattering phase shift—48
Hynek, Allen. Dynamical parallaxes and the apparent failure of the mass luminosity law—114(T)

Iberall, A. S. and W. A. Wildhack. Linear-resistance flowmeter—1229(A)
Imai, Isao. On a refinement of the W. K. B. method—113(L)
Infeld, L. (see Hull, T. E.)—905
Inghram, Mark G. (see Hess, David C., Jr.)—1531(L), 1724(L)
—— **and D. C. Hess, Jr.** Radioactive lanthanum and cerium isotopes of mass 137—627(L)
——, **David C. Hess, Jr., Harrison S. Brown, and Edward Goldberg.** On the isotopic composition of meteoritic and terrestrial gallium—343(L)
——, **David C. Hess, Jr., and Richard J. Hayden.** Isotopic constitution of praseodymium and neodymium—98(L)
Inglis, D. R. Nuclear spin of B^{10} and spin-orbit coupling in Li^7—1876(L)
—— Theory of the lithium two-alpha-reactions—1227(A)
—— Theory of the lithium two-alpha-reactions. I. Angular distribution of $Li^7(p,\alpha)\alpha$—21
—— (see Heydenburg, N. P.)—405, 1226(A)
——, **N. P. Heydenburg, and E. M. Hafner.** Energy and angle variation of $C^{12}(d,p)C^{13}$—1257(A)
Isenberg, I., B. R. Russell, and R. F. Greene. On the measurement of the Hall effect in semiconductors—1255(A)
Ittner, W. B., III (see Sard, R. D.)—97(L)
Ivey, Henry F. Anomalous values of the thermionic emission constant—983(L)

Jacobs, Harold and A. P. LaRocque. Role of the cathode surface in sparking phenomena—163
Jaffe, A. A. (see Balakrishnan, C.)—410
James, Hubert M. Electronic states in almost periodic systems—1218(A)
—— Structure and behavior of rubberlike materials—1254(T)
Jarmotz, P. and R. Pepinsky. Some observations of Geiger counters for periodically pulsed x-ray photon counting—126(A)
Jarrell, H. A. and T. E. Pardue. Characteristics of curved tubes—121(A)
Jauch, J. M. Spin-orbit effect in the hyperfine structure of the ammonia inversion spectrum—1262(A)
—— (see Watson, K.)—1262(A)
—— **and K. M. Watson.** Phenomenological quantum-electrodynamics—950, 1485
Jen, C. K. Microwave Zeeman spectra of methyl-chloride and some nuclear properties of chlorine—1246(A)
—— Zeeman effect in microwave molecular spectra—1396
Jenkins, F. A. Nuclear spins of the carbon isotopes—355
Jenkins, G. L. and F. T. Rogers, Jr. Compensation of circuits for variations of temperature—120(A)
Jenkins, James F., Jr. East-west asymmetry, zenith angle dependence, and flux measurements of cosmic rays up to 36,000 feet—1214(A)
Jennings, B. (see Shoupp, W. E.)—1233(A)
Jesse, William P. and Harold Forstat. Ionization produced by alpha-particles in argon as a function of their energy—1259(A)
Johnson, C. Y. (see Golian, S. E.)—1215(A)
Johnson, E. A. Magnetization of ancient glacial varves—1204(T)
Johnson, Peter D. and Ferd E. Williams. Magnetic properties of the ZnF_2: Mn phosphor—1241(A)
Johnson, V. A. Theory of electrical resistivity in tellurium—1255(A)
Johnson, W. E. (see Davis, R. E.)—1255(A)
Jones, Emily and F. T. Rogers, Jr. Effects of relaxing materials in force-transmitting linkages—122(A)
Jones, J. G. (see Jones, M. W.)—126(A)
Jones, M. W., J. G. Jones, and A. A. Bless. Correlation of the bioelectric potential of corn seeds with x-ray dosage—126(A)
Jones, Shannon. Effects of milling on zinc beryllium silicate phosphors—116(A)
Jones, Stanley B. (see Wang, Kan-Chang)—1547(L)
Jones, W. B., Jr., Slow neutron cross section of H—364
Jordon, W. H. (see Hoover, J. I.)—864
Judson, L. V. Intercomparisons of the standard meter—1203(T)
Jungerman, J. and S. C. Wright. Fission excitation functions—150
Jurney, E. T. Coincidence experiments on Sc^{46}, Ga^{72}, Au^{198}, and Rb^{86}—1049
Justus, Katharine M. (see Yaffe, L.)—850(L)

Kaesberg, Paul, H. N. Ritland, and W. W. Beeman. Small angle Bragg reflections from collagen—1255(A)
——, **H. N. Ritland, and W. W. Beeman.** Use of the double crystal spectrometer in the analysis of Bragg reflections at very small angles—71
Kankovsky, B. T. (see Hubbard, J. C.)—107(L)
Kankovsky, Thomas (see Fitzpatrick, J. A.)—1227(A)
Kaplan, I. (see Borst, L. B.)—1883(L)
Kaplan, Nathan (see Yagoda, Herman)—1249(A)
Karplus, Robert. Saturation effects in microwave spectroscopy—223(L)
Katcoff, Seymour, John A. Miskel, and Charles W. Stanley. Ranges in air and mass identification of plutonium fission fragments—631, 1225(A)
Katzin, Leonard I. and M. Pobereskin. Isotopes Os^{185} and Os^{193}—264
Kaufmann, S. G. (see Bender, R. S.)—1205(A)
Kê, T'ing-Sui. Internal friction and precipitation from the solid solution of N in tantalum—914
—— Internal friction in the interstitial solid solutions of C and O in tantalum—9
—— Stress relaxation by interstitial atomic diffusion in tantalum—16, 1219(A)
Keighton, W. B. (see Mandeville, C. E.)—601, 888
Keller, K. K. and K. B. Mather. Investigation of samarium and gadolinium by the photographic method—624(L)
Kemmerich, M. (see Haxel, O.)—1886(L)
Kennard, E. H. Hydrodynamic problem: flapping wavemaker—1229(A)
Kenty, Carl. Study of metastable and resonance atom populations in gas discharges—114(T)
Kern, Bernard D. (see Zaffarano, Daniel J.)—105(L), 682
Kerst, D. W. Process aiding the capture of electrons injected into a betatron—503(L)
Kessler, Myer, and Walter Gordy. Methods in microwave spectroscopy—123(A)
Keuffel, J. W. Reaction time of parallel-plate counters—1562(A)
King, Gilbert W. and R. M. Hainer. Analysis of the 2.6-Mu band of H_2S by punched-card methods—1247(A)
Kirkwood, D. H. W., B. Pontecorvo, and G. C. Hanna. Fluctuations of ionization and low energy beta-spectra—497(L)
Kissinger, C. W. and D. Cooper. Decay of mesons in carbon—1237(A)
—— **and D. Cooper.** Mean life of negative mesons in carbon—349(L)
Kittel, Charles. Microwave resonance absorption in ferromagnetic materials—1203(T)
—— Theory of the ferromagnetism of simple tetragonal arrays—1206(A)
—— (see Newton, R. R.)—1604
Knable, N., E. O. Lawrence, C. E. Leith, B. J. Moyer, and R. L. Thornton. Delayed emission of neutrons from the decay of N^{17}—1217(A)
Knight, G. B. and B. T. Feld. Interaction of nuclear qudrupole moments with molecular rotation in slightly asymmetric rotor molecules—354(A)
—— **and R. L. Macklin.** Half-life of UX_1 (Th_{234})—1540(L)
Knop, Harry W., Jr. Emissivity of iron-tungsten and iron-cobalt alloys—1413
—— (see Wahlin, H. B.)—687, 1207(A)

Knorr, H. V. Absorption and fluorescence spectra of tetraphenylisoporphine and tetraphenylisoporphine zinc salt—115(A)
Knowles, A. J., C. Balakrishnan, and J. D. Craggs. Velocity of discharge propagation in Geiger counters—627(L)
Knox, William J. Search for gamma-rays from He^6 and F^{18}—1192(L)
Koch, W. R. Illuminant problem in the spectrophotometry of fluorescent materials—115(A)
Koehler, J. S. Change in the electrical resistance produced by cold-work—1219(A)
Kofoed-Hansen, O. On the theory of the recoil in β-decay—1785
—— (see Horowitz, J. J.)—713
Kofsky, Irving L. and Henry Levinstein. Dynamic method for the determination of the velocity distribution of thermal atoms—500(L)
Kohman, Truman P. Binding energies of α-particles in medium-heavy nuclides—1259(A)
Kohn, W. Variational methods in nuclear collision problems—1763
Kossiakoff, A. (see Foner, S. N.)—1222(A)
Kramer, R. L. (see McMillen, J. Howard)—1882(L)
Krasnican, Milan J. Demonstration of some optical phenomena using 3.2-cm microwave source—114(T)
Krause, E. H. Cosmic rays above the atmosphere—1555(T)
—— (see Perlow, G. J.)—1215(A)
Krisberg, N. L., M. L. Pool, and Carl T. Hibdon. Radioactive europium, gadolinium, and terbium—44, 1249(A)
Kruegel, S. L. (see Plyler, E. K.)—1247(A)
Kruger, P. Gerald (see Phillips, J. A.)—1259(A)
—— (see Smith, Lyle W.)—1258(A)
Krumbein, A. D. (see Friedland, S. S.)—1244(A)
Krumhansl, J. A. (see Beyer, R. T.)—1206(A)
Kryder, S. J. (see Lyons, Harold)—1210(A)
Kuder, M. (see Golian, S. E.)—1215(A)
Kundu, D. N. and M. L. Pool. Tc^{92} and Tc^{93} by relative cross-section measurements—1775
—— **and M. L. Pool.** Use of enriched molybdenum in cross-section measurements of the (p,n): (p,γ) and (d,n): $(d,2n)$ reactions—1574
Kunkel, Wulf. Factors affecting the determination of particles size by the Hopper-Laby Stokes' law method—1557(A)
Kurbatov, J. D. (see Yu, Fu-Chun)—34, 114(T)
Kurie, Franz, N. D. (see Burling, R. L.)—109(L)
—— **and M. Ter-Pogossian.** Some measurements of gamma-ray energies—677
Kusch, P. Intrinsic magnetic moment of the electron—1203(T)
—— **and H. M. Foley.** Magnetic moment of the electron—250

Ladenburg, R., J. Winckler, and C. C. Van Voorhis. Erratum: Interferometric studies of faster-than-sound phenomena. Part I. The gas flow around various objects in a free, homogeneous, supersonic air stream—1884(L)
—— (see Bershader, D.)—1229(A)
——, **C. C. Van Voorhis, and J. Winckler.** Supersonic, intermittent, movable wind tunnel for optical studies—1229(A)
Lagemann, R. T., John Evans, and Newton Underwood. Ultrasonic velocity in some liquid fluoro-carbons—124(A)
Lamb, W. A. and F. W. Brown, III. Fading of the latent image in nuclear emulsions—104(L)
Lamb, W. E. Fine structure of the hydrogen atom by a microwave method—1203(T)
Lamont, H. R. L. Atmospheric absorption of microwaves—353(L)
Lampi, Eugene E. (see Blair, J. Morris)—553, 1594, 1599, 1205(A), 1259(A)
—— (see Sleator, William, Jr.)—1260(A)
Lander, J. J. Measurements of Thomson coefficients for metals at high temperatures and of Peltier coefficients for solid-liquid interfaces of metals—479
Lane, C. T. (see Fairbank, Henry A.)—345(L)
Langer, A. (see Fox, R. E.)—1222(A)
Langer, Lawrence M. (see Cook, C. Sharp)—227(L), 502(L), 548, 1241(A)
——, **C. Sharp Cook, and H. Clay Price, Jr.** Beta-spectrum of C^{14}—1263(A)
Langer, R. M. and Herman Yagoda. Interpretation of dual cosmic-ray events—1238(A)
Langmuir, R. V. Radioactive potassium—1559(A)
—— (see Elder, F. R.)—52
Langsdorf, Alexander S., Jr. Oscillatory method for measuring neutron cross sections by the effect on the reactivity of a chain-reacting pile—1216(A)
—— (see Harris, S. P.)—1216(A)
Lanzl, L. H., J. S. Laughlin, and L. S. Skaggs. Method of measuring ratio of Bremsstrahlung cross sections—1261(A)
Lark-Horovitz, K. (see Davis, R. E.)—1255(A)
LaRocque, A. P. (see Jacobs, Harold)—163
Larsh, A. E., Jr. (see Davidson, Norman)—220(L)
Lassen, N. O. Disintegration of deuterium by gamma-rays from ^{24}Na—1533(L)
Latham, R. (see Cassels, J. M.)—103(L)
LaTorre, Richard (see George, Waller)—1256(A)
Lattes, C. M. G. (see Barkas, Walter H.)—1558(A)
—— (see Bishop, A. S.)—1558(A)
—— (see Gardner, Eugene)—1236(A)
—— **and E. Gardner.** Observations of mesons produced by the 184-inch cyclotron—1555(T)
—— **and Eugene Gardner.** Production of mesons by the 184-inch Berkeley cyclotron. Part II. Mass determination—1236(A)
Lauer, James L. Refractive index of several hydrocarbons in the near ultraviolet wave-length region—1232(A)
Laughlin, J. S. (see Lanzl, L. H.)—1261(A)
Lauritsen, C. C. (see Rubin, S.)—1564(A)
—— (see Snyder, C. W.)—1564(A)
Lauritsen, T. (see Dougherty, C. B.)—712(L)
—— (see Hornyak, W. F.)—1727(L), 1565(A)
——, **C. B. Dougherty, and V. K. Rasmussen.** Gamma-radiation from $Be^9(d,n)B^{10}$—1566(A)
Lawrence, E. O. (see Knable, N.)—1217(A)

Lawson, J. L. and M. L. Perlman. Cross section for the reaction $C^{12}(\gamma,n)C^{11}$—1190(L)
Lazarus, David. Elastic constants of beta-brass—1726(L)
Lehovec, K. Photo-voltaic effect—463
Leith, C. E. (see Knable, N.)—1217(A)
Leitner, A. (see Spence, R. D.)—349(L)
Lengel, J. H. (see Bloom, Evelyn G.)—1222(A)
Leslie, J. K. (see Bernstein, S.)—1258(A)
LeVan, W. I. (see Cunningham, G. L.)—1537(L)
Levine, Harold and Julian Schwinger. On the theory of diffraction by an aperture in an infinite plane screen. I—958
—— **and Julian Schwinger.** Variational principles for diffraction problems—1212(A)
Levinstein, Henry (see Kofsky, Irving L.)—500(L)
Levy, M. G. (see Shamos, M. H.)—1237(A)
Lew, Hin. Hyperfine structure and quadrupole moment of Al^{27}—1550(L)
Liebson, S. H. Discharge spread in Geiger-Mueller counters—694(L)
Lind, David A. Protected multicellular Geiger counter for short-wave-length x-rays and gamma-rays for use in the curved crystal spectrometer—1566(A)
—— (see DuMond, Jesse W. M.)—1561(A)
—— (see Watson, Bernard B.)—1561(A)
——, **Bernard B. Watson, and Jesse W. M. DuMond.** Reflecting power of the (310) planes of a curved quartz crystal for x-rays and gamma-rays from 494 x.u. (Sn $K\alpha$ x-rays) to 30 x.u. (Au^{198} gamma-rays). Experimental results and theoretical interpretation—1561(A)
Lindhard, J. (see Horowitz, J. J.)—713
Ling, D. S. and D. L. Falkoff. Interference effects in angular correlations—1224(A)
Linz, Arthur, Jr. (see Scherrer, V. E.)—120(A)
——, **F. T. Rogers, Jr., and G. W. Crawford.** Cathode-follower type of dual-coincidence circuit—119(A)
—— **and V. E. Scherrer.** Possible method for measurement of speed of brittle fracture in steel—121(A)
Little, Charles A., Jr. Diurnal variations of meteor trails 1875(L)
Lockwood, J. A. (see McCarthy, R. L.)—1243(A)
Loeb, Leonard B. Threshold for spark development by streamer mechanism in uniform fields—210
—— (see Parker, James M.)—1557(A)
—— **and Robert A. Wijsman.** Quantitative relations for the thresholds of pre-onset positive burst pulse corona and of positive streamer advance—1556(A)
Lofgren, Edward J. (see Freier, Phyllis)—213, 1818
—— (see Frick, Walter)—1258(A)
——, **Edward P. Ney, and Frank Oppenheimer.** Data obtained from cosmic-ray cloud-chamber tracks taken at 100,000 feet—1258(A)
London, F. On the problem of the molecular theory of superconductivity—562
—— **and P. R. Zilsel.** Heat transfer in liquid helium II by internal convection—1148
Long, H. M., Jr. and R. Pepinsky. Operation of grid-controlled fine-focus x-ray tube—126(A)
Longmire, Conrad. On the virtual excited state of the Be^9 nucleus—1773
Lopes, J. Leite. On the light and heavy mesons—1722(L)
Loud, Oliver S. Physical science course—114(T)
Loughridge, D. H. (see Millican, F. M.)—66
Low Francis. On the ground state of the deuteron—1885(L)
Lowe, D. S. (see Sponer, H.)—122(A)
Lower, I. S. (see Shamos, M. H.)—1237(A)
Lowry, E. F. Long-term decay of phosphors under ultraviolet excitation—1254(T)
Luttinger, J. M. Note on the magnetic moment of the electron—893
Lyons, Harold. Microwave frequency standards—1203(T)
——, **George Birnbaum, and S. J. Kryder.** Measurements of the complex dielectric constant of gases at microwaves—1210(A)
Lyons, W. James and Irven B. Prettyman. Method for the absolute measurement of dynamic properties of linear structures at sonic frequencies—114(T)

Ma, S. T. and F. C. Yu. Erratum: electromagnetic properties of nuclei in the meson theory—500(L)
Mack, J. E. Prospective means for studying the solar and coronal spectra in the vacuum ultraviolet—1208(A)
—— **and N. Austern.** Electromagnetic shift of S levels in He II—1262(A)
MacKenzie, K. R. Wide range frequency modulation—104(L)
Macklin, R. L. (see Knight, G. B.)—1540(L)
Madsen, C. B. and P. Venkateswarlu. Energy straggling of protons—1782
—— **and P. Venkateswarlu.** Proton stopping power of solid beryllium—648
Majumdar, R. C. and A. S. Apte. Meson field and equations of motion of point particles—538
Maloof, M. (see Rado, G. T.)—1206(A)
Mandeville, C. E. (see Scherb, M. V.)—508(L), 1248(A)
—— **and M. V. Scherb.** Coincidence investigation of lanthanum (140)—1251(A)
—— **and M. V. Scherb.** Radiations from columbium (95)—1266(A)
—— **and M. V. Scherb.** Radiations from gold (199)—1565(A)
—— **and M. V. Scherb.** Study of the radiations of two radioactive isotopes of iridium—1250(A)
——, **M. V. Scherb, and W. B. Keighton.** Radiations from platinum (193) and gold (199)—601
——, **M. V. Scherb, and W. B. Keighton.** Study of the radiations from columbium (95), rhenium (188), osmium (191), and osmium (193)—888
Manfredi, U. (see Belock, H.)—1230(A)
Manfredini, A. (see Bernardini, G.)—845(L)
Manfredini, M. (see Bernardini, G.)—1878(L)
Mann, W. B. (see Hawkings, R. C.)—696(L)
Manring, Edward R., John R. Zimmerman, and Dudley Williams. Variation of the nuclear resonance experiment—1263(A)
Marcus, Paul M. Rigorous expansions of the acoustic radiation field on a vibrating piston in a baffle—1228(A)
—— (see Maxwell, E.)—1234(A)

Margenau, H. Erratum: Theory of high frequency discharges. IV—706(L)
Mariani, Jean. Unitary field theory and cosmic magnetism —1265(A)
Marinelli, L. D. and G. J. Hine. Gamma-ray isodosimeter —1245(A)
Markham, J. J. (see Miller, P. H., Jr.)—1218(A)
—— **and Frederick Seitz.** Binding energy for a self-trapped electron in NaCl—1014
Markstein, George H. Application of the image converter tube as electronic stroboscope—1230(A)
Marlow, Douglas, C. R. Nisewanger, and W. M. Cady. Method for the instantaneous measurement of velocity and temperature in high speed air flow—1228(A)
Marshall, J. F. (see Guth, E.)—834(L)
Marshall, L. Angular distribution of α's coincident with U^{235} fission—1259(A)
Marvin, Robert S., Edwin R. Fitzgerald, and John D. Ferry. Twin transducer for measuring mechanical properties of rubberlike solids at audiofrequencies—1256(A)
Masi, J. F. Heats of vaporization of uranium hexafluoride —1220(A)
Mason, F. D. (see Stephenson, S. T.)—1560(A)
Mason, R. C. Adsorption of mercury by activated carbon—1220(A)
Mason, W. P. Electrostrictive effect in barium titanate ceramics—1134
——, **W. O. Baker, H. J. McSkimin, and J. H. Heiss.** Errata and addenda: Mechanical properties of long chain molecule liquids at ultrasonic frequencies—1873(L)
—— **and B. T. Matthias.** Theoretical model for explaining the ferroelectric effect in barium titanate—1622
Mather, K. B. (see Keller, K. K.)—624(L)
Matossi, Frank and Robert Mayer. Extension of the polarizability theory of Raman effect—449
Matthias, Bernd T. (see Danielson, Gordon C.)—986(L)
—— (see Mason, W. P.)—1622
—— (see Richardson, John M.)—987(L)
Mautz, C. W., F. W. Geiger, and H. T. Epstein. On the investigation of supersonic flow patterns by means of the shock tube—1872(L)
Mayar, C. H. (see Schulkin, M.)—840(L)
Mayer, Maria G. On closed shells in nuclei—235
Mayer, Robert (see Matossi, Frank)—449
Maxwell, E., P. M. Marcus, and J. C. Slater. Surface impedance of tin at 24,000 mc/sec.—1234(A)
Maxwell, Howard N. (see Green, J. B.)—1208(A)
McCarthy, R. L., J. A. Lockwood, P. J. Rice, and H. L. Schultz. Two cavity operations of Yale linear electron accelerator—1243(A)
McCay, M. S. Reversal of secondary series—122(A)
McClure, F. T. (see Foner, S. N.)—1222(A)
McClure, Gordon W. (see Groetzinger, Gerhart)—341
McCormack, R. L., J. Cardell, and W. B. Nottingham. Pulsed emission correlated with low temperature direct-current emission properties of certain oxide-coated cathodes—1204(T)
McCown, D. A. (see Woodward, L. L.)—761, 870, 1263(A)
——, **L. L. Woodward, and M. L. Pool.** Radioactive arsenic isotopes—1315
——, **L. L. Woodward, and M. L. Pool.** Radioactive isotopes of Ga and Ge—1311
——, **L. L. Woodward, M. L. Pool, and H. L. Finston.** Radioactive Ga^{67}, Ge^{69}, As^{73}, and As^{74}—1248(A)
——, **L. L. Woodward, M. L. Pool, and H. L. Finston.** Radioactive isotopes of germanium and arsenic—1263(A)
McCoy, R. (see Belock, H.)—1230(A)
McDaniel, B. D. (see Walker, R. L.)—315
McElhinney, J., A. O. Hanson, and R. B. Duffield. Thresholds for some photo-nuclear reactions—1257(A)
McGinnis, C. L. (see Helmholz, A. C.)—1559(A)
McGowan, F. K. (see DeBenedetti, S.)—728
McInteer, B. B. (see Fairbank, Henry A.)—345(L)
——, **L. T. Aldrich, and Alfred O. Nier.** Concentration of He^3 by thermal diffusion—946
McKay, Kenneth G. Electron bombardment conductivity in diamond—1606
McKinley, William A., Jr. and Herman Feshbach. Coulomb scattering of relativistic electrons by nuclei—1759
McMath, Robert R. (see Goldberg, Leo)—1881(L)
—— (see Mohler, Orren C.)—352(L)
——, **Orren C. Mohler, and Leo Goldberg.** Abundance and temperature of methane in the earth's atmosphere—623(L)
McMillan, D. R., Jr. and W. E. Woolf. Temperature coefficient of ultrasonic velocity—124(A)
McMillan, Edwin M. Survey of recent work at the radiation laboratory in Berkeley—1204(T)
—— (see Chupp, W. W.)—1217(A)
McMillen, J. Howard and R. L. Kramer. High velocity particles produced at impact—1882(L)
McQueen, J. H., J. W. Beams, and L. B. Snoddy. Light scattering in supersonic streams—1551(L)
McSkimin, H. J. (see Mason, W. P.)—1873(L)
Medicus, H., A. Mukerji, P. Preiswerk, and G. de Saussure. Disintegration of Tc^{95} and Tc^{96}—839(L)
Meers, J. T. and L. A. Parduo. Knudsen type vacuum gauge—119(A)
Meggers, W. F. Spectrum lines of Hg 198 as standards of length—1203(T)
Meinke, W. W. (see Ghiorso, A.)—695(L)
Meissner, K. W., L. G. Mundie, and P. H. Stelson. Structure of the ^2D-terms of Li^7—1262(A)
——, **L. G. Mundie, and P. H. Stelson.** Structure of the ^2D terms of the arc spectrum of lithium—932
Melander, Lars and Hilding Slätis. Preparation and radiation of U^{237}—709(L)
Melchor, J. L. (see Parker, J. P.)—121(A)
Mendenhall, H. E. Secondary emission from thoria on platinum and tantalum—1265(A)
Meneghetti, David (see Sidhu, S. S.)—222(L)
—— (see Winsberg, Lester)—1216(A)
Menius, A. C., Jr. and T. J. Turner. Crystal "growth" in the electron microscope—125(A)
Merritt, F. R. (see Townes, C. H.)—1113

Metzger, Franz (see Deutsch, Martin)—1542(L)
—— **and Martin Deutsch.** Disintegration scheme of I^{131}—1640
Meyer, C. F. (see Herman, R. C.)—1242(A)
Meyer, H. A. Theory of internal conversion—979(L)
——, **G. Schwachheim, and Andrea Wataghin.** On the production of showers of penetrating particles—846(L)
Meyer, Lothar (see Band, William)—386, 1235(A)
—— **and William Band.** Relaxation and heat conductivity in liquid helium II—1235(A)
—— **and William Band.** Relaxation theory of thermal conduction in helium II—394
Meyerhof, Walter E. Notes on the beta-spectra of Y^{90} and Sr^{90}—621(L)
—— **and M. Goldhaber.** Notes on the beta-ray spectra from copper 64—348(L)
Michels, Walter C. and Louise Gaus. Temperature dependence of the long period. Phosphorescence of zinc silicate—1241(A)
—— **and Esther D. Redding.** Improved lock-in amplifier—1562(A)
Migeotte, Marcel V. Lines of methane at 7.7μ in the solar spectrum—112(L)
Mihelich, J. W. (see Hill, R. D.)—1874(L)
Miles, John W. On vector transforms—1531(L)
Miller, A. R. (see Daunt, J. G.)—842(L)
Miller, D. R., R. C. Thompson, and B. B. Cunningham. Products of high energy deuteron and helium ion bombardments of copper—347(L)
Miller, David C. Effect of the piezoelectric properties of a crystal on diffuse x-ray reflections—166
Miller, L. C. (see Snell, H.)—1217(A)
Miller, P. H., Jr. and J. J. Markham. Work function and semiconductors at high temperatures—1218(A)
Miller, Walter C. (see Waldman, Bernard)—1225(A)
Millett, Walter E. Focusing in crossed fields of charged particles at relativistic energies—1058
Millican, F. M. and D. H. Loughridge. Mass temperature coefficients of cosmic-ray components—66
Millikan, R. A. Why my stork chose 1868—1204(T)
Mills, M. M. Altitude dependence of Auger showers—1555(A)
Miskel, John A. (see Katcoff, Seymour)—631, 1225(A)
Mitchell, Allan C. G. (see Schelberg, A. D.)—1239(A)
—— (see Zaffarano, Daniel J.)—105(L), 682
Mitra, S. K. Active nitrogen—1637
Mizushima, Masataka. On the ammonia molecule—705(L)
Moak, C. D. (see Hoover, J. I.)—864
—— **and J. W. T. Dabbs.** Cloud-chamber measurements of cadmium capture gamma-rays—1249(A)
Mock, Dana L., Ramond C. Waddel, Lawrence W. Fagg, and Ralph A. Tobin. Photo-induced reactions at 20 Mev—1536(L)
Moe, David (see Owen, George E.)—1879(L)
Mohler, Fred L. (see Bloom, Evelyn G.)—1222(A)
Mohler, Orren C. (see Goldberg, Leo)—1881(L)
—— (see McMath, Robert R.)—623(L)
—— **and W. S. Benedict.** Atmospheric absorption of water vapor between 1.42μ and 2.50μ—702(L)
——, **Leo Goldberg, and Robert R. McMath.** Spectroscopic evidence for ammonia in the earth's atmosphere—352(L)
Molineux, C. E. (see Ramsay, B. P.)—118(A)
Molnar, J. P. and J. A. Hornbeck. Cathode-emission processes in Townsend discharges—1254(T)
Montgomery, C. G. Cosmic-ray showers at low altitudes—354(T)
Moore, D. B. and W. N. English. Point-to-plane impulse corona—1557(A)
Morganstern, K. H., C. L. Cowan, and A. L. Hughes. Note on ethylene self-quenching G-M counters—499(L)
Morris, Peter A., W. F. G. Swann, and H. C. Taylor. Sea level latitude effect of cosmic radiation—1102
Morrish, A. H. (see Allen, James S.)—1224(A)
—— **and J. S. Allen.** Performance of the Allen type multiplier tube for lithium ion counting—1260(A)
Morrison, Adair and Eric Pickup. Primary and secondary meson event in photographic emulsions—706(L)
Morrison, H. L. New data on convection in sands—119(A)
Morrison, P. Nuclear magnetic moments and meson exchange—1224(A)
Moshinsky, Marcos and E. P. Wigner. Boundary conditions as relativistic interaction—1212(A)
Motta, E. E. and G. E. Boyd. Characterization of Tc activities produced by deuteron bombardment of separated Mo isotopes—220(L)
—— **and G. E. Boyd.** Long-lived Tc activities produced by deuteron bombardment of separated Mo isotopes—344(L)
Motz, H. T. (see Humphreys, R. F.)—1232(A)
—— **and R. F. Humphreys.** $Na^{23}(\alpha p)Mg^{26}$ reaction—1232(A)
Moyer, B. J. (see Knable, N.)—1217(A)
Muehlhause, C. O. (see Burson, S. B.)—1264(A)
—— (see Goldhaber, M.)—1248(A), 1877(L)
Muether, H. R. (see Sherr, R.)—1239(A)
Mukerji, A. (see Medicus, H.)—839(L)
Mullaney, J. F., F. Reines, and H. G. Weiss. Excitation time of silver-activated zinc sulfide on electron bombardment—491(L)
Mulliken, Robert S. Molecular orbital method and molecular ionization potentials—736
Mullin, Charles J. (see Guth, Eugene)—832(L), 833(L), 834(L)
Mundie, L. G. (see Meissner, K. W.)—932, 1262(A)
Murakawa, K. and S. Suwa. Isotope effects in the spectrum of Ne II—1535(L)
Mutter, W. E. (see Nottingham, W. B.)—1261(A)
Myers, V. and A. Wattenberg. "Cross-over" transitions in gamma-ray spectra—1264(A)

Nafe, John E. Hyperfine structure of hydrogen and deuterium—1203(T)
—— (see Nelson, Edward B.)—1210(A)
Nelson, Edward B. and John E. Nafe. Comparison of the g value of the electron in hydrogen and deuterium—1210(A)
Nelson, R. C. and W. S. Benedict. Absorption of water vapor between 1.34μ and 1.97μ—703(L)

Nereson, Norris G. Disintegration of mesotrons in B^{10}—509(L)
Newton, R. R. and C. Kittel. Proposal for determining the thickness of the transition layer between ferromagnetic domains by a neutron polarization experiment—1604
Ney, Edward P. (see Freier, Phyllis)—213, 1818
—— (see Frick, Walter)—1258(A)
—— (see Lofgren, Edward J.)—1258(A)
Nicodemus, D. (see Bloch, F.)—1025
Nielsen, Alvin H. (see Talley, Robert M.)—123(A)
Nier, Alfred O. C. Mass spectrometry—1254(T)
—— (see Aldrich, L. T.)—876, 1590, 1225(A)
—— (see Fairbank, Henry A.)—345(L)
—— (see McInteer, B. B.)—946
Nierenberg, W. A. and M. Slotnick. Note on the stark effect in diatomic molecules—1246(A)
Nisewanger, C. R. (see Marlow, Douglas)—1228(A)
Nordheim, L. W. (see Richards, James A.)—1106
Nordsieck, A. T. (see Adams, G. D.)—1255(T)
Norris, L. D. and Arthur H. Snell. Some notes on radioactive carbon of high specific activity—1240(A)
Nottingham, W. B. (see McCormack, R. L.)—1204(T)
—— **and W. E. Mutter.** Photoelectric technique for spectral emissivity determination illustrated by results on tungsten—1261(A)

O'Connor, P. R. and G. T. Seaborg. High energy spallation and fission products of uranium—1189(L)
Olsen, L. O. (see Smith, C. S.)—114(T)
Omer, Guy C., Jr. Non-homogeneous cosmological model with a finite cosmological constant—1564(A)
Onsager, L. and J. E. Robinson. De Haas-van Alphen effect in zinc—1235(A)
Opinsky, A. and R. Smoluchowski. Clustering phenomena in solid solution—343(L)
Oppenheimer, Frank (see Freier, Phyllis)—213, 1818
—— (see Frick, Walter)—1258(A)
—— (see Lofgren, Edward J.)—1258(A)
O'Reilly, J. and R. F. Christy. Energy production in the sun—1559(A)
Osborne, Robert K. (see Berggren, Jane L.)—1240(A)
Owen, G. E. Physical properties of water substance near the critical temperature—114(T)
—— (see Braden, C. H.)—1539(L)
—— (see Townsend, J.)—99(L)
——, **David Moe, and C. Sharp Cook.** Evidence for a complex disintegration of I^{131}—1879(L)
—— **and H. Primakoff.** Relation between apparent shapes of monoenergetic conversion lines and of continuous β-spectra in a magnetic spectrometer—1406

Pake, G. E. and H. S. Gutowsky. Nuclear relaxation in ice at −180°C—979(L)
—— **and E. M. Purcell.** Line shapes in nuclear paramagnetism—1184
Paneth, H. R. (see Allen, James S.)—1224(A)
Panofsky, Wolfgang K. H. Detection of light and heavy mesotrons outside the tank of the 184-in. cyclotron—1558(A)
—— (see Phillips, Robert)—1560(A)
—— **and Robert Phillips.** Evidence for a p, d reaction in carbon—1732(L)
Pardue, L. A. (see Flanary, H. G.)—125(A)
—— (see Hoover, J. I.)—864
—— (see Meers, J. T.)—119(A)
Pardue, T. E. (see Jarrell, H. A.)—121(A)
—— (see Parker, J. P.)—121(A)
Parker, J. P., T. E. Pardue, and J. L. Melchor. Failure of metals subjected to repeated plastic strains—121(A)
Parker, James M. and Leonard B. Loeb. Potential and field distribution in the hemispherically capped cylindrical point to plane corona gap—1557(A)
Parker, W. L. and J. J. Dropkin. Stimulated phosphorescence and photo-conductivity of infra-red phosphors—1242(A)
Parnell, Jack L. and Joseph W. Straley. Infra-red spectrum of HCl in solution with dioxane, di-ethyl ether, and ethyl acetate—123(A)
Parzen G. and L. I. Schiff. Short range repulsion as a mechanism for nuclear saturation—1564(A)
Pauls, F. B. (see Flanary, H. G.)—125(A)
Peacock, Charles L. (see Wilkinson, Roger G.)—1250(A)
—— **and Roger G. Wilkinson.** Disintegration of Sc^{46}—1240(A)
—— **and Roger G. Wilkinson.** Disintegration of scadium[46], gold[198], and tungsten[185,187]—297
Pearce, Willard J. (see Winans, J. Gibson)—1262(A)
Pearson, G. L. (see Shockley, W.)—232(L)
Peaslee, D. C. $d-p$ and $d-n$ cross sections—1223(A)
—— Deuteron-induced reactions—1001
Peck, R. A., Jr. $Al^{27}(dn)$ reaction—1233(A)
Pekeris, C. L. Stability of the laminar parabolic flow of a viscous fluid between parallel fixed walls—191
Pell, E. M. and D. H. Tomboulian. Response of certain inorganic phosphors in the extreme ultraviolet region—1242(A)
Pellam, J. R. Pulsed second sound in liquid helium II—841(L)
Pensak, L. Conductivity induced in thin insulating films by electron bombardment—1204(T)
Pepinsky, R. (see Jarmotz, P.)—126(A)
—— (see Long, H. M., Jr.)—126(A)
—— (see Sayre, D.)—127(A)
—— **and D. Sayre.** Quantitative determination of electron densities and contour line delineation in the Auburn electronic Fourier synthesizer for crystal structure analyses—126(A)
Perlman, I. (see Chubbuck, J. B.)—982(L)
——, **A. Ghiorso, and G. T. Seaborg.** Alpha-decay systematics of the heavy elements—1730(L)
Perlman, M. L. (see Lawson, J. L.)—1190(L)
—— **and G. Friedlander.** Relative yields of some x-ray induced nuclear reactions—442
Perlow, G. J., E. Krause, and C. Schroeder. Rocket borne cloud chamber II—1215(A)
Peters, B. (see Bradt, H. L.)—1828
—— (see Freier, Phyllis)—213
Peterson, Jack M. (see Bockhop, Dorothy)—1559(A)

Petree, B. (see Henkel, R. L.)—1260(A)
Phillips, G. C. (see Bonner, T. W.)—1227(A)
Phillips, J. A. and P. Gerald Kruger. Preliminary data on the production of ± electron pairs in the field of an electron—1259(A)
Phillips, Robert (see Panofsky, Wolfgang K. H.)—1732(L)
—— **and Wolfgang K. H. Panofsky.** Excitation curves of $C^{12}(p, pn)C^{11}$ and $B^{11}(p, n)C^{11}$ up to 32 Mev—1560(A)
Piccioni, Oreste. Search for photons from meson-capture—1754
—— Search for photons from stopped mesons—1236(A)
Pickup, Eric. Production of Li^6 in boron-loaded photographic emulsions—495(L)
—— (see Morrison, Adair)—706(L)
Pieper, A. G. (see Hammer, C. F.)—1262(A)
Pietenpol, William J., John D. Rogers, and Dudley Williams. Saturation effects in microwave spectra—1246(A)
Pippard, A. B. (see Daunt, J. G.)—842(L)
Plumb, Harmon (see Bockstahler, Lester I.)—1235(A)
Plyler, E. K. and S. L. Kruegel. Infra-red absorption spectra of ethyl and of *n*-propyl alcohol—1247(A)
Pobereskin, M. (see Katzin, Leonard I.)—264
Pollard, Ernest and David E. Alburger. Large-angle scattering of Na^{24} gamma-radiation—926
——, **V. L. Sailor, and L. D. Wyly.** Energy levels of Al 28 and Mg 25—1233(A)
Pollock, H. C. (see Elder, F. R.)—52
Pomerance, H. (see Hoover, J. I.)—864
Pontecorvo, B. (see Hincks, E. P.)—697(L)
—— (see Kirkwood, D. H. W.)—497(L)
Pool, M. L. (see Eggen, D. T.)—57, 1248(A)
—— (see Gunlock, H. F.)—1264(A)
—— (see Krisberg, N. L.)—44, 1249(A)
—— (see Kundu, D. N.)—1569, 1775
—— (see McCown, D. A.)—1311, 1315, 1248(A), 1263(A)
—— (see Woodward, L. L.)—761, 870, 1263(A)
Poole, J. H. J. and J. W. Bremner. Emission of alpha-particles from the different faces of a radioactive crystal—836(L)
Post, R. F. Wave guide fast counter—1560(A)
—— (see Hansen, W. W.)—1560(A)
Pound, R. V. Erratum: On the nuclear moments of I^{127}, Ga^{69}, Ga^{71}, and P^{31}—228(L)
—— Structure of nuclear resonance absorption lines in crystals—1203(T)
Powell, J. L. On the Compton effect for protons—1258(A)
—— (see Sachs, R. G.)—1258(A)
Powell, R. W. (see Borst, L. B.)—1883(L)
Powell, W. M. Cloud-chamber measurements of recoil protons in the neutron beam of the 184-inch cyclotron—1555(T)
Preiswerk, P. (see Medicus, H.)—839(L)
Preston, W. M. (see DeBenedetti, S.)—1645
Prettyman, Irven B. (see Lyons, W. James)—114(T)
Price, H. Clay, Jr. (see Cook, C. Sharp)—502(L), 548
—— (see Langer, Lawrence M.)—1263(A)
Prim, R. C. Family of rotational corner flows—1563(A)
Primakoff, H. On γ-induced β-disintegration: Theoretical—110(L)
—— On the momentum distribution of the decay electrons from negative mesons—878
—— (see Owen, G. E.)—1406
Probst, R. E. (see Daunt, J. G.)—495(L)
Purcell, E. M. (see Pake, G. E.)—1184

Quercia, I. F., B. Rispoli, and S. Sciuti. About the positive excess of the hard component of cosmic-ray—1728(L)
Quevedo, José L. García and William V. Smith. Frequency stabilization of microwave oscillators by spectrum lines—123(A)

Rabi, I. I. Recent experiments on the dynamics of the electron in atoms—1555(T)
Rado, G. T., M. Maloof, and H. Rosenblatt. Effect of surface treatment on complex permeability—1206(A)
Rainwater, L. J. (see Havens, W. W., Jr.)—1216(A)
—— (see Wu, C. S.)—1248(A)
Ramsay, B. P., J. H. Buehler, and C. E. Molineux. Controls for generators of influence signals—118(A)
Ramsay, Norman F. Effect of large quadrupole interactions on nuclear radiofrequency spectra at twice Larmor frequency—286
Randolph, M. L. Sampling specimens from an ultracentrifuge by quick freezing—118(A)
Rappaport, George. Specular infra-red spectral reflectance for the analysis of organic materials—115(A)
Rarita, William. Deuteron and triton methods—1799
—— Some deuteron variational methods—1222(A)
Rasmussen, V. K. (see Dougherty, C. B.)—712(L)
—— (see Lauritsen, T.)—1566(A)
Rayski, Jerzy. Negative energies in generalized electrodynamics—629(L)
Redding, Esther D. (see Michels Walter C.)—1562(A)
Reekie, James and T. S. Hutchison. Effect of cold working on the magnetic properties of pure metals—610
Reines, F. Neutron spectra from proton recoils in photographic emulsions—1565(A)
—— (see Mullaney, J. F.)—491(L)
Reynolds, Charles A. (see Fairbank, Henry A.)—345(L)
Reynolds, G. T. and W. D. Hardin. Penetrating power of extensive shower particles—1549(L)
Reynolds, S. E. (see Workman, E. J.)—709(L), 1231(A)
—— **and E. J. Workman.** Small generating voltmeter and generating electrometer—1231(A)
Rhodes, J. E., Jr. Device for determining particle size distribution in smokes—124(A)
Rice, P. J. (see McCarthy, R. L.)—1243(A)
Richards, H. T. (see Baskin, S.)—1260(A)
—— (see Smith, R. V.)—1257(A), 1871(L)
—— **and R. V. Smith.** Argon and neon (*pn*) thresholds—1870(L)
—— **and R. V. Smith.** Proton-neutron thresholds in Cl^{37} and K^{41}—1257(A)
Richards, James A., Jr. and L. W. Nordheim. Energy distribution in cosmic-ray showers—1106
Richards, Paul I. Notes on Feenberg's series—Rearrangements—835(L)
Richardson, J. M. On a course-grained density in phase space and its relation to transport phenomena—1214(T)

Richardson, J. Reginald. Lifetime of the heavy meson—1720
Richardson, John M. (see Danielson, Gordon C.)—986(L)
—— **and Bernd T. Matthias.** Theory of the dielectric behavior of $BaTiO_3$—987(L)
Ring, Harold (see Gordy, Walter)—1191(L)
—— (see Smith, A. G.)—123(A), 370
Rispoli, B. (see Quercia, I. F.)—1728(L)
Ritland, H. N. (see Kaesberg, Paul)—71, 1255(A)
Rivier, D. and E. C. G. Stueckiberg. Convergent expression for the magnetic moment of the neutron—218(L); Erratum—986(L)
Robertson, J. H. (see Deal, L. J.)—127(A)
Roberts, Arthur. Nuclear spins and moments obtained from microwave spectra—1254(T)
Robinson, C. V. Neutral region in the space charge of a self-quenching G-M counter—1261(A)
Robinson, J. E. (see Onsager, L.)—1235(A)
Rogers, F. T., Jr. Considerations on the use of field-deflections for determining the mass of the meson—128(A)
—— Quantitative data from a slow-bend test of mild steel—122(A)
—— (see Auld, Mary Jane)—128(A)
—— (see Barlow, J. S.)—700(L)
—— (see Byatt, W. J.)—121(A), 699(L)
—— (see Caldwell, E. E.)—120(A)
—— (see Crawford, G. W.)—118(A)
—— (see Jenkins, G. L.)—120(A)
—— (see Jones, Emily)—122(A)
—— (see Linz, Arthur, Jr.)—119(A)
—— (see Scherrer, V. E.)—119(A)
—— (see Waltner, Arthur)—699(L)
Rogers, John D. (see Pietenpol, William J.)—1246(A)
Rogers, Marguerite M. Creeping cracks in slow-bend fracturing of mild steels—121(A)
—— Strain-aging effects in the slow-bend fracturing of mild steels—122(A)
Rohrlich, F. Classification of the odd terms of Ti I—1381
—— On the configuration of d^2sp, d^3p, and d^7p—1372
Rollefson, R. (see Hammer, C. F.)—1262(A)
Rollin, B. V. and J. Hatton. Concentration of He^3 by evaporation of liquid helium at temperatures below the λ-point—508(L)
—— **and J. Hatton.** Nuclear paramagnetism at low temperatures—346(L)
Rose, M. E. and M. M. Shapiro. Statistical error in absorption experiments—1853
—— **and M. M. Shapiro.** Statistical error in transmission measurements—1213(A)
Rosen, Nathan. Composite particles—128(A)
Rosenbaum, Alma (see Rusk, Rogers D.)—110(L)
—— **and Rogers D. Rusk.** Effects of absorption and scattering of mesons on coincidence-anticoincidence counts—354(A)
Rosenblatt, H. (see Rado, G. T.)—1206(A)
Rossi, Bruno. Interpretation of cosmic-ray phenomena—354(T)
—— (see Bridge, H. S.)—1083
Rothstein, Jerome. Errata and addendum: On the mechanism of electron emission at the cathode spot of an arc—228(L)
Roy, R. R. (see Champion, F. C.)—5
Ruark, Arthur E. Formation of spiral marks on fractures—120(A)
Rubin, S. (see Snyder, C. W.)—1564(A)
——, **C. W. Snyder, C. C. Lauritsen, and W. A. Fowler.** Inelastic scattering of protons from Li^7—1564(A)
Rusinow, K. (see Dailey, B. P.)—1245(A)
Rusk, Rogers D. (see Rosenbaum, Alma)—354(A)
—— **and Alma Rosenbaum.** Attempt to detect neutral particles produced by exchange of charge with cosmic-ray mesons—110(L)
Russek, A. (see Shamos, M. H.)—1545(L)
Russell, B. R. (see Isenberg, I.)—1255(A)
Russell, Henry Norris. Configurations of the low terms of Ti II—689

Sachs, R. G. Exchange currents in nuclei—1223(A)
—— Interpretation of the magnetic moments of light nuclei—1255(T)
—— Phenomenological theory of exchange currents in nuclei—433
—— (see Avery, R.)—1320
—— **and J. L. Powell.** On the Bremsstrahlung produced by protons—1258(A)
Saibel, Edward. Theoretical approach to the strength of materials under cyclic loading—1220(A)
Sailor, V. L. (see Pollard E.)—1233(A)
Sala, O. (see Herb, R. G.)—1256(A)
——, **P. Axel, and M. Goldhaber.** Internal conversion electrons accompanying slow neutron capture in Gd—1249(A)
—— **and R. G. Herb.** Design of electrostatic generator for the University of São Paulo, Brazil—1260(A)
Salant, E. O., J. Hornbostel, and E. M. Dollmann. Tracks in emulsions at 100,000 feet—694(L)
Sampson, M. B. (see Cook, C. S.)—502(L)
—— (see Schelberg, A. D.)—1239(A)
Sanderson, J. A., J. A. Curcio, and Dorothy V. Estes. Photoelectric pyrometer for the measurement of luminous flame temperatures—1221(A)
Sands, Matthew. Slow mesons in the atmosphere—1237(A)
Sard, R. D. and E. J. Althaus. Search for delayed photons from stopped sea-level cosmic-ray mesons—1364
—— **and A. H. Benade.** Time distribution of decay electrons from mesons stopped in magnesium at 3500-m altitude—1237(A)
——, **W. B. Ittner III, A. M. Conforto, and M. F. Crouch.** Evidence for neutrons associated with the stopping of sea level mesons in lead—97(L)
Saxton, D. Beta-spectrum of $Hg^{(\frac{203}{205})}$—849(L)
—— Beta-spectra of W^{185} and Os^{191}—1264(A)
Sayre, D. (see Pepinsky, R.)—126(A)
—— **and R. Pepinsky.** Photoelectric two-dimensional Fourier analyzer—127(A)
Scharff-Goldhaber, G. (see Friedlander, G.)—981(L)

Schein, Marcel. Problem of low energy mesotrons in the cosmic radiation—1555(T)
Schelberg, A. D., M. B. Sampson, and A. C. G. Mitchell. Method for measuring short period activities—1239(A)
Schenck, J. (see Winckler, J. R.)—837(L)
Scherb, M. V. (see Mandeville, C. E.)—601, 888, 1250(A), 1251(A), 1266(A), 1565(A)
—— **and C. E. Mandeville.** Beta-beta-coincidence curves for Ir^{192} and Ta^{182}—508(L)
—— **and C. E. Mandeville.** Radiations from the long period activity of zirconium—1248(A)
Scherrer, Victor E. (see Linz, Arthur, Jr.)—121(A)
—— **and Arthur Linz, Jr.** Speed of propagation of fractures in glass plates—120(A)
—— **and F. W. Rogers, Jr.** Incremental regulation by carbon-pile type of voltage-regulator—119(A)
—— **and Joseph W. Straley.** Conditions for brittle fracture of mild steel—121(A)
Schiff, L. I. Capture of sea-level negative mesons by nuclei—1556(A)
—— (see Parzen, G.)—1564(A)
Schönberg, Mario. Elimination of divergences in the meson theory. I—748
—— Quantum theory of the point electron. I—738
Schroeder, C. (see Perlow, G. J.)—1215(A)
Schulkin, M., F. T. Haddock, K. M. Decker, C. H. Mayar, and J. P. Hagen. Observation of a solar noise burst at 9500 Mc/sec. and a coincident solar flare—840(L)
Schultz, H. L. (see McCarthy, R. L.)—1243(A)
Schwachheim, G. (see Meyer, H. A.)—846(L)
Schwarz, Guenter and J. A. Bearden. Determination of h/e by x-rays—1209(A)
Schweinler, H. C. (see Weinberg, A. M.)—851
Schwinger, Julian. Invariant quantum electrodynamics—1212(A)
—— Quantum electrodynamics: I. A covariant formulation—1439
—— (see Feshbach, H.)—1223(A)
—— (see Levine, Harold)—958, 1212(A)
Sciuti, S. (see Quercia, I. F.)—1728(L)
Scott, E. J. Beta-ray spectrum of P^{32}—1240(A)
Scott, W. T. (see Goudsmit, S. A.)—1537(L)
Seaborg, G. T. (see Ghiorso, A.)—695(L)
—— (see O'Conner, P. R.)—1189(L)
—— (see Perlman, I.)—1730(L)
Segrè, Emilio. Experiments on high energy neutron-proton scattering—1204(T)
Seitz, Frederick. On the theory of vacancy diffusion in alloys—1513
—— (see Falk, C. E.)—1226(A)
—— (see Markham, Jordon J.)—1014
Serber, R. Interpretation of the radiation laboratory meson experiments—1555(T)
Setlow, R. B. High energy states of N_2^+ and N_2—153
Seyfert, C. K. Densely crowded group of galaxies in Serpens—129(A)
Shamos, M. H., M. G. Levy, and I. S. Lower. On the energy dependence of the positive meson excess—1237(A)
—— **and A. Russek.** On the range of decay electrons from mesons—1545(L)
Shapiro, M. M. (see Rose, M. E.)—1853, 1213(A)
Sharbaugh, A. Harry. Microwave determination of the molecular structure of chlorosilane—1870(L)
Sharp, D. E. (see Arner, W. J.)—116(A)
Shaw, A. E. Mass deposition of completely resolved samarium isotopes—980(L)
Shaw, C. H. (see Cooper, J. N.)—114(T)
—— **and J. N. Cooper.** Vacuum double crystal x-ray spectrometer—114(T)
Shaw, J. H., G. B. B. M. Sutherland, and T. W. Wormell. Nitroux oxide in the earth's atmosphere—978(L)
Sherr, R., H. R. Muether, and M. G. White. New 20-second activity induced in boron by high energy protons—1239(A)
Shockley, W. and G. L. Pearson. Modulation of conductance of thin films of semi-conductors by surface charges—232(L)
Shoemaker, F. C. (see Bender, R. S.)—1205(A)
Shoenberg, D. (see Daunt, J. G.)—842(L)
Shoupp, W. E. and B. Jennings. Threshold and resonances in the $C^{14}(pn)$ reaction—1233(A)
Shreffler, R. G. (see Cork, J. M.)—240, 1657, 1249(A)
Shull, C. G. (see Siegel, Sidney)—1255(A)
Shull, Franklin B. Beta-ray spectra of europium and tungsten—917
—— (see Braden, C. H.)—1539(L)
Shulman, R. G. (see Dailey, B. P.)—1245(A)
——, **B. P. Dailey, and C. H. Townes.** Preliminary analysis of the microwave spectrum of ethylene oxide—846(L)
Sidhu, S. S. (see Winsberg, Lester)—1216(A)
——, **L. Winsberg, and D. Meneghetti.** Phase of scattering of thermal neutrons by titanium—222(L)
Siegel, Sidney (see Davis, R. E.)—1255(A)
—— (see Ekstein, H.)—625(L)
—— **and C. G. Shull.** Observations on superlattices in order-disorder alloys using neutron diffraction—1255(A)
Siegert, A. J. F. (see Frerichs, Rudolf)—1875(L)
Silsbee, F. B. Absolute electrical units—1203(T)
Simmons, James W. (see Gordy, Walter)—243
—— **and Walter Gordy.** Structure of the inversion spectrum of ammonia—123(A)
——, **Walter Gordy, and A. G. Smith.** Microwave determination of the molecular structures and nuclear couplings of methyl chloride, methyl bromide, and methyl iodide—1246(A)
Simpson, J. A., Jr. Neutron densities in the atmosphere as a function of latitude and altitude—1214(A)
Singer, S. F. Density spectrum and latitude dependence of extensive air showers at sea level—1214(A)
—— On the lateral extension of Auger showers—844(L)
Skaggs, L. S. (see Lanzl, L. H.)—1261(A)
Slack, C. M., L. F. Ehrke, C. Zavales, D. Dickson, and R. G. Young. High speed x-ray motion pictures—1230(A)
Slater, J. C. (see Maxwell, E.)—1234(A)
Slätis, Hilding (see Melander, Lars)—709(L)
Sleator, William, Jr. (see Blair, J. Morris)—553, 1594, 1599, 1205(A), 1259(A)

——, **J. M. Blair, George Freier, Eugene Lampi, and J. H. Williams.** Angular distribution of 1- to 4-Mev deuterons scattered by deuterons—1260(A)
Slotnick, M. (see Nierenberg, W. A.)—1246(A)
Small, H. (see Wolf, H. E.)—118(A)
Smart, J. S. On the formation of shielded isobars by the nuclear photo-effect—1882(L)
Smith, A. G. (see Gordy, Walter)—243
—— (see Simmons, James W.)—1246(A)
——, **H. Ring, W. V. Smith, and W. Gordy.** Microwave spectra of cyanogen halides—123(A)
——, **Harold Ring, W. V. Smith, and Walter Gordy.** Interatomic distances and nuclear quadrupole couplings in ClCN, BrCN, and ICN—370
Smith, C. S., J. C. Hart, E. C. Crittenden, and L. O. Olsen. Structure of evaporated cobalt films—114(T)
Smith, DeForest F. Pressure broadening in ammonia at centimeter wave-lengths—506(L)
Smith, Lloyd P. (see Caldwell, Wallace C.)—1207(A)
Smith, Lyle W. and P. Gerald Kruger. Absolute thick target yields from several (D, n) reactions—1258(A)
Smith, Paul L. (see Burstein, Elias)—229(L), 1880(L)
Smith, R. V. (see Richards, H. T.)—1257(A), 1870(L)
—— **and H. T. Richards.** Deuterium (pn) threshold—1870(L)
—— **and H. T. Richards.** Proton-neutron thresholds in V^{51} and Mn^{55}—1257(A)
Smith, S. R. (see Daunt, J. G.)—495(L)
Smith, William V. (see Carter, Robert L.)—123(A)
—— (see Quevedo, José L. García)—123(A)
—— (see Smith, A. G.)—123(A), 370
—— (see Opinsky, A.)—343(L)
Smythe, W. R. (see Andrew, Alan)—496(L)
Snell, Arthur H. (see Norris, L. D.)—1240(A)
Snell, H. and L. C. Miller. On the radioactive decay of the neutron—1217(A)
Snoddy, L. B. (see McQueen, J. H.)—1551(L)
—— **and J. W. Beams.** Production of short x-ray pulses by a resonant cavity electron accelerator—126(A)
Snowden, S. C. (see Herb, R. G.)—1256(A)
Snyder, C. W. (see Rubin, S.)—1564(A)
——, **C. C. Lauritsen, W. A. Fowler, and S. Rubin.** Double-focusing magnetic spectrograph—1564(A)
Snyder, R. L. Status of large scale computing devices in the United States—1204(T)
Solomon, A. K. (see Cobb, Jock)—354(A)
—— (see Glendenin, L. E.)—700(L)
Somers, H. S., Jr., P. R. Weiss, and W. Halpern. Precision magnetic field stabilizer—1210(A)
Spence, J., J. Castle, and J. H. Webb. Tracks of low ionizing particles in photographic emulsions—704(L)
Spence, R. D. and A. Leitner. Diffraction by circular disks and apertures—349(L)
Spencer, Charles D. "Brittleness" testing device for small glass tubing—115(A)
Sperduto, A. (see Buechner, W. W.)—1348, 1569, 1226(A)
—— (see Strait, E. N.)—1226(A)
Sponer, H. (see Bass, Arnold M.)—1247(A)
—— **and D. S. Lowe.** Absorption spectrum of benzotrifluoride vapor in the near ultraviolet—122(A)
Spotz, Ellen L. (see Hirschfelder, Joseph O.)—1265(A)
Stanford, C. P. (see Bernstein, S.)—1258(A)
Stanley, Charles W. (see Katcoff, Seymour)—631, 1225(A)
Staub, Hans H. High precision determination of the ratio of the nuclear magnetic moments of proton and neutron—1203(T)
—— (see Bloch, F.)—1025
Steele, M. C. (see de Launay, Jules)—1235(A)
Stein, P. R. (see de Hoffmann, F.)—1330
Steinberger, J. On the range of the electrons in meson decay—500(L)
—— **and G. C. Wick.** Neutron polarization—1207(A)
Stelson, P. H. (see Meissner, K. W.)—932, 1262(A)
Stephens, W. E. (see Cornog, I. C.)—1
—— (see Franzen, W.)—1234(A)
Stephenson, S. T. and F. D. Mason. Continuous spectrum of x-rays to 13A—1560(A)
Stergiopoulos, C. G. (see Buechner, W. W.)—1569, 1226(A)
—— (see Strait, E. N.)—1226(A), 1257(A)
Sternheimer, R. Resonance scattering of slow neutrons in crystals—335
Stevens, W. H. (see Hawkings, R. C.)—696(L)
Stimson, H. F. Proposed revision of the international temperature scale—1203(T)
Stout, J. W. Second-order transformations in two-component systems. Application to solutions of He^3 in He^4—605
Strait, E. N. (see Buechner, W. W.)—1569, 1226(A)
——, **C. G. Stergiopoulos, and W. W. Buechner.** Protons from the $Li^7(d, p)Li^8$ reaction—1257(A)
——, **C. G. Stergiopoulos, A. Sperduto, and W. W. Buechner.** Energy relations in the $Be^9(d, \alpha)Li^7$ reaction—1226(A)
Straley, Joseph W. (see Parnell, Jack L.)—123(A)
—— (see Scherrer, Victor)—121(A)
Strandberg, M. W. P. Microwave rotational absorption in D_2O—1245(A)
—— Rotational spectra of linear molecules—1203(T)
Strauser, W. A. (see Good, W. M.)—1225(A)
Street, J. C. Application of crystal counters to cosmic-ray studies—354(T)
—— (see Fowler, E. C.)—101(L), 850(L)
Strong, H. M. (see Bundy, F. P.)—1221(A)
—— **and F. P. Bundy.** Measurement of gas temperatures in the exhaust flames of rocket motors by spectroscopic methods. I—1221(A)
Strong, J. D. (see Hoover, J. I.)—864
Stroud, W. G. (see Winckler, J. R.)—837(L)
Studer, Frank J. and Gorton R. Fonda. Optical properties and constitution of calcium silicate-lead phosphors—1241(A)
Studier, Martin H. and Earl K. Hyde. New radioactive series—the protactinium series—591
Stuecklberg, E. C. G. (see Rivier, D.)—218(L), 986(L)
Stuhlman, Otto, Jr. Mechanical analysis of the closure movements of Benus' fly trap—119(A)
Sutherland, G. B. B. M. (see Shaw, J. H.)—978(L)
Suwa, S. (see Murakawa, K.)—1535(L)

Svartholm, N. Velocity and two-directional focusing of charged particles in crossed electric and magnetic fields—108(L)
Swann, Charles P. (see Hudspeth, Emmett L.)—1722(L), 1227(A)
—— **and E. L. Hudspeth.** Compact electrostatic generator for positive ion acceleration—1243(A)
Swann, W. F. G. Mass-energy relation—200
—— Possible circulation of cosmic-ray helium particles around the earth—1215(A)
—— (see Morris, Peter A.)—1102
Sweeney, D. W. (see Goldstein, L.)—1565(A)
Szalay, A. and Eva Csongor. Contributions to the nuclear processes induced in magnesium by polonium alpha-particles—1063
Szilard, L., S. Bernstein, B. Feld, and J. Ashkin. Inelastic scattering of fast neutrons—1216(A)

Taft, E. (see Apker, L.)—1462
Talbott, F. L. (see Bernstein, S.)—1258(A)
Talley, Robert M. and Alvin H. Nielsen. Some new measurements on the infra-red spectrum of HF—123(A)
Taschek, Richard F. and H. T. Gittings. Observations of naphthalene scintillations caused by tritium beta-rays—1553(L)
—— **and Arthur Hemmendinger.** Reaction constants for $Li^7(p, n)Be^7$—373
Taub, A. H. Relativistic Rankine-Hugoniot equations—328, 1230(A)
Taylor, H. C. (see Morris, Peter A.)—1102
Teichmann, T. Comparison of recent methods in the theory of nuclear reactions—1223(A)
Teller, E. (see Goldhaber, M.)—1046
Ter-Pogossian, M. (see Kurie, Franz, N. D.)—677
Thaler, William J. (see Fitzpatrick, J. A.)—1227(A)
—— (see Hubbard, J. C.)—107(L), 708(L)
Thamer, B. J. (see Voigt, A. F.)—1264(A)
—— **and A. F. Voigt.** Multivibrator quenching of Geiger-Mueller tubes—1261(A)
Thomas, H. C. (see Haynes, S. K.)—128(A)
—— **and N. Underwood.** Counter for low energy ionizing particles—127(A)
Thomas, Roy. Existence of tensor interactions between nucleons—1564(A)
Thompson, R. C. (see Miller, D. R.)—347(L)
Thompson, R. W. Cloud-chamber study of meson disintegration—490(L)
Thornton, R. L. (see Knable, N.)—1217(A)
Ticho, Harold K. Capture probability of negative mesotrons—1337
—— Mean life of negative mesotrons in sulfur—492(L)
Tinlot, John. Further data concerning the variation of penetrating showers with altitude—1197(L)
Tisza, L. Irreversibility and quantum mechanics—1213(A)
Tobin, Ralph A. (see Mock, Dana L.)—1536(L)
Tollestrup, A. V. Counting efficiency of scintillating counter—1561(A)
Tomboulian, D. H. Radiative x-ray transition within the *L* shell of sulphur—1887(L)
—— (see Pell, E. M.)—1242(A)
Tomlinson, E. P. Wide range field control system for a magnetic spectrograph—1231(A)
Tomonaga, Sin-Itiro. On infinite field reactions in quantum field theory—224(L)
Tongiorgi, V. Cocconi (see Cocconi, G.)—1867
Townes, C. H. Nuclear properties determined from microwave spectroscopy—1203(T)
—— Nuclear quadrupole moments of N^{14} and I^{127}—1245(A)
—— (see Dailey, B. P.)—1245(A)
—— (see Shulman, R. G.)—846(L)
—— **and S. Geschwind.** Spin and quadrupole moment of S^{32}—626(L)
——, **A. N. Holden, and F. R. Merritt.** Microwave spectra of some linear *XYZ* molecules—1113
Townsend, J. (see Braden, C. H.)—1539(L)
——, **Marshall Cleland, and A. L. Hughes.** Disintegration of Cs^{137}—499(L)
——, **G. E. Owen, Marshall Cleland, and A. L. Hughes.** Beta- and gamma-spectra of Cs^{137}—99(L)
Treat, J. E. and K. I. Greisen. Penetrating particles in extensive air showers—414
Trischka, J. W. Nuclear quadrupole interaction in CsF—718
Trolander, Hardy. Description of a klystron oscillator for microwave demonstrations and measurements—114(T)
Turner, T. J. (see Menius, A. C., Jr.)—125(A)

Ufford, C. W. (see Aller, L. H.)—1208(A)
Underwood, Newton. Characteristics of an acoustic interferometer—124(A)
—— (see Lagemann, R. T.)—124(A)
—— (see Thomas, H. C.)—127(A)

Valatin, J. G. Isotopic effect of the potential function of molecular states—346(L)
—— On the dissociation energy of carbon monoxide and the heat of sublimation of carbon—350(L)
Vallarta, M. S. On the energy of cosmic radiation allowed by the earth's magnetic field—1837
Van de Graaff, R. J. (see Buechner, W. W.)—1348, 1226(A)
Van der Grinten, W. Particle tracks in emulsions showing grain gradation—1244(A)
Van Vleck, J. H. Line-breadths in radiofrequency and microwave absorption spectra—1254(T)
—— Dipolar broadening of magnetic resonance lines in crystals—1168
—— (see Aller, L. H.)—1208(A)
—— (see Henderson, R. S.)—106(L)
—— (see Wheatley, John)—1211(A)
Van Voorhis, C. C. (see Ladenburg, R.)—1229(A), 1884(L)
Vassamillet, L. F. (see Brocklehurst, R. E.)—114(T)
Venkateswarlu, P. (see Madsen, C. B.)—648, 1782
Victoreen, John A. Absorption of incident quanta by atoms—114(T)
Vineyard, George H. Interpretation of small angle x-ray scattering observed from argon—1209(A)
—— Small angle x-ray scattering from amorphous materials—1076

Voigt, A. F. (see Hein, R. E.)—1265(A)
—— (see Thamer, B. J.)—1261(A)
—— **and B. J. Thamer.** Studies on the radiation of Hf^{181}—1264(A)

Waddel, Ramond C. (see Mock, Dana L.)—1536(L)
Wadey, Walter G. Alpha-ray spectrum of polonium—1846
Wäffler, H. (see Hirzel, O.)—1553(L)
Wahlin, H. B. and Harry W. Knop, Jr. Spectral emissivity of iron and cobalt—687, 1207(A)
Waldman, Bernard and Walter C. Miller. Ratio of deuterium to beryllium photo-disintegration thresholds—1225(A)
Walker, R. L. and B. D. McDaniel. Gamma-ray spectrometer measurements of fluorine and lithium under proton bombardment—315
Wallace, J. (see Burgy, M.)—1207(A)
Waltner, Arthur. Effect of rapidity of expansion on cloud-chamber operation—129(A)
—— Simplified low pressure cloud chamber—127(A)
—— (see Byatt, W. J.)—699(L)
—— **and F. T. Rogers, Jr.** Cloud-chamber observation on low energy portion RaE beta-spectrum—699(L)
Wang, Kan-Chang and Stanley B. Jones. On the disintegration of mesotrons—1547(L)
Warburton, F. W. Average negative gradient of potential energy—1562(A)
Wataghin, Andrea (see Meyer, H. A.)—846(L)
Wataghin, G. On the multiple production of mesons—975(L)
Watanabe, Satosi. On the possible types of interaction between spinorial and tensorial fields—1865
Watson, Bernard B. (see DuMond, Jesse W. M.)—1561(A)
—— (see Lind, David)—1561(A)
——, **David A. Lind, and Jesse W. M. DuMond.** Method of studying the gamma-ray spectrum of annihilation radiation from a source of positrons using the focusing curved crystal spectrometer—1561(A)
Watson, K. M. (see Jauch, J. M.)—950, 1485
—— **and J. M. Jauch.** Phenomenological quantum-electrodynamics—1262(A)
Watenberg, A. (see Myers, V.)—1264(A)
Watts, R. J. Slave sweep circuits for nuclear research—114(T)
Wayland, Harold and Saul Baker. Behavior of spherically tipped bodies in the early stage of water entry—1563(A)
Weber, Louis R. (see Bever, Renate S.)—1562(A)
Webb, J. H. Photographic plates for use in nuclear physics—511
—— (see Spence, J.)—704(L)
Weidner, R. T. (see Whitmer, C. A.)—1478
——, **P. R. Weiss, and C. A. Whitmer.** Microwave resonance absorption in potassium chrome alum—1211(A)
Weimer, Paul K. Measurement of secondary emission of insulators at low primary energies—1221(A)
Weinberg, A. M. and H. C. Schweinler. Theory of oscillating absorber in a chain reactor—851
Weinberg, Joseph W. Special property of the electron's gyromagnetic ratio—1212(A)
Weinstein, M. (see Bohm, D.)—1789
Weiss, H. G. (see Mullaney, J. F.)—491(L)
Weiss, P. R. Application of the Bethe-Peierls method to ferromagnetism—1493
—— Microwave resonance absorption in paramagnetic salts—1203(T)
—— (see Somers, H. S., Jr.)—1210(A)
—— (see Weidner, R. T.)—1211(A)
—— (see Whitmer, C. A.)—1478
Weissler, Alfred. Ultrasonic velocity in liquid halides—1228(A)
Weissler, Pearl G. (see Cook, Richard K.)—1714
Weisz, P. B. Starting potential of the Geiger-Mueller counter discharge—1807
Welton, Theodore A. Some observable effects of the quantum-mechanical fluctuations of the electromagnetic field—1157
Wentzel, Gregor. Remarks on recent developments in quantum electrodynamics—1254(T)
—— New aspects of the photon self-energy problem—1070
Wheatley, John (see Halliday, David)—1712, 1724(L), 1210(A)
——, **David Halliday, and J. H. Van Vleck.** Paramagnetic resonance absorption line shapes for single crystals of $CuSO_4 \cdot 5H_2O$—1211(A)
White, J. R. and A. E. Cameron. Natural abundance of isotopes of stable elements—991
White, M. G. (see Gugelot, P. C.)—1215(A)
—— (see Sherr, R.)—1239(A)
——, **H. W. Fulbright, P. Gugelot, and R. R. Bush.** Redesign of the Princeton cyclotron to yield 18-Mev protons—1242(A)
White, M. W. Utilization of physicists and other scientists during world war II—1254(T)
Whitehead, W. D., Jr. (see Heydenburg, N. P.)—405, 1226(A)
Whitehurst, Robert N. Study of short-distance propagation of 147-mc radio-waves—124(A)
Whitmer, C. A. (see Weidner, R. T.)—1211(A)
——, **R. T. Weidner, J. S. Hsiang, and P. R. Weiss.** Magnetic resonance absorption in the chrome alums—1478
Whitmer, Robert M. Extremals of impedance elements in wave guide equivalent circuits—1231(A)
Wick, G. C. (see Steinberger, J.)—1207(A)
Wickenden, Roger C. Utilizing the Vernier principle for precise readings of slide rule settings—116(A)
Wiedenbeck, M. L. (see Chu, K. Y.)—494(L)
Wightman, A. Note on polarization effects in Compton scattering—1813
Wigner, E. P. Nuclear reactions and level widths—1254(T)
—— (see Moshinsky, Marcos)—1212(A)
Wijsman, Robert A. (see Loeb, Leonard B.)—1556(A)
Wilcox, Howard A. Experimental determination of rate of energy loss for slow H^1, H^3, He^4, Li^8 nuclei in Au and Al—1743
—— (see Allison, S. K.)—1233(A)
Wildhack, W. A. Pneumatic flow type pressure controller—1229(A)
—— (see Iberall, A. S.)—1229(A)

Wilkinson, D. H. Geiger discharge—1417
Wilkinson, Geoffrey and Harry G. Hicks. Some new radioactive isotopes of Tb, Ho, Tm, Lu, Ta, W, and Re—1733(L)
Wilkinson, Roger G. (see Peacock, Charles L.)—297, 1240(A)
—— **and Charles L. Peacock.** Beta- and gamma-radiation of W^{187} and Au^{198}—1250(A)
Williams, A. O., Jr. (see Davis, W. H.)—1208(A)
Williams, C. (see Borst, L. B.)—1883(L)
Williams, Dudley. Methods of observing microwave absorption lines—114(T)
—— (see Manring, Edward R.)—1263(A)
—— (see Pietenpol, William J.)—1246(A)
—— (see Zimmerman, John R.)—1885(L)
Williams, Ferd E. (see Johnson, Peter D.)—1241(A)
Williams, John H. (see Blair, J. Morris)—553, 1594, 1599, 1205(A), 1259(A)
—— (see Sleator, William, Jr.)—1260(A)
Williams, Robert W. Structure of the large cosmic-ray air showers—1689
—— (see Bridge, H. S.)—1083
Wilson, E. Bright. Use of microwave spectroscopy for studies of molecular structure—1203(T)
Wilson, H. A. Rotation vibration levels of the Fe^{57} and Ni^{59} nuclei—351(L)
—— Rotation vibration levels of the Si^{28} and Al^{28} nuclei—352(L)
Wilson, M. Carr and G. F. Hull, Jr. On the Faraday effect of microwave frequencies—711(L)
Wilts, Charles H. (e/m_0) for free electrons by use of resonant cavity—1560(A)
Winans, J. Gibson and Willard J. Pearce. Band spectrum of HgTl—1262(A)
Winckler, John R. Directional distribution of the total cosmic radiation at atmospheric heights up to 10-cm Hg at Princeton—1214(A)
—— (see Ladenburg, R.)—1229(A), 1884(L)
——, **W. G. Stroud, and J. Schenck.** Directional intensity of cosmic rays at high altitudes—837(L)
Wineland, W. C., T. M. Hahn, Jr., and L. R. Boyd. Coil system for producing longitudinal magnetic gradients—118(A)
Winn, E. B. Self-diffusion coefficient of nitrogen—698(L)
Winsberg, Lester (see Sidhu, S. S.)—222(L)
——, **David Meneghetti, and S. S. Sidhu.** Total neutron cross sections of compounds with different crystalline structures—1216(A)
Winsche, W. E. (see Borst, L. B.)—1883(L)
Wise, C. E. (see Bloom, Evelyn G.)—1222(A)
Witmer, Enos E. Explicit formula for the energy levels of the asymmetric rotator according to quantum mechanics—1250(A)
—— Explicit solution of the problem of the asymmetric rotator according to quantum mechanics—1247(A)
Wohlfarth, E. P. Anomalous values of the thermionic emission constant—984(L)
Wolf, H. E., H. Small, and J. H. Buehler. Current amplifiers for use with magnetic generators—118(A)
Wolfenstein, Lincoln. Proposed nuclear reactions involving polarized protons—1224(A)
Wollan, Abner. Infra-red spectrum of dimethylacetylene—114(T)
Wollan, E. O. (see Goods, W. M.)—1225(A)
—— (see Hoover, J. I.)—864
Woodward, L. L. (see McCown, D. A.)—1311, 1315, 1248(A), 1263(A)
——, **D. A. McCown, and M. L. Pool.** Radioactive Br isotopes—870
——, **D. A. McCown, and M. L. Pool.** Radioactive Kr isotopes—761
——, **D. A. McCown, M. L. Pool, and H. L. Finston.** Artificial radioactivity from enriched Se^{74} and Se^{76}—1263(A)
Woodward, W. M. and I. Halpern. On the angular distribution of protons from the photo-disintegration of the deuteron—1225(A)
Woolf, W. E. (see McMillan, D. R., Jr.)—124(A)
Woolley, Harold W. Force constant calculations for the X_4Y_6 molecule—1247(A)
Wooten, L. A. Sorption of gases by metals at low pressure—a study of getters—1254(T)
Workman, E. J. (see Reynolds, S. E.)—1231(A)
—— **and S. E. Reynolds.** Electrical activity as related to thunderstorm cell growth—1231(A)
—— **and S. E. Reynolds.** Suggested mechanism for the generation of thunderstorm electricity—709(L)
Wormell, T. W. (see Shaw, J. H.)—978(L)
Wouters, Louis F. Pulse characteristics of anthracene scintillation counters—489(L)
Wright, S. C. (see Jungerman, J.)—150
Wu, C. S. (see Albert, R. D.)—847(L)
—— (see Havens, W. W., Jr.)—1216(A)
——, **W. W. Havens, Jr., and L. J. Rainwater.** Beta- and gamma-radiations of arsenic^{76}—1248(A)
Wyly, L. D. (see Pollard E.)—1233(A)

Yaffe, L. and Jean M. Grunlund. Half-life of C^{14}—696(L)
—— **and Katharine M. Justus.** Erratum: A rapid method for the determination of the maximum energies of β-emitters with simple spectra—850(L)
Yagoda, Herman (see Langer, R. M.)—1238(A)
—— **and Nathan Kaplan.** Background eradication of nuclear emulsions by accelerated fading of the latent image—1249(A)
Yang, C. N. On the angular distribution in nuclear reactions and coincidence measurements—764
—— (see Allison, S. K.)—1233(A)
Yevick, G. J. Symmetry properties of χ-functions—1213(A)
Young, R. G. (see Slack, C. M.)—1230(A)
Yu, F. C. (see Ma, S. T.)
Hu, Fu-Chun and J. D. Kurbatov. Disintegration by consecutive electron capture in nucleus—114(T)
—— **and J. D. Kurbatov.** Energy quanta emitted in disintegration of ground state of Ba^{133}—34
Yuan, Luke C. L. Neutron density in the free atmosphere up to 67,000 feet—504(L)

Zabel, Carroll W. (see Davis, Luther, Jr.)—1211(A)
Zacharias, J. R. Molecular beam experiments with chlorine —1203(T)
Zaffarano, Daniel J., Bernard D. Kern, and Allan C. G. Mitchell. Beta- and gamma-rays of Rb^{86}—682
——, Bernard D. Kern, and Allan C. G. Mitchell. Energy of the Be^{7} gamma-ray—105(L)
Zagor, H. (see Belock, H.)—1230(A)
Zar, Jacob L., Joseph Hershkowitz, and Evelyn Berezin. Cloud-chamber study of electrons from meson decay—111(L)
Zavales, C. (see Slack, C. M.)—1230(A)
Zener, C. Theory of strain interaction of solute atoms—639
Zilsel, P. R. (see London, F.)—1148
Zimmerman, John R. (see Manring, Edward R.)—1263(A)
—— and Dudley Williams. Magnetic moment of $boron^{11}$—1885(L)

PHYSICAL REVIEW VOLUME 74, NUMBER 12 DECEMBER 15, 1948

Analytic Subject Index to Volume 74

References with (A) are to abstracts of papers presented at meetings of the American Physical Society. References with (L) are to Letters to the Editor.

Absorption of radiation
Coefficients for gamma-rays, Charlotte M. Davisson and Robley D. Evans—1239(A); Arthur L. Hughes and Clyde L. Cowan—1238(A); Clyde L. Cowan—1841
High energy quanta I, G. D. Adams—1707
Absorption coefficient (see also **Scattering of electrons,** etc.; **X-ray, absorption**)
Statistical error in absorption, M. E. Rose and M. M. Shapiro—1853
Acoustics (see also **Ultrasonics**)
Interpretation of interferometer data, Joseph L. Hunter —116(A)
Radiation field, vibrating piston in baffle, Paul M. Marcus —1234(A)
Second sound in helium II, velocity, J. R. Pellam —841(L)
Two-velocity field model of helium II, William Band and Lothar Meyer—386
Activated gases
Active nitrogen, S. K. Mitra—1637
Adsorption
Of Hg by activated carbon, R. C. Mason—1220(A)
Astrophysics
Dense group of galaxies in Serpens, C. K. Seyfert—129(A)
Energy production in sun, J. O'Reilly and R. F. Christy —1559(A)
Field theory and cosmic magnetism, Jean Mariani—1265(A)
Lines of methane in solar spectrum, Marcel V. Migeotte —112(L)
Magnetic variable stars as sources of cosmic rays, Horace W. Babcock—489(L)
Magnetism of celestial bodies, M. Forró—218(L)
Meteor trials, Charles A. Little, Jr.—1875(L)
Model with finite cosmological constant, Guy C. Omer, Jr.—1564(A)
Origin of elements, separation of galaxies, G. Gamow —505(L)
Production of He in meteorites by cosmic radiation, Carl August Bauer—501(L)
Solar noise burst at 9500 Mc/s, M. Schulkin, F. T. Haddock, K. M. Decker, C. H. Mayar, and J. P. Hagen—840(L)
Source of solar magnetic field, James W. Follin, Jr.—1232(A)
Thermonuclear reactions in expanding universe, R. A. Alpher, R. Herman, and G. A. Gamow—1198(L)
Atmosphere (see **Meteorology**)
Atmospheric electricity (see **Meteorology**)
Atomic structure (see also **Energy states of atoms; Spectra**)
Configurations of d^2sp, d^3p, and d^7p, F. Rohrlich—1372
Aurora
Spectra showing broad hydrogen lines, C. W. Gartlein —1208(A)

Barkhausen effect (see **Magnetic properties**)
Biophysics
Bioelectric potential of corn seeds with x-ray dosage, M. W. Jones, J. G. Jones, and A. A. Bless—126(A)
Closure movements of Venus' fly trap, Otto Stuhlman, Jr.—119(A)
Gamma-ray isodosimeter, L. D. Marinelli and G. J. Hine—1245(A)
Potentials as index of x-ray action, A. A. Bless—1209(A)
Broadening of spectral lines
In NH_3 at cm wave-lengths, DeForest F. Smith —506(L)

Chemical reactions
Theory of reaction rates, C. F. Curtiss and J. O. Hirschfelder—1265(A)
Colloids
Low angle scattering, Peter G. Bergmann—1209(A)
Compton effect (see **X-rays, diffraction, scattering**)
Conductivity, electrical (see **Electrical conductivity, Discharge of electricity in gases**)
Conductivity, thermal (see **Thermal conductivity**)

Constants, physical, standards
Charge of positron, J. Barnóthy—844(L)
(e/m_0) for free electrons, Charles H. Wilts—1560(A)
h/e by x-rays, Guenter Schwarz and J. A. Bearden—1209(A)
Contact potentials
Of semiconductors, L. Apker, E. Taft, and J. Dickey—1462
Cosmic radiation
Absorption and scattering of mesons, Alma Rosenbaum and Rogers D. Rusk—354(A)
Absorption in meteorites, production of He, Carl August Bauer—225(L)
Absorption of nucleonic component, G. Bernardini, G. Cortini, and M. Manfredini—1878(L)
Air showers at sea level, S. F. Singer—1214(A)
Altitude dependence of Auger showers, M. M. Mills—1555(A)
Auger showers, S. F. Singer—844(L)
Beta-decay of light meson, E. C. Fowler, R. L. Cool, and J. C. Street—101(L), 850(L)
Beta-decay of mesons, J. J. Horowitz, O. Kofoed-Hansen, and J. Lindhard—713
Bursts, analysis of, H. S. Bridge, W. E. Hagen, B. Rossi, and R. W. Williams—1083
Bursts at sea level, H. Carmichael—1667; Chang-Ning Chou—1659
Calculations on cascade theory, H. J. Bhabha and S. K. Chakrabarty—1352
Capture of negative mesons, L. I. Schiff—1556(A)
Capture probability of negative mesotrons, Harold K. Ticho—1337
Charged particles from 2.2-μ sec. meson decay, E. P. Hincks and B. Pontecorvo—697(L)
Circulation of He particles around earth, W. F. G. Swann—1215(A)
Directional distribution of radiation at 10 cm Hg, John Winckler—1214(A)
Directional intensity, J. R. Winckler, W. G. Stroud, and J. Schenck—837(L)
Distribution of decay electrons from mesons, R. D. Sard and A. H. Benade—1237(A)
East-west asymmetry, A. G. Fenton and D. W. P. Burbury—589
East-west asymmetry at 33,000 feet, W. C. Barber—1556(A)
East-west asymmetry, etc., up to 36,000 ft., James F. Jenkins, Jr.—1214(A)
Electrons from meson decay, Jacob L. Zar, Joseph Hershkowitz, and Evelyn Berezin—111(L)
Energy allowed by earth's field, M. S. Vallarta—1837
Energy distribution in showers, J. A. Richards, Jr. and L. W. Nordheim—1106
Energy spectrum of protons and stars, Harriet H. Forster—1556(A)
Field deflections for determining mass of meson, F. T. Rogers, Jr.—128(A)
Hard component, I. F. Quércia, B. Rispoli, and S. Sciuti—1728(L)
Heavy component of primary, Phyllis Freier, E. J. Lofgren, E. P. Ney, F. Oppenheimer, H. L. Bradt, and B. Peters—213; Phyllis Freier, E. J. Lofgren, E. P. Ney, and F. Oppenheimer—1818
Heavy mesons to lighter, R. M. Langer and Herman Yagoda—1238(A)
Large air showers, Robert W. Williams—1689
Magnetic variable stars as sources, Horace W. Babcock—489(L)
Mass of mesons and other particles, E. G. Cullwick—707(L)
Mean life of mesotrons in S, Harold K. Ticho—492(L)
Meson disintegration, R. W. Thompson—490(L)
Mesons in C, C. W. Kissinger and D. Cooper—1237(A)
Momentum distribution of electrons from negative mesons, H. Primakoff—878
Multiple production of mesons, G. Wataghin—975(L)
Neutral decay-products, J. Barnóthy and M. Forro—1300
Neutral particles produced by exchange, Rogers D. Rusk and Alma Rosenbaum—110(L)
Neutron density in the atmosphere, Luke C. L. Yuan—504(L); J. M. Simpson, Jr.—1214(A)
Neutrons associated with sea level mesons in Pb, R. D. Sard, W. B. Ittner, III, A. M. Conforto, and M. F. Crouch—97(L)
Neutrons in penetrating showers, G. Cocconi, V. Cocconi Tongiorgi, and K. Greisen—1867
Nuclear evaporations, G. Bernardini, G. Cortini, and A. Manfredini—845(L)
Nuclear plates in magnetic field, determination of sign of particles, Ian G. Barbour—507(L)
Origin of neutrons in showers, Vanna Tongiorgi Cocconi—226(L)
Particles from stopped mesons, W. Y. Chang—1236(A)
Penetrating showers, G. Cocconi and K. Greisen—62; J. E. Treat and K. I. Greisen—414; H. A. Meyer, G. Schwachheim, and Andrea Wataghin—846(L); G. T. Reynolds and W. D. Hardin—1549(L); John Tinlot—1197(L)
Photographing cloud-chamber tracks at 100,000 ft., Walter Frick, Edward J. Lofgren, Frank Oppenheimer, and Edward P. Ney—1258(A)
Photons from meson capture, O. Piccioni—1754
Photons from sea-level mesons, R. D. Sard and E. J. Althaus—1364
Plasma oscillations, acceleration of particles, D. Bohm and E. P. Gross—624(L)
Positive excess, meson component, C. Ballario, M. Benini, and G. Calamai—1729(L); M. H. Shamos, M. G. Levy, and I. S. Lower—1237(A)
Primary and secondary mesons, Adair Morrison and Eric Pickup—706(L)
Primary radiation, photographic emulsions, H. L. Bradt and B. Peters—1828
Production of He in meteorites, Carl August Bauer—501(L)
Production of neutrons at sea level, Gerhart Groetzinger and Gordon W. McClure—341

Range of electrons in meson decay, J. Steinberger—500(L)
Rocket borne cloud chamber, S. E. Golian, C. Y. Johnson, and M. Kuder—1215(A); G. J. Perlow, E. Krause, and C. Schroeder—1215(A)
Scattering in air showers, L. Eyges—1801
Sea level latitude effect, Peter A. Morris, W. F. G. Swann, and H. C. Taylor—1102
Separation of low energy mesotrons from electrons, P. C. Bhattacharya—38
Shower production at 14,000 ft., H. Bridge and W. Hazen—579
Showers by penetrating particles, C. Y. Chao—492(L)
Slow mesons in atmosphere, Matthew Sands—1237(A)
Temperature coefficients, F. M. Millican and D. H. Loughridge—66
Tracks in emulsions at 100,000 ft., E. O. Salant, J. Hornbostel, and E. M. Dollmann—694(L)
Tracks taken at 100,000 ft., Edward J. Lofgren, Edward P. Ney, and Frank Oppenheimer—1258(A)

Cosmology
Model with finite cosmological constant, Guy C. Omer, Jr.,—1564(A)

Cross section, measurements, theory
(α, n) of Be, Mg, and Al, I. Halpern—1234(A)
For $C^{12}(\gamma, n)C^{11}$, J. L. Lawson and M. L. Perlman—1190
d-p and d-n cross sections, D. C. Peaslee—1223(A)
Elastic scattering of nucleons by deuterons calculation, Geoffrey F. Chew—809
Of H for slow neutrons, W. B. Jones, Jr.—364
Low energy $C^{13}(p, \gamma)$ cross section, W. A. Fowler and R. N. Hall—1558(A)
Neutron absorption, pile oscillator, J. I. Hoover, W. H. Jordon, C. D. Moak, L. Pardue, H. Pomerance, J. D. Strong, and E. O. Wollan—864
Of (p, n): (p, γ) and (d, n): (d, $2n$) reactions, D. N. Kundu and M. L. Pool—1574
Of Tc^{98} and Tc^{99}, D. N. Kundu and M. L. Pool—1775

Crystal structure
Auburn electronic Fourier synthesizer, R. Pepinsky and D. Sayre—126(A)
Table of interplanar spacings in terms of 2θ, Suzanne Van Dijke Beatty—625(L)

Crystalline state
Clustering phenomena in solid solution, A. Opinsky and R. Smoluchowski—343(L)
Cold working magnetic properties, James Reekie, and T. S. Hutchison—610
Crystal "growth" in electron microscope, A. C. Menius, Jr. and T. J. Turner—125(A)
Dielectric behavior of $BaTiO_3$, Gordon C. Danielson, Bernd T. Matthias, and John M. Richardson—986(L)
Electron bombardment conductivity in diamond, Kenneth G. McKay—1606
Electronic states in almost period systems, Hubert M. James—1218(A)
Electrostrictive effect in barium titanate ceramics, W. P. Mason—1134
Energy of self-trapped electron in NaCl, J. J. Markham and F. Seitz—1014
Ferroelectric effect in barium titanate, W. P. Mason and B. T. Matthias—1622
Internal friction and precipitation, T'ing-Sui Kê—914
Internal friction, interstitial solid solutions of C and O in Ta, T'ing-Sui Kê—9
Non-rectifying germanium, W. C. Dunlap, Jr. and E. F. Hennelly—976(L)
Nuclear paramagnetism at low temperatures, B. V. Rollin and J. Hatton—346(L)
Nuclear relaxation in ice at −180°C, G. E. Pake and H. S. Gutowsky—979(L)
Paramagnetic resonance absorption in chrome alum, David Halliday and John Wheatley—1712
Paramagnetic resonance absorption in single crystals, David Halliday and John Wheatley—1210(A)
Photoelastic properties of cubic crystals, Elias Burstein and Paul L. Smith—229(L)
Photoelastic properties of diamond, Elias Burstein and Paul L. Smith—1880(L)
Radioactivity from different crystal faces, J. H. J. Poole and J. W. Bremner—836
Recrystallization of Zn at room temperature, Norman Goss—116(A)
Resonance absorption in chrome alums, C. A. Whitmer, R. T. Weidner, J. S. Hsiang, and P. R. Weiss—1478
Resonance absorption in potassium chrome alum, R. T. Weidner, P. R. Weiss, and C. A. Whitmer—1211(A)
Resonance absorption line shapes, John Wheatley, David Halliday, and J. H. Van Vleck—1211(A)
Sintering process, H. Christensen and C. J. Calbick—1219(A)
Strain interaction of solute atoms, C. Zener—639
Stress relaxation by interstitial diffusion, T'ing-Sui Kê—1219(A)
Superlattices in order-disorder alloys, Sidney Siegel and C. G. Shull—1255(A)
Tests of metal single crystal surfaces, H. E. Farnsworth—1219(A)
Thermal voltages of quartz crystal, Richard K. Cook, Martin Greenspan, and Pearl G. Weissler—1714
Vacancy diffusion in alloys, Frederick Seitz—1513
Vibrations of two-dimensional crystals, Nicholas Chako—126(A)

Dielectric constants (see **Dielectrics and dielectric properties**)

Dielectrics and dielectric properties
Of $BaTiO_3$, Gordon C. Danielson, Bernd T. Matthias, and John M. Richardson—986(L)
Of $BaTiO_3$, theory, John M. Richardson and Bernd T. Matthias—987(L)
Dielectric constant of gases at 9340 megacycles, C. M. C. M. Crain—691
Of gases at microwave frequencies, Harold Llyons, George Birnbaum, and S. J. Kryder—1210(A)

Diffraction of neutrons (see **Neutron diffraction**)

Diffraction of radiation
By an aperture in infinite plane screen, Harold Levine and Julian Schwinger—958
By circular disks and apertures, R. D. Spence and A. Leitner—349(L)
Diffraction pattern in plane of apertures, C. L. Andrews —1231(A)
Variational principles for diffraction problems, Harold Levine and Julian Schwinger—1212(A)
Diffusion (see also **Thermal diffusion**)
Concentration of He_3, B. B. McInteer, L. T. Aldrich, and Alfred O. Nier—946
Self-diffusion coefficient of N_2, E. B. Winn—698(L)
Discharge of electricity in gases
Breakdown at microwave frequencies, Melvin A. Herlin and Sanborn C. Brown—291, 910, 1209(A), 1650
Conductivity gas at microwave frequencies, Edgar Everhart and Sanborn C. Brown—1210(A)
Corona from water drop, W. N. English—179
Current density in cathode spot, J. D. Cobine and C. J. Gallagher—1524
Cylindrical point to plane corona gap, James M. Parker and Leonard B. Loeb—1557(A)
Discharge spread in counters, C. Balakrishnan, J. D. Craggs, and A. A. Jaffe—410; S. H. Liebson—694(L)
Effect of point material on corona onset, W. N. English —1556(A)
Electrode vapor jets, Wolfgang Finkelnburg—1475
Electron emission at cathode, errata, Jerome Rothstein —228(L)
Erratum: High frequency discharges, H. Margenau —706(L)
Frictional electricity, E. W. B. Gill—842(L)
Geiger discharge, D. H. Wilkinson—1417
Point-to-plane corona, W. N. English—170; H. W. Bandel and W. W. English—1557(A); D. B. Moore and W. N. English—1557(A)
Positive burst pulse corona, Leonard B. Loeb and Robert A. Wijsman—1556(A)
Role of cathode surface, Harold Jacobs and A. P. LaRocque—163
Spark development in uniform fields, Leonard B. Loeb —210
Vapor jets in arc and spark discharges, Wolfgang Finkelnburg—222(L)
Velocity of discharge in counters, A. J. Knowles, C. Balakrishnan, and J. D. Craggs—627(L)
Discharge of electricity in high vacua (see also **Thermionic emission**)
High frequency loading, Nicholas Begovich—1563(A)
Disintegration and excitation of nucleus (see also **Radioactivity**)
Absolute determinations of three nuclear reactions, R. G. Herb, S. C. Snowden, and O. Sala—1256(A)
Al^{27} (dn) reaction, R. A. Peck, Jr., —1233(A)
Angular distribution in reactions, C. N. Yang—764
Angular distribution of alphas from $Li^6(d, \alpha)\alpha$ and $Li^7(p, \alpha)\alpha$, N. P. Heydenburg, C. M. Hudson, D. R. Inglis, and W. D. Whitehead, Jr.—405
Angular distribution of D-on D, William Sleator, Jr., J. M. Blair, Goerge Freier, Eugene Lampi, and J. H. Williams—1260(A)
Angular distribution of $Li^7(p, \alpha)a$, theory, D. R. Inglis —21
Angular distribution of neutrons from (d, n), C. E. Falk, E. Creutz, and F. Seitz—1226(A)
Angular distribution of products from D−D reaction, J. M. Blair, W. Sleator, Jr., George Freier, E. E. Lampi, and J. H. Williams—1259(A)
Argon and neon (pn) thresholds, H. T. Richards and R. V. Smith—1870(L)
$B^{11}(d, p)$ reaction, β-rays, mass, energy, E. L. Hudspeth and C. P. Swann—1722(L)
Of Ba^{133}, energy quanta emitted, Fu-Chun Yu and J. D. Kurbatov—34
Of Be, electron multiplier tube, Leticia del Rosario—304
Be^9+p resonances, E. Richard Cohen and R. F. Christy —1566(A)
Coincidence experiments on Sc^{46}, Ga^{72}, Au^{198}, and Rb^{86}, E. T. Jurney—1049
Complex disintegration of I^{131}, George E. Owen, David Moe, and C. Sharp Cook—1879(L)
"Cross-over" transitions in gamma-ray spectra, V. Myers and A. Wattenberg—1264(A)
Cross section for $C^{12}(\gamma, n)C^{11}$, J. L. Lawson and M. L. Perlman—1190(L)
Cross-section measurements of (p, n): (p, γ) and (d, n): $(d, 2n)$ reactions, D. N. Kundu and M. L. Pool—1574
Deuterium (pn) threshold, R. V. Smith and H. T. Richards—1871(L)
Deuteron bombardment of B and F, γ-rays, E. L. Hudspeth and C. P. Swann—1227(A)
Deuteron-induced reactions, D. C. Peaslee—1001
Disintegration scheme of I^{131}, Franz Metzger and Martin Deutsch—1641
Double beta-decay, E. Fireman—1238(A)
Electrodisintegration of Be^9, E. Guth, C. J. Mullin, and J. F. Marshall—834(L)
Electrons accompanying slow neutron capture in Gd, O. Sala, P. Axel, and M. Goldhaber—1249(A)
Energy and angle variation in $Li^6(d, \alpha)\alpha$, N. P. Heydenburg, C. M. Hudson, D. R. Inglis, and W. D. Whitehead, Jr.—1226(A)
Energy and angle variation of $C^{12}(d, p)C^{13}$, D. R. Inglis, N. P. Heydenburg, and E. M. Hafner—1257(A)
Energy relations in $Be^9(d, \alpha)Li^7$ reaction, E. N. Strait, C. G. Stergiopoulos, A. Sperduto, and W. W. Buechner —1226(A)
Excitation curves of $C^{12}(p, pn)C^{11}$ and $B^{11}(p, n)C^{11}$, Robert Phillips and Wolfgang K. H. Panofsky—1560 (A); Wolfgang K. H. Panofsky and Robert Phillips —1732(L)
Excited state of Be^9, Conrad Longmire—1773
γ-induced β-disintegration, experimental, R. L. Burling and F. N. D. Kurie—109(L)
γ-induced β-disintegration, theoretical, H. Primakoff —110(L)
γ-radiation from Be^8, S. Devons and M. G. N. Hine —976(L)

γ-radiation from $Be^9(d, n)B^{10}$, T. Lauritsen, C. B. Dougherty, and V. K. Rasmussen—1566

γ-ray from $F^{19} + H^1$, Gerson Goldhaber—1725(L)

γ-rays from F and Li under proton bombardment, R. L. Walker and B. D. McDaniel—315

γ-rays from $H^1(n, \gamma)D^2$, R. E. Bell and L. G. Elliott —1552(L)

High energy deuteron and helium ion bombardments of Cu, D. R. Miller, R. C. Thompson, and B. B. Cunningham—347(L)

Interaction of high energy neutrons and heavy nuclei, M. L. Goldberger—1269

$Li^7(d, p)Li^8$, E. N. Strait, C. G. Stergiopoulos, and W. W. Buechner—1257(A)

Monoenergetic conversion lines, continuous β-spectra, G. E. Owen and H. Primakoff—1406

Neutron spectra from proton recoils in emulsions, F. Reines—1565(A)

Nuclear reactions involving polarized protons, Lincoln Wolfenstein—1224(A)

Polarization and direction of successive quanta, Donald R. Hamilton—782

Processes induced in Mg by alpha-particles, A. Szalay and Eva Csongor—1063

Production of Li^8 in boron-loaded photographic emulsions, E. Pickup—495(L)

Proton-neutron thresholds in Cl^{37} and K^{41}, H. T. Richards and R. V. Smith—1257(A)

Proton-neutron thresholds in V^{51} and Mn^{55}, R. V. Smith and H. T. Richards—1257(A)

Protons from light nuclei bombarded by α-particles, F. C. Champion and R. R. Roy—5

Range data, interpretations, R. F. Humphreys and H. T. Motz—1232(A)

Range data, $Na^{23}(\alpha p)Mg^{26}$ reaction, H. T. Motz and R. F. Humphreys—1232(A)

Range-energy curve, $N^{14}(n, p)$ reaction, W. Franzen, I. C. Cornog, and W. E. Stephens—1234(A)

Range of protons from $N^{14}(n, p)C^{14}$, I. C. Cornog, W. Franzen, and W. E. Stephens—1

Ratio of deuterium to Be photo-disintegration thresholds, Bernard Waldman and Walter C. Miller—1225(A)

Reaction constants for $Li^7(p, n)Be^7$, Richard Taschek and Arthur Hemmendinger—373

Resonances in $C^{14}(p, n)N^{14}$, W. E. Shoupp and B. Jennings—1233(A)

Resonances in disintegration of C by deuterons, T. W. Bonner, J. E. Evans, J. C. Harris, and G. C. Phillips —1227(A)

Resonances in $Li^7(p, n)Be^7$, G. Breit and I. Bloch—397

$S(dp)$ reaction, Perry W. Davison—1233(A)

Short-lived isomers of nuclei, S. DeBenedetti and F. K. McGowan—728

Short-range nuclear recoils, light elements, S. K. Allison, H. V. Argo, W. R. Arnold, L. del Rosario, H. A. Wilcox, and C. N. Yang—1233(A)

Spectroscopy of gamma-rays, Jesse W. M. DuMond, David Lind, and Bernard B. Watson—1561(A)

Theory of internal conversion, H. A. Meyer—979(L)

Theory of $Li^7(p, \alpha)\alpha$, D. R. Inglis—1227(A)

Yields of x-ray induced reactions, M. L. Perlman and G. Friedlander—442

Dissociation, energy of (see also **Molecular structure and constants**)

Of CO, sublimation of carbon, J. G. Valatin—350(L)

Dynamics

Generalized virial theorems, Harvey Einbinder—803

High velocity particles produced at impact, J. Howard McMillen and R. L. Kramer—1882(L)

Integral equations of motion, Elliot T. Benedikt—1213(A)

Elasticity

Brittle fracture of steel, Victor Scherrer and Joseph W. Straley—121(A)

Constants of beta-brass, David Lazarus—1726(L)

Curved tubes, behavior, H. A. Jarrell and T. E. Pardue —121(A)

Failure of metals, repeated plastic strains, J. P. Parker, T. E. Pardue, and J. L. Melchor—121(A)

Fracture of liquids, John C. Fisher—1256

Internal friction in Ta, T'ing-Sui Kê—9

Interpretation of interferometer data, Joseph L. Hunter —116(A)

Propagation of fractures in glass, V. E. Scherrer and Arthur Linz, Jr. —120(A)

Relaxing materials in force-transmitting linkages, Emily Jones and F. T. Rogers, Jr.—122(A)

Slow-bend fracturing of steels, Marguerite M. Rogers —121(A)

Slow-bend fracturing of steels, strain-aging, Marguerite M. Rogers—122(A)

Slow-bend test of mild steel, F. T. Rogers, Jr.—122(A)

Speed of brittle fracture in steel, Arthur Linz, Jr. and V. E. Scherrer—121(A)

Spiral marks on fractures, Arthur E. Ruark—120(A)

Strain interaction of solute atoms, C. Zener—639

Strength dispersion in nylon yarns, Waller George and Richard LaTorre—1256(A)

Strength of materials under cyclic loading, Edward Saibel—1220(A)

Stress relaxation by interstitial diffusion, T'ing-Sui Kê —16, 1219(A)

Stresses in steel during bending, W. J. Byatt and F. T. Rogers, Jr.—121(A)

Vibration in contoured quartz plates, Renate S. Bever, Virgil E. Bottom, and Louis R. Weber—1562(A)

Vibrations of two-dimensional crystals, Nicholas Chako 126(A)

Electrical circuits (see **Methods and instruments**)

Electrical conductivity and resistance

Breakdown in LiF, J. W. Davisson—1218(A)

Cathode spark velocities in $CuSO_4$ solutions, Hugh F. Henry—1232(A)

Change produced by cold work, J. S. Koehler—1219(A)

Conductivity pulses in liquid argon, Norman Davidson and A. E. Larsh, Jr.—220(L)

Electron bombardment conductivity in diamond, Kenneth G. McKay—1606

Electrical conductivity and resistance (continued)
Forward current in germanium point contacts, W. H. Brattain and J. Bardeen—231(L)
Impedance of tin at 24,000 mc/sec., E. Maxwell, P. M. Marcus, and J. C. Slater—1234(A)
Magnetic threshold curves of superconductors, J. G. Daunt—985(L)
Modulation of conductance of thin films by surface charges, W. Shockley and G. L. Pearson—232(L)
Molecular theory of superconductivity, F. London—562
Neutron-bombarded Ge semiconductors, R. E. Davis, W. E. Johnson, K. Lark-Horovitz, and S. Siegel—1255(A)
Non-rectifying Ge, W. C. Dunlap, Jr. and E. F. Hennelly—976(L)
Of Ge, electric field, Ralph Bray—1218(A)
Penetration depth in superconductors, temperature dependence, Jules de Launay and M. C. Steele—1235(A)
Penetration depth of field in superconductors, J. G. Daunt, A. R. Miller, A. B. Pippard, and D. Shoenberg—842(L); J. G. Daunt—985(L)
Photo-conductivity of Cd crystals, Rudolf Frerichs and A. J. F. Siegert—1875(L)
Rectification of insulating layer, H. Y. Fan—1505
Semiconductor triode, transistor, J. Bardeen and W. H. Brattain—230(L)
Semiconductors at high temperatures, P. H. Miller, Jr. and J. J. Markham—1218(A)
Theory of resistivity in Te, V. A. Johnson—1255(A)
Electrodynamic (see **Electromagnetic theory**)
Electromagnetic theory
Capture of electrons injected into betatron, D. W. Kerst—503(L)
Čerenkov radiation, John M. Harding and Joseph E. Henderson—1560(A)
Comparison between traveling wave tubes and linear accelerators, L. Brillouin—90
Diffraction by an aperture in infinite plane screen, Harold Levine and Julian Schwinger—958
Diffraction pattern in plane of apertures, C. L. Andrews—1231(A)
Dipole, quadrupole, and octupole field and search coils using loops and solenoids, W. M. Garrett—1231(A)
Electron motion in field of magnetic pole, Harish-Chandra—883
Electron's gyromagnetic ratio, Joseph W. Weinberg—1212(A)
Equations of motion of point charges, Peter Havas—456
First-order variational principle, F. J. Belinfante—779
Quantum-mechanical fluctuations of field, T. A. Welton—1157
Focusing in crossed fields of charged particles, Walter E. Millett—1058
Generalized electrodynamics, negative energies, Jerzy Rayski—629(L)
Impedance elements in wave guide equivalent circuits, Robert M. Whitmer—1231(A)
Invariant quantum electrodynamics, Julian Schwinger—1212(A)
Magnetic moment of the electron, J. M. Luttinger—893
Mass-energy relation, W. F. G. Swann—200
Motion of point electrons, U. Haber-Schaim—836(L)
Negative gradient of potential energy, F. W. Warburton—1562(A)
New magneto-electric effect, Elliot T. Benedikt—1563(A)
Phenomenological quantum-electrodynamics, J. M. Jauch and K. M. Watson—950
Photon self-energy problem, G. Wentzel—1070
Quantum electrodynamics, covariant formulation, Julian Schwinger—1439
Quantum theory of point electron, Mario Schönberg—738
Radiation from electrons accelerated in a synchrotron, F. R. Elder, R. V. Langmuir, and H. C. Pollock—52
Relativistic cut-off quantum electrodynamics, R. P. Feynman—939, 1212(A)
Single magnetic poles, P. A. M. Dirac—817
Space-charge wave amplification, Andrew V. Haeff—1532(L)
Theory of Čerenkov effect, Guido Beck—795
Electron diffraction
Electron microscopy of monolayers, H. T. Epstein—1256(A)
Electrons, positive (see **Positrons**)
Electrons, scattering of
Polarization of electrons, L. J. F. Broer—1887(L)
Electrons, secondary
By fast neutral molecules, H. W. Berry—848(L)
From insulators at low primary energies, Paul K. Weimer—1221(A)
From thoria on Pt and Ta, H. E. Mendenhall—1265(A)
Electro-optical effects (see also **Photoelectric effect and properties**)
Kerr effects at microwave frequencies, S. P. Cooke—701(L)
Electrostriction
Electrostrictive effect in barium titanate ceramics, W. P. Mason—1134
Elements
Alpha-decay systematics of heavy elements, I. Perlman, A. Ghiorso, and G. T. Seaborg—1730(L)
Formation of shielded isobars, J. S. Smart—1882(L)
Natural abundance of isotopes, J. R. White and A. E. Cameron—991
Neutron-capture theory of formation, R. A. Alpher—1577
Origin of elements, separation of galaxies, G. Gamow—505(L)
Relative abundance, Ralph A. Alpher and Robert Herman—1737
Energy states of atoms (see also **Spectra, atomic**)
Configurations of d^2sp, d^3p, and d^7p, F. Rohrlich—1372
Errata
Achromatization of Debye-Scherrer lines, H. Ekstein and S. Siegel—625(L)
Alkali halide scintillation counters, Robert Hofstadter—628(L)

Convergent expression for the magnetic moment of the neutron, D. Rivier and E. C. G. Stueckiberg—986(L)
Electromagnetic properties of nuclei in the meson theory, S. T. Ma and F. C. Yu—500(L)
On fine structure in the inversion spectrum of ammonia, R. S. Henderson—626(L)
Interferometric studies of faster-than-sound phenomena, R. Ladenburg, J. Winckler, and C. C. Van Voorhis —1884(L)
Magnetic threshold curves of superconductors, J. G. Daunt—985(L)
Mechanical properties of long chain molecule liquids at ultrasonic frequencies, W. P. Mason, W. O. Baker, H. J. McSkimin, and J. H. Heiss—1873(L)
On mechanism of electron emission at cathode spot of an arc, Jerome Rothstein—228(L)
On nuclear moments of I^{127}, Ga^{69}, Ga^{71}, and P^{31}, R. V. Pound—228(L)
Radial dependence of the tensor force in the deuteron, William G. Guindon—699(L)
Rapid method for the determination of the maximum energies of β-emitters with simple spectra, L. Yaffe and Katharine M. Justus—850(L)
Solid state interpretation of the structure near the limit of the continuous x-ray spectrum, Jesse W. M. DuMond—1883(L)
Theory of high frequency discharges, H. Margenau—706(L)
Thermal consequences of the capture of neutrinos by the earth, A. E. Benfield—1192(L)

Ferromagnetism (see **Magnetic properties**)
Fission of nucleus
Distribution of α's coincident with U^{235} fission, L. Marshall—1259(A)
Coincidences between fission neutrons, S. DeBenedetti, J. E. Francis, Jr., W. M. Preston, and T. W. Bonner —1645
Delayed neutrons from U^{235}, F. de Hoffmann, B. T. Feld, and P. R. Stein—1330
Excitation functions, J. Jungerman and S. C. Wright —150
Identification of Pu fission fragments, Seymour Katcoff, John A. Miskel, and Charles W. Stanley—631
Products of U, P. R. O'Conner and G. T. Seaborg—1189(L)
Ranges of plutonium fission fragments, S. Katcoff, J. A. Miskel, and C. W. Stanley—1225(A)
Stopping of fission fragments, W. M. Good, E. O. Wollan, and W. A. Strauser—1225(A)
Fluid dynamics (see **Hydrodynamics**)
Fluorescence
Of fluorobenzene, Arnold M. Bass and H. Sponer—1247(A)
Friction
Frictional electricity, E. W. B. Gill—842(L)
Internal friction and precipitation from solid solution, T'ing-Sui Kê—914

Gases (see also **Kinetic theory**)
Two-dimensional supersonic flow, D. Bershader and R. Ladenburg—1229(A)
Geophysics
Decay constants of K^{40} from accumulation of Ca^{40} in minerals, L. H. Ahrens and Robley D. Evans—279
Decay of K^{40}, L. B. Borst and J. J. Floyd—989(L)
Significance of K^{40}, T. Gráf—831(L)
Thermal consequences of capture of neutrinos by the earth, A. E. Benfield—621(L)

Hall effect
At microwave frequencies, S. P. Cooke—701(L)
Non-rectifying germanium, W. C. Dunlap, Jr. and E. F. Hennelly—976(L)
In semiconductors, I. Isenberg, B. R. Russell, and R. F. Greene—1255(A)
In Te, Virgil E. Bottom—1218(A)
Heat conduction (see **Thermal conductivity**)
Heat of vaporization
Of uranium hexafluoride, J. F. Masi—1220(A)
Hydrodynamics
Convention in sands, H. L. Morrison—119(A)
Hydrodynamic problem: flapping wave maker, E. H. Kennard—1229(A)
Rotational corner flows, R. C. Prim—1563(A)
Steady diabatic flows, B. L. Hicks—1230(A)
Turbulence by light diffraction, J. C. Hubbard, J. A. Fitzpatrick, W. J. Thaler, Laura Cheng, and R. J. Beeber—708(L)
Viscous fluid between parallel walls, C. L. Pekeris—191
Water entry of spherically tipped bodies, Harold Wayland and Saul Baker—1563(A)
Hyperfine structure (see also **Nuclear moments and spin**)
Intrinsic magnetic moment of electron, G. Breit—656
Spin-orbit effect, ammonia inversion spectrum, J. M. Jauch—1262(A)
Of Zn^{67}, O. H. Arroe—1263(A)

Ionization
By α-particles in A, William P. Jesse and Harold Forstat—1259(A)
Fluctuations of ionization, beta-spectra, D. H. W. Kirkwood, B. Pontecorvo, and G. C. Hanna—497(L)
Polarization effects in ionization loss, Frank L. Hereford —1224(A)
Specific primary ionization by electrons, Frank L. Hereford—574
Ionization potentials
Appearance potential of metastable ions, R. E. Fox, A. Langer, and J. A. Hipple—1222(A)
Ionization efficiency curves, S. N. Foner, A. Kossiakoff, and F. T. McClure—1222(A)
Molecular ionization potentials, Robert S. Mulliken—736
Ionosphere
Solar noise burst at 9500 Mc/sec., coincident solar flare, M. Schulkin, F. T. Haddock, K. M. Decker, C. H. Mayar, and J. P. Hagen—840(L)

Mesotrons (continued)
Electromagnetic properties of nuclei in the meson theory, erratum, S. T. Ma and F. C. Yu—500(L)
Emission of radiation, disintegration of mesons, Daniel B. Feer—1238(A)
Field deflections for determining mass, F. T. Rogers, Jr. —128(A)
Heavy mesons to lighter, R. M. Langer and Herman Yagoda—1238(A)
Lifetime of heavy meson, J. Reginald Richardson—1720
Light and heavy mesons, J. Leite Lopes—1722(L)
Mass estimation by grain counting, Walter H. Barkas, Eugene Gardner, and C. M. G. Lattes—1558(A)
Mass of mesons and other particles, E. C. Cullwick —707(L)
Mean life in C, C. W. Kissinger and D. Cooper—349(L)
Mean life in S, Harold K. Ticho—492(L)
Meson field and equations of motion of point particles, R. C. Majumdar and A. S. Apte—538
Mixed meson theory and divergence, Gentaro Araki—985(L)
Momentum distribution of electrons from negative mesons, H. Primakoff—878
Particles from stopped mesons, W. Y. Chang—1236(A)
Photons from meson-capture, O. Piccioni—1754
Photons from sea-level mesons, R. D. Sard and E. J. Althaus—1364
Photons from stopped mesons, Oreste Piccioni—1236(A)
Positive component in cosmic radiation, C. Ballario, M. Benini, and G. Calamai—1729(L)
Positive meson excess, M. H. Shamos, M. G. Levy, and I. S. Lower—1237(A)
Positive mesons produced by cyclotron, A. S. Bishop, John Burfening, Eugene Gardner, and C. M. G. Lattes—1558(A)
Production by cyclotron, experimental arrangement, Eugene Gardner and C. M. G. Lattes—1236(A)
Production by cyclotron, mass determination, C. M. G. Lattes and Eugene Gardner—1236(A)
Pseudovector meson theory, Gentaro Araki—986(L)
Range of decay electrons, M. H. Shamos and A. Russek —1545(L)
Range of electrons in meson decay, J. Steinberger—500(L)
Slow mesons in atmosphere, Matthew Sands—1237(A)
Trajectories of meson test particles, Banesh Hoffmann —1238(A)

Metals (see **Crystalline state**)

Meteorology
Atmospheric absorption of microwaves, H. R. L. Lamont —352(L)
Electrical activity related to thunderstorm growth, E. J. Workman and S. E. Reynolds—1231(A)
Generation of thunderstorm electricity, E. J. Workman and S. E. Reynolds—709(L)
Isotopes of C and O in atmosphere, Leo Goldberg, Orren C. Mohler, and Robert R. McMath—1881(L)
Meteor trials, diurnal variations, Charles A. Little, Jr. —1875(L)
Methane in the earth's atmosphere, Robert R. McMath, Orren C. Mohler, and Leo Goldberg—623(L)
N_2O in earth's atmosphere, J. H. Shaw, G. B. B. M. Sutherland, and T. W. Wormell—978(L)

Methods and instruments
Acoustic interferometer, Newton Underwood—124(A)
Alkali halide counters, Robert Hofstadter—100(L), 628(L)
All electronic, cloud-chamber control circuit, S. Bashkin and H. T. Richards—1260(A)
Amplifiers for use with magnetic generators, H. E. Wolf, H. Small, and J. H. Buehler—118(A)
Analysis of band of H_2S by punched-card methods, Gilbert W. King and R. M. Hainer—1247(A)
Analysis of organic materials, infra-red spectral reflectance, George Rappaport—115(A)
Analysis of solids by mass spectrometer, W. M. Hickam —1222(A)
Anthracene scintillation counters, Louis F. Wouters —489(L)
Auburn electronic Fourier synthesizer, R. Pepinsky and D. Sayre—126(A)
Auger electrons in coincidence experiments, S. K. Haynes and H. C. Thomas—128(A)
Axial magnetic suspension, J. F. Dillon and J. W. Beams —117(A)
Background eradication of nuclear emulsions, Herman Yagoda and Nathan Kaplan—1249(A)
Band width in electrostatic analyzer, Mary Jane Auld and F. T. Rogers, Jr. —128(A)
Barkhausen noise in circuit elements, R. T. Beyer and J. A. Krumhansl—1206(A)
Beam splitters, durable non-absorbing, R. W. Boydston —125(A)
"Brittleness" testing device, Charles D. Spencer—115(A)
Capture of electrons injected into a betatron, D. W. Kerst—503(L)
Carbon-pile type of voltage-regulator, V. E. Scherrer and F. W. Rogers, Jr.—119(A); E. E. Caldwell and F. T. Rogers, Jr. —120(A)
Cathode-follower type of dual-coincidence circuit, Arthur Linz, Jr., F. T. Rogers, Jr., and G. W. Crawford—119(A)
Cavity impedance, W. W. Hansen and R. F. Post—1560(A)
Characteristics of string galvanometer, G. W. Crawford and F. T. Rogers, Jr.—118(A)
Coil for producing longitudinal magnetic gradients, W. C. Wineland, T. M. Hahn, Jr., and L. R. Boyd—118(A)
Compensation of circuits for temperature, G. L. Jenkins and F. T. Rogers, Jr.—120(A)
Concentrating of He^3, B. B. McInteer, L. T. Aldrich, and Alfred O. Nier—946
Counter for low energy particles, H. C. Thomas and N. Underwood—127(A)
Crystal "growth" in electron microscope, A. C. Menius, Jr. and T. J. Turner—125(A)

Curved quartz crystal for x-rays and gamma-rays, David Lind, Bernard B. Watson, and Jesse W. M. DuMond—1561(A)
Deadtime theory of counters, S. S. Friedland and A. D. Krumbein—1244(A)
Detection of beta-radiation by photographic film, Jock Cobb and A. K. Solomon—354(A)
Determination of velocity distribution of atoms, Irving L. Kofsky and Henry Levinstein—500(L)
Detonation temperatures in high explosives, R. L. Boyer —1221(A)
Development of thick emulsions, M. Blau and J. A. DeFelice—1198(L)
Dipole, quadrupole, and octupole field and search coils, W. M. Garrett—1231(A)
Direct current analog computer, H. Belock, E. Bromberg, S. Fifer, U. Manfredi, R. McCoy, and H. Zagor —1230(A)
Discharge spread in counters, S. H. Liebson—694(L)
Double-focusing magnetic spectrograph, C. W. Snyder, C. C. Lauritsen, W. A. Fowler, and S. Rubin—1564(A)
Electron multiplier tube, disintegration experiments, Leticia del Rosario—304
Electrostatic analyzer, Samuel K. Allison and Harold V. Argo—1561(A); Mary Jane Auld—129(A); W. A. Bowers—128(A)
Electrostatic generator for positive ion acceleration, C. P. Swann and E. L. Hudspeth—1243(A)
Electrostatic generator for University of São Paul, O. Sala and R. G. Herb—1260(A)
Energy dependence of film meters, L. J. Deal, J. H. Roberson, and F. H. Day—127(A)
Error in absorption experiments, M. E. Rose and M. M. Shapiro—1853
Ethylene self-quenching counters, K. H. Morganstern, C. L. Cowan, and A. L. Hughes—499(L)
Fading of latent image, W. A. Lamb and F. W. Brown, III—104(L)
Fading of latent images of proton tracks, J. S. Cheka —127(A)
Field control system for magnetic spectrograph, E. P. Tomlinson—1231(A)
Flapping wave maker, E. H. Kennard—1229(A)
Flow type pressure controller, W. A. Wildhack—1229(A)
Fluctuations of ionization, beta-spectra, D. H. W. Kirkwood, B. Pontecorvo, and G. C. Hanna—497(L)
Focusing curved crystal spectrometer, annihilation radiation, Bernard B. Watson, David A. Lind, and Jesse W. M. DuMond—1561(A)
Focusing in crossed fields, Walter E. Millett—1058
Front surfaced mirrors, thermal evaporation, R. W. Boydston—124(A)
Gamma-ray isodosimeter, L. D. Marinelli and G. J. Hine—1245(A)
Gas pressures in exhaust flames of rocket motors, F. P. Bundy, A. B. Gregg, and H. M. Strong—1221(A)
Gas scattering in electron synchrotron, J. Mayo Greenberg and T. H. Berlin—1243(A)
Gas temperatures in exhaust flames of rocket motors, H. M. Strong and F. P. Bundy—1221(A)
Geiger counters for pulsed x-ray photon counting, P. Jarmotz and R. Pepinsky—126(A)
Geiger discharge, D. H. Wilkinson—1417
Generating voltmeter and electrometer, S. E. Reynolds and E. J. Workman—1231(A)
Generators of influence signals, B. P. Ramsay, J. H. Buehler, and C. E. Molineux—118(A)
High frequency loading, Nicholas Begovich—1563(A)
High frequency proton source, R. N. Hall—1558(A)
High pressure ion chamber, H. W. Fulbright and R. J. Britten—1251(A)
Image converter tube as electronic stroboscope, George H. Markstein—1230(A)
Integrator for small currents, H. G. Flanary, F. B. Pauls, and L. A. Pardue—125(A)
Intensity as factor in measurements in ultrasonics, J. A. Fitzpatrick, Thomas Kankovsky, and William J. Thaler—1227(A)
Ionization chamber cosmic-ray bursts, H. S. Bridge, W. E. Hazen, B. Rossi, and R. W. Williams—1083
Knudsen type vacuum gauge, J. T. Meers and L. A. Pardue—119(A)
Life of self-quenching counters, S. S. Friedland—898
Linear accelerator, electron ballistics, C. L. Clark—1243(A)
Linear electron accelerator, R. L. McCarthy, J. A. Lockwood, P. J. Rice, and H. L. Schultz—1243(A)
Linear-resistance flowmeter, A. S. Iberall and W. A. Wildhack—1229(A)
Liquid air as low temperature bath, Lester I. Bockstahler and Harmon Plumb—1235(A)
Lock-in amplifier, Walter C. Michels and Esther D. Redding—1562(A)
Loss of protons in synchrotron, Nelson M. Blachman and Ernest D. Courant—140
Low ionizing particles in photographic emulsions, J. Spence, J. Castle, and J. H. Webb—704(L)
Low pressure cloud chamber, Arthur Waltner—127(A)
Luminous flame temperatures, photoelectric pyrometer, J. A. Sanderson, J. A. Curcio, and Dorothy V. Estes —1221(A)
Magnetic analysis of disintegration products, W. W. Buechner, R. J. Van de Graaff, E. N. Strait, C. G. Stergiopoulos, and A. Sperduto—1226(A)
Magnetic field stabilizer, H. S. Somers, Jr., P. R. Weiss, and W. Halpern—1210(A)
Mass spectrometer for negative ions, Willard H. Bennett —1222(A)
Maximum energies of β-emitters, erratum, L. Yaffe and Katharine M. Justus—850(L)
Measurement of velocity and temperature in high speed air flow, Douglas Marlow, C. R. Nisewanger, and W. M. Cady—1229(A)
Methane-filled counters, Earle C. Farmer and Sanborn C. Brown—902
Method of studying nuclear energy levels, H. W. Fulbright and R. R. Bush—1205(A)

Methods and instruments (continued)
Modulation of chain reactor, A. M. Weinberg and H. C. Schweinler—851
Multicellular counter, David A. Lind—1566(A)
Multiplier tube for Li ion counting, A. H. Morrish and J. S. Allen—1260(A)
Multivibrator quenching of counter tubes, B. J. Thamer and A. F. Voigt—1261(A)
Naphthalene scintillations, R. F. Taschek and H. T. Gittings—1553(L)
Neutron spectra from proton recoils in emulsions, F. Reines—1565(A)
Noise and rectification in CbN bolometer, Donald H. Andrews—1234(A)
Nuclear plates in a magnetic field, determination of sign of particles, Ian G. Barbour—507(L)
Nuclear reactions involving polarized protons, Lincoln Wolfenstein—1224(A)
Nuclear reactor at Brookhaven, L. B. Borst, M. Fox, D. H. Gurinsky, I. Kaplan, R. W. Powell, C. Williams, and W. E. Winsche—1883(L)
Nuclear resonance experiment, Edward R. Manring, John R. Zimmerman, and Dudley Williams—1263(A)
Oscillatory method for measuring neutron cross sections, Alexander Langsdorf, Jr.—1216(A)
Parallel *T* resistance-capacitance network, C. E. Bergman and G. H. Fett—1206(A)
Particle size by the Hopper-Laby Stokes' law method, Wulf Kunkel—1557(A)
Particle size distribution in smokes, J. E. Rhodes, Jr. —124(A)
Particle tracks in emulsions, W. Van der Grinten—1244(A)
Photoelectric two-dimensional Fourier analyzer, D. Sayre and R. Pepinsky—127(A)
Photographic plates for nuclear physics, J. H. Webb —511
Photographic cloud-chamber tracks at 100,000 ft., Walter Frick, Edward J. Lofgren, Frank Oppenheimer, and Edward P. Ney—1258(A)
Proportional counter for beta-rays, C. J. Borkowski and E. Fairstein—1243(A)
Proton stopping power of Be, C. B. Madsen and P. Venkateswarlu—648
Rapid expansion of cloud chamber, Arthur Waltner —129(A)
Reaction time of counters, J. W. Keuffel—1562(A)
Recording microwave refractometer, George Birnbaum —1211(A)
Redesign of Princeton cyclotron, M. G. White, H. W. Fulbright, P. Gugelot, and R. R. Bush—1242(A)
Removal of latent image, Joseph De Felice—1244(A)
Rocket borne cloud chamber, G. J. Perlow, E. Krause, and C. Schroeder—1215(A); S. E. Golian, C. Y. Johnson, and M. Kuder—1215(A)
Scattering of particle tracks, S. A. Goudsmit and W. T. Scott—1537(L)
Scintillation counter, A. V. Tollestrup—1561(A)
Scintillation counting with anthracene, P. R. Bell and R. C. Davis—1245(A)
Self-controlled cloud chamber, Martin J. Cohen—1244(A)
Semiconductor triode, transistor, J. Bardeen and W. H. Brattain—230(L)
Short half-life determination, Martin H. Studier and Earl K. Hyde—591
Short period activities, A. D. Schelberg, M. B. Sampson, and A. C. G. Mitchell—1239(A)
Short x-ray pulses by a resonant cavity, L. B. Snoddy and J. W. Beams—126(A)
Sintering process, H. Christensen and C. J. Calbick —1219(A)
Slide rule settings, Vernier principle, Rodger C. Wickenden—116(A)
Slow neutron velocity spectrometer, W. W. Havens, Jr., L. J. Rainwater, C. S. Wu, and J. R. Dunning—1216(A)
Solar and coronal spectra in ultraviolet, J. E. Mack —1208(A)
Source charging in beta-spectrometers, C. H. Braden, G. E. Owen, J. Townsend, C. S. Cook, and F. B. Shull—1539(L)
Space charge of self-quenching counter, C. V. Robinson —1261(A)
Space-charge wave amplification, Andrew V. Haeff—1532(L)
Specimens from an ultra-centrifuge by quick freezing, M. L. Randolph—118(A)
Spectral emissivity determination, W. B. Nottingham and W. E. Mutter—1261(A)
Spectrometer measurement of gamma-radiation, David E. Alburger—1240(A)
Spectroscopy of gamma-rays, Jesse W. M. DuMond, David Lind, and Bernard B. Watson—1561(A)
Speed of brittle fracture in steel, Arthur Linz, Jr. and V. E. Scherrer—121(A)
Stabilization of microwave oscillators, José L. García Quevedo and William V. Smith—123(A)
Stabilized high voltage supply, R. L. Henkel and B. Petree—1260(A)
Starting potential of counter, P. B. Weisz—1807
Statistical error in transmission measurements, M. E. Rose and M. M. Shapiro—1213(A)
Superconducting bolometers, infra-red sensitivity, Nelson Fuson—1234(A)
Supersonic flow patterns by means of shock tube, C. W. Mautz, F. W. Geiger, and H. T. Epstein—1872(L)
Supersonic wind tunnel for optical studies, R. Ladenburg, C. C. Van Voorhis, and J. Winckler—1229(A)
Table of interplanar spacings in terms of 2θ, Suzanne Van Dijke Beatty—625(L)
Temperature in panel heated house, Clyde B. Crawley —120(A)
Tensiometer for small wires, G. W. Crawford—119(A)
Thickness of transition layer between ferromagnetic domains, C. Kittel and R. R. Newton—1604
Time-of-flight mass spectrometer, S. A. Goudsmit—622(L)

Transducer for measuring mechanical properties, Robert S. Marvin, Edwin R. Fitzgerald, and John D. Ferry —1256(A)
Traveling wave tubes and linear accelerators, L. Brillouin—90
Turbulence by light diffraction, J. C. Hubbard, J. A. Fitzpatrick, W. J. Thaler, Laura Cheng, and R. J. Beeber—708(L)
Variational methods in collision problems, W. Kohn —1763
Vector transforms, John W. Miles—1531(L)
Velocity and two-directional focusing of charged particles, N. Svartholm—108(L)
Velocity of discharge in counters, A. J. Knowles, C. Balakrishnan, and J. D. Craggs—627(L)
Wave guide fast counter, R. F. Post—1560(A)
Wide-range frequency modulation, K. R. MacKenzie— 104(L)

Microwaves (see also **Electromagnetic theory**, and **Spectra, microwave**)
Breakdown between coaxial cylinders, Melvin A. Herlin and Sanborn C. Brown—910
Conductivity of a gas at microwave frequencies, Edgar Everhart and Sanborn C. Brown—1210(A)
Dielectric constant of gases at 9340 megacycles, C. M. Crain—691
Electron microscopy of monolayers, H. T. Epstein— 1256(A)
Pressure broading in NH_3, DeForest F. Smith—506(L)
Recording microwave refractometer, George Birnbaum —1211(A)
Spectra of linear XYZ molecules, C. H. Townes, A. N. Holden, and F. R. Merritt—1113

Molecular structure and constants (see also **Spectra, molecular, etc.**, and **Raman spectra**)
Ammonia molecule, inversion spectrum, Masataka Mizushima—705(L)
Of chlorosilane, microwave determination, A. Harry Sharbaugh—1870(L)
Coupling of electron spins, R. S. Henderson and J. H. Van Vleck—106(L)
Distances and nuclear quadrupole couplings in ClCN, BrCN, and ICN, A. G. Smith, Harold Ring, W. V. Smith, and Walter Gordy—370
Force constant calculations for X_4Y_6, Harold W. Woolley—1247(A)
High energy states of N_2+ and N_2, R. B. Setlow—153
Interaction of nuclear electric quadrupole moments with molecular rotation, J. K. Bragg—533
Isotopic effect on potential function, J. G. Valatin— 346(L)
Molecular ionization potentials, Robert S. Mulliken— 736
Nuclear quadrupole moments, rotation in asymmetric molecules, G. Knight and B. T. Feld—354(A)
Rotational energy levels of H_2O and D_2O, N. Ginsburg —1052
Structures and nuclear couplings of methyl halides, Walter Gordy, James W. Simmons, and A. G. Smith —243

Moments, of particles (see also **Nuclear moments and spin**)
Magnetic moment of neutron, D. Rivier and E. C. G. Stueckiberg—218(L), 986(L)
Moment of electron, J. Barnóthy—113(L); P. Kusch and H. M. Foley—250

Neutrino (see also **Radioactivity; Scattering of electrons, neutrons, and ions**)
Preliminary results of He^6 neutrino experiment, James S. Allen, H. R. Paneth, and A. H. Morrish—1224(A)
Thermal consequences of capture of neutrinos by the earth, A. E. Benfield—621(L), 1192(L)

Neutrons
Absorption cross sections with pile oscillator, J. I. Hoover, W. H. Jordan, C. D. Moak, L. Parude, H. Pomerance, J. D. Strong, and E. O. Wollan—864
Absorption in Sa, A. J. Dempster—505(L)
Associated with sea level mesons in Pb, R. D. Sard, W. B. Ittner, III, A. M. Conforto, and M. F. Crouch 97(L)
In cosmic-ray showers, G. Cocconi, V. Cocconi Tongiorgi, and K. Greisen—1867
Cross sections of compounds, crystalline structures, Lester Winsberg, David Meneghetti, and S. S. Sidhu—1216(A)
Delayed emission from N^{17}, N. Knable, E. O. Lawrence, C. E. Leith, B. J. Moyer, and R. L. Thornton— 1217(A)
Density in atmosphere, Luke C. L. Yuan—504(L); J. A. Simpson, Jr.—1212(A)
Depolarization during diffusion, S. Borowitz—1215(A); Sidney Borowitz and Morton Hamermesh—1285
Depolarization of neutrons, M. Burgy, D. J. Hughes, and J. Wallace—1207(A)
Diffusion in medium with isotropic scattering, M. A. Greenfield—1215(A)
Diffusion in shielding materials, P. C. Gugelot and M. G. White—1215(A)
From U^{235} after short irradiation, F. de Hoffmann, B. T. Feld, and P. R. Stein—1330
High energy neutrons and heavy nuclei, M. L. Goldberger—1269
Inelastic scattering, J. M. Cassels and R. Latham— 103(L); L. Szilard, S. Bernstein, B. Feld, and J. Ashkin—1216(A)
Magnetic moment, F. Bloch, D. Nicodemus, and H. H. Staub—1025
Oscillating absorber in chain reactor, A. M. Weinberg and H. C. Schweinler—851
Oscillatory method of measuring cross sections, Alexander Langsdorf, Jr.—1216(A)
Photo-neutrons from fission products in Be, S. Bernstein, F. L. Talbott, J. K. Leslie, and C. P. Stanford —1258(A)
Polarization, J. Steinberger and G. C. Wick—1207(A)
Polarization by magnetized iron, J. M. Cassels—111(L)
Radioactive decay of neutron, H. Snell and L. C. Miller —1217(A)
Resonance scattering in crystals, R. Sternheimer—335

Neutrons (continued)
Scattering resonances in Sc to As, S. P. Harris and A. S. Langsdorf, Jr.—1216(A)
Yields from (D, n) reactions, Lyle W. Smith and P. Gerald Kruger—1258(A)
Neutron diffraction
By superlattices in order-disorder alloys, Sidney Siegel and C. G. Shull—1255(A)
Nuclear moments and spin (see also **Hyperfine structure**)
Of B^{10}, David R. Inglis—1876(L)
Of B^{11}, John R. Zimmerman and Dudley Williams—1885(L)
Broadening of magnetic resonance lines in crystals, J. H. Van Vleck—1168
Of Cl, C. K. Jen—1246(A)
Of H^3 and He^3, R. Avrami and R. G. Sachs—1320
Of I^{127}, Ga^{69}, Ga^{71}, and P^{31}, erratum, R. V. Pound—228(L)
Interaction with molecular rotation, J. K. Bragg—533
Line shapes in nuclear paramagnetism, G. E. Pake and E. M. Purcell—1184
Magnetic moment of nucleons, Gentaro Araki—986(L)
Of neutron and proton, Kenneth M. Case—1884(L)
Of N^{14} and I^{127}, C. H. Townes—1245(A)
Nuclear magnetic moments and meson exchange, P. Morrison—1224(A)
Nuclear relaxation in ice at −180°C, G. E. Pake and H. S. Gutowsky—979(L)
Nuclear resonance experiment, Edward R. Manring, John R. Zimmerman, and Dudley Williams—1263(A)
Of nuclei of mass ten, M. Goldhaber—1194(L)
Quadrupole interaction in CsF, J. W. Trischka—718
Quadrupole moment of Al^{27}, Hin Lew—1550(L)
Quadrupole moments of B^{10} and B^{11}, Walter Gordy, Harold Ring, and Anton B. Burg—1191(L)
Quadrupole moments of Cl, Luther Davis, Jr. and Carroll W. Zabel—1211(A)
Of Na^{22}, Luther Davis, Jr.—1193(L)
Spin and quadrupole moment of S^{33}, C. H. Townes and S. Geschwind—626(L)
Spins of carbon isotopes, F. A. Jenkins—355
Nuclear structure (see also **Disintegration of nucleus** and **Radioactivity**)
Abundance of elements, Ralph, A. Alpher and Robert Herman—1737
Binding energy of deuteron, R. E. Bell and L. G. Elliott—1552(L)
Closed shells in nuclei, Maria G. Mayer—235; Cecil B. Ellis—1547(L)
Composite particles, Nathan Rosen—128(A)
Double isomer in Rh^{103}, H. F. Gunlock and M. L. Pool 1264(A)
Energy levels in Mg, R. R. Bush and H. W. Fulbright—1206(A)
Energy levels of Al 28 and Mg 25, E. Pollard, V. L. Sailor, and L. D. Wyly—1233(A)
Exchange currents in nuclei, R. G. Sachs—433
Excited level in Li^7 from Li^6 (d, p) Li^7 and Be^9 (d, α) Li^7, W. W. Buechner, E. N. Strait, C. G. Stergipoulos, and A. Sperduto—1569
Excited state of Be^9, Conrad Longmire—1773
Formation of shielded isobars, J. S. Smart—1882(L)
Of Au^{199}, C. E. Mandeville and M. V. Scherb—1565(A)
Ground state of deuteron, Francis Low—1885(L)
Of He^3 nucleus from D-D reaction, Harold V. Argo—1293
Isomers of In, G. J. Goldsmith—1249(A)
Of Li^7, W. F. Hornyak and T. Lauritsen—1565(A)
Mean life of Li^{7*}, L. G. Elliott and R. E. Bell—1869(L)
Metastable state of Sc^{46}, M. Goldhaber and C. O. Muehlhause—1877(L)
Models for Be^9, Eugene Guth and Charles J. Mullin 832(L)
Neutron-proton force, John M. Blatt—92
Rotation vibration levels of Fe^{57} and Ni^{59}, H. A. Wilson—351(L)
Rotation vibration levels of Si^{28} and Al^{28}, H. A. Wilson—352(L)
Short-range repulsion, nuclear saturation, G. Parzen and L. I. Schiff—1564(A)
Spin of B^{10}, and spin-orbit coupling in Li^7, David R. Inglis—1876(L)
Tensor interactions between nucleons, Roy Thomas—1564(A)
Thermonuclear reactions in expanding universe, R. A. Alpher, R. Herman, and G. A. Gamow—1198(L)

Optical constants and properties
Of curved glass, D. W. Dunipace—116(A)
Infra-red dispersion of N_2O and C_2H_4, C. F. Hammer, A. G. Pieper, and R. Rollefson—1262(A)
Photoelastic properties of diamond, Elias Burstein and Paul L. Smith—1880(L)
Refractive index of hydrocarbons in near ultraviolet, James L. Lauer—1232(A)
Optical instruments (see **Methods and instruments**)

Packing fraction (see also **Isotopes**)
Of heavy elements, A. J. Dempster—1225(A)
Pair production
Cloud-chamber data, J. A. Phillips and P. Gerald Kruger—1259(A)
Internal conversion in carbon, C. B. Dougherty, W. F. Hornyak, T. Lauritsen, and V. K. Rasmussen—712(L)
Peltier effect (see **Thermoelectric effect**)
Phosphorescence
Of calcium silicate-lead phosphors, optical properties, Frank J. Studer and Gorton R. Fonda—1241(A)
Electron retrapping in infra-red phosphors, R. C. Herman, C. F. Meyer, and H. S. Hopfield—1242(A)
Excitation time on electron bombardment, J. F. Mullaney, F. Reines, and H. G. Weiss—491(L)
Inorganic phosphors, extreme ultraviolet region, E. M. Pell and D. H. Tomboulian—1242(A)
Photo-conductivity of infra-red phosphors, W. L. Parker and J. J. Dropkin—1242(A)
Of ZnF_2: Mn, Peter D. Johnson and Ferd E. Williams—1241(A)

Zinc beryllium silicate phosphors, Shannon Jones —116(A)
Of zinc silicate, temperature dependence, Walter C. Michels and Louise Gaus—1214(A)
Photo-conductivity
Of Cd crystals, Rudolf Frerichs and A. J. F. Siegert—1875(L)
Of cadmium sulfide, J. C. M. Brentano and D. H. Davis —711(L)
Effects of Cl and S in AgCl, Floyd R. Banks, Jr.—1207(A)
Of infra-red phosphors, W. L. Parker and J. J. Dropkin —1242(A)
Of AgCl and TlBr, Wallace C. Caldwell and Lloyd P. Smith—1207(A)
Photodisintegration
Angular distribution of protons from disintegration of deuteron, W. M. Woodward and I. Halpern—1225(A)
Of Be^9, Eugene Guth and Charles J. Mullin—833(L)
Of deuterium by gamma-rays from Na^{24}, N. O. Lassen —1533(L)
(γ, n) reactions, relative yields, W. A. Bowers—1538(L)
Production of protons in nuclei, E. D. Courant—1226(A)
Ratio of deuterium to beryllium thresholds, Bernard Waldman and Walter C. Miller—1225(A)
Reactions at 20 Mev, Dana L. Mock, Raymond C. Waddel, Lawrence W. Fagg, and Ralph A. Tobin —1536(L)
Thresholds for reactions, J. McElhinney, A. O. Hanson, and R. B. Duffield—1257(A)
Photoelasticity
Of diamond, Elias Burstein and Paul L. Smith—1880(L)
Properties of cubic crystals, Elias Burstein and Paul L. Smith—229(L)
Photoelectric effect and properties; cells
In semiconductors, L. Apker, E. Taft, and J. Dickey —1462
Photography
Background eradication of nuclear emulsions, Herman Yagoda and Nathan Kaplan—1249(A)
Development of thick emulsions, M. Blau and J. A. De Felice—1198(L)
Fading of latent image, W. A. Lamb and F. W. Brown III—104(L)
Fading of latent images of proton tracks, J. S. Cheka —127(A)
Low ionizing particles in photographic emulsions, J. Spence, J. Castle, and J. H. Webb—704(L)
Particle tracks in emulsions, W. Van der Grinten—1244(A)
Plates for nuclear physics, J. H. Webb—511
Removal of latent image, Joseph De Felice—1244(A)
Photons
Theory of elliptically polarized photons, Gentaro Araki —472
Photovoltaic effect
Basic concepts, barrier layer, K. Lehovec—463
Polymerization, properties of polymers
Radioactive zinc dimethyl dithiocarbamate in vulcanization of rubber, I. G. Geib—117(A)
ZnS in activated rubber vulcanizates, W. L. Davidson —116(A)
Positrons
Angular distribution of pair-produced electrons, P. V. C. Hough—80
Specific charge, J. Barnóthy—844(L)
Proceedings of the American Physical Society
Ohio Section, Columbus, Ohio, Meeting March 13, 1948 —114
Metropolitan Section, Brookhaven National Laboratory, March 26, 1948—1735
Southeastern Section, Oak Ridge, Tennessee, Meeting April 9–10, 1948—117
Washington, D. C., Meeting April 29–May 1, 1948 —1201
Ohio Section, Toledo, Ohio, Meeting May 8, 1948—114
New England Section, Cambridge, Massachusetts, Meeting May 29, 1948—354
Madison, Wisconsin, Meeting June 21–23, 1948—1253
Pasadena, California, Meeting June 24–26, 1948—1555

Quantum mechanics (see **Mechanics, quantum**)

Radiation (see also **Thermal radiation**)
Angular distribution of pair-produced electrons and bremsstrahlung, P. V. C. Hough—80
Čerenkov radiation, K. Watson and J. M. Jauch—1262(A)
Emissivity of Fe and Co, H. B. Wahlin and Harry W. Knop, Jr.—687
Emissivity of Fe-W and Fe-Co alloys, Harry W. Knop, Jr.—1413
From electrons accelerated in a synchrotron, F. R. Elder, R. V. Langmuir, and H. C. Pollock—52
Theory of Čerenkov effect, Guido Beck—795
Radio (see also **Ionosphere**)
Propagation of 147-mc radio waves, Robert N. Whitehurst—124(A)
Solar noise burst at 9500 Mc/sec., coincident solar flare, M. Schulkin, F. T. Haddock, K. M. Decker, C. H. Mayar, and J. P. Hagen—840(L)
Radioactivity (see also **Disintegration of nucleus**)
α-decay systematics of heavy elements, I. Perlman, A. Ghiorso, and G. T. Seaborg—1730(L)
α-ray spectrum of Po, Walter G. Wadey—1846
Of Al^{25} and Al^{26}, Hugh Bradner and J. D. Gow—1559(A)
Angular correlation of successive quanta, Edward L. Brady and Martin Deutsch—1541(L)
Angular distribution in reactions, C. N. Yang—764
Of As, D. A. McCown, L. L. Woodward, and M. L. Pool —1315
Auger electrons following K-capture in Cu^{64}, C. Sharp Cook and Lawrence M. Langer—1241(A)
Be^7 gamma-ray, Daniel J. Zaffarano, Bernard D. Kern, and Allan C. G. Mitchell—105(L)

Methods and instruments (continued)
Modulation of chain reactor, A. M. Weinberg and H. C. Schweinler—851
Multicellular counter, David A. Lind—1566(A)
Multiplier tube for Li ion counting, A. H. Morrish and J. S. Allen—1260(A)
Multivibrator quenching of counter tubes, B. J. Thamer and A. F. Voigt—1261(A)
Naphthalene scintillations, R. F. Taschek and H. T. Gittings—1553(L)
Neutron spectra from proton recoils in emulsions, F. Reines—1565(A)
Noise and rectification in CbN bolometer, Donald H. Andrews—1234(A)
Nuclear plates in a magnetic field, determination of sign of particles, Ian G. Barbour—507(L)
Nuclear reactions involving polarized protons, Lincoln Wolfenstein—1224(A)
Nuclear reactor at Brookhaven, L. B. Borst, M. Fox, D. H. Gurinsky, I. Kaplan, R. W. Powell, C. Williams, and W. E. Winsche—1883(L)
Nuclear resonance experiment, Edward R. Manring, John R. Zimmerman, and Dudley Williams—1263(A)
Oscillatory method for measuring neutron cross sections, Alexander Langsdorf, Jr.—1216(A)
Parallel *T* resistance-capacitance network, C. E. Bergman and G. H. Fett—1206(A)
Particle size by the Hopper-Laby Stokes' law method, Wulf Kunkel—1557(A)
Particle size distribution in smokes, J. E. Rhodes, Jr. —124(A)
Particle tracks in emulsions, W. Van der Grinten—1244(A)
Photoelectric two-dimensional Fourier analyzer, D. Sayre and R. Pepinsky—127(A)
Photographic plates for nuclear physics, J. H. Webb —511
Photographic cloud-chamber tracks at 100,000 ft., Walter Frick, Edward J. Lofgren, Frank Oppenheimer, and Edward P. Ney—1258(A)
Proportional counter for beta-rays, C. J. Borkowski and E. Fairstein—1243(A)
Proton stopping power of Be, C. B. Madsen and P. Venkateswarlu—648
Rapid expansion of cloud chamber, Arthur Waltner —129(A)
Reaction time of counters, J. W. Keuffel—1562(A)
Recording microwave refractometer, George Birnbaum —1211(A)
Redesign of Princeton cyclotron, M. G. White, H. W. Fulbright, P. Gugelot, and R. R. Bush—1242(A)
Removal of latent image, Joseph De Felice—1244(A)
Rocket borne cloud chamber, G. J. Perlow, E. Krause, and C. Schroeder—1215(A); S. E. Golian, C. Y. Johnson, and M. Kuder—1215(A)
Scattering of particle tracks, S. A. Goudsmit and W. T. Scott—1537(L)
Scintillation counter, A. V. Tollestrup—1561(A)
Scintillation counting with anthracene, P. R. Bell and R. C. Davis—1245(A)
Self-controlled cloud chamber, Martin J. Cohen—1244(A)
Semiconductor triode, transistor, J. Bardeen and W. H. Brattain—230(L)
Short half-life determination, Martin H. Studier and Earl K. Hyde—591
Short period activities, A. D. Schelberg, M. B. Sampson, and A. C. G. Mitchell—1239(A)
Short x-ray pulses by a resonant cavity, L. B. Snoddy and J. W. Beams—126(A)
Sintering process, H. Christensen and C. J. Calbick —1219(A)
Slide rule settings, Vernier principle, Rodger C. Wickenden—116(A)
Slow neutron velocity spectrometer, W. W. Havens, Jr., L. J. Rainwater, C. S. Wu, and J. R. Dunning—1216(A)
Solar and coronal spectra in ultraviolet, J. E. Mack —1208(A)
Source charging in beta-spectrometers, C. H. Braden, G. E. Owen, J. Townsend, C. S. Cook, and F. B. Shull—1539(L)
Space charge of self-quenching counter, C. V. Robinson —1261(A)
Space-charge wave amplification, Andrew V. Haeff—1532(L)
Specimens from an ultra-centrifuge by quick freezing, M. L. Randolph—118(A)
Spectral emissivity determination, W. B. Nottingham and W. E. Mutter—1261(A)
Spectrometer measurement of gamma-radiation, David E. Alburger—1240(A)
Spectroscopy of gamma-rays, Jesse W. M. DuMond, David Lind, and Bernard B. Watson—1561(A)
Speed of brittle fracture in steel, Arthur Linz, Jr. and V. E. Scherrer—121(A)
Stabilization of microwave oscillators, José L. García Quevedo and William V. Smith—123(A)
Stabilized high voltage supply, R. L. Henkel and B. Petree—1260(A)
Starting potential of counter, P. B. Weisz—1807
Statistical error in transmission measurements, M. E. Rose and M. M. Shapiro—1213(A)
Superconducting bolometers, infra-red sensitivity, Nelson Fuson—1234(A)
Supersonic flow patterns by means of shock tube, C. W. Mautz, F. W. Geiger, and H. T. Epstein—1872(L)
Supersonic wind tunnel for optical studies, R. Ladenburg, C. C. Van Voorhis, and J. Winckler—1229(A)
Table of interplanar spacings in terms of 2θ, Suzanne Van Dijke Beatty—625(L)
Temperature in panel heated house, Clyde B. Crawley —120(A)
Tensiometer for small wires, G. W. Crawford—119(A)
Thickness of transition layer between ferromagnetic domains, C. Kittel and R. R. Newton—1604
Time-of-flight mass spectrometer, S. A. Goudsmit—622(L)

Transducer for measuring mechanical properties, Robert S. Marvin, Edwin R. Fitzgerald, and John D. Ferry —1256(A)
Traveling wave tubes and linear accelerators, L. Brillouin—90
Turbulence by light diffraction, J. C. Hubbard, J. A. Fitzpatrick, W. J. Thaler, Laura Cheng, and R. J. Beeber—708(L)
Variational methods in collision problems, W. Kohn —1763
Vector transforms, John W. Miles—1531(L)
Velocity and two-directional focusing of charged particles, N. Svartholm—108(L)
Velocity of discharge in counters, A. J. Knowles, C. Balakrishnan, and J. D. Craggs—627(L)
Wave guide fast counter, R. F. Post—1560(A)
Wide-range frequency modulation, K. R. MacKenzie— 104(L)

Microwaves (see also **Electromagnetic theory**, and **Spectra, microwave**)
Breakdown between coaxial cylinders, Melvin A. Herlin and Sanborn C. Brown—910
Conductivity of a gas at microwave frequencies, Edgar Everhart and Sanborn C. Brown—1210(A)
Dielectric constant of gases at 9340 megacycles, C. M. Crain—691
Electron microscopy of monolayers, H. T. Epstein— 1256(A)
Pressure broading in NH_3, DeForest F. Smith—506(L)
Recording microwave refractometer, George Birnbaum —1211(A)
Spectra of linear XYZ molecules, C. H. Townes, A. N. Holden, and F. R. Merritt—1113

Molecular structure and constants (see also **Spectra, molecular, etc.**, and **Raman spectra**)
Ammonia molecule, inversion spectrum, Masataka Mizushima—705(L)
Of chlorosilane, microwave determination, A. Harry Sharbaugh—1870(L)
Coupling of electron spins, R. S. Henderson and J. H. Van Vleck—106(L)
Distances and nuclear quadrupole couplings in ClCN, BrCN, and ICN, A. G. Smith, Harold Ring, W. V. Smith, and Walter Gordy—370
Force constant calculations for X_4Y_6, Harold W. Woolley—1247(A)
High energy states of N_2+ and N_2, R. B. Setlow—153
Interaction of nuclear electric quadrupole moments with molecular rotation, J. K. Bragg—533
Isotopic effect on potential function, J. G. Valatin— 346(L)
Molecular ionization potentials, Robert S. Mulliken— 736
Nuclear quadrupole moments, rotation in asymmetric molecules, G. Knight and B. T. Feld—354(A)
Rotational energy levels of H_2O and D_2O, N. Ginsburg —1052
Structures and nuclear couplings of methyl halides, Walter Gordy, James W. Simmons, and A. G. Smith —243

Moments, of particles (see also **Nuclear moments and spin**)
Magnetic moment of neutron, D. Rivier and E. C. G. Stueckiberg—218(L), 986(L)
Moment of electron, J. Barnóthy—113(L); P. Kusch and H. M. Foley—250

Neutrino (see also **Radioactivity; Scattering of electrons, neutrons, and ions**)
Preliminary results of He^6 neutrino experiment, James S. Allen, H. R. Paneth, and A. H. Morrish—1224(A)
Thermal consequences of capture of neutrinos by the earth, A. E. Benfield—621(L), 1192(L)

Neutrons
Absorption cross sections with pile oscillator, J. I. Hoover, W. H. Jordan, C. D. Moak, L. Parude, H. Pomerance, J. D. Strong, and E. O. Wollan—864
Absorption in Sa, A. J. Dempster—505(L)
Associated with sea level mesons in Pb, R. D. Sard, W. B. Ittner, III, A. M. Conforto, and M. F. Crouch 97(L)
In cosmic-ray showers, G. Cocconi, V. Cocconi Tongiorgi, and K. Greisen—1867
Cross sections of compounds, crystalline structures, Lester Winsberg, David Meneghetti, and S. S. Sidhu—1216(A)
Delayed emission from N^{17}, N. Knable, E. O. Lawrence, C. E. Leith, B. J. Moyer, and R. L. Thornton— 1217(A)
Density in atmosphere, Luke C. L. Yuan—504(L); J. A. Simpson, Jr.—1212(A)
Depolarization during diffusion, S. Borowitz—1215(A); Sidney Borowitz and Morton Hamermesh—1285
Depolarization of neutrons, M. Burgy, D. J. Hughes, and J. Wallace—1207(A)
Diffusion in medium with isotropic scattering, M. A. Greenfield—1215(A)
Diffusion in shielding materials, P. C. Gugelot and M. G. White—1215(A)
From U^{235} after short irradiation, F. de Hoffmann, B. T. Feld, and P. R. Stein—1330
High energy neutrons and heavy nuclei, M. L. Goldberger—1269
Inelastic scattering, J. M. Cassels and R. Latham— 103(L); L. Szilard, S. Bernstein, B. Feld, and J. Ashkin—1216(A)
Magnetic moment, F. Bloch, D. Nicodemus, and H. H. Staub—1025
Oscillating absorber in chain reactor, A. M. Weinberg and H. C. Schweinler—851
Oscillatory method of measuring cross sections, Alexander Langsdorf, Jr.—1216(A)
Photo-neutrons from fission products in Be, S. Bernstein, F. L. Talbott, J. K. Leslie, and C. P. Stanford —1258(A)
Polarization, J. Steinberger and G. C. Wick—1207(A)
Polarization by magnetized iron, J. M. Cassels—111(L)
Radioactive decay of neutron, H. Snell and L. C. Miller —1217(A)
Resonance scattering in crystals, R. Sternheimer—335

Neutrons (continued)
Scattering resonances in Sc to As, S. P. Harris and A. S. Langsdorf, Jr.—1216(A)
Yields from (D, n) reactions, Lyle W. Smith and P. Gerald Kruger—1258(A)
Neutron diffraction
By superlattices in order-disorder alloys, Sidney Siegel and C. G. Shull—1255(A)
Nuclear moments and spin (see also **Hyperfine structure**)
Of B^{10}, David R. Inglis—1876(L)
Of B^{11}, John R. Zimmerman and Dudley Williams—1885(L)
Broadening of magnetic resonance lines in crystals, J. H. Van Vleck—1168
Of Cl, C. K. Jen—1246(A)
Of H^3 and He^3, R. Avrami and R. G. Sachs—1320
Of I^{127}, Ga^{69}, Ga^{71}, and P^{31}, erratum, R. V. Pound—228(L)
Interaction with molecular rotation, J. K. Bragg—533
Line shapes in nuclear paramagnetism, G. E. Pake and E. M. Purcell—1184
Magnetic moment of nucleons, Gentaro Araki—986(L)
Of neutron and proton, Kenneth M. Case—1884(L)
Of N^{14} and I^{127}, C. H. Townes—1245(A)
Nuclear magnetic moments and meson exchange, P. Morrison—1224(A)
Nuclear relaxation in ice at −180°C, G. E. Pake and H. S. Gutowsky—979(L)
Nuclear resonance experiment, Edward R. Manring, John R. Zimmerman, and Dudley Williams—1263(A)
Of nuclei of mass ten, M. Goldhaber—1194(L)
Quadrupole interaction in CsF, J. W. Trischka—718
Quadrupole moment of Al^{27}, Hin Lew—1550(L)
Quadrupole moments of B^{10} and B^{11}, Walter Gordy, Harold Ring, and Anton B. Burg—1191(L)
Quadrupole moments of Cl, Luther Davis, Jr. and Carroll W. Zabel—1211(A)
Of Na^{23}, Luther Davis, Jr.—1193(L)
Spin and quadrupole moment of S^{33}, C. H. Townes and S. Geschwind—626(L)
Spins of carbon isotopes, F. A. Jenkins—355
Nuclear structure (see also **Disintegration of nucleus** and **Radioactivity**)
Abundance of elements, Ralph, A. Alpher and Robert Herman—1737
Binding energy of deuteron, R. E. Bell and L. G. Elliott—1552(L)
Closed shells in nuclei, Maria G. Mayer—235; Cecil B. Ellis—1547(L)
Composite particles, Nathan Rosen—128(A)
Double isomer in Rh^{103}, H. F. Gunlock and M. L. Pool 1264(A)
Energy levels in Mg, R. R. Bush and H. W. Fulbright—1206(A)
Energy levels of Al 28 and Mg 25, E. Pollard, V. L. Sailor, and L. D. Wyly—1233(A)
Exchange currents in nuclei, R. G. Sachs—433
Excited level in Li^7 from Li^6 (d, p) Li^7 and Be^9 (d, α) Li^7, W. W. Buechner, E. N. Strait, C. G. Stergipoulos, and A. Sperduto—1569
Excited state of Be^9, Conrad Longmire—1773
Formation of shielded isobars, J. S. Smart—1882(L)
Of Au^{199}, C. E. Mandeville and M. V. Scherb—1565(A)
Ground state of deuteron, Francis Low—1885(L)
Of He^3 nucleus from D-D reaction, Harold V. Argo—1293
Isomers of In, G. J. Goldsmith—1249(A)
Of Li^7, W. F. Hornyak and T. Lauritsen—1565(A)
Mean life of Li^{7*}, L. G. Elliott and R. E. Bell—1869(L)
Metastable state of Sc^{46}, M. Goldhaber and C. O. Muehlhause—1877(L)
Models for Be^9, Eugene Guth and Charles J. Mullin 832(L)
Neutron-proton force, John M. Blatt—92
Rotation vibration levels of Fe^{57} and Ni^{59}, H. A. Wilson—351(L)
Rotation vibration levels of Si^{28} and Al^{28}, H. A. Wilson—352(L)
Short-range repulsion, nuclear saturation, G. Parzen and L. I. Schiff—1564(A)
Spin of B^{10}, and spin-orbit coupling in Li^7, David R. Inglis—1876(L)
Tensor interactions between nucleons, Roy Thomas—1564(A)
Thermonuclear reactions in expanding universe, R. A. Alpher, R. Herman, and G. A. Gamow—1198(L)

Optical constants and properties
Of curved glass, D. W. Dunipace—116(A)
Infra-red dispersion of N_2O and C_2H_4, C. F. Hammer, A. G. Pieper, and R. Rollefson—1262(A)
Photoelastic properties of diamond, Elias Burstein and Paul L. Smith—1880(L)
Refractive index of hydrocarbons in near ultraviolet, James L. Lauer—1232(A)
Optical instruments (see **Methods and instruments**)

Packing fraction (see also **Isotopes**)
Of heavy elements, A. J. Dempster—1225(A)
Pair production
Cloud-chamber data, J. A. Phillips and P. Gerald Kruger—1259(A)
Internal conversion in carbon, C. B. Dougherty, W. F. Hornyak, T. Lauritsen, and V. K. Rasmussen—712(L)
Peltier effect (see **Thermoelectric effect**)
Phosphorescence
Of calcium silicate-lead phosphors, optical properties, Frank J. Studer and Gorton R. Fonda—1241(A)
Electron retrapping in infra-red phosphors, R. C. Herman, C. F. Meyer, and H. S. Hopfield—1242(A)
Excitation time on electron bombardment, J. F. Mullaney, F. Reines, and H. G. Weiss—491(L)
Inorganic phosphors, extreme ultraviolet region, E. M. Pell and D. H. Tomboulian—1242(A)
Photo-conductivity of infra-red phosphors, W. L. Parker and J. J. Dropkin—1242(A)
Of ZnF_2: Mn, Peter D. Johnson and Ferd E. Williams—1241(A)

Zinc beryllium silicate phosphors, Shannon Jones —116(A)
Of zinc silicate, temperature dependence, Walter C. Michels and Louise Gaus—1214(A)
Photo-conductivity
Of Cd crystals, Rudolf Frerichs and A. J. F. Siegert—1875(L)
Of cadmium sulfide, J. C. M. Brentano and D. H. Davis —711(L)
Effects of Cl and S in AgCl, Floyd R. Banks, Jr.—1207(A)
Of infra-red phosphors, W. L. Parker and J. J. Dropkin —1242(A)
Of AgCl and TlBr, Wallace C. Caldwell and Lloyd P. Smith—1207(A)
Photodisintegration
Angular distribution of protons from disintegration of deuteron, W. M. Woodward and I. Halpern—1225(A)
Of Be^9, Eugene Guth and Charles J. Mullin—833(L)
Of deuterium by gamma-rays from Na^{24}, N. O. Lassen —1533(L)
(γ, n) reactions, relative yields, W. A. Bowers—1538(L)
Production of protons in nuclei, E. D. Courant—1226(A)
Ratio of deuterium to beryllium thresholds, Bernard Waldman and Walter C. Miller—1225(A)
Reactions at 20 Mev, Dana L. Mock, Raymond C. Waddel, Lawrence W. Fagg, and Ralph A. Tobin —1536(L)
Thresholds for reactions, J. McElhinney, A. O. Hanson, and R. B. Duffield—1257(A)
Photoelasticity
Of diamond, Elias Burstein and Paul L. Smith—1880(L)
Properties of cubic crystals, Elias Burstein and Paul L. Smith—229(L)
Photoelectric effect and properties; cells
In semiconductors, L. Apker, E. Taft, and J. Dickey —1462
Photography
Background eradication of nuclear emulsions, Herman Yagoda and Nathan Kaplan—1249(A)
Development of thick emulsions, M. Blau and J. A. De Felice—1198(L)
Fading of latent image, W. A. Lamb and F. W. Brown III—104(L)
Fading of latent images of proton tracks, J. S. Cheka —127(A)
Low ionizing particles in photographic emulsions, J. Spence, J. Castle, and J. H. Webb—704(L)
Particle tracks in emulsions, W. Van der Grinten—1244(A)
Plates for nuclear physics, J. H. Webb—511
Removal of latent image, Joseph De Felice—1244(A)
Photons
Theory of elliptically polarized photons, Gentaro Araki —472
Photovoltaic effect
Basic concepts, barrier layer, K. Lehovec—463
Polymerization, properties of polymers
Radioactive zinc dimethyl dithiocarbamate in vulcanization of rubber, I. G. Geib—117(A)
ZnS in activated rubber vulcanizates, W. L. Davidson —116(A)
Positrons
Angular distribution of pair-produced electrons, P. V. C. Hough—80
Specific charge, J. Barnóthy—844(L)
Proceedings of the American Physical Society
Ohio Section, Columbus, Ohio, Meeting March 13, 1948 —114
Metropolitan Section, Brookhaven National Laboratory, March 26, 1948—1735
Southeastern Section, Oak Ridge, Tennessee, Meeting April 9–10, 1948—117
Washington, D. C., Meeting April 29–May 1, 1948 —1201
Ohio Section, Toledo, Ohio, Meeting May 8, 1948—114
New England Section, Cambridge, Massachusetts, Meeting May 29, 1948—354
Madison, Wisconsin, Meeting June 21–23, 1948—1253
Pasadena, California, Meeting June 24–26, 1948—1555

Quantum mechanics (see **Mechanics, quantum**)

Radiation (see also **Thermal radiation**)
Angular distribution of pair-produced electrons and bremsstrahlung, P. V. C. Hough—80
Čerenkov radiation, K. Watson and J. M. Jauch—1262(A)
Emissivity of Fe and Co, H. B. Wahlin and Harry W. Knop, Jr.—687
Emissivity of Fe-W and Fe-Co alloys, Harry W. Knop, Jr.—1413
From electrons accelerated in a synchrotron, F. R. Elder, R. V. Langmuir, and H. C. Pollock—52
Theory of Čerenkov effect, Guido Beck—795
Radio (see also **Ionosphere**)
Propagation of 147-mc radio waves, Robert N. Whitehurst—124(A)
Solar noise burst at 9500 Mc/sec., coincident solar flare, M. Schulkin, F. T. Haddock, K. M. Decker, C. H. Mayar, and J. P. Hagen—840(L)
Radioactivity (see also **Disintegration of nucleus**)
α-decay systematics of heavy elements, I. Perlman, A. Ghiorso, and G. T. Seaborg—1730(L)
α-ray spectrum of Po, Walter G. Wadey—1846
Of Al^{28} and Al^{26}, Hugh Bradner and J. D. Gow—1559(A)
Angular correlation of successive quanta, Edward L. Brady and Martin Deutsch—1541(L)
Angular distribution in reactions, C. N. Yang—764
Of As, D. A. McCown, L. L. Woodward, and M. L. Pool —1315
Auger electrons following K-capture in Cu^{64}, C. Sharp Cook and Lawrence M. Langer—1241(A)
Be^7 gamma-ray, Daniel J. Zaffarano, Bernard D. Kern, and Allan C. G. Mitchell—105(L)

Radioactivity (continued)
Of Be^{10}, C. Eggler, D. J. Hughes, and C. Huddleston—1239(A)
β- and γ-radiation of W^{187} and Au^{198}, Roger G. Wilkinson and Charles L. Peacock—1250(A)
β- and γ-radiations of As^{76}, C. S. Wu, W. W. Havens, Jr., and L. J. Rainwater—1248(A)
β- and γ-rays of Rb^{86}, Daniel J. Zaffarano, Bernard D. Kern, and Allan C. G. Mitchell—682
β- and γ-spectra of Cs^{137}, J. Townsend, G. E. Owen, Marshall Cleland, and A. L. Hughes—99(L); J. Townsend, Marshall Cleland, and A. L. Hughes—499(L)
β- and γ-spectra of Ga^{70} and Ga^{72}, S. K. Haynes—423
β- and γ-spectrum of Sc^{46}, Charles L. Peacock and Roger G. Wilkinson—1240(A)
Beta-beta-coincidence for Ir^{192} and Ta^{182}, M. V. Scherb and C. E. Mandeville—508(L)
β-decay spectra of B^{12} and Li^{8}, W. F. Hornyak, C. B. Dougherty, and T. Lauritsen—1727(L)
β-decay theory at low energies, Eugene P. Cooper—1565(A)
β-ray spectra from Cu^{64}, W. E. Meyerhof and M. Goldhaber—348(L)
β-ray spectrum of P^{32}, E. J. Scott—1240(A)
β-spectra of C^{14} and S^{35}, C. Sharp Cook, Lawrence M. Langer, and H. Clay Price, Jr.—548; L. E. Glendenin and A. K. Solomon—700(L); Jane L. Berggren and Robert K. Osborne—1240(A)
β-spectra of Y^{90} and Sr^{90}, Walter E. Meyerhof—621(L)
β-spectrometers, source charging, C. H. Braden, G. E. Owen, J. Townsend, C. S. Cook, and F. B. Shull—1539(L)
β-spectrum of Be^{10}, D. J. Hughes and C. Eggler—1239(A)
β-spectrum of C^{14}, Lawrence M. Langer, C. Sharp Cook, and H. Clay Price, Jr.—1263(A)
β-spectrum of S^{35}, R. D. Albert and C. S. Wu—847(L)
Binding energies of α-particles, Truman P. Kohman—1259(A)
Of Br isotopes, L. L. Woodward, D. A. McCown, and M. L. Pool—870
Of Cd isomers, A. C. Helmholz and C. L. McGinnis—1559(A)
Of Ce and La, J. B. Chubbuck and I. Perlman—982(L)
Coincidences between beta-rays and conversion electrons in Eu, K. Y. Chu and M. L. Wiedenbeck—494(L)
Collateral chains to thorium and actinium families, A. Ghiroso, W. W. Meinke, and G. T. Seaborg—695(L)
Of Cb^{95}, C. E. Mandeville and M. V. Scherb—1266(A)
Of Cb^{95}, Re^{188}, Os^{191}, and Os^{193}, C. E. Mandeville, M. V. Scherb, and W. B. Keighton—888
Converted gamma-radiation from Ag, Cd, In, Pr, and Re, J. M. Cork, R. G. Schreffler, and C. M. Fowler—1657
Correlation between direction and polarization of quanta, Martin Deutsch and Franz Metzger—1542(L)
"Cross-over" transitions in gamma-ray spectra, V. Myers and A. Wattenberg—1264(A)
Decay constants of K^{40}, L. H. Ahrens and Robley D. Evans—279
Decay of neutron, H. Snell and L. C. Miller—1217(A)
Decay of tritium, W. J. Byatt, F. T. Rogers, Jr., and Arthur Waltner—699(L)
Decay times of scintillations, George B. Collins—1543(L)
Detection of beta-radiation by photographic film, Jock Cobb and A. K. Solomon—354(A)
From different crystal faces, J. H. J. Poole and J. W. Bremner—836(L)
From enriched Se^{74} and Se^{76}, L. L. Woodward, D. A. McCown, M. L. Pool, and H. L. Finston—1263(A)
Discoloration of glass, W. J. Arner and D. E. Sharp—116(A)
Of Eu, Gd, and Tb, N. L. Krisberg, M. L. Pool, and Carl T. Hibdon—44, 1249(A)
Of Eu and W, Franklin B. Shull—917
Of 47-hr. Sm^{153}, S. B. Burson and C. O. Muehlhause—1264(A)
Of Ga and Ge, D. A. McCown, L. L. Woodward, and M. L. Pool—1311
Of Ga^{67}, Ge^{69}, As^{73}, and As^{74}, D. A. McCown, L. L. Woodward, M. L. Pool, and H. L. Finston—1248(A)
γ-induced β-disintegration, experimental, R. L. Burling and F. N. D. Kurie—109(L)
γ-induced β-disintegration, theoretical, H. Primakoff—110(L)
Gamma-ray energies, positron emission, Franz N. D. Kurie and M. Ter-Pogossian—677
γ-ray transitions in Co^{60} and Se^{46}, R. G. Fluharty and Martin Deutsch—1241(A)
γ-rays from Cd, C. D. Moak and J. W. T. Dabbs—1249(A)
Gamma-rays from He^{6} and F^{18}, William J. Knox—1192(L)
γ-rays from Te and Sa, J. M. Cork, R. G. Shreffler, and C. M. Fowler—1249(A)
Half-life of C^{14}, L. Yaffe and Jean M. Grunlund—696(L); R. C. Hawkings, R. F. Hunter, W. B. Mann, and W. H. Stevens—696(L)
Half-life of K^{40}, T. Gráf—831(L)
Half-life of Rb^{87}, O. Haxel, F. G. Houtermans, and M. Kemmerich—1886(L)
Half-life of UX_1 (Th_{234}), G. B. Knight and R. L. Macklin—1540(L)
High energy deuteron bombardment of Cu, Dorothy Bockhop, A. C. Helmholz, and J. M. Peterson—1559(A)
High specific activity of carbon compounds, L. D. Norris and Arthur H. Snell—1240(A)
Induced in elements, J. M. Cork, R. G. Shreffler, and C. M. Fowler—240
Of I^{131}, Franz Metzger and Martin Deutsch—1641
Of Ir, C. E. Mandeville and M. V. Scherb—1250(A)
Isomers by slow neutron capture, M. Goldhaber and C. O. Muehlhause—1248(A)
Isotopes of Ge and As, D. A. McCown, L. L. Woodward, M. L. Pool, and H. L. Finston—1263(A)

Of isotopes of Y, Ru, Ce, 61, Sr, Ba, and La, Richard J. Hayden—650
Of Kr isotopes, L. L. Woodward, D. A. McCown, and M. L. Pool—761
Of La^{137} and Ce^{137}, M. G. Inghram and D. C. Hess, Jr. —627(L)
Of La, coincidence investigation, C. E. Mandeville and M. V. Scherb—1251(A)
Low energy portion RaE beta-spectrum, Arthur Waltner and F. T. Rogers, Jr.—699(L)
Of $Hg^{(203)}_{(205)}$, D. Saxon—849(L)
Metastable state of Sc^{46}, M. Goldhaber and C. O. Muehlhause—0000(L)
N^{17}, 4-second neutron emitter, Luis W. Alvarez—1217(A)
Of Os^{185} and Os^{193}, Leonard I. Katzin and M. Pobereskin —264
Of Pt^{193} and Au^{199}, C. E. Mandeville, M. V. Scherb, and W. B. Keighton—601
Of Pu fission fragments, Seymour Katcoff, John A. Miskel, and Charles W. Stanley—631
Polarization and direction of successive quanta, Donald R. Hamilton—782
Positive particles from P^{32}, J. S. Barlow and F. T. Rogers, Jr.—700(L)
Positron spectrum of Cu^{61}, C. Sharp Cook and Lawrence M. Langer—227(L)
Positron spectrum of N^{13}, C. S. Cook, L. M. Langer, H. C. Price, Jr., and M. B. Sampson—502(L)
Of K, L. T. Aldrich and Alfred O. Nier—876; L. B. Borst and J. J. Floyd—989; O. Hirzel and H. Wäffler —1553 (L); T. Gráf—1199(L); R. V. Langmuir—1559(A)
K^{40} β-spectrum, S. Franchetti and M. Giovanozzi—102(L)
Preparation and radiation of U^{237}, Lars Melander and Hilding Slätis—709(L)
Production of N^{17} by deuterons, W. W. Chupp and E. M. McMillan—1217(A)
Protactinium series, Martin H. Studier and Earl K. Hyde—591
Radiation of Hf^{181}, A. F. Voigt and B. J. Thamer—1264(A)
Radiations from Te^{121}, R. D. Hill and J. W. Mihelich 1874(L)
Of RaC, and RaC′, W. Y. Chang—1195(L)
Of RdTh, ThC, and ThC′, W. Y. Chang and T. Coor 1196(L)
Recoil in β-decay, O. Kofoed-Hansen—1785
Of Ru and Tc, D. T. Eggen and M. L. Pool—1248(A)
Of Ru and Tc isotopes, D. T. Eggen and M. L. Pool—57
Of Sm and Gd, K. K. Keller and K. B. Mather—624(L)
Of Sm^{153}, internal conversion electrons, R. D. Hill—78
Of Sc^{46}, Au^{198}, and $W^{185\ 187}$, Charles L. Peacock and Roger G. Wilkinson—297
Scintillations due to tritium β-rays, R. F. Taschek and H. T. Gittings—1537(L)
Short-lived isomers of nuclei, S. DeBenedetti and F. K. McGowan—728
Short period activities, A. D. Schelberg, M. B. Sampson, and A. C. G. Mitchell—1239(A)
Tc activities, E. E. Motta and G. E. Boyd—220(L)
Tc activities, deuteron bombardment of Mo, E. E. Motta and G. E. Boyd—344(L)
Of Tc^{95} and Tc^{98}, H. Medicus, A. Mukerji, P. Preiswerk, and G. de Saussure—839(L)
Of Te^{125}, metastable state, G. Friedlander, M. Goldhaber, and G. Scharff-Goldhaber—981(L)
Of Tb, Ho, Tm, Lu, Ta, W, and Re, Geoffrey Wilkinson and Harry G. Hicks—1733(L)
Of TiO_2, neutron bombardment, R. E. Hein and A. F. Voigt—1265(A)
Of W^{185} and Os^{193}, D. Saxon—1264(A)
Twenty-second activity in B, C^{10}, R. Sherr, H. R. Muether, and M. G. White—1239(A)
Of Zr^{95}, M. V. Scherb and C. E. Mandeville—1248(A)

Raman spectra
Polarizability theory of effect, Frank Matossi and Robert Mayer—449

Relativity
Boundary conditions as relativistic interaction, Marcos Moshinsky and E. P. Wigner—1212(A)
Coulumb scattering of relativistic electrons, William A. McKinley, Jr. and Herman Feshbach—1759
Field theories, T. S. Chang—1250(A)
Mass-energy relations, W. F. G. Swann—200
Quantization of space and time, H. T. Flint—209
Relativistic cut-off for quantum electrodynamics, R. P. Feynman—1430, 1212(A)

Scattering of electrons, neutrons, and ions (see also **Electrons, scattering of; Electron diffraction; Cross section**)
(α, n) cross sections of Be, Mg, and Al, I. Halpern —1234(A)
Analysis of proton-proton scattering, Charles L. Critchfield—1205(A)
Angular distribution, deuterons by deuterons, J. Morris Blair, George Freier, Eugene Lampi, William Sleator, Jr., and J. H. Williams—1594
Angular distribution, products of D−D reaction, J. Morris Blair, George Freier, Eugene Lampi, William Sleator, Jr., and J. H. Williams—1599
Boundary value condition for proton-proton scattering, G. Breit and W. G. Bouricius—1546(L)
Coulumb scattering of relativistic electrons, William A. McKinley, Jr., and Herman Feshbach—1759
Elastic scattering of nucleons by deuterons, calculation, Geoffrey F. Chew—809
Elastic scattering of protons by Al, R. S. Bender, F. C. Shoemaker, S. G. Kaufmann, and G. M. B. Bouricius —1205(A)
Energy loss for H^1, H^2, He^4, Li^6, Howard A. Wilcox —1743
Energy straggling of protons, C. B. Madsen and P. Venkateswarlu—1782
Inelastic scattering of fast neutrons, L. Szilard, S. Bernstein, B. Feld, and J. Ashkin—1216(A)

Scattering of electrons, neutrons, and ions (continued)
Inelastic scattering of neturons, J. M. Cassels and R. Latham—103(L)
Inelastic scattering of protons, H. W. Fulbright and R. R. Bush—1323
Multiple scattering with energy loss, Leonard Eyges—1534(L)
Neutron cross sections of compounds, crystalline structures, Lester Winsberg, David Meneghetti, and S. S. Sidhu—1216(A)
Neutron helium resonance scattering, L. Eisenbud —1206(A)
Neutron-proton force, John M. Blatt—1205(A)
Neutron-proton scattering models, L. Goldstein and D. W. Sweeney—1565(A)
Neutron scattering resonances in Sc to As, S. P. Harris and A. S. Langsdorf, Jr.—1216(A)
Of particles in synchrotron, Nelson M. Blachman and Ernest D. Courant—140
Phase of scattering of thermal neutrons by Ti, S. S. Sidhu, L. Winsberg, and D. Meneghetti—222(L)
Proton stopping power of Be, C. B. Madsen and P. Venkateswarlu—648
Protons by protons, 2.4- to 3.5-Mev, J. Morris Blair, George Freier, Eugene E. Lampi, William Sleator, Jr., and John H. Williams—553, 1205(A)
Of protons from Li^7, S. Rubin, C. W. Snyder, C. C. Lauritsen, and W. A. Fowler—1564(A)
Of slow neutrons by H, W. B. Jones, Jr.—364
Of slow neutrons in crystals, R. Sternheimer—335
Theory of scattering processes, Eugene Feenberg—664; Paul I. Richards—835(L)
Variational methods in collision problems, W. Kohn —1763
Scattering of radiation (see also **Raman spectra**)
In colloidal solutions, Peter G. Bergmann—1209(A)
Of Na^{24} gamma-radiation, Ernest Pollard and David E. Alburger—926
In supersonic streams, J. H. McQueen, J. W. Beams, and L. B. Snoddy—1551(L)
Secondary electrons (see **Electrons, secondary**)
Semiconductors (see **Electrical conductivity and resistance**)
Shock waves (see also **Explosion phenomena**)
Relativistic Rankine-Hugoniot equations, A. H. Taub —1230(A)
Supersonic flow patterns, C. W. Mautz, F. W. Geiger, and H. T. Epstein—1872(L)
Solid state (see **Crystalline state**)
Spectra, absorption
Of benzotrifluoride vapor in ultraviolet, H. Sponer and D. S. Lowe— 122(A)
Of ethyl and of *n*-propyl alcohol, E. K. Plyler and S. L. Kruegel—1247(A)
Of He atom, Su-Shu Huang—1262(A)
Isotopes of C and O in atmosphere, Leo Goldberg, Orren C. Mohler, and Robert R. McMath—1881(L)
Lines of methane in solar spectrum, Marcel V. Migeotte —112(L)
Microwave rotational in D_2O, M. W. P. Strandberg—1245(A)
N_2O in earth's atmosphere, J. H. Shaw, G. B. B. M. Sutherland, and T. W. Wormell—978
Pressure broadening in NH_3, DeForest F. Smith—506(L)
Reversal of secondary series, M. S. McCay—122(A)
Of tetraphenylisoporphine zinc salt, H. V. Knorr—115(A)
Of water vapor between 1.34μ and 1.97μ, R. C. Nelson and W. S. Benedict—703(L)
Of water vapor between 1.42μ and 2.50μ, Orren C. Mohler and W. S. Benedict—702(L)
Spectra, atomic
^2D terms of Li, K. W. Meissner, L. G. Mundie, and P. H. Stelson—932
^2D-terms of Li^7, K. W. Meissner, L. G. Mundie, and P. Stelson—1262(A)
Forbidden lines in O II, L. H. Aller, C. W. Ufford, and J. H. Van Vleck—1208(A)
g value of electron in hydrogen and deuterium, Edward B. Nelson and John E. Nafe—1210(A)
Intensity ratio of H_α and of D_α, Chao-Wang Hsueh —670
Isotope effects in Ne II, K. Murakawa and S. Suwa —1535(L)
Isotopic shift in He, Alan Andrew and W. W. Carter —838(L)
Low terms of Ti II, Henry Norris Russell—689
Nuclear dipole vibrations, M. Goldhaber and E. Teller —1046
Nuclear motion, fine structure of hydrogen, G. Breit and G. E. Brown—1278
Odd terms of Ti I, F. Rohrlich—1381
Rydberg denominators, J. G. Hirschberg, Jr.—1262(A)
Self-consistent field for Ca XIII, W. H. Davis, A. O. Williams, Jr., and R. T. Beyer—1208(A)
Shift of *S* levels in He II, J. E. Mack and N. Austern —1262(A)
S-level shift in ionized He, G. R. Fowles—219(L)
Spectra, general
Microwave spectroscopy, Myer Kessler and Walter Gordy—123(A)
Nuclear quadrupole interaction in CsF, J. W. Trischka —718
Nuclear radiofrequency spectra, quadrupole interactions, Norman F. Ramsay—286
Spectral emissivity of Fe and Co, H. B. Wahlin and Harry Knop—1207(A)
Stabilization of microwave oscillators, José L. García Quevedo and William V. Smith—123(A)
Theory of elliptically polarized photons, Gentaro Araki —472
Spectra, microwave
Absorption line frequencies of methyl alcohol, Donald K. Coles—1194(L)
Absorption line shapes for single crystals, John Wheatley, David Halliday, and J. H. Van Vleck—1211(A)
Atmospheric absorption, H. R. L. Lamont—352(L)
Of cyanogen halides, A. G. Smith, H. Ring, W. V. Smith, and W. Gordy—123(A)
In D_2O, M. W. P. Strandberg—1245(A)

Of ethylene oxide, R. G. Shulman, B. P. Dailey, and C. H. Townes—846(L)
Inversion spectrum of NH_3, James W. Simmons and Walter Gordy—123(A)
Of CH_3Cl, CH_3Br, and CH_3I, James W. Simmons, Walter Gordy, and A. G. Smith—1246(A)
Of linear *XYZ* molecules, C. H. Townes, A. N. Holden, and F. R. Merritt—1113
Of methyl-chloride, C. K. Jen—1246(A)
Quadrupole moments of B^{10} and B^{11}, Walter Gordy, Harold Ring, and Anton B. Burg—1191(L)
Resonance absorption in ferromagnetic semiconductors, William H. Hewitt, Jr.—1211(A)
Resonance absorption in potassium chrome alum, R. T. Weidner, P. R. Weiss, and C. A. Whitmer—1211(A)
Resonance absorption in single crystals, David Halliday and John Wheatley—2110(A)
Saturation effect, NH_3, Robert L. Carter and William V. Smith—123(A)
Saturation effects, Robert Karplus—223(L); William J. Pietenpol, John D. Rogers, and Dudley Williams —1246(A)
Structures and nuclear couplings of methyl halides, Walter Gordy, James W. Simmons, and A. G. Smith —243
Zeeman effect, C. K. Jen—1396

Spectra, molecular see also **Molecular structure and constants**)
Analysis of band of H_2S by punched-card methods, Gilbert W. King and R. M. Hainer—1247(A)
Aurora spectra, C. W. Gartlein—1208(A)
Band spectrum of HgTl, J. Gibson Winans and Willard J. Pearce—1262(A)
Of ethylene oxide, G. L. Cunningham, W. I. LeVan, and William D. Gwinn—1537(L)
Evidence for Sr isotopes, L. H. Ahrens—74
Infra-red of HCl in solution, Jack L. Parnell and Joseph W. Straley—123(A)
Infra-red of HF, Robert M. Talley and Alvin H. Nielsen —123(A)
Inversion spectrum of NH_3, fine structure, R. S. Henderson—107(L), 626(L)
Rotational of AsF^3, B. P. Dailey, K. Rusinow, R. G. Shulman, and C. H. Townes—1245(A)
Of water vapor, W. S. Benedict—1246(A)

Spectroscopy, technique
Spectrophotometry of fluorescent materials, W. R. Koch —115(A)

Stark effect
In diatomic molecules, W. A. Nierenberg and M. Slotnick —1246(A)
In methyl alcohol, Donald K. Coles—1194(L)

Statistical mechanics (see **Mechanics, statistical**)

Superconductivity (see **Electrical conductivity and resistance**)

Supersonics (see **Acoustics and Ultrasonics**)

Surface tension
Length of capillary, capillary rise of polar liquids, George Antonoff—1227(A)

Thermal conductivity
In liquid helium II, F. London and P. R. Zilsel—1148
Relaxation and heat conductivity in He II, Lothar Meyer and William Band—1235(A)
Relaxation theory, helium II, Lothar Meyer and William Band—394

Thermal radiation (see also **Radiation**)
Emissivity of Fe and Co, H. B. Wahlin and Harry W. Knop, Jr.—687
Emissivity of iron-tungsten and iron-cobalt alloys, Harry W. Knop, Jr.—1413
Temperature in panel heated house, Clyde B. Crawley —120(A)

Thermionic emission; Emitting surfaces
Anomalous values of emission constant, Henry F. Ivey —983(L); E. P. Wohlfarth—984(L)

Thermodynamics
Irreversibility and quantum mechanics, L. Tisza— 1213(A)
Irreversible processes in He, C. J. Gorter—1544(L)
Quantum statistics and **H** theorem, Harvey Einbinder —805
Redefinition of thermodynamic scale, F. G. Brickwedde —1220(A)
Second-order transformations, application to solutions of He^3 in He^4, J. W. Stout—605

Thermoelectric effects
Thomson for metals at high temperatures and Peltier coefficients, solid-liquid interfaces, J. J. Lander—479

Ultrasonics (see also **Acoustics**)
Absorption in resonant liquid column, Joseph L. Hunter —1228(A)
Concentration of beams by curved reflectors, F. E. Fox and V. Griffing—1228(A)
Distortion of ultrasonic waves, J. C. Hubbard, J. A. Fitzpatrick, B. T. Kankovsky, and William J. Thaler —107(L)
Intensity as factor in measurements, J. A. Fitzpatrick, Thomas Kankovsky, and William J. Thaler—1227(A)
Relativistic Rankine-Hugoniot equations, A. H. Taub —328
Supersonic wind tunnel for optical studies, R. Ladenburg, C. C. Van Voorhis, and J. Winckler—1229(A)
Temperature coefficient of velocity, D. R. McMillan, Jr. and W. E. Woolf—124(A)
Two-dimensional supersonic flow, D. Bershader and R. Ladenburg—1229(A)
Velocity and temperature measurement, Douglas Marlow, C. R. Nisewanger, and W. M. Cady—1228(A)
Velocity in liquid fluoro-carbons, R. T. Lagemann, John Evans, and Newton Underwood—124(A)
Velocity in liquid halides, Alfred Weissler—1228(A)

Vapor pressure
Of He^3, Henry A. Fairbank, Charles A. Reynolds, C. T. Lane, B. B. McInteer, L. T. Aldrich, and Alfred O. Nier—345(L)
Of O_3 from triple point to critical point, Harold J. Hoge —1221(A)

Viscosity
Of D_2O and of H_2O from 5° to 125°C, R. C. Hardy and R. L. Cottington—1220(A)

Wave guide (see **Electromagnetic theory**)

X-rays, absorption, diffraction, scattering, reflection, refraction, and polarization
Achromatization of Debye-Scherrer lines, H. Ekstein and S. Siegel, erratum—625(L)
Bragg reflections at small angles, Paul Kaesberg, H. N. Ritland, and W. W. Beeman—71
Compton effect for protons, J. L. Powell—1258(A)
Diffraction by three-dimensional lattices, Otto Halpern and Edward Gerjuoy—1562(A)
Diffuse reflections, piezoelectrically oscillating quartz, David C. Miller—166
MnK absorption edges, H. P. Hanson and W. W. Beeman—1261(A)
Polarization in Compton scattering, A. Wightman —1813
Small angle Bragg reflections, Paul Kaesberg, H. N. Ritland, and W. W. Beeman—1255(A)
Small angle scattering from amorphous materials, George H. Vineyard—1076
Small angle scattering from argon, George H. Vineyard —1209(A)

X-rays, emission (see also **X-rays, spectra and spectroscopy, etc.**)
Bremsstrahlung produced by protons, R. G. Sachs and J. L. Powell—1258(A)
Continuous spectrum, S. T. Stephenson and F. D. Mason—1560(A)
Continuous x-ray spectrum, Jesse W. M. DuMond—1883(L)
Ratio of bremsstrahlung cross sections, L. H. Lanzl, J. S. Laughlin, and L. S. Skaggs—1261(A)
Thick-target production, 1250 to 2350 kilovolts, W. W. Buechner, R. J. Van de Graaff, E. A. Burrill, and A. Sperduto—1348
Transition within L shell of S, D. H. Tomboulian—1887(L)

X-rays, spectra and spectroscopy, wave-length measurements (see also **X-rays, emission**)
Curved quartz crystal for x-rays and gamma-rays, David Lind, Bernard B. Watson, and Jesse W. M. DuMond—1566(A)
Table of interplanar spacings in terms of 2θ, Suzanne Van Dijke Beatty—625

X-rays, tubes, apparatus
Electron diffraction and x-ray tube, John E. Edwards and Karl A. Davis—116(A)
Grid-controlled fine-focus x-ray tube, H. M. Long, Jr. and R. Pepinsky—126(A)
High speed motion pictures, C. M. Slack, L. F. Ehrke, C. Zavales, D. Dickson, and R. G. Young—1230(A)
Short x-ray pulses by a resonant cavity, L. B. Snoddy and J. W. Beams—126(A)

Zeeman effect
In Au, J. B. Green and Howard N. Maxwell—1208(A)
In microwave molecular spectra, C. K. Jen—1396

THE

PHYSICAL REVIEW

Second Series

DECEMBER 15

Published for the

AMERICAN PHYSICAL SOCIETY

by the

AMERICAN INSTITUTE OF PHYSICS

Lancaster, Pa., and New York

THE PHYSICAL REVIEW

A journal of experimental and theoretical physics established by E. L. Nichols in 1893

Published by the American Institute of Physics
for the
AMERICAN PHYSICAL SOCIETY

Officers

President

J. R. Oppenheimer
Institute for Advanced Study
Princeton, New Jersey

Vice-President

F. W. Loomis
University of Illinois
Urbana, Illinois

Secretary

K. K. Darrow
Bell Telephone Laboratories
Office:
Columbia University
New York 27, New York

Treasurer

G. B. Pegram
Columbia University
New York 27, New York

Local Secretary
for the Pacific Coast

J. Kaplan
University of California at Los Angeles
Los Angeles, California

Managing Editor

John T. Tate
University of Minnesota
Minneapolis, Minnesota

BOARD OF EDITORS

Associate Editors

H. A. Bethe
L. A. Ellenour
W. H. Zachariasen

S. A. Goudsmit
E. M. Purcell
V. F. Weisskopf

All manuscripts for publication should be submitted to John T. Tate, [illegible], University of Minnesota, Minneapolis, Minnesota.

All correspondence concerning papers in the process of publication should be addressed to the Publication Manager, American Institute of Physics, [illegible] 55 Street, New York 22, New York.

Subscription Price

[illegible] States and Canada $15.00
[illegible] $16.50

Back Numbers

Complete sets, Series 2, Vol. 1, 1913–Vol. 72, 1947—$630.00
[illegible] $20.00
[illegible] $2.00 each, price to July, 1929;
[illegible] $1.00 each, July, 1929–December, 1941;
[illegible] $2.00 each, January, 1942–December, 1946.
[illegible] $1.00 each.

[illegible] and orders for back numbers should be addressed to the [illegible], Lancaster, Pennsylvania, or to the American Institute of Physics, [illegible] 55 Street, New York 22, New York.

[illegible] in the case of members of the American Physical Society should be addressed to the Treasurer; in the case of other subscribers to the Business Manager, American Institute of Physics.

[illegible] Department of Physics, Cornell University, Ithaca, New York.

The Physical Review is published [illegible] Ritter and Lemon Streets, Lancaster, Pennsylvania.

Entered as second-class matter March 6, 1917, [illegible] at Lancaster, Pennsylvania, under the Act of March 3, 1879.

Acceptance for mailing at special rate of [illegible] provided for in section 538, P. L. & R., authorized January 27, 1925.